# Development of unconventional biocatalytic strategies for the synthesis of sulfoxides

Silvia Anselmi

**University College London (UCL)**

**2023**

Supervised by Dr. Daniele Castagnolo (primary) and
Dr. Sarah M. Barry (secondary)

*Submitted in partial fulfilment of the requirements for the degree of Doctor of Philosophy (PhD)*

***"This is the Golden Age of Biocatalysis"***

*Prof N. J. Turner and Dr R. Kumar, Current Opinion in Chemical Biology, 2018.*[1]

## Declaration

I, Silvia Anselmi, confirm that the work presented in this thesis is my own. Where information has been derived from other sources, I confirm that this has been indicated in the thesis and in the Author contribution statement on page vi.

## Author contribution statement

The author of this thesis and Ms Jingyue Wu contributed equally to the development of the project illustrated in Chapter 3.

In Chapter 4, the *in silico* modelling, docking and MD simulations were carried out by Dr Alexandra Carvalho, from the department of Biocatalysis & Isotope Chemistry, Almac. Ms Angela Serrano-Sanchez carried out the protein NMR experiments and data interpretation under the supervision of Dr Jose L. Ortega-Roldan, School of Biosciences, University of Kent.

## Abstract

The synthesis of sulfoxides represents an ongoing challenge for the scientific community as these molecules find many applications in chemistry, varying from organic synthesis to medicinal chemistry. With the aim of providing a solution to the toxic and hazardous methods classically used for the synthesis of sulfoxides, biocatalysis has emerged in the past several decades as an alternative green and sustainable strategy to obtain both racemic and enantiopure sulfoxides. However, the use of enzymes still has some drawbacks, especially in terms of industrial applicability, as they often work on laboratory scale only, may lead to the production of other oxidative side products, or require the use of expensive cofactors and effective oxygenation.

In this thesis, three different biocatalytic approaches for the synthesis of sulfoxides applicable in both academic and industrial settings are illustrated. First, the immobilised enzyme *Candida antarctica* lipase B (CALB) was exploited to develop a mild, chemoselective and sustainable biocatalytic method, suitable for industrial use, for the preparation of sulfoxides from sulfides. Second, Baeyer-Villiger and flavine monooxygenases (BVMOs and FMOs respectively) were investigated for the production of enantiopure sulfoxides that display multiple functional groups. Lastly, the reductive enzyme methionine sulfoxide reductase A (MsrA) from *Saccharomyces cerevisiae* was employed for the kinetic resolution (KR) of racemic sulfoxides using the inexpensive recycling co-substrate dithiothreitol and a total of 23 (*R*)-sulfoxides were obtained with excellent enantiomeric excess and yields. Additionally, the catalytic mechanism of the enzyme was investigated in depth via structural biology, mutagenesis, and *in silico* studies, which also led to the development of a new engineered MsrA biocatalyst capable of reducing bulky substrates.

## Impact statement

With this research the authors intended to achieve a slowly growing and long-lasting impact on the scientific society, showcasing alternative biocatalytic routes for the synthesis of essential chemical functional groups. In fact, there is a global urge to find greener routes for chemical transformations that have a milder impact on the environment. Being based on the use of biodegradable and non-toxic enzymes, biocatalysis offers substantial benefits from an environmental point of view compared to the traditional methods that are generally more toxic, hazardous and based on the use of fossil fuel derived materials.

Therefore, in this thesis, three novel biocatalytic methodologies are reported for the synthesis of sulfoxides, organosulfur compounds that find application in many areas of chemistry and are also common in active pharmaceutical ingredients.

The impact of the research carried out in this thesis has so far been documented in a research paper on the use of immobilised CALB for the synthesis of racemic sulfoxides, a methodology developed in an academic environment but that has the potential of being applied in industry too. This work, which is illustrated in Chapter 1, has a positive impact on the environment and human health because, among its benefits, it avoids the use of stoichiometric amounts of explosive oxidants, such as *m*CPBA.

The research showed in Chapter 3 on the identification of new monooxygenase enzymes that carry out chemo- and stereoselective sulfoxidations on multifunctional substrates was instead predicted to have an impact especially in the broader context of research. In particular, it would allow the scientific community to expand the knowledge on this class of biocatalysts and consecutively develop novel enzymes for the production of complex chiral sulfoxides.

Lastly, with the development of a methodology for the enantioselective production of (*R*)-sulfoxides explained in Chapter 4, we aimed at impacting the scientific society by adding knowledge to and expanding the toolbox of the field of biocatalysis. The reductive enzymes utilised in this chapter require dithiothreitol as an inexpensive recycling sacrificial co-substrate, an advantage compared to enzymes that instead need expensive cofactors and their relative recycling systems. This therefore has a positive economic impact on the cost of the reaction process. Additionally, more awareness was brought to the potential of reductive enzymes for the synthesis of enantiopure sulfoxides in a review paper.

# UCL Research Paper Declaration Form: referencing the doctoral candidate's own published work(s)

Please use this form to declare if parts of your thesis are already available in another format, e.g. if data, text, or figures:

- have been uploaded to a preprint server;
- are in submission to a peer-reviewed publication;
- have been published in a peer-reviewed publication, e.g. journal, textbook.

*This form should be completed as many times as necessary. For instance, if you have seven thesis chapters, two of which containing material that has already been published, you would complete this form twice.*

| | | |
|---|---|---|
| **1.** For a research manuscript that has already been published (if not yet published, please skip to section 2): | | |
| **a)** Where was the work published? (e.g. journal name) | Organic and Biomolecular Chemistry | |
| **b) Who published the work?** (e.g. Elsevier/Oxford University Press): | Royal Society of Chemistry | |
| **c)** When was the work published? | 06/11/2020 | |
| **d)** Was the work subject to academic peer review? | Yes | |
| **e)** Have you retained the copyright for the work? | No - a CC BY licence was required by the funding body.<br>"If the third party work is licensed under a Creative Commons licence, or other terms of use that allow a licensee to make copies available publicly, you do not need permission."<br>https://www.ucl.ac.uk/library/ucl-copyright-advice/copyright-research | |
| [If no, please seek permission from the relevant publisher and check the box next to the below statement]:<br>☒ I acknowledge permission of the publisher named under 1b to include in this thesis portions of the publication named as included in 1a. | | |
| **2.** For a research manuscript prepared for publication but that has not yet been published (if already published, please skip to section 3): | | |
| **a)** Has the manuscript been uploaded to a preprint server? (e.g. medRxiv): | Please select. | **If yes, which server?** Click or tap here to enter text. |
| **b) Where is the work intended to be published?** (e.g. names of journals that you are planning to submit to) | Click or tap here to enter text. | |
| **c)** List the manuscript's authors in the intended authorship order: | Click or tap here to enter text. | |
| **d)** Stage of publication | Please select. | |
| **3.** For multi-authored work, please give a statement of contribution covering all authors (if single-author, please skip to section 4): | | |

| | | | |
|---|---|---|---|
| Silvia Anselmi and Daniele Castagnolo developed the methodology. Silvia Anselmi, Siyu Liu and Seong-Heun Kim contributed to the expansion of the scope of the biocatalytic methodology. The manuscript was drafted by Silvia Anselmi and it was revised by Sarah M. Barry, Thomas S. Moody and Daniele Castagnolo and other contributing authors. | | | |
| **4.** In which chapter(s) of your thesis can this material be found? | | | |
| Chapter 2 | | | |
| **5. e-Signatures confirming that the information above is accurate** (this form should be co-signed by the supervisor/ senior author unless this is not appropriate, e.g. if the paper was a single-author work): | | | |
| Candidate: | Silvia Anselmi | Date: | 22/02/2023 |
| Supervisor/ Senior Author (where appropriate): | Daniele Castagnolo | Date: | 22/02/2023 |

| | | | |
|---|---|---|---|
| **1.** For a research manuscript that has already been published (if not yet published, please skip to section 2): | | | |
| **a)** Where was the work published? (e.g. journal name) | ChemBioChem | | |
| **b) Who published the work?** (e.g. Elsevier/Oxford University Press): | Wiley-VCH GmbH | | |
| **c)** When was the work published? | 31/07/2020 | | |
| **d)** Was the work subject to academic peer review? | Yes | | |
| **e)** Have you retained the copyright for the work? | No - a CC BY licence was required by the funding body.<br>"If the third party work is licensed under a Creative Commons licence, or other terms of use that allow a licensee to make copies available publicly, you do not need permission."<br>https://www.ucl.ac.uk/library/ucl-copyright-advice/copyright-research | | |
| [If no, please seek permission from the relevant publisher and check the box next to the below statement]:<br>☒ I acknowledge permission of the publisher named under 1b to include in this thesis portions of the publication named as included in 1a. | | | |
| **2.** For a research manuscript prepared for publication but that has not yet been published (if already published, please skip to section 3): | | | |
| **e)** Has the manuscript been uploaded to a preprint server? (e.g. medRxiv): | Please select. | **If yes, which server?** Click or tap here to enter text. | |
| **f) Where is the work intended to be published?** (e.g. names of journals that you are planning to submit to) | Click or tap here to enter text. | | |
| **g)** List the manuscript's authors in the intended authorship order: | Click or tap here to enter text. | | |
| **h)** Stage of publication | Please select. | | |
| **3.** For multi-authored work, please give a statement of contribution covering all authors (if single-author, please skip to section 4): | | | |
| Silvia Anselmi and Nandini Aggarwal drafted the manuscript, which was revised by Thomas S. Moody and Daniele Castagnolo. | | | |
| **4.** In which chapter(s) of your thesis can this material be found? | | | |
| Chapter 2 and Chapter 4 | | | |
| **5. e-Signatures confirming that the information above is accurate** (this form should be co-signed by the supervisor/ senior author unless this is not appropriate, e.g. if the paper was a single-author work): | | | |
| Candidate: | Silvia Anselmi | Date: | 22/02/2023 |
| Supervisor/ Senior Author (where appropriate): | Daniele Castagnolo | Date: | 22/02/2023 |

| | | | |
|---|---|---|---|
| **1.** For a research manuscript that has already been published (if not yet published, please skip to section 2): | | | |
| **a)** Where was the work published? (e.g. journal name) | Click or tap here to enter text. | | |
| **b) Who published the work?** (e.g. Elsevier/Oxford University Press): | Click or tap here to enter text. | | |
| **c)** When was the work published? | Click or tap to enter a date. | | |
| **d)** Was the work subject to academic peer review? | Please select. | | |
| **e)** Have you retained the copyright for the work? | Please select. | | |
| [If no, please seek permission from the relevant publisher and check the box next to the below statement]:<br>☐ I acknowledge permission of the publisher named under 1b to include in this thesis portions of the publication named as included in 1a. | | | |
| **2.** For a research manuscript prepared for publication but that has not yet been published (if already published, please skip to section 3): | | | |
| **i)** Has the manuscript been uploaded to a preprint server? (e.g. medRxiv): | No | **If yes, which server?** Click or tap here to enter text. | |
| **j) Where is the work intended to be published?** (e.g. names of journals that you are planning to submit to) | ACS Catalysis | | |
| **k)** List the manuscript's authors in the intended authorship order: | Silvia Anselmi, Alexandra Carvalho, Angela Serrano-Sanchez, Jose L. Ortega-Roldan, Jill Caswell, Iman Omar, Gustavo Perez-Ortiz, Sarah M. Barry, Thomas S. Moody and Daniele Castagnolo | | |
| **l)** Stage of publication | Undergoing revision after peer review | | |
| **3.** For multi-authored work, please give a statement of contribution covering all authors (if single-author, please skip to section 4): | | | |
| The biocatalytic methodology was developed by Silvia Anselmi and Daniele Castagnolo. Alexandra Carvalho performed all in silico studies. Angela Serrano-Sanchez and Jose L. Ortega-Roldan carried out the NMR studies. Silvia Anselmi, Alexandra Carvalho, Jill Caswell, Iman Omar and Gustavo Perez-Ortiz contributed to the production and purification of the enzymes. The manuscript was drafted by Silvia Anselmi and Daniele Castagnolo and was revised by Sarah M. Barry, Thomas S. Moody and other contributing authors. | | | |
| **4.** In which chapter(s) of your thesis can this material be found? | | | |
| Chapter 4 | | | |
| **5. e-Signatures confirming that the information above is accurate** (this form should be co-signed by the supervisor/ senior author unless this is not appropriate, e.g. if the paper was a single-author work): | | | |
| Candidate: | Silvia Anselmi | Date: | 22/02/2023 |
| Supervisor/ Senior Author (where appropriate): | Daniele Castagnolo | Date: | 22/02/2023 |

## Acknowledgements

The past four years have been an incredible journey full of ups and (lock)downs that allowed me to grow both as a scientist and as a person and culminated with the writing of this thesis. This odyssey, however, would have not been possible without the help and encouragement of a few people, who have been vital for my PhD survival.

First and foremost, I would like to thank my supervisor, Daniele, whose advice, guidance, positive attitude, and always-open door have been essential for the completion of this PhD. Dan's actions have also shown me what it truly means to empower women in science, by allowing me to develop my own thoughts and ideas and pushed me to never give up even when I couldn't see the light at the end of the 'project tunnel'. His support had also extended beyond work, as he has listened and supported me when I was at my lowest moments during this journey. I will miss our procrastination friendly chats in your office! I would also like to profoundly thank my secondary supervisor, Sarah, who welcomed me into her lab and gave me the opportunity to learn and love molecular biology.

Just like Ulysses had his comrades in his adventures, I had my group to keep me company during my PhD odyssey. These are the people that brightened the day-to-day lab life and, also, made a pretty awesome lunch crew. Amber, Domi, Vladimir, Fei, Michele, Kate, Ariane, Gui, Chuhan, Krisztina, Blaz, Gustavo, Sophie and everyone else who has been part of the group, we all started off as colleagues but I am now proud of calling you all my friends and I hope our paths will cross again in the future. Two special thank yous go to Sabina and Iman, my PhD sisters. Sab, I will always remember that 1st of October 2018 when we, two strangers, stepped together into corridor 5D not knowing how important our friendship would become to face together all that the PhD would throw at us. Iman, you have been such a great friend since the day you joined the group, you always had my back and never hesitated to help anyone (me) in need of advice. It's been an honour embarking on this journey with you both!

This PhD would have not been the same without the partnership with Almac, through which I met some inspiring people, including Tom, Jill, Alexandra and Lyndsey, who have been very patient with me during my placements and have shown me the true potential of what can be achieved through academia and industry multidisciplinary collaborations.

I would also like to spend a few words to thank Billy, my boyfriend. You were in my master's acknowledgements as my friend and lab mate and have upgraded to boyfriend and life partner in my PhD ones. Who knew all it took was a drunken wish, and now you

are stuck with me! You truly are my rock and I would have not been able to get through this without your love and support. There is so much I could say on how important you have been to me and how much you have changed my life in the past four years, but I know you hate these things so I will just say: I love you.

These acknowledgements could not be completed without thanking my parents, Stefania and Bruno, who have been nothing but encouraging of me and my dreams and when I hit the very emotional and mental rock bottom in this journey, I don't know what I would have done if you hadn't been there. Our family arrangements have been less than ideal in the past 10 years, but despite that you continue to show me and my brother the importance of perseverance and resilience to achieve what really matters in life. You are incredible parents, and I would like to dedicate this thesis to you both.

# Table of Contents

Declaration ..... v

Author contribution statement ..... vi

Abstract ..... vii

Impact statement ..... viii

UCL Research Paper Declaration Form: referencing the doctoral candidate's own published work(s) ..... ix

Acknowledgements ..... xiii

Table of Contents ..... xv

I. Table of tables ..... xix

II. Table of figures ..... xx

III. Table of schemes ..... xxii

IV. Abbreviations ..... xxv

Chapter 1. General introduction ..... 1

1.1 Sulfoxides ..... 1

1.2 Green chemistry ..... 5

1.2.1 The environmental movement ..... 5

1.2.2 The 12 Principles of Green Chemistry ..... 6

1.2.3 Biocatalysis as a green solution ..... 8

1.3 General Aims ..... 12

Chapter 2. A mild and chemoselective CALB biocatalysed synthesis of sulfoxides exploiting the dual role of EtOAc as solvent and reagent ..... 13

2.1 Introduction ..... 13

2.1.1 Traditional methods for the synthesis of sulfoxides ..... 13

2.1.2 Alternative green methods for the synthesis of sulfoxides: enzymatic transformations ..... 20

2.2 Aims of the project ..... 28

2.3 Results and discussion ..... 29

2.3.1 Oxidation of sulfides with CALB in EtOAc in the presence of UHP ..... 29

2.3.2 *In situ* production of $H_2O_2$ for the generation of peracids ..... 39

2.3.3 Development of a methodology to obtain chiral sulfoxides ..... 47

2.4 Final considerations and conclusions ..... 51

Chapter 3. Stereoselective oxidation of functionalised sulfides using flavoprotein monooxygenases ..... 53

3.1 Introduction ..... 53

3.1.1 Classification, structural features, and mechanism of flavoprotein monooxygenases ..... 54

3.1.2 Reactivity of BVMOs and FMOs ..... 59

3.2 Aims of the project ..... 67

3.3 Results and discussion ..... 68
3.3.1 Screening of the BVMO and FMO panel ..... 68
3.3.2 Optimisation of the BVMO145 biocatalysed (*S*)-sulfoxidation reaction conditions ..... 69
3.3.3 Scope of the BVMO145 biocatalysed sulfoxidation ..... 71
3.4 Preliminary conclusions and future work ..... 74
Chapter 4. Enhancing the synthetic scope and potentiality of methionine reductase enzymes in the biocatalytic synthesis of enantiomerically pure sulfoxides: mechanistic and mutagenesis studies ..... 76
4.1 Introduction ..... 76
4.1.1 Enzymatic kinetic resolution by methionine sulfoxide reductases ..... 79
4.2 Aims of the project ..... 89
4.3 Results and discussion ..... 90
4.3.1 Msr02 biocatalysed kinetic resolution of sulfoxides ..... 90
4.3.2 Structural and functional studies on MsrA02 ..... 100
4.3.3 Mutagenesis studies and development of new Msr mutants ..... 108
4.3.4 Development of a deracemization method ..... 115
4.4 Final considerations and conclusions ..... 121
Chapter 5. General final remarks ..... 123
Chapter 6. Experimental ..... 126
6.1 General methods ..... 126
6.2 Chapter 2. Methods ..... 127
Synthetic methods ..... 127
6.2.1 General procedure for the synthesis of sulfides 27 ..... 127
6.2.2 General procedure for the synthesis of sulfides 38a-c ..... 131
6.2.3 General procedure for the synthesis of sulfides 38d-f ..... 132
6.2.4 General procedure for the synthesis of sulfides 40 ..... 133
6.2.5 Synthesis of (but-3-en-1-yloxy)benzene 33[396] ..... 134
6.2.6 Synthesis of chiral acids 47 and 52 ..... 135
Biocatalytic methods ..... 136
6.2.7 General procedure for the biocatalytic oxidation of sulfides using CALB ..... 136
6.2.8 CALB recycling experiments ..... 144
6.2.9 General procedure for the two step-one pot photocatalytic production of $H_2O_2$ and sulfoxidation by CALB ..... 145
6.2.10 General procedure for the synthesis of chiral sulfoxides using chiral acids ..... 145
6.3 Chapter 3. Methods ..... 147
Synthetic methods ..... 147

6.3.1 General procedure for the synthesis of sulfides 27 and 38 ..... 147
6.3.2 General procedure for the synthesis of racemic sulfoxides standards 28 ..... 149
Biocatalysis methods ..... 153
6.3.3 Screening of BVMO and FMO enzymes panel using 27s ..... 153
6.3.4 General procedure for the asymmetric oxidation of substrates 27 and 38 using BVMO145 ..... 154
Computational methods ..... 154
6.4 Chapter 4. Methods ..... 155
Synthetic methods ..... 155
6.4.1 General procedure for the synthesis of sulfides 27 ..... 155
6.4.2 General procedure for the synthesis of racemic sulfoxides 28a-af ..... 157
6.4.3 Synthesis of riboflavin tetraacetate (RFTA)[380] ..... 161
Molecular biology and biocatalysis methods ..... 162
6.4.4 Preparation of Msr WT enzymes panel ..... 162
6.4.5 Purification of *S. cerevisiae* MsrA02 from CFE ..... 162
6.4.6 General procedure for the kinetic resolution of substrates 28 using MsrA02 ..... 163
6.4.7 Preparation of C28S and C68S MsrA02 ..... 164
6.4.8 Activity assay of C25S and C68S MsrA02 ..... 166
6.4.9 Activity assay of C23S, C44S and C176S MsrA02 ..... 166
6.4.10 Identification of other Msrs for the kinetic resolution of bulkier sulfoxides ..... 166
6.4.11 General procedure for the kinetic resolution of sulfoxides using MsrA33 ..... 167
Computational methods ..... 167
6.4.12 Modelling ..... 167
6.4.13 Molecular Docking ..... 168
6.4.14 Molecular Dynamics Simulations ..... 168
6.4.15 Quantum Chemistry Calculations ..... 168
NMR studies methods ..... 168
6.4.16 Production of $^{15}N$ and $^{13}C$ labelled MsrA02 and MsrA02_C25S ..... 168
6.4.17 NMR spectroscopy ..... 169
Development of a deracemization method ..... 169
6.4.18 Screening of commercially available photocatalysts for the oxidation of sulfides in the enzymatic reaction conditions ..... 169
6.4.19 Photobiocatalytic deracemization method using eosin Y 96 ..... 170
6.4.20 Use of riboflavin and riboflavin tetraacetate (RFTA) for the oxidation of sulfides in the enzymatic reaction conditions ..... 170

References ..... 171
Appendices ..... 190
Appendix I. Copies of NMR spectra ..... 190
Sulfides NMR spectra ..... 190
Sulfoxides NMR spectra ..... 220
Other compounds spectra ..... 270
Appendix II. Isolated yields and optical rotation data of (*R*)-sulfoxides 28 (Chapter 4) ..... 275
Appendix III. Table of retention times and chiral column specification for compounds 28 (Chapter 3) ..... 276
Appendix IV. Table of retention times and chiral column specification for compounds 28 (Chapter 4) ..... 277
Appendix V. HPLC traces ..... 278
Chapter 3 ..... 278
Chapter 4 ..... 286
Appendix VI. Calibration curves for HPLC conversions ..... 318
Appendix VII. Bradford assay calibration curve ..... 324

# I. Table of tables


**Table 1.1.** Typical *E*-factors for the chemical industry sectors as of 2015. ..... 7

**Table 1.2.** Biocatalysis and the 12 Principles of Green Chemistry. ..... 9

**Table 2.1.** Optimisation of the CALB biocatalysed sulfoxidation of **27a**. ..... 30

**Table 2.2.** Scope of the CALB biocatalysed sulfoxidation ..... 33

**Table 2.3.** CALB biocatalysed synthesis of sulfoxides bearing carbonyl groups. ..... 36

**Table 2.4.** First screening of conditions for the photo- and biocatalysed sulfoxidation of **27a**. ..... 44

**Table 2.5.** Second screening of conditions for the photo- and biocatalysed sulfoxidation of **27a**. ..... 46

**Table 2.6.** Screening of commercially available acids for the asymmetric synthesis of **28a**. ..... 49

**Table 3.1.** Screening of the BVMO and FMO enzymes panel. ..... 69

**Table 3.2.** Optimisation of the conditions of the BVMO145 biocatalysed **27s** sulfoxidation. ..... 70

**Table 3.3.** Scope of the BVMO145 biocatalysed sulfoxidation. ..... 71

**Table 4.1.** Screening of Msr enzymes with sulfoxide **28af**. ..... 91

**Table 4.2.** Optimisation of the MsrA02 biocatalysed KR of **28af**..... 93

**Table 4.3.** Substrate scope of the EKR of sulfoxides **28a-e**. ..... 95

**Table 4.4.** Screening of Msr enzymes with bulkier sulfoxides. ..... 99

**Table 4.5.** Results of MsrA02 cysteine mutants catalysed reduction of **28af**..... 105

**Table 4.6.** New panel of structurally different MsrA enzymes containing 12 mutant enzymes from WT MsrA02 and MsrA10 and 7 new WT MsrAs. ..... 110

**Table 4.7.** Screening of MsrA mutants and new WT MsrA. ..... 111

**Table 4.8.** Optimisation of reaction conditions with MsrA33. ..... 113

**Table 4.9.** Scope of the MsrA33 biocatalysed KR of larger sulfoxides. ..... 115

**Table 4.10.** Screening of organic photocatalysts for the racemic oxidation of **27af** to **28af**. ..... 117

**Table 4.11.** Photobiocatalytic method and control reactions for the deracemization of **28af**..... 118

**Table 4.12.** Screening of conditions for the sulfoxidation of **27af** catalysed by flavine photocatalysts. ..... 119

# II. Table of figures


**Figure 1.1.** Resonance structure displaying the distorted tetrahedral arrangement of substituents around the sulfur atom and chiral sulfoxides. ..... 1

**Figure 1.2.** FDA approved sulfide containing drugs. Courtesy of Topics in Current Chemistry, Springer.[13] ..... 3

**Figure 1.3.** FDA approved sulfoxide containing drugs. Stereochemistry indicated for the sulfoxides sold as the single enantiomer drug. ..... 4

**Figure 1.4.** Structure of the novel sulfoxide tetrahydropyridine analogue **7**, active against *M. catarrhalis* and *S. pyogenes* by Prachayasittikul *et al.*.[15] ..... 5

**Figure 2.1.** Interaction of lipases with natural substrates or hydrophobic solid supports for immobilisation. ..... 21

**Figure 2.2.** Mechanism of hydrolysis of esters or acids catalysed by CALB. Two transition states and intermediate are shown.[168] ..... 25

**Figure 2.3.** Concentration or peracetic acid formed *in situ* over time. ..... 32

**Figure 2.4.** Recycling experiments of CALB. ..... 39

**Figure 2.5.** Three essential steps of photocatalytic transformations: i) absorption of photon; ii) excitation of electrons to high energy states and iii) transfer of electrons to chemical species. ..... 41

**Figure 3.1.** Differences in the mechanism of oxidation between monooxygenases and peroxygenases. ..... 53

**Figure 3.2.** Summary of the different groups of FPMOs (A-H). ..... 55

**Figure 3.3.** Electrostatic potential surface (EPS) map for **27z** and **27ac**. ..... 72

**Figure 3.4.** New sulfide substrates for the expansion of the BVMO145 biocatalysed sulfoxidation. ..... 75

**Figure 4.1.** Schematic representation of EKR and EDKR with their relative energy diagram. In black is the $\Delta G_{rac}$ of a EKR process while in blue is the $\Delta G_{rac}$ of an EDKR. ..... 76

**Figure 4.2.** Diagram of DMSO reductase in *E. coli* where the catalytic subunits, namely the hydrophilic catalytic subunit (DmsA) that bears a pterin molybdenum cofactor (MoCo), the hydrophilic subunit (DmsB) that contains four cysteine groups individually bonded to four [4Fe-4S] clusters and the hydrophobic subunit (DmsC) that anchors the protein to the cell membrane are shown. DmsA and DmsB are orientated towards the cytoplasmic phase of the cell, while DmsC anchors the protein onto the membrane and mediates the electron transfer from menaquinol ($MQH_2$) to DmsAB for the reduction of DMSO to take place.[317] ..... 78

**Figure 4.3.** Schematic representation of the different classes of Msr and their mode of action. ..... 80

**Figure 4.4.** Biocatalytic approaches for the deracemization of sulfoxides using MsrAs. ..... 89

**Figure 4.5.** Proposed mechanism for the reduction of sulfoxides by MsrA biocatalysts. ..... 94

**Figure 4.6.** Steric hindrance effects of aromatic substituents on the nucleophilic attack of cysteine to the sulfoxide moiety. ..... 96

**Figure 4.7.** Behaviour of naphthyl moieties in comparison to *meta* and *ortho* substituents. ..... 96

**Figure 4.8.** Electrostatic potential surface (EPS) for **28v** and **28t**. ..... 97

**Figure 4.9.** Sequence alignment of MsrAs from *S. cerevisiae* (UPID: B3LS55, PDB: 3PIL), *N. meningitidis* (UPID: Q9K1N8), *E. coli* (UPID: P0A744) and *M. tuberculosis* (UPID: P9WJM5). *N. meningitidis* is an AB hybrid Msr so the sequence showed here corresponds to the MsrA domain of the enzyme (from residues Asn196 to Thr378). Cys25 and Cys176 are highlighted in yellow, while the hydrophobic pocket formed by Phe26 and Trp27 and the hydrophilic pocket formed by Tyr64, Glu76 and Tyr116 are highlighted in green and cyan respectively. In *S. cerevisiae*, other cysteine residues are represented by blue triangles. Secondary structure features are shown for *S. cerevisiae*. Figure prepared using ESPript.[366] ..... 101

**Figure 4.10.** Crystal structure of MsrA02 (PDB: 3PIL) with the five cysteine residues highlighted as sticks. C25 and C176 are key residues in the active site. Generated with Pymol. ..... 104

**Figure 4.11.** Comparison between the active sites of the WT enzyme (purple) and the C23S variant (magenta). The serine hydroxide sidechain makes an H bond with Thr29, significantly changing the loop of the Cys25. ..... 106

**Figure 4.12.** $^{15}$N HSQC spectrum of MsrA02. Part A) Assigned $^{15}$N HSQC of MsrA02 in its free, reduced form. Part B) $^{15}$N SOFAST HMQC of MsrA02 collected at increasing **28af** concentration of 0 mM (black), 0.5 mM (blue) and 1 mM (red). ..... 107

**Figure 4.13.** Cartoon representation of the MsrA02 structure (PDB: 3PIL) with the residues involved in the catalytic cycle of **28af** highlighted. Residues with resonances undergoing significant intensity losses upon addition of 0.5 mM or 1 mM of **28af** are labelled in blue or red, respectively. Residues with resonances undergoing significant chemical shift differences between the free and bound forms are labelled in cyan. Cys25 and Cys176 sidechains are shown for clarity. ..... 108

**Figure 4.14.** a) Docking of sulfoxide **28ag** in MsrA02; Tyr174 keeps Cys25 close to the sulfoxide group. b) Docking of the sulfoxide **28j** in MsrA02. c) Overlap of MsrA10 (light green) over MsrA02 (grey). The second cysteine residue of MsrA10 is not in C-terminal region. ..... 109

**Figure 4.15.** The binding pose of **28j** and mutant MsrA33 (adapted from PDB: 3PIL) ..... 112

## III. Table of schemes


**Scheme 1.1.** Pummerer reaction of sulfoxide **1** to obtain the uracil functionalised thioribose intermediate **2** in the DIPEA-catalysed total synthesis of albomycins by Lin *et al.*.[8] ..... 2

**Scheme 1.2.** Synthesis of asymmetric ketones **5** using a Rh-based catalyst and the chiral sulfoxide ligand **6** by Lang *et al.*.[12] ..... 2

**Scheme 1.3.** New chemoenzymatic route for the manufacturing process of Pregabalin.[41] ..... 11

**Scheme 2.1.** $HNO_3$ and nitromethane Biphasic system for the oxidation of sulfides reported by Gasparrini in 1990.[46] ..... 13

**Scheme 2.2.** Oxidation of sulfides in $HNO_3$ in the presence of $FeBr_3$ by Suarez *et al.*. [47,48] ..... 14

**Scheme 2.3.** Oxidation of 1-thiacyclooctan-5-one1-oxide **12** in aqueous $NaIO_4$ by Leonard and Johnson. [52] ..... 15

**Scheme 2.4.** Oxidation of allyl-aryl sulfides using $Ca(OBr)_2$ by Pace *et al.*.[61] ..... 15

**Scheme 2.5.** In flow production of sulfoxides using Oxone by Silva *et al.*.[65] ..... 16

**Scheme 2.6.** Chemoselective synthesis of sulfoxides using Cu-*Calendula*@$Fe_3O_4$ nanocomposite material in 30% $H_2O_2$.[105] ..... 18

**Scheme 2.7.** Green oxidation of sulfides using $H_2O_2$ and TFAP in *t*-BuOH and buffer by Voutyritsa *et al.*.[99] ..... 18

**Scheme 2.8.** First reported example of esterification and hydrolysis of five-, six- and seven-membered *meso*-dials or the corresponding diacetates using the immobilised enzyme Novozym 435 by Johnson and Bis.[135] ..... 22

**Scheme 2.9.** Examples of CALB catalysed ammonolysis. Part A) Formation of aliphatic amides from triglycerides proposed by Griffin *et al.*.[164] Part B) Synthesis of the amide intermediate **26** in the synthesis of Saxagliptin.[165] ..... 23

**Scheme 2.10.** Proposed mechanism of action of the Knoevenagel condensation reaction catalysed by immobilised CALB by Wang *et al.*.[166] ..... 24

**Scheme 2.11.** Oxidation of limonene by immobilised CALB via production of peroctanoic acid by Melchiors *et al.*.[181] ..... 26

**Scheme 2.12.** Exploitation of EtOAc as reaction solvent and peracid precursor for the synthesis of lactones by Chávez *et al.*.[183] ..... 27

**Scheme 2.13.** Proposed cycle for the CALB biocatalysed sulfide oxidation in EtOAc. ..... 31

**Scheme 2.14.** Titration of peracetic acid formed by CALB. ..... 32

**Scheme 2.15.** Biocatalysed epoxidation of alkene-bearing ether **33**. ..... 35

**Scheme 2.16.** CALB biocatalysed synthesis of sulfoxides bearing hydroxyl groups. ..... 37

**Scheme 2.17.** Part A: Gram-scale synthesis of sulfoxide **28a**; Part B: Synthesis of omeprazole **43** *via* CALB biocatalysed oxidation. ..... 38

**Scheme 2.18.** Industrial production of $H_2O_2$ from AQ ..... 40

**Scheme 2.19.** Envisioned photo- and biocatalytic synthesis of **28a**. ..... 43

**Scheme 2.20.** CALB biocatalysed oxidation of **27a** in toluene/water 4:1 and benzoic acid **44**. ..... 45

**Scheme 2.21.** Proposed S-oxidation mechanism for the photocatalytic oxidation of **27a**. ..... 47

**Scheme 2.22.** Reaction of the asymmetric chemo-enzymatic Baeyer-Villiger oxidation of 4-methylcyclohexanone.[179] ..... 48

**Scheme 2.23.** Asymmetric synthesis of **39a**. Part A) Predicted mechanism. Part B) Scheme of reaction. ..... 50

**Scheme 3.1.** Proposed mechanism of action of Group B FPMOs using flavin and NAD(P)H cofactors. ..... 57

**Scheme 3.2.** Formation of the three peroxyflavin species in FPMOs. ..... 58

**Scheme 3.3.** Large scale production of trimethyl-ε-caprolactones **56** using CHMO from *T. municipal*e by Solé *et al.*.[279] ..... 60

**Scheme 3.4.** Bayer-Villiger oxidation of aliphatic keto acids **57** to ester products **58** using a BVMO from *G. sihwensis* by Zhang *et al.*.[275] ..... 60

**Scheme 3.5.** Oxidation of bicyclo[3.2.0]hept-2-en-6-one **60** using the novel FMOA from *Pimelobacter* sp. by Löwe *et al.*.[271] Part A) regeneration NADPH using stoichiometric formate. Part B) *in situ* regeneration NADPH exploiting microalgae, light, water, and $CO_2$. ..... 61

**Scheme 3.6.** Synthesis of the *N*-oxide metabolite **62** of the antidepressant drug Moclobemide using the human FMO isoform 3 by Hanlon *et al*..[288] ..... 62

**Scheme 3.7.** *N*-oxidation of indole **63** using M446G PAMO and subsequent spontaneous indigo blue formation by Torres-Pazmiño *et al*..[293] ..... 63

**Scheme 3.8.** OTEMO catalysed oxidation of sulfides **66** to sulfoxides **(*S*)-67** and sulfones **68** by de Gonzalo *et al.*.[301] ..... 64

**Scheme 3.9.** Type II FMO catalysed enantioselective oxidation of thioanisole **69** to (*R*)- or (*S*)-methyl phenyl sulfoxide **70**.[302] ..... 65

**Scheme 3.10.** Synthesis of (*R*)-lansoprazole **71** in 99% and >99% conversion using the novel *cb*BVMO by Liu *et al*..[303] ..... 65

**Scheme 3.11.** Plant scale synthesis of drug intermediate 19 in the synthesis of AZD6738 **74** using Codexis' BVMO-P1/D08 by Goundry and colleagues, AstraZeneca.[299] ..... 66

**Scheme 4.1.** Indirect EKR methods to access enantiopure sulfoxides Part A) EKR of (*E*)-γ-Hydroxy-α,β-unsaturated *p*-tolylsulfoxides **75** using a lipase from *Pseudomonas cepacia* by Guerrero de la Rosa *et al.*.[315] Part B) Synthesis of β-hydroxysulfoxides **78** by Chen *et al.*.[316] ..... 77

**Scheme 4.2.** Synthesis of sulfoxides using a whole *E. coli* cell system overexpressing *pm*MsrA by Yang *et al.*.[349] ..... 81

**Scheme 4.3.** Conversions of racemic sulfoxides using the crude *pm*MsrA-DTT system by Chen and Yang.[351] ..... 82

**Scheme 4.4.** Conversions of racemic sulfoxides using the crude *pa*MsrA-DTT system by Chen *et al.*.[352] ..... 83

**Scheme 4.5.** Conversions of racemic sulfoxides using whole *E. coli* BL21 (DE3) cell system overexpressing *ak*MsrB by Chen *et al.*.[354] ..... 84

**Scheme 4.6.** Deracemization of racemic sulfoxides in a biphasic aqueous buffer/decane system using whole cell MsrA and oxaziridine **18** by Nosek and Míšek.[355] ..... 85

**Scheme 4.7.** Photo-biocatalytic deracemization of racemic sulfoxides using *pa*MsrA and photocatalyst **92** by Bierbaumer *et al.*.[356] ..... 86

**Scheme 4.8.** Multienzymatic deracemization of racemic sulfoxides using MsrA and SMO by Peng *et al.*.[357] ..... 87

**Scheme 4.9.** Rearrangement mechanism for the degradation of **28l** in a basic aqueous environment. ..... 100

**Scheme 4.10.** Proposed mechanism of MetSO reduction and sulfenic acid formation (PDB: 3PIL). ..... 102

**Scheme 4.11**. Schematic representation of a deracemization protocol using MsrAs and chemical oxidation methods. ..... 116

## IV. Abbreviations

| | |
|---|---|
| (*R*)- | Rectus |
| (*S*)- | Sinister |
| $^{o}$C | Celsius |
| 2D | Bi dimensional |
| Ac | Acetyl |
| AE | Atom economy |
| AHQ | Anthrahydroquinone |
| API | Active pharmaceutical ingredient |
| AQ | Anthraquinone |
| Asp | Asparagine |
| auc | Area under the curve |
| Bn | Benzyl |
| BVMO | Baeyer-Villiger monooxygenase |
| CALB | Candida antarctica lipase B |
| CFE | Cell free extract |
| CHMO | Cyclohexanone monooxygenase |
| CLEA | Cross-linked enzyme aggregate |
| Cys | Cysteine |
| DCM | Dichloromethane |
| DDT | Dichlorodiphenyltrichloroethane |
| DIPEA | Diisopropylethylamine |
| DMS | Dimethyl sulfide |
| DmsABC | Dimethyl sulfoxide reductase |
| DMSO | Dimethyl sulfoxide |
| DTT | Dithiotheitol |
| EAQ | 2-Ethylanthraquinone |
| EDG | Electron donating group |
| EDKR | Enzymatic dynamic kinetic resolution |
| ee | Enantiomeric excess |
| EKR | Enzymatic kinetic resolution |
| EQ | Environmental quotient |
| eq. | Equivalent |
| *et al.* | And others |
| Et | Ethyl |
| EtOAc | Ethyl acetate |
| EtOH | Ethanol |

| | |
|---|---|
| EWG | Electron withdrawing group |
| FAD | Flavin adenine dinucleotide |
| FMN | Flavin mononucleotide |
| FMO | Flavin-containing monooxygenases |
| Fmoc | Fluorenylmethyloxycarbonyl protecting group |
| FPMO | Flavoprotein monooxygenase |
| frMsr | Free methionine sulfoxide reductase |
| g | Grams |
| GABA | γ-aminobutyric acid |
| GDH | Glucose dehydrogenase |
| h | Hour |
| $H_2O$ | Water |
| $H_2O_2$ | Hydrogen peroxide |
| His | Histidine |
| HOMO | Highest occupied orbital |
| HPLC | High performance liquid chromatography |
| *i-* | *iso-* |
| IL | Ionic liquid |
| IPA | Isopropanol |
| KPI | Potassium phosphate |
| L | Liter |
| *m-* | *meta-* |
| M | Molar |
| *m*CPBA | Meta-chloroperbenzoic acid |
| Me | Methyl |
| MeOH | Methanol |
| Met | Methionine |
| MetSO | Methionine sulfoxide |
| min | Minute |
| mL | Millilitre |
| mM | Millimolar |
| mol | Moles |
| MPS | Methyl phenyl sulfide |
| MPSO | Methyl phenyl sulfoxide |
| $MQH_2$ | Menaquinol |
| Msr | Methionine sulfoxide reductase |
| MsrA | Methionine sulfoxide reductase A |

| | |
|---|---|
| MsrB | Methionine sulfoxide reductase B |
| MTS | Methyl *p*-tolyl sulfide |
| MTSO | Methyl *p*-tolyl sulfoxide |
| MW | Microwave |
| *n*- | *normal* |
| NAD(P)H | Nicotinamide adenine dinucleotide (phosphate) |
| NMR | Nuclear magnetic resonance |
| NP | Nanoparticle |
| *o*- | *ortho*- |
| OD | Optical density |
| OTEMO | 2-Oxo-$\Delta^3$-4,5,5-trimethylcyclo-pentenylacetyl-CoA 1,2-monooxygenase |
| *p*- | *para*- |
| Ph | Phenyl |
| PPI | Protein pump inhibitor |
| ppm | part per million |
| Pr | Propyl |
| Pro | Proline |
| PTDH | Phosphate dehydrogenase |
| Py | Pyridyl |
| RFTA | Riboflavin tetraacetate |
| ROS | Reactive oxygen species |
| rt | room temperature |
| Ser | Serine |
| SMO | Styrene monooxygenase |
| $S_N2$ | Bimolecular nucleophilic substitution |
| *t*- | *tert*- |
| TBHP | *tert*-Butyl hydroperoxide |
| t-BuOH | *tert*-Butanol |
| TEMPO | (2,2,6,6-Tetramethylpiperidin-1-yl)oxy |
| Tf | Triflate |
| TFA | Trifluoroacetic acid |
| TFAP | 2,2,2-trifluoroacetophenone |
| TLC | Thin layer chromatography |
| TMS | Trimethylsilyl |
| Trx | Thioredoxin |
| $Trx_{red}$ | Thioredoxin reductase |
| UHP | Urea hydrogen peroxide |

| | |
|---|---|
| Val | Valine |
| W | Watt |
| w/v | weight over volume |
| w/w | weight over weight |
| WT | Wild type |

# Chapter 1. General introduction

The development of green and sustainable methodologies for the synthesis of fine chemicals remains one of the major challenges in modern scientific research. There is an ever more pressing need to find alternative solutions that do not rely on fossil fuel and that have the smallest possible carbon footprint and impact on global pollution. In recent years, biocatalysis has emerged as a promising solution to this problem as it provides a much safer and generally more environmentally friendly alternative to traditional synthetic methods. Therefore, this thesis will focus on the development of new and unconventional biocatalytic strategies specifically for the synthesis of sulfoxides, a class of fine chemicals that find many applications in chemistry, varying from organic synthesis to medicinal chemistry.

## 1.1 Sulfoxides

Sulfoxides are organosulfur compounds with an $R_1SOR_2$ motif that have been known since the origins of modern organic chemistry. In sulfoxides, the sulfur atom is bonded to an oxygen atom through a polarised double-dative hybrid bond and the sulfur lone pair forces the geometrical arrangement of the atoms around the sulfur centre into a distorted tetrahedral shape (Figure 1.1). Sulfoxides are configurationally stable and, depending on the identity of the R groups, can be non-chiral when $R_1=R_2$, or chiral when $R_1\neq R_2$ (Figure 1.1). The strong polarisation of the S-O bond is responsible for the unique and prominent reactivity of these organosulfur molecules. Among the numerous chemical transformations developed through the years that involve a sulfoxide moiety, it is possible to name the Pummerer rearrangement,[2–4] the Mislow−Braverman−Evans rearrangement[5] and the Johnson−Corey−Chaykovsky epoxidation and cyclopropanation.[6,7] For instance, in 2018 Lin *et al.* used a Pummerer reaction to synthesise the uracil functionalised thioribose intermediate **2** from sulfoxide **1** in the total synthesis of the promising natural antibacterial albomycins (Scheme 1.1).[8]

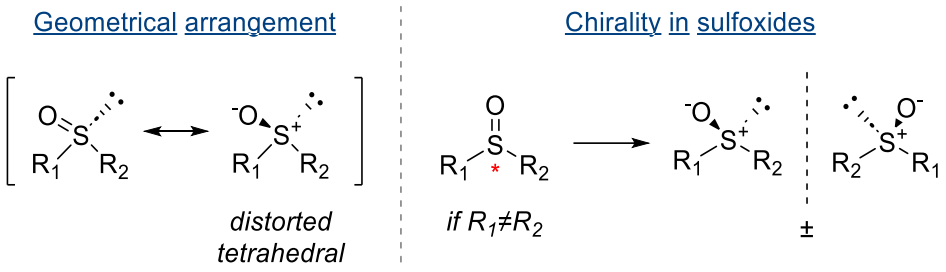


**Figure 1.1.** Resonance structure displaying the distorted tetrahedral arrangement of substituents around the sulfur atom and chiral sulfoxides.

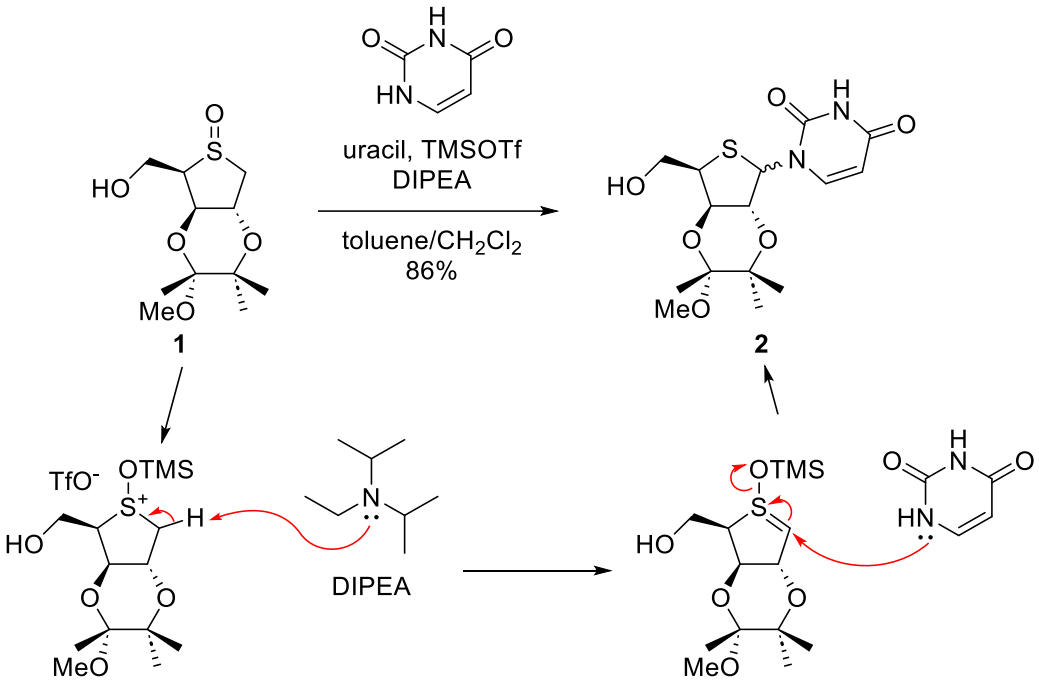


**Scheme 1.1.** Pummerer reaction of sulfoxide **1** to obtain the uracil functionalised thioribose intermediate **2** in the DIPEA-catalysed total synthesis of albomycins by Lin *et al.*.[8]

In this synthetic route, trimethylsilyl trifluoromethanesulfonate (TMSOTf) was used as the sulfoxide activator, while the bulky base *N,N*-diisopropylethylamine (DIPEA) was chosen to avoid competitive nucleophilic addition, observed when using smaller bases, such as triethylamine. Achiral and enantiopure sulfoxides have also been used as ligands[9,10] and auxiliaries.[11] For example, Lang *et al.* in 2010 reported the catalytic asymmetric 1,4-addition of arylboronic acids **3** to electron-deficient olefins **4** in *enantiomeric excesses* (ees) up to 98% and yields up to 99% using a rhodium-based catalyst and the chiral sulfoxide ligand **6** (Scheme 1.2).[12]

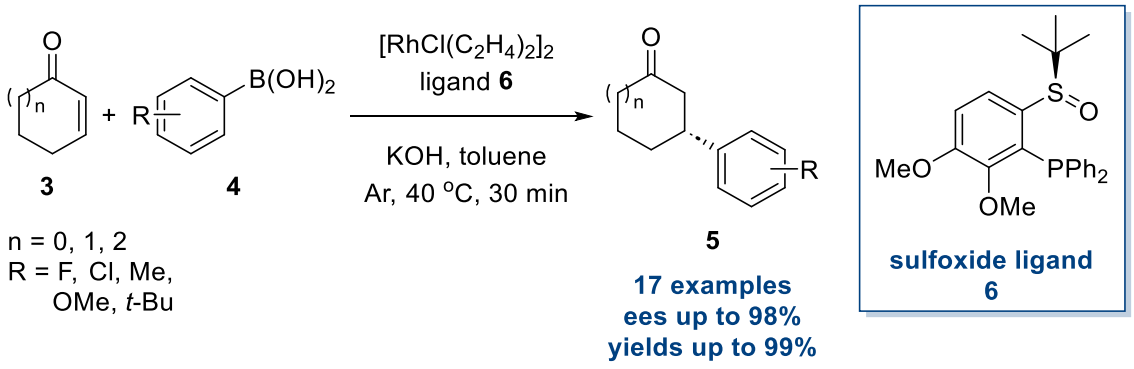


**Scheme 1.2.** Synthesis of asymmetric ketones **5** using a Rh-based catalyst and the chiral sulfoxide ligand **6** by Lang *et al.*.[12]

Another important area of research in both academia and industry where sulfoxides have received a lot of attention is medicinal chemistry. Indeed, the healing properties of sulfur containing compounds have been known since ancient times and their importance has been proven with their recurrence as active functional groups in modern pharmaceutical agents.[13] The importance of sulfur in drugs is now well-established and there are 288 FDA approved drugs that contain a sulfur moiety (Figure 1.2), of which twelve are sulfoxide-containing active pharmaceutical ingredients (API).[13] Five sulfoxide-containing APIs are sold as the pure enantiomer while the remaining seven as the racemate (Figure 1.3). The first sulfoxide-containing drug to be approved by the FDA was sulfinpyrazone in 1959.[13] It was marketed as an antiplatelet agent with the sulfoxide reducing the anti-inflammatory side effects.

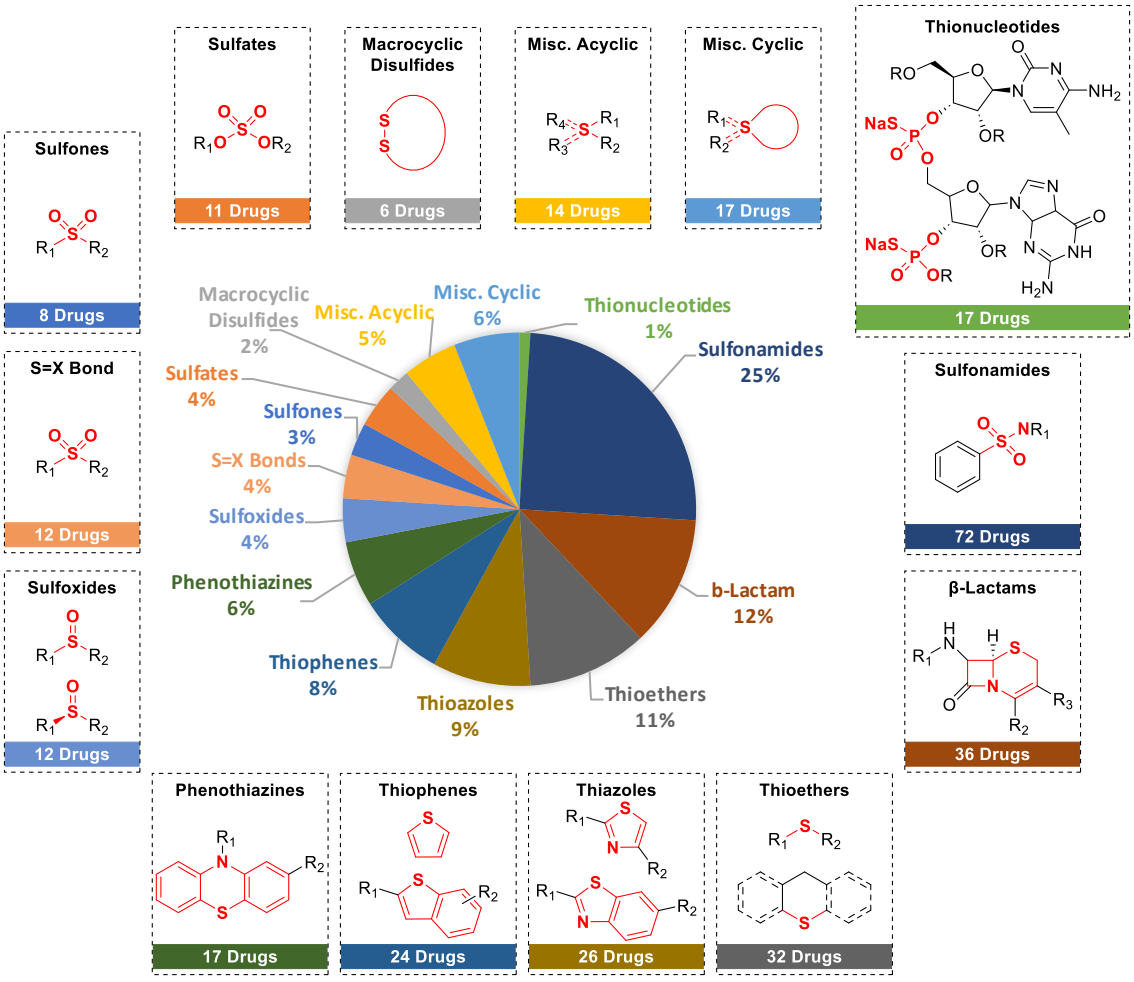


**Figure 1.2.** FDA approved sulfide containing drugs. Courtesy of Topics in Current Chemistry, Springer.[13]

In 1989 instead, the blockbuster drug omeprazole was approved as a proton pump inhibitor (PPI) for the treatment of gastroesophageal reflux diseases well as duodenal and gastric ulcers.[14] Omeprazole was the first drug in the PPI series to make it to market, while in 2001 esomeprazole, the (*S*)-form of omeprazole, was the first sulfoxide drug to be sold as a pure enantiomer. Another drug that experienced chiral switching through the years is modafinil, a dopamine reuptake inhibitor used to treat sleeping disorders. Initially approved in 1998 as the racemate, it was relaunched in the market in 2007 as armodafinil, the (*R*)-enantiomer. These are some examples of FDA approved sulfoxide containing APIs. However, there are more than twelve sulfoxides that have shown promising activity against diseases.

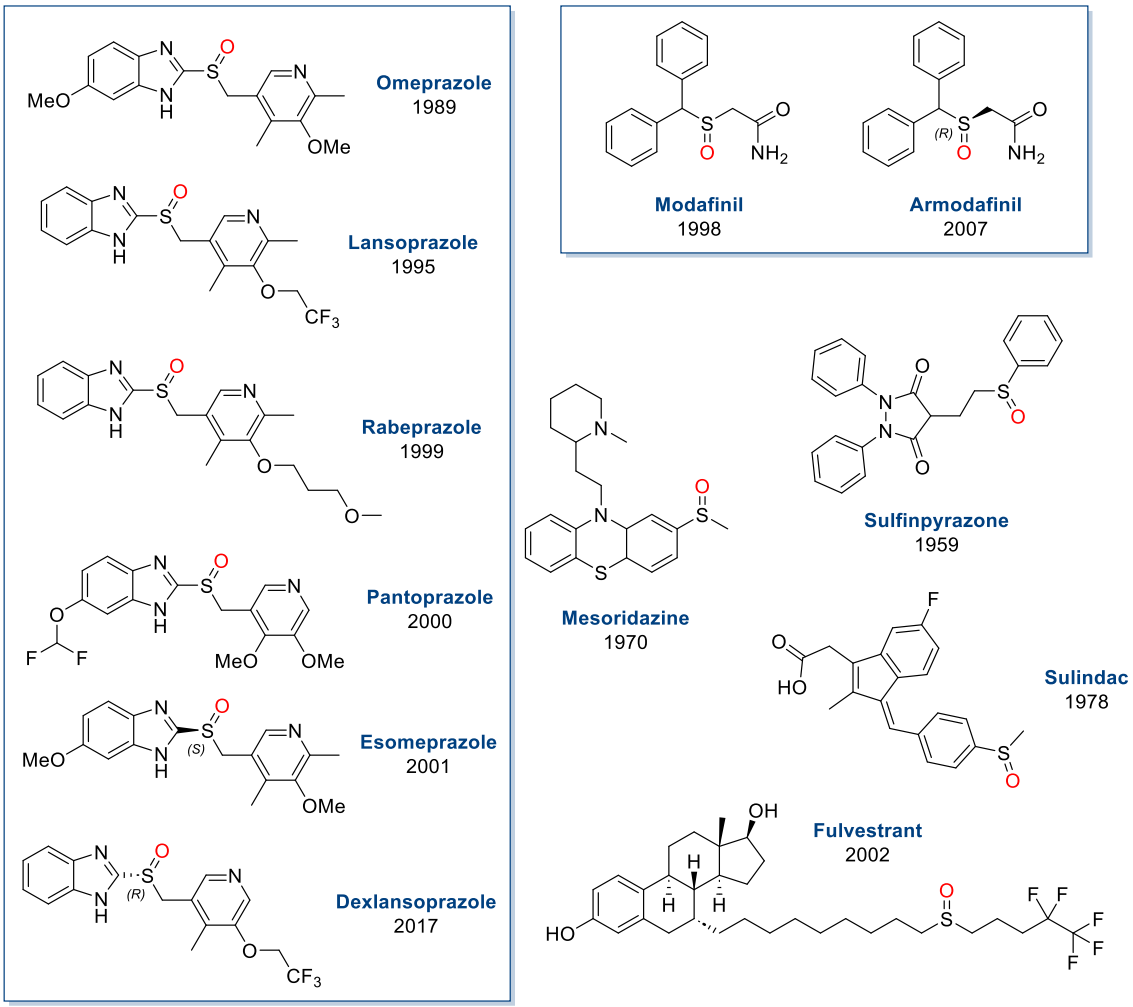


**Figure 1.3.** FDA approved sulfoxide containing drugs. Stereochemistry indicated for the sulfoxides sold as the single enantiomer drug.

For instance, in 2010 Prachayasittikul *et al.* reported a novel sulfoxide analogue **7** of the bioactive tetrahydropyridine family that possessed antiviral activity against *Moraxella catarrhalis* and *Streptococcus pyogenes* (Figure 1.4).[15] This was an example where the sulfoxide moiety was directly responsible for antimicrobial activity as the sulfide derivatives **8** and **9** were found to be inactive.

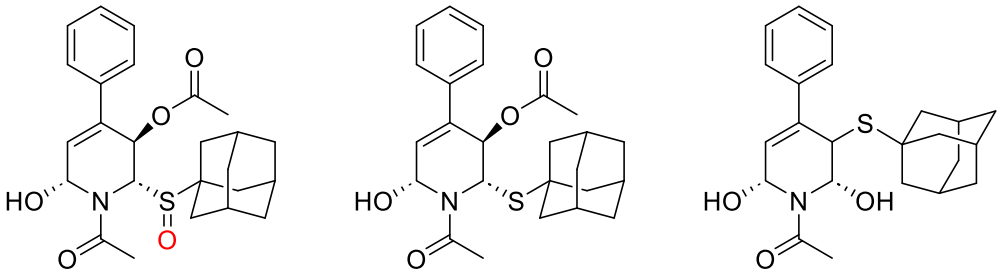


**7**
*active against M. catarrhalis and S. pyogenes*

**8**
*inactive*

**9**
*inactive*

**Figure 1.4.** Structure of the novel sulfoxide tetrahydropyridine analogue **7**, active against *M. catarrhalis* and *S. pyogenes* by Prachayasittikul *et al.*.[15]

Due to the outstanding applications that sulfoxides find in both academia and industry, it is not surprising that, over the years an abundance of methodologies for the synthesis of sulfoxide moieties as racemates and as enantiopure compounds have emerged in the literature.[16] Among these, in the last three decades biocatalysis, the branch of (green) chemistry that studies the use of enzymes as reaction catalysts, has been the centre of attention of many research groups as an alternative strategy to develop greener and more sustainable sulfoxidation protocols.[17] In fact, biocatalysis allows researchers to control the impact that the chemical industry has on the environment and human health. The use of enzymes also presents considerable advantages over traditional methods due to their intrinsic chemo-, regio- and stereoselectivity that arose from millions of years of evolution.

## 1.2 Green chemistry

### 1.2.1 The environmental movement

Whether it is air, land or water, pollution has become a global issue that if left untreated will change life on Earth as we know it.[18,19] Pollution can be defined as the release of harmful materials and chemicals into the environment and, for this reason, in the past

century the chemical industry has often been the target of criticisms and allegations for inadequate regulations to prevent or minimise pollution.[20] A turning point for the awareness of the damage that the uncontained release of harmful chemicals into the environment can cause was 1962, when Rachel Carson published *Silent Spring*,[21] a book where the author documented the detrimental effects of the uncontrolled use of pesticides, especially DDT, on the flora and fauna in the affected areas. This initiated the environmental movement, which gradually pushed for new laws and regulations such as the Pollution Prevention Act passed in 1990 by the US government,[22] stating that pollution needs to be prevented and limited at the source where possible. Therefore, pushed by these new regulations and by a sense of responsibility towards the preservation of the environment, a new chemical discipline started to arise from the late 1980's, where research groups investigated the environmental impact and safety of chemical processes. This is known today as *Green chemistry*, defined as the sustainable design of synthetic and manufacturing processes for the production of chemicals that aims to minimise any negative environmental effects.[23]

### 1.2.2 The 12 Principles of Green Chemistry

In 1998, the pioneers of this relatively modern field of chemistry, Paul T. Anastas and John C. Warner, developed a set of twelve rules, the *12 Principles of Green Chemistry*.[23] For the last 25 years, these principles functioned as a guideline for the design of more sustainable and green chemical processes:

1. Prevention
2. Atom economy
3. Less hazardous chemical syntheses
4. Designing safer chemicals
5. Safer solvents and auxiliaries
6. Design for energy efficiency
7. Use of renewable feedstocks
8. Reduce derivatives
9. Catalysis
10. Design for degradation
11. Real-time analysis for pollution prevention
12. Inherently safer chemistry for accident prevention

These 12 Principles outline that for a synthetic process to be green there is the need for waste prevention and minimisation, reduction of the overall toxicity of the process and use of renewable feedstock where possible. In some cases, such as replacing a highly toxic reagent for an equivalent safer one, the changes to increase the "grenness" of a reaction can be straightforward and easily implemented. However, improving the

"grenness" of overall synthetic processes can be complicated, especially at an industrial scale. Therefore, green chemistry metrics,[24,25] a collection of mathematical equations established to help quantify the environmental performance of chemical processes, can be a useful tool to identify where change is needed. For instance, in 1991 the concept of atom economy (AE) was presented by Barry Trost,[26,27] who defined it as the ratio expressed as a percentage of the mass of the desired product over the overall mass of all the products (Equation (1)). A large AE value indicates that most of the mass of the reactants was incorporated in the products, hence causing little waste.

$$\text{Atom economy (AE)} = \frac{\text{molecular weight of desired product}}{\text{molecular weight of all products}} \times 100\% \qquad (1)$$

Another important metric was introduced by Roger Sheldon in 1992, who described the environmental factor (*E*-factor) as a measure for the assessment of the environmental impact of a chemical process based on the mass of waste.[28–30] This differs from AE because it is calculated by taking the mass of all waste produced in a process and dividing it by the mass of the final product (Equation (2)).

$$E\text{-factor} = \frac{\text{mass of total waste}}{\text{mass of product}} \qquad (2)$$

Ideally, *E*-factors should have values of zero and the larger the value the less environmentally benign the process is. The typical *E*-factors of chemical industries are illustrated in Table 1.1,[31] showing that production of pharmaceuticals and fine chemicals are the processes that causes the most waste.

**Table 1.1.** Typical *E*-factors for the chemical industry sectors as of 2015.

| Sector | Product tonnage | *E*-factor (kg waste per kg product) |
|---|---|---|
| Oil refining | $10^6$-$10^8$ | <0.1 |
| Bulk chemicals | $10^4$-$10^6$ | <0.1 – 5 |
| Fine chemicals | $10^4$-$10^2$ | 5 – >50 |
| Pharmaceuticals | 10-$10^2$ | 25 – >100 |

While an *E*-factor provides a fast indication of how wasteful a chemical process, one of its shortcomings is that all types of waste are assigned the same weighting regardless of their toxicity. The *E*-factor can consequently be misleading as a measure of "grenness" of a process as, for example, one kilogram of sodium chloride does not have the same

environmental impact as one kilogram of dichloromethane. Therefore, in an attempt at quantifying the toxicity of waste, the environmental quotient (EQ) was introduced,[30] and it is obtained by multiplying the *E*-factor (E) by an arbitrary multiplier for the unfriendliness or weighting of each kind of waste (Q) (Equation (3)). Different Q values are independently set by each company and can vary from process to process.

$$\text{Environmental quotient (EQ)} = E\text{-factor} \times Q \quad (3)$$

### 1.2.3 Biocatalysis as a green solution

One considerable source of waste in chemical processes is the use of stoichiometric reagents that do not contribute to the mass of the final product. In fact, principle no. 9 clearly states that 'Catalytic reagents (as selective as possible) are superior to stoichiometric reagents' as at the end-of-life of a chemical reaction, catalysts will contribute to a much lower percentage of waste compared to stoichiometric reagents. Traditionally, transition metal-based catalysts have been one of the most popular choices for catalysed chemical transformations.[29] However, while the use of these catalysts is still preferred over the use of stoichiometric reagents, transition metals come with a lot of disadvantages. The most apparent one is that transition metal catalysts are generally prohibitively expensive to purchase due to their mining and production costs and because some elements, including Ag, Ru, Rh, and Ir, are increasingly becoming more endangered, with a real threat to their future supply.[32] Additionally, metal-based catalysts may require specific reaction conditions, such as water and oxygen-free environment and difficult storage conditions, which result in the need of (costly) specialist apparatus to guarantee safe and effective handling. Lastly, traces of metal catalysts require tedious and expensive protocols to be removed to non-toxic ppm levels when used in later stage reactions in the production of pharmaceuticals, food, and cosmetic additives and therefore their use is often limited to transformations only in early stages of synthetic routes.[29] An answer to this problem has been provided by the ever-growing field of biocatalysis, which is the use of enzymes, nature's (bio)catalysts, for organic synthesis purposes. Because of their nature, enzymes are inherently biocompatible, biodegradable, essentially non-hazardous, non-toxic and they also avoid the use of scarce precious metals. Indeed, biocatalysis fits well with the 12 principles of green chemistry (Table 1.2) and its implementation in chemical processes, especially at industrial level, is key to achieve green processes with maximum source utilisation and

**Table 1.2.** Biocatalysis and the 12 Principles of Green Chemistry.

| | Principles of Green Chemistry | Biocatalysis |
|---|---|---|
| 1 | **Prevention** | The use of enzymes significantly reduces waste as the use of stoichiometric reagents is avoided. *E*-factor values also lowered as there is minimal use of organic solvents |
| 2 | **Atom economy** | Enzymes can carry out biotransformations in a more atom and step economical way |
| 3 | **Less hazardous chemical syntheses** | Enzymes are derived from renewable resources and are bio-compatible, biodegradable, essentially non-hazardous and non-toxic |
| 4 | **Designing safer chemicals** | Highly reactive and unsafe products are generally not compatible with biocatalysis as the enzymes may be susceptible to degradation by such species |
| 5 | **Safer solvents and auxiliaries** | Reaction often carried out in aqueous media at physiological pH |
| 6 | **Design for energy efficiency** | Mild conditions and atmospheric pressure require far less energy than traditional organic synthesis |
| 7 | **Use of renewable feedstocks** | Precious scarce metals are not used in biocatalysis. Enzymes are derived from biomass (fermentation) |
| 8 | **Reduce derivatives** | Extra steps for protection and deprotection of functional groups can be bypassed due to the high regio- and chemoselectivity of enzymes |
| 9 | **Catalysis** | Enzymes have developed through millions of years to effortlessly catalyse complex reactions |
| 10 | **Design for degradation** | Enzymes are proteins that can easily degrade in the environment |
| 11 | **Real-time analysis for pollution prevention** | Applicable to biocatalysis |
| 12 | **Inherently safer chemistry for accident prevention** | The mild conditions required by production or use of enzymes cause negligible chances of chemical leakage, thermal runways, and explosions |

minimal waste production.[33] In the early days of biocatalysis, this discipline was severely limited by the availability and diversity of biocatalysts, which were mainly lipases and hydrolases of animal origin, and hence was regarded as having niche applications of primarily academic interest.[34] However, in the second half on the 1980's, two concomitant events triggered a new wave of interest for the development of synthetic routes based on the use of biocatalysts. Firstly, in 1984 Zaks and Klibanov published a paper[35] in which it was reported that certain enzymatic reactions exhibited a much higher stability in organic media, such as toluene, at higher temperatures than under physiological conditions, leading to the realisation that biocatalysis had a much broader scope in organic synthesis than anticipated. Secondly, at around the same time, the FDA outlined a series of guidelines for the production of drugs with chiral centres, whereby the enantiomers had to be tested individually regardless of the final marketing (single enantiomers or racemates) to avoid unwanted side effects.[29,36] Since then, the advances of modern technologies such as DNA sequencing of genomes, enzyme engineering and enzyme directed evolution, for which Prof Arnold won the Nobel prize in 2018,[37] have enabled scientists to develop novel, robust and stable enzymes with pre-defined properties, such as activity, selectivity and substrate specificity.

Therefore, in the last 30 years, biocatalysis has evolved from only a fascinating academic interest to a valuable tool for the synthesis and manufacturing of fine chemicals and pharmaceuticals at industrial level.[29,33,34,38–40] An outstanding example of how biocatalysis replaced a traditional synthetic route for the synthesis of an API was reported in 2008 by Martinez and colleagues at Pfizer, who introduced the use of Lipolase, an economical lipase enzyme, for the manufacturing process for Pregabalin (Scheme 1.3), a γ-aminobutyric acid (GABA) analogue used to treat central nervous system disorders.[41] The only steps shared between the first-generation classical route and the new chemoenzymatic one were an initial Knoevenagel condensation of isovaleraldehyde and diethyl malonate, followed by cyanation to give intermediate **10**. After these two initial steps, the team at Pfizer used the enzyme Lipolase to perform the kinetic resolution of **10** through a chemoselective hydrolysis to afford the chiral acid salt **11** leaving **(*R*)-10** untouched. The conditions of this biocatalytic transformations were quite remarkable as 3 M **10** was quantitatively resolved by Lipolase at a concentration of 8% *w/v* enzyme. The team also developed a method to racemise **(*R*)-10** using EtONa in toluene under reflux so that a deracemization system would be achieved and the overall yield increased (Scheme 1.3). With **11** in hand, the team could then complete the manufacturing process to Pregabalin by carrying out a heat induced decarboxylation followed by a chemical hydrolysis and a CN reduction.

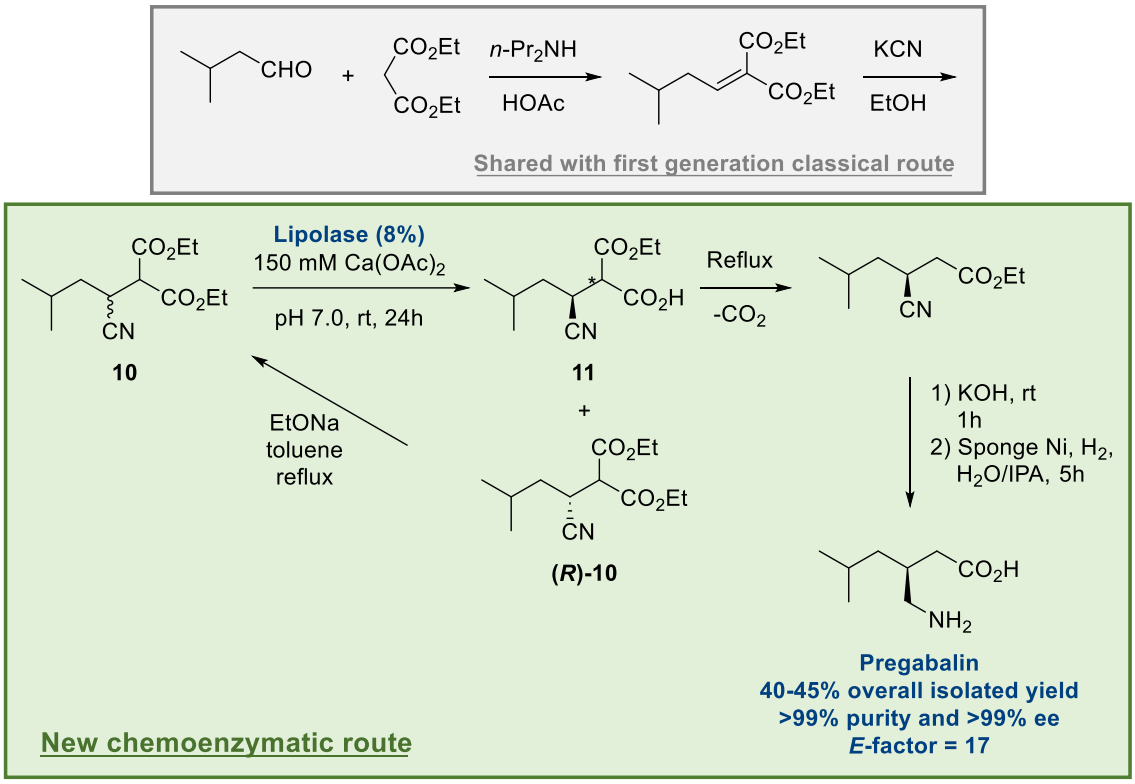


**Scheme 1.3.** New chemoenzymatic route for the manufacturing process of Pregabalin.[41]

With this new manufacturing protocol, Pregabalin could be obtained in an overall 40-45% yield, >99% purity and ee on a 1000 kg scale. An *E*-factor of 17 was obtained when using the chemoenzymatic route, which is a 5-fold improvement relative to the 86 for the first-generation classical route.

This example, and many more in the literature, highlight the importance for the continuous discovery and development of novel enzymatic strategies that could have applications in both academia and industry.

## 1.3 General Aims

The aim of the research presented in this PhD thesis was to develop *unconventional* biocatalytic methodologies for the synthesis of sulfoxides, a large class of organic compounds, which find application in many sectors of chemistry. Three different projects were developed within this PhD work, and each of them demonstrated the possibility to obtain chiral and non-chiral sulfoxide compounds by exploiting different biocatalysts. Each project illustrated in the following chapters possesses its unique *unconventional* features, distinguishing them from publications on biocatalytic sulfoxidations currently available in scientific literature.

Chapter 2 describes the development of a chemo-biocatalytic green racemic oxidative protocol for the facile and scalable synthesis of sulfoxides using immobilised enzyme *Candida antarctica* lipase B (CALB) and urea hydrogen peroxide (UHP) in ethyl acetate. The *unconventional* character of this project was the use of ethyl acetate as well as CALB, a well-known hydrolytic enzyme, in an oxidation reaction.

Chapter 3 provides a comprehensive review of Almac's commercial Baeyer-Villiger monooxygenases (BVMO) and flavine-containing monooxygenase (FMO), with the goal of identifying an *unconventional* enzyme that could chemo- and stereoselectively afford enantiopure sulfoxides in substrates containing diverse oxidisable functional groups.

Lastly, Chapter 4 discloses the use of reductive methionine sulfoxide reductase (Msr) enzymes for the kinetic resolution of racemic sulfoxide substrates to obtain enantiopure (*S*)-sulfoxides. The use of reductive rather than oxidising enzymes is an *unconventional* and new route for accessing chiral sulfoxides that has been only partially explored in the past five years. Additionally, through directed mutagenesis studies, we generated mutant Msr enzymes that could reduce bulky substrates.

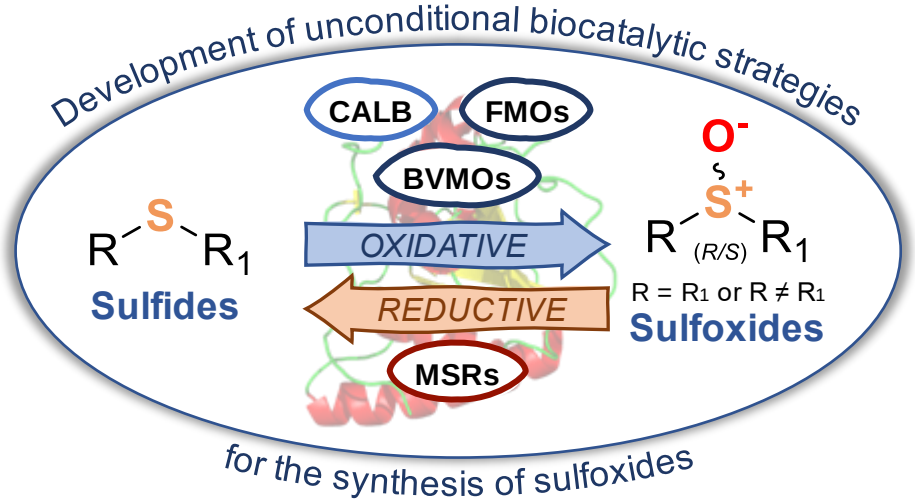

# Chapter 2. A mild and chemoselective CALB biocatalysed synthesis of sulfoxides exploiting the dual role of EtOAc as solvent and reagent

## 2.1 Introduction

### 2.1.1 Traditional methods for the synthesis of sulfoxides

Sulfoxides play an important role in organic chemistry as they are found not only in pharmaceuticals, but are also used as chiral auxiliaries, metal complexes ligands and directing groups for C-C and C-H reactions. To date, the most common methods adopted by research laboratories for the synthesis of achiral sulfoxides often involve the oxidation of sulfides using toxic and explosive reagents that require harsh reaction conditions and have a poor atom economy. Some examples include the use of nitric acid ($HNO_3$), hypohalites, oxone, peracids and peroxides.

#### *2.1.1.1 Sulfoxidation by nitric acid*

Perhaps one of the oldest methods, the synthesis of sulfoxides using $HNO_3$ was first reported in 1866 by Saytzeff.[42–44] This was one of the very first examples of sulfoxide synthesis and isolation, unknown until then, and marked the beginning of studies on this new class of compounds. Many other attempts and examples of synthesis of sulfoxides using $HNO_3$ have emerged[45] and to this day the use of $HNO_3$ to aid novel sulfoxidation processes is still appreciated by research groups. For instance, in 1990 Gasparrini *et al.* published a report on the synthesis of sulfoxides in a nitromethane/$HNO_{3(aq)}$ biphasic system catalysed by tetrabutylammonium tetrabromoaurate(III) ($TBA^+AuBr_4^-$)[46] (Scheme 2.1). The scope of this reaction included a diverse range of sulfoxides, including the more hindered aryl-aryl substrates.

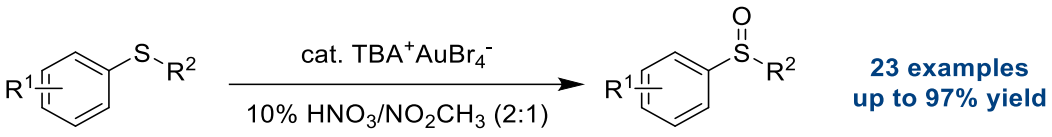


**Scheme 2.1.** $HNO_3$ and nitromethane Biphasic system for the oxidation of sulfides reported by Gasparrini in 1990.[46]

The method proved to be selective for the oxidation to sulfoxides only, showing no trace overoxidation to sulfone. A similar report where a biphasic organic solvent/$HNO_{3(aq)}$ system was adopted emerged in 1995, when Suárez *et al.* observed that the oxidation of sulfides could also be achieved using 10 mol % of the much cheaper $FeBr_3$ or $(FeBr_3)_2(DMSO)_3$ metal catalysts (Scheme 2.2).[47,48] Other sulfoxidation strategies involving $HNO_3$ include the reports by Hajipour and Khodaei in 2005 and 2010 respectively.[49,50] The former group showed that sulfides could be oxidised in a solvent-free system composed of $P_2O_5$ and silica in the presence of 1 equivalent of $HNO_3$, while the latter group revealed that a homogeneous mixture of $H_2O_2$, $HNO_3$ and EtOH led to the chemoselective oxidation of sulfides.

**Scheme 2.2.** Oxidation of sulfides in $HNO_3$ in the presence of $FeBr_3$ by Suarez *et al.*. [47,48]

### *2.1.1.2 Sulfoxidation by hypohalites*

Oxidation of sulfides using hypohalites was initially observed in the 1940's,[51] but it was only later in the 1960's that this class of oxidants became a popular method to access sulfoxides. Indeed in 1962, Leonard *et al.* were investigating the synthesis of 1-thiacyclooctan-5-one1-oxide **12** and found that when a sulfide is exposed to a solution of aqueous sodium meta periodate ($NaIO_4$) the corresponding sulfoxide **13** was afforded (Scheme 2.3).[52] The highly oxidative nature of $NaIO_4$ meant that it could have been difficult to maintain chemoselective control over what functional group was oxidised.[53–55] Therefore, the focus shifted towards slightly milder hypohalite oxidants, such as sodium hypochlorite (NaOCl) and calcium hypobromite ($Ca(OBr)_2$). These new methods still presented some challenges such as the overoxidation to the sulfone, which in some cases was avoided by shortening the reaction time as seen in the report by Khurana

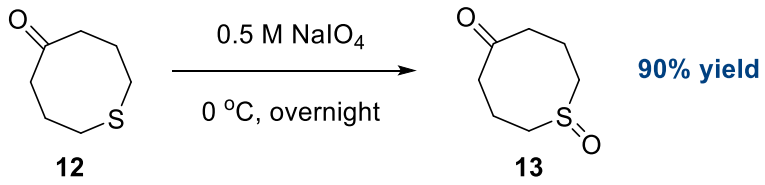


**Scheme 2.3.** Oxidation of 1-thiacyclooctan-5-one1-oxide **12** in aqueous $NaIO_4$ by Leonard and Johnson. [52]

*et al.*,[56] or by using catalysts such as metalloporphyrins[57] and 2,2,6,6-tetramethyl-piperidine-1-oxyl (TEMPO)[58] as demonstrated by Amoozadeh *et al.* and Huang *et al.* respectively. Furthermore, Okada *et al.* showed that using the safer crystalline $NaOCl{\cdot}5H_2O$ also improved the chemoselectivity of the reaction.[59,60] They attributed this improvement to the difference in basicity of the reaction mixture compared to when $NaOCl_{(aq)}$ was used. In fact, when the crystals were used, the solution had an ideal pH of 11 and only sulfide oxidation was observed, while the commercially available aqueous NaOCl solution had a pH of 13, which instead led to sulfone overoxidation. Another example was proposed by Pace and colleagues, who in 2012 developed a methodology for the synthesis of allyl-aryl sulfoxides based on $Ca(OBr)_2$ (Scheme 2.4).[61] This specific class of sulfoxides is generally prone to overoxidation not only on the sulfur centre but also on the activated allylic olefin.

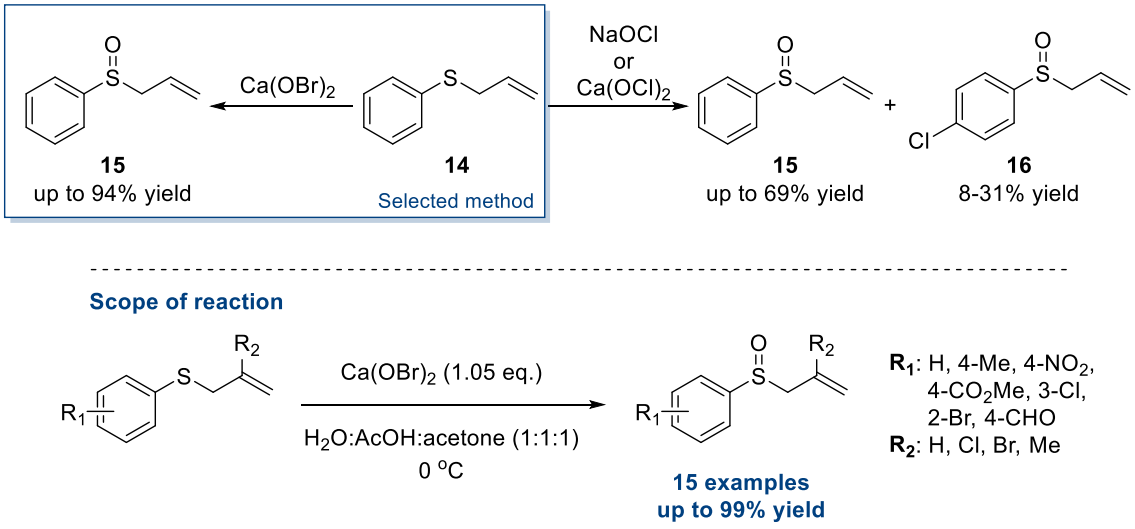


**Scheme 2.4.** Oxidation of allyl-aryl sulfides using $Ca(OBr)_2$ by Pace *et al.*.[61]

At the preliminary stages of this work, they explained that while the use of NaOCl showed chemoselectivity for the formation of the sulfoxide over olefin oxidation of compound **14**, it also promoted *para*-chlorination on the phenol (compound **16**). Therefore, switching to $Ca(OBr)_2$ completely removed any chlorinating ability of the oxidant while maintaining excellent chemoselectivity and activity across a variety of allyl-aryl sulfides.

### *2.1.1.3 Sulfoxidation by Oxone*

Oxone ($2KHSO_5 \cdot KHSO_4 \cdot K_2SO_4$) is a readily available mild and safe solid oxidant, which has been used in the functionalisation of various groups.[45,62–67] The first report on its use for the oxidation of sulfides was released in 2000 when Kropp *et al.* discovered that when Oxone is dispersed on alumina or silica gel, it efficiently oxidises sulfides to sulfoxides, with some overoxidation to the sulfone.[68] This new oxone-$SiO_2$ method afforded sulfoxides even when used as a solvent-free system. However, the scope of this reaction was very limited to aliphatic sulfides until 2003, when Chen *et al.* applied the methodology on glycosyl sulfides reporting good yields and no interference with the protecting groups on glycosides.[69] Another example of a heterogeneous system was reported in 2018, when Silva and colleagues used a packed-bed reactor for the oxidation of sulfides in flow chemistry in the presence of trifluoroacetic acid (TFA) (Scheme 2.5).[65] The insoluble Oxone was packed in the column and as dichloromethane (DCM), containing the sulfide and TFA, was pumped through, the oxidation would successfully take place without causing overoxidation or side reactivities. A common feature among these protocols is that an acid, $SiO_2$ or TFA, is required to activate Oxone. In 2012 and 2017 two independent groups published two reports on the use of Oxone in an acid-free environment.[70,71] However, harsher, and longer reaction conditions were needed to achieve the oxidation of sulfides.

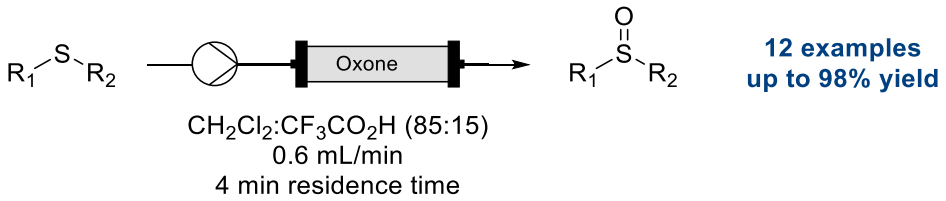


**Scheme 2.5.** In flow production of sulfoxides using Oxone by Silva *et al.*.[65]

#### *2.1.1.4 Sulfoxidation by peracids*

Peracids are probably the most effective and convenient sulfide oxidants but are notoriously explosive and have a poor atom economy, as only one oxygen atom of these oxidants gets incorporated in the product while the rest of the molecule accounts for waste. The most common peracid used for the synthesis of sulfoxides is *meta*-chloroperbenzoic acid (*m*CPBA) as it is easy to handle and commercially available.[72,73] *m*CPBA is a very effective generic oxidant, which makes it only compatible with simple sulfide molecules because it can oxidise multiple functional groups, including ketones and olefins, and can promote C-C functionalisation reactions.[72] *m*CPBA is generally used in aprotic solvents, like DCM, and affords sulfoxides in good yields if used stoichiometrically, with some overoxidation to the sulfone. Other peracids have been evaluated for the synthesis of alkyl aryl sulfoxides by Davies and Deary in 1996,[74] who were able to determine the kinetics of reaction of different peracids depending on their interaction with cyclodextrin. Despite the effectiveness of these oxidants, not much is reported in the literature regarding other peracids besides *m*CPBA. This is likely due to their synthesis and isolation which leads to rather explosive and shock sensitive compounds.[75,76]

#### *2.1.1.5 Sulfoxidation by peroxides*

The use of peroxides has probably been the most widely reported method for the synthesis of sulfoxides. In fact, there is a plethora of publications on sulfoxidation based on the use of peroxides, a lot of which have been summarised in excellent review papers.[67,77–82] The general trend for this class of oxidants is that peroxides are usually too mild to effectively react with sulfides and need a catalyst to be activated, usually in the form of an acid. Hydrogen peroxide ($H_2O_2$) is often the peroxide of choice because it is considered the greenest oxidant as it is mild, and its decomposition product is water. Alone, it requires heating to >70 $^oC$ up to reflux to effectively oxidise sulfides, which is usually avoided, especially on large scale, as it could cause thermal runways and explosions.[83–85] Therefore, throughout the years many catalysts have found applications in the activation of $H_2O_2$ to render it an effective safe oxidant, including the use of i) metal complexes, such as cobalt, tantalum and vanadium[86–94], ii) Lewis and Brönsted acids,[83,95–99] iii) silica and other solid supports[100–105] and iv) ultrasound sonication[106,107]. Due to the heavy interest this topic has received in the past few decades, several greener and more environmentally friendly protocols have been published. For instance, in the field of metal catalysed sulfoxidation, heterogeneous reaction systems that utilise magnetic nanoparticles (NPs) have become popular in recent years.[73,93,104] For example,

in 2021 Elgorban *et al.* reported the chemoselective synthesis of sulfoxides using Cu-*Calendula*@$Fe_3O_4$ nanocomposite material in 30% $H_2O_{2(aq)}$.[105] $Fe_3O_4$ nanoparticles were first coated in a biolayer of calendula extracts, which provided a lipophilic coating that reduces the reactivity of the NPs making them more biocompatible, and then the copper catalyst was absorbed onto the *Calendula*@$Fe_3O_4$ NPs (Scheme 2.6).

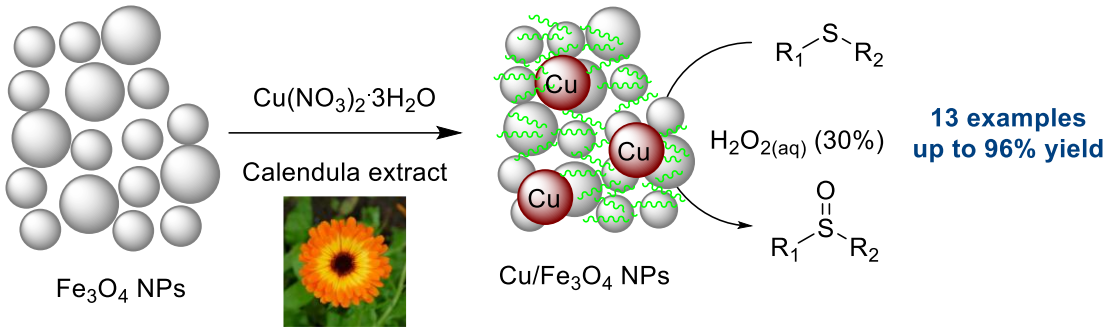


**Scheme 2.6.** Chemoselective synthesis of sulfoxides using Cu-*Calendula*@$Fe_3O_4$ nanocomposite material in 30% $H_2O_2$.[105]

With this method, the group selectively oxidised a panel of sulfides to sulfoxides with no observed overoxidation to sulfones. Moreover, due to the magnetic nature of the NPs, the heterogeneous catalyst was easily recovered from the reaction mixture using a magnet and was reused with no drop in activity for eight consecutive cycles. Similar works on NPs supported metal catalysts have also been reported by Veisi *et al.*[104] and Bezaatpour *et al.*[93] in 2018 and 2017 respectively, where this time oxo-vanadium and molybdenum Schiff bases were absorbed onto $Fe_3O_4$ NPs. Metal-free examples of greener sulfoxidations include the use of organocatalysts to activate $H_2O_2$. In 2017, Voutyritsa *et al.* used the cheap and commercially available 2,2,2-trifluoroacetophenone (TFAP) in aqueous $H_2O_2$ and *t*-BuOH to yield sulfoxides.[99] Moreover, they demonstrated that by tuning the reaction conditions they could selectively obtain either the sulfoxide or the sulfone, making this protocol fully flexible (Scheme 2.7).

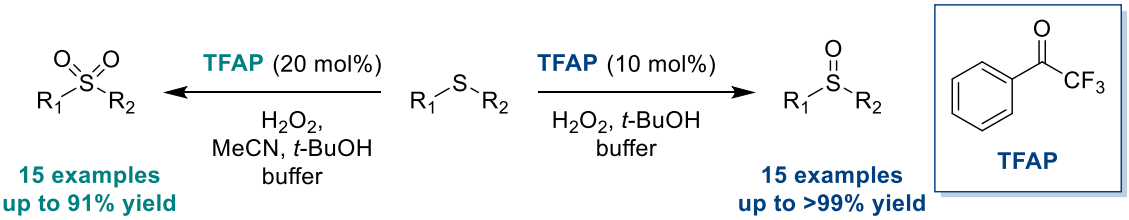


**Scheme 2.7.** Green oxidation of sulfides using $H_2O_2$ and TFAP in *t*-BuOH and buffer by Voutyritsa *et al.*.[99]

Borax[98] and boronic acid[83] have also found some interest in the scientific community for $H_2O_2$ activation as they are cheap, easy to handle and environmentally friendly salts. Lastly, a few examples where $H_2O_2$ was activated by mechanical force rather than chemical interaction have been described. Indeed, Mahamuni *et al.* presented works[106,107] where the activation of $H_2O_2$ was achieved by ultrasound. Here, methyl phenyl sulfide was placed in a bath with 30% $H_2O_{2(aq)}$ and upon sonication the desired sulfoxide was afforded with only minimal overoxidation.

Other peroxides have been studied, such as *tert*-butyl hydroperoxide (TBHP),[68,108–111] but have not gained as much popularity as $H_2O_2$ as they cause more waste at the end of the reaction and are generally less stable.

#### *2.1.1.6 Limitations of classic oxidation methods*

All these traditional methods afforded sulfoxides in varying success and have been extensively used on laboratory scale, especially *m*CPBA and other peroxides. However, when it comes to their scalability for industrial production of sulfoxides, most of these protocols present unnegotiable limitations. The use of some of these oxidants, like $HNO_3$ and NaOCl, is highly toxic, not only because they are harsh chemicals, but also because they can degrade into toxic gases such as HBr, NO, $Br_2$ and $Cl_2$. Also, especially in older publications, the organic solvents selected were toxic and often chlorinated. Therefore, these solvents would be unsafe to use in large scale reactors. Additionally, a common pattern found across the different methodologies is that often the oxidants led to overoxidation to sulfones if not properly controlled and they were incompatible with sulfides bearing multiple functional groups due to side reactivity. Perhaps, the use of peroxides, especially $H_2O_{2(aq)}$, can be considered among the greenest approaches to the synthesis of sulfoxides, but it still presents some disadvantages. For instance, several of the reported protocols that use $H_2O_{2(aq)}$ relied on the use of transition metals for effective sulfoxidation, which can be very costly at a large-scale production and could complicate the disposal of the end-of-reaction material. Also, aqueous $H_2O_2$ is generally sold as a 30% v/v solution, which is stable at cool temperatures. However, when used in large volumes for industrial purposes it may still have the potential to explode. Peracids, instead, are highly avoided because of their well-known explosive and shock sensitive nature, which becomes extremely dangerous for large scale use. Lastly, many of these oxidants have a poor atom economy as most of the molecular weight accounts for waste at the end of the reaction.

### 2.1.2 Alternative green methods for the synthesis of sulfoxides: enzymatic transformations

Despite the efforts and advances made in the last decade for the sustainable synthesis of sulfoxides, traditional methods still present substantial disadvantages that make their use unfavourable in industry. A sustainable and generally safer solution to this problem is biocatalysis, which exploits Nature's machinery, enzymes, to carry out chemical transformations.[34] Biocatalytic sulfoxidations have been extensively studied in the years and the large number of publications that arose as a result of this interest have been summarised in a number of excellent reviews.[16,17,112–115] Reports include enzymes such as cytochromes P450, monooxygenases, chloroperoxidases, laccase, as well as reductive enzymes,[115] all of which provide more sustainable, cheaper and ultimately safer methodologies to access sulfoxide compounds.[17,67] However, despite the excellent conversions, these approaches still have poor industrial applicability because of the low recyclability, high costs and stability of the enzymes. In addition, some enzymatic oxidations also require toxic and flammable additives and effective aeration of the system, all of which represent drawbacks in industry.[38,116–118] Ultimately, due to the intrinsic stereoselectivity of enzymes, most of the reports focus on the formation of enantiopure or enantioenriched sulfoxides, which from an industrial standpoint may not always be needed or favourable. One of the strategies that research groups have adopted in order to increase the stability, recyclability and hence cost effectiveness of enzymes is immobilisation of enzymes on a solid support.[119–121] The most famous and fruitful example of immobilised enzyme is *Candida antarctica lipase B* (CALB).[122]

#### *2.1.2.1 Immobilised Candida antarctica lipase B*

Lipases are probably the most widely used enzymes with the highest number of publications on search engines (5000 articles as per September 2022).[123,124] The natural substrates of lipases are lipids, phospholipids and triglycerides to name a few, which are transformed by this class of enzyme through a variety of reactions, such as hydrolysis, esterification and transesterification.[125,126] These natural substrates, however, are often insoluble in physiological conditions and hence, lipases adapted through years of evolutions to be able to interact with heterogeneous substrates. As a result, lipases have developed a broad substrate specificity which makes them appealing from a biocatalysis point of view.[122] For this reason, a lot of attention was dedicated to transforming lipases into enzymes that could perform at their maximum rate in non-physiological environment, a quality especially favoured at industrial level where continuous maximum efficiency is desired. One of the first approaches at improving performance and stability of lipases in

organic media was immobilisation on a solid support.[127] This was found to be particularly efficient with this class of enzymes due to their unique mode of action that relies on interfacial activation.[128,129] This, in fact, allows for an easy absorption on hydrophobic surfaces, oil droplets in the case of substrates, nanoparticles or natural and polymeric supports for immobilisation purposes instead (Figure 2.1). Furthermore, thanks to interfacial activation, when the enzyme is absorbed onto the support, the active site remains open allowing for efficient catalysis of the substrates.[130,131] Some of the advantages of immobilising lipases include increased stability, activity, selectivity, and specificity but also compatibility with organic or non-physiological media, increased resistance to harsh chemicals and recyclability.[122] Out of the many lipases commercially available, *Candida antarctica lipase B* (CALB) showed remarkable stability, broad selectivity, and ease of immobilisation due to its active site shape, all characteristics which made it a superior lipase.[126,129,132–134] As a result, CALB has been the mostly used lipase in the literature both as a free form and immobilised. The first manuscript describing the use of immobilised CALB dates back to 1992,[135] when Johnson and Bis described the enantioselective esterification or hydrolysis of five-, six- and seven-membered *meso*-diols **17a-c** or the corresponding diacetates **18a-c** using Novozym 435,

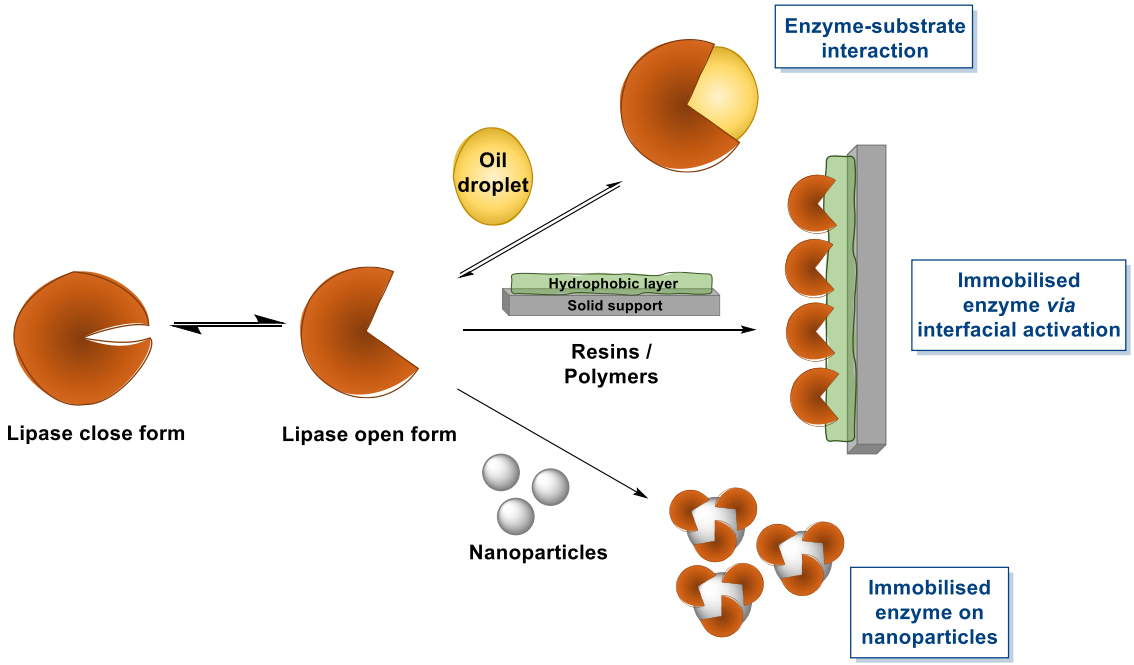


**Figure 2.1.** Interaction of lipases with natural substrates or hydrophobic solid supports for immobilisation.

a CALB enzyme immobilised by interfacial absorption on Lewatit VP OC 1600, a macroporousacrylic polymer resin supplied by Novozymes (Scheme 2.8). Since then, immobilised CALB found many other applications in biocatalysis,[136–138] some of which will be highlighted below, and due to its popularity, many companies have commercialised their own versions of immobilised CALB.

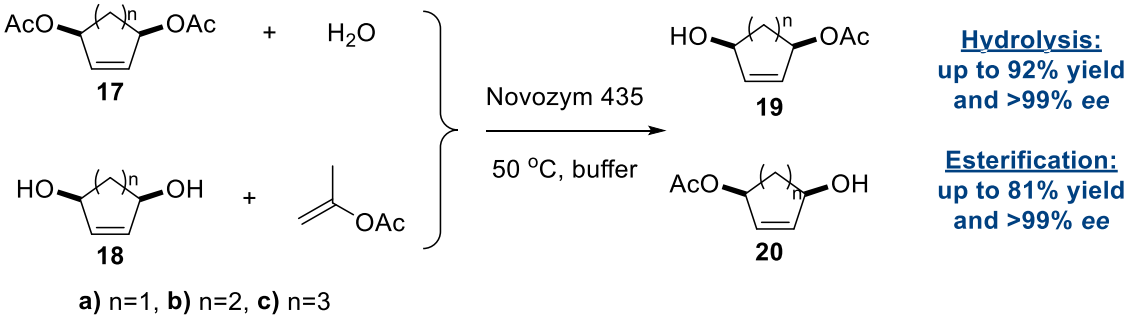


**a)** n=1, **b)** n=2, **c)** n=3

**Scheme 2.8.** First reported example of esterification and hydrolysis of five-, six- and seven-membered *meso*-dials or the corresponding diacetates using the immobilised enzyme Novozym 435 by Johnson and Bis.[135]

### *2.1.2.2 Reactivity of CALB*

Despite the many functionalisation strategies CALB has been the protagonist of, the reactivity of this enzyme can be categorised into two reaction classes: hydrolysis and esterification.[139,140] Both reaction profiles have been adopted for transformations such as kinetic resolutions, derivatisations, synthesis of new glycerides, biodiesel formation and oxidation.[132,141–163] In 2016 Griffin *et al.* reported the first case of ammonolysis of triglycerides in liquid ammonia using immobilised CALB.[164] This protocol, which would normally require high temperatures (>180 °C) and pressures, afforded a series of amides starting from the corresponding triglycerides at room temperature and pressure (Scheme 2.9, Part A).

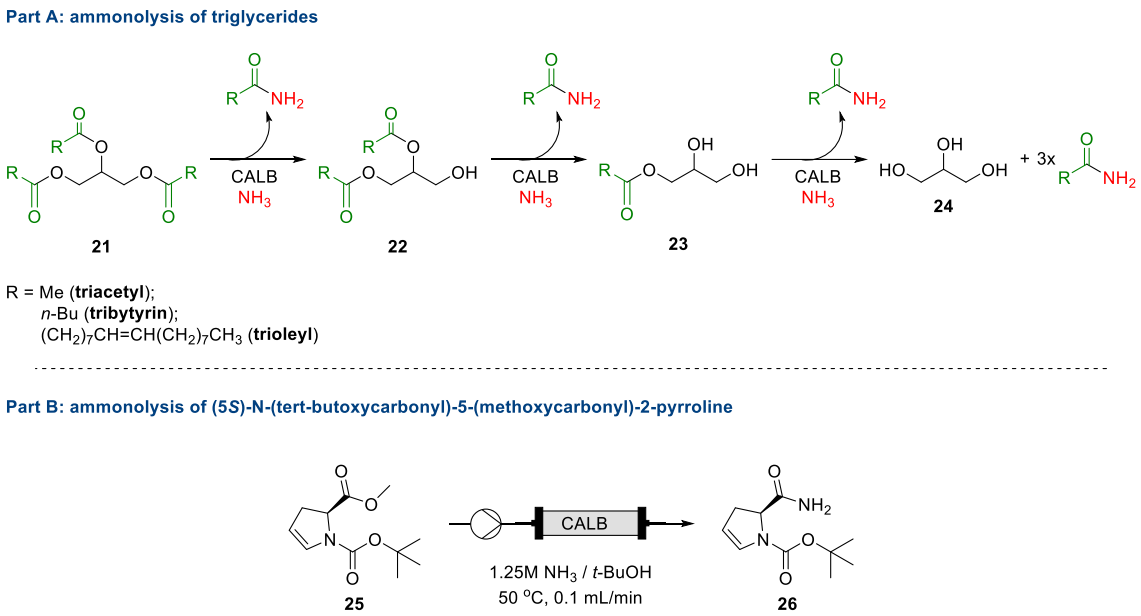


**Scheme 2.9.** Examples of CALB catalysed ammonolysis. Part A) Formation of aliphatic amides from triglycerides proposed by Griffin *et al.*.[164] Part B) Synthesis of the amide intermediate **26** in the synthesis of Saxagliptin.[165]

In 2018, Harini *et al.* also reported a CALB catalysed ammonolysis protocol,[165] where (5*S*)-N-(*tert*-butoxycarbonyl)-5-(methoxycarbonyl)-2-pyrroline **25**, a peptidase inhibitor intermediate, was converted into its corresponding amide **26** (Scheme 2.9, Part B) after passing 1.25 M ammonia in anhydrous *tert*-butanol through a packed bed reactor containing immobilised CALB at 50 °C. Another unique example of the use of immobilised CALB was reported by Wang *et al.* in 2018, who utilised the enzyme immobilised on a chitosan coated acrylic resin for a Knoevenagel condensation reaction,[166] a tandem esterification and transesterification, for the production of a benzopyran compound (Scheme 2.10). Remarkably, the immobilised CALB could be recycled for five consecutive cycles until its relative activity dropped to 60%. Another area where lipases and CALB have found a lot of applications is esterification of glycerol with long chain acids to form glycerides. For instance, in 2017 Yadav *et al.* reported the synthesis of glycerine monoundecylenate, an emulsifier used in the food and cosmetic industries, from glycerol and undecylenic acid.[167] It was shown that this reaction could afford the product at 60 °C after 2 hours when in batch, or in 10 minutes if performed in flow with only up to 10% diacylation of glycerol.

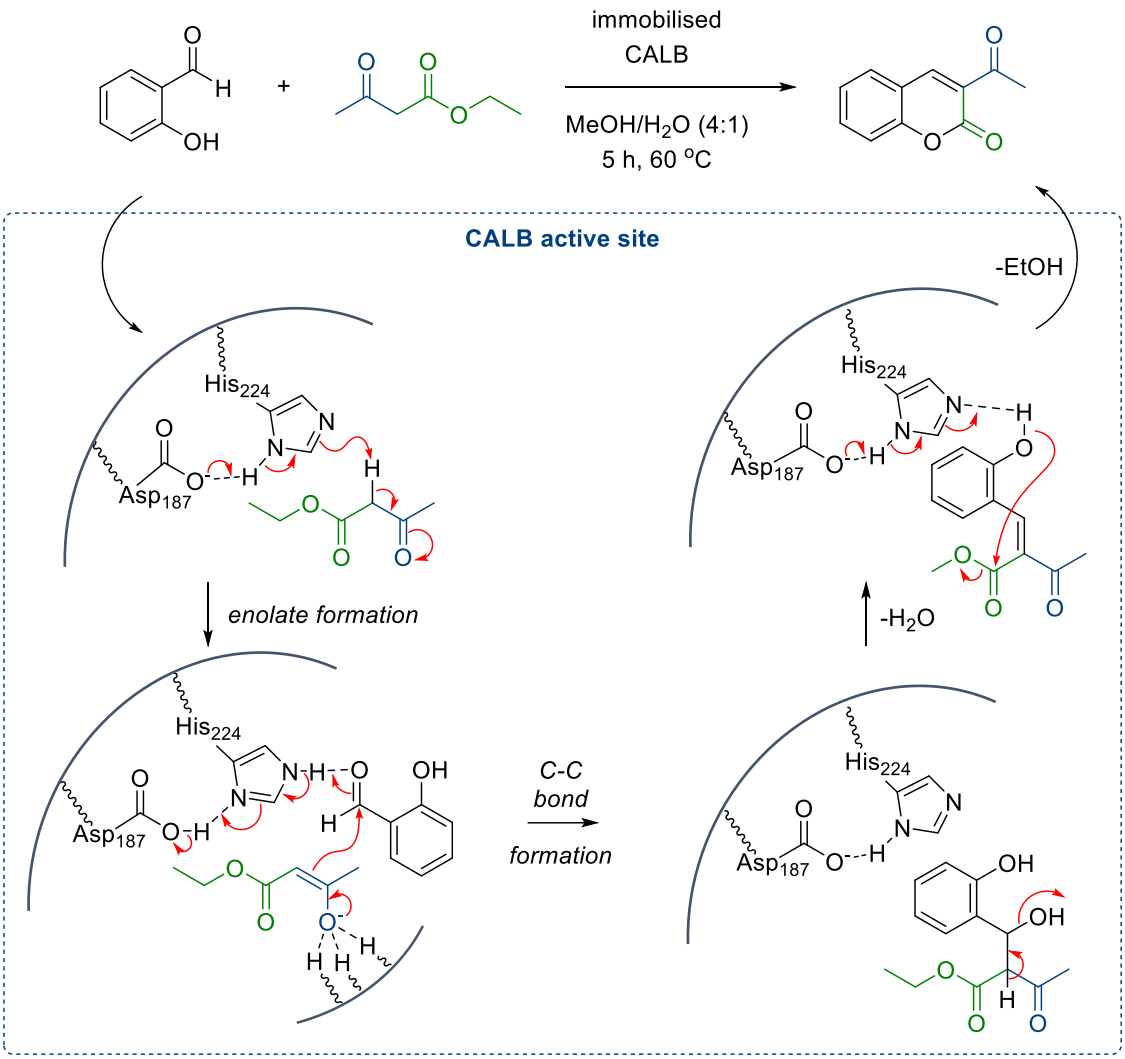


**Scheme 2.10.** Proposed mechanism of action of the Knoevenagel condensation reaction catalysed by immobilised CALB by Wang *et al.*.[166]

Another crucial reactivity of CALB is the ability to catalyse perhydrolysis, the formation of peracids from acids or ester precursors in the presence of $H_2O_2$. The mechanism of action for this transformation is believed to proceed in the same way as for hydrolysis, which involves Ser105, His224 and Asp187,[168,169] except that one molecule of $H_2O_2$ is integrated into the molecule instead of $H_2O$ (Figure 2.2).

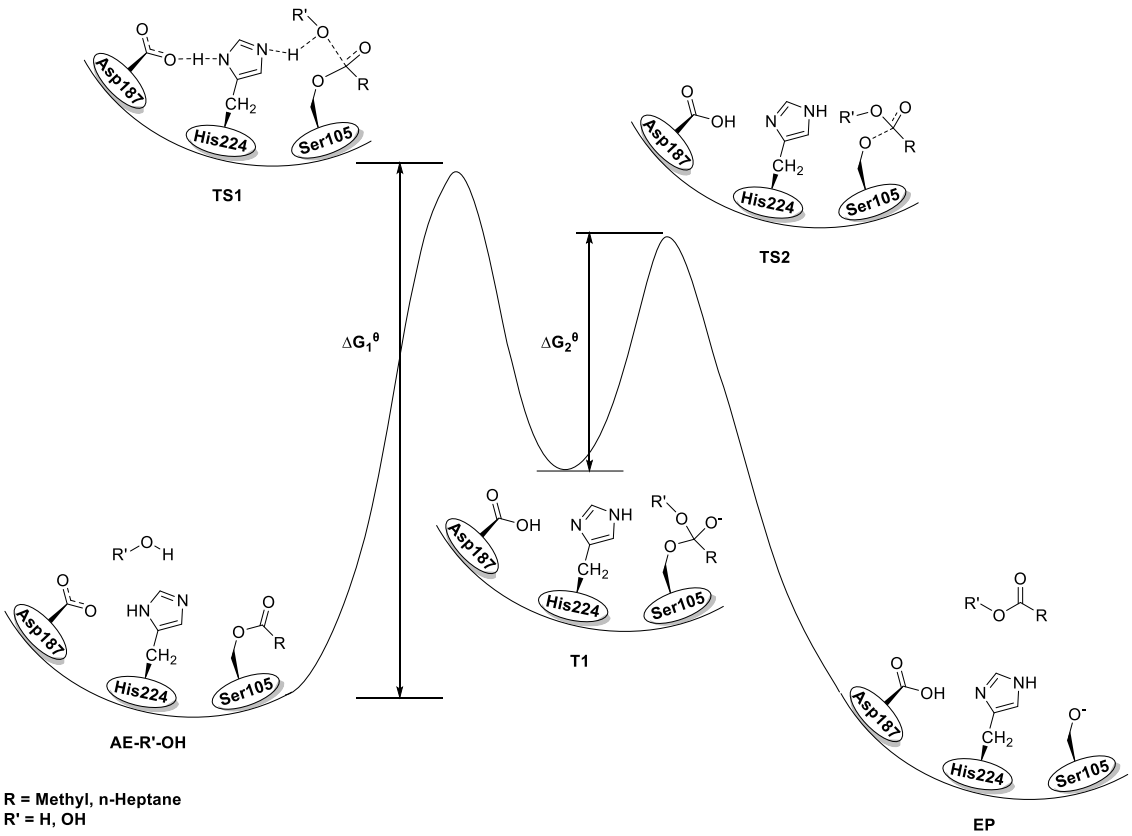


**Figure 2.2.** Mechanism of hydrolysis of esters or acids catalysed by CALB. Two transition states and intermediate are shown.[168]

The peracids formed *in situ* are then used for epoxidations,[170–175] Baeyer-Villiger lactonisations and esterifications[171,176–179] as well as amine oxidations.[180] In 2019, Melchiors *et al.* reported the use of an immobilised CALB for the mono epoxidation of limonene,[181] an oil which can be extracted from citrus food waste and used for food and cosmetics. In this study the peracid oxidant was formed *in situ* from octanoic acid and $H_2O_2$ in toluene with 5% immobilised CALB at 50 °C. They also demonstrated that the enzyme could be used for 3 consecutive cycles until $H_2O_2$ induced degradation occurred (Scheme 2.11).

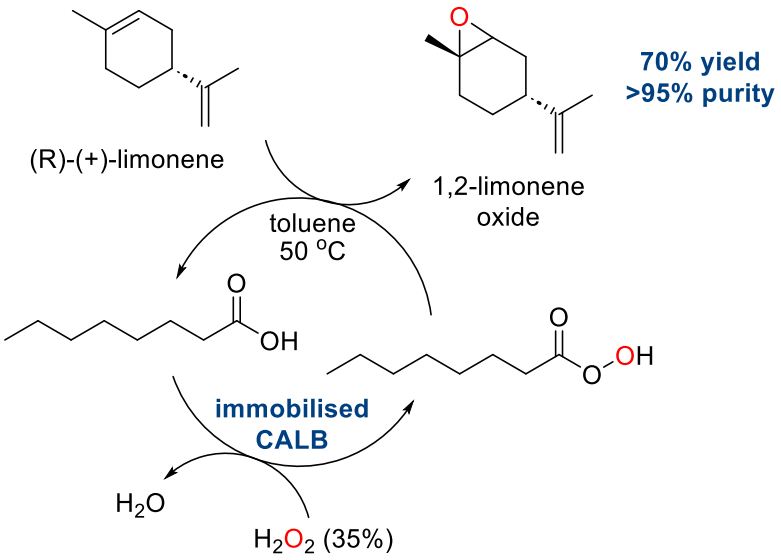


**Scheme 2.11.** Oxidation of limonene by immobilised CALB via production of peroctanoic acid by Melchiors *et al.*.[181]

So far, all the examples presented were focused on acrylic resin immobilised CALB. However, other immobilisation strategies have been successfully adopted for CALB transformations. For instance, in 2014 Zanette *et al.* published a protocol for the epoxidation of oleic and linoleic acids using a semisolid CALB immobilised in a lecithin-based microemulsion-based organogel.[182] This methodology, compared to the more traditional polymer supported enzymes, has the benefit of reduced deactivation of the enzyme by $H_2O_2$ because it is hypothesised that the biocatalyst is more protected and less susceptible to deactivation in the gel-like matrix. It was also demonstrated that running the reaction in EtOAc would increase the rate of reaction as the media acted as a co-oxidant reacting with $H_2O_2$ to give peracetic acid. This is not the only example where the media of the reaction has been used as the oxidant for a biotransformation. In fact, in 2012 Chávez *et al.* reported the lactonization of small cyclic ketones using cross-linked enzyme aggregate (CLEA) CALB in EtOAc at 40 °C (Scheme 2.12).[183] The "greenness" and low boiling point of EtOAc make it a suitable solvent for industrial use and it is therefore often used in green chemistry transformations. Moreover, the authors demonstrated that the use of CLEA-CALB is comparable to the one of Novozyme® 435 with the added benefit of not suffering from enzyme leaching.

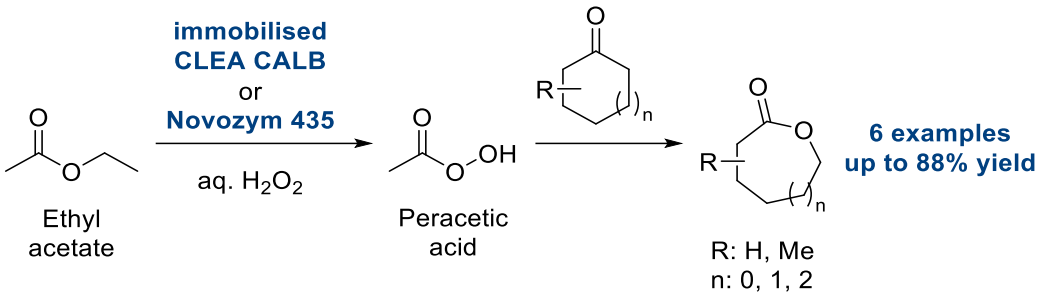


**Scheme 2.12.** Exploitation of EtOAc as reaction solvent and peracid precursor for the synthesis of lactones by Chávez *et al.*.[183]

Despite the well-known ability of peracids to carry out sulfoxidations (as escribed in section 2.1.1.4), to our surprise the use of CALB as a biocatalyst in the oxidation of sulfide substrates into sulfoxides had never been investigated. Therefore, in this chapter of this thesis, it is demonstrated how the ability of CALB to catalyse the formation of peracids *in situ* can be exploited for sulfoxide synthesis.

## 2.2 Aims of the project

The main aim of this research project was to demonstrate that a facile, chemoselective and scalable biocatalytic protocol for the synthesis of sulfoxides could be achieved by exploiting the ability of CALB to catalyse perhydrolysis. Additionally, driven by the interest of our group in the development of industrially applicable green methodologies, EtOAc was used in the dual role of solvent and CALB substrate, avoiding the use of extra acid additives. The choice of EtOAc as solvent/reagent improves the industrial sustainability of the method as, when considering all factors in choosing a solvent for a chemical process such as the health, environment, and safety scores,[184–186] EtOAc is considered a safer and more economical alternative to other widely used solvents, such as halogenated or high boiling point solvents. Thus, EtOAc was deemed ideal for the development of this sulfoxidation methodology, where it can serve as a solvent and CALB substrate, in turn contributing to the atom economy of the process.

Furthermore, in order to increase the "grenness" of the process, the *in situ* production of $H_2O_2$ via photocatalytic means was investigated, with the aim to prevent the hazards associated with handling $H_2O_2$ at large scale.

Lastly, the production and use of chiral peracids from commercially available substrates and their effect on the stereochemistry of the CALB sulfoxidation was investigated.

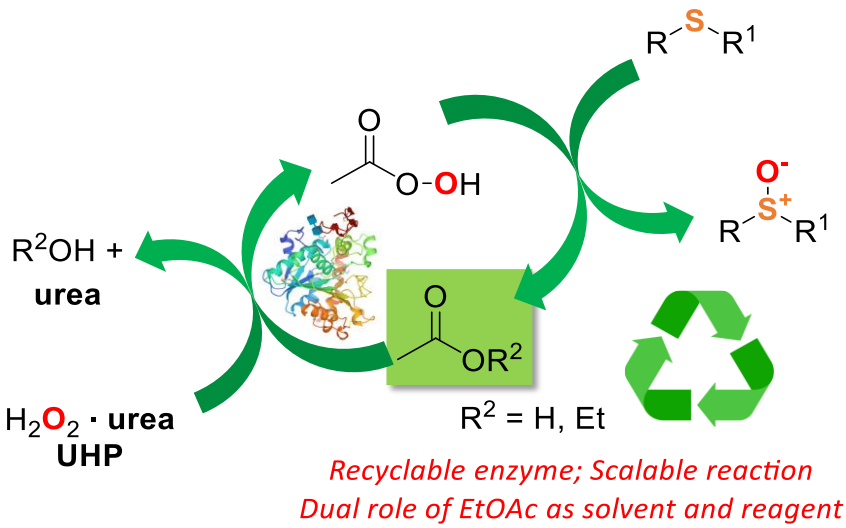

## 2.3 Results and discussion

### 2.3.1 Oxidation of sulfides with CALB in EtOAc in the presence of UHP

#### *2.3.1.1 Optimisation of the reaction conditions*

Based on a report given to us by Almac, where immobilised CALB was used in EtOAc in the presence of $H_2O_2$ or urea hydrogen peroxide (UHP) to form epoxides, this project commenced by proving that the *in situ* formation of peracetic acid from EtOAc could be exploited for the oxidation of sulfides to sulfoxides. Therefore, the commercially available methyl phenyl sulfide (MPS) **27a** was selected as substrate and the commercially available recombinant CALB from *Aspergillus oryzae* immobilised on Immobead 150 was the biocatalyst of choice to develop the sulfoxidation methodology. Sulfide **27a** was initially treated with CALB (20% w/w) and 1.1 equivalents of $H_2O_2$ in EtOAc (400 mM) leading to an 83:17 mixture of the desired sulfoxide **28a** and the over-oxidation sulfone by-product **29a** within 24 h (Table 2.1, *Entry 1*). Replacement of $H_2O_2$ with UHP,[187] which is often used as a more stable alternative to $H_2O_2$, led to the full oxidation of **27a** in only 2 h and to the formation of the sulfoxide **28a** as the major product in an improved 93:7 ratio against **29a** (Table 2.1, E*ntry 2*). Reducing the concentration of **27a** to 200 mM (Table 2.1, *Entry 3*) led to a small improvement in the sulfoxide/sulfone ratio (94:6), while a lower ratio (92:8) was observed in more concentrated conditions (Table 2.1, *Entry 4*). Thus, the optimal reaction concentration of **27a** was kept at 400mM. All the reactions were carried out under open air conditions. In order to confirm that the oxidation of sulfide **27a** was biocatalysed by CALB rather than being promoted by UHP only or by air, a series of control experiments (Table 2.1, E*ntries 5-7*) were performed. Upon the removal of CALB and in the presence of UHP only, both in stoichiometric amount and in excess (5.0 eq.), negligible formation of **28a** was observed, clearly accounting for the key role of CALB for the *in situ* generation of the peroxyacid oxidant intermediate **30** (Scheme 2.13).[183]

**Table 2.1.** Optimisation of the CALB biocatalysed sulfoxidation of **27a**.

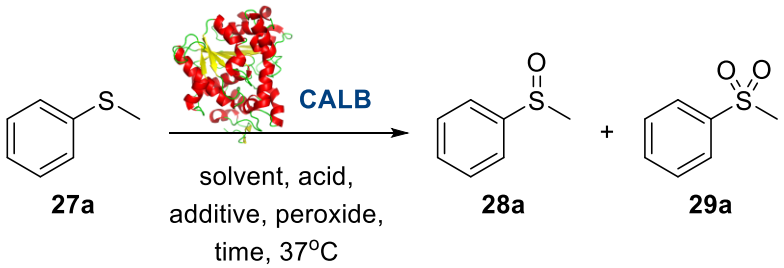


| Entry | 27a (mM) | CALB (%*w/w*) | Peroxide[a] | Solvent | Acid additive | Time (h) | Conv. (%)[b] | Ratio 28a/29a[c] |
|---|---|---|---|---|---|---|---|---|
| *1* | 400 | 20 | $H_2O_2$ | EtOAc | - | 24 | 99 | 83:17 |
| ***2*** | **400** | **20** | **UHP** | **EtOAc** | **-** | **2** | **>99[d]** | **93:7** |
| *3* | 200 | 20 | UHP | EtOAc | - | 2 | >99 | 94:6 |
| *4* | 600 | 20 | UHP | EtOAc | - | 2 | >99 | 92:8 |
| *5* | 400 | - | UHP | EtOAc | - | 2 | 8 | ND |
| *6* | 100 | - | UHP (5.0 eq.) | EtOAc | - | 24 | 30 | ND |
| *7* | 400 | 20 | - | EtOAc | - | 2 | 4 | ND |
| *8* | 400 | 20 | UHP | DCM | - | 2 | 1 | ND |
| *9* | 400 | 20 | UHP | Toluene | - | 2 | 4 | ND |
| *10* | 400 | 20 | $H_2O_2$ | DCM | 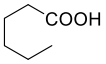 | 20 | 44 | ND |
| *11* | 400 | 20 | UHP | Toluene | | 2 | 17 | ND |
| *12* | 160 | 20 | UHP | Toluene | | 20 | 81 | 66:34 |
| *13* | 160 | 20 | UHP | Toluene | 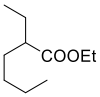 | 2 | 16 | ND |

[a]1.1 eq. of $H_2O_2$ or UHP were used unless indicated differently; [b]Determined by analysis of the $^1$H-NMR crude mixture and referred to the conversion of **27a** into **28a-29a** together; [c]Determined by $^1$H-NMR; [d]Compound **28a** was obtained with 89% isolated yield.

Similarly, when UHP was omitted from the reaction, only a small amount of **28a** was obtained and 96% of **27a** was recovered. Finally, no sulfoxidation was observed when DCM or toluene (Table 2.1, *Entries 8,9*) were used as solvents, further supporting the key dual role of EtOAc as solvent and CALB substrate and precursor of peroxyacid **30**. As an additional confirmation of the key dual functionality of EtOAc over the use of inert solvents such as DCM and toluene, a series of experiments using acid additives as

precursors of the peroxyacid oxidant were carried out. The treatment of **27a** with CALB in DCM or toluene in presence of stoichiometric hexanoic acid and 2-ethylhexanoic acid (Table 2.1, E*ntries 10,11*) led to **28a** with poor conversion after 2 h. Interestingly, in the presence of 2-methylbutyric acid, **27a** was converted at 81%, but with poor 66:34 sulfoxide/sulfone ratio (Table 2.1, E*ntry 12*), while in the presence of the ester additive ethyl (2-ethyl)-hexanoate in toluene, **28a** was obtained in low amount (Table 2.1, E*ntry 13*).

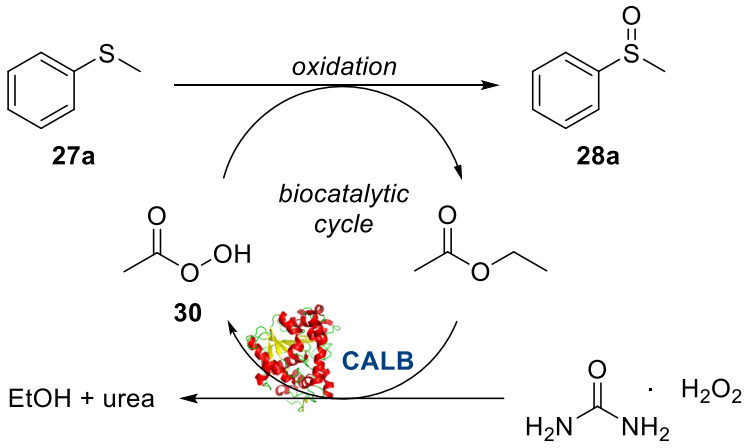


**Scheme 2.13.** Proposed cycle for the CALB biocatalysed sulfide oxidation in EtOAc.

### *2.3.1.2 Titration of peracetic acid formed by CALB*

To further confirm the S-oxidation mechanism and the formation of the peracetic acid, a series of titrations experiments based on the report by Chávez *et al.*[183] were carried out to determine the concentration of peracetic acid over time. The reaction mixture containing 270 mM UHP and 20-24% CALB was incubated at 37 °C without the sulfide **27a** and aliquots were taken at time intervals of 30 min, 1, 2 and 4 h. These were then treated with the commercially available catalase from Sigma Aldrich to remove leftover $H_2O_2$ from UHP, reacted with KI and $H_2SO_4$ to reduce the peracid with the concomitant formation of $I_2$, which was then titrated with a 0.05 M solution of sodium thiosulfate using starch as an indicator (Scheme 2.14). From the titration curve (Figure 2.3), it was clear that the production of peracetic acid was fast within the first hour, with a rate of reaction of 1.3764 mM/h and more than half of the UHP transformed into peracid. The reaction then plateaued after 2 h, reaching a concentration of approximately 180 mM, which follows a standard enzyme kinetics profile.

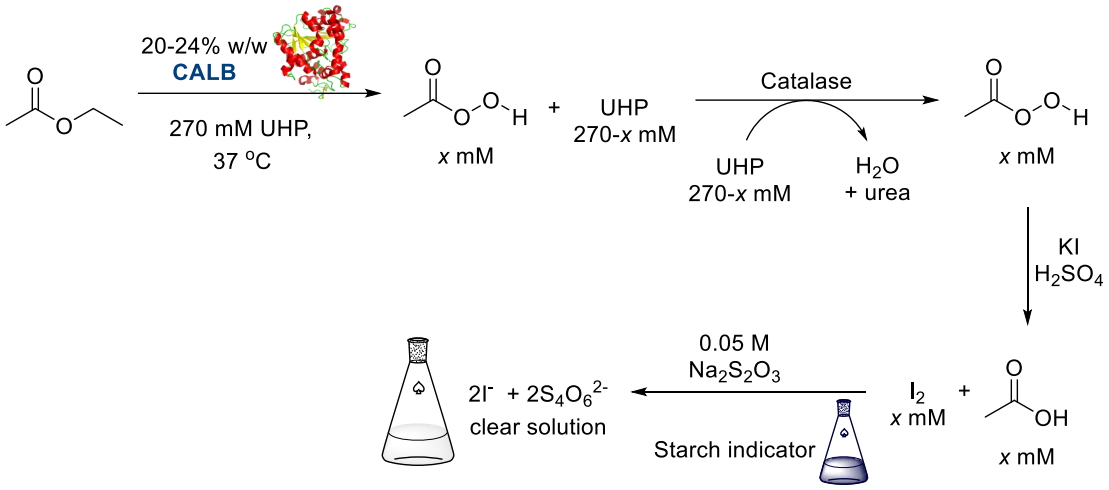


**Scheme 2.14.** Titration of peracetic acid formed by CALB.

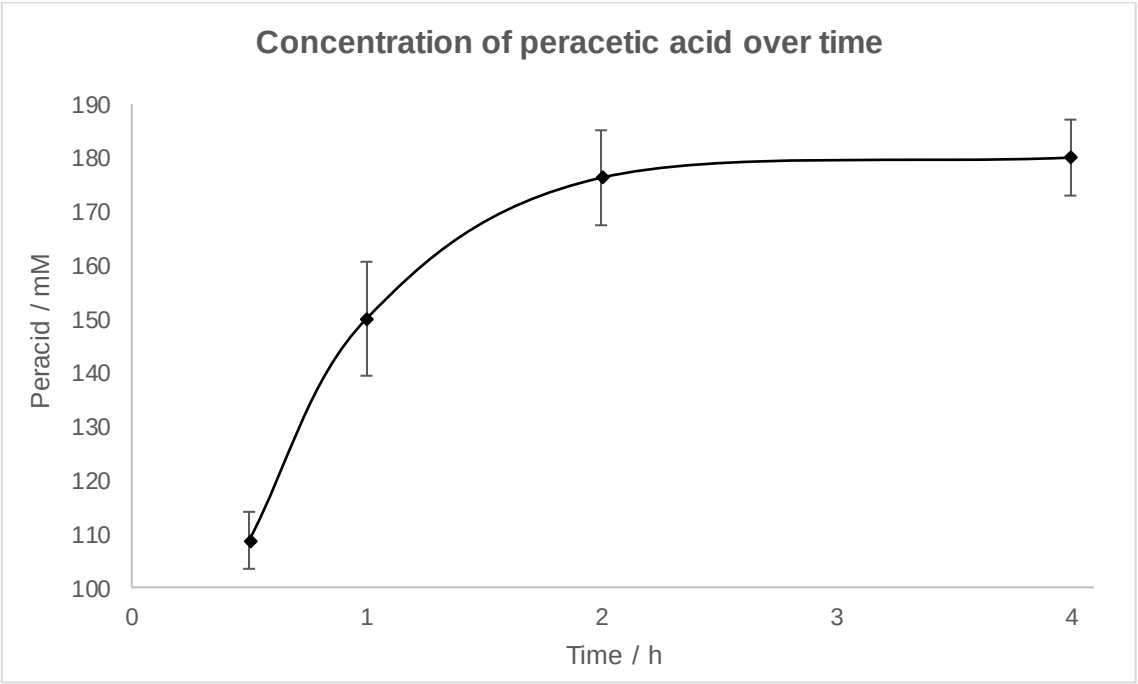


**Figure 2.3.** Concentration or peracetic acid formed *in situ* over time.

### *2.3.1.3 Scope of the reaction*

With the optimised reaction conditions in hand (**27a** 400 mM, 20% w/w CALB, 1.1 eq. UHP in EtOAc at 37 °C), the scope of the CALB biocatalysed sulfoxidation was investigated. A series of alkyl-aryl(benzyl) sulfides **27a-r** were synthesised from the appropriate thiophenol or benzylthiol precursors **31a-h** through an $S_N2$ reaction of the appropriate alkyl halide in water under microwave irradiation at 140 °C at intervals of 5

minutes. All substrates **27** were converted into the corresponding sulfoxides **28** with high yields as shown in Table 2.2. In most cases, only a low amount of the sulfone by-product was formed, and high isolated yields were obtained regardless of the size of the alkyl substituent (Me, Et, Pr) on the sulfoxide moiety. Excellent conversions and high yields were also obtained for the allylic sulfoxide **28l** (Table 2.2, E*ntry 11*), benzyl sulfoxides **28o** and **28p** (Table 2.2, E*ntry 14*), the chiral nitrile **28q** (Table 2.2, E*ntry 16*) and the dialkyl derivative **28r** (Table 2.2, E*ntry 17*).

**Table 2.2.** Scope of the CALB biocatalysed sulfoxidation

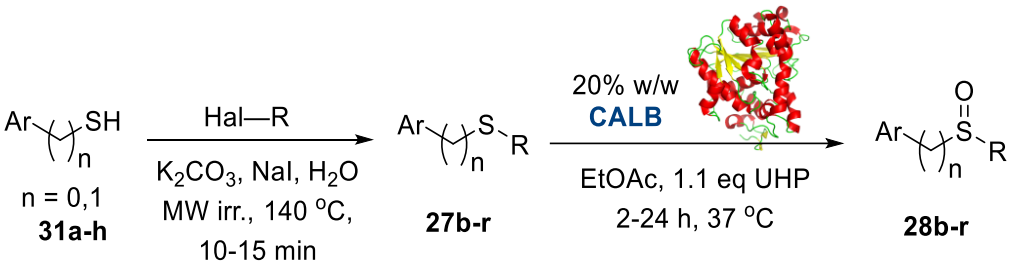


| Entry | Compound | | Conv. (%)[a] | Yield (%)[b,c,d] | Ratio SO/SO$_2$ |
|---|---|---|---|---|---|
| *1* | **28b** | 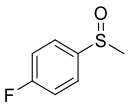 | >99[e] | 85 | 88:12 |
| *2* | **28c** | 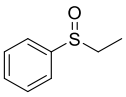 | 99 | 63 | 66:34 |
| *3* | **28d** | 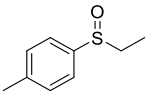 | 90 | 71 | 80:20 |
| *4* | **28e** | 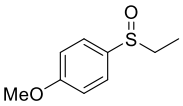 | 97[e] | 60 | 70:30 |
| *5* | **28f** | 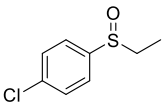 | 90 | 67 | 80:20 |
| *6* | **28g** | 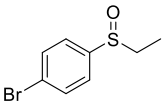 | 97 | 67 | 76:24 |
| *7* | **28h** | 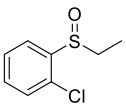 | 99 | 81 | 83:17 |
| *8* | **28i** | 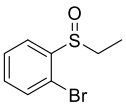 | 99 | 80 | 90:10 |

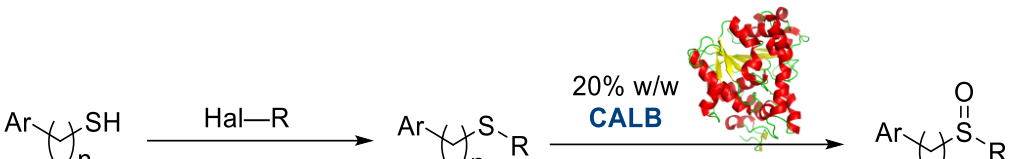


| Entry | Compound | | Conv. (%)[a] | Yield (%)[b,c,d] | Ratio SO/SO$_2$ |
|---|---|---|---|---|---|
| *9* | **28j** | 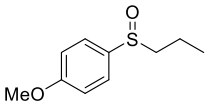 | 98 | 79 | 80:20 |
| *10* | **28k** | 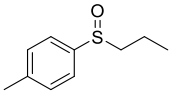 | 88 | 68 | 80:20 |
| *11* | **28l** | 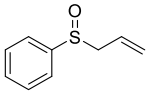 | 90 | 68 | 100:0 |
| *12* | **28m** | 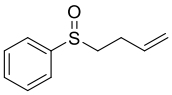 | 67 | 58 | 100:0 |
| *13* | **28n** | 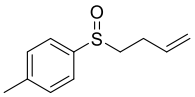 | 85 | 73 | 100:0 |
| *14* | **28o** | 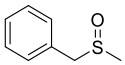 | 90 | 82 | 83:17 |
| *15* | **28p** | 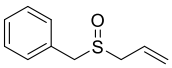 | 96 | 86 | 92:8 |
| *16* | **28q** | 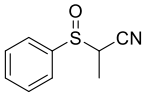 | 94 | 78[f] | 95:5 |
| *17* | **28r** | 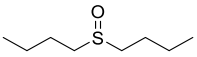 | >99[e] | 89 | 94:6 |

[a]Determined by the crude $^1$H-NMR mixture and referred to the conversion of **27** in **28-29** together. [b]All the reactions were carried out for 24 h, unless completed before as revealed by TLC. [c]Isolated yields reported refer to the pure sulfoxides. [d]Isolated yields refer to the biocatalytic step only. [e]The reaction was completed in 2 h. [f]Obtained as a 3:2 mixture of diastereoisomers.

As described in Section 2.1.2.2, when CALB is in the presence of a peroxide and an ester/acid, epoxidations and Baeyer-Villiger reactions are known to occur due to the formation of peracids. However, the methodologies reported in the literature are mostly carried out on simple compounds that bear only one type of functional group, either an alkene or a ketone, highlighting a lack of investigation on the chemoselectivity when multi-functional group molecules are exposed to the conditions of CALB catalysed perhydrolysis. Therefore, sulfide derivatives **27m** and **27n** bearing a non-allylic double

bond were also synthesised to test whether epoxidation or sulfoxidation was favoured. Sulfoxides **28m** and **28n** were obtained chemoselectively in high yields (Table 2.2, E*ntries 12,13*) and no traces of epoxide (by)-products were detected, indicating the chemoselectivity of this reaction and the preferred oxidation of sulfur over alkenes. In order to understand why sulfoxidation was favoured over epoxidation, ether **33** was synthesised as shown in Scheme 2.15 and subsequently reacted with CALB and UHP in EtOAc. Surprisingly, after 48 h reaction time, full recovery of **34** was determined by crude $^{1}$H NMR with no oxidation to the epoxide observed, even after doubling the equivalents of UHP and CALB and increasing the reaction temperature to 50 $^{o}$C. Interestingly, other reports in the literature where terminal alkenes are exposed to peracids formed in situ do not report the formation of the epoxide, as in the case of limonene.[181,188,189] It was then hypothesised that the terminal alkene was not reactive enough to react with the peracetic acid formed due to lack of interaction of adjacent filled C-C and C-H σ orbitals of parallel bonds with the π* antibonding orbital of the alkene.[190] This interaction stabilises the double bonds, and makes them significantly more nucleophilic towards electrophiles, as the electron donation raises the energy of the HOMO. For instance, there is a 21-fold increase in reactivity between a mono- and a disubstituted alkene with *m*CPBA.[190]

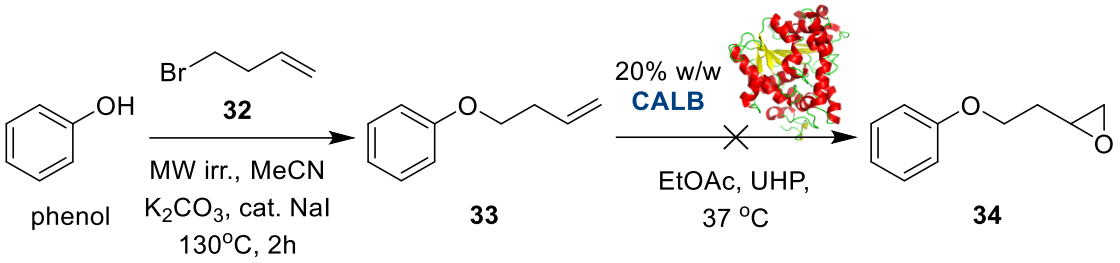


**Scheme 2.15.** Biocatalysed epoxidation of alkene-bearing ether **33**.

With the aim to further investigate the chemoselectivity of this transformation, namely S-oxidation versus Baeyer-Villiger oxidation, a series of sulfide substrates **38a-f** bearing a carbonyl moiety was also synthesised from thiophenol **35** through either a Michael addition with αβ-unsaturated ketones **36** or an $S_N2$ reaction with α-chloro ketones **37**. All carbonyl containing substrates **38a-f** were selectively oxidised at the sulfur atom, as determined by NMR, affording the corresponding sulfoxides **39a-f** with excellent conversions (up to 99%) and high yields after 24 h (Table 2.3).

**Table 2.3.** CALB biocatalysed synthesis of sulfoxides bearing carbonyl groups.

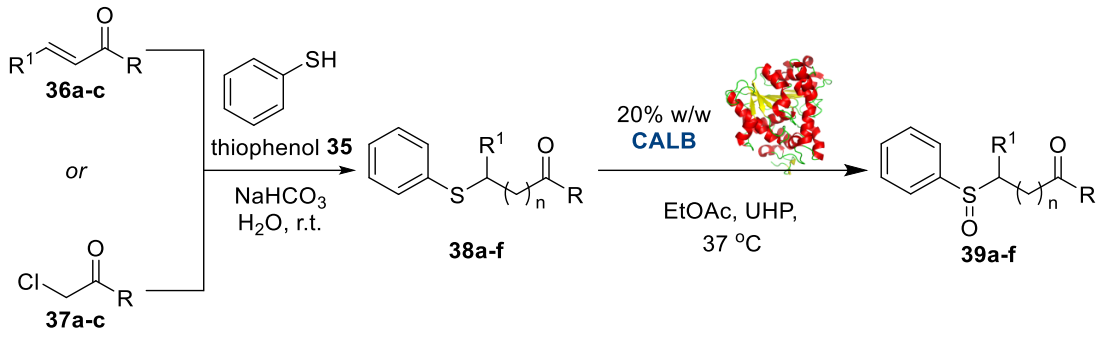


| Entry | Compound | R | $R^1$ | n | Conv. (%)[a] | Yield (%)[b,c] | Ratio $SO/SO_2$ |
|---|---|---|---|---|---|---|---|
| *1* | **39a** | Me | H | 1 | 89 | 71 | 100:0 |
| *2* | **39b** | Me | Me | 1 | 68[d] | 42 | 100:0 |
| *3* | **39c** | H | Me | 1 | 0 | 0 | 100:0 |
| *4* | **39d** | Me | H | 0 | 99 | 67 | 80:20 |
| *5* | **39e** | Et | H | 0 | 96 | 81 | 85:15 |
| *6* | **39f** | *i*Pr | H | 0 | 93 | 68 | 89:11 |

[a]Determined by $^1$H-NMR of the crude mixture and referred to the conversion of **39** in $SO/SO_2$ products together; [b]Reported isolated yields refer to the pure sulfoxides. [c]Isolated yields refer to the biocatalytic step only.

The only exception was represented by the aldehyde substrate **39c** (Table 2.3, *Entry 3*) which degraded during the reaction and no sulfoxide or other oxidation by-products were obtained from the reaction mixture. In all cases, the oxidation was highly selective towards the formation of the sulfoxide over the sulfone. Remarkably, no Baeyer-Villiger oxidation side products were observed in any reaction, further proving the high chemoselectivity of the methodology. Finally, to further investigate the compatibility of this method with other functional groups, compounds **38a** and **38c** were reduced to their alcohol derivatives **40a,c** using $NaBH_4$ (Scheme 2.16). Alcohols are also substrates of CALB and, especially in a water free environment, tend to undergo esterification reactions if either acids or esters, like EtOAc, are present (Section 2.1.2.2). Therefore, **40a,c** were subjected to the CALB catalysed sulfoxidation and led to products **41a,c** with excellent conversions and yields (Scheme 2.16). Predictably, in the case of **41b**, CALB also catalysed the acetylation of the primary hydroxyl group in addition to the S-oxidation, showing that there are two concomitant reactions taking place. Instead, in the case of **41a**, no acylation was observed due to the steric hindrance and decreased reactivity of the secondary alcohol.

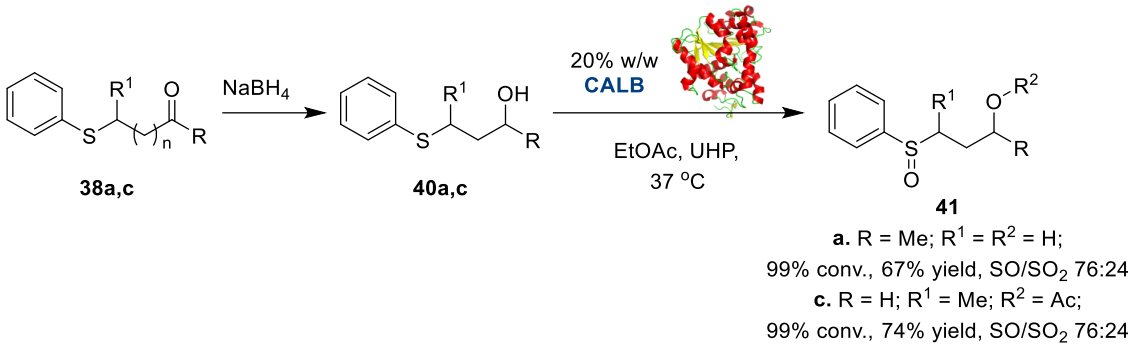


**Scheme 2.16.** CALB biocatalysed synthesis of sulfoxides bearing hydroxyl groups.

### *2.3.1.4 Industrial applicability*

One of the main drawbacks of the synthetic methodologies developed within an academic environment is that they often fail to translate to industrial scale use as they are not easily scalable and/or applicable to pharmaceutical ingredients (APIs). Initially, the scalability of the CALB S-oxidation was investigated through the of 3 g of sulfide **27a** (Scheme 2.17, Part A), a 100-fold increase in scale compared to the scope of the reaction. **27a** was treated with the same conditions as for laboratory scale synthesis but, in order to avoid the overoxidation of **27a** due to high amounts of UHP used, as well as for safety reasons, the peroxide was added to the reaction mixture in two portions every 30 min. The sulfoxide **28a** was obtained with 93% conversion and 88% isolated yield, with an excellent E-factor of 33. This was calculated using Equation 2 as shown below:

$$\text{E-factor} = \frac{\text{mass of total waste}}{\text{mass of product}} = \frac{\text{EtOAc+urea+H}_2\text{O}}{\text{Sulfoxide}} \qquad (2)$$

Note that immobilised CALB was not included in the calculation of E-factor, because it can be recycled at the end of the reaction. Secondly, applicability of the method to the synthesis of APIs was investigated through the synthesis of omeprazole **43** (Scheme 2.17, Part B). The sulfide precursor **42** was treated with CALB and UHP under standard condition with the addition of 1% DCM due to the poor solubility of **42** and the selective oxidation of the sulfur to sulfoxide was quantitatively completed within 2 hours, leading to omeprazole **43** in 73% isolated yield. No trace of the sulfone or other by-products were observed. Even after considering the addition of DCM, the E-factor of the transformation was found to be an optimal 35 (calculated using Equation 2), confirming the high industrial applicability of the CALB oxidation method.

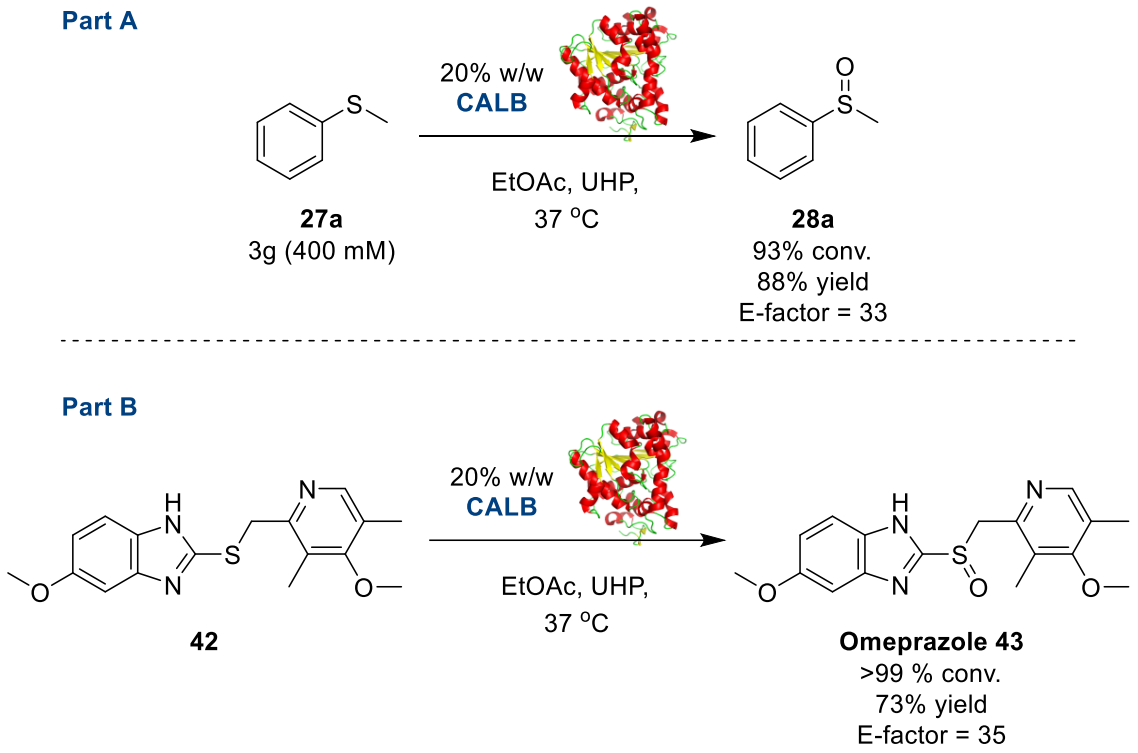


**Scheme 2.17.** Part A: Gram-scale synthesis of sulfoxide **28a**; Part B: Synthesis of omeprazole **43** *via* CALB biocatalysed oxidation.

Interestingly, most of the current approaches reported in literature for the synthesis of omeprazole **43** are carried out under harsher reaction conditions and longer reaction times,[191–193] highlighting the potential impact of this method on the synthesis of sulfoxide containing pharmaceutical ingredients at industrial level.

### *2.3.1.5 Recyclability of the immobilised CALB*

One of the many advantages of using immobilised enzymes is their recoverability at the end of reaction, as the solid beads can easily be filtered from the liquid phase. Hence, we set out to determine how many cycles the immobilised CALB used for this protocol could withstand before losing activity. Therefore, a series of recyclability experiments were performed where sulfide **27a** was dissolved in EtOAc (400 mM) with 20% *w/w* CALB and 1.1 equivalents of UHP and stirred for 24 h. At the end of each reaction, CALB was filtered off and washed with a 9:1 mixture of $CH_3CN$/water (9:1) to remove leftover urea from UHP.[175] CALB, obtained with a recovery yield of 75-96%, was then re-used in a subsequent sulfoxidation reaction of **27a**. The catalytic activity of CALB was maintained through four reaction cycles without significant loss in oxidation activity and specificity

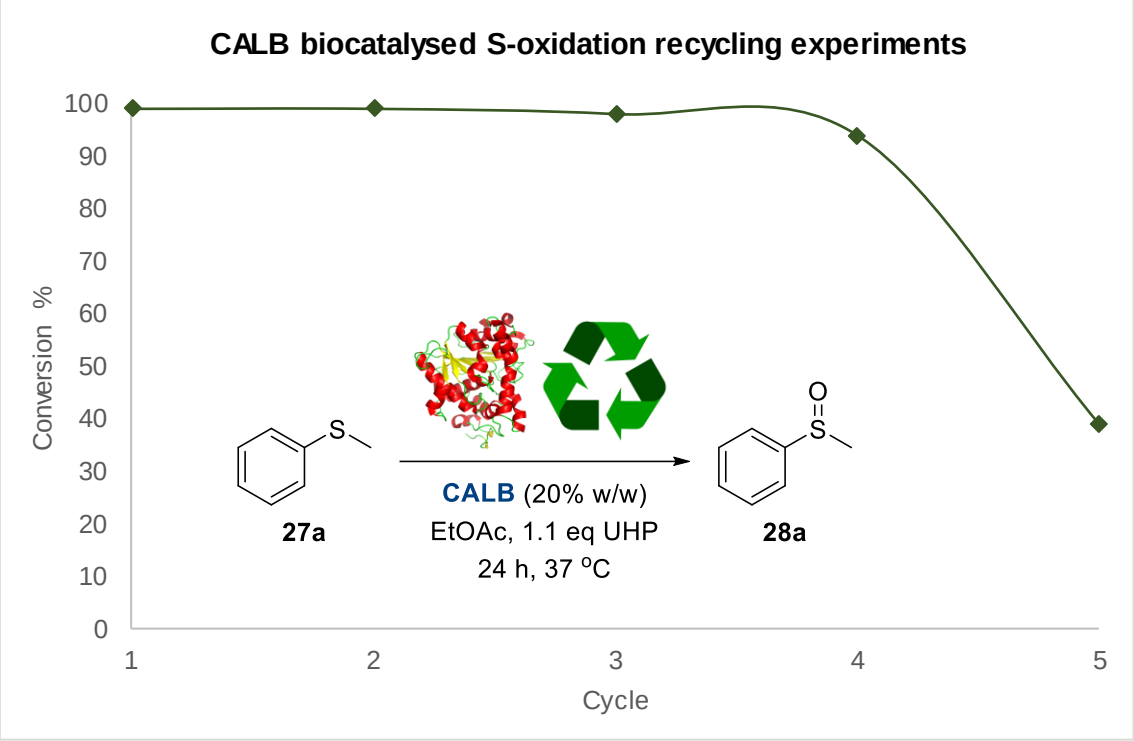


**Figure 2.4.** Recycling experiments of CALB.

(99-94% conversions of **27a**, Figure 2.4) until a drop to 39% of activity was observed in the fifth cycle. The possibility of recycling CALB makes this protocol even cheaper, hence even more appropriate for industrial use.

### 2.3.2 *In situ* production of $H_2O_2$ for the generation of peracids

The CALB sulfoxidation method developed uses a recyclable enzyme, a green solvent and a mild oxidant, all features which make it a green and sustainable protocol. However, the use of UHP presents the main drawback of this method especially when handled at large scale, because even if it is a stable form of $H_2O_2$ it could still result in explosions. Therefore, in our quest to maximise the "grenness" and safety of our S-oxidation, we attempted to remove the need for any stoichiometric peroxide by producing it *in situ*. The main process for industrial production of $H_2O_2$ involves cycles of reduction and oxidation of anthraquinone (AQ) and anthrahydroquinone (AHQ), followed by distillation and concentration to give the desired 30-35% $H_2O_2$ (Scheme 2.18). Notably, the reduction and oxidation cycles must be carried out separately, as the reaction between $H_2$ and $O_2$

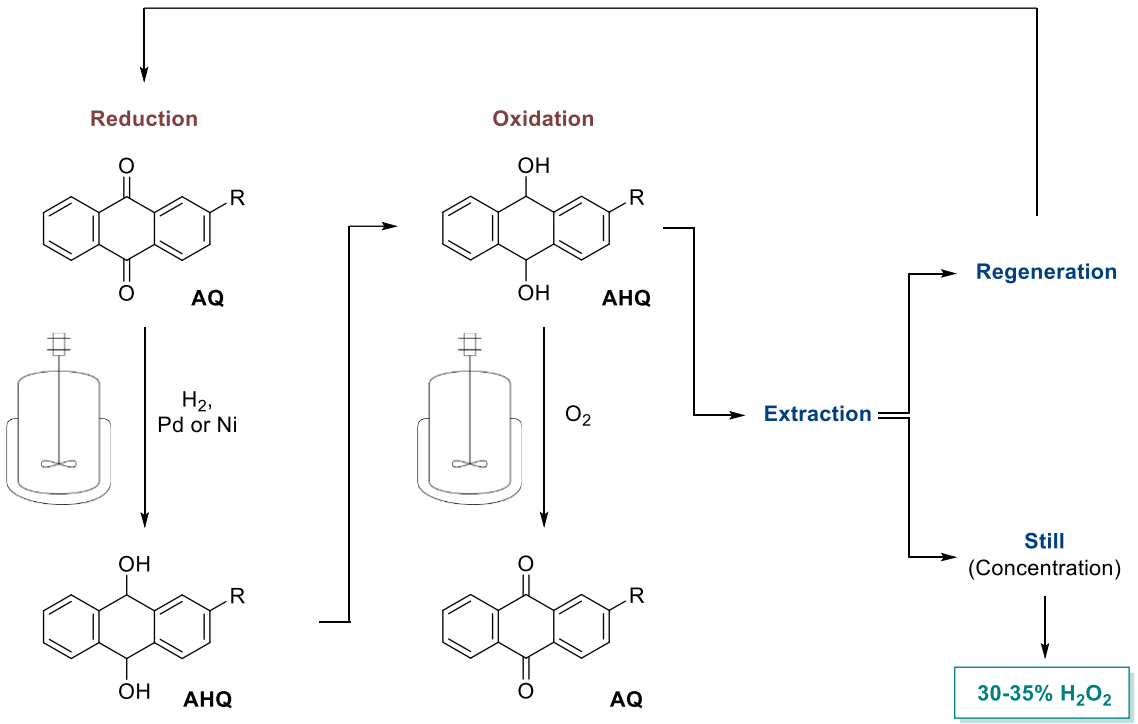


**Scheme 2.18.** Industrial production of $H_2O_2$ from AQ.

would cause explosions, which makes this multistep process energy inefficient and costly. Moreover, AQ oxidation is not an environmentally friendly process because it produces large volumes of wastewater, solid waste and exhaust gas.[194] Therefore, through the years, several more sustainable methodologies have emerged for the production of $H_2O_2$ *in situ*, including electrochemistry,[195–202] direct synthesis[198,203–205] and photocatalysis.[194,206–212] From a green chemistry perspective photocatalysis is the most appealing as it has the advantage to be fully compatible with the use of enzymes and organic solvents, and therefore compatible with CALB.

### *2.3.2.1 Photocatalysed generation of $H_2O_2$*

Photocatalysis is a unique class of chemical transformations where thermodynamically unfavourable reactions are driven to completion using optical energy. Specifically, a photocatalyst is a chemical or material that can absorb light and change the kinetics of any given reaction by establishing new thermodynamically favourable routes.[213] When it comes to alternative ways to produce $H_2O_2$, photocatalytic methodologies boast the second largest number of publications after electrochemical methods. In fact, over the past decade, the production of $H_2O_2$ via photocatalytic routes has grown exponentially, as it only needs Earth-abundant $H_2O$ and $O_2$ as bulk materials and it relies on light as the energy supply. As a result, there is a plethora of publications focused on the use of

light to produce $H_2O_2$, which are elegantly summarised in excellent review papers.[194,198,205,209,210,212]

Like all photochemical transformations, production of $H_2O_2$ has to follow three essential steps: i) absorption of a photon on the photocatalyst; ii) excitation of electrons form low energy states to high energy states and iii) transfer of the electron to the chemical species via charge carriers (Figure 2.5). Then, regardless of the method used, it is generally accepted that the photocatalytic production of $H_2O_2$ can proceed via two generic routes: i) the direct one step, 2 electron reduction (Equation (1)) or ii) the indirect sequential two step, single electron reduction (Equation (2)-(5)). Both routes can be summarised in Equation (6).

$$O_2 + 2\,H^+ + 2\,e^- \rightarrow H_2O_2 \quad (1)$$

$$O_2 + e^- \rightarrow O_2^{\bullet-} \quad (2)$$

$$O_2^{\bullet-} + H^+ \rightarrow HO_2^{\bullet} \quad (3)$$

$$HO_2^{\bullet} + e^- \rightarrow HO_2^- \quad (4)$$

$$HO_2^- + H^+ \rightarrow H_2O_2 \quad (5)$$

$$2\,H_2O + O_2 \xrightarrow{h\nu} 2\,H_2O_2 \quad (6)$$

The most common photocatalyst investigated for the photocatalytic production of $H_2O_2$ is $TiO_2$, as it is highly structurally stable, biocompatible and has interesting physical, optical and electric properties.[214,215]

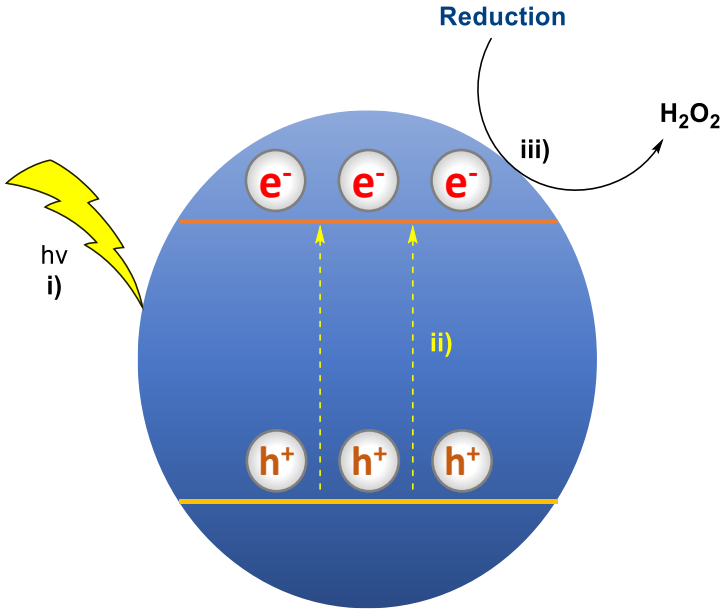


**Figure 2.5.** Three essential steps of photocatalytic transformations: i) absorption of photon; ii) excitation of electrons to high energy states and iii) transfer of electrons to chemical species.

However, pure $TiO_2$ has some heavy drawbacks, such as bad light absorption due to the large band gap between its low and high energy states, which requires high frequency wavelengths such as UV to promote electrons, and it can be easily decomposed. Therefore, modification strategies have been implemented to design better $TiO_2$ based photocatalysts, including surface complexation with anions and cations,[216,217] loading of Nobel metals NPs,[218–220] modifications with quantum dots[221,222] and heterogenization with graphene oxide.[223–225] A novel photocatalyst class that has gained substantial interest in recent years is graphite-like carbon nitrides (g-$C_3N_4$), metal-free polymers analogues of graphite with a similar 2D layered structure that gives them unique electrical, optical, structural, and physiochemical properties.[226,227] Compared to $TiO_2$ based photocatalysts, these have a lower band gap that absorbs in the visible light and have been shown to both oxidise and reduce water,[228–230] making them ideal for $H_2O_2$ production. However, the use of g-$C_3N_4$ is still limited for $H_2O_2$ production because of disadvantages such as low surface area and low efficiency in light absorption.[230] Other photocatalysts include more inorganic-based materials, metal-organic materials, supramolecular coordination complexes, coordination polymers and metal free polymers.[194] Despite presenting valuable alternative solutions to the synthesis of $H_2O_2$, the majority of these protocols use materials that are not commercially available and are often difficult and/or expensive to synthesise. Combined with the low $H_2O_2$ yields, poor response to light and decomposition of the photocatalyst, the use of these photocatalytic protocols is unfeasible in many laboratories.

However, in 2016 Xu *et al.* reported the continuous photocatalytic production of $H_2O_2$ using 2-ethylanthraquinone (EAQ) and full-spectrum light.[206] This was the first cheap and accessible methodology for the synthesis of $H_2O_2$ *in situ*, as EAQ is an economical commercially available by-product of the production of $H_2O_2$ using AQ.[194] In their protocol, Xu *et al.* reported that when under full-spectrum light irradiation and a steady air flow, after 6 h EAQ could produce up to 366 mM $H_2O_2$ in an EtOH monophasic system or 478, 500 and 574 mM in toluene/water, xylene/water and mesitylene/water biphasic systems respectively. Even at the lowest final concentration of $H_2O_2$ in EtOH, this system could provide enough peroxide for the CALB catalysed sulfoxidation. It was envisioned that the best media for the photocatalytic production of $H_2O_2$ would be a mixture of EtOH and EtOAc, because EtOH would behave as a H-donor for the excited state of EAQ, and EtOAc would still react with the immobilised CALB to make the peracid species (Scheme 2.19). Additionally, the two solvents should be compatible with each other as EtOH is a product of EtOAc perhydrolysis.

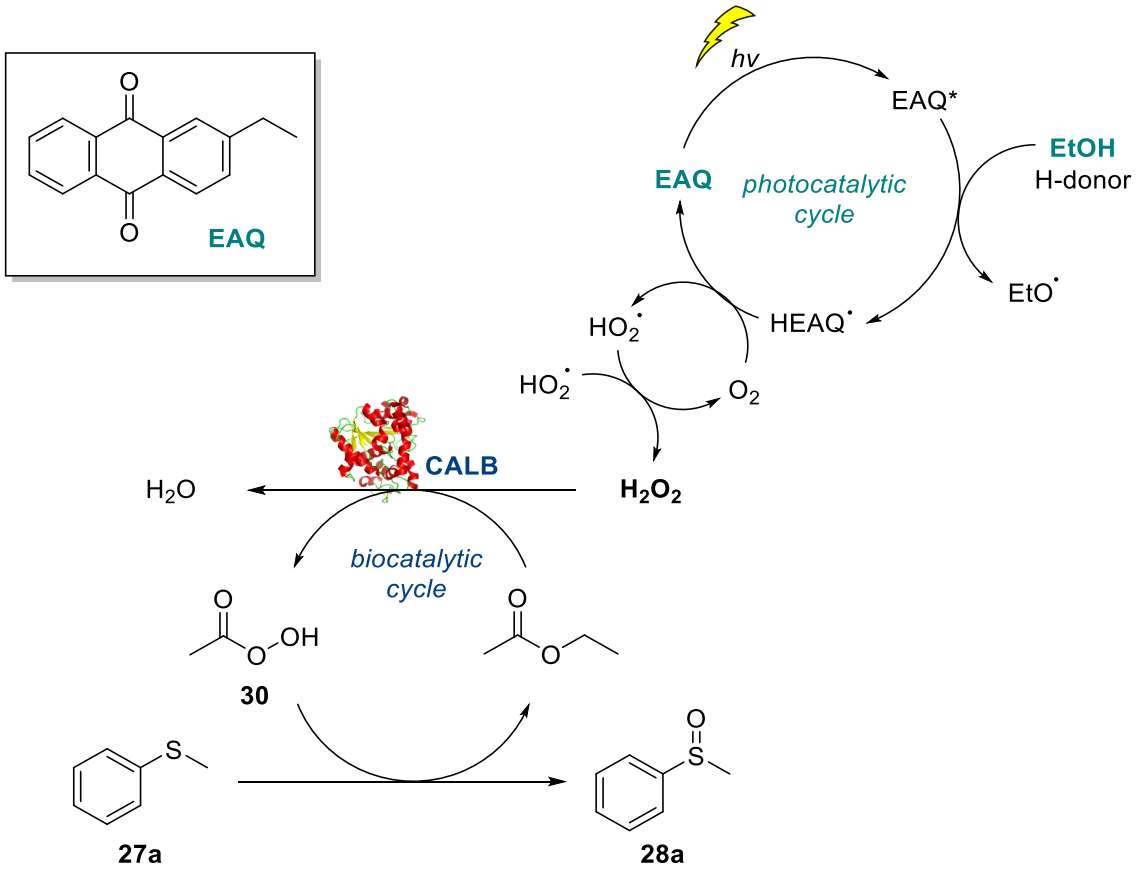


**Scheme 2.19.** Envisioned photo- and biocatalytic synthesis of **28a**.

Therefore, sulfide **27a** was placed in a 95:5 mixture of EtOAc and EtOH at 37 °C with 20% w/w CALB and irradiated under white light (5W) over 24 h (Table 2.4, *Entry 1*). However, only 15% conversion to **28a** was observed by $^1$H NMR and it was also found that increasing the temperature to 50 °C would only approximately double the conversion to 34% (Table 2.4, *Entry 2*). As these results were not satisfactory, different solvent ratios were tried to rule out poor reactivity of the photocatalyst due to the low 5% H-donor alcohol content. Interestingly, while a 1:1 ratio of EtOH and EtOAc did not show any improvement (Table 2.4, *Entry 3*), carrying out the reaction in 100% EtOH and catalytic amounts of EtOAc afforded **28a** in 72 and 85% conversion after 4 and 24 h respectively (Table 2.4, *Entries 4,5*). However, it was soon realised that, when in EtOH, the sulfoxidation of **27a** would proceed spontaneously, probably due to the reaction of free radicals formed in the photocatalytic process with $O_2$, as **28a** was obtained almost quantitatively in the absence of CALB (Table 2.4, *Entry 6*). A weeklong experiment was carried out to assess the photocatalytic S-oxidative activity of EAQ alone in the 95:5 mixture of EtOAc and EtOH (Table 2.4, *Entry 7*). The rationale behind this experiment

**Table 2.4.** First screening of conditions for the photo- and biocatalysed sulfoxidation of **27a**.

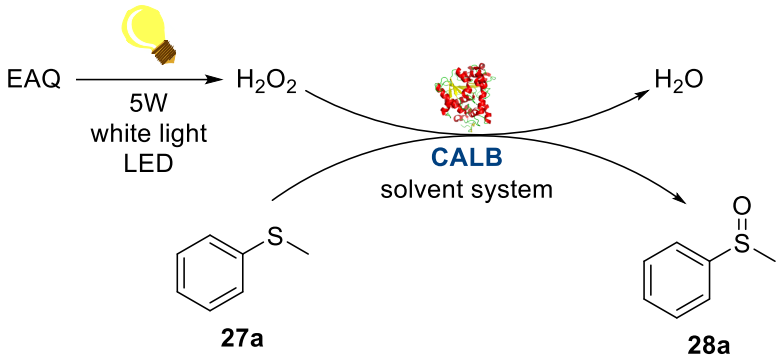


| Entry | CALB (% w/w) | Solvent system | T (°C) | Time (h) | Conv. (%)[a] |
|---|---|---|---|---|---|
| *1* | 20 | EtOAc/EtOH 95:5 | 37 | 24 | 15 |
| *2* | 20 | EtOAc/EtOH 95:5 | 50 | 24 | 34 |
| *3* | 20 | EtOAc/EtOH 1:1 | 37 | 24 | 16 |
| *4* | 20 | EtOH (cat. EtOAc) | 37 | 4 | 72 |
| *5* | 20 | EtOH (cat. EtOAc) | 37 | 24 | 85 |
| ***6*** | **0** | **EtOH** | **37** | **24** | **98** |
| *7* | 0 | EtOAc/EtOH 95:5 | 37 | 1 week | 97 |

[a]Determined by $^1$H-NMR of the crude mixture.

was to understand whether CALB could at least facilitate the oxidation of **27a** over a long period of time when in less favourable reaction media. However, after a week the conversion of **27a** to **28a** was 97%, indicating that the system does not need CALB and the peracid formation to oxidise sulfides.

The results for the sulfide oxidation obtained in the monophasic EtOH system clearly indicate that CALB is not required for the formation of the sulfoxide. Therefore, the oxidation was attempted in a biphasic toluene/water system, as it was foreseen that the reactive radical species would be more soluble in the aqueous phase while the sulfide **27a** would prefer the apolar toluene layer, hence limiting the surface area of reaction and promoting the CALB catalysed perhydrolysis over the photocatalytic oxidation. It was also predicted that no addition of acid or ester CALB substrate was needed because in the paper the authors described a possible oxidative pathway of toluene leading to benzoic acid **44**. In fact, toluene, and the other organic solvents xylene and mesitylene, behaves as the H-donor for the photocatalytic cycle of EAQ, but compared to EtOH, it then undergoes a series of oxidative transformations with the excited EAQ* until the fully oxidised product, benzoic acid **44**, is obtained (Equations 7-9). The formation of **44** was confirmed by isolation of pure product after EAQ was irradiated under white light (5W) for 24 h in a mixture of toluene/water 4:1.

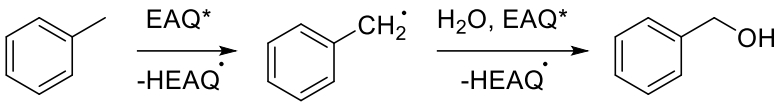


(7)

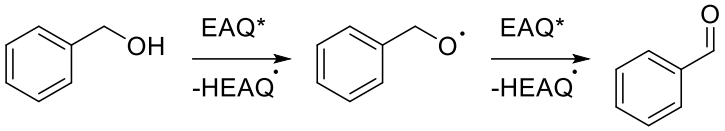


(8)

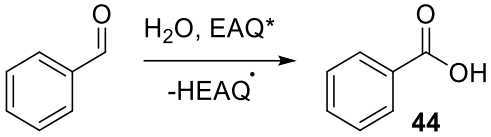


(9)

Next, a reaction with **27a**, CALB, stoichiometric $H_2O_2$ and benzoic acid **44** in toluene/water 4:1 was carried out to verify that the CALB catalysed sulfoxidation could occur under these conditions, and after 24 h 85% conversion to **28a** was calculated by $^1$H NMR (Scheme 2.20). With this data in hand, **27a** was placed in a 4:1 toluene/water biphasic system with EAQ and CALB and it was irradiated under white light (5W). After 24 h, a 29% conversion to **28a** was observed by NMR (Table 2.5, *Entry 1*), which was improved to 92% after irradiating for 48 h instead (Table 2.5, *Entry 2*). In order to prove that this sulfoxidation was indeed photobiocatalysed, a control reaction was carried out in DCM/water 4:1, since DCM is not a proton donor and therefore no reaction should take place. Unfortunately, the conversion to **28a** reached 50% after only 24 h (Table 2.5, *Entry 3*) and upon removal of CALB it even increased to 70% after 24 h (Table 2.5, *Entry 4*), indicating that somehow CALB might be inhibiting the photocatalytic sulfoxidation.

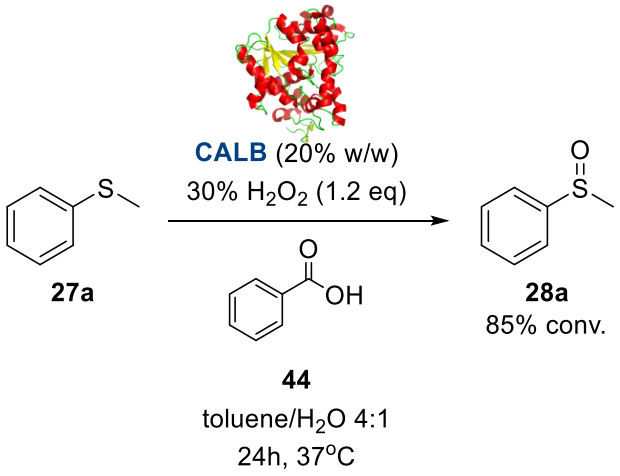


**Scheme 2.20.** CALB biocatalysed oxidation of **27a** in toluene/water 4:1 and benzoic acid **44**.

**Table 2.5.** Second screening of conditions for the photo- and biocatalysed sulfoxidation of **27a**.

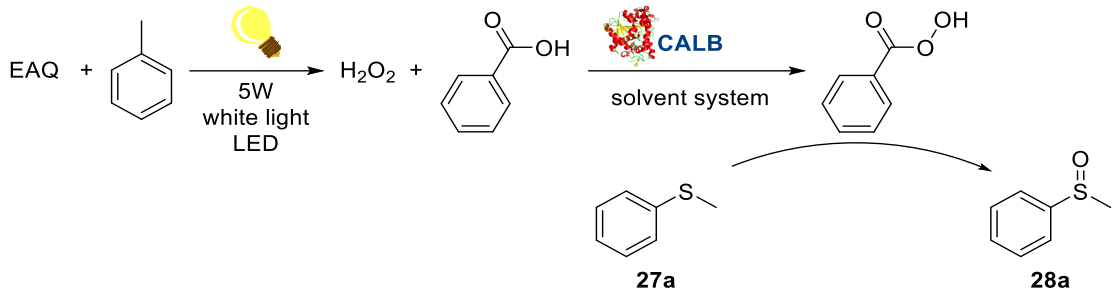


| Entry | CALB (% w/w) | Solvent system | T (°C) | Time (h) | Conv. (%)[a] |
|---|---|---|---|---|---|
| *1* | 20 | Toluene/$H_2O$ 4:1 | 37 | 24 | 29 |
| *2* | 20 | Toluene/$H_2O$ 4:1 | 37 | 48 | 92 |
| *3* | 20 | DCM/$H_2O$ 4:1 | 37 | 24 | 50 |
| *4* | 0 | DCM/$H_2O$ 4:1 | 37 | 24 | 70 |

[a]Determined by $^1$H-NMR of the crude mixture.

The control reactions clearly highlighted that the sulfoxidation is achieved exclusively via photocatalytic means and, as $H_2O_2$ alone isn't strong enough to oxidise **27a**, that the mechanism of oxidation probably proceeds through the activation of $O_2$ into a reactive oxygen species that attacks the sulfide to form the sulfoxide. Photocatalytic sulfoxidation is a well-documented process and by combining photocatalytic cycles reported by other groups[231–233] with the EAQ one proposed by Xu *et al.*,[206] in Scheme 2.21 it was possible to hypothesise how the S-sulfoxidation may be catalysed by light. Despite the promising results from the photocatalytic S-oxidation using only EAQ, which still hasn't been considered for this oxidative process, it was decided to not pursue this part of the project further as our focus was on industrially applicable methodologies and CALB with stoichiometric UHP still offered the more appropriate approach. In fact, at large scale production, it is difficult to provide uniform irradiation of light to large batch reactions and relatively expensive specialist equipment would be required. This would have also been true if the initial prediction for the bio- photocatalytic cycle had worked, but the production of $H_2O_2$ *in situ* and hence avoiding handling peroxides would have outweighed the extra costs and efforts of ensuring even light irradiation. Therefore, the use of EAQ for sulfoxidations was halted and the focus shifted back to the original CALB biocatalysed method.

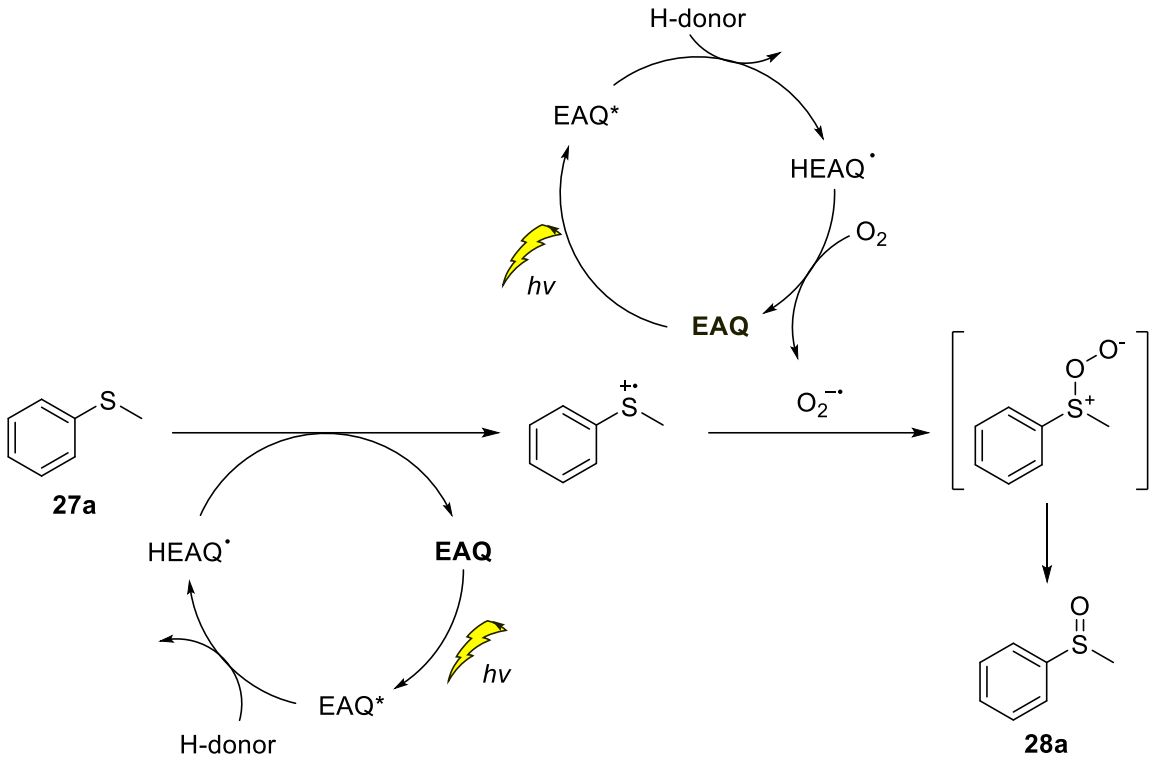


**Scheme 2.21.** Proposed S-oxidation mechanism for the photocatalytic oxidation of **27a**.

### 2.3.3 Development of a methodology to obtain chiral sulfoxides

The CALB catalysed oxidation of sulfides has proved to be efficient at both academic and industrial scale to afford racemic sulfoxides in high yields. The lack of chirality of the method is derived by the fact that CALB is not active on the sulfide, but on EtOAc, which is achiral and will exclusively lead to racemic sulfoxides. Therefore, we decided to investigate whether a method to obtain enantiopure sulfoxides could be achieved whilst maintaining the high efficiency, selectivity, and industrial applicability of the biocatalytic CALB method.

#### *2.3.3.1 Stereoselective oxidation via the use of chiral acids*

Chirality induces chirality. Based on this statement and on a report by Drozdz and Chrobok, where a stereoselective CALB catalysed Baeyer-Villiger oxidation of 4-methylcyclohexanone was achieved using (*R*)-4-methyloctanoic acid to afford (*R*)-4-methylcaprolactone in 97% yield and 96% ee after 8 days (Scheme 2.22),[179] the natural progression for the development of a chiral CALB biocatalysed sulfoxidation was to look

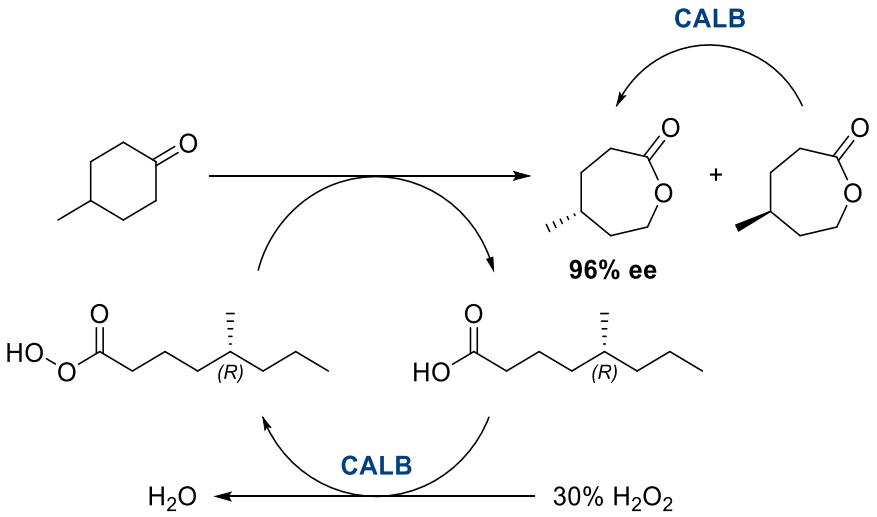


**Scheme 2.22.** Reaction of the asymmetric chemo-enzymatic Baeyer-Villiger oxidation of 4-methylcyclohexanone.[179]

for commercially available chiral acids or esters which could be transformed to chiral peracids by CALB. Therefore, commercially available chiral acids **45-53** were selected for the stereoselective oxidation of **27a**. Results are reported in Table 2.6. The general pattern observed was that the bulkier the acid was around the carboxylic acid moiety, the less efficient the S-oxidation was, which is in line with what was reported by Drozdz and Chrobok.[179] Initially, the stereoselective sulfoxidation was attempted with a series of amino acids **45-37**. It was found that when proline **45** was used as the unprotected version, a poor 39% conversion to **28a** was obtained in 24 h (Table 2.6, *Entry 1*). Instead, upon protecting the free amine, the conversion to **28a** increased to 70% with **46** in 24 h (Table 2.6, *Entry 2*) and a 15% conversion was also observed after 2.5 h when **47** was used (Table 2.6, *Entry 3*). Although 15% conversion can be classified as low, it was achieved after only 2.5 h indicating that there was an increase of reaction rate compared to *Entry 1*. A further increase was obtained moving from the cyclic prolines **45-36** to the linear Fmoc-valine **47**, which yielded **28a** in 83% conversion. A series of non-amino acid carboxylic acids was also studied (Table 2.6, *Entries 4-9*). The most promising oxidations of **27a** were achieved using acids **50**, **51** and **53** that afforded **28a** in 99, 94 and 81% conversion respectively. These acids are in fact the smallest and less hindered of the series, which probably facilitated the perhydrolysis process by CALB. Larger acids **49** and **52** instead led to **28a** in 9 and 11% conversion respectively. Unfortunately, no enantioselective oxidation was obtained with any of the acids, as negligible ees were observed by chiral HPLC.

**Table 2.6.** Screening of commercially available acids for the asymmetric synthesis of **28a**.

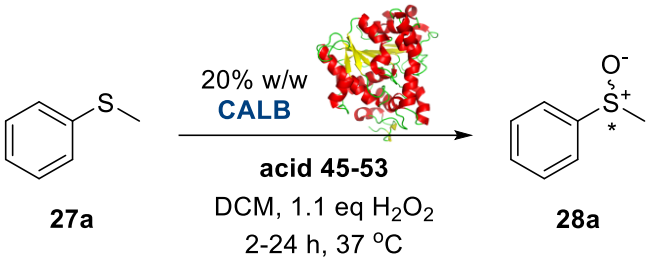


**27a** **28a**

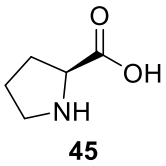

**45**

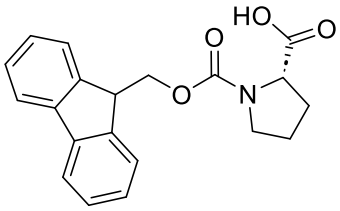

**46**

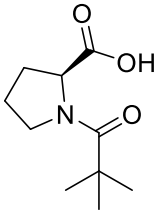

**47**

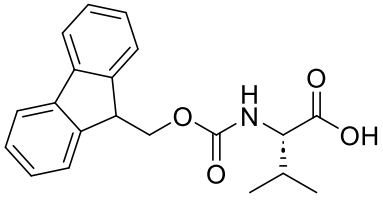

**48**

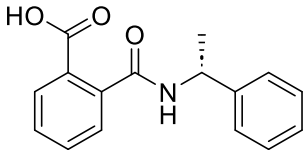

**49**

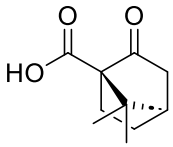

**50**

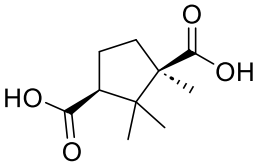

**51**

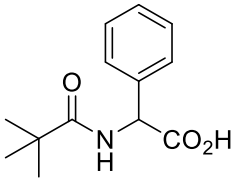

**52**

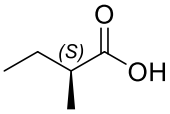

**53**

| Entry | Acid | Time (h) | Conv. (%)[a] | ee (%)[b] |
|---|---|---|---|---|
| 1 | Proline **45** | 24 | 39 | 2 |
| 2 | Fmoc-Pro **46** | 24 | 70 | 2 |
| 3 | **47**[d] | 2.5 | 15 | <1 |
| 4 | Fmoc-Val **48** | 24 | 83 | 2 |
| 5 | **49** | 2 | 9 | <1 |
| 6 | **50** | 24 | 99 | <1 |
| 7 | **51** | 24 | 94 | <1 |
| 8 | **52**[d] | 2.5 | 11 | 1 |
| 9 | **53**[c] | 24 | 81 | 1 |

[a]Determined by $^1$H-NMR of the crude mixture; [b]Determined by chiral HPLC using an IG/IC Chiracel column; [c]Reaction was carried out in toluene; [d]Derived from the commercially available amino acid after treatment with pivaloyl chloride (see Experimental 6.2.9 for details).

The complete absence of enantioselectivity was initially attributed to the sulfide **27a** being too small and lacking handles for the acids to interact with. Therefore, the focus

shifted towards sulfides containing other functional groups, such as sulfides **38** from the substrate scope of the racemic oxidation of CALB. Particularly, it was predicted that sulfide **38a** would interact strongly with proline **45** forming a stable enamine intermediate **43**, which would then form the peracid after reacting with CALB and UHP. As the geometrical arrangement of the peracid and sulfide would now be fixed, **(*S*)-39a** should be obtained (Scheme 2.23, Part A). However, when **38a** was reacted with **45**, CALB, UHP in THF and water, only a disappointing 21% conversion and negligible ee were obtained (Scheme 2.23, Part B).

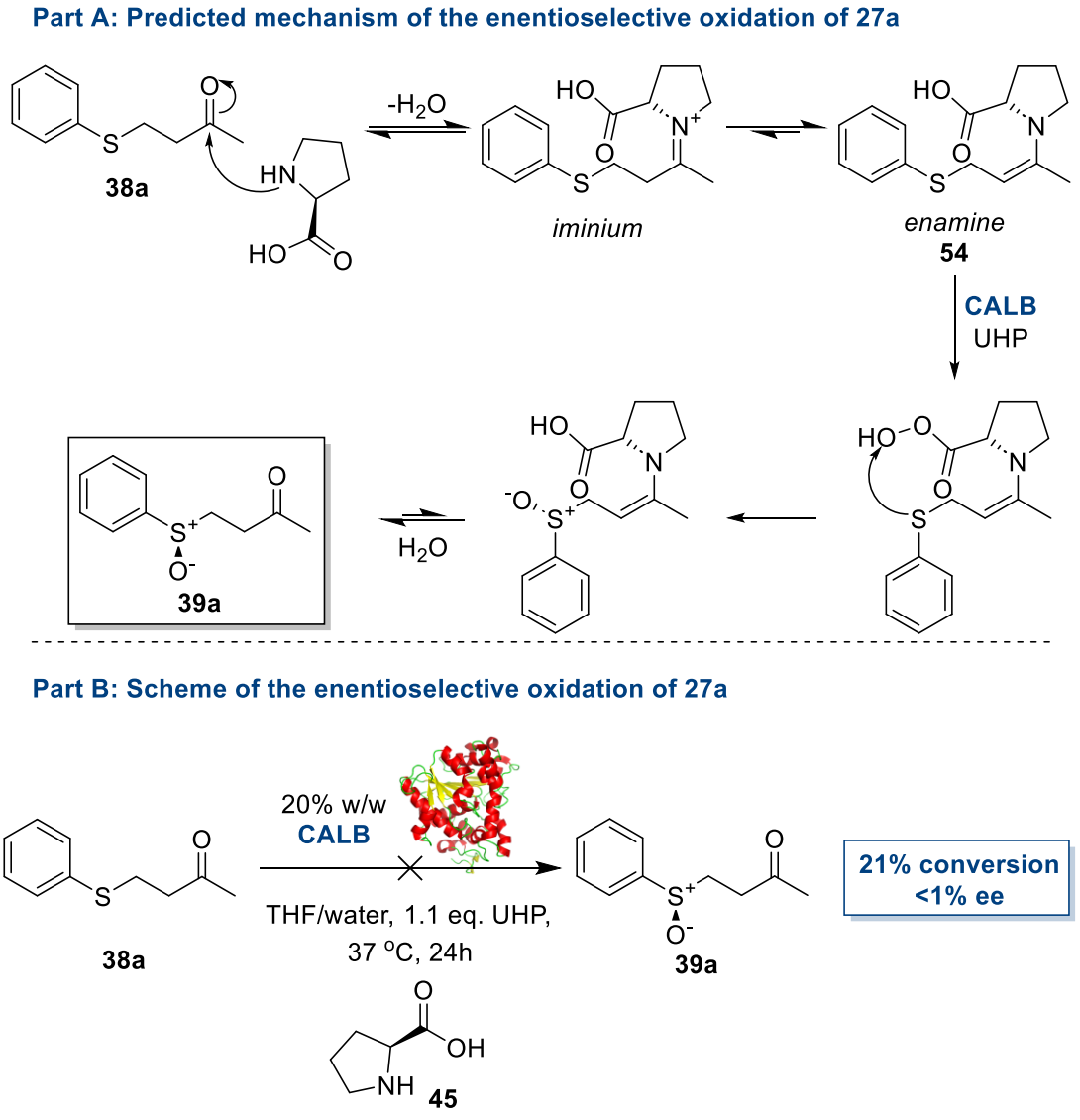


**Scheme 2.23.** Asymmetric synthesis of **39a**. Part A) Predicted mechanism. Part B) Scheme of reaction.

## 2.4 Final considerations and conclusions

In this project, a mild, green, and scalable methodology for the synthesis of sulfoxides was developed using immobilised CALB and UHP in EtOAc. With this method, a total of 17 alkyl-aryl sulfoxides, 6 carbonyl- and 2 hydroxyl- containing sulfoxides and omeprazole were obtained in excellent conversions and yields with little-to-no sulfone overoxidation by-products. Furthermore, this method is highly chemoselective as no epoxidation or Baeyer-Villiger side reaction products were observed. Among the benefits that this protocol offers, its industrial applicability is what elevates this methodology above other reports in the literature. For instance, the use of EtOAc with the dual role of green solvent and substrate for CALB greatly increases the sustainability and safety of the methodology. In fact, EtOAc has a low environmental impact and toxicity, is cheap, readily available, and easy to purify by distillation after completion of reaction, which make it one of the best solvents for use at industrial scale production.[185,234] Additionally, EtOAc is converted by CALB into peracetic acid, the oxidative species, which means no acid or ester additives were required to promote the oxidation of the sulfide. This allowed the overall reduction of end-of-life waste and contributed to a better atom economy. The EtOAc decomposition products, EtOH and acetic acid, are also considered non-toxic and, once separated by distillation, can potentially be recycled for other processes as solvents or reagents. The use of immobilised CALB also increases the appeal of the method for industrial use. In fact, the commercially available CALB used in this protocol is a biocatalyst that can easily be recycled up to four times just by filtration without any significant loss in activity, which reduces the costs of production and improves its sustainability. Moreover, despite commercial CALB being already affordable, in order to further reduce the expenses at industrial level, the immobilisation of the enzyme can easily be done in-house, as the structural features of CALB allow for an easy and well documented immobilisation strategy onto acrylic resins. Lastly, the more stable, easy to handle and ultimately safer UHP is used in place of aqueous $H_2O_2$. The end product urea and $H_2O$ can easily be separated from the final reaction mix during the workup phase and recovery of sulfoxide and are themselves innocuous.

Efforts to further improve the sustainability and scope of the reaction were made. Firstly, with the intention to avoid the use of stoichiometric amounts of peroxide, the production of $H_2O_2$ *in situ* was attempted via photocatalytic methods, using EAQ. Reported by Xu *et al.*,[206] it was found that EAQ could produce $H_2O_2$ under full spectrum irradiation. EAQ itself was regarded an ideal photocatalyst as it is an end-of-production waste derivative of AQ in the industrial production of $H_2O_2$, which makes it cheap and readily available in

tonne scales. Also, its use allows recycling of waste chemical that otherwise would contribute to waste. EAQ was therefore applied to produce $H_2O_2$ in the CALB catalysed synthesis of sulfoxides. Whether in a EtOH monophasic system or a toluene-water biphasic system, unfortunately EAQ always gave the same results: negligible $H_2O_2$ formation and direct photocatalytic oxidation of sulfides by activation of molecular oxygen. After assessing the parameters of this photocatalysed sulfoxidation, it was decided that despite the promising results, this transformation would find fewer industrial applications compared to CALB and therefore the focus shifted back to the original methodology.

Secondly, given the effectiveness of the protocol to produce sulfoxides in high conversions and yields, the use of chiral acid additives for the enantioselective oxidation of sulfides was attempted to expand the scope of the reaction. Therefore, based on a report by Drozdz and Chrobok,[179] who described the enantioselective synthesis of lactones starting from the chiral (*R*)-4-methyloctanoic acid, a series of commercially available chiral acids were employed in S-oxidations. Unfortunately, regardless of the nature of both the acid and sulfide, no enantioselectivity or enantioenrichment were observed despite achieving good conversions. This was probably due to lose interactions between the oxidant and substrate that resulted in racemic oxidations.

# Chapter 3. Stereoselective oxidation of functionalised sulfides using flavoprotein monooxygenases

## 3.1 Introduction

Despite the remarkable success and applicability of the CALB catalysed sulfoxidation protocol, all attempts at developing an enantioselective strategy were unsuccessful. Therefore, our attention turned to a different and more traditional approach, which entailed the use of oxidative enzymes capable of interacting directly with prochiral sulfide substrates. Historically, enzymes such as peroxygenases[235–239] and monooxygenases[240–243] have been used for the synthesis of enantiopure sulfoxides because of their ability to catalyse the addition of one oxygen atom to their substrates. One of the main differences between these two classes of enzymes, which also determines the mode of action, is the source of atomic oxygen, since peroxygenases take advantage of $H_2O_2$ produced by metabolic pathways and reactive oxygen species (ROS) in cells, while monooxygenases rely on a supply of molecular oxygen to carry out oxidative transformations (Figure 3.1). While both classes of enzymes were proven valuable tools for the biocatalytic oxidation of various substrates, peroxygenases require stoichiometric amounts of $H_2O_2$, which as explained in the previous chapter, can be disadvantageous when large scale syntheses are performed. Additionally, not all peroxygenases are stable at high levels of $H_2O_2$, as it can lead to their deactivation, and therefore labour-intensive stepwise additions[236] or the development of a parallel biocatalytic production of $H_2O_2$ *in situ*[244] are necessary for efficient oxidative processes.

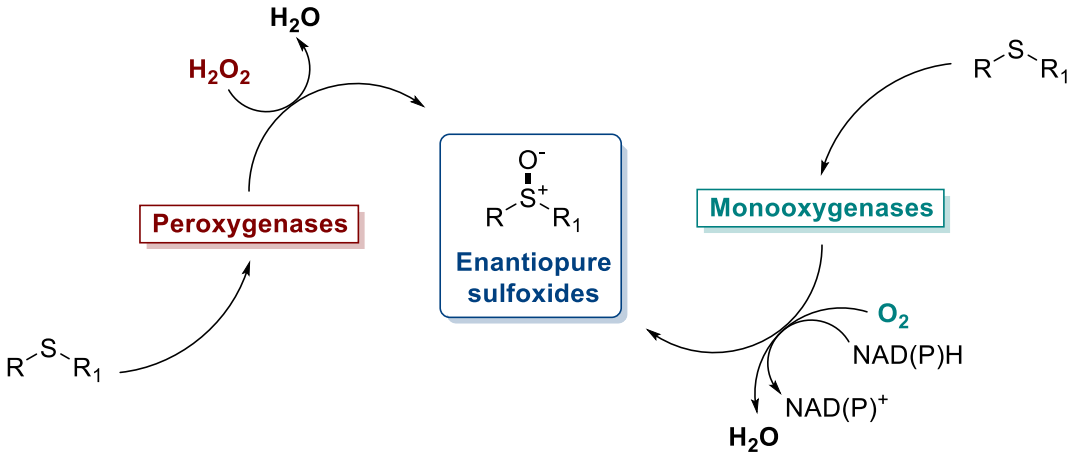


**Figure 3.1.** Differences in the mechanism of oxidation between monooxygenases and peroxygenases.

Meanwhile, monooxygenases have shown to be active in the presence of just atmospheric oxygen,[245] making them a more appealing class of enzymes to study. Therefore, in this project, two subclasses of flavoprotein monooxygenases (FPMO), namely the Baeyer-Villiger (BVMO) and flavine-containing monooxygenases (FMO), were investigated for the synthesis of enantiopure sulfoxides.

### 3.1.1 Classification, structural features, and mechanism of flavoprotein monooxygenases

As already mentioned, BVMOs and FMOs are oxidative enzymes that belong to a broader class of enzymes called flavoprotein monooxygenases (FPMO). To date, there are eight subclasses of FPMOs (Groups A to H), which are differentiated by both structural and functional features.[245–248] For instance, enzymes in Groups A and B rely on the tightly bound flavin adenosine dinucleotide (FAD) prosthetic group and nicotinamide adenine (phosphorylated) dinucleotide (NAD(P)H) as electron donor for their oxidative activity.[245,247] FPMOs in Groups A and B are also single-component enzymes, meaning that they are capable of regenerating the active site without the need for external recycling systems. Instead, enzymes in Groups C to F are coupled with a flavin reductase system which facilitates the electron transfer from NAD(P)H to the oxidised form of the flavin prosthetic group.[245,247] For this reason, these FPMOs are called two component systems. Up until recently, Groups A to F made up the entirety of FPMOs. However, as more enzymes were discovered, two new classes were added to the classification of these enzymes, namely Groups G and H, which comprise the so-called 'internal' FPMOs, biocatalysts that, just like those in Groups A and B, are single component systems but are also self-sufficient and do not need an external electron donor.[247] Together, Groups A to H contain a plethora of FPMOs that can perform different oxidative reactions, which are found in a brief summary in Figure 3.2. The vast majority of BVMOs and FMOs can be classified as Group B FPMOs.[245–248] These enzymes, even in cases of low degree of sequence similarity, share common structural features such as a Rossmann-like three-layer ββα sandwich domain for FAD binding, and a further ββα sandwich binding domain for NAD(P)H.[245,247] Within Group B FPMOs there are other subclasses, including Group B1 and Group B2, where BVMOs and FMOs are found, respectively. The BVMOs found in Group B1 are classified as Type I BVMOs and can perform Baeyer-Villiger oxidations on a wide scope of ketones and aldehydes as well as oxidations on heteroatoms. There is another class of BVMOs, Type II, which also catalyse Baeyer-Villiger oxidations, but these are two-component enzymes belonging to Group C and are not discussed here.[245]

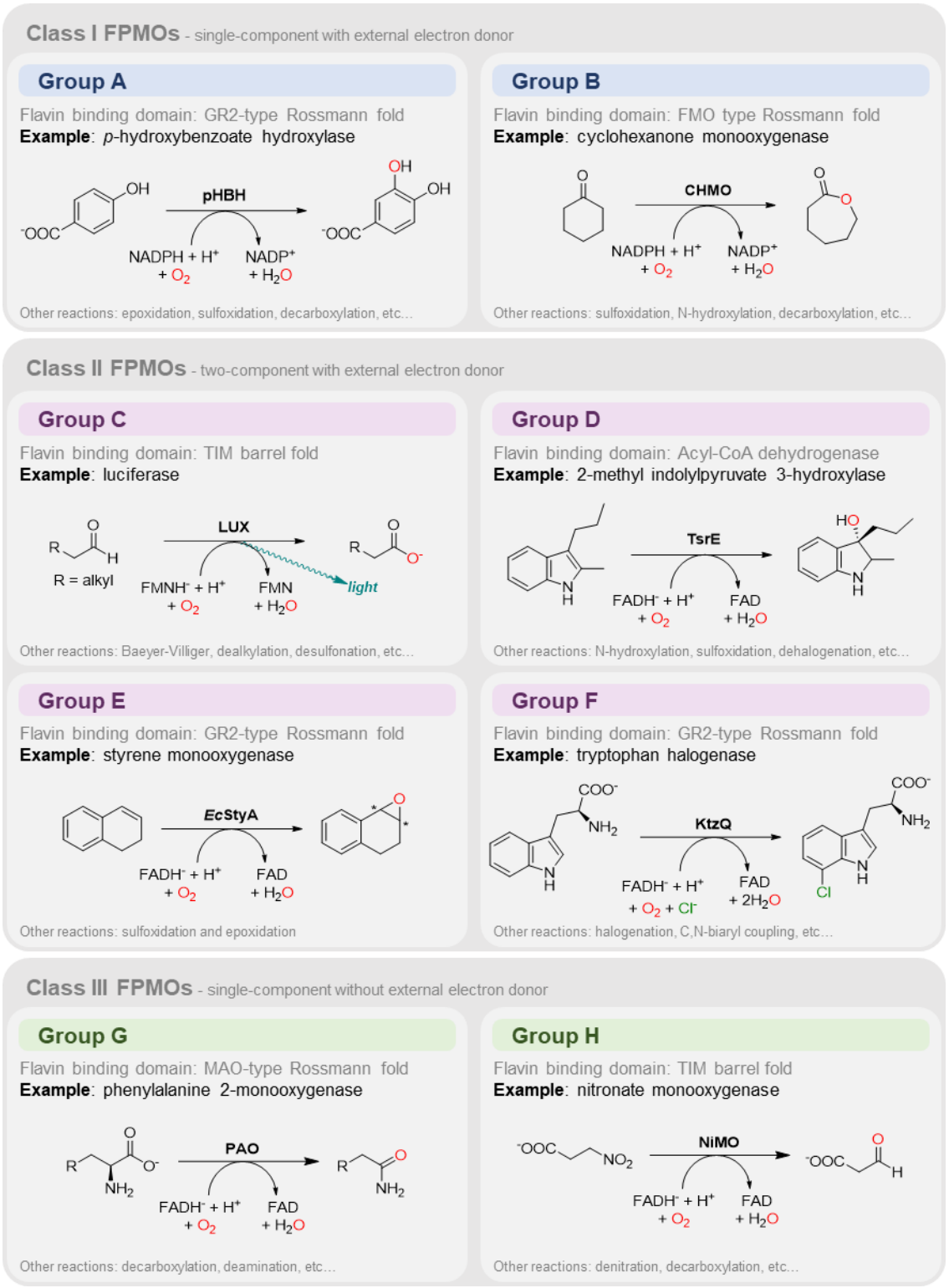


**Figure 3.2.** Summary of the different groups of FPMOs (A-H).

The first BVMO activity was observed in 1948 by Turfitt,[249] who described the oxidative degradation of steroids and cholesterol by *Actinomyces* (formerly known as *Proactinomyces*) bacteria from soil. However, it was only later in 1971 that Norris *et al.*

identified a NADPH and molecular oxygen-dependent enzyme capable of catalysing Baeyer-Villiger oxidations of cyclohexanone to ε-caprolactone in *Nocardia globerula* CL1.[250] The enzyme was subsequently isolated from *Acinetobacter calcoaceticus* and characterised as cyclohexanone monooxygenase (*Ac*CHMO).[251] Since then, several eukaryotic and prokaryotic BVMOs have been found and these play essential roles in the metabolism of toxins, steroids, hydrocarbons and terpenes to name a few.[246] Instead, the FMOs found in group B2 can be further classified as type I FMOs and type II FMOs, which can both carry out Baeyer-Villiger transformations and heteroatom oxidations. Even though FMOs are found in all kingdoms of life, plant FMOs, such as YUCCA enzymes, have attracted significant interest in the last two decades due to their large diversity and unexplored physiological function.[245,252] The first FMO was described in 1972 by Ziegler and Mitchell,[253] who reported the *N*-oxidation of lipophilic *sec*- and *tert*-amines to the corresponding hydroxylamines and amine oxides using a FMO extracted from pig liver.

Since their discoveries, these Group B FPMO enzymes have attracted a lot of attention in the scientific community because they provide safer, chemo- and stereoselective, and overall, more sustainable alternatives to the traditional methods for Baeyer-Villiger transformations, notoriously dangerous due to the explosive nature of peracids, and S- and *N*-heteroatom oxidations.[245,246] Therefore, due to the ever-increasing interest, modern techniques such as gene mining[254] and gene evolution allowed the discovery and design of several new BVMOs and FMOs. Interestingly, a 30-year gap separates the discoveries of the first BVMO and FMO enzyme from the full resolution of their crystal structures. In fact, in 2004 Malito *et al.* reported the first crystal structure of a BVMO from the thermophilic bacterium *Thermobifida fusca*,[255] while the first FMO crystal structure was reported in 2006 by Eswaramoorthy *et al.*,[256] who analysed the mechanism and structure of a FMO extracted from the fungus *Schizosaccharomyces pombe.* Following these initial breakthroughs, several other groups[257] also reported crystal structures of new BVMOs and FMOs, which together with mechanistic studies allowed the determination of the mechanism of action[245,247,258–262] of these biocatalysts. The biocatalytic cycle of Group B FPMOs starts when NADPH binds to its binding domain in the active site (Scheme 3.1, **a**). This then triggers a two-electron reduction of the FAD prosthetic group ($FADH^-$) that reacts with molecular oxygen through a radical mechanism pathway to form a peroxyflavin oxidative species ($FAD_{OO(H)}$) (Scheme 3.1, **b**).

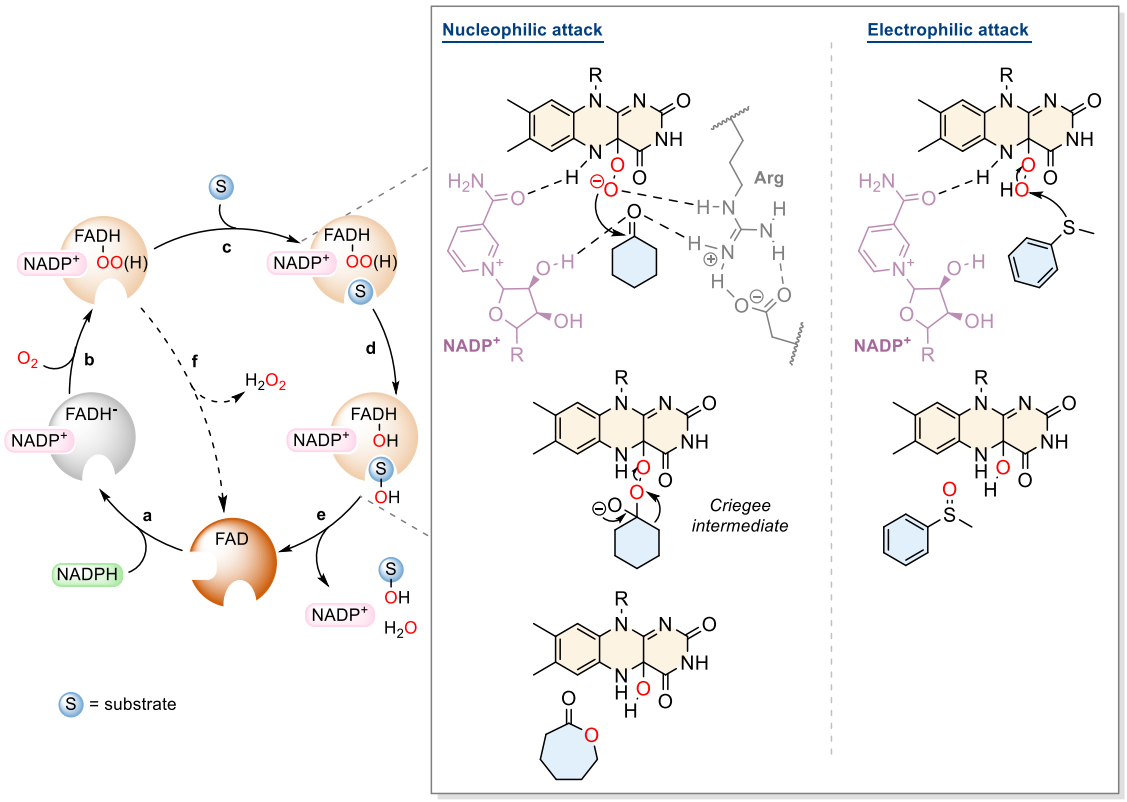


**Scheme 3.1.** Proposed mechanism of action of Group B FPMOs using flavin and NAD(P)H cofactors.

To date there are three accepted forms of peroxyflavin species that have all been observed through UV-vis spectroscopy studies, thanks to their unique absorption profiles, and crystallography studies (Scheme 3.2).[245,259] For a long time, $FAD_{C4aOO(H)}$ was believed to be the only form of oxygenating $FAD_{OO(H)}$ species and has been extensively studied as a result. Depending on the environmental conditions, this species can be found in both its protonated and deprotonated form (Scheme 3.2), which affects the reactivity of the enzyme. While $FAD_{C4aOO(H)}$ still remains the most common oxidating $FAD_{OO(H)}$ species for oxidative transformations, recently researchers have also identified two forms, namely the $FAD_{N5OO}$ and $FAD_{N5O}$ (Scheme 3.2), which suggest that FPMOs may have a broader applicability to diverse substrates and mechanistic complexity than anticipated.[259] Due to the large volume of publications on the biocatalytic mechanism based on $FAD_{C4aOO(H)}$, this species will be used to describe the full catalytic cycle of Group B FPMOs.

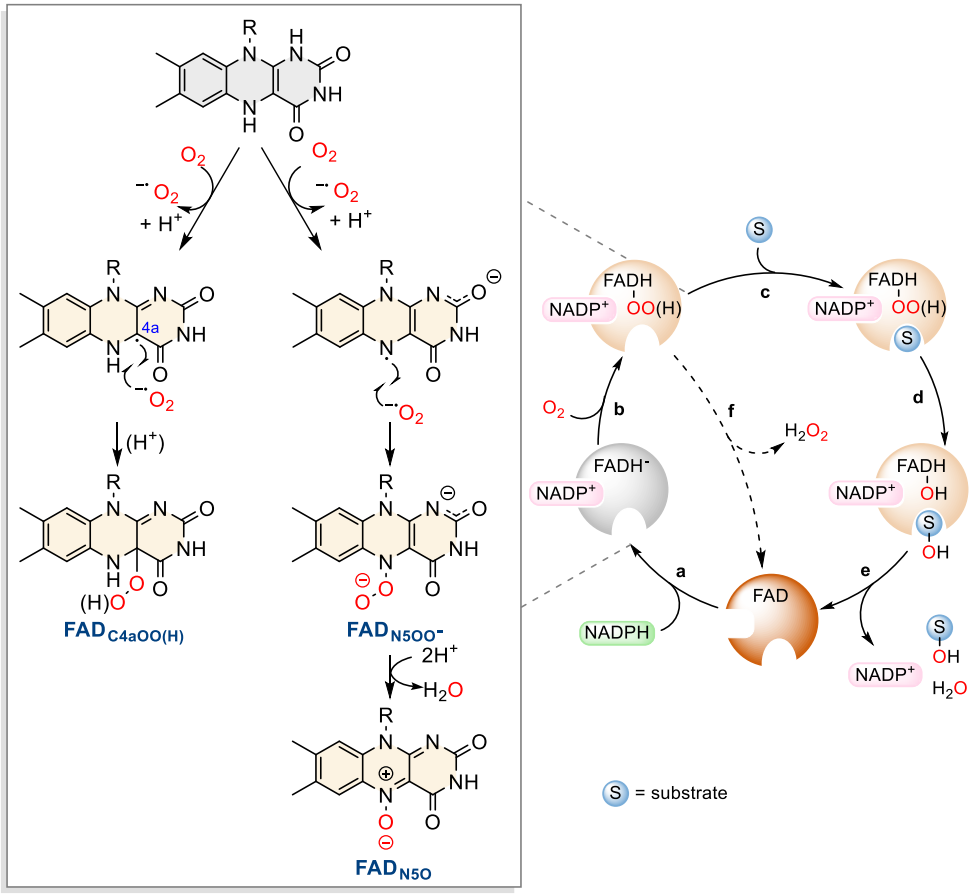


**Scheme 3.2.** Formation of the three peroxyflavin species in FPMOs.

While free peroxyflavins are highly unstable in solution, enzyme bound $FAD_{OO(H)}$ is stabilised through interactions in the active site of FPMOs. Unfortunately, the exact factors that influence the mechanism of stabilisation of peroxyflavin are not well known, as the lifetime of this species can vary from milliseconds in some FPMOs to several hours in FMOs.[245] Some *in silico* and crystallography studies seem to suggest that the amide oxygen of the oxidised $NADP^+$ may form a hydrogen bond with the flavin's N5.[263] This is further supported by a study in which omission of the nicotinamide cofactor in certain BVMO and Group B enzymes sped up the decay process of $FAD_{OO(H)}$.[264] Finally, an arginine in the active site forms another key interaction for the stabilisation of $FAD_{OO(H)}$ in its deprotonated form ($FAD_{OO}$) (Scheme 3.1). After $FAD_{OO(H)}$ is stabilised, if a suitable substrate, such as a ketone or sulfide, is present, the next step in the biocatalytic cycle is either a nucleophilic or electrophilic attack on the substrate depending on the protonation state of the peroxyflavin (Scheme 3.1, **d**). In fact, if protonated, $FAD_{OOH}$ will perform an electrophilic attack on soft nucleophiles such as sulfur, amines, or C-C double bonds; whilst, if deprotonated, $FAD_{OO}$ will react with electrophilic substrates, such as

ketones and aldehydes, to perform Baeyer-Villiger oxidations (very common in BVMOs). Just as for the traditional synthesis, formation of an ester or acid during a biocatalysed Baeyer-Villiger oxidation occurs via a Criegee intermediate (Scheme 3.1, **d**).[247,259] In the absence of a substrate, peroxyflavin instead decays to form $H_2O_2$ in the so-called 'uncoupling' reaction (Scheme 3.1, **f**). After the oxygen transfer from the peroxyflavin to the substrate has occurred, a hydroxy-flavin species is formed ($FAD_{OH}$), whose spontaneous dehydration reforms FAD. The last step in the catalytic cycle is the ejection of the oxidised $NADP^+$ from the NADPH binding domain so that another NADPH molecule can then trigger a new cycle (Scheme 3.1, **e**).

### 3.1.2 Reactivity of BVMOs and FMOs

BVMOs and FMOs have been used since the 1960s and 1970s to catalyse a variety of oxidative transformations and several extensive reviews that summarise the use of these enzymes can be found in the literature.[265–269] As mentioned in 3.1.1, depending on the nature of the substrate and the protonation state of peroxyflavin, BVMOs and FMOs can catalyse either nucleophilic or electrophilic additions of oxygen onto their substrates.

#### *3.1.2.1 Nucleophilic peroxyflavin $FAD_{C4aOO}$- reactions*

Undoubtedly the most common nucleophilic addition of oxygen, FPMO-catalysed Baeyer-Villiger transformations of ketone and aldehyde substrates to afford the corresponding ester or acids have been extensively studied since the discovery of CHMO. Within the last five years, a multitude of new and improved BVMO methodologies have emerged in the literature.[270–278] For example, in 2019 Solé *et al.* proposed a scale-up procedure for the industrial synthesis of trimethyl-ε-caprolactones **56** starting from 3,3,5-trimethyl-cyclohexanone **55** using cyclohexanone monooxygenase of *Thermocrispum municipal*e (*tm*CHMO) (Scheme 3.3).[279] The group carried out a sequence of increasingly larger reaction volumes starting at 30 mL, where the biocatalytic transformation was optimised for quantitative conversion, to reach a final batch reaction volume of 100 L, obtaining 85% conversion and 76% yield after 9 h. Additionally, the industrial applicability of this process was further enhanced because the enzyme was used as fermentation broth, which requires the least amount of biocatalyst preparation effort, and hence production cost.

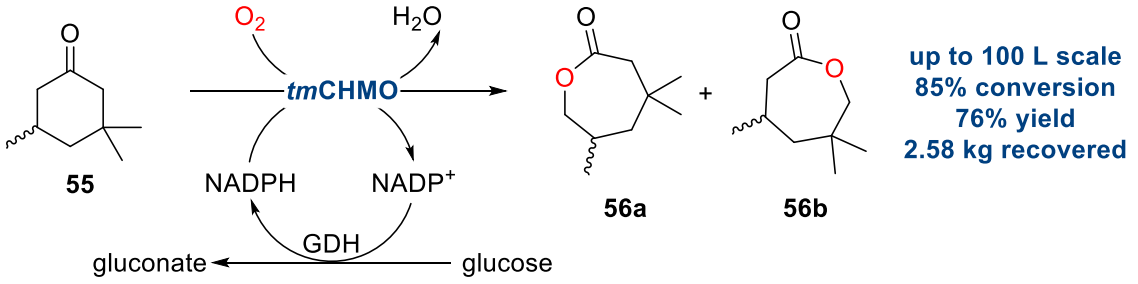


**Scheme 3.3.** Large scale production of trimethyl-ε-caprolactones **56** using CHMO from *T. municipal*e by Solé *et al.*.[279]

One of the limitations of BVMOs is that often two regioisomers can be obtained during Baeyer-Villiger transformations when the bonds rearrange in the Criegee intermediate. The regioisomers are defined as 'normal', if the product follows the bond migration rules, or 'abnormal' if the migration of the bonds does not follow the migration rules. Therefore in 2021, Zhang *et al.* identified and engineered a novel BVMO biocatalyst from *Gordonia sihwensis* (*gs*BVMO) with high selectivity for the normal regioisomer products after a homology search initiated with the known sequence of BVMO from *Pseudomonas putida* (*pp*BVMO).[275] The use of *gs*BVMO for the Bayer-Villiger oxidation of aliphatic keto acids **57** afforded the ester product **58** with a normal to abnormal ratio of 97:3 (Scheme 3.4). These products could then be further processed to obtain ω-hydroxy fatty acids **59** that have important applications as fragrances, adhesives, antiseptics, and pharmaceutical intermediates. Despite being known to catalyse Bayer-Villiger oxidations, there are not as many reports on the use of FMOs for the synthesis of esters or alcohols and many date to over a decade ago. However, in 2019 Löwe *et al.* reported the isolation of three new Type II FMOs from the hydrocarbon degrading bacterium *Pimelobacter* sp. (*ps*FMOA-C).[271]

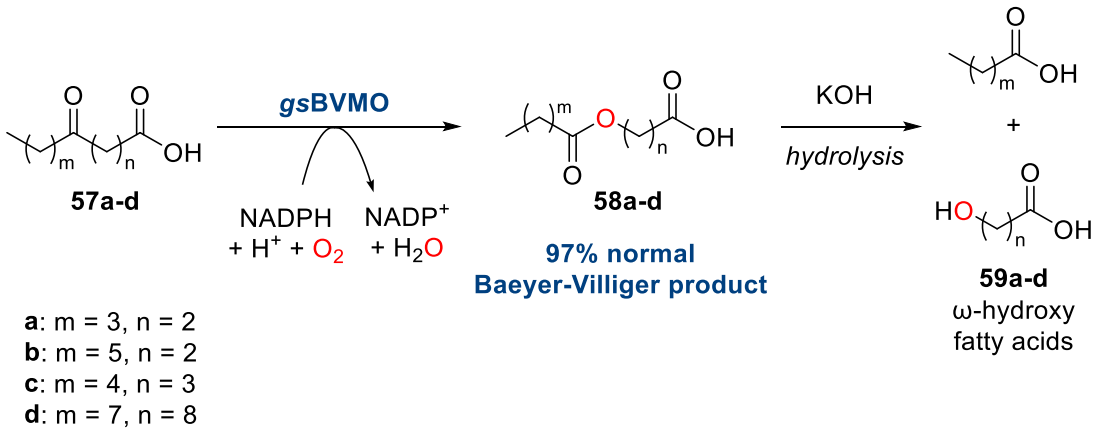


**Scheme 3.4.** Bayer-Villiger oxidation of aliphatic keto acids **57** to ester products **58** using a BVMO from *G. sihwensis* by Zhang *et al.*.[275]

After cloning and expressing the genes in *E. coli*, *ps*FMOA was found to be the most active of the three, converting 5.0 mM bicyclo[3.2.0]hept-2-en-6-one **60** to its corresponding lactone **61** in 85% conversion and >99% ee for the normal 1*R*-5*S* enantiomer **61a** and 34% ee for the abnormal 1*R*-5*S* enantiomer **61b** after 66 h (Scheme 3.5, Part A). Furthermore, the group proposed a photobiocatalytic *in situ* production of formate, required for the NADPH recycling system, from $CO_2$, water, light and microalgae which, when combined with *ps*FMOA and formate dehydrogenase (FDH), led to the production of **1*R*-5*S*-61** in 94% conversion and >99% ee for **61a** or 57% ee for **61b** (Scheme 3.5, Part B).

Other BVMO-catalysed nucleophilic additions of oxygen but with far fewer reports in the literature include oxidations of boronic acids,[280,281] sulfonations[282] and the very uncommon phosphite oxidation.[283,284]

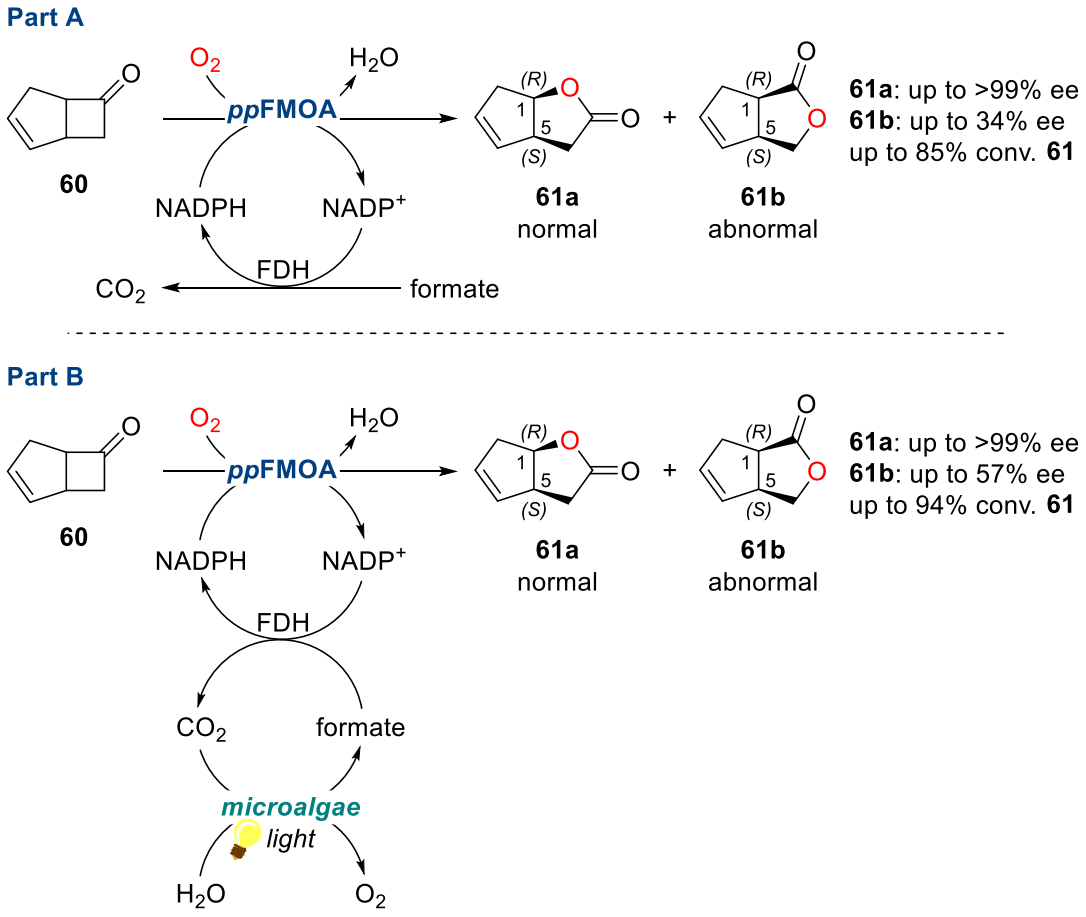


**Scheme 3.5.** Oxidation of bicyclo[3.2.0]hept-2-en-6-one **60** using the novel FMOA from *Pimelobacter* sp. by Löwe *et al.*.[271] Part A) regeneration NADPH using stoichiometric formate. Part B) *in situ* regeneration NADPH exploiting microalgae, light, water, and $CO_2$.

### *3.1.2.2 Electrophilic peroxyflavin $FAD_{C4aOOH}$ reactions*

The two most frequently reported reactivities of BVMOs and FMOs for the electrophilic addition of $O_2$ onto soft nucleophilic substrates are *N*-oxidations and sulfoxidations. Whilst both enzyme classes have been shown to carry out these oxidations efficiently, *N*-oxidations are more common in FMOs, as their physiological role is to metabolise nitrogen-containing toxins in organisms.[247,252] However, most publications on FMOs that involve their ability to catalyse the formation of *N*-oxides are focused on understanding their biological pathways and for the synthesis of drug metabolites.[285–287] For instance, in 2012 Hanlon *et al.* utilised the human FMO isoform 3 (*h*FMO3) for the milligram scale synthesis of the *N*-oxide metabolite **62** of Moclobemide, routinely prescribed for depression (Scheme 3.6).[288] Instead in 2018, Chen *et al.* demonstrated that FMO1 in *Arabidopsis thaliana* plants could catalyse the oxidation of pipecolic acid to *N*-hydroxy-pipecolic acid, a metabolite responsible for triggering systemic disease resistance in *Arabidopsis* plants.[289] Despite the far fewer reports on their oxidative activity towards amines and *N*-heterocycles, BVMOs have been used as biocatalysts for synthesis of small and building block *N*-oxide molecules.[290–292] In 2007, Torres-Pazmiño and colleagues reported the discovery of the M446G mutant of the thermostable phenylacetone monooxygenase (PAMO), which showed substantial improvement in its substrate specificity.[293] Compared to the WT parent, the mutant could oxidise a variety of ketones, sulfides, and secondary amines, including indole **63**. The oxidation of indole **63** was especially interesting as the authors hypothesised that, due to the poor ability of BVMOs to catalyse hydroxylations and epoxidations, PAMO M446G carried out the *N*-oxidation of **63** to indole oxide **64**, which was then converted to the indoxyl intermediate **65** and subsequently dimerised to indigo blue (Scheme 3.7).[294]

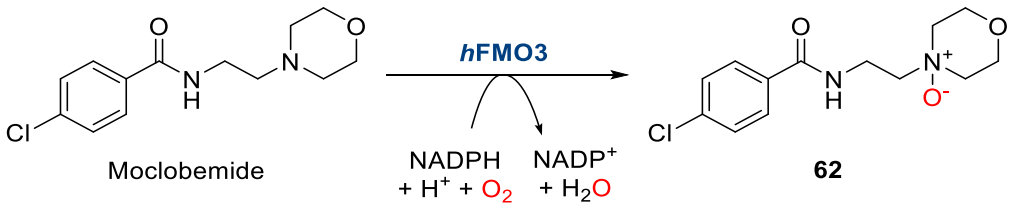


**Scheme 3.6.** Synthesis of the *N*-oxide metabolite **62** of the antidepressant drug Moclobemide using the human FMO isoform 3 by Hanlon *et al*..[288]

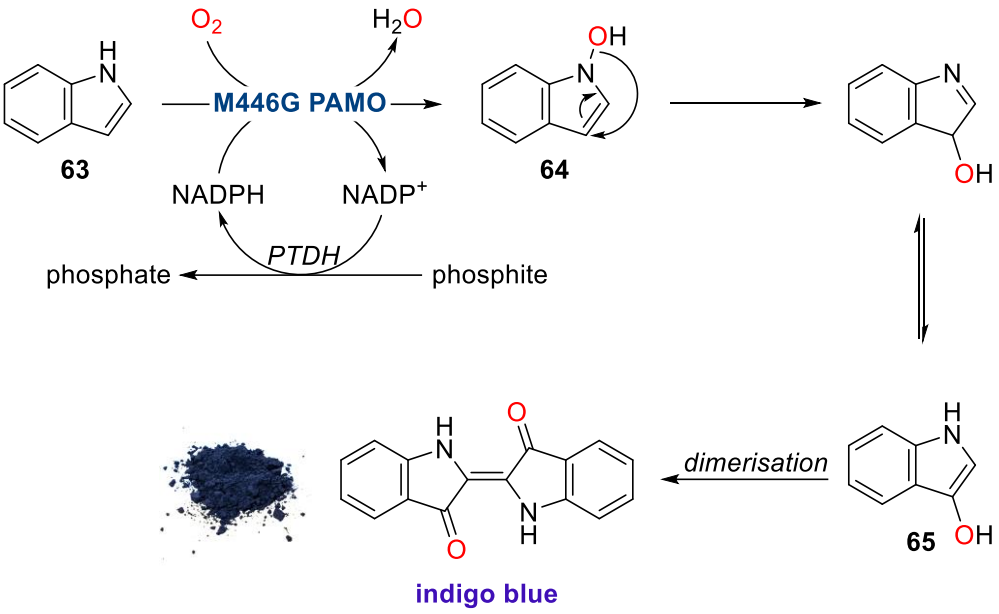


**Scheme 3.7.** *N*-oxidation of indole **63** using M446G PAMO and subsequent spontaneous indigo blue formation by Torres-Pazmiño *et al*..[293]

Compared to the overall low volume of publications on the well-established *N*-oxidative ability of BVMOs and FMOs and with over fifty articles published in the last decade, there is a consistently increasing number of reports for the BVMO and FMO biocatalysed synthesis of enantiopure sulfoxides, perhaps due to the importance of the sulfoxide moiety in all areas of chemistry. Between the two FPMOs, BVMO-catalysed sulfoxidations make up most of the works reported in the literature, as these enzymes have traditionally been under scrutiny for their biocatalytic properties far more than FMOs. The stereoselective sulfur oxidations can be categorised into three groups: discovery of new biocatalysts for the synthesis of small molecule sulfoxides,[17,295,296] synthesis of pharmaceutically active ingredients (API),[243,297,298] and large-scale production of enantiopure sulfoxides.[299,300] For instance, de Gonzalo *et al.* reported the stereoselective synthesis of (*S*)-alkyl aryl sulfoxides **67** in moderate to good ees (up to 93%) using the Baeyer-Villiger monooxygenase 2-Oxo-$\Delta^3$-4,5,5-trimethylcyclopentenylacetyl-CoA 1,2-monooxygenase (OTEMO) from *Pseudomonas putida*.[301] The enzyme was used as a PTDH-OTEMO fusion biocatalyst, where PTDH (phosphate dehydrogenase) was used as the NADPH recycling enzyme at the expense of a phosphite molecule (Scheme 3.8). In the course of the study, it was observed that sulfides **66** with electron donating group (EDG) substituents generally afforded (*S*)-sulfoxides with higher ee compared to those with electron withdrawing group (EWG) substituents.

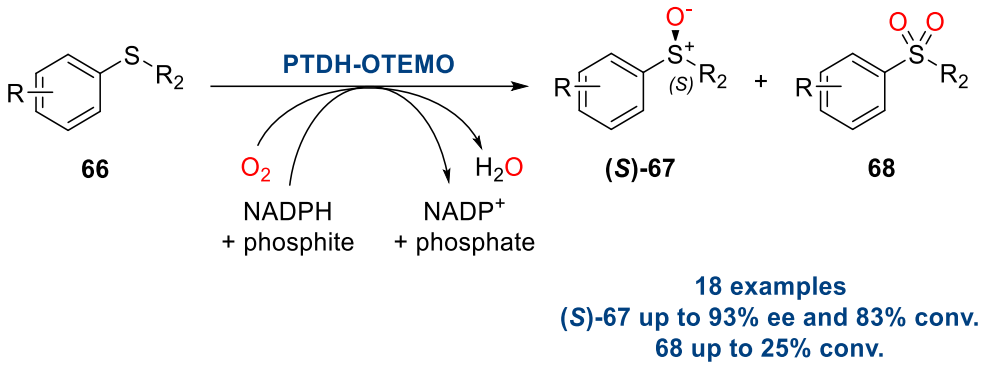


**Scheme 3.8.** OTEMO catalysed oxidation of sulfides **66** to sulfoxides **(*S*)-67** and sulfones **68** by de Gonzalo *et al.*.[301]

Furthermore, the authors reported that, in most cases, around 10% sulfone **68** overoxidation was obtained, which was subsequently exploited for the development of the KR of racemic sulfoxides. However, OTEMO showed a low enantiopreference towards sulfoxide oxidation, which led to enantioenriched sulfone:sulfoxide mixtures with ees up to only 54%. The FMO-catalysed sulfoxidation of thioanisole **70** was also reported by the same group, who identified eight new FPMOs from *Rhodococcus jostii* RHA1 and tested them for their oxidative ability.[302] The sequence of seven of these new enzymes formed an isolated cluster of proteins that presented similar structural motifs to FMOs, and therefore were classified as a new FMO subclass, the type II FMOs (FMO-A to G). Of these newly discovered biocatalysts, FMO-A-F only partially converted **69** to (*R*)-methyl phenyl sulfoxide **70** in low to moderate ees (up to 33%), while FMO-G provided **(*S*)-70** in the highest observed ee (57%), but only in a mere 21% conversion (Scheme 3.9). BVMOs, in particular, have been largely investigated for API synthesis, especially for the prazole-family. For example, in 2021 Liu *et al*. reported the synthesis of (*R*)-lansoprazole **71** in 99% ee and >99% conversion in 35 h using a novel BVMO from *Cupriavidus basilensis* (*cb*BVMO) as a whole cell catalyst (Scheme 3.10).[303] After virtual sequence filtering, gene cloning and expression, *cb*BVMO was selected among 10,000 homologues of BVMO from *Bradyrhizobium oligotrophicum*, which was known to selectively oxidise lansoprazole sulfide to the corresponding (*R*)-sulfoxide enantiomer. BVMO-catalysed large-scale production protocols of enantiopure sulfoxides have also recently emerged in the literature. In 2017 the team led by Goundry from AstraZeneca reported the development of a protocol that uses Codexis' BVMO-P1/D08 for the plant scale manufacturing of sulfoxide **(*R,R*)-73**, an intermediate in the synthesis of the lead candidate AZD6738 **74** for an oncology project (Scheme 3.11).[299]

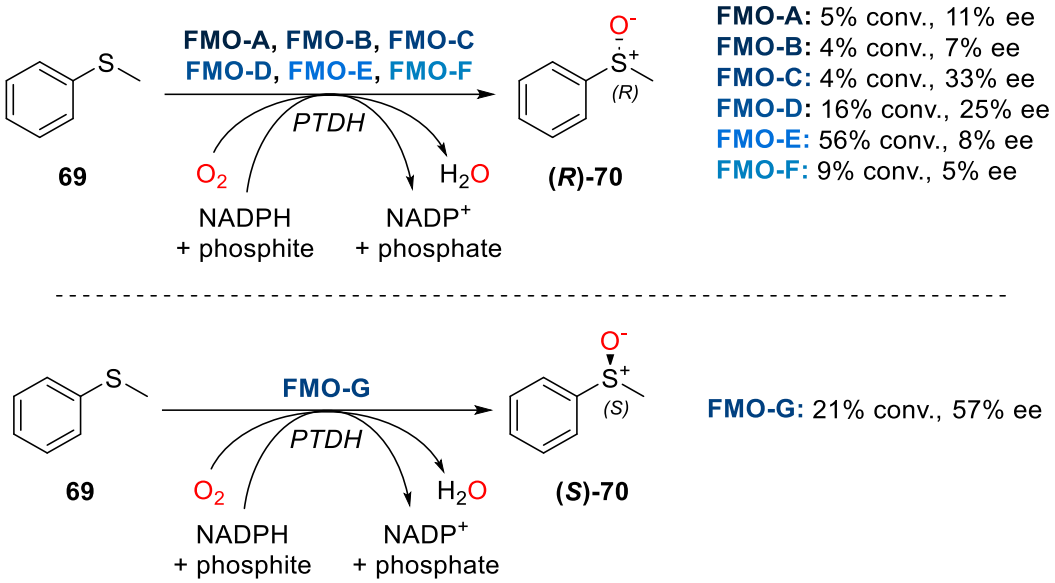


**Scheme 3.9.** Type II FMO catalysed enantioselective oxidation of thioanisole **69** to (*R*)- or (*S*)-methyl phenyl sulfoxide **70**.[302]

During the development of the process, the transfer of gas-liquid mass of $O_2$ to the reaction mixture was found to be responsible for the low biocatalytic efficiency of BVMO-P1/D08 and low **73** yields. Therefore, after a series of around 30 kilogram-scale batch reactions and performing at least two plant scale pilot reactions, the team managed to obtain **73** from **72** in 72% yield (83 kg) at plant scale production level.

Other electrophilic oxidations catalysed by BVMOs and FMOs include oxidative halogenations, rare heteroatom oxidations, and epoxidations. However, publications on these topics are scarce as these reactions are more commonly catalysed by FPMOs in other groups.[245,247]

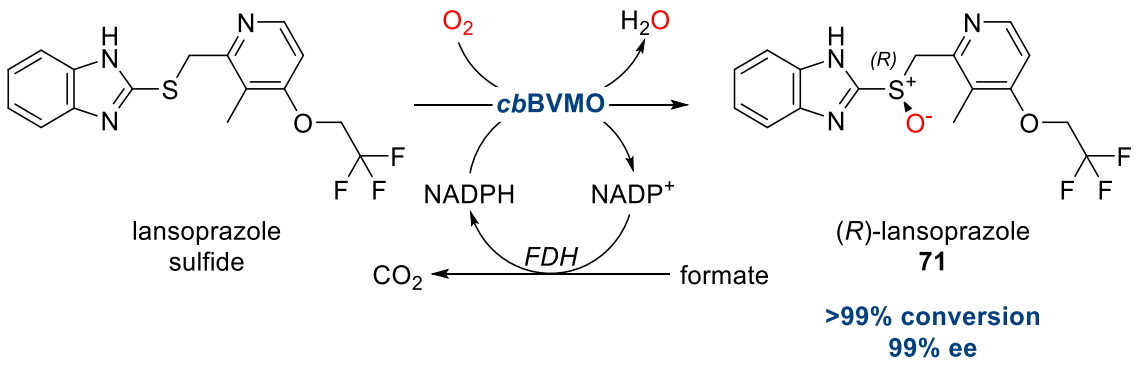


**Scheme 3.10.** Synthesis of (*R*)-lansoprazole **71** in 99% and >99% conversion using the novel *cb*BVMO by Liu *et al*..[303]

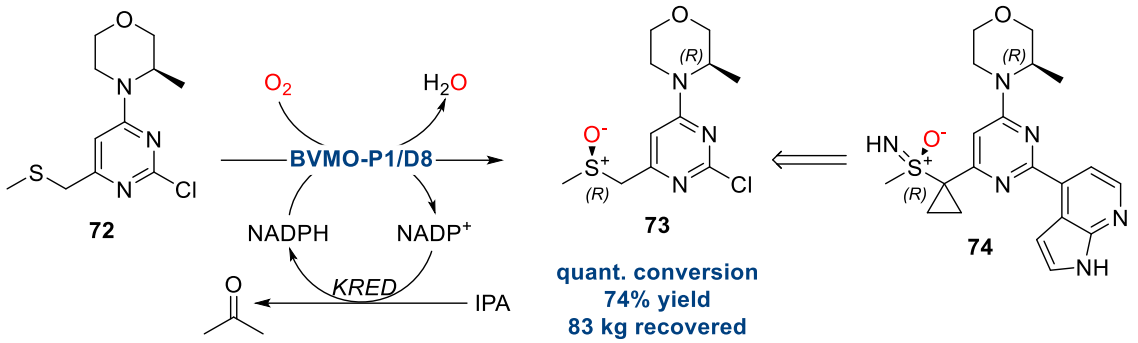


**Scheme 3.11.** Plant scale synthesis of drug intermediate 19 in the synthesis of AZD6738 **74** using Codexis' BVMO-P1/D08 by Goundry and colleagues, AstraZeneca.[299]

Although the ability of BVMOs to perform enantioselective sulfoxidations has been proven throughout the decades, the full biocatalytic potential of FMOs for the synthesis of enantiopure sulfoxides remains largely unexplored. Additionally, most reports on the chiral production of sulfoxides focus on substrates that do not bear other functional groups that could potentially lead to the formation of other oxidative side products, such as amines and ketones. Therefore, the lack of a detailed study on the chemoselectivity of BVMOs and FMOs when reacted with multifunctional substrates means that the applicability of these FPMOs remains limited to simple prochiral sulfides.

## 3.2 Aims of the project

This project began as an investigation in collaboration with Almac aimed at finding oxidative enzymes capable of chemo- and stereoselectively oxidising sulfides in molecules bearing nitrogen heterocycles. Therefore, this project wanted to investigate the ability of a panel of BVMO and FMO enzymes to stereoselectively catalyse the S-oxidation of sulfide substrates bearing nitrogen heterocycles without generating *N*-oxide side products. Additionally, to determine the commercial relevance of the identified BVMOs and FMOs, we aimed at providing a more complete account on both the chemoselectivity of these biocatalysts when reacted with carbonyl-containing substrates and their general applicability when used for the enantioselective synthesis of simpler sulfoxides.

## 3.3 Results and discussion

### 3.3.1 Screening of the BVMO and FMO panel

The project began by screening a panel of over 80 commercial BVMO and FMO enzymes provided by Almac as freeze-dried cell free extracts (CFE). This panel comprised a variety of both WT and engineered biocatalysts, which for intellectual property (IP) reasons cannot be disclosed at this stage of the project. The pyridine-containing sulfide **21a** was the ideal initial substrate to identify enzymes capable of carrying out chemo- and stereoselective sulfoxidations on compounds bearing functional groups prone to oxidation by FPMOs and was therefore selected to perform the screening of the panel. The initial reaction conditions were set to Almac's enzyme kit instructions, which required 1.2 mM **21a**, 10 $gL^{-1}$ of enzyme CFE, 2.0 $gL^{-1}$ glucose dehydrogenase (GDH), 5.5 eq. glucose and 2.0 mM $NADP^+$ in 50 mM Tris-HCl buffer at pH = 8.0 with 2.0% $CH_3CN$ to solubilise **21a**. Due to the large number of BVMOs and FMO in the panel, only the best results of the screening have been reported in Table 3.1. All the enzymes selectively oxidised **21a** to the (*S*)-sulfoxide **(*S*)-22a** except for FMOD9, which provided **(*R*)-22a** in 65% ee and full conversion (Table 3.1, *Entry 16*). Among the enzymes that afforded the (*S*)-enantiomer, BVMO145 stood out as the most promising biocatalyst as it led to **(*S*)-22a** in >99% ee and 75% conversion (Table 3.1, *Entry 7*). Additionally, BVMO145 showed remarkable chemoselectivity for sulfide oxidation as no traces of sulfone **23a** were observed with this enzyme. This is in contrast to, for instance, the results obtained with BVMO129, which showed negligible stereoselectivity for the oxidation of **21a** and the major reaction product was **23a** (Table 3.1, *Entry 4*), which means that this enzyme would be a good candidate for biocatalysed sulfone synthesis of pyridine bearing sulfides. Interestingly, no *N*-oxidation of the pyridine ring was observed in any of the enzymes screened. Therefore, enzymes BVMO145 and FMOD9 were selected for the development of two complementary methodologies for the oxidation of multi-functional group sulfides. It has to be noted that in the initial screening of the FMO enzymes, it was not possible to determine the sulfone content at the end of the reaction and due to time constraints, a second screening has not been performed. However, as FMOD9 showed good opposite enantioselectivity to BVMO145, it was still considered for the development of a sulfoxidation method.

**Table 3.1.** Screening of the BVMO and FMO enzymes panel.

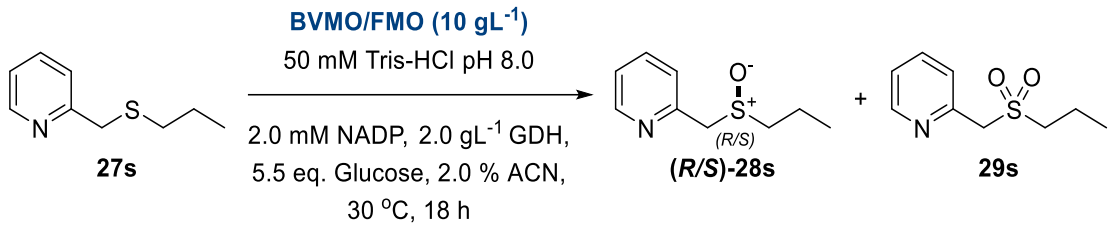


| Entry | Enzyme | Code | 28s conv. %[a] | 29s conv. %[a] | 28s ee %[b] | Enantiomer[c] |
|---|---|---|---|---|---|---|
| *1* | BVMO | 113 | 36 | - | 32 | (*S*) |
| *2* | BVMO | 114 | 67 | 4 | 54 | (*S*) |
| *3* | BVMO | 128 | 48 | - | 6 | (*S*) |
| *4* | BVMO | 129 | 24 | 53 | 3 | (*S*) |
| *5* | BVMO | 138 | 66 | 14 | 54 | (*S*) |
| *6* | BVMO | 141 | 10 | 70 | 39 | (*S*) |
| ***7*** | **BVMO** | **145** | **75** | **-** | **>99** | **(*S*)** |
| *8* | BVMO | 148 | 49 | 2 | 75 | (*S*) |
| *9* | BVMO | 149 | 63 | 3 | 72 | (*S*) |
| *10* | FMO | A3 | 99 | n.d.[d] | 53 | (*S*) |
| *11* | FMO | A4 | 70 | n.d.[d] | 9 | (*S*) |
| *12* | FMO | A5 | 80 | n.d.[d] | 41 | (*S*) |
| *13* | FMO | A6 | 76 | n.d.[d] | 61 | (*S*) |
| *14* | FMO | D10 | 53 | n.d.[d] | 40 | (*S*) |
| *15* | FMO | D12 | 99 | n.d.[d] | 47 | (*S*) |
| ***16*** | **FMO** | **D9** | **99** | **n.d.[d]** | **65** | **(*R*)** |
| *17* | FMO | E2 | 99 | n.d.[d] | 9 | (*S*) |

[a]Determined by reversed phase HPCL using a Kromasil C18 column, monitored at 254 nm. [b]Determined by chiral HPLC using Chiralpak IC column, monitored at 254 nm. [c]Enantiomer determined by comparison with the literature. [d]n.d. = not determined.

### 3.3.2 Optimisation of the BVMO145 biocatalysed (*S*)-sulfoxidation reaction conditions

Once the two best enzymes which gave best conversion and ees were identified, the sulfoxidation reaction conditions were optimised, focussing first on the use of BVMO145. Firstly, the concentration of $NADP^+$ suggested by the kit instructions was optimised. The initial 2.0 mM $NADP^+$ equalled 1.7 eq. with respect to the concentration of **27s**, which was unnecessarily high stoichiometric amount of expensive cofactor as GDH and glucose were also utilised in the biocatalytic system to continuously produce NADPH from $NADP^+$. Therefore, when the concentration of $NADP^+$ was set to 5 mol % (0.06 mM), the conversion of **27s** to **(*S*)-28s** was improved from 75% to 90% after 18 h without affecting the ee (>99%) (Table 3.2, *Entry 1*).

**Table 3.2.** Optimisation of the conditions of the BVMO145 biocatalysed **27s** sulfoxidation.

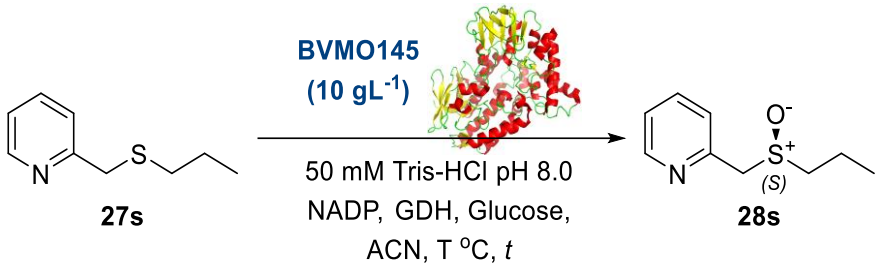


| Entry | 27s / mM | NADPH / mM | GDH / gL$^{-1}$ | pH | T / °C | *t* / h | Conv. %[a] | ee %[b] |
|---|---|---|---|---|---|---|---|---|
| *1* | 1.2 | 0.06 | 2 | 8.0 | 30 | 18 | 90 | >99 |
| *2* | 1.2 | 0.06 | 5 | 8.0 | 30 | 18 | 40 | >99 |
| *3* | 1.2 | 0.06 | 1 | 8.0 | 30 | 18 | 93 | >99 |
| *4* | 5.0 | 0.06 | 1 | 8.0 | 30 | 18 | 42 | >99 |
| *5* | 10 | 0.06 | 1 | 8.0 | 30 | 18 | 12 | >99 |
| *6* | 20 | 0.06 | 1 | 8.0 | 30 | 18 | 12 | >99 |
| *7* | 40 | 0.06 | 1 | 8.0 | 30 | 18 | 10 | >99 |
| *8* | 5.0 | 0.25 | 1 | 8.0 | 30 | 18 | 93 | >99 |
| *9* | 10 | 0.50 | 1 | 8.0 | 30 | 18 | 70 | >99 |
| *10*[c] | 5.0 | 0.25 | 1 | 8.0 | 30 | 18 | <1 | n.d.[d] |
| *11*[e] | 5.0 | 0.25 | 1 | 8.0 | 30 | 18 | <1 | n.d.[d] |
| *12* | - | 0.25 | 1 | 8.0 | 30 | 18 | - | - |
| *13* | 5.0 | 0.25 | 1 | 7.0 | 30 | 18 | 93 | >99 |
| *14* | 5.0 | 0.25 | 1 | 9.0 | 30 | 18 | >99 | >99 |
| *15* | 5.0 | 0.25 | 1 | 9.0 | 37 | 18 | >99 | >99 |
| ***16*** | **5.0** | **0.25** | **1** | **9.0** | **37** | **4** | **>99** | **>99** |
| *17* | 5.0 | 0.25 | 1 | 9.0 | 37 | 1 | 71 | >99 |

[a]Determined by reversed phase HPCL using a Kromasil C18 column, monitored at 254 nm. [b]Determined by chiral HPLC using Chiralpak IC column, monitored at 254 nm. [c]Empty vector *E. coli* CFE. [d]n.d. = not determined. [e]Enzyme-free reaction.

It was also found that the higher the concentration of GDH, the lower the overnight conversion of **27s** would be, as 5.0 gL$^{-1}$ GDH led to 40% **(*S*)-28s** (Table 3.2, *Entry 2*), while 1.0 gL$^{-1}$ GDH led to a slightly improved 93% **(*S*)-28s** instead (Table 3.2, *Entry 3*). Hence, the concentration of GDH was set to 1.0 gL$^{-1}$ for the rest of the optimisation experiments. Then, the optimal concentration of **27s** was investigated. Despite obtaining >99% ee in all cases, when the concentration of NADP$^+$ was kept at 0.06 mM, any increase in **27s** concentration would unsurprisingly lead to much lower overnight conversions (Table 3.2, *Entries 4-7*). However, if the concentration of NADP$^+$ was kept at 5 mol % (hence increased with the concentration of **27s**), the concentration of **27s** could be increased to 5.0 mM as **(*S*)-28s** was once again obtained in 93% conversion and >99% ee (Table 3.2, *Entry 8*). Unfortunately, the enzyme did not seem to tolerate substrate concentrations higher than 5.0 mM (Table 3.2, *Entry 9*), which was selected as the optimal **27s** concentration. Three control experiments were then performed, where

empty pET28a(+) vector *E. coli* CFE, enzyme-free and substrate **27s**-free reactions were carried out (Table 3.2, *Entries 10-12*). In all three cases no sulfoxide **28s** formation was observed. Lastly the pH and reaction temperature were analysed (Table 3.2, *Entries 13-17*), and it was found that at a higher pH of 9.0 and 37 °C, **(*S*)-28s** was obtained in quantitative conversion (>99%) and >99% ee in only 4 h (Table 3.2, *Entry 16*).

### 3.3.3 Scope of the BVMO145 biocatalysed sulfoxidation

With the best conditions in hand (Table 3.2, *Entry 16*), the scope of the BVMO145 biocatalysed sulfoxidation was then investigated. Results are reported in Table 3.3. Conversion of the other two pyridine containing sulfides drastically changed depending on the size of the other sulfur substituent, as the ethyl substituted sulfide **27t** was fully

**Table 3.3.** Scope of the BVMO145 biocatalysed sulfoxidation.

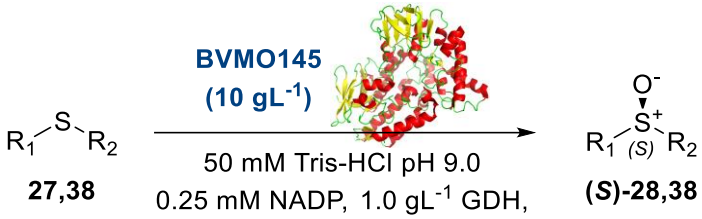


| Entry | Substrate | $R_1$ | $R_2$ | Time / h | Conv. %[a] | ee %[b] |
|---|---|---|---|---|---|---|
| *1* | **27t** | 2-Py$CH_2$ | Et | 4 | >99 | >99 |
| *2* | **27u** | 2-Py$CH_2$ | $CH_2$Ph | 4 | <1 | n.d.[c] |
| *3* | **27v** | Bn | Et | 4 | >99 | >99 |
| *4* | **27o** | Bn | Me | 4 | <1 | n.d.[c] |
| *5* | **27w** | Ph$(CH_2)_2$ | Et | 4 | <1 | n.d.[c] |
| *6* | **27a** | Ph | Me | 4 | 76 | >99 |
| *7* | **21h** | 4-F-$C_6H_4$ | Me | 4 | 53 | >99 |
| *8* | **27x** | 4-Br-$C_6H_4$ | Me | 4 | <1 | n.d.[c] |
| *9* | **27y** | 4-Cl-$C_6H_4$ | Me | 4 | <1 | n.d.[c] |
| *10* | **27z** | 3-Cl-$C_6H_4$ | Me | 4 | <1 | n.d.[c] |
| *11* | **27aa** | 2-Cl-$C_6H_4$ | Me | 4 | <1 | n.d.[c] |
| *12* | **27ab** | 4-Ac-$C_6H_4$ | Me | 4 | <1 | n.d.[c] |
| *13*[d] | **27ac** | 3-Me-$C_6H_4$ | Me | 4 | 82 | >99 |
| *14* | **27ad** | 2,4-Me-$C_6H_3$ | Me | 4 | <1 | n.d.[c] |
| *15* | **27g** | 4-Br-$C_6H_4$ | Et | 4 | 3 | >99 |
| *16* | **27j** | 4-MeO-$C_6H_4$ | Et | 4 | <1 | n.d.[c] |
| *17* | **38a** | Ph | $(CH_2)_2COCH_3$ | 4 | >99 | n.d.[c] |
| *18* | **38d** | Ph | $CH_2COCH_3$ | 4 | >99 | n.d.[c] |
| *19* | **38f** | Ph | $CH_2COCH(CH_3)_2$ | 4 | <1 | n.d.[c] |

[a]Determined by reversed phase HPCL using a Kromasil C18 column, monitored at 254 nm. [b]Determined by chiral HPLC using Chiralpak IG or IC column, monitored at 254 nm. [c]n.d. = not determined. [d](*R*)-enantiomer obtained instead.

oxidised to **(*S*)-28t** in >99% ee, while **27u**, which has a bulkier methylphenyl $R_2$ group, showed no conversion to the sulfoxide (Table 3.3, *Entries 1,2*). Interestingly, the benzyl substituted **27v**, an analogue of **27t**, also showed >99 % conversion to **(*S*)-28v** in >99% ee but no conversion for the smaller methyl substituted **27o** was observed after 4 h (Table 3.3, *Entries 3,4*). This may suggest that the alkyl chain may be involved in anchoring the substrate in the active site through hydrophobic interactions, and it needs to be longer than a methyl group. However, despite having an ethyl chain, no conversion was detected for sulfide **27w** (Table 3.3, *Entry 5*), probably due to the size of the bulkier phenethyl substituent. A series of small phenyl and methyl substituted sulfides **27a-o** were also reacted with BVMO145 (Table 3.3, *Entries 6-14*). Interestingly, while the equal sized **21g** and **27b** were partially converted to the corresponding (*S*)-sulfoxides in 76% and 53% conversion respectively (Table 3.3, *Entries 6,7*), larger para-substituents of sulfides **27x**, **27y**, **27ab** and **27ad** did not seem to be tolerated by BVMO145, indicating that steric hindrance may play a role in substrate binding. Additionally, the slightly electron withdrawing nature of halogen substituents seemed to also affect the conversion of sulfides. In fact, while the 3-methylphenyl substituted **27ac** showed 82% conversion to **28ac** in 4 h (Table 3.3, *Entry 13*), no oxidation of the 3-chlorophenyl **27z** was detected (Table 3.3, *Entry 10*). Interestingly, the enantioselectivity for **28ac** is reversed as the (*R*)-enantiomer was obtained instead. From the electrostatic potential surface (EPS) map of the two sulfides (Figure 3.3), it is clear that when the *meta* substituent is a halogen,

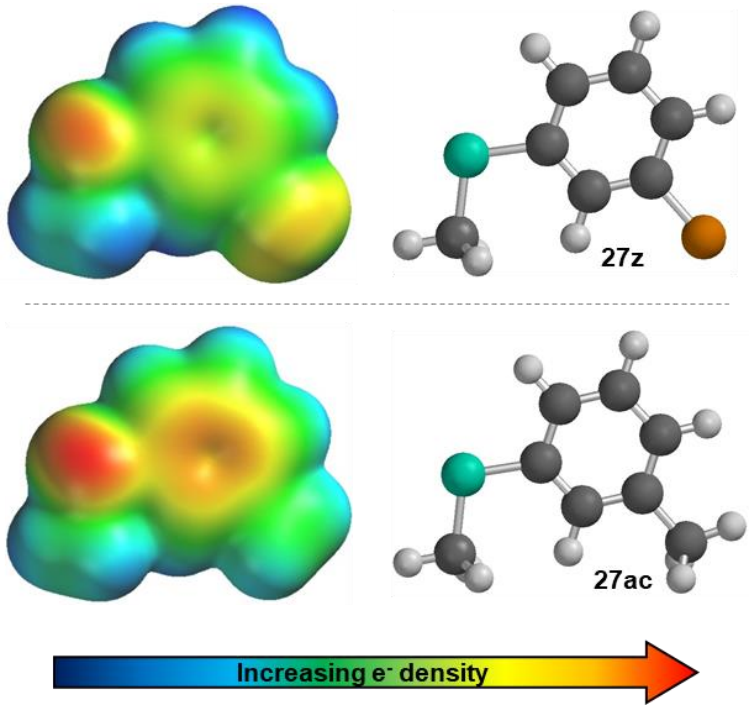


**Figure 3.3.** Electrostatic potential surface (EPS) map for **27z** and **27ac**.

the electron density on the sulfur atom is much lower compared to that of the methyl substituent. Therefore, **27ac** had better nucleophilic properties and could react with the protonated peroxyflavin species of BVMO145 in the oxidative reaction. The EWG effect of substituents was marginally counterbalanced when the $R_2$ group was an ethyl chain, as a very small 3% conversion of **27g** to **(*S*)-28g** was observed (Table 3.3, *Entry 15*). This further enforces the hypothesis that a longer alkyl chain may help the substrate bind to the active site. Instead for **27j** with a larger para methoxy group, no conversion was observed despite the ethyl chain (Table 3.3, *Entry 16*). Lastly, a series of carbonyl containing sulfides was analysed. For compounds **38a-s**, which have a linear carbonyl chain, full conversion of the substrate was observed (Table 3.3, *Entries 17,18*). However, no sulfoxide or sulfone were detected by HPLC, indicating that the competing Baeyer-Villiger reactions may have taken place instead. The characterisation of the side products proved to be challenging and it is currently ongoing in the group. The branched carbonyl sulfide **38f** was fully recovered at the end of the reaction instead (Table 3.3, *Entry 19*).

## 3.4 Preliminary conclusions and future work

In this project, a panel of over 80 enzymes containing a mixture of WT and mutant commercial BVMOs and FMOs from Almac was screened and BVMO145 and FMOD9 were selected for the development of two parallel complementary oxidative protocols for the chemo- and stereoselective synthesis of sulfoxides bearing other functional groups. Unfortunately, due to time constraints, this project could not be completed before submission of this thesis. However, from the data obtained to date, it was possible to draw some preliminary conclusions on the catalytic activity of BVMO145. In fact, BVMO145 was the first biocatalyst to be studied because it showed remarkable enantioselectivity for pyridyl-containing (*S*)-sulfoxides without generating sulfone overoxidation by-products. Therefore, having optimised the reaction conditions, the chemo- and stereoselective preference of BVMO145 was investigated on a series of 20 structurally different prochiral sulfides. Even though only 7 compounds were oxidised to the corresponding (*S*)-sulfoxides in low to excellent conversions, the enantioselectivity was found to be exceptional as in all cases >99% ee was observed. Additionally, full conversion of 2 carbonyl containing sulfides was also observed, but in these instances, it was postulated that the Baeyer-Villiger products were formed instead as no sulfoxide or sulfone formation was detected by HPLC. The initial assessment of the scope of BVMO145 identified characteristics substrates need to have to react with the enzyme:

- the prochiral substrate may require an alkyl chain substituent of two or more carbon chain length to induce non-polar interactions with the active site of the enzyme,
- whilst an aromatic ring is tolerated, para and EWG substituents have detrimental effects on the sulfoxidation due to steric hindrance and deactivation of the sulfide as a soft nucleophile,
- an ethylene spacer between the aromatic ring and the sulfur may be beneficial for the binding of the substrate into the active site of the enzyme.

In order to prove these observations, the sulfides showed in Figure 3.4 will be synthesised and reacted with BVMO145, and an *in silico* docking study of the sulfide substrates will also accompany these experimental findings. Furthermore, the chemoselectivity of BVMO145 for Baeyer-Villiger reactions over sulfoxidations and preference for normal or abnormal regioisomer in carbonyl-containing sulfides will need to be confirmed by analytical methods. Finally, the efficiency of FMOD9 as an oxidative biocatalyst for stereo- and chemoselective sulfoxidations will be assessed for the development of an enantiocomplementary methodology.

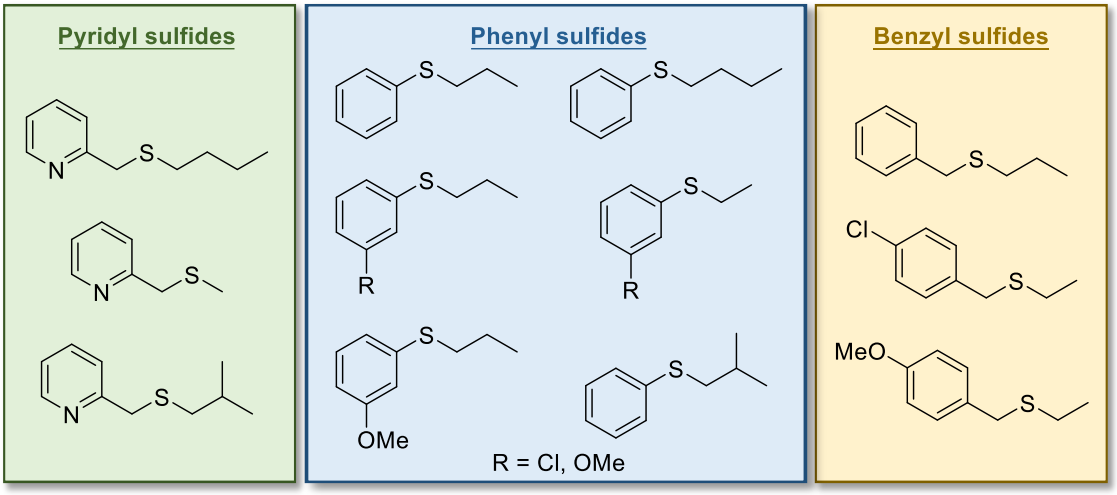


**Figure 3.4.** New sulfide substrates for the expansion of the BVMO145 biocatalysed sulfoxidation.

# Chapter 4. Enhancing the synthetic scope and potentiality of methionine reductase enzymes in the biocatalytic synthesis of enantiomerically pure sulfoxides: mechanistic and mutagenesis studies

## 4.1 Introduction

The most common biocatalytic route to access chiral sulfoxides is oxidative, meaning that a prochiral sulfide is oxidised using enzymes such as monooxygenases[16,245,246,270,304–308] and peroxygenases.[236–238] However, even if these oxidative enzymatic methodologies are highly efficient and stereoselective, they present drawbacks, especially in terms of industrial applicability. Such drawbacks include the use of expensive NAD(P)H to regenerate the FAD or FMN cofactors in monooxygenases, the use of stoichiometric amounts of $H_2O_2$ in peroxygenases and the need of effective oxygenation to promote the S-oxidation. Also, in certain scenarios, oxidising species like peroxides can be produced during the reaction and they need to be effectively removed to avoid enzyme degradation and the formation of overoxidation side products.[309] However, the oxidative route is not the only option in the biocatalysis toolbox available to researchers as, in fact, it has been possible to obtain enantiopure sulfoxides through enzymatic kinetic resolutions (EKR) or the even better enzymatic dynamic kinetic resolution (EDKR). KR occurs when two enantiomers are irreversibly differentiated from a racemic mixture as they react at different rates with chiral catalysts, enzymes in EKR, resulting in a 1:1 mixture of product and enantiopure unreacted starting material (Figure 4.1).[262]

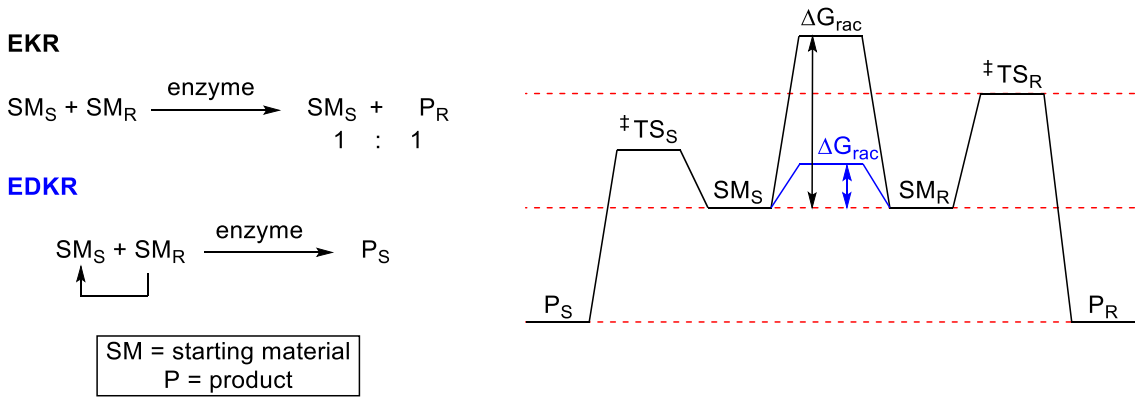


**Figure 4.1.** Schematic representation of EKR and EDKR with their relative energy diagram. In black is the $\Delta G_{rac}$ of a EKR process while in blue is the $\Delta G_{rac}$ of an EDKR.

This separation is possible because the energies of the two transition states of the enantiomers are different and the Gibbs free energy change for the racemisation ($\Delta G_{rac}$) is greater than the activation energy of the unreacted enantiomer (Figure 4.1, $\Delta G_{rac}$ in black). Meanwhile, DKR differs from KR in that there is accumulation of only one enantiopure product at the end of the reaction, because the two enantiomers of the starting material can easily epimerise as the $\Delta G_{rac}$ is lower than the activation energy of the reacted enantiomer (Figure 4.1, $\Delta G_{rac}$ in blue).[262] A few examples have been proposed where EKR of sulfoxides takes place via manipulation of other moieties in the molecule.[310–314] For example, in 2000 Guerrero de la Rosa *et al.* reported the EKR of (*E*)-γ-Hydroxy-α,β-unsaturated *p*-tolylsulfoxides **75** using a lipase from *Pseudomonas cepacia*, which was active on the hydroxyl group of the molecule (Scheme 4.1, Part A).[315]

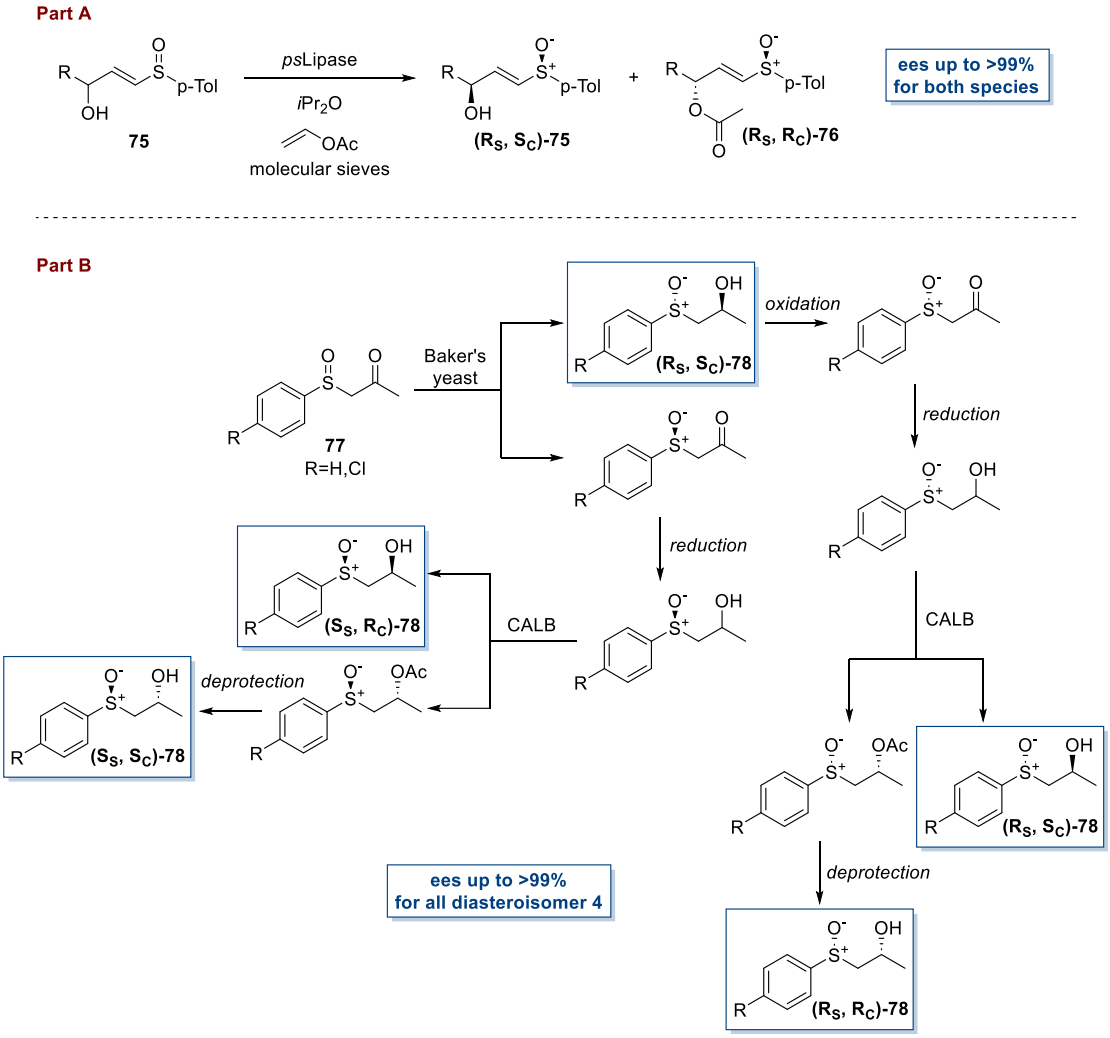


**Scheme 4.1.** Indirect EKR methods to access enantiopure sulfoxides Part A) EKR of (*E*)-γ-Hydroxy-α,β-unsaturated *p*-tolylsulfoxides **75** using a lipase from *Pseudomonas cepacia* by Guerrero de la Rosa *et al.*.[315] Part B) Synthesis of β-hydroxysulfoxides **78** by Chen *et al.*.[316]

With this method they managed to separate and isolate the individual diastereomers for full characterisation and analysis. Another instance of indirect EKR of sulfoxides was reported in 2008 by Chen and colleagues, who managed to synthesise and isolate the four diastereomers of β-hydroxysulfoxides **78** using a combination of Baker's yeast and CALB in multi-step syntheses starting from **77** (Scheme 4.1, Part B).[316] Remarkably, the biocatalytic transformations were carried out in diisopropyl ether with 7% water, which allowed for an easy isolation of the reaction products. All these EKR methods to obtain enantiopure sulfoxides require other functional groups that react with enzymes and are not always applicable to substrates that lack hydroxyl or carbonyl moieties. More recently, the focus on EKR of sulfoxides shifted towards a new approach where enantiopure sulfoxides are obtained via reductive biocatalytic mechanisms using reductive enzymes that catalyse the kinetic resolution of sulfoxide racemates by selectively reducing one of the two enantiomers into the corresponding sulfide. However, unlike the large pool of oxidative enzymes from which the researcher can chose from, the range of reductive enzymes is still rather small and currently limited to only two classes: the dimethyl sulfoxide (DMSO) reductases (DmsABCs) and the methionine sulfoxide reductases (Msrs). Most DmsABCs compared to Msrs are membrane bound enzymes[317] (Figure 4.2) and have mostly been used as whole cell biocatalysts, resulting in suboptimal substrate loadings (only up to 1 $gL^{-1}$) to avoid toxicity to the cells.[318–321]

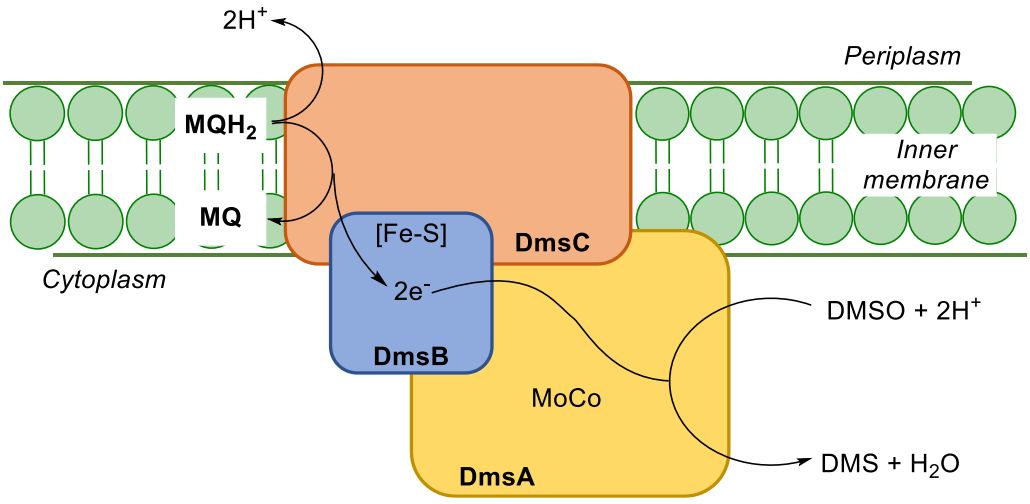


**Figure 4.2.** Diagram of DMSO reductase in *E. coli* where the catalytic subunits, namely the hydrophilic catalytic subunit (DmsA) that bears a pterin molybdenum cofactor (MoCo), the hydrophilic subunit (DmsB) that contains four cysteine groups individually bonded to four [4Fe-4S] clusters and the hydrophobic subunit (DmsC) that anchors the protein to the cell membrane are shown. DmsA and DmsB are orientated towards the cytoplasmic phase of the cell, while DmsC anchors the protein onto the membrane and mediates the electron transfer from menaquinol ($MQH_2$) to DmsAB for the reduction of DMSO to take place.[317]

Some soluble DmsABCs have been identified,[322] but as DmsABCs are trimeric enzymes made up of three non-identical subunits (DmsA, DmsB and DmsC, Figure 4.2), we predicted that they might present challenging expression and purification procedures compared to the monomeric Msrs. In addition, DmsABC catalysed biotransformations must be carried out under inert atmosphere ($N_2$ or Ar) to ensure anaerobic growth of the bacteria and upregulation of the reductase; however, complete oxygen depletion could be a complication if this new methodology is to be used at industrial level. Therefore, due to the drawback that DmsABCs present, we decided to focus on the use of Msrs for the development of a reductive procedure for the kinetic resolution of racemic sulfoxides.

### 4.1.1 Enzymatic kinetic resolution by methionine sulfoxide reductases

The other class of enzymes that can perform EKRs by reducing racemic sulfoxides are methionine sulfoxide reductase (Msr) enzymes, a large class of reductive enzymes found in many organisms.[323]

#### *4.1.1.1 Biological relevance of Msrs*

The fundamental biochemical role of these enzymes is the ability to restore the functionality of damaged proteins containing methionine sulfoxides. The oxidation of surface exposed or free methionine (Met) residues is a posttranslational modification that happens when the cell is under an oxidative stress environment and is generally caused by reactive oxygen species (ROS) produced as by-products of metabolism, apoptotic mechanisms, and other external factors as changes in the environment.[324–327] These result in the formation of diastereomeric mixtures of Met-(*S*)-sulfoxide ((*S*)-MetSO) and Met-(*R*)-sulfoxide ((*R*)-MetSO).[328] The original functionality of proteins containing (*S*)-MetSO and (*R*)-MetSO is then restored by two subfamilies of Msr enzymes, the methionine sulfoxide reductases A (MsrAs) and the methionine sulfoxide reductases B (MsrBs), which respectively reduce (*S*)-MetSO and (*R*)-MetSO back to the original amino acid Met (Figure 4.3).[329,330] Another class of Msr has been identified more recently, namely the free (*R*)-Msr (frMsr), which is instead capable of reducing free (unbound) (*R*)-MetSO (Figure 4.3).[331,332] Although structurally different, the proposed mechanism of action of Msr enzymes *in vivo* involves at least two catalytic cysteine (Cys) residues, one of which attacks and reduces the sulfoxide moiety of MetSO and is simultaneously converted into a cysteine sulfenic acid (Cys-SOH), which subsequently reacts with the second cysteine residue forming an intramolecular disulfide bond (Figure 4.3).

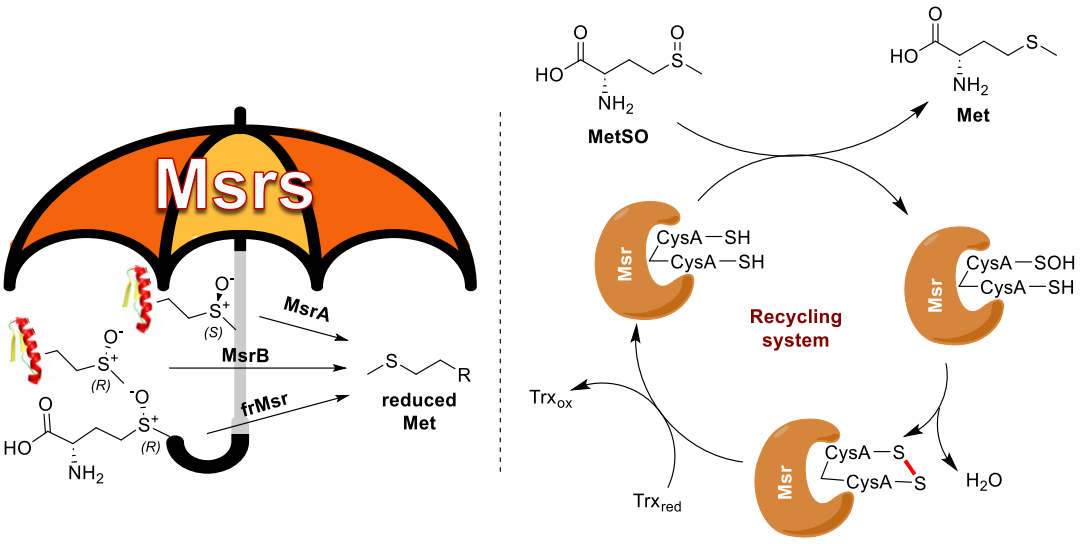


**Figure 4.3.** Schematic representation of the different classes of Msr and their mode of action.

The final step in the Msr enzyme cycle is the regeneration of the active site by reducing the Cys-Cys disulfide bond. In cells this involves the oxidoreductase thioredoxin (Trx) in its reduced form ($Trx_{red}$), which becomes oxidised ($Trx_{ox}$) upon reduction of the Cys-Cys bond in Msr (Figure 4.3).[333–337]

MetSO residues are themselves considered the main signalling molecules for the upregulation of Msrs in cells and tissues[338,339] and the total level of MetSO is regulated by the Msr system, which not only includes Msr enzymes but also thioredoxin (Trx) and Trx reductase ($Trx_{red}$).[327] Levels of expression of each of these individual components can influence the overall reduction of MetSO and the stronger the Msr system, the more resistant the cells are to oxidative stress. It has been shown that a malfunctioning Msr system can have deleterious effects on various signalling pathways. For instance, it has been shown both *in vitro* and *in vivo* that MetSO interferes with the ability of proteins to phosphorylate, in turn causing a cascade of downstream events associate with signal transduction pathways.[340–342] Additionally, high levels of MetSO residues in the calcium/calmodulin-dependent protein kinase II ($Ca^{2+}$/CaM) have been associated with compromised cardiac functions as the enzyme $Ca^{2+}$/CaM remains constantly active and fails to regulate the cellular levels of calcium.[343] Other examples where MetSO residues have been shown to have a negative effect on the physiological activity of cells are glucose homeostasis and mitochondrial function, inflammation and protein degradation.[327] The Msr system has also been associated with age-related diseases as Msr expression levels in mammals have shown to decrease with age.[325,326] Specifically, there is a strong correlation between a less efficient Msr system with a lower antioxidant

capacity and lower levels of MsrAs and MsrBs and neurodegenerative diseases such as Alzheimer and Parkinson diseases.[327] Unfortunately, it is not well understood how the Msr system is affecting ageing and there are no known small molecule inhibitors or activators that can help regulate it.[344] Therefore, due to its physiological and pathophysiological relevance, more in depth investigations on the regulation events of the Msr system are required to lead to new therapeutic approaches.

### *4.1.1.2 Use of Msrs for EKRs*

Following their natural biochemical reactivity, Msrs have also been investigated as biocatalysts to perform the kinetic resolution (KR) of exogenous racemic sulfoxide substrates. Despite their activity being known for decades,[345] only in 1992 Broth *et al.* first sequenced and expressed a recombinant Msr enzyme after cloning the gene from *E. coli*.[346] In 1996 the same group reported the cloning, sequencing and expression of the mammalian homologue of *E. coli* MsrA and showed that this enzyme was active on both natural and synthetic substrate,[347] being able to reduce a variety of sulfoxide containing compounds including (*S*)-(–)-methyl *p*-tolyl sulfoxide. Despite this, advancements in the kinetic resolution of racemic sulfoxides using Msr enzymes happened only in the last few years as the progress and development of more advanced chemical biology techniques allowed research groups to re-evaluate this class of enzymes as biocatalysts. In 2014, Chen and co-workers observed that a strain of *Pseudomonas monteilii* CCTCC M2013683 was capable of synthesising chiral sulfoxides with 99% ee.[348] Later, the same authors reported the cloning and expression of the MsrA gene from *P. monteilii* CCTCC M2013683 (*pm*MsrA).[349] In order to assess the ability of *pm*MsrA to lead to optically pure sulfoxides, the recombinant protein was expressed in *E. coli* BL21(DE3), harvested in the resting phase and subsequently subjected to an activity assay using racemic sulfoxide **79a** (Scheme 4.2).

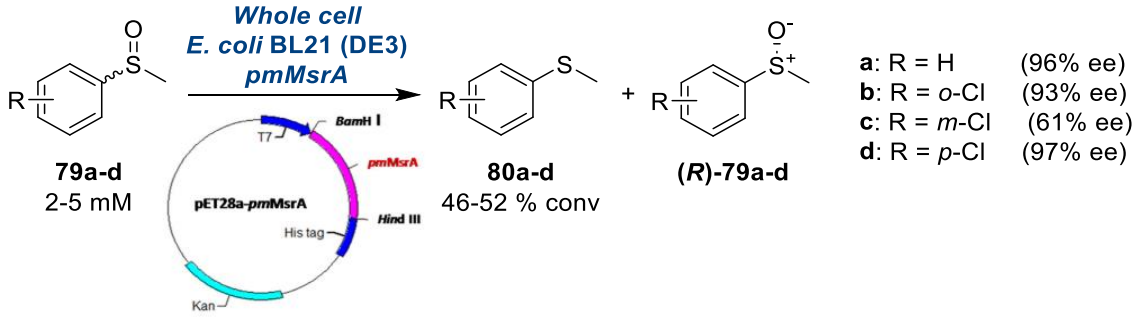


**Scheme 4.2.** Synthesis of sulfoxides using a whole *E. coli* cell system overexpressing *pm*MsrA by Yang *et al.*.[349]

After 24 hours, this whole cell system led to the formation of sulfide **80a** with 51% conversion, leaving sulfoxide **(*R*)-79a** unreacted with >99% ee. Further investigation of *pm*MsrA revealed that the system could tolerate substrate concentrations up to 5.0 mM with an optimal cell density of 40 $g_{cdw}L^{-1}$ yielding 46% **(*R*)-79a** after 16 h reaction and maintaining an excellent 96% ee. The biocatalyst proved to tolerate halogen substitutions on the aromatic ring **79b-d** retaining good-to-excellent ees and conversions. In 2017 Minetti *et al*. reported a recombinant mammalian MsrA showing a similar level of activity and enantioselectivity to Chen's biocatalyst.[350] In this work, a highly stereoselective kinetic resolution of racemic alkyl-aryl-sulfoxides using purified MsrA regenerated by the cheap and widely available dithiothreitol (DTT) was achieved, demonstrating that isolated Msrs and the use of commercial dithiol reducing agents are equally efficient for the synthesis of chiral sulfoxides. Following this work, Chen and Yang developed a crude *pm*MsrA-DTT system that could tolerate substrate concentrations up to 200 mM (37 $gL^{-1}$),[351] and was found to reduce 50 mM and 200 mM **7a** in 30 minutes and 4 hours respectively, retaining >99% ee in both cases (Scheme 4.3).

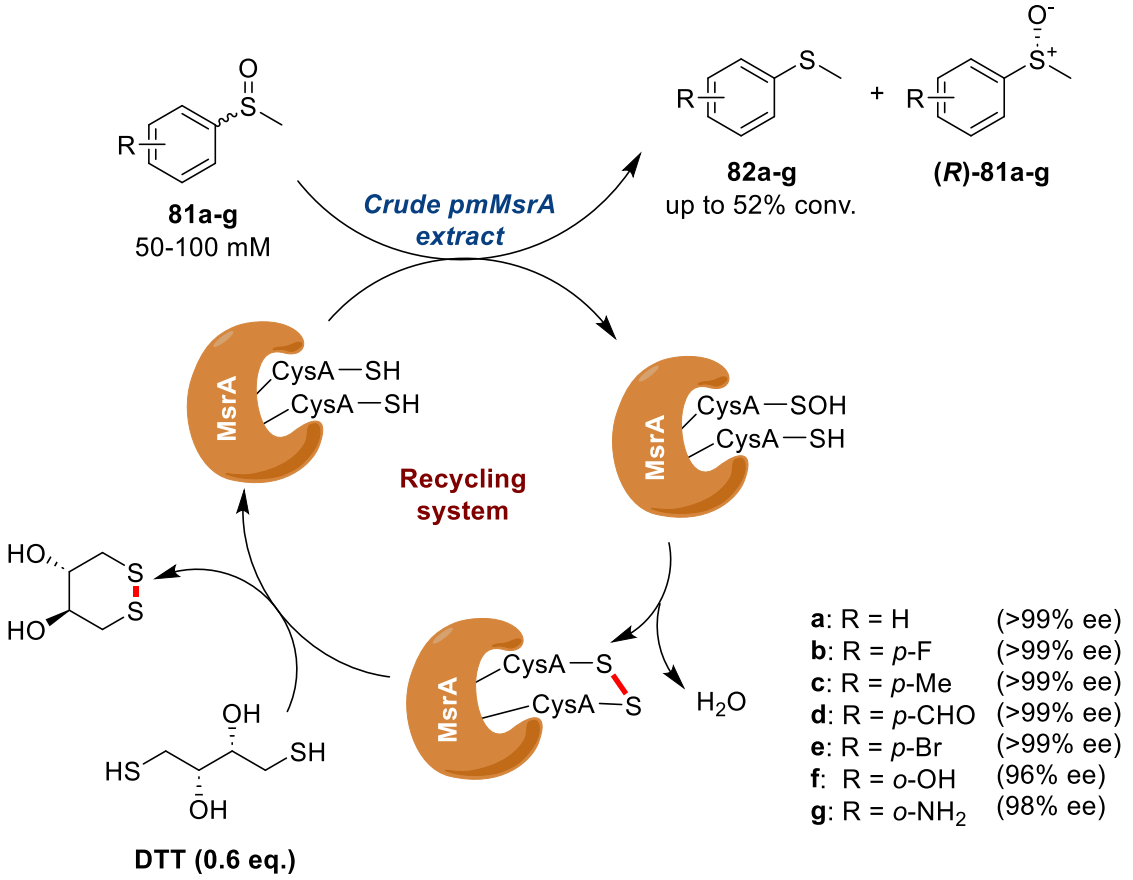


**Scheme 4.3.** Conversions of racemic sulfoxides using the crude *pm*MsrA-DTT system by Chen and Yang.[351]

Theoretically, in this system, only 0.5 equivalents of DTT should be necessary, as **(*R*)-81a** is only half of the overall amount of **81a**. However, it was shown that moving from 0.5 to 0.6 equivalents of DTT was necessary as it was hypothesised that other cellular components in the crude enzyme extract may react and sequester the reducing agent from the regeneration of *pm*MsrA. Chen's *pm*MsrA-DTT system was found to be active on several sulfoxides **81a-g** with excellent conversions and ee (Scheme 4.3). In 2019, Chen's group reported a homologue of *pm*MsrA enzyme from *Pseudomonas alcaliphila*, the biocatalyst *pa*MsrA, that could tolerate substrate loadings up to 320 mM (45 $gL^{-1}$).[352] Four homologues of *pm*MsrA, namely *pc*MsrA, *pf*MsrA, *pa*MsrA and *vh*MsrA sharing 60-90% sequence identities, were identified and all showed similar biocatalytic activity to the parent enzyme in reducing **83a-k** (Scheme 4.4). The crude *pa*MsrA-DTT system exhibited much better catalytic activity and stereoselectivity than other homologues.

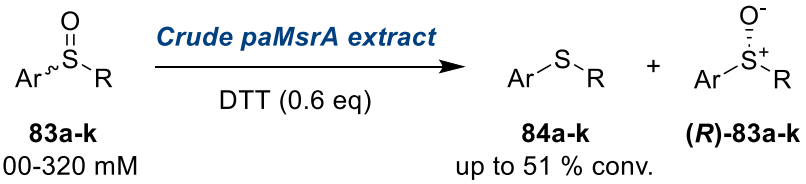


**a**: Ar = Ph, R = Me (>99% ee)
**b**: Ar = *p*-F-$C_6H_4$, R = Me (99% ee)
**c**: Ar = *p*-Me-$C_6H_4$, R = Me (95% ee)
**d**: Ar = *p*-CHO-$C_6H_4$, R = Me (>99% ee)
**e**: Ar = *p*-Br-$C_6H_4$, R = Me (>99% ee)
**f**: Ar = *o*-OH-$C_6H_4$, R = Me (>99% ee)
**g**: Ar = *o*-$NH_2$-$C_6H_4$, R = Me (>99% ee)
**h**: Ar = *m*-$NH_2$-$C_6H_4$, R = Me (>99% ee)
**i**: Ar = *o*-NHAc-$C_6H_4$, R = Me (95% ee)
**j**: Ar = napthyl, R = Me (69% ee)
**k**: Ar = Ph, R = Et (>99% ee)

**Scheme 4.4.** Conversions of racemic sulfoxides using the crude *pa*MsrA-DTT system by Chen *et al.*.[352]

While MsrAs are selective biocatalysts for the reduction of (*S*)-MetSO and other (*S*)-sulfoxides, MsrB enzymes instead are selective for the opposite enantiomer of MetSO, (*R*)-MetSO. However, MsrB enzymes have been shown to be far less active and to have a much higher substrate specificity than MsrAs, thus limiting their use in the synthesis of (*S*)-sulfoxides.[353] In 2020, Chen and co-workers reported the first example of kinetic resolution of alkyl aryl sulfoxides using whole cell *ak*MsrB from *Acidovorax sp.* KKS102.[354] The biocatalyst *ak*MsrB was found among a pool of 6 enzymes that shared 55-92% sequence identity, out of which *ak*MsrB was able to convert the (*R*)-enantiomers of sulfoxides **85a-c** into the corresponding sulfides **86a-c** yielding **(*S*)-85a-c** with >90% ee (Scheme 4.5). Unfortunately, when the same biocatalytic transformation was attempted with the purified enzyme, all activity was lost.

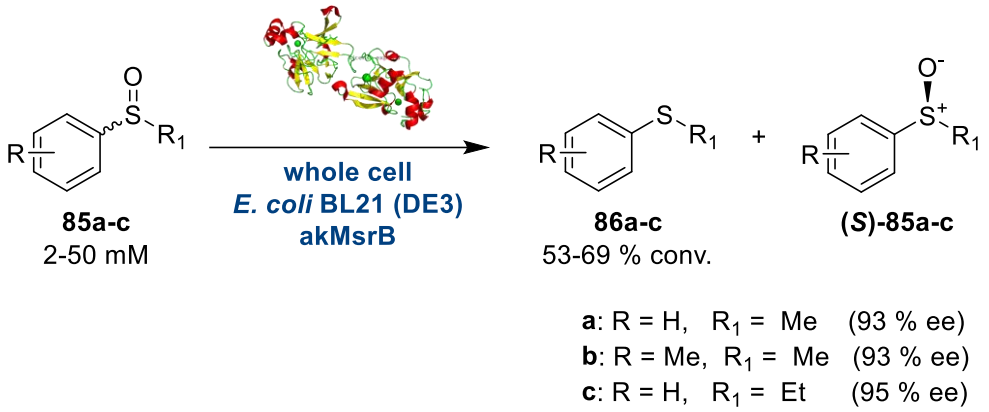


**Scheme 4.5.** Conversions of racemic sulfoxides using whole *E. coli* BL21 (DE3) cell system overexpressing *ak*MsrB by Chen *et al.*.[354]

### *4.1.1.3 Use of Msrs for enzymatic deracemizations*

The main drawback with the use of Msr catalysed processes is that the yield of the enantiopure sulfoxide can only be 50% maximum. Even if the sulfoxide/sulfide products of these biotransformations can be easily separated by chromatography, this may represent a major limitation at industrial level. One of the strategies for improving the conversion and yields of KRs is the deracemization of sulfoxide racemates, where a chemoselective reduction by Msr is coupled with a racemic oxidation using various oxidants. To date only three deracemization of sulfoxides using Msrs have been reported as chemo-enzymatic, photo-enzymatic, or multi-enzyme systems. In 2018, Míšek's group reported a chemo-enzymatic dynamic deracemization of sulfoxides **87a-l** using whole cell *E. coli* BL21(D3) overexpressing MsrA combined with an oxaziridine-type oxidant **89** in a biphasic system (Scheme 4.6).[355] The rationale behind the use of a biphasic system was that once the stereoselective reduction of **87** happened in the aqueous buffer, the oxidation of sulfide **88** using the oxidant **89** could occur in the decane phase (5% *v/v*), without inactivating the biocatalytic system. Sulfoxides **87a-l** were converted into **(*R*)-87a-l** with excellent ee (>99%) and moderate-to-good conversions (55-93%) (Scheme 4.6). The deracemization of the anti-inflammatory drug sulindac was also carried out using this method, leading to (*R*)-enantiomer with 93% ee and 75% conversion. The use of different oxidants (aliphatic peroxides) proved to be detrimental for the biotransformation.[355]

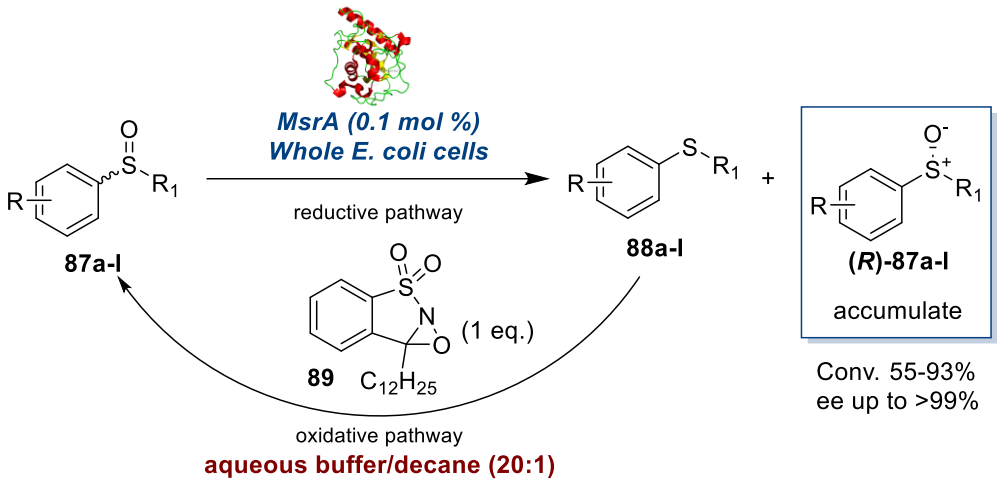


**a:** R = H, $R_1$ = Me; **d:** R = *p*-Me, $R_1$ = Et; **g:** R = *p*-Me, $R_1$ = Me; **j:** R = Bn, $R_1$ = Me;
**b:** R = *m*-Me, $R_1$ = Me; **e:** R = *p*-Br, $R_1$ = Me; **h:** R = *p*-OMe, $R_1$ = Me; **k:** R = Bn, $R_1$ = Et;
**c:** R = *o*-Me, $R_1$ = Me; **f:** R = *p*-CN, $R_1$ = Me; **i:** R = *p*-OH, $R_1$ = Me; **l:** R = $Ph(CH_2)_2$, $R_1$ = Me

**Scheme 4.6.** Deracemization of racemic sulfoxides in a biphasic aqueous buffer/decane system using whole cell MsrA and oxaziridine **18** by Nosek and Míšek.[355]

In 2022 a photo-biocatalytic deracemization of racemic sulfoxides **90a-h** was instead reported by Bierbaumer *et al.*,[356] where the enzyme *pa*MsrA was chosen as the most promising biocatalyst from a pool of Msr enzymes previously studied by Chen *et al.*,[352] and coupled with the photocatalyst **92** isolated from the purple bacterium *Rhodobacter capsulatus* ZY5 for the non-selective oxidation of the sulfide products **91a-h** (Scheme 4.7). Notably, the photocatalyst was shown to be compatible in the aqueous environment of the biocatalytic transformation, achieving excellent ees up to >99%. Other photocatalysts including porphyrin derivatives, $[Ru(bpy)_3]Cl_2$ and Eosin Y were investigated, but lower ees were achieved when coupled with *pa*MsrA. Sulfoxides **90a-i** were converted into **(*R*)-90a-i** with excellent ee (>99%) and good HPLC recoveries (59-91%) Interestingly, when the deracemization of sulindac was attempted using this method, the (*R*)-enantiomer was obtained with 99% ee but with only 43% recovery, indicating that perhaps in this case a KR was occurring. Consequently, the low recovery rate of (*R*)-sulindac and the lack of reported isolated yield, highlight the need for further investigation to ascertain a deracemization over a KR only.

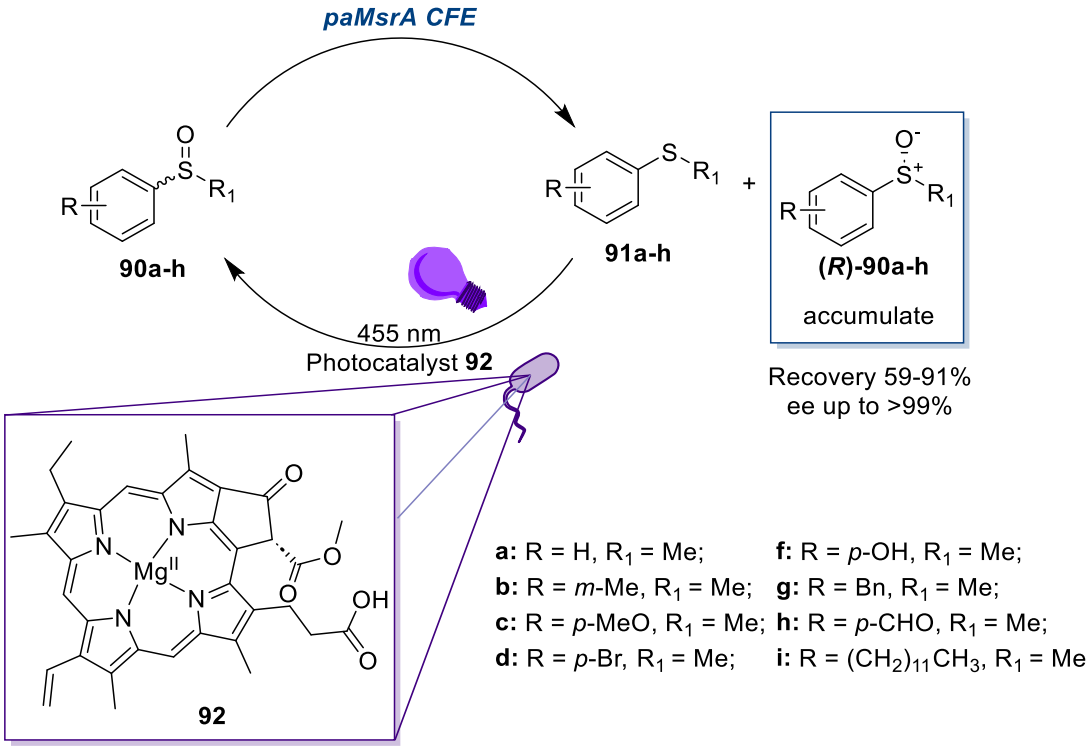


**Scheme 4.7.** Photo-biocatalytic deracemization of racemic sulfoxides using *pa*MsrA and photocatalyst **92** by Bierbaumer *et al.*.[356]

The latest deracemization protocol was published by Peng *et al.*, who reported a 'one-pot one-step' biocatalytic cascade using a highly enantioselective MsrA and a non-selective styrene monooxygenase (SMO) from *Pseudomonas sp.* coupled with a trienzymatic recycling system shared between both biocatalysts (Scheme 4.8).[357] The Msr was chosen from their previous works as it showed excellent enantioselectivity and high substrate scope and tolerance,[348,349,351,352] while the SMO from *Pseudomonas sp.* LQ26 was selected because of its high conversion rates and low stereoselectivity after screening five genetically different enzymes. A combination of the two biocatalytic processes was initially tested on sulfoxide **93a** using whole cell MsrA and SMO as well as stoichiometric NADPH. The deracemization product **(*R*)-93a** was obtained with >99% ee and 72% isolated yield. After proving that the two enzymes can work together for the deracemization of sulfoxides, the focus shifted towards the development of a multienzyme system containing MsrA/Trx/$Trx_{red}$/GDH/SMO as individual CFEs. Glucose dehydrogenase (GDH) was selected to regenerate NADPH for both MsrA and SMO allowing the use of catalytic amounts of the cofactor, while thioredoxin (Trx) and thioredoxin reductase ($Trx_{red}$) were used as the regenerating system for MsrA.

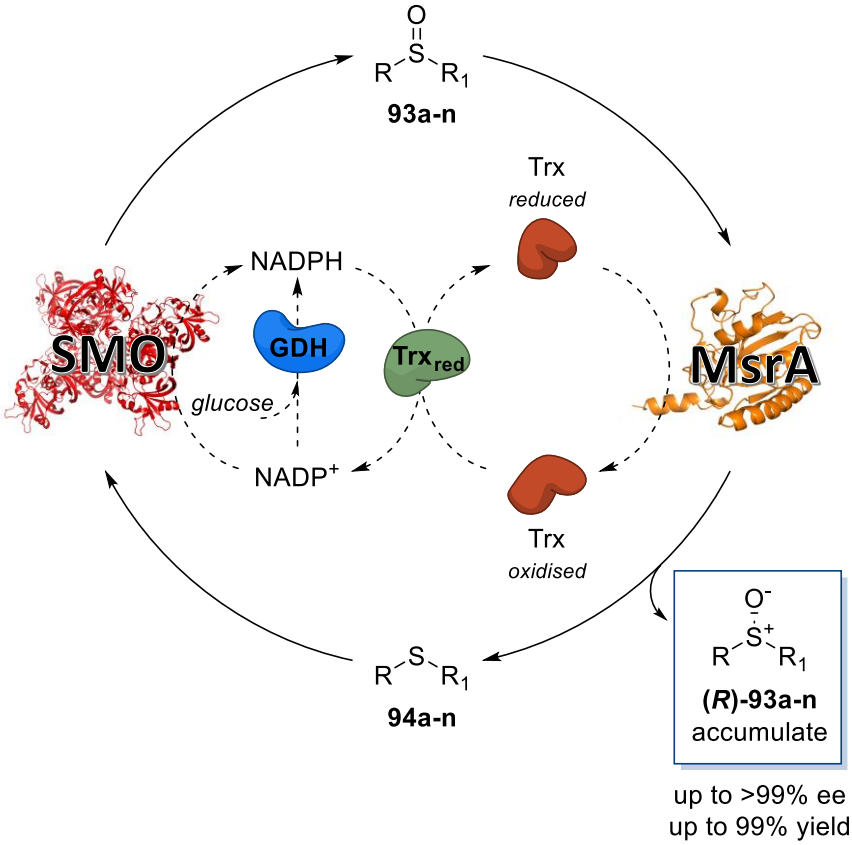


**a:** R = Ph, $R_1$ = Me; **f:** R = 2-OH-$C_6H_4$, $R_1$ = Me; **k:** R = 2-pyrimidine, $R_1$ = Me;
**b:** R = 2-F-$C_6H_4$, $R_1$ = Me; **g:** R = Ph, $R_1$ = Et; **l:** R = $CH_3(CH_2)_2$, $R_1$ = Me;
**c:** R = 2-Cl-$C_6H_4$, $R^1$ = Me; **h:** R = 2-napth, $R_1$ = Me; **m:** R = $CH_3(CH_2)_2$, $R_1$ = Et;
**d:** R = 2-Br-$C_6H_4$, $R_1$ = Me; **i:** R = 4-F-$C_6H_4$, $R_1$ = Me **n:** R = $CH_3SCH_2$, $R_1$ = Me
**e:** R = 2-$NH_2$-$C_6H_4$, $R_1$ = Me; **j:** R = Fn($CH_2$), $R_1$ = Me

**Scheme 4.8.** Multienzymatic deracemization of racemic sulfoxides using MsrA and SMO by Peng *et al.*.[357]

Upon combination of the enzyme, the group reported the successful deracemizations of **93a-n** to afford **(*R*)-93a-l** in excellent ees (89-99%) and yields (86-99%). A scaleup experiment was also carried out with **93m** on a 1 L volume reaction and the enantiopure product **(*R*)-93m** was obtained with 99% ee and 84% isolated yield. Although all these pioneering studies show the remarkable efficacy of MsrA enzymes in the production of (*R*)-sulfoxides via a reductive pathway, additional work is still needed to expand the scope and industrial applicability of these biocatalysts. The main disadvantage is perhaps the applicability of these protocols to only sulfoxides bearing methyl or, in some cases, ethyl alkyl chains on the sterically unhindered part of the molecule. Additionally, the enzymes so far studied as biocatalysts have been sourced only from *Pseudomonas sp.*, mammals, and *E. coli*, indicating the potential discovery of even better catalysts from different species. Furthermore, while the Msr mechanism of reduction of MetSO has

been widely explored, there are currently no studies on the mechanism of the enzymes in which non-natural substrates, like small molecule sulfoxides, are reduced. Lastly, no investigation has been reported on how the features of the three-dimensional structure of Msrs and the modifications thereof affect the biocatalytic process.

## 4.2 Aims of the project

The aim of this research project was to identify novel Msr enzymes that would be used for the kinetic resolution of structurally diverse sulfoxides while simultaneously cultivating a detailed understanding of the mechanism of action of this biocatalytic transformation. This task was initially approached by screening a panel of Msrs from different microorganisms and assessing their use as biocatalysts in the reduction of chiral sulfoxides, which led to the discovery of the highly performing MsrA02 from *Saccharomyces cerevisiae.* Due to the crystallography data of MsrA02 being available in the literature, mutagenesis of cysteine residues and structural NMR studies were subsequently performed as part of a series of mechanistic studies with the aim to understand how the enzyme and sulfoxide substrates interact together and to have a real time analysis of the conformational changes that occur at the active site during the kinetic resolution of racemic sulfoxides. With the mechanistic knowledge in hand, further *in silico* engineering and mutagenesis approaches enabled the rational design and successful development of a series of mutant MsrA biocatalysts with the aim to overcome the limited substrate scope of the currently available MsrAs. This led to the identification of MsrA33, a mutant of MsrA02, which was shown to reduce propyl-containing sulfoxides.

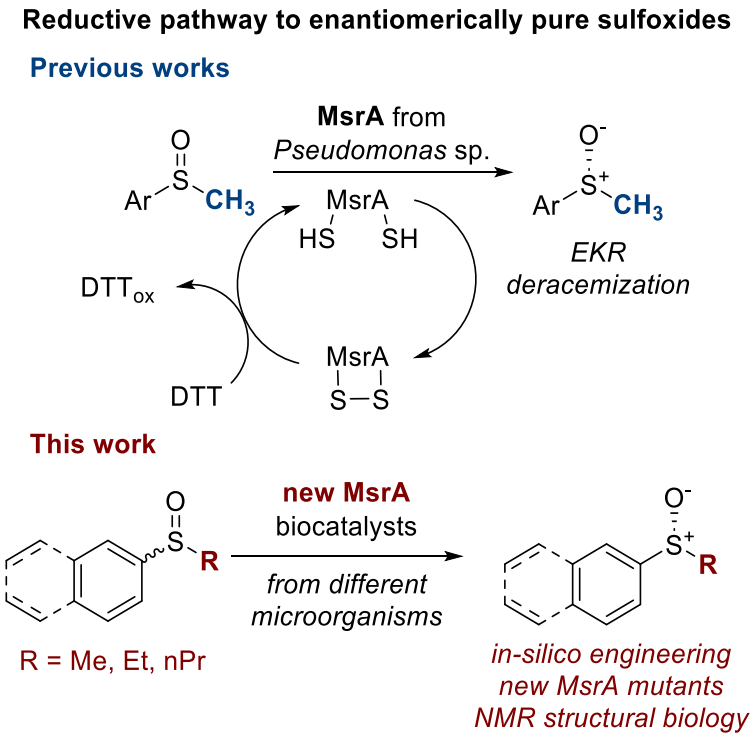


**Figure 4.4.** Biocatalytic approaches for the deracemization of sulfoxides using MsrAs.

## 4.3 Results and discussion

### 4.3.1 Msr02 biocatalysed kinetic resolution of sulfoxides

#### *4.3.1.1 Screening of the Msr panel from Almac*

This project commenced by identifying new Msrs from organisms that could perform KRs of racemic small molecule sulfoxides. A library of 15 Msr enzymes selected from literature and homology searching in public databases was first prepared by Almac and consisted of a panel of diverse biocatalysts from different organisms as well as different Msr types. These enzymes were then cloned into pET28a(+), transformed into BL21(DE3) *E. coli* expression strain and protein production was induced by addition of 1 mM IPTG at 25 °C. After expression, the 15 Msr enzymes were harvested and freeze dried as cell free extracts (CFE) to best preserve their activity over time. The Msrs were then screened for the resolution of the racemic sulfoxide **28af**, with the goal to identify the best biocatalysts able to afford the enantiomer **(*R*)-28af** in high yields and ee.

The biotransformation conditions for the screening were initially adopted from previous works.[351,352] Substrate **28af** was dissolved in *i*PrOH (IPA) and added to a 100 mM KPi buffer solution at pH = 8.0 containing 1.6 $gL^{-1}$ Msr CFE and 4.0 eq. of dithiothreitol (DTT) to regenerate the enzyme. It was postulated that DTT might interact with the cell debris in the CFE and oxidise to the cyclic form, becoming unavailable for the regeneration of the enzymes and leading to a false negative result of the screening. Hence, an excess of DTT was initially used to promote full regeneration of the biocatalyst. The mixture was then shaken at 30 °C for 24 h, after which the yields and ees of the enantiomer **(*R*)-28af** were calculated. The results are shown in Table 4.1. Most of the MsrA enzymes showed excellent enantiospecificity and the enantiomer **(*R*)-28af** was obtained in high yields (up to 50%), except for MsrA18 (Table 4.1, *Entry 14*). Interestingly, all the AB hybrid Msr enzymes showed identical enantioselectivity to MsrAs, affording **(*R*)-28af** still in high ees but generally lower yields than MsrAs indicating that **(*R*)-28af** started being reduced too. Instead, MsrB03, frMsr05 and MsrB21 proved to be unable to reduce the racemic sulfoxide **28af** (Table 4.1, *Entries 3,4 and 15*). This is however unsurprising because both the species of Msr enzymes, B and fr, are believed to be far more specific to their endogenous substrates, protein bound (*R*)-MetSO and free (*R*)-MetSO respectively, and therefore a lower substrate acceptance was expected. After scrutinising the screening of the Msrs, MsrA02 from *Saccharomyces cerevisiae* (Table 4.1, *Entry 2*) was selected as the best enzyme for further studies not only due to the excellent yield and ee, but also because compared to the other promising MsrAs, MsrA02 was the only enzyme that was

not of bacterial origin, as *S. cerevisiae* is a yeast (Baker's yeast) and belongs to the fungi kingdom. It was therefore expected to behave the most different compared to what was reported in the literature already. Furthermore, Baker's yeast is a very commonly studied organism as it is used in daily activities that vary from scientific research to bread making and has the added benefit that several of its enzymes have been fully characterised, including MsrA02. Therefore, it was envisioned that the mechanistic studies would greatly benefit from the structural crystallographic data of Msr02 available in the literature.[335]

**Table 4.1.** Screening of Msr enzymes with sulfoxide **28af**.

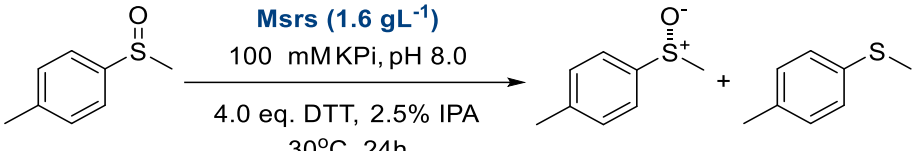


**28af** **(*R*)/(*S*)-28af** **27af**

| Entry | Msr | Msr type | Msr species | 28af yield[a] % | 28af ee[b] % | 28af enant.[b] |
|---|---|---|---|---|---|---|
| *1* | 01 | A | *Escherichia coli* | 51 | >99 | (*R*) |
| ***2*** | **02** | **A** | ***Saccharomyces cerevisiae*** | **50** | **>99** | **(*R*)** |
| *3* | 03 | B | *Escherichia coli* | 90 | 4 | (*S*) |
| *4* | 05 | Free R | *Saccharomyces cerevisiae* | >99 | <1 | n.d.[c] |
| *5* | 07 | A | *Mycobacterium tuberculosis* | 44 | >99 | (*R*) |
| *6* | 08 | AB hybrid | *Neisseria meningitidis* | 44 | >99 | (*R*) |
| *7* | 09 | A | *Staphylococcus aureus* | 55 | >99 | (*R*) |
| *8* | 10 | AB hybrid | *Thermococcus kodakarensis* | 31 | >99 | (*R*) |
| *9* | 11 | A | *Streptomyces griseochromogenes* | 54 | >99 | (*R*) |
| *10* | 13 | AB hybrid | *Streptococcus pneumoniae* | 48 | >99 | (*R*) |
| *11* | 15 | AB hybrid | *Treponema denticola* | 54 | >99 | (*R*) |
| *12* | 16 | A | *Klebsiella pneumoniae* | 50 | >99 | (*R*) |
| *13* | 17 | A | *Salmonella schwarzengrund* | 53 | >99 | (*R*) |
| *14* | 18 | A | *Serratia symbiotica* | >99 | 4 | (*R*) |
| *15* | 21 | B | *Klebsiella oxytoca* | >99 | 1 | n.d.[c] |

[a]HPLC yields are reported. Calculated using an Agilent Eclipse Plus C18 column and methyl phenyl sulfoxide as internal standard (see Appendix VI for calibration curve data). [b]Determined by chiral HPLC using a Chiralpak IC column. [c]Not determined.

*4.3.1.2 Optimisation of the reaction conditions*

Once MsrA02 was selected as the best enzyme, the enzymatic kinetic resolution of **28af** was optimised. The optimal concentration of the biocatalyst was investigated keeping the concentration of **28af** fixed at 8.0 mM and using 4.0 eq. of DTT. Firstly, the time of reaction was shortened to 4 h as the $^{1}$H-NMR yield of the enantiomer **(*R*)-28af** at 18 h and 4 h (Table 4.2, *Entries 1,2*) was identical to the 24 h long experiment from the Msr screening. Therefore, the reactions were carried out at 30 °C for 4 h (Table 4.2, *Entries 2-6*). In general, after 4 h a 50% $^{1}$H-NMR yield of **(*R*)-28af** was observed, suggesting completion of the enzymatic kinetic resolution reaction. The best concentration for MsrA02 was found at 1.0 $gL^{-1}$ (Table 4.2, *Entry 5*) while lower concentrations led to poorer ees and yields. When the reaction was carried out without the enzyme, the sulfoxide **28af** was fully recovered as the racemate (Table 4.2, E*ntry 6*). The optimal concentration of the substrate was then investigated (Table 4.2, *Entries 7-10*). Remarkably, the biocatalytic transformation tolerates concentrations of substrate **28af** up to 32-64 mM, while at higher concentrations **28af** was recovered as a racemic mixture (Table 4.2, E*ntry 10*).

It was also noted that MsrA02 could tolerate changes in some parameters and the outcome of the reduction would not be affected. For instance, a higher temperature (37 $^{o}$C) led to **(*R*)-28af** after 1 h with yield and ee (Table 4.2, E*ntry 11*), which is comparable to the conversion observed at 30 $^{o}$C. Changing the cosolvent IPA with MeOH, EtOH or $CH_3CN$ also did not seem to perturb enzymatic activity (Table 4.2, E*ntries 12-15*). Interestingly, when the reaction was carried out without any cosolvent or in the presence of DMSO, sulfoxide **28af** was recovered as racemate indicating that no reduction took place (Table 4.2, E*ntries 16,17*). It is plausible that DMSO could act as competitive substrate for MsrA02, while in the absence of an organic cosolvent the substrate **28af** is not soluble enough in the buffer media to interact with the biocatalyst. A series of experiments were performed to determine the optimal concentration of DTT. Even though theoretically 0.5 eq. of DTT should suffice to reduce **(*S*)-28af** to **27af** (as it is only half of **28af** racemate), it was found that at least 1.0 eq. of DTT was needed for the regeneration of MsrA02 (Table 4.2, *Entries 18,19*). It was then decided that 1.1 eq. of DTT would be more appropriate conditions to move forward with the scope, as the slight increase would ensure complete regeneration of the enzyme for each EKR reaction. Unsurprisingly, no biocatalytic transformation occurred when no DTT was added to the reaction mixture, confirming its crucial role in MsrA02 regeneration (Table 4.2, *Entry 20* and Figure 4.5). The optimal reaction conditions were combined and set at 1.0 $gL^{-1}$ of biocatalyst, 32 mM of **28af**, 1.1 eq. of DTT and 30 $^{o}$C, leading to **(*R*)-28af** with 48%

isolated yield and 99% ee (Table 4.2, *Entry 21*). Similar results were obtained when a higher concentration of the substrate (64 mM) was used (Table 4.2, *Entry 22*) proving the robustness of the biotransformation. However, for the scope of reaction, the substrate concentration was maintained at 32 mM, as different species of sulfoxides could have poisoned the enzyme at higher concentrations. Lastly, the use of MsrA02 as whole cell biocatalyst (Table 4.2, E*ntry 23*) or as pure enzyme (Table 4.2, E*ntry 24*) led to enantiomerically pure **(*R*)-28af** in identical conversion and ee to the CFE. Where possible, the use of CFE is favoured over whole cell or purified enzymes.

**Table 4.2.** Optimisation of the MsrA02 biocatalysed KR of **28af**.

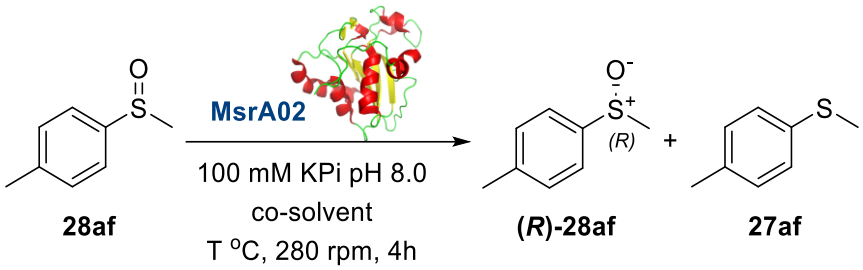


**28af** **(*R*)-28af** **27af**

| Entry | *sc*MsrA[a] ($gL^{-1}$) | 28af (mM) | DTT (eq.) | Co-solvent | Temp °C | (*R*)-28af yield[b] % | ee[c] % |
|---|---|---|---|---|---|---|---|
| *1*[d] | 1.6 | 8.0 | 4.0 | IPA | 30 | 52 | >99 |
| *2* | 1.6 | 8.0 | 4.0 | IPA | 30 | 51 (51)[e] | 98 (>99) |
| *3* | 1.0 | 8.0 | 4.0 | IPA | 30 | 54 (51)[e] | 99 (>99) |
| *4* | 0.4 | 8.0 | 4.0 | IPA | 30 | 53 (52)[e] | 98 (97) |
| *5* | 0.1 | 8.0 | 4.0 | IPA | 30 | 71 (86)[e] | 40 (30) |
| *6* | - | 8.0 | 4.0 | IPA | 30 | >99 | <1 |
| *7* | 1.6 | 16 | 4.0 | IPA | 30 | 54 | 99 |
| *8* | 1.6 | 32 | 4.0 | IPA | 30 | 52 | 99 |
| *9* | 1.6 | 64 | 4.0 | IPA | 30 | 52 (48)[e] | 99 (>99) |
| *10*[f] | 1.6 | 128 | 4.0 | IPA | 30 | 97 | 5 |
| *11* | 1.6 | 8.0 | 4.0 | IPA | 37 | 47 | 99 |
| *12* | 1.6 | 8.0 | 4.0 | MeOH | 30 | 46 | >99 |
| *13* | 1.6 | 8.0 | 4.0 | EtOH | 30 | 50 | >99 |
| *14* | 1.6 | 8.0 | 4.0 | IPA | 30 | 54 | >99 |
| *15* | 1.6 | 8.0 | 4.0 | $CH_3CN$ | 30 | 49 | >99 |
| *16* | 1.6 | 8.0 | 4.0 | DMSO | 30 | 90 | 5 |
| *17* | 1.6 | 8.0 | 4.0 | Neat | 30 | >99 | 5 |
| *18* | 1.6 | 8.0 | 1.0 | IPA | 30 | 45 | 99 |
| *19* | 1.6 | 8.0 | 0.5 | IPA | 30 | 69 (62)[e] | 64 |
| *20* | 1.6 | 8.0 | - | IPA | 30 | >99 | <1 |
| ***21*** | **1.0** | **32** | **1.1** | **IPA** | **30** | **53 (48)[g]** | **99** |
| *22* | 1.0 | 64 | 1.1 | IPA | 30 | 46 | 99 |
| *23* | 10[h] | 32 | 1.1 | IPA | 30 | (52)[e] | >99 |
| *24* | 2.3[i] | 32 | 1.1 | IPA | 30 | (52)[e] | >99 |

[a] MsrA02 used as CFE. [b] $^1$H-NMR yields are reported. [c]Determined by chiral HPLC using Chiralpak IC column. [d]The biocatalytic reaction was carried out for 18 h. [e]HPLC conversion is reported. [f]1h reaction time. [g]Isolated yield. [h]Whole cell MsrA02 10 $gL^{-1}$ was used. [i]Pure MsrA02 enzyme 100 µM was used.

In fact, when using whole cell, not only was the process more sensitive to changes in the reaction environment, but it also resulted in a much more difficult reaction workup and product extraction as the broken cells tend to create emulsions that are very difficult to separate. Instead, while the use of purified enzymes is acceptable in academia, in industry it is largely avoided because the purification process is long compared to the preparation of CFE (1 week vs 2 days) and the purified proteins also need to be stored at lower temperatures compared to the freeze dried CFEs, which results in a less efficient and more expensive production of enzymes.

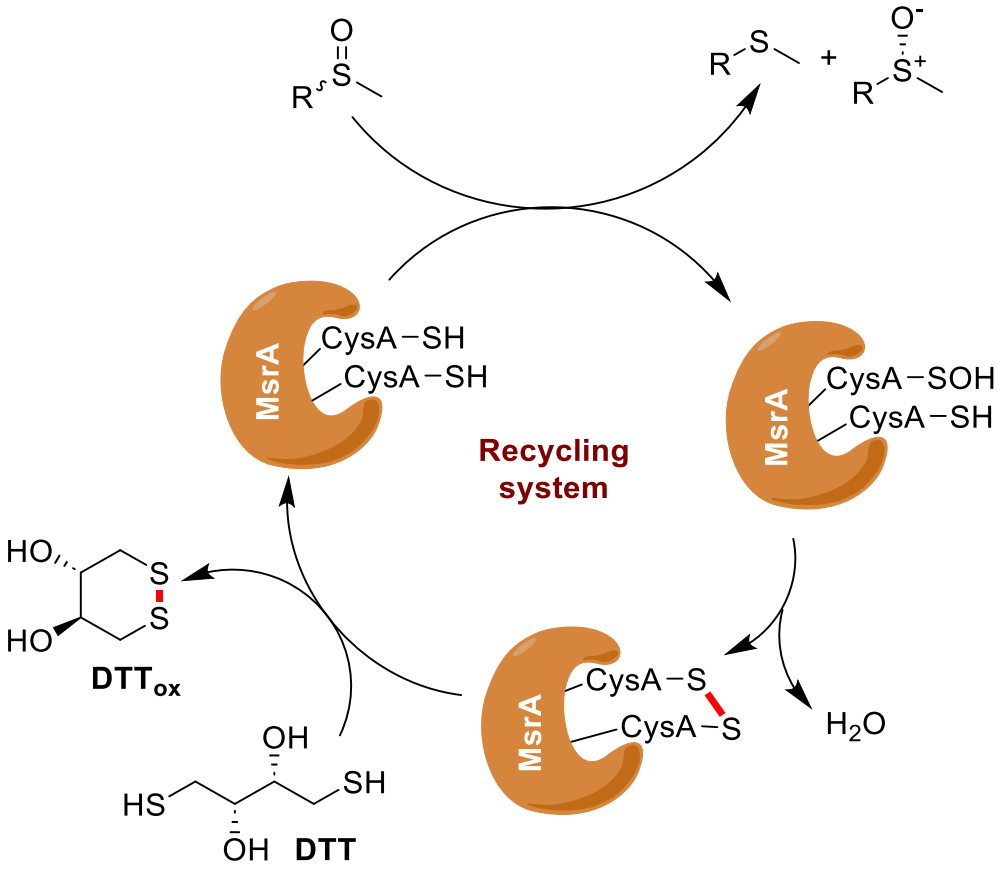


**Figure 4.5.** Proposed mechanism for the reduction of sulfoxides by MsrA biocatalysts.

### *4.3.1.3 Scope of the reaction*

Once the best conditions of the biocatalytic reduction of **28af** were identified, the substrate scope for the MsrA02 biocatalysed reaction was investigated. Results are reported in Table 4.3. The reactions were carried out using 1.0 $gL^{-1}$ of MsrA02 CFE biocatalysts and 32 mM of the sulfoxide substrate unless stated otherwise. Isolated yields are reported for the reaction products. Sulfoxides bearing a small methyl group **28a-ad** (Table 4.3, *Entries 1-11*) were all kinetically resolved by MsrA02 with excellent

ee (99%) and high isolated yields. Interestingly, while the electron donating or withdrawing nature of the phenyl ring substituents did not significantly alter the outcome of the reduction, their position on the phenyl ring seemed to affect the kinetics of the rate of reaction, with sulfoxides **21aa** and **21ad** bearing groups in *ortho* position having the longest reaction times of 28 and 81 h respectively. The effect of the substituents on the reaction time can be explained from a steric hindrance perspective as *ortho* substituents are much closer to the sulfoxide moiety compared to *meta* or *para*, making the first nucleophilic attack from

**Table 4.3.** Substrate scope of the EKR of sulfoxides **28a-e**.

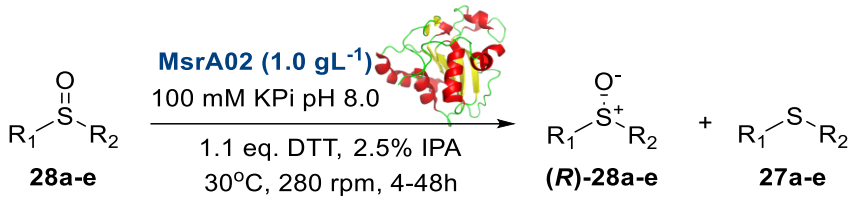


**28a-e** **(*R*)-28a-e** **27a-e**

| Entry | Substrate | $R_1$ | $R_2$ | Time (h) | Isolated yield[a] % | ee[b] % |
|---|---|---|---|---|---|---|
| *1* | **28a** | Ph | Me | 4 | 35 | >99 |
| *2* | **28b** | 4-F-$C_6H_4$ | Me | 6 | 26 | >99 |
| *3* | **28x** | 4-Br-$C_6H_4$ | Me | 6 | 41 | >99 |
| *4* | **28y** | 4-Cl-$C_6H_4$ | Me | 4 | 38 | >99 |
| *5* | **28z** | 3-Cl-$C_6H_4$ | Me | 6 | 40 | >99 |
| *6* | **28aa** | 2-Cl-$C_6H_4$ | Me | 28 | 30 | >99 |
| *7* | **28ab** | 4-Ac-$C_6H_4$ | Me | 4 | 50 | >99 |
| *8* | **28ag** | 4-MeO-$C_6H_4$ | Me | 4 | 43 | >99 |
| *9* | **28ah** | 3-MeO-$C_6H_4$ | Me | 6 | 35 | >99 |
| *10* | **28ac** | 3-Me-$C_6H_4$ | Me | 6 | 48 | >99 |
| *11* | **28ad** | 4,2-Me-$C_6H_3$ | Me | 81 | 41 | >99 |
| *12* | **28ai**[c] | 2-Naph | Me | 28 | n.d.[f] | 74 |
| *13* | **28aj** | 1-Naph | Me | 24 | n.d.[f] | 16 |
| *14* | **28o** | Bn | Me | 24 | 29 | 94 |
| *15* | **28ak** | Dodecyl | Me | 24 | 46 | >99 |
| *16* | **28al** | $CH_3CO(CH_2)_2$ | Me | 24 | n.d.[f] | >99 |
| *17* | **28am** | $PhSO(CH_2)_2$ | Me | 8 | 49 | >99 |
| *18* | **28c** | Ph | Et | 48 | 47 | 90 |
| *19* | **28d**[c] | 4-Me-$C_6H_4$ | Et | 48 | 36 | 98 |
| *20* | **28g**[c] | 4-Br-$C_6H_4$ | Et | 48 | 55 | 80 |
| *21* | **28v**[e] | Bn | Et | 24 | 36 | 96 |
| *22* | **28w** | $Ph(CH_2)_2$ | Et | 8 | 40 | 99 |
| *23* | **28t**[e] | 2-Py$CH_2$ | Et | 24 | n.d.[f] | 54 |
| *24* | **28an**[d] | Ph | *n*Pr | 24 | n.d.[f] | <1 |
| *25* | **28j**[d] | 4-MeO-$C_6H_4$ | *n*Pr | 24 | n.d.[f] | <1 |
| *26* | **28e** | Ph | Allyl | 7d | n.d.[f] | 16 |

[a]Isolated yields after chromatographic purification of the (*R*)-sulfoxide [b]Determined by chiral HPLC using Chiralpak column IG or IC. [c]2.0 $gL^{-1}$ CFE MsrA02. [d]8 mM substrate, 10 $gL^{-1}$ CFE MsrA02. [e]10 $gL^{-1}$ CFE MsrA02. [f]n.d. not determined.

the Cys residue in the active site kinetically unfavourable (Figure 4.6). Effects of the steric hindrance can also be seen in the resolution of naphthyl-bearing sulfoxides **28ai** and **28aj** (Table 4.3, *Entries 12,13*). In both instances the biocatalytic reduction proved to be less efficient compared to **28a-ad**, as **(*R*)-28ai** was obtained in 74% ee and **(*R*)-28aj** in only 16% ee after 28 and 24 h respectively, results attributed to the much bulkier aromatic moieties. It could be hypothesised that the 2-naph group behaves as a phenyl ring with a *pseudo-meta* substituent for **28ai**, and similarly the 1-naph as a *pseudo-ortho* for **28aj** (Figure 4.7). The sulfoxides **28o-am** (Table 4.3, *Entries 14-17*) bearing spacers between the aromatic ring and sulfoxide moiety or alkyl $R^1$ groups on the sulfur atom were also reduced by MsrA02 affording the corresponding (*R*)-enantiomers with high isolated yields (up to 49%) and excellent ee (up to 99%). The diastereomers **(*R*),(*R*)-28am** and **(*S*),(*R*)-28am** were obtained in a 1:1 ratio (see Appendix IV) indicating that only the terminal (*S*)-sulfoxide was fully reduced by the enzyme. MsrA02 showed excellent activity also on the substrates **28c-w** bearing an Et substituent on the sulfur atom with high yields and excellent ees (Table 4.3, *Entries 18-22*).

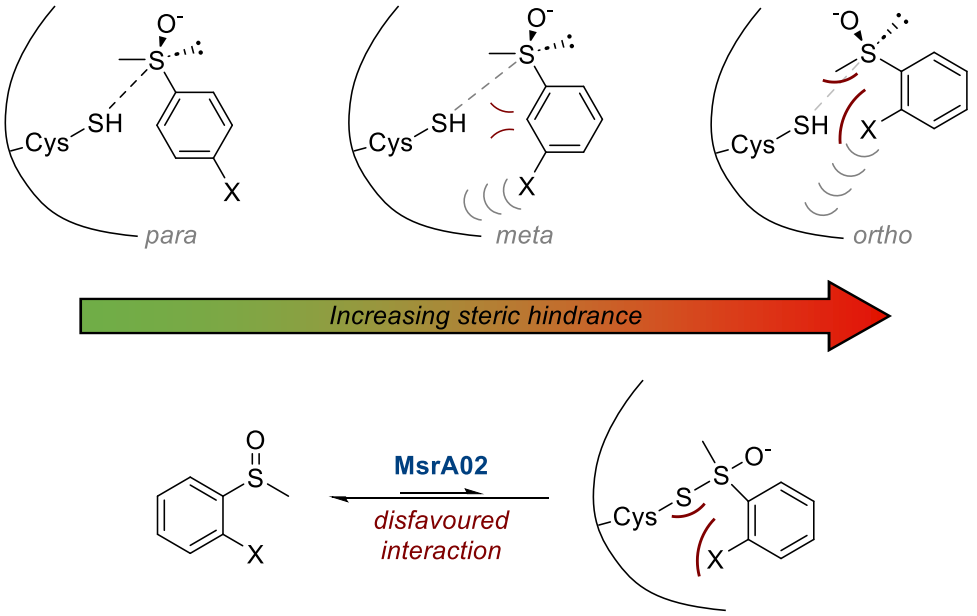


**Figure 4.6.** Steric hindrance effects of aromatic substituents on the nucleophilic attack of cysteine to the sulfoxide moiety.

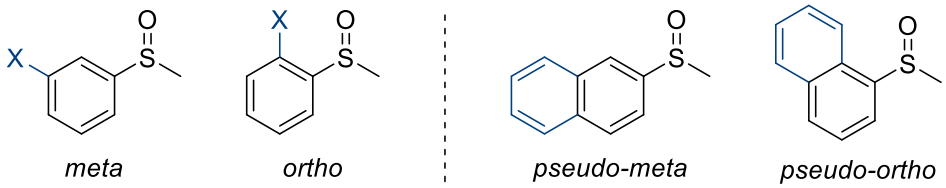


**Figure 4.7.** Behaviour of naphthyl moieties in comparison to *meta* and *ortho* substituents.

Remarkably, for phenyl-bearing **28c-ae** the reaction time was 48 h, which reduced to 24 h for **28v** and 8 h for **28w**. One hypothesis for this behaviour is that the longer the spacing chain between the aromatic ring and the sulfoxide (as for **28v-w**), the more flexible the molecule is and, because the $R^2$ group for these substrates is an Et chain, the added flexibility allows the molecule to easily access the catalytic Cys in the active site whilst avoiding steric hindrance clashes. This also allowed **28v-w** to be obtained in higher ees. However, this cannot be said for the pyridyl derivative **(*R*)-28t**, an analogue of **(*R*)-28v**, which was obtained with only 54% ee after 24 h (Table 4.3, E*ntry 23*). One plausible explanation is that due to the heteroaromatic ring, the electron distribution on the molecule combined with the Et group disfavoured the reduction of the substrate. This is also supported by the comparison between the electron distribution maps of **28t** and **28v** (Figure 4.8) where it is shown that due to the pyridine ring, the electron density of the sulfur atom is slightly increased making it less electrophilic. Lastly, the propyl derivatives **28an** and **28j** as well as the allyl substate **28l** were not reduced by MsrA02 (Table 4.3, *Entries 24-26*).

After the investigation of the scope of the biocatalysed KR, MsrA02 proved to be a valuable addition to the reductive enzymes toolbox as a total of 23 (*R*)-sulfoxides (**(*R*)-28af-t**) were obtained in good to excellent ees up to >99% and yields of up to 50%. This is so far the largest scope of any MsrA enzyme reported in the literature.

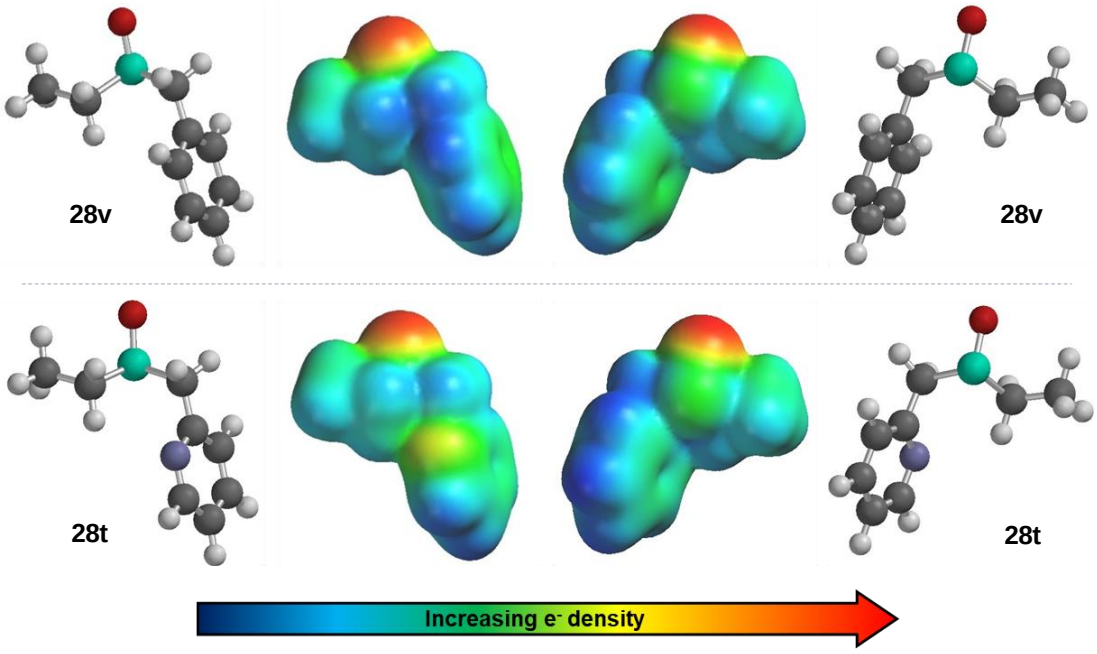


**Figure 4.8.** Electrostatic potential surface (EPS) for **28v** and **28t**.

It must be noted that even if the maximum theoretical yield expected for these reactions was 50%, the empirical isolated yield detected after chromatographic purification was slightly lower due to the difficulties associated with the extraction of the sulfoxide compounds from the buffer media with EtOAc. Nevertheless, in most case the isolated yields obtained were well above 40%. MsrA02 was not deemed a suitable biocatalyst for the reduction of propyl, and allyl sulfoxides **28an-l** but also for the naphthyl derivatives **28ai-aj**. Therefore, the identification of an additional enzyme for the resolution of larger and bulkier substrates was the next logical step in this research project.

#### *4.3.1.4 Identification of other Msrs from Almac panel for the KR of larger substrates*

The search for a biocatalyst capable of resolving the substrates that MsrA02 could not effectively reduce began with an investigation of other enzymes from the initial panel. Four Msrs were selected based on their initial performance with **28af** and on their relevant publications in the literature. For instance, MsrA01 had already been used by other groups for the EKR of non-natural sulfoxides, but the scope had always been limited to less than 10 substrates and hence was chosen to assess its use with larger ones. Instead, MsrAB08 and MsrAB10 were selected because of their structural differences from MsrAs. Furthermore, MsrAB08 had a variety of publications on its structural characterisation in the literature, while MsrAB10 was the only enzyme that furnished **(*R*)-28af** in substantially lower yields (31%) compared to the remaining enzymes, which signified a more efficient reduction activity. MsrA16 instead was selected because it performed very similarly to MsrA02 but did not benefit from structural characterisation. With this selection in hand, screening reactions were performed using the optimised reaction conditions for MsrA02 (32 mM substrate, 1.0 $gL^{-1}$ Msr and 1.1 eq. DTT) for 24 h. The results are reported in Table 4.4. In general, these WT enzymes did not show a significant improvement from MsrA02. However, MsrA10 proved to be highly effective in the reduction of **28ai** when used at 8 mM concentration, affording the (*R*)-enantiomer with excellent >99% ee (Table 4.4, *Entry 1*), whilst still being inactive on the opposite sterically hindered regioisomer 1-naphtyl derivative **28aj** (Table 4.4, *Entry 2*). Some reductive activity was detected for sulfoxide **28l**, where low ees were observed up to 24% with MsrA01 (Table 4.4, *Entry 5*).

**Table 4.4.** Screening of Msr enzymes with bulkier sulfoxides.

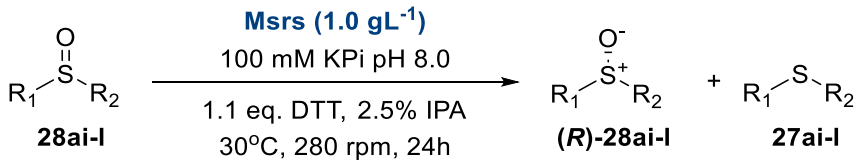


**28ai-l** **(*R*)-28ai-l** **27ai-l**

| Entry | Substrate | $R_1$ | $R_2$ | Msr | ee[a] % |
|---|---|---|---|---|---|
| *1* | **28ai** | 2-Naph | Me | 01 | 9 |
| | | | | 08 | 9 |
| | | | | 10 | 30 |
| | | | | 10[b] | >99 |
| | | | | 16 | 32 |
| *2* | **28aj** | 1-Naph | Me | 01 | <1 |
| | | | | 08 | <1 |
| | | | | 10 | <1 |
| | | | | 16 | 10 |
| *3* | **28t** | 2-PyCH$_2$ | Et | 01 | 20 |
| | | | | 08 | 8 |
| | | | | 10 | <1 |
| | | | | 16 | 14 |
| *4* | **28j** | 4-Me-C$_6$H$_4$ | *n*Pr | 01 | 10 |
| | | | | 08 | <1 |
| | | | | 10 | <1 |
| | | | | 16 | 4 |
| *5* | **28l** | Ph | Allyl | 01 | 24 |
| | | | | 08 | 4 |
| | | | | 10 | <1 |
| | | | | 16 | 18 |

[a]Determined by chiral HPLC using Chiralpak column IG or IC. [b]8 mM substrate.

It was hypothesised that this allylic sulfoxide could have been unstable in the basic aqueous enzymatic environment and had undergone a [2,3]-sigmatropic rearrangement reaction which led to its degradation (Scheme 4.9).

Due to the unsuccessful results from the screening of the panel, rational mutagenesis approaches and structural studies of MsrA02 were adopted for the development of an alternative enzyme to broaden the scope of this biocatalytic transformation.

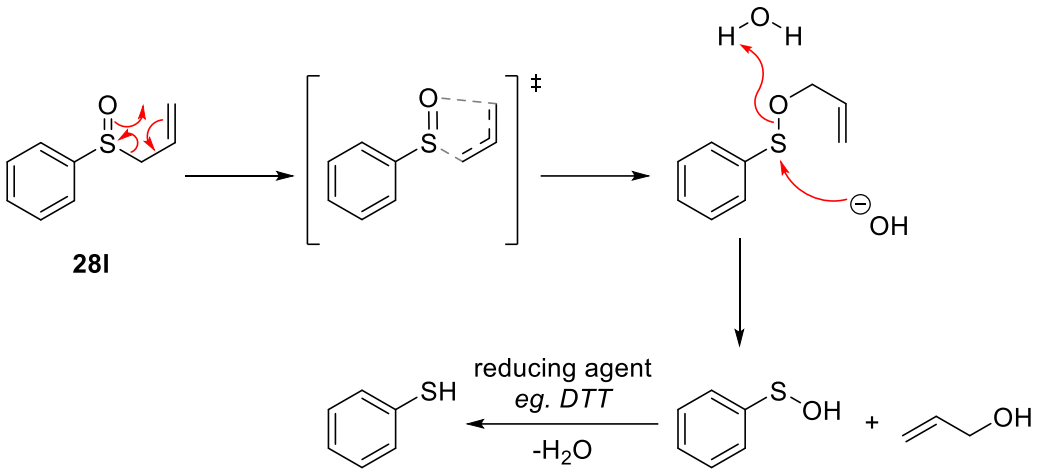


**Scheme 4.9.** Rearrangement mechanism for the degradation of **28l** in a basic aqueous environment.

### 4.3.2 Structural and functional studies on MsrA02

The substrate scope study of this biocatalytic transformation clearly shows the ability of MsrA02 to catalyse the kinetic resolution of sulfoxides bearing a methyl and an ethyl substituent on the sulfur atom. However, bulkier substrates bearing a propyl or an allyl substituent were not reduced by MsrA02 or other MsrA wild type (WT) enzymes in adequate yields and ees. Therefore, the next step in the expansion of substrate scope was to engineer MsrA02 (and potentially other WT enzymes) using rational mutagenesis to develop mutants capable of reducing bulkier sulfoxides. In order to proceed with the mutagenesis studies, single point mutagenesis of Cys residues of MsrA02 and NMR studies of the biocatalytic transformation were carried out with the aim of fully understanding the catalytic cycle of MsrA02 and hence assessing which mutations could be beneficial and which would have deleterious effects on the MsrA activity.

#### *4.3.2.1 MsrA02 homology models for the structural analysis of the active site and mechanism of catalysis*

Although several sequences of MsrAs have been identified, structural characterisation and investigation of the mechanism of action have only been resolved for a few species including *E. coli*,[334,358] *M. tuberculosis*,[359] *N. meningitidis*[333,360–362] and coincidentally *S. cerevisiae.*[335] The alignment of the MsrA sequences from these species is shown in Figure 4.9. It is apparent that the core structures of the MsrA enzymes are conserved and that the alignment shows a great degree of similarity, with the greatest differences in the C-terminal loop. Several crystallography and NMR studies contributed to the

elucidation of the mechanism of action and the identification of the residues responsible for activity. As mentioned previously, all Msr enzymes reduce MetSO in three defined steps: first, in the reductive phase, a Cys residue binds to the MetSO substrate forming a Michaelis-like complex, which then collapses into a sulfenic acid intermediate with the concomitant release of one molecule of Met, then the sulfenic acid forms an intramolecular disulfide bond with a Cys in the C-terminal loop and finally the enzyme is reduced to its original form by thioredoxin (Trx).[323,363–365] For some MsrA enzymes, such as *E. coli*,[334] an extra Cys residue is involved in the mechanism by forming an additional disulfide bridge prior to the regeneration by Trx. In particular, in *S. cerevisiae*, and hence in MsrA02, the active Cys residues are Cys25 and Cys176 (highlighted in yellow in Figure 4.9).[332] Interestingly, in all crystal and NMR structures of the various MsrAs, these two Cys residues (three for *E. coli*) are too far apart for easy interaction, indicating that major

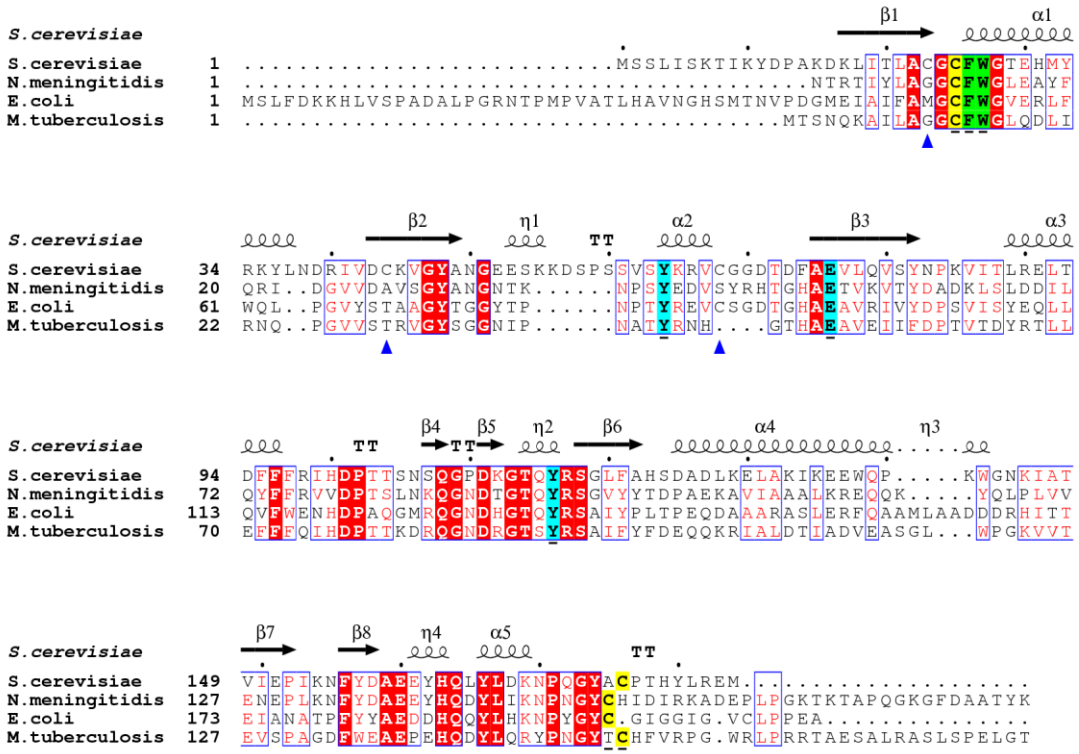


**Figure 4.9.** Sequence alignment of MsrAs from *S. cerevisiae* (UPID: B3LS55, PDB: 3PIL), *N. meningitidis* (UPID: Q9K1N8), *E. coli* (UPID: P0A744) and *M. tuberculosis* (UPID: P9WJM5). *N. meningitidis* is an AB hybrid Msr so the sequence showed here corresponds to the MsrA domain of the enzyme (from residues Asn196 to Thr378). Cys25 and Cys176 are highlighted in yellow, while the hydrophobic pocket formed by Phe26 and Trp27 and the hydrophilic pocket formed by Tyr64, Glu76 and Tyr116 are highlighted in green and cyan respectively. In *S. cerevisiae*, other cysteine residues are represented by blue triangles. Secondary structure features are shown for *S. cerevisiae*. Figure prepared using ESPript.[366]

conformational changes during the catalytic cycle must take place to allow the formation of the disulfide bond. There are three more Cys residues (represented by blue triangles in Figure 4.9), but they are not believed to be involved in the mechanism as they are not conserved in all species.[332] In addition to the cysteine residues, the active site of MsrA02 (and other MsrAs) is also characterised by Phe26 and Trp27 (highlighted in green in Figure 4.9), which form a hydrophobic pocket on one side of the cavity, and Tyr64, Glu76 and Tyr116 (highlighted in cyan in Figure 4.9), which instead constitute a local hydrophilic region on the opposite side.[333,360,365] These two pockets play essential roles in the stabilisation of MetSO during the initial two phases of the catalytic cycle (Scheme 4.10).

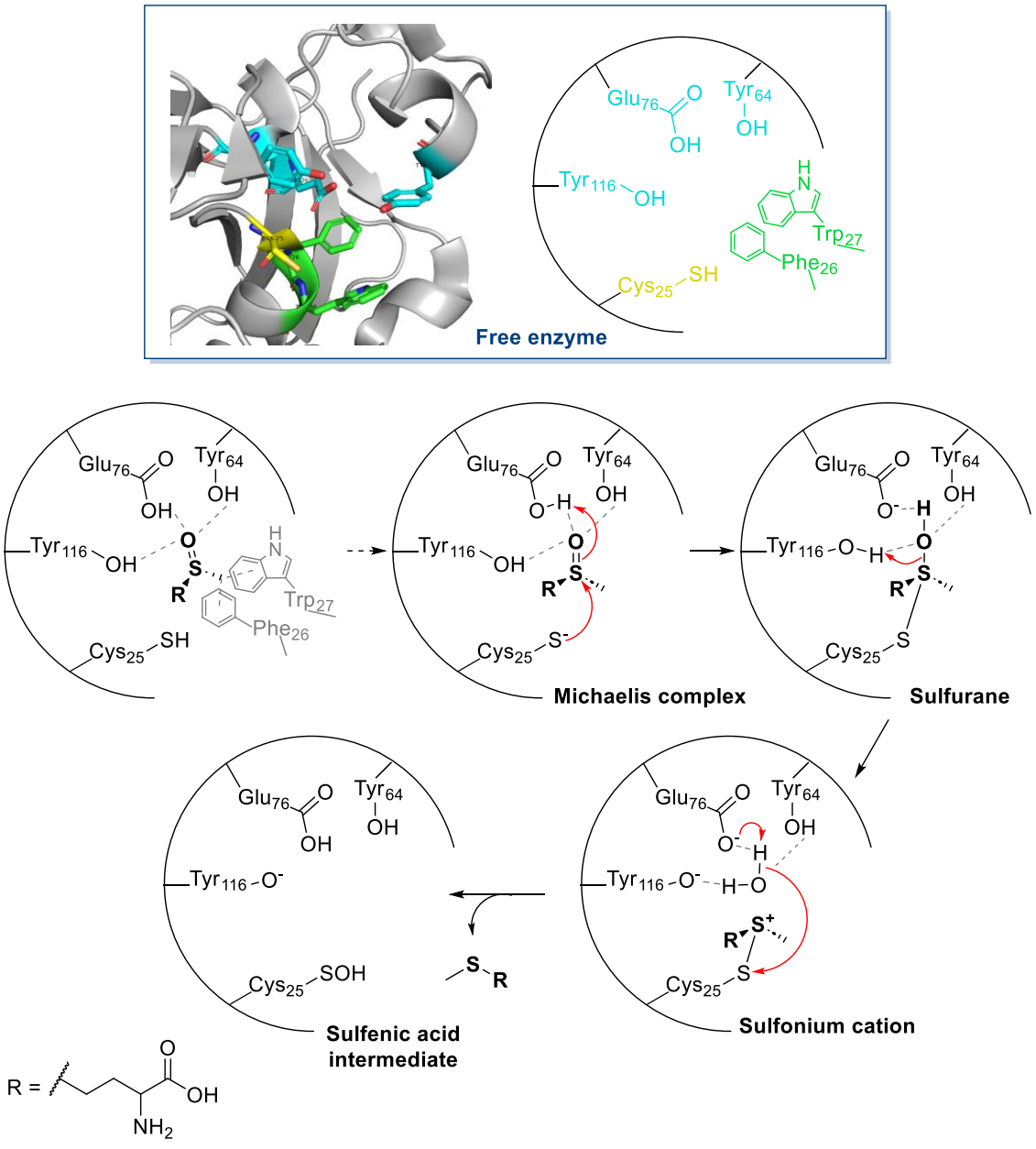


**Scheme 4.10.** Proposed mechanism of MetSO reduction and sulfenic acid formation (PDB: 3PIL).

In fact, the methyl group of MetSO interacts with the hydrophobic pocket formed by Phe26 and Trp27, while Tyr64, Glu76 and Tyr116 are responsible for forming H-bonding interactions with the oxygen of the sulfoxide (Scheme 4.10). Due to these anchoring interactions, the electrophilic sulfur atom on the substrate is now in close proximity (3.3 Å in *N. meningitidis*[333]) to Cys25 forming a Michaelis-like complex. The nucleophilic attack is also favoured because the single S-O bond has now become highly polarised due to the H-bonding interactions of the oxygen and the hydrophilic pocket.[365] Following the nucleophilic attack of Cys25, a sulfurane intermediate is formed in the rate determining step in the reduction of MetSO *via* a proton transfer from the carbonyl of Glu76. A further proton transfer from one of the two Tyr leads to the formation of a sulfonium cation with the concomitant release of a water molecule. This, in turn, is activated by Glu76 and attacks the catalytic cysteine forming the sulfenic acid intermediate and one equivalent of the reduced Met is released.[365]

Interestingly, in all these stages of the reduction, no conformational changes were detected in the structure of MsrA from *S. cerevisiae* and *N. meningitidis*. There are two plausible explanations for these observations. The first is that the conformational changes are happening very quickly and are not observed on NMR timescale. The second is that the active sites of Msrs are optimised to bind the substrate efficiently without the requirement of any conformational rearrangement. The latter is considered the most probable explanation, because, coupled with the shallow shape of the active site on the surface of the enzymes, is what allows MsrAs to access oxidised methionine residues on structurally different peptides.[335]

The second general step in the catalytic cycle of MsrA02 is the formation of a disulfide bridge between Cys25 and Cys176. Crystal and NMR structures of MsrAs show drastic global conformational changes in the backbone of the C-terminal loop, which completely leaves its place and closes towards the active site to bring the second catalytic Cys (Cys176 for MsrA02) into close proximity of Cys25-OH to form a disulfide bond.[333,335] This change in conformation comes with the unwinding of the α2 helix and the movement of the α3-β4 segment. Also, in *N. meningitidis*, the loop where Cys25 is found undergoes a slight reorientation and repositions the residue for a nucleophilic attack by Cys176.[335]

In the final regeneration phase, MsrAs interact with Trx to form an intermolecular disulfide bond that ultimately regenerates the two free catalytic Cys residues. In MsrA02, the disulfide bond exchange happens between Cys176 and Cys31 of Trx and it is believed that the Ala159-His179 segment is directly involved with the binding to Trx.[335]

#### *4.3.2.2 Cysteine to serine single point mutations*

MsrA02 bears five cysteine residues in the protein sequence, namely Cys23, Cys25, Cys44, Cys68 and Cys176. It has been postulated through crystallography and NMR studies that Cys25 and Cys176 are directly involved in the reduction of MetSO, while Cys23, Cys44 and Cys68 do not seem to be involved in the catalytic cycle. It also becomes evident that these residues are not involved in the reduction mechanism when looking at the crystal structure of MsrA02 (PDB: 3PIL), as Cys23, although close to Cys25, is pointing away from the active site and Cys44 is buried in the structure of the enzyme (Figure 4.10). Additionally, Cys23 and Cys44 are completely non-conserved across MsrA species. Instead, Cys68 is much closer to the active site (Figure 4.10) and in some reports, it is hypothesised to interact with the active site in the oxidised crystal form of the enzyme.[335] This is also supported by the fact that Cys68 is conserved in higher organisms, while it is not found in lower ones. Therefore, to confirm the role of the five cysteines in the reduction of **28af**, single point mutations were carried out on MsrA02, where each cysteine was individually mutated into a serine amino acid and five MsrA02 mutants (C23S, C25S, C44S, C68S and C176S) were then produced in *E. coli* T7 express cells. Serine was chosen because it has a similar shape and size to cysteine but is unable to form disulfide bonds.

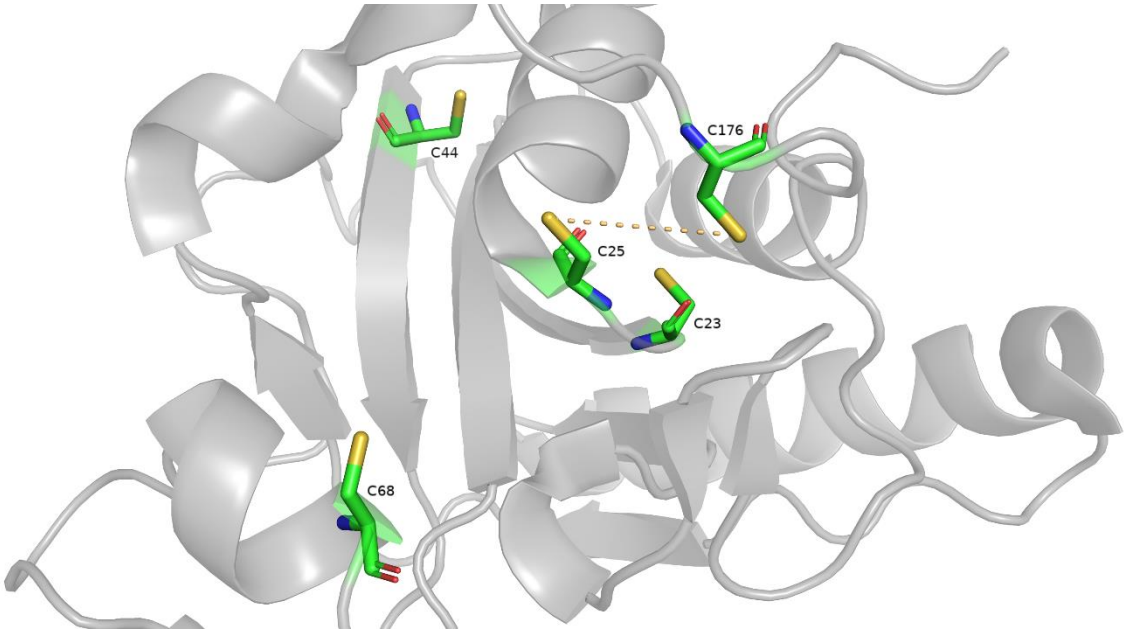


**Figure 4.10.** Crystal structure of MsrA02 (PDB: 3PIL) with the five cysteine residues highlighted as sticks. C25 and C176 are key residues in the active site. Generated with Pymol.

The results of the reactions using Msr02 cysteine mutants on **28af** are reported in Table 4.5. Even though reactions were initially carried out using the optimised conditions of reactions found for WT MsrA02, experiments were also carried out at higher concentrations of the biocatalysts to avoid negative results potentially due to lower enzyme concentration in the CFE and lower reaction rates of the mutants. As predicted, the sulfoxide reducing activity of MsrA02_C25S and MsrA02_C176S was significantly affected and, in both cases, **28af** was recovered as a racemate (Table 4.5, *Entries 2,5*). Interestingly, when MsrA02_C176S was used at 40 $gL^{-1}$, a 36% ee was obtained. It was hypothesised that this was due to the catalytic activity of the untouched Cys25, which could still reduce **28af** in a stoichiometric fashion. These results once again confirm that Cys25 and Cys176 are the two key residues involved in the catalytic cycle, even when non-natural sulfoxides like **28af** are used. Then, the KR of **28af** was not affected when the MsrA02_C44S mutant was employed and **(*R*)-28af** was obtained with 99% ee at 10 $gL^{-1}$ of mutant CFE (Table 4.5, *Entry 1*), which is in line with the reported literature and confirms that Cys44 has no role in the catalytic cycle of MsrA02.

**Table 4.5.** Results of MsrA02 cysteine mutants catalysed reduction of **28af**.

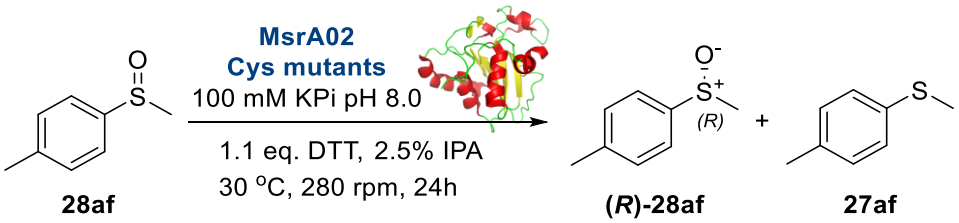


**28af** **(*R*)-28af** **27af**

| Entry | Single point mutation | Enzyme conc. / $gL^{-1}$ | ee%[a] |
|---|---|---|---|
| *1* | C23S | 1.0 | 26 |
| | | 10 | 67 |
| | | 40 | 80 |
| *2* | C25S[b,c] | 0.23 | <1 |
| | | 2.3 | 8 |
| | | 9.2 | 21 |
| *3* | C44S | 1.0 | 9 |
| | | 10 | 99 |
| | | 40 | >99 |
| *4* | C68S[b,c] | 0.23 | >99 |
| | | 2.3 | >99 |
| | | 9.2 | >99 |
| *5* | C176S | 1.0 | 4 |
| | | 10 | 26 |
| | | 40 | 36 |
| *6* | WT | 1.0 | >99 |

[a]Determined by chiral HPLC using Chiralpak column IG. [b]Purified mutant MsrA02 enzyme used. [c]$gL^{-1}$ of protein concentration calculated from 10, 100 and 400 µM.

MsrA02_C68S also seemed to have no negative effects on the catalytic activity of the enzyme, as even at low concentrations (0.23 $gL^{-1}$ of pure enzyme) >99% ee is obtained (Table 4.5, *Entry 4*). Interestingly, instead, the mutation of the other totally unconserved cysteine residue, Cys23, led to **(*R*)-28af** with poor ees (Table 4.5, *Entry 1*), especially at low concentration of the enzyme. An overlap of the structure of the WT enzyme with the C23S MsrA02 mutant one revealed that while Cys23 is not directly involved in the catalytic cycle for the reduction of sulfoxide **28af**, the replacement of this cysteine with a serine residue destabilises the binding pocket (Figure 4.11). In fact, in MsrA02_C23S, the hydroxide group on the serine side chain binds to Thr29 through an H-bond interaction (Figure 4.11), leading to a significant conformational change in the nucleophilic Cys25, which is now oriented away from the active site and is probably less available for nucleophilic attack on the sulfoxide substrate (computational studies performed by Dr. Carvalho, Almac).

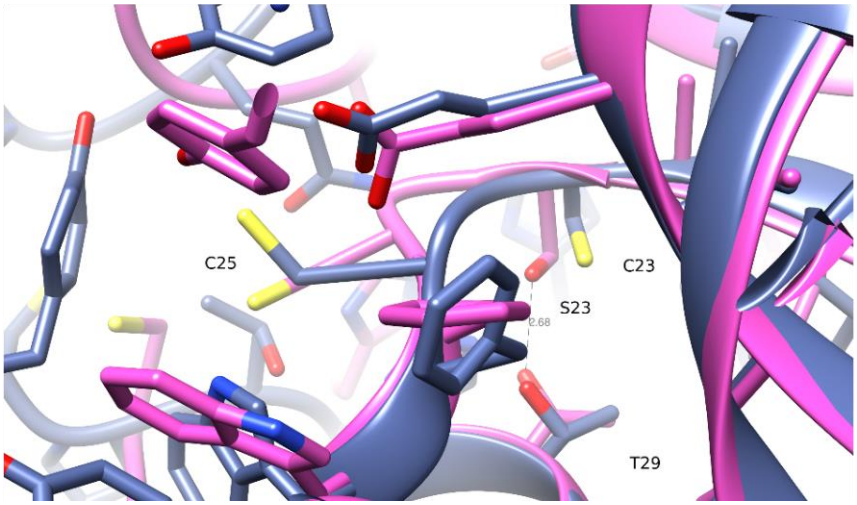


**Figure 4.11.** Comparison between the active sites of the WT enzyme (purple) and the C23S variant (magenta). The serine hydroxide sidechain makes an H bond with Thr29, significantly changing the loop of the Cys25.

### *4.3.2.3 NMR structural and mechanistic studies*

To further investigate and elucidate the dynamics of the catalytic cycle, an NMR structural study of the biocatalyst MsrA02 was carried out in collaboration with Dr Ortega-Roldan and Ms Serrano-Sanchez from the University of Kent. The $^{15}N$- and $^{13}C$- labelled MsrA02 enzymes were prepared at King's College London and the biocatalytic reduction of the sulfoxide **28af** was studied by $^{15}N$-NMR. The $^{13}C$,$^{15}N$-labelled MsrA02 was used to assign most of the peaks of the protein in the NMR spectrum (Figure 4.12, Part A).

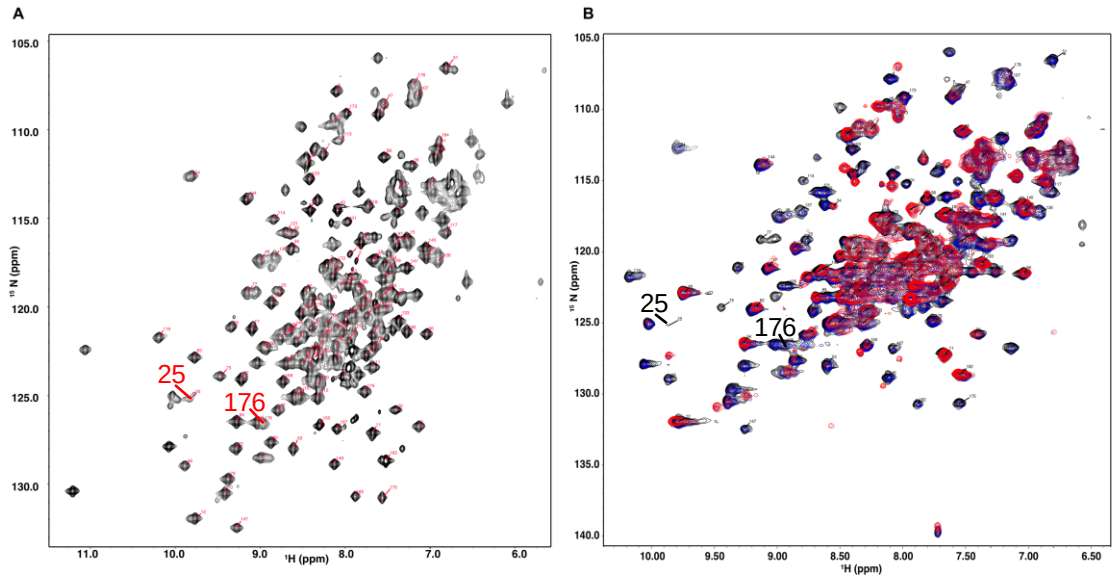


**Figure 4.12.** $^{15}$N HSQC spectrum of MsrA02. Part A) Assigned $^{15}$N HSQC of MsrA02 in its free, reduced form. Part B) $^{15}$N SOFAST HMQC of MsrA02 collected at increasing **28af** concentration of 0 mM (black), 0.5 mM (blue) and 1 mM (red).

The $^{15}$N-HSQC spectrum, containing one cross peak for every amide bond in the protein, was collected and, using a standard suit of triple resonance NMR experiments, around 70% of the backbone resonances were identified, allowing us to identify residues involved in the catalytic activity. SOFAST HMQC experiments were subsequently collected at increasing substrate **28af** concentrations in the presence of DTT, resulting in modulation of both intensities and chemical shift positions of a subset of NMR resonances following a slow exchange regime (Figure 4.12, Part B). A comparison of the decay of intensities upon substrate addition at 0.5 and 1.0 mM shows that at the lower concentration of **28af** the most affected region of the protein is around Cys25, including the beta strand at positions Phe74-Glu76 (Figure 4.13, in blue), suggesting that the catalytic activity starts with the engagement of Cys25 with the substrate. In fact, a large change in the chemical shift of amino acid residues usually is a result of substantial change in the conformation of parts of the protein, indicating potential interactions of the enzyme with the substrate. At 1.0 mM of **28af**, large intensity changes extend from the Cys25 to the whole beta strand between residues Phe74-Val80 and the area around it, reaching Cys176 and its neighbouring residues (Figure 4.13, in red). Such changes suggest that once the substrate is bound to Cys25, the area around Cys176 is involved in the catalytic cycle, supported by the changes occurring in the helical region between residues Glu161 to Gln172. The largest chemical shift changes between the free and bound state are also found in the patch surrounding Cys25, Cys176, and the central beta strand (Figure 4.13, in cyan). The spectrum for the bound state of the protein shows

broader peaks, indicating that substrate binding induces significant dynamics on the structure of MsrA02. Further addition of DTT reverts the spectrum of MsrA02 back to the apo form one.

**Figure 4.13.** Cartoon representation of the MsrA02 structure (PDB: 3PIL) with the residues involved in the catalytic cycle of **28af** highlighted. Residues with resonances undergoing significant intensity losses upon addition of 0.5 mM or 1 mM of **28af** are labelled in blue or red, respectively. Residues with resonances undergoing significant chemical shift differences between the free and bound forms are labelled in cyan. Cys25 and Cys176 sidechains are shown for clarity.

### 4.3.3 Mutagenesis studies and development of new Msr mutants

Once the role of the cysteine residues of MsrA02 was confirmed by mutagenesis and the structural changes of the enzymes upon substrate binding were resolved using NMR, the generation of mutant enzymes able to accept sulfoxide substrates bearing substituents on the sulfur atom different from a methyl group was then investigated.

#### *4.3.3.1 In silico studies: docking of **28ag** and **28j** and design of new mutants*

The first step towards the design of new mutant MsrA enzymes began with an *in silico* investigation on the difference in the binding between smaller and larger substrates with the WT MsrA02 active site. Therefore, the substrates **28ag** and **28j**, bearing respectively a methyl and a *n*-propyl chain on the sulfur atom, were docked by Dr Carvalho, from

Almac, into the active site of WT MsrA02 (Figure 4.14). As previously mentioned, other than the two key cysteines Cys25 and Cys176, the hydrophobic pocket formed by Phe26 and Trp27 and the hydrophilic region formed by Tyr64, Glu76 and Tyr116 play a key role in the selectivity of the reaction as well as on the stability of the active site of the enzyme. In the case of **28ag**, the docking simulations showed that Tyr174 was also important to position the catalytic Cys25 at a distance of 3.55 Å from the S=O group of **28ag** and facilitates the nucleophilic attack on the substrate (Figure 4.14, a). However, when substrate **28j** was docked into the MsrA02 active site, the sulfoxide group was now at a distance of 6.60 Å from Cys25, which is too far for the nucleophilic attack to effectively take place (Figure 4.14, b), thus explaining the lack of activity of MsrA02. This was likely due to steric hindrance clashes between the bulkier *n*-propyl side chain and the residues of the active site, particularly with Phe26 and Trp27 in the hydrophobic pocket. Therefore, a series of nine mutant enzymes of WT MsrA02 (Table 4.6, *Entries 1-9*) were computationally designed, targeting different areas of the enzyme with the aim of allowing a shorter distance between the sulfoxide group of **28j** and the Cys25 residue.

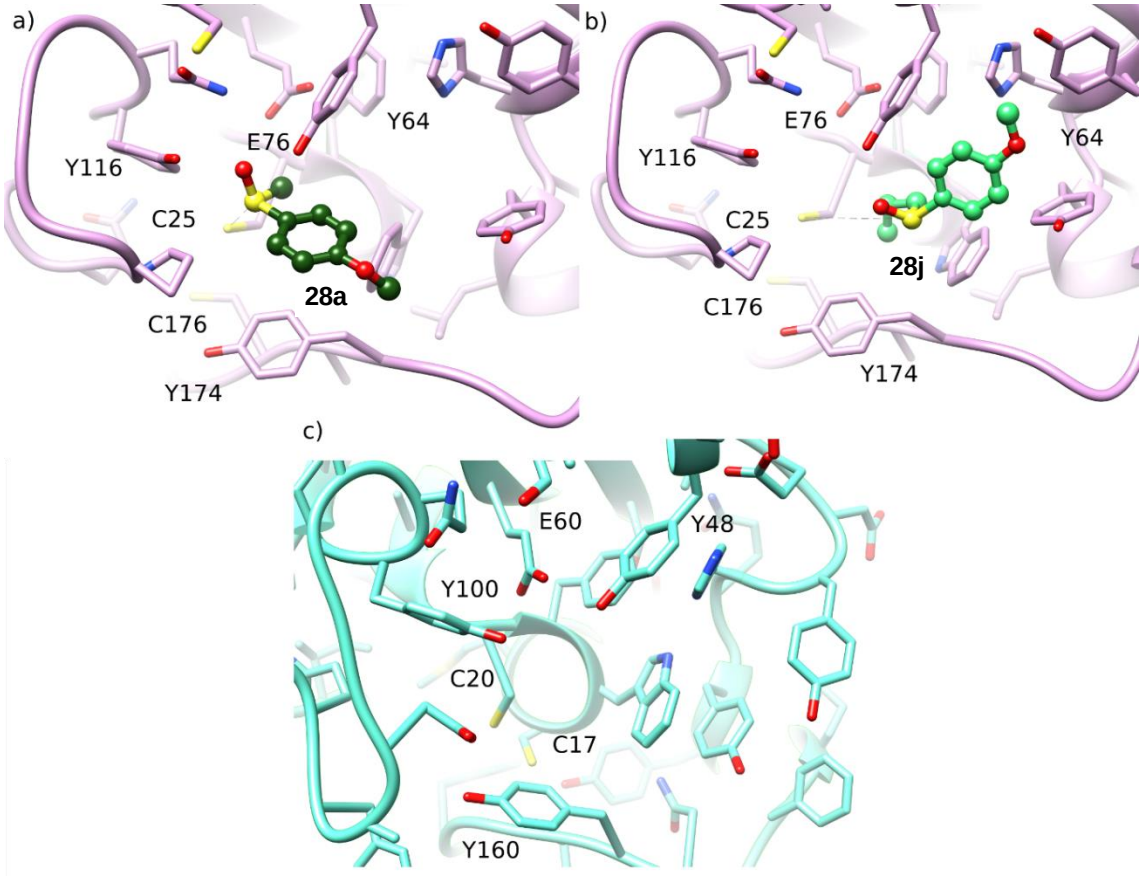


**Figure 4.14.** a) Docking of sulfoxide **28ag** in MsrA02; Tyr174 keeps Cys25 close to the sulfoxide group. b) Docking of the sulfoxide **28j** in MsrA02. c) Overlap of MsrA10 (light green) over MsrA02 (grey). The second cysteine residue of MsrA10 is not in C-terminal region.

**Table 4.6.** New panel of structurally different MsrA enzymes containing 12 mutant enzymes from WT MsrA02 and MsrA10 and 7 new WT MsrAs.

| Entry | Mutant MsrA code | WT MsrA | WT residue | Mutant residue | Position |
|---|---|---|---|---|---|
| *1* | MsrA31 | 02 | Cys68 | Thr | α2-helix |
| *2* | MsrA32 | 02 | Trp27 | Phe | Pocket |
| *3* | MsrA33 | 02 | Phe26 | Tyr | Pocket |
| *4* | MsrA34 | 02 | Gly28 | Cys | α1-helix |
| *5* | MsrA35 | 02 | Leu167 | Phe | C-terminal loop |
| *6* | MsrA36 | 02 | Tyr174 | Lys | C-terminal loop |
| *7* | MsrA37 | 02 | Tyr174 | Leu | C-terminal loop |
| *8* | MsrA38 | 02 | H179 | Arg | C-terminal loop |
| *9* | MsrA39 | 02 | Gly28<br>Tyr174 | Cys<br>Lys | Pocket and C-terminal loop |
| *10* | MsrA40 | 10 | Ser52 | Thr | α2-helix |
| *11* | MsrA41 | 10 | Phe18 | Tyr | Pocket |
| *12* | MsrA42 | 10 | Tyr169 | Lys | C-terminal loop |

| Entry | New WT Msr | Organism |
|---|---|---|
| *13* | MsrA43 | Unspecified bacterium |
| *14* | MsrA44 | *S. piezotolerans* |
| *15* | MsrA45 | *B. solimangrovi* |
| *16* | MsrA46 | *Archaeon* |
| *17* | MsrA47 | *C. Aenigmarchaeota archaeon* |
| *18* | MsrA49 | *Lentisphaerae* bacterium |

The design of appropriate mutants proved to be more complicated than predicted because of the high degree of flexibility of the enzyme active site. In fact, single point mutations would affect the ability of the enzyme to maintain flexibility and activity was lost. In particular, mutations in the pocket seemed to affect the selectivity of the reduction, while alterations in the C-terminal loop would be detrimental to the stability of the enzyme. MsrA10, another novel enzyme that showed good activity on the substrate **21m**, was also investigated for rational mutagenesis. Interestingly, when the structures of MsrA02 and MsrA10 were overlapped (Figure 4.14, c), it was realised that the second cysteine recycling was found on the same α1-helix as Cys25 and not in the C-terminal loop as in MsrA02. Therefore, mutations in the C-terminal region were expected to not affect the stability and activity of MsrA10 mutants. Thus, three additional MsrA10 mutants bearing mutations in different areas of the enzyme were designed and produced (Table 4.6, *Entries 10-12*). Finally, six new WT MsrA enzymes that show different C-terminal regions of MsrA02 were also selected from the literature and homology searches in public databases (Table 4.6, *Entries 13-18*) and added to the new panel of MsrA prepared for screening on substrate **28j**.

### *4.3.3.2 Screening of novel mutant and WT enzymes Almac panel*

The new MsrA02 and MsrA10 mutants and WT enzymes were cloned and expressed in *E. coli* BL21(DE3) under the same conditions as the original panel of Msr enzymes and prepared as CFE in 96-well plates. The **28j** *n*-propyl substrate was used at a concentration of 8 mM, while the enzymes were diluted to 10 $gL^{-1}$ in 100 mM KPi at pH 8.0 containing 1.1 eq. DTT. The plates were incubated for 24 h at 30 °C and 1000 rpm and the ees were analysed by normal phase chiral chromatography. The results of the screening are reported in Table 4.7. The best mutant enzyme was found to be MsrA33, followed by MsrA31 and MsrA32, all of which afforded **(*R*)-28j** in moderate ees of 46%, 34% and 18% respectively. Unfortunately, the rest of the panel including MsrA10 mutants and new WT MsrAs did not appear to be active towards the reduction of **28j**. Interestingly, MsrA32 and MsrA33, which partially reduced **28j,** bear mutations in the hydrophobic pocket responsible for anchoring the methyl group of MetSO into the active site.

**Table 4.7.** Screening of MsrA mutants and new WT MsrA.

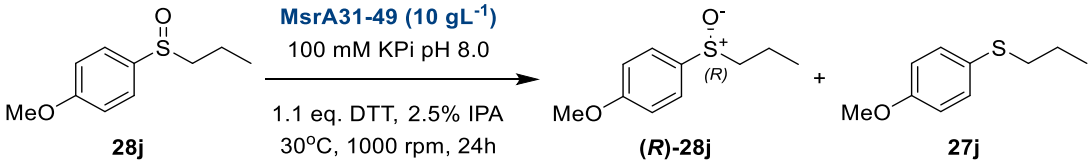


| Entry | Enzyme | (*R*)-28j ee[a] % |
|---|---|---|
| *1* | MsrA02 WT | <1 |
| *2* | MsrA31 | 34 |
| *3* | MsrA32 | 18 |
| *4* | MsrA33 | 46 |
| *5* | MsrA34 | <1 |
| *6* | MsrA35 | 13 |
| *7* | MsrA36 | <1 |
| *8* | MsrA37 | <1 |
| *9* | MsrA38 | <1 |
| *10* | MsrA39 | <1 |
| *11* | MsrA40 | <1 |
| *12* | MsrA41 | <1 |
| *13* | MsrA42 | <1 |
| *14* | MsrA43 | <1 |
| *15* | MsrA44 | <1 |
| *16* | MsrA45 | <1 |
| *17* | MsrA46 | <1 |
| *18* | MsrA47 | 6 |
| *19* | MsrA49 | <1 |

[a]Determined by chiral HPLC using Chirapak IC column.

One hypothesis for the improved activity of these two mutants is that by changing the shape of the hydrophobic pocket (potentially enlarging it), bulkier alkyl substituents, such as *n*-propyl groups, can now dock themselves deeper into the active site, bringing the sulfoxide moiety in close proximity to Cys25. To further confirm this, MD simulations were performed by docking **28j** in both WT MsrA02 and MsrA33, the best mutant of the screening. The F26Y mutation allows **28j** to be at 5.00 Å from Cys25 in MsrA33 (Figure 4.15), which compared to the previous 6.60 Å in MsrA02, is a good distance for the nucleophilic attack to take place. It is also possible to see how the arrangement of **28j** in the active site changes between the WT and the F26Y mutant. In fact, when docked into the WT site, the *n*-propyl chain points in the opposite direction of the hydrophobic pocket and into the solvent-exposed region, with the bulky 4-methoxy phenyl ring preventing a good interaction between the S=O moiety and Cys25. Instead, when docked into MsrA33, the *n*-propyl chain is buried into the hydrophobic pocket, restoring the anchoring interactions that allow **28j** and Cys25 to react together.

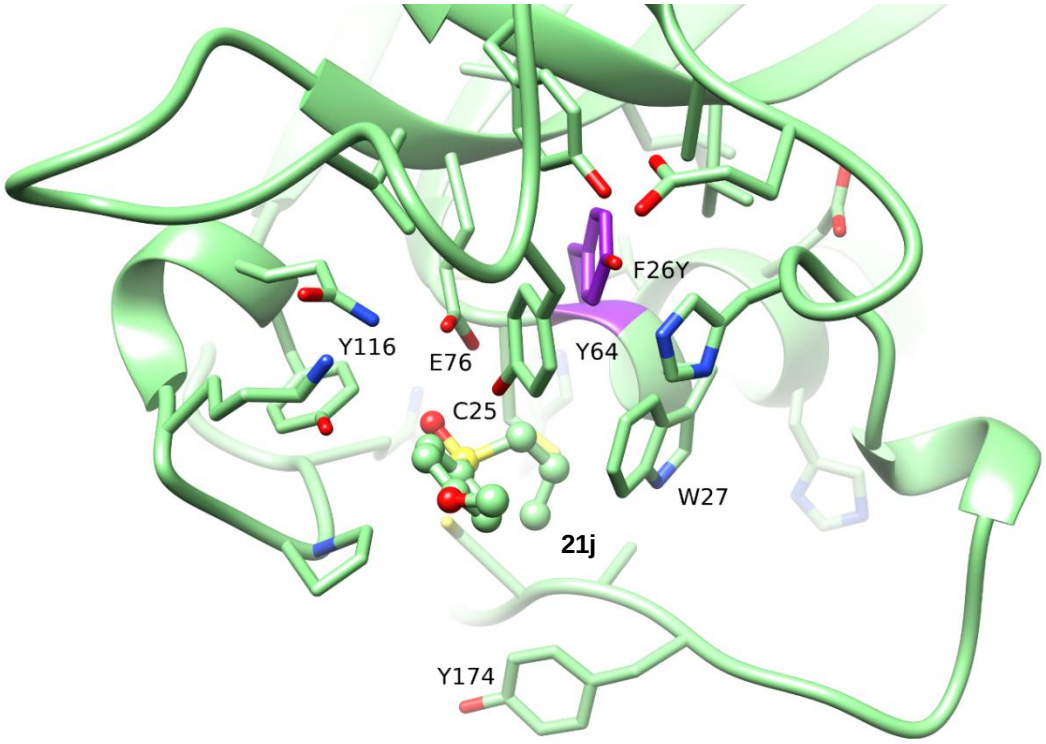


**Figure 4.15.** The binding pose of **28j** and mutant MsrA33 (adapted from PDB: 3PIL).

### *4.3.3.3 Optimisation of the rection conditions using MsrA33*

With the best mutant for the reduction of bulkier substrates in hand, the optimisation of the MsrA33 biocatalysed reduction of **28j** began by investigating whether the optimised reaction conditions for the WT MsrA02 reaction could be applied in this scenario. Unfortunately, when the mutant catalyst was used at a concentration of 1.0 $gL^{-1}$ and exposed to 32 mM substrate (Table 4.8, *Entries 1-3*), **28j** was recovered as a racemate. However, the outcome of this first set of optimisation reactions was to be expected, because it is known that, while enzymes engineered through rational mutagenesis can present an improved activity towards a larger variety of substrates, these are often less efficient compared to their parent WT enzyme. This is also why for the optimisation of reaction conditions with MsrA33, the quantity of DTT was increased from 1.1 to 4.0, as it was predicted that saturating the environment of reaction with the regenerating agent would maximise the reducing activity of the enzyme and would also avoid false negative results due to slow kinetics.

**Table 4.8.** Optimisation of reaction conditions with MsrA33.

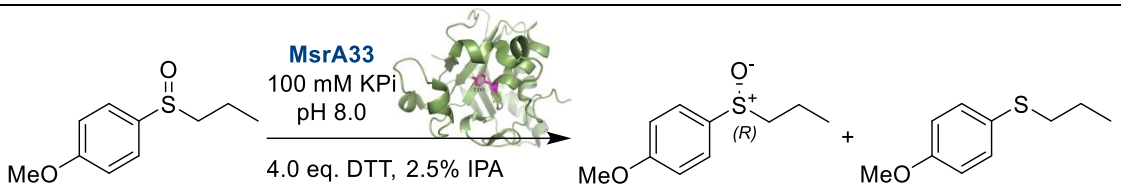


**28j** **(*R*)-28j** **27j**

| Entry | MsrA33 conc. / $gL^{-1}$ | 28j conc. / mM | T / °C | Time / h | (*R*)-28j ee[a,b] % |
|---|---|---|---|---|---|
| *1* | 1.0 | 8.0 | 30 | 24 | 4 |
| *2* | 1.0 | 32 | 30 | 24 | <1 |
| *3* | 10 | 32 | 30 | 24 | 6 |
| *4* | 10 | 8.0 | 30 | 24 | 40 |
| *5* | 10 | 8.0 | 30 | 48 | 66 |
| *6* | 10 | 8.0 | 30 | 72 | 66 |
| *7* | 10 | 4.0 | 30 | 24 | 50 |
| *8* | 10 | 4.0 | 30 | 48 | 70 |
| *9* | 10 | 2.0 | 30 | 24 | 54 |
| *10* | 10 | 2.0 | 30 | 48 | 50 |
| *11* | 10 | 1.0 | 30 | 24 | 28 |
| *12* | 10 | 1.0 | 30 | 48 | 28 |
| *13* | 20 | 8.0 | 30 | 24 | 78 |
| *14* | 20 | 8.0 | 30 | 48 | 82 |
| *15* | 40 | 8.0 | 30 | 24 | 92 |
| ***16*** | **40** | **8.0** | **30** | **48** | **>99 (42)[c]** |
| *17* | 20 | 8.0 | 37 | 24 | 6 |

[a]Determined by chiral HPLC using a Chiralpak IC column. [b]Reactions run in duplicates. [c]HPLC yield is reported. Calculated using an Agilent Eclipse Plus C18 column and methyl *p*-tolyl sulfoxide as internal standard (see Appendix VI for calibration curve data).

A series of time point experiments at 24, 48 and 72 h keeping the enzyme at 10 $gL^{-1}$ and **28j** at 8.0 mM (Table 4.8, *Entries 4-6*) revealed that the optimal reaction time was 48 h, as **(*R*)-28j** was obtained in 66% ee at 48 h, a 25% increase from the 24 h mark, after which no further change in ee was observed. Similar results were obtained for the 24 and 48 h time points when **28j** was used at 4.0 mM (Table 4.8, *Entries 7,8*). Interestingly, when **28j** was used at 2.0 or 1.0 mM (Table 4.8, *Entries 9-12*) no improvement in ee was observed after 24 h and for 1.0 mM **28j,** the ee only reached 28%. The decreased enzymatic activity as the substrate concentration is also reduced can be rationalised in terms of collision theory, where the suboptimal **28j** concentration is too dilute and cannot trigger the activation of the enzyme. After selecting 8.0 mM as the most suitable concentration of **28j**, the concentration of MsrA33 was also assessed. A series of reactions at 20 $gL^{-1}$ and 40 $gL^{-1}$ MsrA33 (Table 4.8, *Entries 13-16*) were monitored at 24 and 48 h and generally afforded **(*R*)-28j** in much higher ees. Specifically, *Entry 16* shows that when 40 $gL^{-1}$ MsrA33 was reacted with 8.0 mM **28j** for 48 h, **(*R*)-28j** was obtained in >99% ee and 42% HPLC yield. In *Entry 17*, a reaction at 20 $gL^{-1}$ MsrA33 was carried out at 37 $^{o}$C to verify whether a slightly higher temperature and a lower enzyme loading also would provide **(*R*)-28j** in excellent ee. Unexpectedly, the 7 $^{o}$C increase in reaction temperature proved to be deleterious for biotransformation, as **28j** was recovered as a racemate after 24 h. Hence, the conditions in *Entry 16* were deemed optimal for the KR of larger substrates by MsrA33.

#### *4.3.3.4 Scope of the MsrA33 biocatalysed KR of large sulfoxides*

After finding the ideal reaction conditions, the substrate scope of the biocatalytic reduction of various sulfoxides with the mutant MsrA33 was finally investigated. The results are reported in Table 4.9. All the sulfoxides **28j**, **28an**, **28k-ar** bearing an *n*-propyl substituent on the sulfur atom were obtained in good to high yields (Table 4.9, *Entries 1-6*). The (*R*)-enantiomers of the derivatives **28j**, **28k** and **28ao** were afforded with excellent ees, while **28an**, **28ap** and **28aq** were reduced less selectively. For instance, **(*R*)-28an** was obtained in 37% yield with an ee of 65%, which clearly indicates that MsrA33 was quite active on the substrate but was not very selective for the reduction of **(*S*)-28an** compared to other sulfoxides. Instead, **28ap** and **28aq** were obtained in about 50% yield but the ee only reached 64 and 76% respectively.

**Table 4.9.** Scope of the MsrA33 biocatalysed KR of larger sulfoxides.

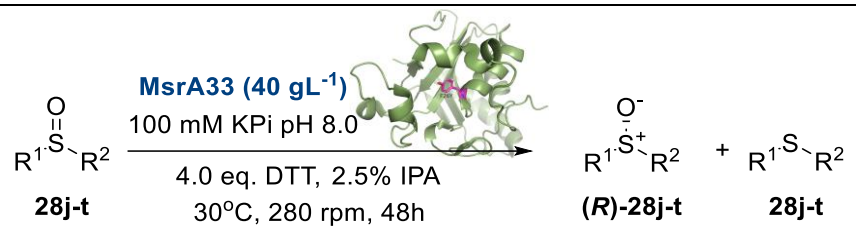


| Entry | Substrate | $R^1$ | $R^2$ | (*R*)-21 yield[a] % | ee[b] % |
|---|---|---|---|---|---|
| *1* | **28j** | 4-MeO-$C_6H_4$ | *n*Pr | 42 | >99 |
| *2* | **28an** | Ph | *n*Pr | 37 | 65 |
| *3* | **28k** | 4-Me-$C_6H_4$ | *n*Pr | 40 | 99 |
| *4* | **28ao** | 4-Cl-$C_6H_4$ | *n*Pr | 46 | 92 |
| *5* | **28ap** | 4-Br-$C_6H_4$ | *n*Pr | 56 | 76 |
| *6* | **28aq** | 3-MeO-$C_6H_4$ | *n*Pr | 51 | 64 |
| *7* | **28ar** | 4-MeO-$C_6H_4$ | *n*Bu | 87 | 12 |
| *8* | **28g** | 4-Br-$C_6H_4$ | Et | 39 | >99 |
| *9* | **28t** | 2-Py$CH_2$ | Et | 44 | >99 |

[a]HPLC yield is reported. Calculated using an Agilent Eclipse Plus C18 column and methyl *p*-tolyl sulfoxide as internal standard (see Appendix VI for calibration curve data). [b]Determined by chiral HPLC using Chiralpak columns IG, IC or ID or Chiracel OD-H.

Unfortunately, when moving from a *n*-propyl to a *n*-butyl chain, as for sulfoxide **28ar**, the enzyme could no longer reduce the substrate as **(*R*)-28ar** was recovered in 12% ee and 87% yield (Table 4.9, *Entry 7*). Sulfoxides **28g** and **28t**, which were poorly resolved by MsrA02, were reacted with MsrA33 to assess whether the enzyme would retain selectivity and activity for smaller substrates too. Interestingly, both **(*R*)-28g** and **(*R*)-28t** were formed with ees of >99% and HPLC yields of 39% and 44% respectively (Table 4.9, *Entries 8,9*). The fact that the mutant enzyme showed promiscuity between the two enantiomers explains why the recorded HPLC yields of the (*R*)-sulfoxides with excellent ees are lower than 50%, as both enantiomers can be reduced by MsrA33.

### 4.3.4 Development of a deracemization method

In the course of the PhD, the photobiocatalytic[356] and multienzymatic[357] deracemization publications aforementioned were released. While the 'one-pot one-step' biocatalytic cascade proposed by Peng *et al.*[357] proved to be a robust scalable protocol that could be applied on a large substrate scope, the photobiocatalytic presented by Bierbaumer *et al.*[356] had a restricted scope and it was limited to analytical scale production of (*R*)-sulfoxides. In the photobiocatalytic methodology, the authors were also suspicious that in some instances their method might have only kinetically resolved some of the

substrates rather than fully deracemized them. Another disadvantage of this photobiocatalytic protocol was that the sulfide photocatalyst used for the oxidation had to be harvested from the purple bacterium *Rhodobacter capsulatus* ZY5, which was described as a laborious, time consuming and expensive process that only yielded 40 mg of photocatalyst per litre of cell culture. Therefore, we wanted to try the development of a simplified deracemization methodology using our MsrA02 enzymes (WT and mutant) and cheap commercially available organic photocatalysts (Scheme 4.11). In comparison to the ones in the literature, this protocol would, in fact, provide a simplified alternative for the deracemization of sulfoxides, applicable to a large substrate scope.

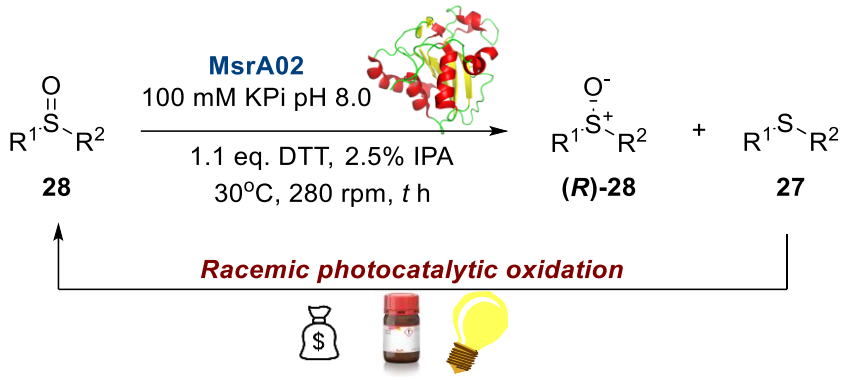


**Scheme 4.11**. Schematic representation of a deracemization protocol using MsrAs and chemical oxidation methods.

### *4.3.4.1 Identification of best commercially available photocatalyst for the deracemization of **28af** and optimisation of the reaction conditions*

The investigation began by assessing which commercially available photocatalysts could furnish racemic sulfoxides in the conditions of the MsrA02 biotransformation. The focus was on organic photoactivators because it was predicted that these would be the most compatible with enzymes and would also avoid the use of transition metals. It is also worth mentioning that heterogeneous photocatalysts based on $TiO_2$ were also found to be quite effective for racemic sulfoxidation protocols, but in most reports, they required manipulations to maximise their performance.[233,367–372] Therefore, as the goal was to keep the deracemization process simple and effortless, the use of $TiO_2$ based catalysts was avoided. Based on the literature,[373] rose Bengal **95**,[374–376] eosin Y **96**[231,377,378] and NHPI **97** [232] were chosen as photocatalysts, as they all provided racemic sulfoxides from sulfide precursors in excellent yields and selectivity, with only traces of sulfone reported in all cases. Furthermore, fluorescein **98** was selected as well because, despite the lack of reports on its ability to oxidise sulfides, it is structurally similar to rose Bengal and eosin

Y. Methyl *p*-tolyl sulfoxide **27af** was selected as the starting sulfide for the development of the photocatalytic sulfoxidation. The starting conditions were set identical to those of the optimised MsrA02 KR, except that DTT was initially omitted to avoid interference with the sulfoxidation and IPA was substituted with $CH_3CN$ as this did not seem to affect the performance of MsrA02 (Section 4.3.1.2, Table 4.2) but it appeared to be a more suitable cosolvent for the photocatalysts. Results of the screening are reported in Table 4.10. After irradiating under visible light for 1.5 h, it was found that the organic dyes **95-98** led to either quantitative conversion in case of rose Bengal and eosin Y (Table 4.10, *Entries 2,3*) or partial conversion with fluorescein (Table 4.10, *Entry 4*). Interestingly, full recovery of starting sulfide **27af** was observed when NHPI **97** was used as a photocatalyst instead. A series of experiments in which EDTA was added to the reaction as a sacrificial electron donor was also performed to see whether it would lead to an improvement in the sulfoxidation. Unfortunately, in all cases, addition of EDTA led to poorer TLC conversions and no improvement was found for NHPI either (Table 4.10, *Entries 5-8*).

**Table 4.10.** Screening of organic photocatalysts for the racemic oxidation of **27af** to **28af**.

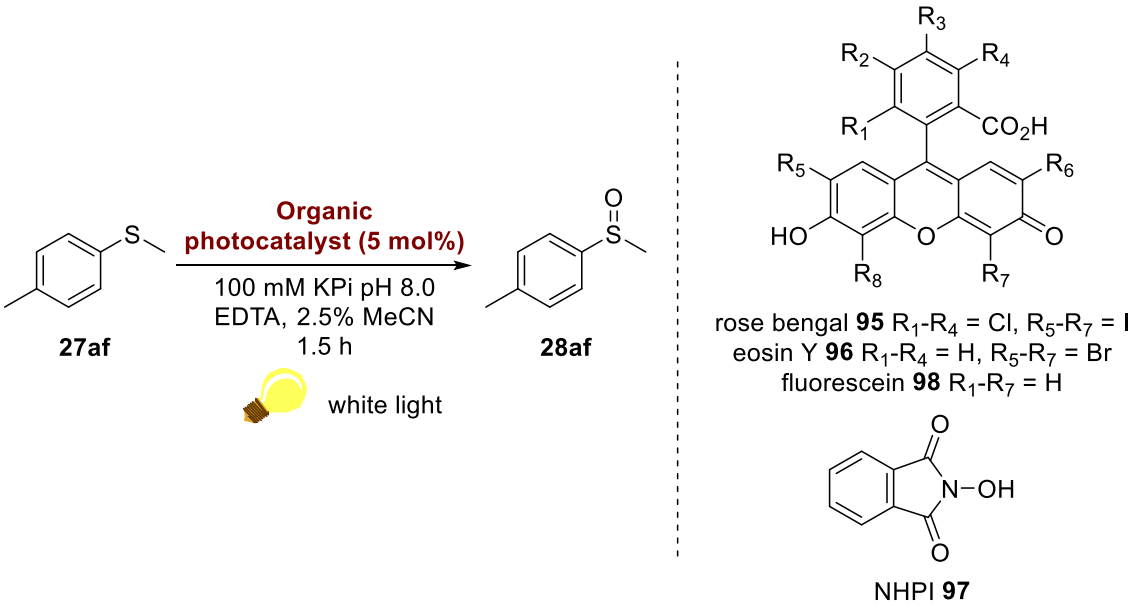


| Entry | Photocatalyst | EDTA | TLC conversion[a] |
|---|---|---|---|
| *1* | NHPI[b] | - | No |
| *2* | Rose bengal | - | Quant. |
| *3* | Eosin Y[c] | - | Quant. |
| *4* | Fluorescein | - | Yes |
| *5* | NHPI[b] | 1.0 eq | No |
| *6* | Rose bengal | 1.0 eq | Yes |
| *7* | Eosin Y[c] | 1.0 eq | Yes |
| *8* | Fluorescein | 1.0 eq | Yes |

[a]Qualitative TLC conversion for fast analysis. [b]10 mol % of catalyst used. [c]Green light used.

Therefore, rose Bengal and eosin Y were then selected for the development of the photobiocatalytic deracemization protocol. The next step was then to combine the selected photocatalysts with MsrA02. As expected, the biocatalytic reaction without any photocatalysts led to **(*R*)-28af** in 99% ee (Table 4.11, *Entry 1*). Upon addition of **96** and **96**, the ee of **(*R*)-28af** dropped to 14% and 26% respectively (Table 4.11, *Entries 2,3*). This indicated either that the photobiocatalytic reaction kinetics were slower and the system was quenched too early resulting in poor ees, or that the photocatalyst was poisoning the enzyme, thus resulting in lower ees. To rule out the latter hypothesis, a sequence of control reactions was carried out using eosin Y **96** as it performed better. Initially, increasing the concentration of MsrA02 (Table 4.11, *Entries 4-6*) resulted in progressively higher ees, peaking at 97% when 8.0 $gL^{-1}$ of MsrA02 was used (Table 4.11, *Entry 6*). Unfortunately, the approximate HPLC conversion of this reaction was around 50%, indicating that even in this case a kinetic resolution was obtained. The fact that a high ee was only achieved when the MsrA02 concentration was increased by 8-fold emphasised that the low ee observed in *Entry 3* was indeed caused by inactivation of the enzyme by the photocatalyst.

**Table 4.11.** Photobiocatalytic method and control reactions for the deracemization of **28af**.

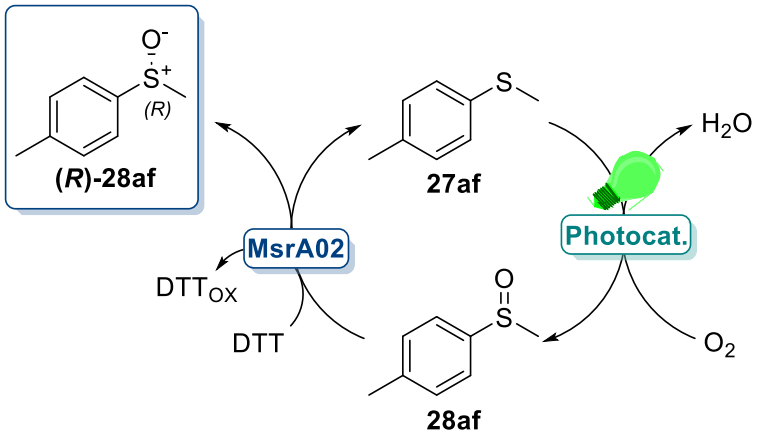


| Entry | Photocatalyst | MsrA02 /$gL^{-1}$ | (*R*)-28af ee[a] % |
|---|---|---|---|
| *1* | No | 1.0 | 99 |
| *2* | Rose Bengal[b] | 1.0 | 14 |
| *3* | Eosin Y | 1.0 | 26 |
| *4* | Eosin Y | 3.0 | 28 |
| *5* | Eosin Y | 4.0 | 40 |
| *6* | Eosin Y | 8.0 | 97 |
| *7* | Eosin Y | 1.0 | 13[c] |

[a]Conditions of reaction: 1.1 eq. DTT, 100 mM KPi pH 8.0, 2.5% ACN, 5 mol % photocatalyst, 45 min intervals of light irradiation, 15 min darkness. Overall time 18 h. [b]White light used. [c]Reaction in the dark

In fact, as the concentration of MsrA02 was increased, the percentage of active enzyme also increased, giving a higher ee. This was further confirmed with an overnight reaction carried out in the dark in the presence of eosin Y **96**, where only 13% ee was obtained (Table 4.11, *Entry 7*) clearly suggesting enzyme inactivation by the photocatalyst. Hence, eosin Y **96** was inadequate for the development of a photobiocatalytic deracemization protocol. Another strategy for the photocatalytic oxidation of sulfoxides was published by Neveselý *et al.*, where the photocatalyst riboflavin or its derivative, riboflavin tetraacetate (RFTA), successfully catalysed the oxidation of a broad range of sulfides under blue light irradiation in a mixture of 15:85 water:$CH_3CN$ with no overoxidation observed.[379,380] Riboflavin is commonly synthesised by most organisms as it is the precursor for the coenzymes flavin adenine dinucleotide (FAD) and flavin mononucleotide (FMN), which are used for redox reaction processes.[381] Therefore, it was envisioned that, as riboflavin is endogenous to both *E. coli* and *S. cerevisiae* cells,[381,382] MsrA02 should be able to tolerate both riboflavin and RFTA as photocatalysts. As MsrA02 was found to be inactive in the reaction conditions reported by Neveselý and colleagues (85% $CH_3CN$), a series of reactions was carried out to verify whether riboflavin or RFTA could catalyse the oxidation of **27af** in a more water-based environment. The results are reported in Table 4.12. When riboflavin was reacted in 100-85% water no oxidation to **28af** was observed (Table 4.12, *Entries 1,2*). Similar results were obtained for RFTA in 85% water (Table 4.12, *Entry 3*).

**Table 4.12.** Screening of conditions for the sulfoxidation of **27af** catalysed by flavine photocatalysts.

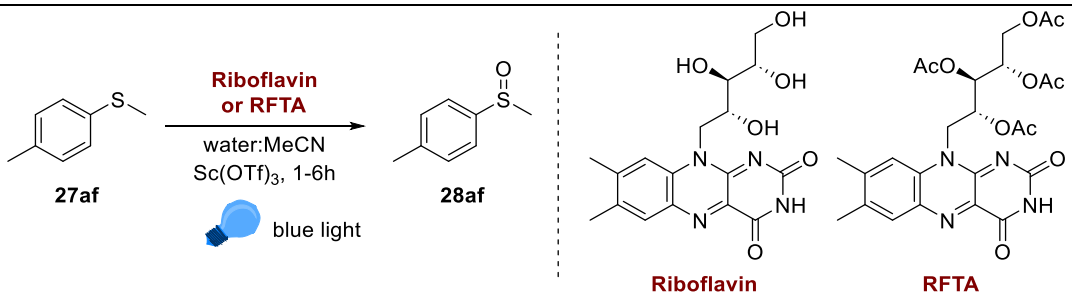


| Entry | Photocat. | Photocat. / mol% | Water:$CH_3CN$ | $Sc(OTf)_3$ / mol % | TLC conv.[a] |
|---|---|---|---|---|---|
| *1* | Riboflavin | 5 | 100:0 | - | - |
| *2* | Riboflavin | 10 | 85:15 | - | - |
| *3* | RFTA | 10 | 85:15 | - | - |
| *4* | Riboflavin | 10 | 85:15 | 20 | - |
| *5* | Riboflavin | 10 | 1:1 | 20 | - |
| *6* | Riboflavin | 10 | 97.5:2.5 | 20 | - |
| *7* | RFTA | 10 | 85:15 | 20 | - |
| *8* | RFTA | 2 | 15:85 | - | Quant. |
| *9* | Riboflavin | 1 | 15:85 | - | Quant. |

[a]Qualitative TLC conversion for fast analysis.

The addition of scandium triflate $Sc(OTf)_3$ as a cocatalyst, which forms a complex with riboflavin and was shown to aid electron transfers between reacting species in the photocatalytic aerobic oxidation of ethylbenzene by Mühldorf and Wolf,[383] did not improve the oxidative ability of the photocatalysts in varying ratios of water:$CH_3CN$ (Table 4.12, *Entries 4-7*). Finally, two reactions using riboflavin and RFTA were set up under the conditions of the reported paper to verify whether the results could be reproduced and, in both cases, quantitative conversion to **28af** was observed on TLC (Table 4.12, *Entries 8,9*). Therefore, the results from the optimisation of the sulfoxidation conditions clearly highlight the incompatibility of both riboflavin and RFTA as photocatalysts under the conditions of the biocatalysed KR of MsrA02.

## 4.4 Final considerations and conclusions

In this project, the enantioselective synthesis of a wide range of aromatic and aliphatic (*R*)-sulfoxides was achieved through the kinetic resolution of racemic sulfoxides starting materials utilising the novel MsrA02 enzyme from *S. cerevisiae*. Methionine sulfoxide reductases are unconventional biocatalysts for the synthesis of chiral sulfoxides as, traditionally, oxidative enzymes such as peroxidases and peroxygenases have been used to access such molecules instead. The use of reductive instead of oxidative enzymes in the synthesis of enantiomerically pure sulfoxides offers substantial advantages from a synthetic point of view, such as the use of the cheap co-substrate DTT at low concentrations in place of the expensive cofactor NADPH and related recycling systems, or even avoiding peroxide reagents which can lead to overoxidation by-products. Also, while existing oxidative enzymes are often incompatible with substrates bearing multiple oxidation sites, MsrAs can be used on substrates that present a wide range of other functional groups as they are specific exclusively for sulfoxide moieties. Other benefits of this methodology include the use of MsrA02 CFE, which allowed for much lower dry powder loadings per volume compared to the whole cell freeze dried powder, and its production was much less process intensive compared to the purified form. The use of the enzyme as a CFE also allowed for quite high substrate concentrations, up to 64 mM, which are often avoided when using either whole cell or purified biocatalysts due to enzyme inactivation.

This project also aimed to understand the mechanism of action of MsrA02 for the reduction of non-natural substrates. Hence, in the first step of this investigation, single point mutants, where the five cysteine residues (Cys23, Cys25, Cys44, Cys68, and Cys147) were mutated to serine, confirmed that the highly conserved Cys25 and Cys176 were responsible for the catalytic activity. It was also revealed that the C23S mutation had a detrimental effect on activity because modelling suggested it caused a conformational change in the active site, misplacing Cys25 from its ideal position and preventing a good interaction with the substrate. The role of Cys25 and Cys176 was also confirmed by NMR studies, where the significant shift of the residue signals upon substrate binding indicated high activity and conformational changes around the two residues.

One of the main limitations of the protocol developed in this project was that MsrA02 was mainly active on methyl- and some ethyl-substituted sulfoxides, but it showed no activity on bulkier ones. Through *in silico* and MD studies, it was found that the longer alkyl chains of some substrates prevented a close interaction between the S=O moiety and

Cys25, explaining why MsrA02 would not be able to reduce larger sulfoxides. Therefore, 9 MsrA02 and 3 MsrA10 mutants holding mutations on different parts of their structure were designed and developed into a new enzyme panel along with 6 new WT MsrAs from different species, which had significantly different C-terminal regions. Among these novel enzymes, MsrA33 was identified as the most promising biocatalyst as it led to the production of **28j** in 46% ee, improved to >99% and 42% HPLC yield after optimising the reaction conditions. It was hypothesised that the improved substrate scope of MsrA33 was due to the F26Y mutation in the hydrophobic pocket of the active site. This is in fact responsible for interacting with the aliphatic substituent of the substrate, and it was demonstrated *in silico* that it allowed the larger substrates to be in close proximity with the catalytic Cys25. While MsrA33 appeared to be a less robust enzyme compared to MsrA02, as for instance it was very sensitive to the reaction environment, its discovery and development demonstrates the unexplored potential of MsrA enzymes.

The development of a simple photobiocatalytic deracemization strategy based on commercially available photocatalysts was attempted. While such a deracemization process was proposed by Bierbaumer *et al.*,[356] the group had to employ a photocatalyst isolated from a cyanobacterium, whose production is lengthy and tedious, resulting in a process that is overall too expensive to pursue in industry. Therefore, a series of commercially available organic dyes, namely rose Bengal **95**, eosin Y **96** and fluorescein **98**, the organic photo-inducer NHPI **97** and the FAD precursor riboflavin with its tetraacetate derivative, RFTA, were selected from the literature and assessed for their ability to catalyse photoinduced oxidations under the same conditions as MsrA02. Unfortunately, none of these photocatalysts led to the expected deracemization results. In fact, while the organic dyes promoted sulfide oxidation in buffer but inactivated MsrA02, NHPI **97**, riboflavin and RFTA were found to be completely inactive in aqueous solutions.

# Chapter 5. General final remarks

Sulfoxides are ubiquitous organosulfur molecules that find applications in many areas of chemistry. For example, they can be essential intermediates in the synthesis of other target compounds or can also be crucial moieties in molecules such as ligands and drugs. Over the years, a plethora of new methodologies emerged in the literature for the efficient synthesis of both chiral and achiral sulfoxides. However, driven by the need to find greener and safer alternatives to traditional synthetic routes, researchers turned to biocatalysis for the development of more environmentally friendly sulfoxidation strategies. Biocatalysis is the application of wild type or engineered enzymes as biodegradable, biocompatible and non-toxic feedstock-derived catalysts for chemical transformations. Furthermore, the use of enzymes can offer advantages over traditional catalysts, such as excellent regio-, chemo- and enantioselectivity gained through millions of years of evolution or, in recent years, enzyme mutagenesis. Therefore, in this thesis, three different biocatalytic approaches to the synthesis of sulfoxides were investigated. Each project presented unique unconventional features that made the research stand out from other reports already presented in the literature.

In the first project described in Chapter 2, immobilised *Candida antarctica* lipase B (CALB) was utilised in combination with ethyl acetate (EtOAc) for the development of a novel, green and scalable synthesis of racemic sulfoxides. In this protocol, the commercially available CALB catalysed the formation of the peracetic acid *in situ* from urea hydrogen peroxide (UHP) and EtOAc, which served both as reaction solvent and enzyme substrate. A total of 17 alkyl-aryl sulfoxides, 6 carbonyl- and 2 hydroxyl- bearing sulfides and the active pharmaceutical ingredient omeprazole sulfide were successfully and, in most cases, quantitatively oxidised to the corresponding sulfoxides. Moreover, scale-up and CALB recyclability experiments demonstrated the applicability of this protocol for the industrial production of sulfoxides. One of the benefits of this methodology is the overall improved atom economy as the use of EtOAc as solvent and CALB substrate avoids the need of both stoichiometric amounts of potentially explosive oxidants, such as *m*CPBA, and acid or ester additives as peracid precursors. Additionally, EtOAc is considered a green solvent compared to the chlorinated ones, usually employed for the synthesis of sulfoxides.

In Chapter 3, two flavoprotein monooxygenases from Almac's own in-house library, namely Baeyer-Villiger monooxygenase (BVMO) 145 and flavine-containing monooxygenase (FMO) D9, were identified for the enantioselective and enantiocomplementary synthesis of chiral sulfoxides that carry multiple functional groups

prone to oxidation. In this project, only BVMO145 has been investigated due to time constraints and it showed excellent enantioselectivity for the synthesis of 7 alkyl-aryl (*S*)-sulfoxides, which were obtained in varying conversions. Whilst additional investigation is currently undergoing in the group, some preliminary conclusions emerged from this project. For instance, it was observed that the prochiral sulfide substrates may require a longer alkyl chain substituent to induce hydrophobic interactions with the active site of the enzyme, and that an ethylene spacer between the sulfur atom and aromatic ring may facilitate the binding of the substrate in the active site. Additionally, although an aromatic ring was tolerated, it was postulated that para and electron withdrawing substituents may have detrimental effects on the sulfoxidation activity of BVMO145 due to steric hindrance and reduction of the nucleophilicity of sulfide substrates, an essential property that sulfides need to have to react with flavoprotein monooxygenases. All these hypotheses will soon be tested through *in silico* docking of the substrates and by expanding the scope of BVMO145. It was then predicted that when the full assessment of these biocatalyst is completed, the information provided by this study will be the foundations for the further development of improved engineered enzymes that have an improved chemoselectively towards the oxidation of sulfides.

The final project presented in Chapter 4 focused on the use of a relatively new class of reductive biocatalysts, the methionine sulfoxide reductase A (MsrA) enzymes, for the production of (*R*)-sulfoxides. The use of these enzymes is advantageous compared to traditional oxidative enzymes because MsrAs need a much simpler and cheaper recycling system based on the sacrificial co-substrate dithiothreitol. Additionally, they are active exclusively on sulfoxide moieties and hence they can be used with substrates that have other functional groups. Therefore, the project began with the identification of the novel MsrA02 from *Saccharomyces cerevisiae*, which was selected from a panel of wild type MsrAs, for the development and optimisation of the kinetic resolution of sulfoxide racemates. With a total of 24 alkyl aryl sulfoxides resolved with enantiomeric excesses of up to >99%, MsrA02 has the largest scope reported in the literature to date. However, not all sulfoxides were substrates of MsrA02, especially those bearing an alkyl chain longer than an ethyl group. This was found to be a common drawback among all MsrA procedures, and therefore we decided to develop an engineered enzyme through rational mutagenesis capable of resolving bulkier sulfoxide substrates. First, an assessment of the key residues for activity was carried out by both by enzyme mutagenesis and NMR studies, which confirmed that Cys25 and Cys176 are the two cysteine residues essential for enzyme activity. Then *in silico* substrate docking and molecular dynamics studies were carried out with wild type MsrA02 to understand why larger substrates were not

tolerated in the active site. Finally, a panel of 13 mutants was developed and it was found that MsrA33, which bears the F26Y mutation in the hydrophobic pocket of the active site, could resolve propyl-containing sulfoxides in enantiomeric excesses of up to >99%. This is the first example of directed mutagenesis of MsrA enzymes.

These three biocatalytic methodologies have demonstrated that it is possible to find new and alternative green protocols for the synthesis of sulfoxides. I hope that this research, along with the many other groups that choose to work within biocatalysis, can be one small step forward towards the change of the chemical industry for a greener, safer, and sustainable future.

# Chapter 6. Experimental

## 6.1 General methods

Reagents and solvents were used as supplied from the vendor without further purification. Thin layer chromatography plates (Merk, silica gel 60 $F_{254}$, aluminium backed) were viewed under UV light and stained using $KMnO_4$ developed using heat. $MgSO_4$ (Sigma Aldrich, anhydrous ≥ 98.0 %) was used as the drying agent. Column chromatography was performed on silica gel for flash chromatography (Sigma Aldrich, 40-63 µm particle size, 60 Å pore size). Microwave irradiations were conducted using a CEM Discover Synthesis Unit. Products were characterised by $^{1}H$ NMR, $^{13}C$ NMR and $^{19}F$ NMR spectra where applicable obtained from one of the following: a) Bruker (Germany) Ascend400 Spectrometer ($\delta_H$ 400 MHz, $\delta_C$ 101 MHz, $\delta_F$ 376 MHz) at 300 K; b) Bruker (Germany) Avance III 400 ($\delta_H$ 400 MHz, $\delta_C$ 101 MHz) at 300 K; c) Bruker (Germany) Avance Neo 500 ($\delta_H$ 500 MHz, $\delta_C$ 126 MHz) at 300 K. Chemical shifts are reported in ppm relative to the reference peaks of the solvents: $CDCl_3$ ($^{1}H$ NMR 7.26 and $^{13}C$ NMR 77.16) unless stated otherwise. Coupling constants (*J*) are reported in Hz, multiplicities are specified as singlet (s), doublet (d), triplet (t), quartet (q), pentet (p), sextet (sx), septet (h), multiplet (m).

HPLC/UPLC and LC-MS analysis was carried out using one of the following: a) Agilent series 1100 LC/MSD system coupled with UV detector at l = 254 nm, 2 = 240 nm, 3 = 210 nm, and an atmospheric pressure chemical ionization (APCI) source; b) Agilent series 1250 UPLC system coupled with UV detector at 1 = 254 nm, 2 = 240 nm, 3 = 210 nm. The columns used are specified in each section of the Experimental chapter. High resolution mass spectra were acquired on a Waters LCT Premier XE instrument or an Agilent 6510 QToF, using electrospray ionisation methods in the positive mode (ESI+). Infrared spectra were obtained using a Perkin Elmer Spectrum 100 FTIR Spectrometer operating in ATR mode. Optical rotation data was obtained using a Bellingham + Stanley ADP430 polarimeter.

Protein purification was performed on an ÄKTA Fast Protein Liquid Chromatography (FPLC) Instrument (GE Healthcare) with a UV detector set at 280 nm. Purification was carried out a 5 mL His-Trap™ Fast Flow nickel affinity column (GE) and a HiLoadTM 16/600 Superdex 200pg size exclusion chromatography column (GE) where appropriate.

## 6.2 Chapter 2. Methods

## Synthetic methods

### 6.2.1 General procedure for the synthesis of sulfides 27

Sulfides **27a**, **27b**, **27o** and **27r** were purchased and used without any further purification. For the remaining sulfides, the appropriate thiophenol or benzylthiol (1.36 mmol) and haloalkane (2.04 mmol) were added to a microwave (MW) vial and dissolved in water (2 mL), $K_2CO_3$ (1.36 mmol) and, for bromo- and chloro- alkanes, NaI (0.13 mmol) were then added to the vial and the resulting reaction mixture was stirred at 140 ºC in intervals of 5 minutes under microwave irradiation until completion was observed on TLC. The reaction was then extracted in EtOAc (3 x 2mL) and the collected organic layers were washed with water (1 x 2mL), brine (2 x 2mL), dried on $MgSO_4$ and evaporated under vacuum. The desired sulfides **27** were obtained as pale yellow oils and proved to be pure enough to be used in the next step without any further purification.

#### *6.2.1.1 Ethyl(phenyl)sulfane (**27c**)*[384]

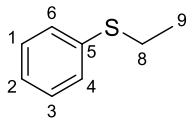


Synthesised from thiophenol and bromoethane. Yellow oil, >99% yield. $^1$H NMR (400 MHz, $CDCl_3$) δ 7.40 – 7.16 (m, 5H, *Ar*), 2.97 (q, J = 7.4 Hz, 2H, 8-H), 1.35 (t, J = 7.4 Hz, 3H, 9-H) ppm. $^{13}$C NMR (101 MHz, $CDCl_3$) δ 136.7 (5), 129.0 (4,6), 128.9 (1,3), 125.8 (2), 27.7 (8), 14.4 (9) ppm.

#### *6.2.1.2 Ethyl(p-tolyl)sulfane (**27d**)*[385]

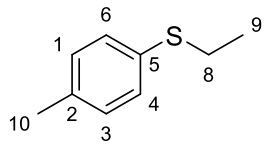


Synthesised from thiocresol and bromoethane. Oil, 64% yield. $^1$H NMR (400 MHz, Chloroform-d) δ 7.77 (d, J = 8.2 Hz, 2H, 4,6-H), 7.35 (d, J = 8.2 Hz, 2H, 1,3-H), 3.09 (q, J = 7.3 Hz, 2H, 8-H), 2.44 (s, 3H, 10-H), 1.25 (t, J = 7.3 Hz, 3H, 9-H) ppm. $^{13}$C NMR (101 MHz, $CDCl_3$) δ 144.61 (5), 135.7 (4,6), 129.7 (1,3), 128.23 (2), 50.7 (8), 21.6 (10), 7.48 (9).

*6.2.1.3 Ethyl(4-methoxyphenyl)sulfane (**27e**)*[386]

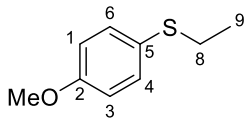


Synthesised from thiophenol and bromoethane. Yellow oil, 22% yield. $^{1}$H NMR (400 MHz, Chloroform-d) δ 7.35 (d, J = 8.8 Hz, 2H, 4,6-H), 6.85 (d, J = 8.8 Hz, 2H, 1,3-H), 3.79 (s, 3H, OMe), 2.84 (q, J = 7.4 Hz, 2H, 8-H), 1.25 (t, J = 7.4 Hz, 3H, 9-H) ppm. $^{13}$C NMR (101 MHz, $CDCl_3$) δ 158.9 (2), 133.3 (4,6), 126.6 (1,3), 114.6 (5), 55.4 (OMe), 29.9 (8), 14.7 (9) ppm.

*6.2.1.4 (4-Chlorophenyl)(ethyl)sulfane (**27f**)*[386]

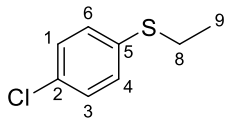


Synthesised from 4-chlorothiophenol and bromoethane. Colourless oil, 68% yield. $^{1}$H NMR (400 MHz, $CDCl_3$) δ 7.26 (s, 4H, Ar), 2.93 (q, J = 7.4 Hz, 2H, 8-H), 1.31 (t, J = 7.4 Hz, 3H, 9-H) ppm. $^{13}$C NMR (101 MHz, $CDCl_3$) δ 135.2 (5), 131.7 (2), 130.3 (4,6), 129.0 (1,3), 27.9 (8), 14.3 (9) ppm.

*6.2.1.5 (4-Bromophenyl)(ethyl)sulfane (**27g**)*[386]

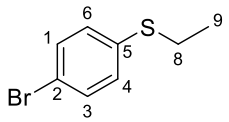


Synthesised from 4-bromothiophenol and bromoethane. Oil, 68% yield. 1H NMR (400 MHz, Chloroform-d) δ 7.40 (d, J = 8.6 Hz, 2H, 4,6-H), 7.19 (d, J = 8.6 Hz, 2H, 1,3-H), 2.93 (q, J = 7.4 Hz, 2H, 8-H), 1.32 (t, J = 7.4 Hz, 3H, 9-H) ppm. $^{13}$C NMR (101 MHz, $CDCl_3$) δ 136.0 (5), 131.9 (4,6), 130.4 (1,3), 119.5 (2), 27.7 (8), 14.3 (9) ppm.

*6.2.1.6 (2-Chlorophenyl)(ethyl)sulfane (**27h**)*

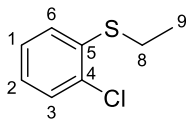


Synthesised from 2-chlorothiophenol and bromoethane. Pale yellow oil, 99% yield. $^{1}$H NMR (400 MHz, $CDCl_3$) δ 7.38 (dd, J = 7.9, 1.5 Hz, 1H, Ar), 7.31 – 7.20 (m, 2H, Ar), 7.15 – 7.06 (m, 1H, Ar), 2.98 (q, J = 7.4 Hz, 2H, 8-H), 1.38 (t, J = 7.4 Hz, 3H, 9-H) ppm. $^{13}$C

NMR (101 MHz, $CDCl_3$) δ 136.3 (5), 132.8, 129.5, 127.6, 127.0, 126.0, 26.3 (8), 13.6 (9) ppm.

### *6.2.1.7 (2-Bromophenyl)(ethyl)sulfane (**27i**)*

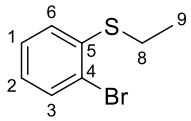


Synthesised from 2-bromothiophenol and bromoethane. Pale yellow oil, 99% yield. $^1$H NMR (400 MHz, $CDCl_3$) δ 7.55 (dd, J = 8.0, 1.6 Hz, 1H, Ar), 7.31 – 7.19 (m, 2H, Ar), 7.02 (ddd, J = 8.0, 7.0, 1.6 Hz, 1H, Ar), 2.97 (q, J = 7.4 Hz, 2H, 8-H), 1.39 (t, J = 7.4 Hz, 3H, 9-H) ppm. $^{13}$C NMR (101 MHz, $CDCl_3$) δ 138.4 (5), 132.9, 127.7, 127.4, 126.2, 123.0, 26.8 (8), 13.7 (9) ppm.

### *6.2.1.8 (4-Methoxyphenyl)(propyl)sulfide (**27j**)*[386]

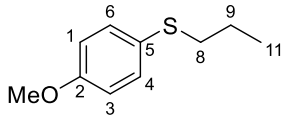


Synthesised from 4-methoxythiophenol and iodopropane. Pale yellow oil, 95% yield. $^1$H NMR (400 MHz, $CDCl_3$) δ 7.40 (d, J = 8.9 Hz, 2H, 4,6-H), 6.89 (d, J = 8.9 Hz, 2H, 1,3-H), 3.81 (s, 3H, OMe), 2.85 (t, J = 7.3 Hz, 2H, 8-H), 1.67 (sx, J = 7.3 Hz, 2H, 9-H), 1.06 (t, J = 7.3 Hz, 3H, 11-H) ppm. $^{13}$C NMR (101 MHz, $CDCl_3$) δ 158.8 (2), 133.0 (4,6), 127.0 (5), 114.5 (1,3), 55.2 (OMe), 37.8 (8), 22.7 (9), 13.3 (11) ppm.

### *6.2.1.9 Propyl(p-tolyl)sulfane (**27k**)*[387]

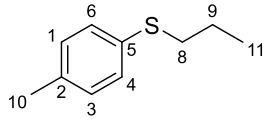


Synthesised from thicresol and iodopropane. Pale yellow oil, 51% yield. $^1$H NMR (400 MHz, $CDCl_3$) δ 7.33 (d, J = 8.3 Hz, 2H, 4,6-H), 7.15 (d, J = 8.3 Hz, 2H, 1,2-H), 2.92 (t, J = 7.3 Hz, 2H, 8-H), 2.38 (s, 3H, 10-H), 1.72 (h, J = 7.3 Hz, 2H, 9-H), 1.09 (t, J = 7.3 Hz, 3H, 11-H) ppm. $^{13}$C NMR (101 MHz, $CDCl_3$) δ 135.8 (5), 133.2 (2), 129.9 (4,6), 129.6 (1,3), 36.4 (8), 22.7 (10), 21.0 (9), 13.4 (11) ppm.

*6.2.1.10 Allyl(phenyl)sulfane (**27l**)*[384]

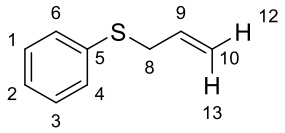


Synthesised from thiophenol and allylbromide. Pale yellow oil, 60% yield. $^{1}$H NMR (400 MHz, $CDCl_3$) δ 7.38 – 7.15 (m, 5H, Ar), 5.88 (ddt, J = 17.0, 10.0, 6.8 Hz, 1H, 9-H), 5.14 (dd, *J* = 17.0, 1.5 Hz, 1H, 12-H), 5.07 (ddd, *J* = 10.0, 1.5, 0.9 Hz, 1H, 13-H), 3.55 (d, J = 6.8 Hz, 2H, 8-H) ppm. $^{13}$C NMR (101 MHz, $CDCl_3$) δ 135.9 (5), 133.6 (9), 129.9 (4,6), 128.8 (1,3), 126.2 (2), 117.7 (10), 37.2 (8).

*6.2.1.11 But-3-en-1-yl(phenyl)sulfane (**27m**)*[388]

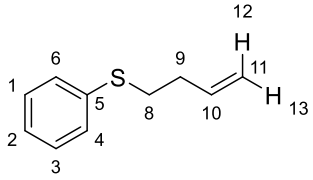


Synthesised from thiophenol and 4-bromo-1-butene. Oil, 65% yield. $^{1}$H NMR (400 MHz, Chloroform-d) δ 7.38 – 7.33 (m, 2H, Ar), 7.32 – 7.25 (m, 2H, Ar), 7.21 – 7.16 (m, 1H, Ar), 5.86 (ddt, J = 16.9, 10.2, 6.7 Hz, 1H, 10-H), 5.13 – 5.04 (m, 2H, 12,13-H), 2.99 (t, J = 7.9 Hz, 2H, 8-H), 2.40 (td, *J* = 7.9, 6.7 Hz, 2H, 9-H) ppm. $^{13}$C NMR (101 MHz, $CDCl_3$) δ 136.5 (5), 129.4, 129.0, 126.1 (2), 116.4 (11), 33.5 (8), 33.2 (9) ppm.

*6.2.1.12 But-3-en-1-yl(p-tolyl)sulfane (**27n**)*[389]

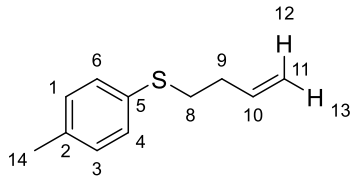


Synthesised from thicresol and 4-bromo-1-butene. Pale yellow oil, 72% yield. $^{1}$H NMR (400 MHz, $CDCl_3$) δ 7.27 (dd, *J* = 7.1, 2.0 Hz, 2H, 4,6-H), 7.10 (d, J = 8.1 Hz, 2H, 1,3-H), 5.90 – 5.78 (m, 1H, 10-H), 5.11 – 5.01 (m, 2H. 12,13-H), 2.94 (t, J = 7.1 Hz, 2H, 8-H), 2.36 (dt, *J* = 8.3, 7.1 Hz, 2H, 9-H), 2.32 (s, 3H, 14-H) ppm. $^{13}$C NMR (101 MHz, $CDCl_3$) δ 136.5 (5), 132.6 (10), 130.2 (2), 129.7 (1,3), 128.6 (4,6), 116.1 (11), 33.8 (14), 33.5 (8), 21.0 (9) ppm.

*6.2.1.13 Allyl(benzyl)sulfane (**27p**)*[390]

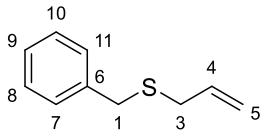


Synthesised from benzylmercaptan and allylbromide. Yellow oil, 55% yield. $^{1}$H NMR (400 MHz, $CDCl_3$) δ 7.36 – 7.19 (m, 5H, Ar), 5.88 – 5.73 (m, 1H, 4-H), 5.18 – 5.03 (m, 2H, 5-H), 3.67 (s, 2H, 1-H), 3.04 (d, J = 7.1 Hz, 2H, 3-H) ppm. $^{13}$C NMR (101 MHz, $CDCl_3$) δ 138.3 (6), 134.2 (4), 129.0 (7,11), 128.5 (8,10), 127.0 (9), 117.3 (5), 34.9 (1), 34.1 (3) ppm.

*6.2.1.14 2-(Phenylthio)propanenitrile (**27q**)*[391]

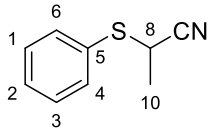


Synthesised from thiophenol and 2-bromopropionitrile. Yellow oil, 76% yield. $^{1}$H NMR (400 MHz, $CDCl_3$) δ 7.64 – 7.60 (m, 2H, 4,6-H), 7.42 – 7.37 (m, 3H, 1-3-H), 3.80 (q, J = 7.3 Hz, 1H, 8-H), 1.61 (d, J = 7.3 Hz, 3H, 10-H) ppm. $^{13}$C NMR (101 MHz, $CDCl_3$) δ 134.8 (5), 130.5 (4,6), 129.7 (1,3), 129.5 (2), 119.9 (CN), 31.4 (8), 18.8 (10) ppm.

### 6.2.2 General procedure for the synthesis of sulfides 38a-c

Thiophenol (14.3 mmol) was added to a solution of $NaHCO_3$ (14.3 mmol) in water (8 mL) at RT, followed by the appropriate α,β-unsaturated ketone/aldehyde **21** (7.14 mmol). The resulting mixture was stirred until the reaction was completed as observed on TLC. The reaction was then extracted in EtOAc (3x10 mL), the collected organic layers were washed with water (1x20 mL) and brine (2x20 mL), dried on $MgSO_4$ and evaporated under reduced pressure. The crude product was purified by column chromatography using a hexane/EtOAc (10:1) eluting system to afford the desired sulfides **27a-c**.

*6.2.2.1 4-(Phenylthio)butan-2-one (**38a**)*[392]

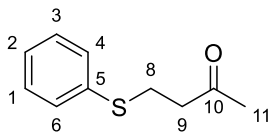


Synthesised from thiophenol and 3-buten-2-one. Yellow oil, 92% yield. $^{1}$H NMR (400 MHz, $CDCl_3$) δ 7.42 – 7.15 (m, 5H, Ar), 3.15 (t, *J* = 7.3 Hz, 2H, 9-H), 2.77 (t, *J* = 7.3 Hz,

2H, 8-H), 2.15 (s, 3H, 11-H) ppm. $^{13}$C NMR (101 MHz, $CDCl_3$) δ 206.5 (10), 135.7 (5), 129.6 (4,6), 129.0 (1,3), 126.3 (2), 43.1 (9), 30.1 (11), 27.5 (8) ppm.

*6.2.2.2 4-(Phenylthio)pentan-2-one (**38b**)*[393]

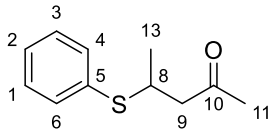


Synthesised from thiophenol and 4-chloropentan-2-one. Pale yellow oil, 82% yield. $^1$H NMR (400 MHz, $CDCl_3$) δ 7.42 (d, *J* = 7.0 Hz, 2H, 4,6-H), 7.29 (dt, *J* = 14.7, 7.0 Hz, 3H, 1,3-H), 3.70 (m, 1H, 8-H), 2.76 (dd, *J* = 15.3, 6.9 Hz, 1H, 9-H), 2.57 (dd, *J* = 15.3, 6.9 Hz, 1H, 9-H), 2.14 (s, 3H, 11-H), 1.30 (d, *J* = 6.7 Hz, 3H, 13-H) ppm. $^{13}$C NMR (101 MHz, $CDCl_3$) δ 206.6 (11), 134.2 (5), 132.4(2), 129.0 (4,6), 127.3 (1,3), 50.4 (8), 38.2 (9), 30.6 (11), 21.0 (13) ppm.

*6.2.2.3 3-(Phenylthio)butanal (**38c**)*[394]

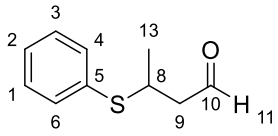


Synthesised from thiophenol and crotonaldehyde. Colourless oil, 73% yield. $^1$H NMR (400 MHz, $CDCl_3$) δ 9.66 (d, *J* = 1.9 Hz, 1H, 11-H), 7.34 (d, *J* = 6.4 Hz, 2H, 4,6-H), 7.27 – 7.14 (m, 3H, 1,3-H), 3.60 (sx, *J* = 6.8 Hz, 1H, 8-H), 2.66 – 2.43 (m, 2H, 9-H), 1.27 (d, *J* = 6.8 Hz, 3H, 13-H) ppm. $^{13}$C NMR (101 MHz, $CDCl_3$) δ 200.3 (10), 133.6 (5), 133.0 (4,6), 129.1 (1,3), 127.7 (2), 50.1 (8), 37.6 (9), 21.2 (13) ppm.

### 6.2.3 General procedure for the synthesis of sulfides 38d-f

Thiophenol (1.95 mmol) and the appropriate 1-bromoketone **22** (1.50 mmol) were consecutively added to a solution of $NaHCO_3$ (3.45 mmol) previously dissolved in water (8 mL). The reaction mixture was stirred at RT until completion was observed on TLC. The reaction was extracted in ethyl acetate (3x4 mL), the collected organic layers were washed with water (1x10 mL) and brine (2x10 mL), dried on $MgSO_4$ and evaporated under reduced pressure. The crude product was then purified by column chromatography using a hexane/EtOAc (10:1) eluting system to afford the desired sulfides **27d-f**.

*6.2.3.1 3-(Phenylthio)-2-propanone (**38d**)*[395]

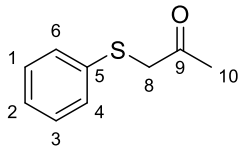


Synthesised from thiophenol and 1-bromoacetone. Yellow solid, 85% yield. $^{1}$H NMR (400 MHz, $CDCl_3$) δ 7.42 – 7.17 (m, 5H, Ar), 3.69 (s, 2H, 8-H), 2.30 (s, 3H, 10-H) ppm. $^{13}$C NMR (101 MHz, $CDCl_3$) δ 203.5 (9), 134.7 (5), 129.5 (4,6), 129.2 (1,3), 126.9 (2), 44.7 (8), 28.0 (10) ppm.

*6.2.3.2 1-(Phenylthio)-2-butanone (**38e**)*[395]

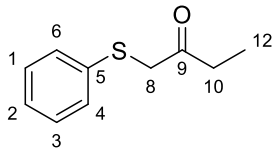


Synthesised from thiophenol and 1-bromo-2-butanone. Pale oil, 98% yield. $^{1}$H NMR (400 MHz, $CDCl_3$) δ 7.39 – 7.19 (m, 5H, Ar), 3.70 (s, 2H, 8-H), 2.64 (q, *J* = 7.3 Hz, 2H, 10-H), 1.08 (t, *J* = 7.3 Hz, 3H, 12-H) ppm. $^{13}$C NMR (101 MHz, $CDCl_3$) δ 206.2 (9), 135.0 (5), 129.5 (4,6), 129.1 (1,3), 126.8 (2), 43.6 (8), 33.9 (10), 7.9 (12) ppm.

*6.2.3.3 1-(Phenylthio)-2-pentanone (**38f**)*[395]

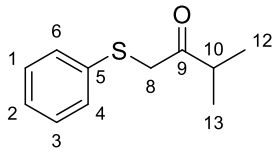


Synthesised from thiophenol and 1-bromo-3-methyl-2-butanone. Colourless oil, 54% yield. $^{1}$H NMR (400 MHz, $CDCl_3$) δ 7.42 – 7.17 (m, 5H, *Ar*), 3.78 (s, 2H), 2.96 (p, *J* = 6.9 Hz, 1H, C*H*), 1.12 (d, *J* = 6.9 Hz, 6H) ppm. $^{13}$C NMR (101 MHz, $CDCl_3$) δ 208.9, 129.6 (2C), 129.1 (2C), 126.8, 42.5, 38.7, 18.4 ppm.

### 6.2.4 General procedure for the synthesis of sulfides 40

Ketones **38a** or **38c** (1.00 mmol) were reduced using $NaBH_4$ (1.50 mmol) previously dissolved in MeOH (20 mL). The resulting mixture was stirred until the reaction was completed as observed on TLC. Upon completion, MeOH was evaporated under reduced pressure and the residue dissolved in EtOAc (20 mL), washed with water (1x20

mL) and brine (2x 20 mL), dried on $MgSO_4$ and evaporated under reduced pressure. The crude product was purified by column chromatography to afford the desired sulfides **40a,c**.

#### *6.2.4.1 4-(Phenylthio)butan-2-ol (**40a**)*[392]

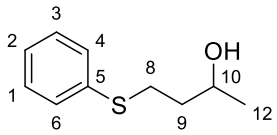


Oil, 97% yield. $^1$H NMR (400 MHz, $CDCl_3$) δ 7.39 – 7.33 (m, 2H, 4,6-H), 7.34 – 7.24 (m, 2H, 1,3-H), 7.23 – 7.15 (m, 1H, 2-H), 3.98 (sx, J = 6.2 Hz, 1H, 10-H), 3.12 – 2.97 (m, 2H, 8-H), 1.83 – 1.73 (m, 2H, 9-H), 1.67 (s, 1H, OH), 1.22 (d, J = 6.2 Hz, 3H, 12-H) ppm. $^{13}$C NMR (101 MHz, $CDCl_3$) δ 136.5 (5), 129.3 (4,6), 129.0 (1,3), 126.1 (2), 67.1 (10), 38.2 (8), 30.3 (9), 23.8 (12) ppm.

#### *6.2.4.2 3-(Phenylthio)butan-1-ol (**40c**)*

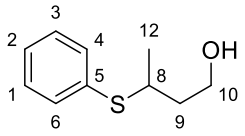


Oil, 68% yield. $^1$H NMR (400 MHz, $CDCl_3$) δ 7.47 – 7.40 (m, 2H, Ar), 7.35 – 7.28 (m, 2H, Ar), 7.28 – 7.21 (m, 1H, Ar), 3.89 – 3.71 (m, 2H, 10-H), 3.41 (sx, J = 6.8 Hz, 1H, 8-H), 2.06 (s, 1H, OH), 1.93 – 1.73 (m, 2H, 9-H), 1.33 (d, J = 6.8 Hz, 3H, 12-H) ppm. $^{13}$C NMR (101 MHz, $CDCl_3$) δ 134.8 (5), 132.3 (4,6), 129.0 (1,3), 127.0 (2), 60.6 (10), 40.4 (8), 39.2 (9), 21.6 (12) ppm.

### 6.2.5 Synthesis of (but-3-en-1-yloxy)benzene 33[396]

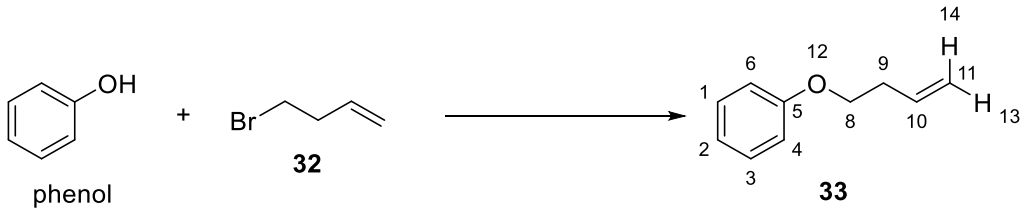


Phenol (1.35 mmol) and 4-bromobut-1-ene **32** (2.70 mmol) were added to a microwave (MW) vial and dissolved in $CH_3CN$ (2 mL). $K_2CO_3$ (3.37 mmol) and NaI (0.13 mmol) were then added to the vial and the resulting reaction mixture was stirred at 120 °C for 2 h. The reaction was then gently evaporated under vacuum to remove $CH_3CN$ and

redissolved in 2 mL EtOAc and 2 mL water. Then, it was extracted in EtOAc (3 x 2mL) and the collected organic layers were washed with water (1 x 2mL), brine (2mL), dried on $MgSO_4$ and evaporated under vacuum. The crude product was then purified by silica flash chromatography using a 95:5 hexane:EtOAc eluent system to afford ether **33** as an oil (80 mg, 40% yield). $^1$H NMR (500 MHz, $CDCl_3$) δ 7.32 – 7.25 (m, 2H, 4,6-H), 6.98 – 6.88 (m, 3H, 1-3-H), 5.92 (ddt, *J* = 17.1, 10.2, 6.8 Hz, 1H, 10-H), 5.18 (dq, *J* = 17.1, 1.6 Hz, 1H, 14-H), 5.11 (dq, *J* = 10.2, 1.6 Hz, 1H, 13-H), 4.02 (t, *J* = 6.8 Hz, 2H, 8-H), 2.55 (qt, *J* = 6.8, 1.6 Hz, 2H, 9-H).

### 6.2.6 Synthesis of chiral acids 47 and 52

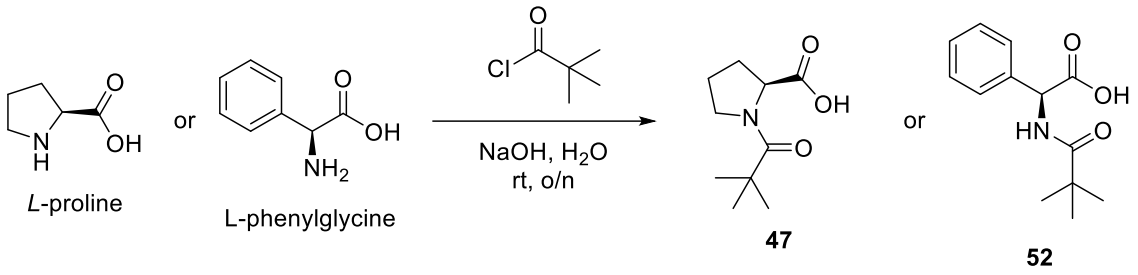


*L*-proline L-phenylglycine **47** **52**

L-proline or L-phenylglycine (0.26 mmol) was dissolved in 500 µL 4% $NaOH_{(aq)}$ solution. Then, pivaloyl chloride (0.31 mmol) was added to the amino acid solution and the resulting mixture was stirred overnight at RT. Then, 3M HCl was used to acidify the solution and the protected amino acid was extracted in EtOAc (3x5 mL) and the collected organic layers washed with water (1x5 mL) and brine (1x5 mL), dried over $MgSO_4$ and dried at the rotary evaporator. The crude material was recrystallised from a mixture of hexane and EtOAc and was then used without any further purification.

#### *6.2.6.1 Pivaloyl-L-proline (**47**)*[397]

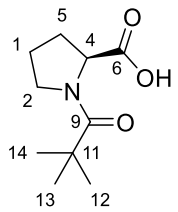

White solid, 58% yield. $^1$H NMR (400 MHz, $CDCl_3$) δ 4.55 (dd, *J* = 8.0, 4.0 Hz, 1H, 4-H), 3.71 (m, 2H, 2-H), 2.17 – 1.91 (m, 4H, 1,5-H), 1.27 (s, 9H, 12-14-H).

*6.2.6.2 Pivaloyl-L-phenylglycine (**52**)*[398]

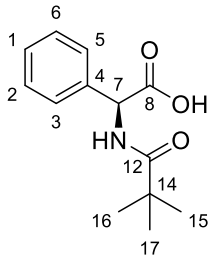


White solid, 65% yield. $^{1}$H NMR (400 MHz, $CDCl_3$) δ 7.42 – 7.28 (m, 5H, Ar), 6.70 (s, 1H, NH), 5.53 (d, *J* = 6.7 Hz, 1H, 7-H), 1.21 (s, 9H, 12-14-H).

## Biocatalytic methods

### 6.2.7 General procedure for the biocatalytic oxidation of sulfides using CALB

The appropriate sulfide (0.22 mmol), CALB (20 % w/w) and UHP or $H_2O_2$ (0.24 mmol) were added to a round bottom flask containing ethyl acetate (1 mL). The reaction was stirred for 2-24 h at 37 $^{o}$C and monitored by TLC until completion. Upon completion, CALB was removed from the reaction mixture by filtration using a celite plug and then rinsed with ethyl acetate (3x2 mL) and quenched with 10 mL 10% $Na_2S_2O_{3(aq)}$ followed by 10 mL of $H_2O$. The collected aqueous layer was then extracted with ethyl acetate (3x5 mL), the collected organic layers were washed with water (1x10 mL) and brine (2x10 mL), dried on $MgSO_4$ and evaporated under reduced pressure. The crude product was then purified by silica flash chromatography using an appropriate hexane:EtOAc eluting system.

*6.2.7.1 Methyl phenyl sulfoxide (**28a**)*[399]

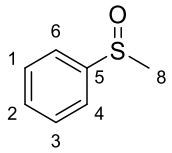


Oil, 89 % yield. $^{1}$H NMR (400 MHz, Chloroform-*d*) δ 7.70 – 7.59 (m, 2H, 4,6-H), 7.57 – 7.45 (m, 3H, 1-3-H), 2.71 (s, 3H, 8-H) ppm. $^{13}$C NMR (101 MHz, $CDCl_3$) δ 145.9 (5), 131.1 (4,6), 129.5 (1,3), 123.6 (2), 44.1 (8) ppm.

*6.2.7.2 1-Fluoro-4-(methylsulfinyl)benzene (**28b**)*[399,400]

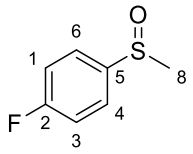


Pale yellow oil, 85% yield. $^{1}$H NMR (400 MHz, Chloroform-*d*) δ 7.67 – 7.60 (m, 2H, 4,6-H), 7.24 – 7.17 (m, 2H,1,3-H), 2.70 (s, 3H, 8-H) ppm. $^{13}$C NMR (101 MHz, $CDCl_3$) δ 164.48 (d, *J* = 251.4 Hz, 5-C), 141.31 (2-C), 125.99 (d, *J* = 8.9 Hz, 4,6-C), 116.83 (d, *J* = 22.6 Hz, 1,3-C), 44.30 (d, *J* = 1.4 Hz, 8-C). $^{19}$F NMR (376 MHz, $CDCl_3$) δ -108.61 (F) ppm.

*6.2.7.3 (Ethylsulfinyl)benzene (**28c**)*[401]

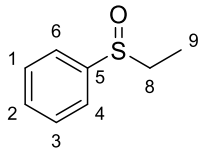


Pale yellow oil, 63 % yield. $^{1}$H NMR (400 MHz, Chloroform-*d*) δ 7.65 – 7.57 (m, 2H, 4,6-H), 7.54 – 7.45 (m, 3H, 1-3-H), 2.96 – 2.83 (m, 1H, 8-H), 2.76 (dq, *J* = 13.2, 7.4 Hz, 1H, 8-H), 1.19 (t, *J* = 7.4 Hz, 3H, 9-H) ppm. $^{13}$C NMR (101 MHz, $CDCl_3$) δ 143.5 (5), 131.0 (2), 129.3 (4,6), 124.3 (1,3), 50.4 (8), 6.1 (9).

*6.2.7.4 (Ethylsulfinyl)-4-methylbenzene (**28d**)*[355]

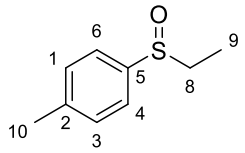


Yellow oil, 71% yield. $^{1}$H NMR (400 MHz, Chloroform-*d*) δ 7.52 – 7.43 (m, 2H, 4,6-H), 7.29 (d, *J* = 7.9 Hz, 2H, 1,3-H), 2.84 (dq, *J* = 13.2, 7.4 Hz, 1H, 8-H), 2.73 (dq, *J* = 13.2, 7.4 Hz, 1H, 8-H), 2.39 (s, 3H, 10-H), 1.16 (t, *J* = 7.4 Hz, 3H, 9-H) ppm. $^{13}$C NMR (101 MHz, $CDCl_3$) δ 141.4 (5), 140.2 (2), 129.9 (4,6), 124.3 (1,3), 50.4 (8), 21.5 (10), 6.1 (9).

*6.2.7.5 1-(Ethylsulfinyl)-4-methoxybenzene (**28e**)*[402]

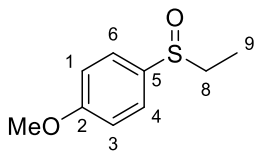

Yellow oil, 60% yield. $^{1}$H NMR (400 MHz, Chloroform-*d*) δ 7.58 – 7.51 (m, 2H, 1,3-H), 7.05 – 6.99 (m, 2H, 4,6-H), 3.85 (s, 3H, OMe), 2.91 – 2.71 (m, 2H, 8-H), 1.17 (t, *J* = 7.4 Hz, 3H, 9-H) ppm. $^{13}$C NMR (101 MHz, $CDCl_3$) δ 162.1 (2), 134.4 (5), 126.2 (4,6), 114.8 (1,3), 55.6 (OMe), 50.6 (8), 6.3 (9) ppm.

### *6.2.7.6 1-Chloro-4-(ethylsulfinyl)benzene (**28f**)*[403]

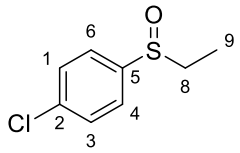


Oil, 67% yield. $^{1}$H NMR (400 MHz, Chloroform-*d*) δ 7.53 (d, *J* = 8.6 Hz, 2H, 1,3-H), 7.48 (d, *J* = 8.6 Hz, 2H, 4,6-H), 2.94 – 2.80 (m, 1H, 8-H), 2.80 – 2.66 (m, 1H, 8-H), 1.17 (t, *J* = 7.4 Hz, 3H, 9-H) ppm. $^{13}$C NMR (101 MHz, $CDCl_3$) δ 142.0 (5), 137.2 (2), 129.5 (4,6), 125.7 (1,3), 50.4 (8), 5.9 (9) ppm.

### *6.2.7.7 1-Bromo-4-(ethylsulfinyl)benzene (**28g**)*[404]

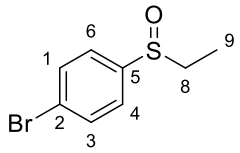


Yellow oil, 67% yield. $^{1}$H NMR (400 MHz, Chloroform-*d*) δ 7.67 – 7.62 (m, 2H, 4,6-H), 7.49 – 7.44 (m, 2H, 1,3-H), 2.88 (dq, *J* = 13.3, 7.4 Hz, 1H, 8-H), 2.72 (dq, *J* = 13.3, 7.4 Hz, 1H, 8-H), 1.18 (t, *J* = 7.4 Hz, 3H, 9-H) ppm. $^{13}$C NMR (101 MHz, $CDCl_3$) δ 142.6 (5), 132.5 (4,6), 125.9 (1,3), 125.5 (2), 50.4 (8), 5.9 (9). MS (APCI): m/z = 232.1, 234.1 $[M+H]^+$.

### *6.2.7.8 1-Chloro-2-(ethylsulfinyl)benzene (**28h**)*[405]

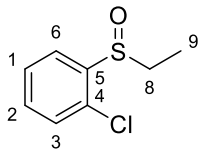


Yellow oil, 81 % yield: $^{1}$H NMR (400 MHz, Chloroform-*d*) δ 7.88 (dd, *J* = 7.8, 1.7 Hz, 1H, Ar), 7.52 (td, *J* = 7.5, 1.5 Hz, 1H, Ar), 7.47 – 7.37 (m, 2H, Ar), 3.13 (dq, *J* = 14.2, 7.4 Hz, 1H, 8-H), 2.86 (dq, *J* = 14.2, 7.4 Hz, 1H, 8-H), 1.25 (t, *J* = 7.4 Hz, 3H, 9-H) ppm. $^{13}$C NMR (101 MHz, $CDCl_3$) δ 141.1 (5), 131.8, 130.1 (4), 129.8, 127.7, 126.6, 47.1 (8), 5.6 (9) ppm. MS (APCI): m/z = 189.1 $[M+H]^+$.

*6.2.7.9 1-Bromo-2-(ethylsulfinyl)benzene (**28i**)*[406]

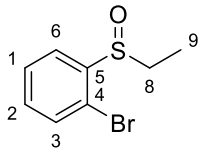


Pale yellow oil, 80 % yield: $^{1}$H NMR (400 MHz, Chloroform-*d*) δ 7.85 (dd, *J* = 8.0, 1.8 Hz, 1H, Ar), 7.62 – 7.50 (m, 2H, Ar), 7.40 – 7.32 (m, 1H, Ar), 3.13 (dq, *J* = 13.6, 7.4 Hz, 1H, 8-H), 2.85 (dq, *J* = 13.6, 7.4 Hz, 1H, 8-H), 1.25 (t, *J* = 7.4 Hz, 3H, 9-H) ppm. $^{13}$C NMR (101 MHz, $CDCl_3$) δ 143.0 (5), 133.1, 132.4, 128.4, 127.1, 118.9 (4), 47.5 (8), 6.0 (9) ppm. MS (APCI): m/z = 232.1-234.1 $[M+H]^+$.

*6.2.7.10 1-Methoxy-4-(propylsulfinyl)benzene (**28j**)*[407]

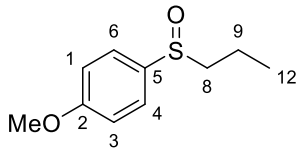


Yellow oil, 79 % yield. $^{1}$H NMR (400 MHz, Chloroform-*d*) δ 7.51 (d, *J* = 8.8 Hz, 2H, 4,6-H), 6.97 (d, *J* = 8.8 Hz, 2H, 1,3-H), 3.79 (s, 3H, OMe), 2.81 – 2.70 (m, 1H, 8-H), 2.70 – 2.59 (m, 1H, 8-H), 1.76 – 1.52 (m, 2H, 9-H), 0.98 (t, *J* = 7.4 Hz, 3H, 12-H) ppm. $^{13}$C NMR (101 MHz, $CDCl_3$) δ 161.9 (2), 134.9 (4,6), 125.9 (1,3), 114.7 (5), 59.4 (OMe), 55.5 (8), 16.0 (9), 13.3 (12) ppm. MS (APCI): m/z = 199.1 $[M+H]^+$.

*6.2.7.11 1-Methyl-4-(propylsulfinyl)benzene (**28k**)*[408]

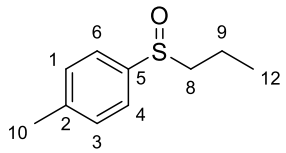


Yellow oil, 68 % yield. $^{1}$H NMR (400 MHz, $CDCl_3$) δ 7.51 (d, *J* = 8.1 Hz, 2H, 4,6-H), 7.31 (d, *J* = 8.1 Hz, 2H, 1,3-H), 2.88 – 2.65 (m, 2H, 8-H), 2.41 (s, 3H, 10-H), 1.85 – 1.56 (m, 2H, 8-H), 1.03 (t, *J* = 7.4 Hz, 3H, 12-H) ppm. $^{13}$C NMR (101 MHz, $CDCl_3$) δ 141.5 (5), 141.0 (2), 130.0 (4,6), 124.2 (1,3), 59.5 (8), 21.5, 16.1, 13.4 (9) ppm. MS (APCI): m/z = 183.1 $[M+H]^+$.

*6.2.7.12 (Allylsulfinyl)benzene (**28l**)*[401]

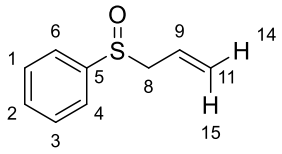


Yellow oil, 68 % yield. $^{1}$H NMR (400 MHz, $CDCl_3$) δ 7.64 – 7.56 (m, 2H, 4,6-H), 7.49 (m, 3H, 1-3-H), 5.63 (m, 1H, 9-H), 5.31 (dd, *J* = 10.2, 1.4 Hz, 1H, 14-H), 5.17 (dd, *J* = 17.0, 1.4 Hz, 1H, 15-H), 3.62 – 3.42 (m, 2H, 8-H) ppm. $^{13}$C NMR (101 MHz, $CDCl_3$) δ 142.9 (5), 131.1 (2), 129.1 (4,6), 125.3 (9), 124.3 (1,3), 123.9 (11), 60.9 (8) ppm.

*6.2.7.13 (But-3-en-1-ylsulfinyl)benzene (**28m**)*[99]

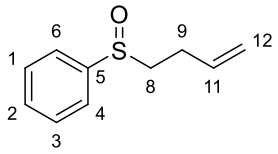


Yellow oil, 58 % yield. $^{1}$H NMR (400 MHz, Chloroform-*d*) δ 7.64 – 7.59 (m, 2H, 4,6-H), 7.55 – 7.46 (m, 3H, 1-3-H), 5.79 (ddt, *J* = 16.9, 10.2, 6.6 Hz, 1H, 11-H), 5.15 – 5.01 (m, 2H, 12-H), 2.94 – 2.76 (m, 2H, 9-H), 2.60 – 2.45 (m, 1H, 8-H), 2.39 – 2.24 (m, 1H, 8-H) ppm. $^{13}$C NMR (101 MHz, $CDCl_3$) δ 143.8 (5), 135.0 (11), 131.1 (2), 129.4 (4,6), 124.2 (1,3), 117.2 (12), 56.2 (8), 26.3 (9) ppm.

*6.2.7.14 1-(But-3-en-1-ylsulfinyl)-4-methylbenzene (**28n**)*[389]

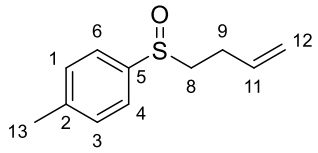


Pale yellow oil, 73 % yield. $^{1}$H NMR (400 MHz, $CDCl_3$) δ 7.51 (d, *J* = 8.1 Hz, 2H, 4,6-H), 7.33 (d, *J* = 8.1 Hz, 2H, 1,3-H), 5.86 – 5.73 (m, 1H, 11-H), 5.14 – 5.03 (m, 2H, 12-H), 2.84 (t, *J* = 7.8 Hz, 2H, 8-H), 2.57 – 2.45 (m, 1H, 9-H), 2.42 (s, 3H, 13-H), 2.39 – 2.27 (m, 1H, 9-H) ppm. $^{13}$C NMR (101 MHz, $CDCl_3$) δ 141.6 (5), 140.7 (2), 135.1 (11), 130.1 (4,6), 124.3 (1,3), 117.1 (12), 56.4 (8), 26.4 (13), 21.6 (9) ppm.

*6.2.7.15 Benzyl methyl sulfoxide (**28o**)*[409]

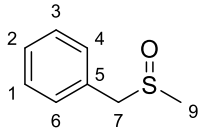

Yellow oil, 82% yield. $^{1}$H NMR (400 MHz, Chloroform-*d*) δ 7.44 – 7.32 (m, 3H, Ar), 7.31 – 7.26 (m, 2H, Ar), 4.07 (d, *J* = 12.8 Hz, 1H, 7-H), 3.93 (d, *J* = 12.8 Hz, 1H, 7-H), 2.46 (s, 3H, 9-H) ppm. $^{13}$C NMR (101 MHz, $CDCl_3$) δ 130.2 (4,6), 129.8 (5), 129.1 (1,3), 128.6 (2), 60.5 (7), 37.4 (90 ppm. MS (APCI): m/z = 155.1 $[M+H]^+$.

*6.2.7.16 Allyl benzyl sulfoxide (**28p**)*[394]

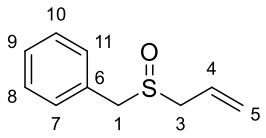


White crystal, 86% yield. $^{1}$H NMR (400 MHz, Chloroform-*d*) δ 7.42 – 7.27 (m, 5H, Ar), 6.00 – 5.85 (m, 1H, 4-H), 5.52 – 5.34 (m, 2H, 5-H), 4.05 – 3.92 (m, 2H, 1-H), 3.43 (ddt, *J* = 13.2, 7.4, 1.1 Hz, 1H, 3-H), 3.27 (ddt, *J* = 13.2, 7.4, 1.1 Hz, 1H, 3-H) ppm. $^{13}$C NMR (101 MHz, $CDCl_3$) δ 130.1, 130.0, 129.0, 128.4, 125.8, 123.7, 56.9, 54.2 ppm.

*6.2.7.17 2-(Phenylsulfinyl)propanenitrile (**28q**)*

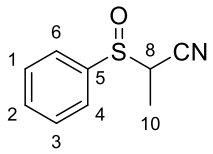


1:1.4 Mixture of diastereoisomers. Colourless oil, 78 % yield. $^{1}$H NMR (400 MHz, $CDCl_3$) δ 7.86 – 7.52 (m, 5H, Ar), 3.71 (q, *J* = 6.7 Hz, 1H, 8-H), 3.63 (q, *J* = 7.3 Hz, 1H, 8-H), 1.60 (d, *J* = 7.3 Hz, 2H, 10-H), 1.56 (d, *J* = 7.2 Hz, 1H, 10-H) ppm. $^{13}$C NMR (101 MHz, $CDCl_3$) δ 140.3 (5), 139.2 (5), 132.9 (2), 132.6 (2), 129.5 (4,6), 129.4 (4,6), 125.0 (1,3), 124.9 (1,3), 115.6 (CN), 115.1 (CN), 51.3 (8), 49.7 (8), 12.2 (10), 10.8 (10) ppm.

*6.2.7.18 1-(Butylsulfinyl)butane (**28r**)*[374]

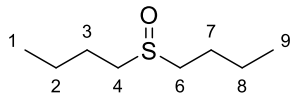


Oil, 89% yield. $^{1}$H NMR (400 MHz, Chloroform-*d*) δ 2.72 – 2.53 (m, 4H, 4,6-H), 1.80 – 1.63 (m, 4H, 3,7-H), 1.57 – 1.35 (m, 4H, 2,8-H), 0.94 (t, *J* = 7.4 Hz, 6H, 1,9-H) ppm. $^{13}$C NMR (101 MHz, $CDCl_3$) δ 52.3 (4,6), 24.7 (3,7), 22.2 (2,8), 13.8 (1,9) ppm.

*6.2.7.19 4-(Phenylsulfinyl)butan-2-one (**39a**)*[410]

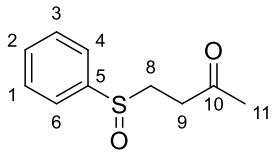


Oil, 71% yield. $^{1}$H NMR (400 MHz, $CDCl_3$) δ 7.60 – 7.39 (m, 5H, Ar), 3.16 (ddd, *J* = 13.5, 8.2, 6.3 Hz, 1H, 8-H), 2.93 (ddd, *J* = 18.0, 8.2, 6.3 Hz, 1H, 8-H), 2.82 (ddd, *J* = 13.5, 8.2, 5.2 Hz, 1H, 9-H), 2.61 (ddd, *J* = 18.0, 8.2, 5.2 Hz, 1H, 9-H), 2.09 (s, 3H, 11-H) ppm. $^{13}$C NMR (101 MHz, $CDCl_3$) δ 205.2 (10), 143.3 (5), 131.1 (2), 129.3 (4,6), 123.9 (1,3), 50.0 (8), 34.7 (9), 29.7 (11) ppm.

*6.2.7.20 4-(Phenylsulfinyl)pentan-2-one (**39b**)*

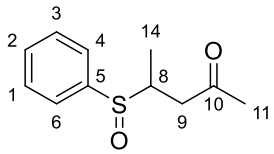


1:1.4 Mixture of diastereoisomers. Oil, 42 % yield. $^{1}$H NMR (400 MHz, $CDCl_3$) δ 7.63 – 7.45 (m, 10H, Ar), 3.27 (dt, *J* = 14.0, 6.5 Hz, 2H, 8-H), 3.18 (dd, *J* = 18.1, 6.5 Hz, 1H, 8-H), 2.85 (dd, *J* = 18.1, 3.8 Hz, 1H, 8-H), 2.49 (ddd, *J* = 18.1, 14.0, 8.1 Hz, 2H, 9-H), 2.21 (s, 3H, 11-H), 2.07 (s, 3H, 11-H), 1.29 (d, *J* = 7.0 Hz, 3H, 14-H), 0.99 (d, *J* = 7.0 Hz, 3H, 14-H) ppm. $^{13}$C NMR (101 MHz, $CDCl_3$) δ 205.4 (10), 205.2 (10), 141.8 (5), 141.2 (5), 131.3 (2), 130.9 (2), 129.1 (4,6), 129.0 (4,6), 124.9 (1,3), 124.7 (1,3), 54.8 (8), 53.6 (8), 43.7 (9), 41.5 (9), 30.5 (11), 29.7 (11), 14.6 (14), 10.3 (14) ppm. HRMS (APCI) m/z calcd. for $C_{11}H_{15}O_2S^+$ $[M+H]^+$ 211.0787; found 211.0785.

*6.2.7.21 1-(Phenylsulfinyl)propan-2-one (**39d**)*[411]

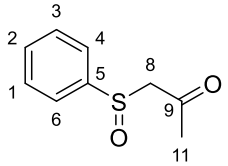


Oil, 67% yield. $^{1}$H NMR (400 MHz, $CDCl_3$) δ 7.73 – 7.63 (m, 2H, 4,6-H), 7.55 (m, 3H, 1-3-H), 3.88 (d, *J* = 13.7 Hz, 1H, 8-H), 3.81 (d, *J* = 13.7 Hz, 1H, 8-H), 2.25 (s, 3H, 11-H) ppm. $^{13}$C NMR (101 MHz, $CDCl_3$) δ 199.5 (9), 143.0 (5), 131.7 (2), 129.6 (4,6), 124.1 (1,3), 68.8 (8), 32.1 (11) ppm.

*6.2.7.22 1-(phenylsulfinyl)butan-2-one (**39e**)*[412]

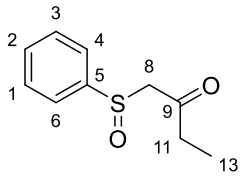


Oil, 81% yield. $^{1}$H NMR (400 MHz, $CDCl_3$) δ 7.67 – 7.59 (m, 2H, 4,6-H), 7.51 (m, 3H, 1-3-H), 3.89 (d, *J* = 13.7 Hz, 1H, 8-H), 3.76 (d, *J* = 13.7 Hz, 1H, 8-H), 2.48 (dq, *J* = 12.1, 7.2 Hz, 2H, 11-H), 0.99 (t, *J* = 7.2 Hz, 3H, 13-H) ppm. $^{13}$C NMR (101 MHz, $CDCl_3$) δ 202.1 (9), 143.2 (5), 131.7 (2), 129.5 (4,6), 124.1 (1,3), 68.0 (8), 38.5 (11), 7.3 (13).

*6.2.7.23 3-Methyl-1-(phenylsulfinyl)butan-2-one (**39f**)*

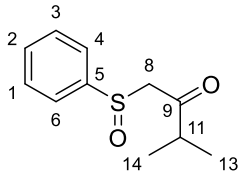


Oil, 68% yield. $^{1}$H NMR (400 MHz, Chloroform-*d*) δ 7.70 – 7.61 (m, 2H, 4,6-H), 7.52 (dd, *J* = 5.2, 2.0 Hz, 3H, 1-3-H), 4.00 (d, *J* = 14.2 Hz, 1H, 8-H), 3.81 (d, *J* = 14.2 Hz, 1H, 8-H), 2.56 (h, *J* = 7.0 Hz, 1H, 11-H), 1.08 (d, *J* = 7.0 Hz, 3H, 13-H), 0.99 (d, *J* = 6.9 Hz, 3H, 14-H) ppm. $^{13}$C NMR (101 MHz, $CDCl_3$) δ 205.6 (9), 143.6 (5), 131.7 (2), 129.5 (4,6), 124.2 (1,3), 67.0 (8), 42.3 (11), 17.5 (13), 17.4 (14) ppm. HRMS (APCI) m/z calcd. for $C_{11}H_{15}O_2S^+$ $[M+H]^+$ 211.0787; found 211.0786.

*6.2.7.24 4-(Phenylsulfinyl)butan-2-ol (**41a**)*

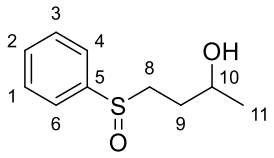


1:1 Mixture of diastereoisomers. Oil, 67% yield. $^{1}$H NMR (400 MHz, Chloroform-*d*) δ 7.69 – 7.43 (m, 10H, Ar), 4.00 – 3.78 (m, 2H, 8-H), 3.15 – 2.96 (m, 2H), 2.96 – 2.80 (m, 2H), 2.01 – 1.88 (m, 1H), 1.80 (p, *J* = 7.8, 7.4 Hz, 2H, 9-H), 1.75 – 1.63 (m, 1H), 1.19 (d, *J* = 6.0 Hz, 6H, 11-H) ppm. $^{13}$C NMR (101 MHz, $CDCl_3$) δ 143.4 (5), 143.2 (5), 131.1 (2), 131.1 (2), 129.4 (4,6), 129.4 (4,6), 124.3 (1,3), 124.2 (1,3), 66.6 (8), 66.4 (8), 53.8 (10), 53.7 (10), 32.1 (9), 31.6 (9), 23.6 (11), 23.6 (11) ppm. HRMS (APCI) m/z calcd. for $C_{10}H_{15}O_2S^+$ $[M+H]^+$ 199.0787; found 199.0784.

*6.2.7.25 3-(Phenylsulfinyl)butyl acetate (**41b**)*

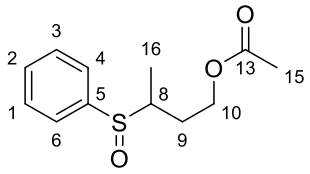

1:1 Mixture of diastereoisomers. Oil, 74% yield. $^{1}$H NMR (400 MHz, Chloroform-*d*) δ 7.64 – 7.43 (m, 5H, Ar), 4.30 (m, 1H, 8-H), 4.22 – 4.05 (m, 1H, 8-H), 4.16 – 4.04 (m, 2H), 2.89 – 2.81 (m, 1H), 2.77 (m, 6.5 Hz, 1H), 2.32 – 2.23 (m, 1H), 2.05 (s, 3H, 15-H), 2.00 (s, 3H, 15-H), 1.74 – 1.62 (m, 3H), 1.21 (d, *J* = 7.0 Hz, 3H, 16-H), 1.06 (d, *J* = 7.0 Hz, 3H, 16-H) ppm. $^{13}$C NMR (101 MHz, $CDCl_3$) δ 171.0 (13), 170.9 (13), 141.4 (5), 141.3 (5), 131.4 (2), 131.0 (2), 129.1 (4,6), 129.1 (4,6), 125.3 (1,3), 124.9 (1,3), 61.6 (10), 61.5 (10), 56.4 (8), 56.1 (8), 29.7 (9), 27.8 (9), 21.1 (15), 21.0 (15), 13.0 (16), 10.6 (16) ppm. HRMS (APCI) m/z calcd. for $C_{12}H_{17}O_3S^+$ $[M+H]^+$ 241.0893; found 241.0886.

*6.2.7.26 Omeprazole **43***[401]

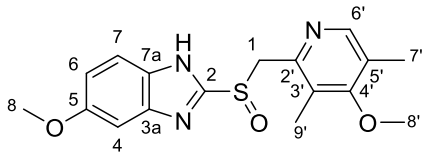

Brown solid, 73% yield. $^{1}$H NMR (400 MHz, Chloroform-*d*) δ 12.01 (br s, 1H, NH), 8.20 (s, 1H, 6'-H), 7.63 (br s, 1H, 4-H), 7.33 – 7.23 (br s, 1H, 6-H), 6.94 (d, *J* = 9.0 Hz, 1H, 7H), 6.88 (s, 0.5H), 4.79 – 4.65 (m, 2H, 1-H), 3.84 (s, 3H, 8-H), 3.63 (s, 3H, 8'-H), 2.22 (s, 3H, 9'-H), 2.14 (s, 3H, 7'-H) ppm. $^{13}$C NMR (101 MHz, $CDCl_3$) δ 164.6, 149.9, 148.9, 127.2, 126.5, 60.8, 60.0, 55.9, 13.5, 11.6 ppm. MS (APCI): m/z = 346.1 $[M+H]^+$.

### 6.2.8 CALB recycling experiments

The sulfide **27a** (20 mmol), CALB (20 % w/w) and UHP (22 mmol) were added to a round bottom flask containing EtOAc (50 mL) stirred at 37 ºC. The reaction was stirred for 24 h and monitored by TLC. Upon completion, CALB was removed through filtration using a Buchner funnel and washed with $CH_3CN/H_2O$ (9:1) (3x10 mL) to remove urea, followed by EtOAc (3x10 mL). The recovered CALB was air dried first and then placed in a desiccator to ensure full dryness for the next cycle. The filtrate was instead cooled to 0 ºC and quenched with 30 mL 10% $Na_2S_2O_{3(aq)}$. The organic layer was washed with water (1x) and brine (2x), dried on $MgSO_4$ and evaporated under reduced pressure. The

crude product analysed by NMR to determine conversion to sulfoxide. Quantities for the next reaction were calculated on the isolated dried CALB.

### 6.2.9 General procedure for the two step-one pot photocatalytic production of $H_2O_2$ and sulfoxidation by CALB

#### *6.2.9.1 Method 1: Monophasic*

Methyl phenyl sulfide **27a** (0.20 mmol) and CALB (20 % w/w) were added to a round bottom flask containing 2-EAQ (0.01 mmol, 5 mol %) suspended in a mix of EtOAc and EtOH (1 mL), which had been previously saturated with oxygen by bubbling compressed air through for 10 min. The reaction was stirred for 2-24 h under white light irradiation (5W) and monitored by TLC. Then, CALB was removed from the reaction mixture by filtration using a celite plug and then rinsed with EtOAc (3x2 mL) and quenched with 5 mL 10% $Na_2S_2O_{3(aq)}$ followed by 5 mL of $H_2O$. The collected aqueous layer was then extracted with EtOAc (3x5 mL), the collected organic layers were washed with water (1x10 mL) and brine (1x10 mL), dried on $MgSO_4$ and evaporated under reduced pressure. The conversion was determined by NMR from the crude product.

#### *6.2.9.2 Method 2: Biphasic*

Methyl phenyl sulfide **27a** (0.20 mmol) and CALB (20 % w/w) were added to a round bottom flask containing 2-EAQ (0.01 mmol, 5 mol %) suspended in a 1:4 water/toluene (or DCM) biphasic system (4 mL), which had been previously saturated with oxygen by bubbling compressed air through for 10 min. The reaction was stirred for 2-24 h under white light irradiation (5W) and monitored by TLC. Then, CALB was removed from the reaction mixture by filtration using a celite plug and then rinsed with toluene or DCM (3x2 mL) and quenched with 5 mL 10% $Na_2S_2O_{3(aq)}$. The collected aqueous layer was then extracted with EtOAc (3x5 mL), the collected organic layers were washed with water (1x10 mL) and brine (1x10 mL), dried on $MgSO_4$ and evaporated under reduced pressure. The conversion was determined by NMR from the crude product.

### 6.2.10 General procedure for the synthesis of chiral sulfoxides using chiral acids

Methyl phenyl sulfide **27a** (0.10 mmol), CALB (20 % w/w) and UHP or $H_2O_2$ (0.11 mmol) were added to a round bottom flask containing toluene (1 mL) and the appropriate chiral acid (0.10 mmol). The reaction was stirred for 2-24 h at 37 $^oC$ and monitored by TLC. Then, CALB was removed from the reaction mixture by filtration using a celite plug and

then rinsed with diethyl ether (3x2 mL) and quenched with 5 mL 10% $Na_2S_2O_{3(aq)}$ followed by 5 mL of $H_2O$. The collected aqueous layer was then extracted with diethyl ether (3x5 mL), the collected organic layers were washed with water (1x10 mL) and brine (2x10 mL), dried on $MgSO_4$ and evaporated under reduced pressure. The conversion was determined by NMR from the crude product and the enantiomeric excess was checked by normal phase chiral HPLC using a Daicel Chiralpak IC® (0.5µm, 4.6mm x 250mm) chiral column.

## 6.3 Chapter 3. Methods

## Synthetic methods

### 6.3.1 General procedure for the synthesis of sulfides 27 and 38

Sulfides **27o** and **27a-b**, **27x-ad** were commercially available. The synthetic methods and characterization of sulfides **27g**, **27j**, **38a**, **38d**, **38f** are described in sections 6.2.1, 6.2.2 and 6.2.3. The remaining sulfides were synthesised using one of the two following methods. Crude sulfides **27** were purified by flash column chromatography using an appropriate eluent mixture of EtOAc or $Et_2O$ and hexane to afford the resulting pure sulfide.

#### *6.3.1.1 Method A: microwave synthesis*

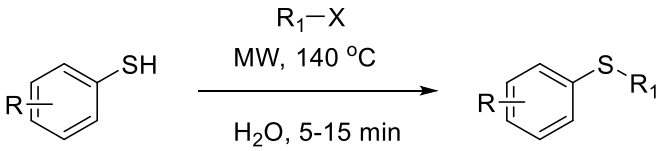


**27**

The appropriate thiophenol or benzylthiol (3.0 mmol) and halo-alkane (3.6 mmol) were added to a microwave (MW) vial and dissolved in water (10 mL). $K_2CO_3$ (4.5 mmol) and NaI (0.3 mmol) were then added to the vial and the resulting reaction mixture was stirred at 140 ºC in intervals of 5 minutes under microwave irradiation until completion was observed on TLC. The reaction was then extracted in EtOAc (3x2 mL) and the collected organic layers were washed with water (1x2 mL), brine (2x2 mL), dried on $MgSO_4$ and evaporated under vacuum.

#### *6.3.1.2 Method B: NaH synthesis*

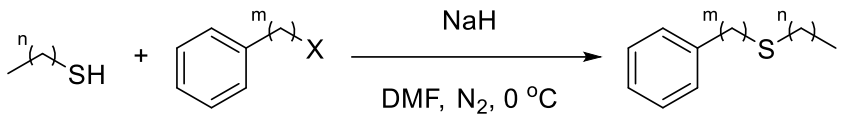


**21**

Methanethiol or ethanethiol (3.0 mmol) and NaH (6.0 mmol) were stirred in anhydrous DMF (10 mL) under $N_2$ for 30 min on ice. Then, a halo-arylalkane (3.6 mmol) was added to the mixture and the reaction was stirred until completion was observed on TLC. The reaction was quenched with ice, extracted with EtOAc (5x5 mL) and the collected organic

layers were washed with water (10x5 mL), brine (2x5 mL) to ensure full removal of DMF from the crude. The collected organic layer was the dried over $MgSO_4$ and evaporated under vacuum.

### *6.3.1.3 2-((Propylthio)methyl)pyridine (**27s**)*

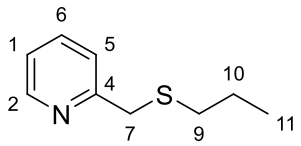


Synthesised using Method B from 2-(bromomethyl)pyridine hydrobromide and propanethiol. Pale yellow oil (62% yield). $\nu_{max}/cm^{-1}$: 2960, 1590, 1433. $^1$H NMR (400 MHz, Chloroform-*d*) δ 8.44 (d, *J* = 4.1 Hz, 1H), 7.57 (td, *J* = 7.7, 1.8 Hz, 1H), 7.30 (d, *J* = 7.9 Hz, 1H), 7.07 (ddd, *J* = 7.6, 4.9, 1.2 Hz, 1H), 3.76 (s, 2H), 2.43 – 2.35 (m, 2H), 1.51 (sx, *J* = 7.3 Hz, 2H), 0.87 (t, *J* = 7.3 Hz, 3H). $^{13}$C NMR (101 MHz, $CDCl_3$) δ 159.0, 149.1, 136.6, 123.0, 121.7, 38.1 (7), 33.7 (9), 22.5 (10), 13.4 (11). HRMS (ESI) m/z calcd. for $C_9H_{14}ON^{32}S^+$ $[M+H]^+$ 168.08415; found 168.0840.

### *6.3.1.4 2-((Ethylthio)methyl)pyridine (**27t**)*

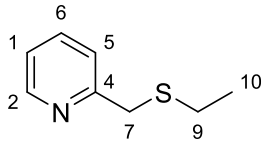


Synthesised using Method B from 2-(bromomethyl)pyridine hydrobromide and ethanethiol. Colourless oil (642 mg, 64% yield). $\nu_{max}/cm^{-1}$: 2925, 1590, 1433. $^1$H NMR (400 MHz, $CDCl_3$) δ 8.45 (ddd, *J* = 4.9, 1.9, 0.9 Hz, 1H, 2-H), 7.60 (td, *J* = 7.6, 1.9 Hz, 1H, 6-H), 7.32 (dt, *J* = 7.8, 1.2 Hz, 1H, 1-H), 7.10 (ddd, *J* = 7.6, 4.9, 1.2 Hz, 1H, 5-H), 3.79 (s, 2H, 7-H), 2.44 (q, *J* = 7.4 Hz, 2H, 9-H), 1.16 (t, *J* = 7.4 Hz, 3H, 11-H). $^{13}$C NMR (101 MHz, $CDCl_3$) δ 159.0 (4), 149.0 (2), 137.1 (6), 123.3 (5), 122.0 (1), 37.8 (7), 25.8 (9), 14.6 (11). HRMS (ESI) m/z calcd. for $C_8H_{12}N^{32}S^+$ $[M+H]^+$ 154.06850; found 154.0685.

### *6.3.1.5 2-((Benzylthio)methyl)pyridine (**27u**)*[413]

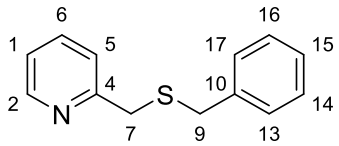


Synthesised using Method B from 2-(bromomethyl)pyridine hydrobromide and benzyl mercaptan. Red oil (46% yield). $^1$H NMR (400 MHz, Chloroform-d) δ 8.43 (ddd, J = 4.9,

1.9, 0.9 Hz, 1H), 7.48 (td, J = 7.7, 1.9 Hz, 1H), 7.23 – 7.14 (m, 4H), 7.13 – 7.07 (m, 1H), 7.01 (ddd, J = 7.5, 4.9, 1.2 Hz, 1H), 3.63 (s, 2H), 3.57 (s, 2H). 13C NMR (101 MHz, CDCl3) δ 158.50, 149.13, 137.95, 136.50, 128.93, 128.34, 126.87, 122.99, 121.73, 37.38, 35.81.

#### *6.3.1.6 Benzyl(ethyl)sulfane (**27v**)*[414]

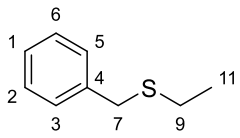


Synthesised using Method B from benzylmercaptan and bromoethane. Colourless oil (476 mg, 95% yield). $^{1}$H NMR (400 MHz, $CDCl_3$) δ 7.34 – 7.28 (m, 4H, Ar), 7.27 – 7.21 (m, 1H, Ar), 3.73 (s, 2H, 7-H), 2.43 (q, *J* = 7.5 Hz, 2H, 9-H), 1.23 (t, *J* = 7.4 Hz, 3H, 11-H). $^{13}$C NMR (126 MHz, $CDCl_3$) δ 138.8 (4), 129.0 (3,5), 128.6 (2,6), 127.0 (1), 36.0 (7), 25.4 (9), 14.5 (11).

#### *6.3.1.7 Ethyl(phenethyl)sulfane (**27w**)*

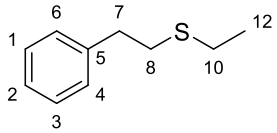


Synthesised using Method B from (2-bromoethyl)benzene and ethanethiol. Pale yellow oil (485 mg, 97% yield). $\nu_{max}$/cm$^{-1}$: 2923, 1452, 1263. $^{1}$H NMR (400 MHz, $CDCl_3$) δ 7.35 – 7.18 (m, 5H, Ar), 2.90 (m, 2H, 8-H), 2.80 (m, 2H, 7-H), 2.57 (q, *J* = 7.4 Hz, 2H, 10-H), 1.28 (t, *J* = 7.4 Hz, 3H, 12-H). $^{13}$C NMR (101 MHz, $CDCl_3$) δ 140.9 (2), 128.6, 126.5 (5), 36.5 (8), 33.3 (7), 26.2 (10), 14.9 (12). HRMS (ESI) m/z calcd. for $C_{10}H_{15}{}^{32}S^{+}$ $[M+H]^{+}$ 167.08890; found 167.0887.

### 6.3.2 General procedure for the synthesis of racemic sulfoxides standards 28

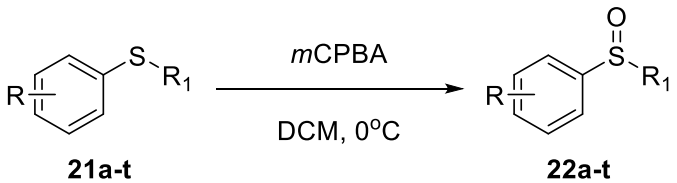


**21a-t** **22a-t**

Sulfoxide **28a** was commercially available. The synthetic methods and characterization of sulfoxides **28o**, **28b**, **28g**, **39a**, **39d**, **39f** are described in sections 6.2.4. Other racemic sulfoxides were synthesised as follows the appropriate sulfide (2.0 mmol, 1.0 eq.) was

dissolved in DCM (10 mL) and stirred at 0 °C. *m*CPBA (2.2 mmol, 1.1 eq) in DCM (10 mL) was added dropwise using a dropping funnel and the reaction was monitored by TLC for 1-24 h until completion. The reaction was dried under reduced pressure and purified by flash column chromatography using an appropriate eluent mixture of EtOAc and hexane to afford the resulting sulfoxide.

#### *6.3.2.1 2-((Propylsulfinyl)methyl)pyridine (**28s**)*

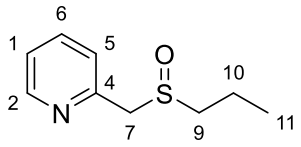


Yellow oil (35% yield). $^{1}$H NMR (400 MHz, $CDCl_3$) δ 8.60 (d, *J* = 4.6 Hz, 1H, Ar), 7.71 (td, *J* = 7.7, 1.8 Hz, 1H, Ar), 7.37 (d, *J* = 7.8 Hz, 1H, Ar), 7.31 – 7.23 (m, 1H, Ar), 4.18 (d, *J* = 12.8 Hz, 1H, 7-H), 4.08 (d, *J* = 12.8 Hz, 1H, 7-H), 2.75 – 2.58 (m, 2H, 9-H), 1.89 – 1.72 (m, 2H, 10-H), 1.05 (t, *J* = 7.4 Hz, 3H, 11-H). $^{13}$C NMR (101 MHz, $CDCl_3$) δ 151.0, 149.9, 137.1, 125.5, 123.2, 59.7, 53.7, 16.4, 13.5. HRMS (ESI) m/z calcd. for $C_9H_{14}ON^{32}S^+$ $[M+H]^+$ 184.07906; found 184.0793.

#### *6.3.2.2 2-((Ethylsulfinyl)methyl)pyridine (**28t**)*

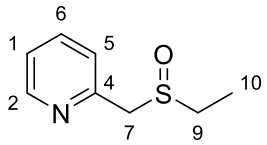


Colourless oil (242 mg, 81% yield). $\nu_{max}$/cm$^{-1}$: 2970, 2930, 1433, 1041. $^{1}$H NMR (400 MHz, $CDCl_3$) δ 8.62 – 8.56 (m, 1H, Ar), 7.70 (td, *J* = 7.8, 1.8 Hz, 1H, Ar), 7.37 (d, *J* = 7.8 Hz, 1H, Ar), 7.30 – 7.22 (m, 1H, Ar), 4.17 (d, *J* = 12.8 Hz, 1H, 7-H), 4.07 (d, *J* = 12.8 Hz, 1H, 7-H), 2.78 (dq, *J* = 13.2, 7.6 Hz, 1H, 9-H), 2.66 (dq, *J* = 13.2, 7.6 Hz, 1H, 9-H), 1.34 (t, *J* = 7.6 Hz, 3H, 11-H). $^{13}$C NMR (101 MHz, $CDCl_3$) δ 151.0 (4), 149.9 (2), 137.01 (6), 125.5 (5), 123.2 (1), 59.0 (7), 45.0 (9), 6.8 (11). HRMS (ESI) m/z $[M+H]^+$ calcd. for $C_8H_{12}ON^{32}S^+$ $[M+H]^+$ 170.0634; found 170.0631.

#### *6.3.2.3 2-((Benzylsulfinyl)methyl)pyridine (**28u**)*

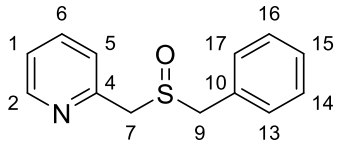

Brown amorphous solid (75% yield). $\nu_{max}/cm^{-1}$: 2918, 1581, 1433. $^{1}H$ NMR (400 MHz, CDCl3) δ 8.59 (ddd, J = 5.0, 1.9, 1.0 Hz, 1H), 7.65 (td, J = 7.7, 1.8 Hz, 1H), 7.40 – 7.26 (m, 6H), 7.22 (ddd, J = 7.6, 4.9, 1.2 Hz, 1H), 4.12 (d, *J* = 9.4 Hz, 1H), 4.09 (d, *J* = 9.4 Hz, 1H), 3.94 (d, *J* = 8.5 Hz, 1H), 3.90 (d, *J* = 8.5 Hz, 1H). $^{13}C$ NMR (101 MHz, CDCl3) δ 150.94, 149.83, 136.74, 130.43, 129.90, 128.84, 128.28, 125.60, 122.98, 57.82, 57.25. HRMS (ESI) m/z $[M+H]^+$ calcd for $C_{13}H_{14}NOS$ 232.07906, found: 232.0791.

### *6.3.2.4 ((Ethylsulfinyl)methyl)benzene (**28v**)*[355,415]

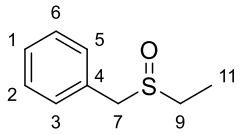


White solid (198 mg, 66% yield). $^{1}H$ NMR (500 MHz, $CDCl_3$) δ 7.40 – 7.32 (m, 3H, Ar), 7.31 – 7.27 (m, 2H, Ar), 4.02 (d, *J* = 13.0 Hz, 1H, 7-H), 3.93 (d, *J* = 13.0 Hz, 1H, 7-H), 2.72 – 2.49 (m, 2H, 9-H), 1.33 (t, *J* = 7.5 Hz, 3H, 11-H). $^{13}C$ NMR (126 MHz, $CDCl_3$) δ 130.2 (4), 130.1 (3,5), 129.1 (2,6), 128.5 (1), 57.9 (7), 44.3 (9), 6.7 (11).

### *6.3.2.5 (2-(Ethylsulfinyl)ethyl)benzene (**28w**)*

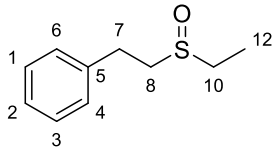


Pale yellow oil (258 mg, 86% yield). $\nu_{max}/cm^{-1}$: 2930, 1452, 1014. $^{1}H$ NMR (400 MHz, $CDCl_3$) δ 7.38 – 7.28 (m, 2H, 4,6-H), 7.28 – 7.20 (m, 3H, 1-3-H), 3.21 – 3.01 (m, 2H, 8-H), 3.02 – 2.82 (m, 2H, 7-H), 2.78 – 2.67 (m, 2H, 10-H), 1.33 (t, *J* = 7.6 Hz, 3H, 12-H). $^{13}C$ NMR (101 MHz, $CDCl_3$) δ 139.1 (5), 128.9 (4,6), 128.7 (1,3), 126.9 (2), 53.2 (8), 45.9 (7), 29.0 (10), 6.8 (12). HRMS (ESI) m/z calcd. for $C_{10}H_{15}O^{32}S^+$ $[M+H]^+$ 183.0838; found 183.0839.

### *6.3.2.6 1-Bromo-4-(methylsulfinyl)benzene (**28x**)*[409]

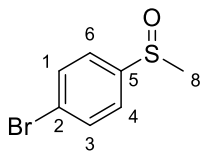


White crystalline solid (193 mg, 90% yield). $^{1}H$ NMR (400 MHz, Chloroform-*d*) δ 7.68 (d, *J* = 8.6 Hz, 2H, 4,6-H), 7.53 (d, *J* = 8.6 Hz, 2H, 1,3-H), 2.72 (s, 3H, 8-H). $^{13}C$ NMR (101 MHz, $CDCl_3$) δ 145.1 (5), 132.8 (4,6), 125.6 (2), 125.3 (1,3), 44.2 (8).

*6.3.2.7 1-Chloro-4-(methylsulfinyl)benzene (**28y**)*[409]

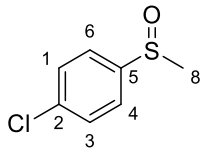

White solid (359 mg, 99% yield). $^{1}$H NMR (400 MHz, Chloroform-*d*) δ 7.62 – 7.57 (m, 2H, 4,6-H), 7.54 – 7.49 (m, 2H, 1,3-H), 2.72 (s, 3H, 8-H). $^{13}$C NMR (101 MHz, $CDCl_3$) δ 144.1 (5), 137.1 (2), 129.5 (4,6), 124.8 (1,3), 43.9 (8).

*6.3.2.8 1-Chloro-3-(methylsulfinyl)benzene (**28z**)*[415]

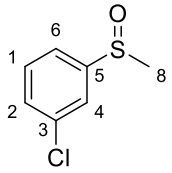

Pale yellow oil (362 mg, 99% yield). $^{1}$H NMR (400 MHz, Chloroform-*d*) δ 7.68 – 7.65 (m, 1H, 4-H), 7.52 – 7.45 (m, 3H, 1,2,6-H), 2.74 (s, 3H, 8-H). $^{13}$C NMR (101 MHz, $CDCl_3$) δ 148.1 (5), 135.9 (3), 131.3, 130.7, 123.8, 121.8, 44.2 (8).

*6.3.2.9 1-Chloro-2-(methylsulfinyl)benzene (**28aa**)*[399]

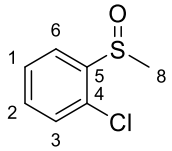

Pale yellow oil (125 mg, 57% yield). $^{1}$H NMR (500 MHz, $CDCl_3$) δ 7.97 (dd, *J* = 7.9, 1.7 Hz, 1H), 7.54 (td, *J* = 7.6, 1.3 Hz, 1H), 7.45 (td, *J* = 7.6, 1.7 Hz, 1H), 7.40 (dd, *J* = 7.9, 1.3 Hz, 1H), 2.83 (s, 3H, 8-H). $^{13}$C NMR (126 MHz, $CDCl_3$) δ 143.8 (5), 132.1, 130.0, 129.9, 128.3, 125.5, 41.8 (8).

*6.3.2.10 (4-(Methylsulfinyl)phenyl)ethan-1-one (**28ab**)*[409,416]

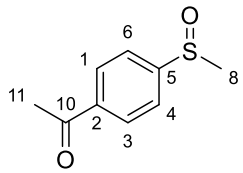

White amorphous solid (434 mg, 87% yield). $^{1}$H NMR (400 MHz, Chloroform-*d*) δ 8.09 – 7.98 (m, 2H, 4,6-H), 7.73 – 7.64 (m, 2H, 1,3-H), 2.70 (s, 3H, 11-H), 2.58 (s, 3H, 8-H). $^{13}$C

NMR (101 MHz, $CDCl_3$) δ 197.0 (10), 150.9 (5), 139.0 (2), 129.1 (4,6), 123.7 (1,3), 43.8 (8), 26.8 (11).

*6.3.2.11 1-Methyl-3-(methylsulfinyl)benzene (**28ac**)*[409]

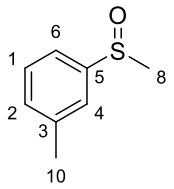


Colourless oil (312 mg, 88% yield). $^1$H NMR (400 MHz, Chloroform-*d*) δ 7.49 (dt, *J* = 1.5, 0.8 Hz, 1H, Ar), 7.43 – 7.38 (m, 2H, Ar), 7.33 – 7.27 (m, 1H, Ar), 2.72 (s, 3H, 8-H), 2.43 (t, *J* = 0.8 Hz, 3H, 10-H). $^{13}$C NMR (101 MHz, $CDCl_3$) δ 145.4, 139.5, 131.7, 129.0, 123.6, 120.5, 43.8 (8), 21.3 (10).

*6.3.2.12 2,4-Dimethyl-1-(methylsulfinyl)benzene (**28ad**)*[406]

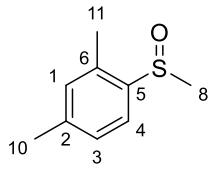


Colourless oil (275 mg, 83% yield). $^1$H NMR (500 MHz, $CDCl_3$) δ 7.83 (d, *J* = 8.0 Hz, 1H, 4-H), 7.25 (dd, *J* = 8.0, 1.8 Hz, 1H, 3-H), 7.01 (d, *J* = 1.8 Hz, 1H, 1-H), 2.66 (s, 3H, 8-H), 2.36 (s, 3H, 10-H), 2.34 (s, 3H, 11-H). $^{13}$C NMR (126 MHz, $CDCl_3$) δ 141.2 (5), 141.0 (2), 134.0, 131.6, 128.3, 123.3, 42.4 (8), 21.3 (11), 18.1 (10).

## Biocatalysis methods

### 6.3.3 Screening of BVMO and FMO enzymes panel using 27s

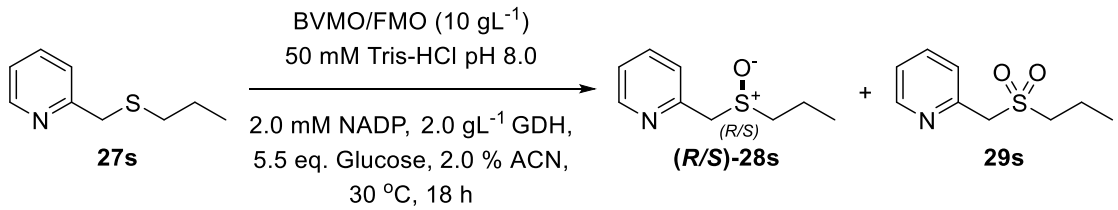


To initiate the reaction, 20 µL of a 60 mM stock solution in $CH_3CN$ of the relevant sulfide substrate **27s** (1.2 mM final concentration) was added to each well in a deep 96-well plate containing NADP (2.0 mM, 1.7 eq.), GDH (2.0 $gL^{-1}$), glucose (27.5 mM, 5.5 eq.)

and the enzyme (10 $gL^{-1}$) in 980 µL 50 mM Tris-HCl buffer pH 8. The reaction was shaken at 30 °C for 18 h. Upon completion, a 30 µL aliquot of each well was extracted with EtOAc (3x50 µL), centrifuged at maximum speed (12500 rpm, 5 min) and the collected organic layers were analysed by normal phase HPLC using Chiralpak IC chiral columns to determine the enantiomeric excess (see Appendix III for conditions). The remaining reaction mixture was quenched with 700 µL of $CH_3CN$ and the conversion was calculated by reversed phase HPLC using a Kromasil C18 column.

### 6.3.4 General procedure for the asymmetric oxidation of substrates 27 and 38 using BVMO145

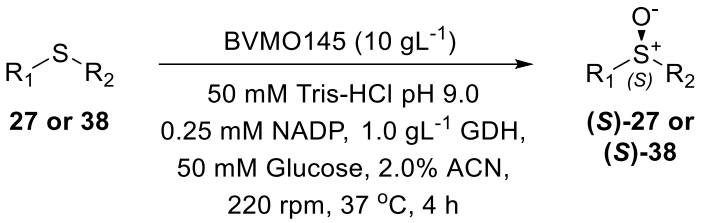


14 µL of a 250 mM stock solution in $CH_3CN$ of the relevant sulfide substrate **27** (5.0 mM final concentration), was added to 686 µL 50 mM Tris-HCl buffer pH 9.0 containing NADP (0.25 mM, 0.05 eq.), GDH (1.0 $gL^{-1}$), glucose (50 mM, 10 eq.) and BVMO145 (10 $gL^{-1}$) to initiate the reaction. The reaction was shaken at 37 °C for 4 h. Upon completion, a 30 µL aliquot was extracted with EtOAc (3x50 µL), centrifuged at maximum speed (12500 rpm, 5 min) and the collected organic layers were analysed by normal phase HPLC using Chiralpak IC or IG chiral columns to determine the enantiomeric excess (see Appendix III for conditions). The remaining reaction mixture was quenched with 700 µL of $CH_3CN$ and the conversion was calculated by reversed phase HPLC using a Kromasil C18 column.

## Computational methods

Quantum chemical computations were performed using Spartan Pro. Two molecular structures were optimised at the Hartree-Fock/6 -31G* level of theory, in the gas phase, while the ESP was calculated using a constant electronic density of 0.002 au. The ESP values were shown by means of coloured maps on isodensity surface (range between -28 and 29 a.u).

## 6.4 Chapter 4. Methods

### Synthetic methods

#### 6.4.1 General procedure for the synthesis of sulfides 27

Sulfides **27af, 27a-b**, **27x-z**, **27aa-ad**, **27o**, and **27al** were commercially available. The synthetic methods and characterization of sulfides **27c**, **27d**, **27g**, **27j**, **27k** and **27l** are described in sections 6.2.1 and sulfides **27v-w**, **27t** in section 6.3.1. The remaining sulfides were synthesised using either Method A or Method B described in section 6.3.1. In both cases, sulfides **27** were used in the next oxidative step to obtain sulfoxides **28** as crude if sufficiently clean on $^{1}$H NMR, otherwise they were purified by flash column chromatography using an appropriate eluent mixture of EtOAc or $Et_2O$ and hexane to afford the resulting sulfide.

##### *6.4.1.1 Methyl(naphthalen-2-yl)sulfane (**27ai**)*[417]

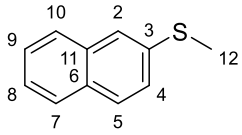


Synthesised using Method B from 2-naphthalenethiol and iodomethane. Amorphous white solid (495 mg, 99% yield). $^{1}$H NMR (400 MHz, $CDCl_3$) δ 7.76 (m, 3H, Ar), 7.63 – 7.57 (m, 1H, Ar), 7.52 – 7.35 (m, 3H, Ar), 2.59 (s, 3H, 12-H). $^{13}$C NMR (101 MHz, $CDCl_3$) δ 136.1, 133.9, 131.3, 128.2, 127.7, 126.8, 126.6, 125.7, 125.2, 123.4, 15.8 (12).

##### *6.4.1.2 Methyl(naphthalen-1-yl)sulfane (**27aj**)*[417]

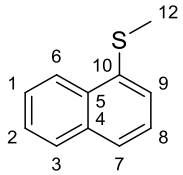


Synthesised using Method A from 1-naphthalenethiol and iodomethane. Pale yellow oil (188 mg, 63% yield). $^{1}$H NMR (400 MHz, $CDCl_3$) δ 8.33 – 8.22 (m, 1H, Ar), 7.90 – 7.80 (m, 1H, Ar), 7.72 – 7.63 (m, 1H, Ar), 7.60 – 7.48 (m, 2H, Ar), 7.46 – 7.36 (m, 2H, Ar), 2.59 (s, 3H, 12-H). $^{13}$C NMR (101 MHz, $CDCl_3$) δ 136.0 (10), 133.8, 131.8, 128.7, 126.4, 126.3, 126.0, 125.8, 124.4, 123.8, 16.4 (12).

*6.4.1.3 Methyl(2-(phenylthio)ethyl)sulfane (**27am**)*

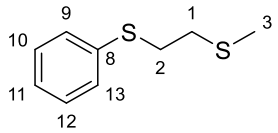


Synthesised using Method A from (2-bromoethyl)(phenyl)sulfane and metanethiol. Colourless oil (324 mg, 68% yield). $\nu_{max}/cm^{-1}$: 2913, 1437, 1024. $^{1}H$ NMR (500 MHz, $CDCl_3$) δ 7.39 – 7.34 (m, 2H, 9,13-H), 7.30 (t, *J* = 7.7 Hz, 2H, 10,12-H), 7.24 – 7.17 (m, 1H, 11-H), 3.16 – 3.07 (m, 2H, 2-H), 2.75 – 2.68 (m, 2H, 1-H), 2.13 (s, 3H, 3-H). $^{13}C$ NMR (126 MHz, CDCl3) δ 135.6, 130.1, 129.2, 126.6, 33.8, 33.8, 15.7. HRMS (ESI) m/z calcd. for $C_{13}H_{12}ON^{32}S_2^+$ $[M+H]^+$ 185.04532; found 185.0452.

*6.4.1.4 (Propylsulfinyl)benzene (**27an**)*[384]

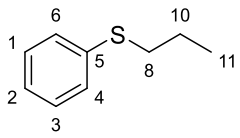


Synthesised using Method A from thiophenol and iodopropane. Pale yellow oil (217 mg, 72% yield). $^{1}H$ NMR (500 MHz, $CDCl_3$) δ 7.34 – 7.23 (m, 4H, Ar), 7.18 – 7.13 (m, 1H, Ar), 2.89 (t, *J* = 7.3 Hz, 2H, 8-H), 1.67 (sx, *J* = 7.3 Hz, 2H, 10-H), 1.02 (t, *J* = 7.3 Hz, 3H, 11-H).

*6.4.1.5 (4-Chlorophenyl)(propyl)sulfane (**27ao**)*[418]

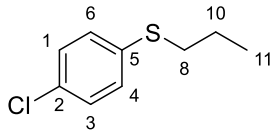


Synthesised using Method A from 4-chlorothiophenol and iodopropane. Pale yellow oil (460 mg, 92% yield). $^{1}H$ NMR (400 MHz, $CDCl_3$) δ 7.34 – 7.27 (m, 4H, Ar), 2.93 (t, *J* = 7.3 Hz, 2H, 8-H), 1.71 (sx, *J* = 7.3 Hz, 2H, 10-H), 1.07 (t, *J* = 7.3 Hz, 3H, 11-H). $^{13}C$ NMR (126 MHz, $CDCl_3$) δ 135.6 (5), 131.8 (2), 130.5 (4,6), 129.1 (1,3), 36.0 (8), 22.6 (10), 13.5 (11).

*6.4.1.6 (4-Bromophenyl)(propyl)sulfane (**27ap**)*[419]

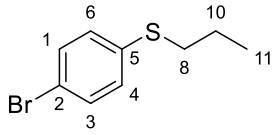

Synthesised using Method A from 4-bromothiophenol and iodopropane. Yellow oil (495 mg, 99% yield). $^{1}$H NMR (500 MHz, $CDCl_3$) δ 7.38 (d, *J* = 8.5 Hz, 2H, 4,6-H), 7.18 (d, *J* = 8.5 Hz, 2H, 1,3-H), 2.87 (t, *J* = 7.3 Hz, 2H, 8-H), 1.66 (sx, *J* = 7.3 Hz, 2H, 10-H), 1.02 (t, *J* = 7.3 Hz, 3H, 11-H). $^{13}$C NMR (126 MHz, $CDCl_3$) δ 136.4 (5), 132,0 (4,6), 130.6 (1,3), 119.5 (2), 35.8 (8), 22.5 (10), 13.5 (11).

#### *6.4.1.7 (3-Methoxyphenyl)(propyl)sulfane (**27aq**)*

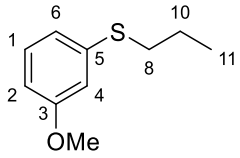


Synthesised using Method A from 3-methoxythiophenol and iodopropane. Yellow oil (419 mg, 84% yield). $\nu_{max}$/cm$^{-1}$: 2960, 1588, 1227, 1039. $^{1}$H NMR (400 MHz, $CDCl_3$) δ 7.19 (t, *J* = 8.0 Hz, 1H, 1-H), 6.93 – 6.85 (m, 2H, Ar), 6.70 (dd, *J* = 8.3, 2.4 Hz, 1H, 2-H), 3.80 (s, 3H, OMe), 2.90 (t, *J* = 7.3 Hz, 2H, 8-H), 1.69 (sx, *J* = 7.3 Hz, 2H, 10-H), 1.03 (t, *J* = 7.4 Hz, 3H, 11-H). $^{13}$C NMR (126 MHz, $CDCl_3$) δ 159.9 (3), 138.5, 129.8, 121.1, 114.3, 111.4, 55.4 (OMe), 35.5 (8), 22.7 (10), 13.6 (11). HRMS (ESI) m/z calcd. for $C_{10}H_{15}O^{32}S^{+}$ $[M+H]^{+}$ 183.08381; found 183.0835.

#### *6.4.1.8 (4-Methoxyphenyl)(butyl)sulfane (**27ar**)*[386]

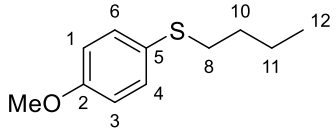


Synthesised using Method A from 4-methoxythiophenol and iodobutane. Pale yellow oil (430 mg, 86% yield). $^{1}$H NMR (500 MHz, $CDCl_3$) δ 7.34 (d, *J* = 8.8 Hz, 2H, 4,6-H), 6.84 (d, *J* = 8.8 Hz, 2H, 1,3-H), 3.80 (s, 3H, OMe), 2.82 (t, *J* = 7.3 Hz, 2H, 8-H), 1.60 – 1.52 (m, 2H, 10-H), 1.46 – 1.37 (m, 2H, 11-H), 0.90 (t, *J* = 7.1 Hz, 3H, 12-H). $^{13}$C NMR (126 MHz, $CDCl_3$) δ 158.8 (2), 133.0 (4,6), 127.1(5), 114.6 (1,3), 55.5 (OMe), 35.6 (8), 31.6 (10), 22.0 (11), 13.8 (12).

### 6.4.2 General procedure for the synthesis of racemic sulfoxides 28

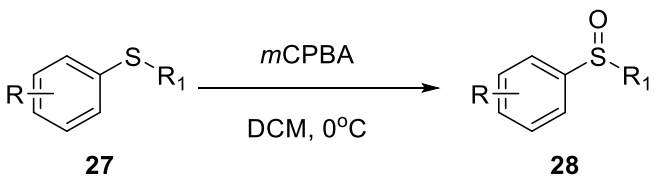


**27** **28**

Sulfoxides **28af**, **28a** and **28ak** were commercially available. The synthetic methods and characterization of sulfoxides **28a-l** and **28o** are described in section 6.2.7 and sulfides **28t** and **28v-ad** in section 6.3.2. The remaining racemic sulfoxides were synthesised as follows: the appropriate sulfide (2.0 mmol, 1.0 eq.) was dissolved in DCM (10 mL) and stirred at 0 °C. *m*CPBA (2.2 mmol, 1.1 eq) in DCM (10 mL) was added dropwise using a dropping funnel and the reaction was monitored by TLC for 1-24 h until completion. The reaction was dried under reduced pressure and purified by flash column chromatography using an appropriate eluent mixture of EtOAc and hexane to afford the resulting sulfoxide.

### *6.4.2.1 Methoxy-4-(methylsulfinyl)benzene (**28ag**)*[409]

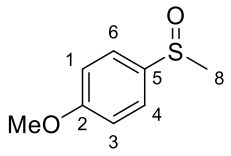


Off white solid (241 mg, 73% yield). $^{1}$H NMR (400 MHz, Chloroform-*d*) δ 7.63 – 7.57 (m, 2H, 4,6-H), 7.06 – 6.99 (m, 2H, 1,3-H), 3.85 (s, 3H, OMe), 2.71 (s, 3H, 8-H). $^{13}$C NMR (101 MHz, $CDCl_3$) δ 162.2 (5), 136.6 (2), 125.7 (4,6), 115.0 (1,3), 55.7 (MeO), 44.1 (8).

### *6.4.2.2 Methoxy-3-(methylsulfinyl)benzene (**28ah**)*[416]

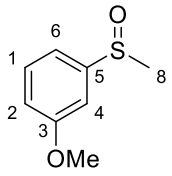


Colourless oil (386 mg, 77% yield). $^{1}$H NMR (400 MHz, Chloroform-*d*) δ 7.44 – 7.38 (m, 1H, 4-H), 7.27 – 7.24 (m, 2H, Ar), 7.13 (ddd, *J* = 7.7, 1.9, 0.9 Hz, 1H, Ar), 7.02 (ddd, *J* = 8.3, 2.6, 0.9 Hz, 1H, Ar), 3.87 (s, 3H, OMe), 2.73 (s, 3H, 8-H). $^{13}$C NMR (101 MHz, $CDCl_3$) δ 160.7 (3), 147.3 (5), 130.5 (1), 117.6, 115.7, 108.1 (4), 55.8 (OMe), 44.2 (8).

### *6.4.2.3 (Methylsulfinyl)naphthalene (**28ai**)*[409]

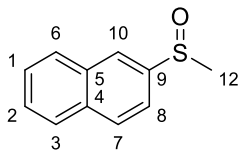


White crystals (170 mg, 57% yield). $^{1}$H NMR (400 MHz, $CDCl_3$) δ 8.22 (d, *J* = 0.7 Hz, 1H, Ar), 7.99 (d, *J* = 0.7 Hz, 1H, Ar), 7.97 – 7.89 (m, 2H, Ar), 7.67 – 7.55 (m, 3H, Ar), 2.80

(s, 3H, 12-H). $^{13}$C NMR (101 MHz, $CDCl_3$) δ 129.8, 128.7, 128.2, 128.0, 127.5, 124.2, 119.6, 44.0 (12). 3 quat carbons.

### *6.4.2.4 (Methylsulfinyl)naphthalene (**28aj**)*[420]

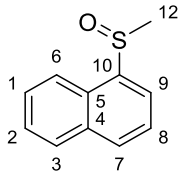


White amorphous solid (106 mg, 85% yield). $^1$H NMR (400 MHz, $CDCl_3$) δ 8.17 (dd, *J* = 7.3, 1.2 Hz, 1H, Ar), 7.99 – 7.86 (m, 3H, Ar), 7.65 (dd, *J* = 8.2, 7.3 Hz, 1H, Ar), 7.61 – 7.51 (m, 2H, Ar), 2.82 (s, 3H, 12-H). $^{13}$C NMR (101 MHz, $CDCl_3$) δ 141.6, 133.5, 131.3, 129.2, 128.6, 127.3, 126.8, 125.8, 122.2, 121.4, 43.0 (12).

### *6.4.2.5 (Methylsulfinyl)butan-2-one (**28al**)*

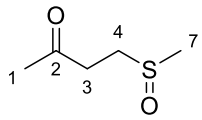


Pale yellow oil (312 mg, 99% yield). $\nu_{max}$/cm$^{-1}$: 2996, 2913, 1709. $^1$H NMR (500 MHz, $CDCl_3$) δ 3.08 – 3.00 (m, 1H), 2.97 (td, *J* = 7.2, 2.6 Hz, 2H), 2.85 – 2.76 (m, 1H), 2.57 (s, 3H, 7-H), 2.23 (d, *J* = 0.9 Hz, 3H, 1-H). $^{13}$C NMR (126 MHz, $CDCl_3$) δ 205.3 (2), 47.7, 39.1, 35.6, 30.0 (1). HRMS (ESI) m/z calcd. for $C_5H_{11}O_2{}^{32}S^+$ $[M+H]^+$ 135.0474; found 135.0475.

### *6.4.2.6 ((2-(Methylsulfinyl)ethyl)sulfinyl)benzene (**28am**)*

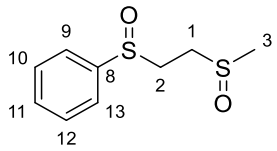


1:1 Mix of diastereomers. White crystalline solid (166 mg, 85% yield). $\nu_{max}$/cm$^{-1}$: 2911, 1421, 1019. $^1$H NMR (500 MHz, $CDCl_3$) δ 7.64 – 7.48 (m, 10H, Ar), 3.43 – 3.32 (m, 2H), 3.23 (ddd, *J* = 13.1, 10.4, 5.3 Hz, 1H), 3.10 – 2.97 (m, 3H), 2.97 – 2.88 (m, 1H), 2.66 (ddd, *J* = 13.1, 10.4, 4.9 Hz, 1H), 2.59 (s, 3H, 3-H), 2.56 (s, 3H, 3-H). $^{13}$C NMR (126 MHz, $CDCl_3$) δ 142.6 (8), 142.4 (8), 131.6 (9,13), 131.6 (9,13), 124.1 (10,12), 124.0 (10,12), 48.8 (2), 48.5 (2), 45.5 (1), 45.4 (1), 39.0 (3), 39.0 (3). HRMS (ESI) m/z calcd. for $C_9H_{13}O_2{}^{32}S^{2+}$ $[M+H]^+$ 217.0352; found 217.0348.

*6.4.2.7 (Propylsulfinyl)benzene (**28an**)*[421]

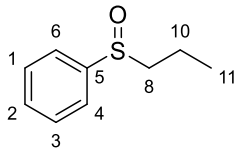


Yellow oil (366 mg, 99% yield). $^{1}$H NMR (500 MHz, $CDCl_3$) δ 7.66 – 7.59 (m, 2H, 4,6-H), 7.55 – 7.46 (m, 3H, 1-3-H), 2.86 – 2.71 (m, 2H, 8-H), 1.87 – 1.74 (m, 1H, 9-H), 1.73 – 1.60 (m, 1H, 9-H), 1.05 (t, *J* = 7.4 Hz, 3H, 11-H). $^{13}$C NMR (126 MHz, $CDCl_3$) δ 144.3 (5), 131.3 (2), 129.6 (4,6), 124.6 (1,3), 59.6 (8), 16.3 (10), 13.6 (11).

*6.4.2.8 1-Chloro-4-(propylsulfinyl)benzene (**28ao**)*[421]

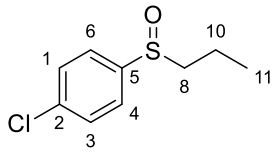


Colourless oil (183 mg, 61% yield). $^{1}$H NMR (500 MHz, $CDCl_3$) δ 7.58 – 7.54 (m, 2H, 4,6-H), 7.52 – 7.47 (m, 2H, 1,3-H), 2.83 – 2.69 (m, 2H, 8-H), 1.87 – 1.73 (m, 1H, 10-H), 1.72 – 1.58 (m, 1H, 10-H), 1.05 (t, *J* = 7.4 Hz, 3H, 11-H). $^{13}$C NMR (126 MHz, $CDCl_3$) δ 142.6 (5), 137.3 (2), 129.7 (4,6), 125.6 (1,3), 59.4 (8), 15.9 (10), 13.4 (11).

*6.4.2.9 1-Bromo-4-(propylsulfinyl)benzene (**28ap**)*

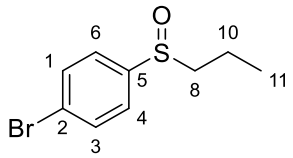


Colourless oil (278 mg, 99% yield). $\nu_{max}$/cm$^{-1}$: 2963, 1470, 1005. $^{1}$H NMR (500 MHz, $CDCl_3$) δ 7.65 (d, *J* = 8.4 Hz, 2H, 4,6-H), 7.49 (d, *J* = 8.5 Hz, 2H, 1,3-H), 2.82 – 2.68 (m, 2H, 8-H), 1.87 – 1.73 (m, 1H, 10-H), 1.71 – 1.58 (m, 1H, 10-H), 1.04 (t, *J* = 7.4 Hz, 3H, 11-H). $^{13}$C NMR (126 MHz, $CDCl_3$) δ 143.3 (5), 132.5 (4,6), 125.8 (1,3), 125.5 (2), 59.3 (8), 15.9 (10), 13.4 (11). HRMS (ESI) m/z calcd. for $C_9H_{12}BrO^{32}S^+$ $[M+H]^+$ 246.9714; found 246.9785, 248.9758.

*6.4.2.10 1-Methoxy-3-(propylsulfinyl)benzene (**28aq**)*

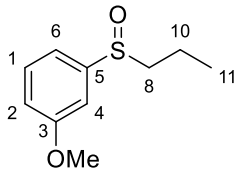


Pale yellow oil (232 mg, 77% yield). $\nu_{max}/cm^{-1}$: 2963, 1479, 1025. $^{1}H$ NMR (400 MHz, $CDCl_3$) δ 7.39 (td, *J* = 7.8, 1.5 Hz, 1H, Ar), 7.23 (dd, *J* = 2.6, 1.5 Hz, 1H, Ar), 7.10 (dt, *J* = 7.8, 1.2 Hz, 1H, Ar), 7.0 (ddd, *J* = 8.3, 2.6, 1.2 Hz, 1H, Ar), 3.86 (s, 3H, OMe), 2.86 – 2.68 (m, 2H, 8-H), 1.87 – 1.73 (m, 1H, 10-H), 1.73 – 1.58 (m, 1H, 10-H), 1.09 – 1.00 (m, 3H, 11-H). $^{13}C$ NMR (101 MHz, $CDCl_3$) δ 160.6 (5), 145.6 (3), 130.2 (4), 117.5 (6), 116.2 (2), 108.6 (1), 59.4 (OMe), 55.7 (8), 16.1 (10), 13.4 (11). HRMS (ESI) m/z calcd. for $C_9H_{15}O_2{}^{32}S^+$ $[M+H]^+$ 199.0787; found 199.0784.

*6.4.2.11 1-Methoxy-4-(butylsulfinyl)benzene (**28ar**)*[422]

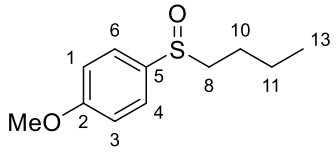


Yellow oil (195 mg, 65% yield). $^{1}H$ NMR (500 MHz, $CDCl_3$) δ 7.56 (d, *J* = 8.8 Hz, 2H, 4,6-H), 7.02 (d, *J* = 8.8 Hz, 2H, 1,3-H), 3.85 (s, 3H, OMe), 2.84 – 2.71 (m, 2H, 8-H), 1.73 – 1.52 (m, 2H, 10-H), 1.51 – 1.34 (m, 2H, 11-H), 0.91 (t, *J* = 7.3 Hz, 3H, 13-H). $^{13}C$ NMR (126 MHz, $CDCl_3$) δ 162.0 (5), 135.0 (2), 126.1 (4,6), 114.9 (1,3), 57.3 (OMe), 55.6 (8), 24.4 (10), 22.0 (11), 13.8 (13).

### 6.4.3 Synthesis of riboflavin tetraacetate (RFTA)[380]

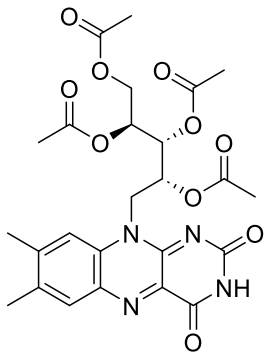


Riboflavin (1.33 mmol, 1.0 eq.) was dissolved in acetic anhydride (10 mL) and pyridine (10 mL) and the resulting solution was stirred under reflux for 20 min. The reaction

mixture was the cooled to rt, diluted with DCM (25 mL) and poured into ice cold 1 M $HCl_{(aq)}$ (15 mL). The aqueous phase was extracted with DCM (3x5 mL) and the combined organic phase was washed with 1 M $HCl_{(aq)}$ (1x5 mL) and water (2x5 mL) and was then dried over $MgSO_4$ and evaporated under reduced pressure. The crude product was purified by silica column chromatography using a 9:1 DCM/MeOH eluent system to afford RFTA as a yellow solid (736 mg, 99% yield). $^1$H NMR (400 MHz, $CDCl_3$) δ 8.31 (s, 1H, NH), 8.05 (d, *J* = 5.2 Hz, 1H, Ar), 7.57 (d, *J* = 7.6 Hz, 1H, Ar), 5.66 (d, *J* = 7.7 Hz, 1H), 5.49 – 5.38 (m, 2H), 4.44 (dd, *J* = 12.4, 2.8 Hz, 2H), 4.28 – 4.21 (m, 2H), 2.57 (d, *J* = 2.8 Hz, 3H), 2.45 (d, *J* = 2.8 Hz, 3H), 2.29 (d, *J* = 1.3 Hz, 3H), 2.22 (d, *J* = 4.6 Hz, 3H), 2.08 (d, *J* = 0.8 Hz, 3H), 1.76 (s, 3H).

## Molecular biology and biocatalysis methods

### 6.4.4 Preparation of Msr WT enzymes panel

The Msr genes were synthesised and cloned in pET28a(+) and used to transform BL21(DE3) *E. coli* competent cells and plated on nutrient agar plates containing 50 µg/mL kanamycin which were incubated at 37 °C overnight. Single colonies for each Msr gene were used to inoculate a 10 mL culture tube containing LB media (10 g tryptone, 5 g yeast extract and 10 g NaCl per litre) and 50 µg/mL kanamycin which was incubated at 37 °C overnight with at 220 rpm. This 10 mL primary culture was then used to inoculate a 1 L culture of LB media containing kanamycin (50 µg/mL) in a 2 L shake flask. The culture was incubated at 37 °C in an orbital shaker until $OD_{600}$ reached ~0.6. At this point the incubation temperature was reduced to 25 °C and 1 mM IPTG added to induce gene expression overnight. Following the incubation, the culture was centrifuged to pellet the bacterial material, and the pellet resuspended in 0.1 M Potassium Phosphate buffer, pH 7.4. The pellet was then subjected to sonication (10 secs on, 10 sec off for 6 cycles) to lyse the *E. coli* cells. The lysate was centrifuged for 15 min at 4000 rpm to pellet the cellular debris. The supernatant was retained and lyophilised to generate freeze dried cell free extract (CFE) to be used in all subsequent experiments.

### 6.4.5 Purification of *S. cerevisiae* MsrA02 from CFE

1.6 g of MsrA02 CFE (Almac) was resuspended in Buffer A (20 mM Tris base pH 8.0, 100 mM NaCl, 20 mM imidazole and 10% *v/v* glycerol and 1 mM DTT) and was centrifuged at 4000 rpm for 20 minutes. A 5 mL His-Trap™ Fast Flow nickel affinity

column was washed with water (7 CV) and equilibrated with Buffer A (7 CV). The filtered supernatant was loaded onto the nickel affinity column and the column was flushed with Buffer A (1.6 CV). The protein was eluted with Buffer B (20 mM Tris base pH 8.0, 100 mM NaCl, 200 mM imidazole and 10% *v/v* glycerol), the fractions of the purification were analysed by SDS-Page (expected molecular weight including the 6xHis tag of 23.3 kDa). The fractions containing the protein of interest were pooled and concentrated, and buffer exchanged in Buffer C (20 mM Tris base pH 8.0, 100 mM NaCl and 10% *v/v* glycerol) by centrifugation on ultrafiltration unit (10 KDa MWCO, Cytiva, Sweden). When the volume reached approximately 1.5 mL, it was mixed with an equal amount of Buffer D (20 mM Tris base pH 8.0, 100 mM NaCl and 30% *v/v* glycerol), divided into 100 µL aliquots, snap frozen and stored at -80 °C. The final concentration was assessed through Bradford method.

### 6.4.6 General procedure for the kinetic resolution of substrates 28 using MsrA02

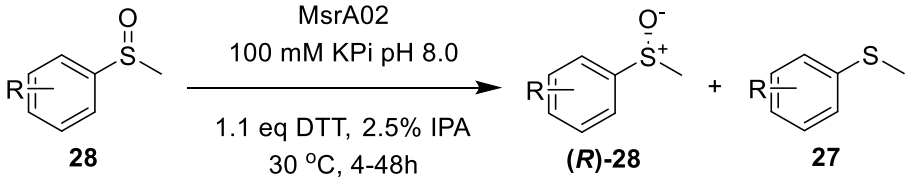


315 µL of a 1.28 M stock solution in IPA of the relevant racemic substrate **28** (32 mM final concentration), was added to 12.3 mL 100 mM KPi buffer pH 8.0 containing DTT (35.2 mM, 1.1 eq.) and MsrA02 to initiate the reaction. The reaction was monitored by taking 10 µL aliquots, which were extracted with EtOAc (3x20 µL) and injected into the appropriate HPLC chiral column. Upon completion, the reaction was extracted with EtOAc (5x5 mL) by centrifugation (5300 rpm, 5 min, 4 °C). The organic phase was dried over $MgSO_4$ and evaporated under reduced pressure and the resulting crude was purified by flash column chromatography using a mixture of EtOAc and hexane to afford the resulting enantiopure (*R*)-sulfoxide. Compounds were purified on neutral alumina ($Al_3O_2$) and the final enantiomeric excess was determined using Chiralpak IC or IG chiral columns (see Appendix VI for conditions). The isolated yields and optical rotation data of (*R*)-sulfoxides are reported in Appendix II.

*6.4.6.1 Synthesis of ethyl(2-(phenylsulfinyl)ethyl)sulfane (**27r**) through the kinetic resolution of ((2-(methylsulfinyl)ethyl)sulfinyl)benzene (**28r**)*

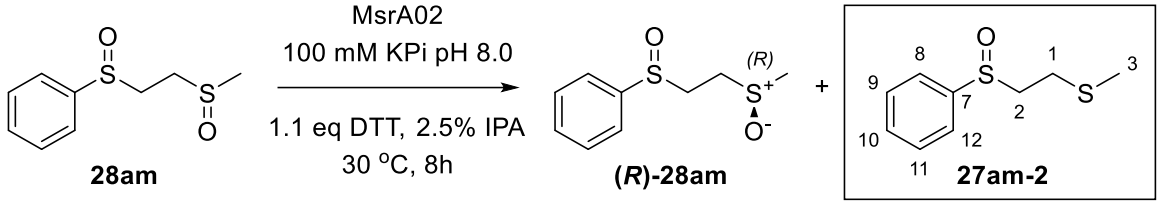


253 µL of a 1.28 M stock solution in IPA of **28am** (32 mM final concentration), was added to 10.0 mL 100 mM KPi buffer pH 8.0 containing DTT (35.2 mM, 1.1 eq.) and MsrA02 to initiate the reaction. The reaction was monitored by taking 10 µL aliquots, which were extracted with EtOAc (3x20 µL) and analysed by HPLC fitted with a Chiralpak IC chiral column. After 8 h, the reaction was extracted with EtOAc (10x5 mL) by centrifugation (5300 rpm, 5 min, 4 °C). The collected organic phase was dried over $MgSO_4$ and evaporated under reduced pressure and the resulting crude was purified on neutral alumina ($Al_3O_2$) by flash column chromatography using 100% EtOAc first followed by 95:5 DCM/MeOH to afford both **(*R*)-28am** (see 6.4.1.15 and Appendix II) and **27am-2** as a yellow oil (32 mg, 49% yield). $\nu_{max}/cm^{-1}$: 3397, 2911, 1440, 1036. $^1$H NMR (500 MHz, $CDCl_3$) δ 7.63 – 7.57 (m, 2H, 8,12-H), 7.54 – 7.46 (m, 3H, 9-11-H), 3.09 – 2.94 (m, 2H, 2-H), 2.87 (ddd, *J* = 13.4, 9.7, 6.3 Hz, 1H, 1-H), 2.64 – 2.58 (m, 1H, 1-H), 2.09 (s, 3H, 3-H). $^{13}$C NMR (126 MHz, $CDCl_3$) δ 143.2 (7), 131.3 (10), 129.5 (8,12), 124.1 (9,11), 56.5 (2), 26.3 (1), 15.7 (3). HRMS (ESI) m/z calcd. for $C_9H_{13}O_2{}^{32}S^{2+}$ $[M+H]^+$ 201.0399; found 201.0402.

### 6.4.7 Preparation of C28S and C68S MsrA02

*6.4.7.1 General considerations*

The plasmid encoding WT MsrA02 gene (pET28a-Msr-XhoI-NdeI) was obtained by Almac. PCR kit QuikChange II was purchased by Agilent Technologies and the primers were purchased from Merk Life Science.

| Desired point mutation | Nucleotide change | Forward primer (5'-3') | Reverse primer (3'-5') |
|---|---|---|---|
| C25S | TGC→T**C**C | CACCCTGGCGTGCGG TT**C**CTTTTGGGGCSC CGAGCACATGTACCG | GACCGCACGCCAA**G**G AAAACCCCGTGGCTC GTGTAC |
| C68S | TGC→T**C**C | AGCTATAAGCGT GTTT**C**CGGTGGC GACACC | TCGATATTCGCA CAAA**G**GCCACCG CTGTGG |

*6.4.7.2 Site directed mutagenesis*

Site directed mutagenesis was performed by PCR according to Phusion High-Fidelity PCR Master Mix manufacturer's instructions using pET28a-Msr-XhoI-NdeI as template. In a PCR tube 12.5 µL of Phusion High-Fidelity PCR Master Mix, 1.25 µL x 10 µM primers (final concentration 0.5 µM), 1 µL WT template DNA and 9 µL sterilised water were added and the PCR sequence started (1) initial denaturation at 95 °C, 30 sec; 2) a: 95 °C, 30 sec, b:55 °C, 1 min, c:68 °C, 6 min. Repeat for 25 cycles; 3) hold at 4 °C). After PCR, the template of the reaction was digested with DpnI (1 hour 1 µL, Thermofisher). On completion, 2 µL of the reaction mixture were used to transform 50 µL of Top10 competent *E. coli* cells. Single colonies were selected and incubated overnight in 15 mL of LB media with 50 µg/mL kanamycin. The DNA plasmid was extracted and purified with the QIAprep® Spin Minikit (QIAGEN). The resulting DNA was analysed by agarose gel after incubation with XhoI, BglI and BssSI digestive enzymes. The mutated sequence was confirmed by sequencing (Genewiz, Azenta Life Sciences).

*6.4.7.3 Gene expression and purification*

The purified MsrA02_C25S or C68S plasmids were used to transform *E. coli* T7 express competent cells and the resulting cell mixture was plated on LB agar (50 $\mu g mL^{-1}$ kanamycin) and incubated overnight at 35 °C. A single colony of transformed cells was used to incolulate 100 mL preculture in LB media with kanamycin (50 $\mu g mL^{-1}$) and incubated overnight at 37 °C and 220 rpm. The overnight precultures were used to inoculate 2x1L cultures in LB media with kanamycin (50 $\mu g mL^{-1}$). When the $OD_{600}$ reached 0.6-0.8 the expression of the protein was induced with 0.5 mM isopropyl-β-D-thiogalactopyranoside (IPTG) and incubated overnight at 25 °C. Cells were harvested by centrifugation (18,000 rpm, 45 min, 4 °C), resuspended in cell lysis buffer (Buffer A, pepstatin, protease cocktail, lysozyme, DNAase, 1 mM DTT) and lysed using a IXT4A (Constant System LTD) cell disruptor (25 psi, 4 °C). After centrifugation (20,000 rpm, 1 h, 4 °C), the CFE was loaded onto a His-Trap™ Fast Flow nickel affinity column and

purified following the procedure described in Section 2.2. The final concentration was assessed through Bradford method.

### 6.4.8 Activity assay of C25S and C68S MsrA02

Reactions were run in duplicates in a final volume of 1.0 mL in microcentrifuge tubes. C25S or C68S MsrA02 was used directly from the previously prepared stock and was diluted to three diffferent concentrations (10, 100 and 400 mM) in 100 mM KPi buffer (pH 8.0) containing 8.8 mM DTT. 25 µL of a 320 mM stock solution of **28af** in IPA were added to the reactions and the microcentrifuge tubes were shaken at 30 °C and 280 rpm for 18 h. The reactions were extracted using 3x250 µL EtOAc and the enantiomeric excess was determined using a Chiralpak IG chiral column.

### 6.4.9 Activity assay of C23S, C44S and C176S MsrA02

Reactions were run in duplicates in a final volume of 500 µL. The CFE of the mutants C23S, C44S and C176S of MsrA02 were provided in 96-well plates containing 10 mg of lyophilised powder each. Each mutant was redissolved in 100 mM KPi buffer (pH 8.0) to 1.0, 10 and 40 mg/mL final concentrations. Then, 12.5 µL 352 mM DTT in buffer and 12.5 µL of a 320 mM stock solution of **28af** in IPA was added to each well to initiate the reaction. The plate was incubated for 18 h at 30 °C and 1000 rpm. 500 µL of $CH_3CN$ was added to each well to quench the reaction and the plates were centrifuged for 20 min at 4000 rpm and 4 °C to get rid of cell debris. To determine the activity of the mutants, 5 µL aliquots were injected into a Phenomenex chiral Lux *i*-Amylose-3 column and the enantiomeric excess was determined.

### 6.4.10 Identification of other Msrs for the kinetic resolution of bulkier sulfoxides

The CFE of 13 Msrs and EVC was provided by Almac in 96-well plates as 10 mg of lyophilised powder. Each well was resuspended in 950 µL 100 mM KPi buffer (pH 8.0) and split into two wells of a fresh 96-well plate (475 µL each). Then, 12.5 µL 352 mM DTT in buffer and 12.5 µL of a 320 mM sulfoxide solution in IPA or $CH_3CN$ were added to each well to initiate the reaction. The plate was shaken for 18 h at 30 °C and 1000 rpm. 500 µL of $CH_3CN$ were added to the wells to quench the reaction and the plates were centrifuged for 20 min at 4000 rpm and 4 °C to get rid of cell debris. To determine the final concentration of the remaining sulfoxide, 1 µL aliquots were injected into a UPLC Agilent Eclipse Plus C18 column and analysed with the following method: 0.5 mL/min,

25 °C; *T0*, water:$CH_3CN$ 90:10; *T4min*, water:$CH_3CN$ 40:60, hold for 1.5 min; *T6min*, water:$CH_3CN$ 90:10, hold for 1 minute. Total time 7 minutes.

### 6.4.11 General procedure for the kinetic resolution of sulfoxides using MsrA33

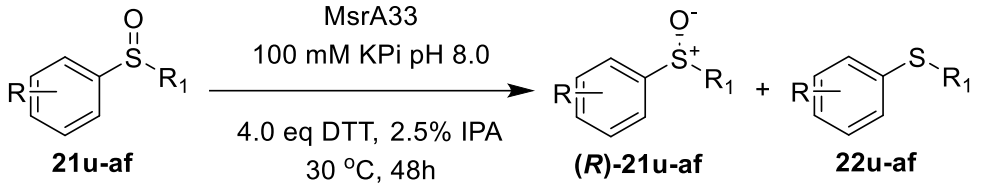


25 µL of a 320 mM stock solution in IPA of the relevant racemic substrate **28** (8.0 mM final concentration), was added to 975 µL 100 mM KPi buffer pH 8.0 containing DTT (16 mM, 4.0 eq.) and MsrA33 (40 $gL^{-1}$) to initiate the reaction. The reaction was shaken at 30 °C for 48 h. Upon completion, a 30 µL aliquot was extracted with EtOAc (3x50 µL), centrifuged (12500 rpm, 5 min) and the collected organic layers were analysed by normal phase HPLC using Chiralpak IC, IG or ID chiral columns to determine the enantiomeric excess. The remaining reaction mixture was quenched with 500 µL of $CH_3CN$ and 25 µL of compound **28af** was added as internal standard. The conversion was calculated by reversed phase HPLC using an Agilent Eclipse Plus C18 column (Calibration curves for the conversion are described in Appendix VI).

## Computational methods

### 6.4.12 Modelling

The crystal structure of MsrA02 from *Saccharomyces cerevisiae* (pdb code 3PIL)[423] was used as the initial structure. The acetate molecule was deleted, and hydrogens were added with Molprobity.[424] For the variants, single point mutations were introduced using a rotamer library. Afterwards, the structures were geometry optimized and subjected to molecular dynamics simulations. GROMACS[425] cluster analysis was conducted to select the most representative structures from the simulations.

The substrates **28ag** and **28j** were optimized with the exchange-correlation functional B3LYP,[426] the 6-31g(d) basis set and Polarizable Continuum Model (PCM).[427] The point charges were calculated resorting to the RESP methodology, from a single point calculation using Hartree-Fock with the 6-31g(d) basis set.

### 6.4.13 Molecular Docking

Molecular docking was performed using Autodock4.2 with the Lamarckian genetic algorithm (LGA)[428] using a grid around the sulfur atom of the nucleophilic cysteine. A total of 1000 LGA runs were carried out per system. The population was 300, the GA elitism=1, the maximum number of generations was 27000 and the maximum number of energy evaluations was 2500000. The top ranked structure corresponds to lowest binding energy structure of the most populated cluster with the lowest mean binding energy.

### 6.4.14 Molecular Dynamics Simulations

Molecular dynamics (MD) simulations were performed with GROMACS[425] with the amber parm99SB[429] force field. One initial energy minimization was performed, followed by two equilibration steps to slowly heat the system from 0 to 300 K (in canonical and isothermal-isobaric ensembles, respectively). Temperature and pressure coupling were 300 K and 1 bar, respectively and periodic boundary conditions (PBC) were used. Production runs were performed in an isothermal-isobaric ensemble. For each enzyme 3 replicas of the production simulations (100 ns) were carried out at 300 K. The time step was set to 2 fs and LINCS[430] constraints were applied to all bonds involving hydrogen atoms. The particle mesh Ewald (PME) method[431] was used to calculate electrostatic interactions.

### 6.4.15 Quantum Chemistry Calculations

Quantum chemical computations were performed using Spartan Pro. Two molecular structures **28v** and **28t** were optimised at the Hartree-Fock/6-31G* level of theory, in the gas phase, while the ESP was calculated using a constant electronic density of 0.002 au. The ESP values were shown by means of coloured maps on isodensity surface (range between -28 and 29 a.u).

## NMR studies methods

### 6.4.16 Production of $^{15}N$ and $^{13}C$ labelled MsrA02 and MsrA02_C25S

The purified MsrA02 and MsrA02_C25S plasmids were transformed into T7 express competent cells and the resulting cell mixture was plated on LB agar (50 $\mu g mL^{-1}$ kanamycin) and incubated overnight at 35 $^{o}C$. A single colony of transformed cells was

used to inoculate 1.0 mL SOC media with kanamycin (50 μgmL$^{-1}$) and incubated at 30 $^{o}$C and 220 rpm until cloudy. Then 150 μL of the SOC media was used to inoculate 50 mL M9 media (100 mM $NaH_2PO_4$, 100 mM $KH_2PO_4$, 100 mM NaCl, 1 mM $MgSO_4$, 0.1 mM $CaCl_2$, 1 mM Thiamine-HCl, 22 mM $^{13}$C glucose, 19 mM $^{15}NH_4Cl$) with kanamycin (50 μgmL$^{-1}$) and incubated overnight at 37 $^{o}$C. The overnight M9 preculture was used to inoculate 500 mL of M9 media and incubated at 30 $^{o}$C. When $OD_{600}$ reached 0.6-0.8 the expression of the protein was induced with 0.5 mM isopropyl-β-D-thiogalactopyranoside (IPTG) and incubated overnight at 25 $^{o}$C. Cells were harvested by centrifugation (18,000 rpm, 45 min, 4 $^{o}$C), resuspended in cell lysis buffer (Buffer A, pepstatin, protease cocktail, lysozyme, DNAase, 1 mM DTT) and lysed using a IXT4A (Constant System LTD) cell disruptor. After centrifugation (20,000 rpm, 1 h, 4 $^{o}$C), the CFE was loaded onto a His-Trap™ Fast Flow nickel affinity column and purified following the procedure described in Section 2.2. The final concentration was assessed through Bradford method.

### 6.4.17 NMR spectroscopy

Spectra were acquired on a Bruker Avance III spectrometer at a proton frequency of 600MHz using a QCIP cryoprobe at 25 $^{o}$C. NMR spectra were processed using NMRPipe[432] and analyzed using NMRView.[433] Backbone $^{1}$HN, $^{15}$N, and $^{13}$C, assignments were obtained from triple resonance HNCA, HN(CO)CA, CBCA(CO)NH, HNCACB, and HNCO spectra collected on $^{15}$N- and $^{13}$C- labelled MsrA02 enzyme. Backbone resonances are deposited on the BMRB (51733).

## Development of a deracemization method

### 6.4.18 Screening of commercially available photocatalysts for the oxidation of sulfides in the enzymatic reaction conditions

Each photocatalyst **95-98** was dissolved in 2.3 mL 100 mM KPi buffer pH 8.0 to a concentration of 5 mol% and 10 mol% for **98**. EDTA (36 nmol) was subsequently added to the mixture if appropriate. Then, methyl *p*-tolyl sulfide **27af** (5 mg, 36 nmol) was dissolved in 575 μL $CH_3CN$ and added to the mixture. The reaction was stirred under white light irradiation (5W) and monitored by TLC for 1.5 h for qualitative conversion to methyl phenyl sulfoxide **28af**.

### 6.4.19 Photobiocatalytic deracemization method using eosin Y 96

To initiate the reaction, 50 µL of a 1.28 M stock solution of **28af** in $CH_3CN$ (32 mM final concentration), was added to 1.950 mL 100 mM KPi buffer pH 8.0 containing DTT (35.2 mM, 1.1 eq.), eosin Y **96** (5 mol %) and MsrA02 in varying concentrations. The reaction was stirred and irradiated using a green LED light (5W) for intervals of 1 h and 15 min darkness. After 18 h, the reaction was quenched and extracted with EtOAc (3x100 µL) and injected into a Daicel Chiralpak IG (0.46 cm x 25 cm) chiral HPLC column to determine the enantiomeric excess.

### 6.4.20 Use of riboflavin and riboflavin tetraacetate (RFTA) for the oxidation of sulfides in the enzymatic reaction conditions

Riboflavin or RFTA were dissolved in 1 mL of a mix of water and $CH_3CN$ in varying ratios to achieve a concentration of 10 mol %. $Sc(OTf)_3$ (20 mol %) was subsequently added to the mixture if needed. Then, methyl *p*-tolyl sulfide **27af** (2 mg, 14 nmol) was added to the mixture and the reaction was stirred under blue light irradiation (15 W) and monitored by TLC for 1-6 h for qualitative conversion to methyl *p*-tolyl sulfoxide **28af**.

## References


1 N. J. Turner and R. Kumar, *Curr. Opin. Chem. Biol.*, 2018, **43**, A1–A3.

2 D. Kaiser, I. Klose, R. Oost, J. Neuhaus and N. Maulide, *Chem. Rev.*, 2019, **119**, 8701–8780.

3 L. H. S. Smith, S. C. Coote, H. E. Sneddon and D. J. Procter, *Angew. Chem., Int. Ed.*, 2010, **49**, 5832–5844.

4 D. Gamba-Sánchez and F. Garzón-Posse, *Pummerer-Type Reactions as Powerful Tools in Organic Synthesis*, John Wiley & Sons, Ltd, 2015, vol. 1.

5 I. Colomer, M. Velado, R. Fernández De La Pradilla and A. Viso, *Chem. Rev.*, 2017, **117**, 14201–14243.

6 E. J. Corey and M. Chaykovsky, *J. Org. Chem.*, 1958, **23**, 29.

7 V. K. Aggarwal and C. L. Winn, *Acc. Chem. Res.*, 2004, **37**, 611–620.

8 Z. Lin, X. Xu, S. Zhao, X. Yang, J. Guo, Q. Zhang, C. Jing, S. Chen and Y. He, *Nat. Commun.*, 2018, **9**, 1–8.

9 B. M. Trost, M. Rao, B. M. Trost and M. Rao, *Angew. Chem., Int. Ed.*, 2015, **54**, 5026–5043.

10 G. Sipos, E. E. Drinkel and R. Dorta, *Chem. Soc. Rev.*, 2015, **44**, 3834–3860.

11 M. Carmen Carreño, G. Hernández-Torres, M. Ribagorda and A. Urbano, *Chem. Commun.*, 2009, **0**, 6129–6144.

12 F. Lang, D. Li, J. Chen, J. Chen, L. Li, L. Cun, J. Zhu, J. Deng and J. Liao, *Adv. Synth. Catal.*, 2010, **352**, 843–846.

13 K. A. Scott and J. T. Njardarson, *Top. Curr. Chem.*, 2018, **376**, 1–34.

14 T. Shimatani, M. Inoue, T. Kuroiwa, J. Xu, H. Mieno and S. Tazuma, *Dig. Liver Dis.*, 2006, **38**, 554–559.

15 S. Prachayasittikul, R. Pingaew, A. Worachartcheewan, S. Ruchirawat and V. Prachayasittikul, *EXCLI J.*, 2010, **9**, 102–107.

16 J. Han, V. A. Soloshonok, K. D. Klika, J. Drabowicz and A. Wzorek, *Chem. Soc. Rev.*, 2018, 47, 1307–1350.

17 W. Maczka, K. Wińska and M. Grabarczyk, *Catalysts*, 2018, **8**, 624–651.

18 R. Naidu, B. Biswas, I. R. Willett, J. Cribb, B. Kumar Singh, C. Paul Nathanail, F. Coulon, K. T. Semple, K. C. Jones, A. Barclay and R. John Aitken, *Environ. Int.*, 2021, **156**, 106616.

19 C. Wyborn, E. Louder, M. Harfoot and S. Hill, *Environ. Conserv.*, 2021, **48**, 8–15.

20 Company fined £650,000 after banned chemical entered Yealm estuary - GOV.UK, https://www.gov.uk/government/news/company-fined-650-000-after-banned-chemical-entered-yealm-estuary, (accessed 3 February 2023).

21 R. Carson, *Silent Spring*, Houghton Mifflin, 1962.

22 Pollution Prevention Act of 1990 | US EPA, https://www.epa.gov/p2/pollution-prevention-act-1990, (accessed 24 January 2023).

23 P. T. Anastas and J. C. Warner, *Green chemistry: theory and practice*, Oxford University Press, Oxford , First., 1998.

24 M. Tobiszewski, M. Marć, A. Gałuszka and J. Namieśnik, *Molecules*, 2015, **20**, 10928–10946.

25 R. A. Sheldon, M. L. Bode and S. G. Akakios, *Curr. Opin. Green Sustainable Chem.*, 2022, **33**, 100569.

26 A. Horowitz, L. Kroitoru, E. Mazor and D. Gilad, *Science (1979)*, 1991, **254**, 1471–1477.

27 B. M. Trost, *Angew. Chem., Int. Ed. Engl.*, 1995, **34**, 259–281.

28 R. A. Sheldon, *Chem Commun.*, 2008, 3352–3365.

29 R. A. Sheldon, *Green Chem.*, 2017, **19**, 18–43.

30 R. A. Sheldon, *ACS Sustainable Chem. Eng.*, 2018, **6**, 32–48.

31 T. V. T. Phan, C. Gallardo and J. Mane, *Green Chem.*, 2015, **17**, 2846–2852.

32 A. J. Hunt, *Element Recovery and Sustainability*, RSC Publishing, Cambridge, 2013.

33 A. R. Alcántara, P. Domínguez de María, J. A. Littlechild, M. Schürmann, R. A. Sheldon and R. Wohlgemuth, *ChemSusChem*, 2022, **15**, e202102709.

34 R. A. Sheldon and J. M. Woodley, *Chem. Rev.*, 2018, **118**, 801–838.

35 A. Zaks and A. M. Klibanov, *Science (1979)*, 1984, **224**, 1249–1251.

36 Development of New Stereoisomeric Drugs | FDA, https://www.fda.gov/regulatory-information/search-fda-guidance-documents/development-new-stereoisomeric-drugs, (accessed 8 February 2023).

37 F. H. Arnold, *Angew. Chem., Int. Ed.*, 2019, **58**, 14420–14426.

38 M. D. Truppo, *ACS Med. Chem. Lett.*, 2017, **8**, 476–480.

39 J. M. Woodley, *Appl. Microbiol. Biotechnol.*, 2019, **103**, 4733–4739.

40 S. Wu, R. Snajdrova, J. C. Moore, K. Baldenius and U. T. Bornscheuer, *Angew. Chem., Int. Ed.*, 2021, **60**, 88–119.

41 C. A. Martinez, S. Hu, Y. Dumond, J. Tao, P. Kelleher and L. Tully, *Org. Process Res. Dev.*, 2008, **12**, 392–398.

42 A. Saytzeff, *Justus Liebigs Ann. Chem.*, 1866, **139**, 354–364.

43 A. Saytzeff, *Justus Liebigs Ann. Chem.*, 1867, **144**, 145–148.

44 D. E. Lewis, *Angew. Chem., Int. Ed.*, 2011, **50**, 6452–6458.

45 R. v. Kupwade, *J. Chem. Rev.*, 2019, **1**, 99–113.

46 F. Gasparrini, M. Giovannoli, D. Misiti, G. Natile and G. Palmieri, *J. Org. Chem.*, 1990, **55**, 1323–1328.

47 A. R. Suárez, L. I. Rossi and S. E. Martín, *Tetrahedron Lett.*, 1995, **36**, 1201–1204.

48 C. O. Kinen, L. I. Rossi and R. H. de Rossi, *J. Org. Chem.*, 2009, **74**, 7132–7139.

49 A. R. Hajipour, B. Kooshki and A. E. Ruoho, *Tetrahedron Lett.*, 2005, **46**, 5503–5506.

50 M. M. Khodaei, K. Bahrami and M. S. Arabi, *J. Sulfur Chem.*, 2010, **31**, 83–88.

51 H. T. Clarke, J. R. Johnson and R. Robinson, *Chemistry of Penicillin*, Princeton University Press, 1949.

52 N. J. Leonard and C. R. Johnson, *J. Org. Chem.*, 1962, **27**, 282–284.

53 P. Kowalski, K. Mitka, K. Ossowska and Z. Kolarska, *Tetrahedron*, 2005, **61**, 1933–1953.

54 D. N. Gupta, P. Hodge and J. E. Davies, *J. Chem. Soc., Perkin Trans. 1*, 1981, **1**, 2970–2973.

55 A. Sudalai, A. Khenkin and R. Neumann, *Org. Biomol. Chem.*, 2015, **13**, 4374–4394.

56 J. M. Khurana, A. K. Panda, A. Ray and A. Gogia, *Org. Prep. Proced. Int.*, 1996, **28**, 234–237.

57 A. Amoozadeh and F. Nemati, *Phosphorus, Sulfur, and Silicon*, 2009, **184**, 2569–2575.

58 J. Y. Huang, S. J. Li and Y. G. Wang, *J. Carbohydr. Chem.*, 2010, **29**, 142–153.

59 T. Okada, H. Matsumuro, S. Kitagawa, T. Iwai, K. Yamazaki, Y. Kinoshita, Y. Kimura and M. Kirihara, *Synlett*, 2015, **26**, 2547–2552.

60 M. Kirihara, T. Okada, Y. Sugiyama, M. Akiyoshi, T. Matsunaga and Y. Kimura, *Org Process Res Dev*, 2017, **21**, 1925–1937.

61 V. Pace, L. Castoldi and W. Holzer, *Tetrahedron Lett.*, 2012, **53**, 967–972.

62 M. Eissen and D. Lenoir, *Chem. - Eur. J.*, 2008, **14**, 9830–9841.

63 H. Hussain, I. R. Green and I. Ahmed, *Chem. Rev.*, 2013, **113**, 3329–3371.

64 S. Alvi, V. Jayant and R. Ali, *ChemistrySelect*, 2022, **7**, e202200704.

65 F. Silva, A. Baker, J. Stansall, W. Michalska, M. S. Yusubov, M. Graz, R. Saunders, G. J. S. Evans and T. Wirth, *Eur. J. Org. Chem.*, 2018, **2018**, 2134–2137.

66 M. Eissen, M. Strudthoff, S. Backhaus, C. Eismann, G. Oetken, S. Kaling and D. Lenoir, *J. Chem. Educ.*, 2011, **88**, 284–291.

67 J. P. Colomer, M. Traverssi and G. Oksdath-Mansilla, *J. Flow Chem.*, 2020, **10**, 123–138.

68 P. J. Kropp, G. W. Breton, J. D. Fields, J. C. Tung and B. R. Loomis, *J. Am. Chem. Soc.*, 2000, **122**, 4280–4285.

69 M. Y. Chen, L. N. Patkar, H. T. Chen and C. C. Lin, *Carbohydr. Res.*, 2003, **338**, 1327–1332.

70 B. Yu, A.-H. Liu, L.-N. He, B. Li, Z.-F. Diao and Y.-N. Li, *Green Chem.*, 2012, **14**, 957–962.

71 R. v Kupwade, S. S. Khot, U. P. Lad, U. v Desai, P. P. Wadgaonkar, S. S. Khot, U. P. Lad, U. v Desai and P. P. Wadgaonkar, *Res. Chem. Intermed.*, 2017, **43**, 6875–6888.

72 H. Hussain, A. Al-Harrasi, I. R. Green, I. Ahmed, G. Abbas and N. U. Rehman, *RSC Adv.*, 2014, **4**, 12882–12917.

73 A. Naeimi and M. Yoosefian, *J.Nanostruct.*, 2019, **9**, 86–93.

74 M. D. Davies and M. E. Deary, *J. Chem. Soc., Perkin Trans. 2*, 1996, 2423–2430.

75 B. E. Winfred Parker, C. Ricciuti, C. L. Ogg and D. Swern, *J. Am. Chem. Soc.*, 1955, **77**, 4037–4041.

76 C. A. Contreras, P. A. A. Ignacio-De Leon and J. M. Notestein, *Microporous and Mesoporous Mater.*, 2016, **225**, 289–295.

77 K. Kaczorowska, Z. Kolarska, K. Mitka and P. Kowalski, *Tetrahedron*, 2005, **61**, 8315–8327.

78 K. Liu, H. Ou, X. Shi, X. Dong, W. Ma and J. Wei, *Chin. J. Org. Chem.*, 2014, 34, 681–692.

79 K. Yoshihiro, *J. Jpn. Pet. Inst.*, 2017, **60**, 159–169.

80 S. Matavos-Aramyan, S. Soukhakian, & Mohammad, H. Jazebizadeh and M. H. Jazebizadeh, *Phosphorus, Sulfur, and Silicon*, 2019, **195**, 181–193.

81 X. B. Liu, Q. Rong, J. Tan, C. Chen and Y. L. Hu, *Front. Chem.*, 2022, 9, 1–17.

82 L. Ji, J. Liu, C. Qian and X. Chen, *Chin. J. Org. Chem.*, 2012, 32, 254–265.

83 A. Rostami and J. Akradi, *Tetrahedron Lett.*, 2010, **51**, 3501–3503.

84 R. B. Wagh, S. H. Gund and J. M. Nagarkar, *J. Chem. Sci.*, 2016, **128**, 1321–1325.

85 F. Shi, M. K. Tse, H. M. Kaiser and M. Beller, *Adv. Synth. Catal.*, 2007, **349**, 2425–2430.

86 M. Kirihara, A. Itou, T. Noguchi and J. Yamamoto, *Synlett* , 2010, **10**, 1557–1561.

87 M. Kirihara, J. Yamamoto, T. Noguchi and Y. Hirai, *Tetrahedron Lett.*, 2009, **50**, 1180–1183.

88 S. Yamazaki, *Bull. Chem. Soc. Jpn.*, 1996, **69**, 2955–2959.

89 C. Yang, Q. Jin, H. Zhang, J. Liao, J. Zhu, B. Yu and J. Deng, *Green Chem.*, 2009, **11**, 1401–1405.

90 A. R. Supale and G. S. Gokavi, *React. Kinet. Catal. Lett.*, 2009, **96**, 83–89.

91 X. F. Wu, *Tetrahedron Lett.*, 2012, **53**, 4328–4331.

92 J. B. Feng, J. L. Gong and X. F. Wu, *RSC Adv.*, 2014, **4**, 29273–29275.

93 A. Bezaatpour, E. Askarizadeh, S. Akbarpour, M. Amiria and B. Babaei, *Mol. Catal.*, 2017, **436**, 199–209.

94 F. Mangiavacchi, L. Crociani, L. Sancineto, F. Marini and C. Santi, *Molecules*, 2020, **25**, 2711–2722.

95 M. Mokhtary, M. Qandalee and M. R. Niaki, *E-J. Chem.*, 2012, **9**, 863–868.

96 M. Azizi, A. Maleki, F. Hakimpoor, R. Ghalavand and · Ali Garavand, *Catal. Lett.*, 2017, **3**, 2173–2177.

97 H. Firouzabadi, N. Iranpoor, A. A. Jafari and E. Riazymontazer, *Adv. Synth. Catal.*, 2006, **348**, 434–438.

98 S. Hussain, S. K. Bharadwaj, R. Pandey and M. K. Chaudhuri, *Eur. J. Org. Chem.*, 2009, 3319–3322.

99 E. Voutyritsa, I. Triandafillidi and C. G. Kokotos, *Synthesis (Stuttg)*, 2017, **49**, 917–924.

100 B. Karimi, M. Ghoreishi-Nezhad and J. H. Clark, *Org. Lett.*, 2005, **7**, 625–628.

101 F. Gregori, I. Nobili, F. Bigi, R. Maggi, G. Predieri and G. Sartori, *J. Mol. Catal. A: Chem.*, 2008, **286**, 124–127.

102 M. Azizi, A. Maleki and F. Hakimpoor, *Catal. Commun.*, 2017, **100**, 62–65.

103 R. Frenzel, D. Morales, G. Romanelli, G. Sathicq, M. Blanco and L. Pizzio, *J. Mol. Catal. A: Chem.*, 2016, **420**, 124–133.

104 H. Veisi, S. Sajjadifar, P. M. Biabri and S. Hemmati, *Polyhedron*, 2018, **153**, 240–247.

105 A. M. Elgorban, N. Marraiki, S. A. Ansari and A. Syed, *J. Organomet. Chem.*, 2021, 954–955.

106 N. N. Mahamuni, P. R. Gogate and A. B. Pandit, *Ind. Eng. Chem. Res.*, 2006, **45**, 8829–8836.

107 N. N. Mahamuni, P. R. Gogate and A. B. Pandit, *Ultrason. Sonochem.*, 2007, **14**, 135–142.

108 F. di Furia, G. Modena and R. Curci, *Tetrahedron Lett.*, 1976, **50**, 4637–4638.

109 F. di Furia, G. Modena and R. Seraglia, *Synthesis (Stuttgart)*, 1984, 325–326.

110 A. Russo and A. Lattanzi, *Adv. Synth. Catal.*, 2009, **351**, 521–524.

111 X. Jiang, C. Yao, C. Tong, R. Bai, T. Zhou and Y. Xie, *Chin. J. Org. Chem.*, 2020, **40**, 1752–1759.

112 T. Matsui, Y. Dekishima and M. Ueda, *Appl. Microbiol. Biotechnol.*, 2014, **98**, 7699–7706.

113 F. Garzón-Posse, L. Becerra-Figueroa, J. Hernández-Arias and D. Gamba-Sánchez, *Molecules*, 2018, 23, 1265–1302.

114 S. Anselmi, N. Aggarwal, T. S. Moody and D. Castagnolo, *ChemBioChem*, 2021, **22**, 298–307.

115 A. Rostami, B. Mohammadi, Z. Shokri and S. Saadati, *Catal. Commun.*, 2018, **111**, 59–63.

116 P. N. Devine, R. M. Howard, R. Kumar, M. P. Thompson, M. D. Truppo and N. J. Turner, *Nat. Rev.*, 2018, **2**, 409–421.

117 R. A. Sheldon and D. Brady, *Chem. Commun*, 2018, **54**, 6088.

118 G. Hughes and J. C. Lewis, *Chem. Rev.*, 2018, 118, 1–3.

119 C. Garcia-Galan, Á. Berenguer-Murcia, R. Fernandez-Lafuente and R. C. Rodrigues, *Adv. Synth. Catal.*, 2011, **353**, 2885–2904.

120 R. K. Singh, M. K. Tiwari, R. Singh and J. K. Lee, *Int. J. Mol. Sci.*, 2013, **14**, 1232–1277.

121 C. Mateo, J. M. Palomo, G. Fernandez-Lorente, J. M. Guisan and R. Fernandez-Lafuente, *Enzyme Microb. Technol.*, 2007, **40**, 1451–1463.

122 C. Ortiz, M. Luján Ferreira, O. Barbosa, J. C. S dos Santos, R. C. Rodrigues, Á. Berenguer-Murcia, L. E. Briand and R. Fernandez-Lafuente, *Catal. Sci. Technol*, 2019, **9**, 2380.

123 P. Villeneuve, J. M. Muderhwa, J. Graille and M. J. Haas, *J. Mol. Catal. B: Enzym.*, 2000, **9**, 113–148.

124 M. T. Reetz, *Curr. Opin. Chem. Biol.*, 2002, **6**, 145–150.

125 R. Zechner, R. Zimmermann, T. O. Eichmann, S. D. Kohlwein, G. Haemmerle, A. Lass and F. Madeo, *Cell Metab.*, 2012, **15**, 279–291.

126 B. Kovács, E. Forró and F. Fülöp, *Tetrahedron*, 2018, **74**, 6873–6877.

127 R. A. Sheldon, *Adv. Synth. Catal.*, 2007, **349**, 1289–1307.

128 R. D. Schmid and R. Verger, *Angew. Chem., Int. Ed.*, 1998, **37**, 1608–1633.

129 T. B. Nielsen, M. Ishii and O. Kirk2, *Biotechnol. Appl. Cold-Adapted Org.*, 1999, 49–61.

130 E. A. Manoel, J. C. S. dos Santos, D. M. G. Freire, N. Rueda and R. Fernandez-Lafuente, *Enzyme Microb. Technol.*, 2015, **71**, 53–57.

131 S. P. Benson and J. Rgen Pleiss, *Langmuir*, 2017, **33**, 3251–3159.

132 A. Kundys, E. Białecka-Florjańczyk, A. Fabiszewska and J. Małajowicz, *J. Polym. Environ.*, 2018, **26**, 396–407.

133 E. M. Anderson, K. M. Larsson and O. Kirk, *Biocatal. Biotransform.*, 1998, **16**, 181–204.

134 O. Kirk and M. W. Christensen, *Org. Process Res. Dev.*, 2002, **6**, 446–451.

135 C. R. Johnson and S. J. Bis, *Tetrahedron Lett.*, 1992, **33**, 7287–7290.

136 E. P. Cipolatti, M. C. C. Pinto, J. de M. Robert, T. P. da Silva, T. da C. Beralto, J. G. F. Santos, R. de P. V. de Castro, R. Fernandez-Lafuente, E. A. Manoel, J. C. Pinto and D. M. G. Freire, *J. Appl. Polym. Sci.*, 2018, **135**, 46726–46739.

137 E. A. Manoel, J. M. Robert, M. C. C. Pinto, A. C. O. Machado, M. D. Besteti, M. A. Z. Coelho, A. B. C. Simas, R. Fernandez-Lafuente, J. C. Pinto and D. M. G. Freire, *RSC Adv.*, 2016, **6**, 4043–4052.

138 K. Engelmark Cassimjee, P. Hendil-Forssell, A. Volkov, A. Krog, J. Malmo, T. v Erik Aune, W. Knecht, I. R. Miskelly, T. S. Moody, M. Svedendahl Humble, V. A. Biosolutions and A. gt, *ACS Omega*, 2017, **2**, 8674–8677.

139 J. Zdarta, L. Klapiszewski, A. Jedrzak, M. Nowicki, D. Moszynski and T. Jesionowski, *Catalysts*, 2017, **7**, 14–35.

140 M. Oláh, S. Suba, Z. Boros, P. Kovács, M. Gosselin, C. Gaudreault and G. Hornyánszky, *Period. Polytech. Chem. Eng.*, 2018, **62**, 519–532.

141 R. T. Otto, H. Scheib, U. T. Bornscheuer, J. Pleiss, C. Syldatk and R. D. Schmid, *J. Mol. Catal. B: Enzym.*, 2000, **8**, 201–211.

142 Y. Watanabe, Y. Shimada, A. Sugihara and Y. Tominaga, *J. Mol. Catal. B: Enzym.*, 2002, **17**, 151–155.

143 Y. Watanabe, S. Sato, S. Sera, C. Sato, K. Yoshinaga, T. Nagai, R. Sato, H. Iwasaka and T. Aki, *J. Am. Oil Chem. Soc.*, 2014, **91**, 1323–1330.

144 E. Passicos, X. Santarelli and D. Coulon, *Biotechnol. Lett.*, 2004, **26**, 1073–1076.

145 A. B. R. Moreira, V. H. Perez, G. M. Zanin and H. F. de Castro, *Energy Fuels*, 2007, **21**, 3689–3694.

146 Y. Yu and S. Lutz, *Biotechnol. Bioeng.*, 2010, **105**, 44–50.

147 J. A. Kralovec, W. Wang and C. J. Barrow, *Aust. J. Chem.*, 2010, **63**, 922–928.

148 M. Kramer, J. C. Cruz, P. H. Pfromm, M. E. Rezac and P. Czermak, *J. Biotechnol.*, 2010, **150**, 80–86.

149 A. K. Singh and M. Mukhopadhyay, *Grasas Aceites*, 2012, **6**, 202–208.

150 Z. Boros, P. Falus, M. Márkus, D. Weiser, M. Oláh, G. Hornyánszky, J. Nagy and L. Poppe, *J. Mol. Catal. B: Enzym.*, 2013, **85–86**, 119–125.

151 S. Devendran and G. D. Yadav, *Chirality*, 2014, **26**, 286–292.

152 K. Bhandari, S. P. Chaurasia and A. K. Dalai, *Chem. Eng. Commun.*, 2015, **202**, 920–926.

153 H. N. Hoang and T. Matsuda, *Tetrahedron Lett.*, 2015, **56**, 639–641.

154 S. Gandomkar, Z. Habibi, M. Mohammadi, M. Yousefi and S. Salimi, *Biocatal Agric Biotechnol*, 2015, **4**, 550–554.

155 S. R. Matkovic, J. F. Nilsson, M. E. Fait, S. R. Morcelle and L. E. Briand, *Catal. Lett.*, 2016, **146**, 2341–2347.

156 J. Zdarta, M. Wysokowski, M. Norman, A. Kołodziejczak-Radzimska, D. Moszyński, H. Maciejewski, H. Ehrlich and T. Jesionowski, *Int. J. Mol. Sci.*, 2016, **17**, 1581–1603.

157 M. P. Pinheiro, N. S. Rios, T. de S. Fonseca, F. de A. Bezerra, E. Rodríguez-Castellón, R. Fernandez-Lafuente, M. Carlos de Mattos, J. C. S. dos Santos and L. R. B. Gonçalves, *Biotechnol. Prog.*, 2018, **34**, 878–889.

158 E. Gianolio, R. Mohan and A. Berkessel, *Adv. Synth. Catal.*, 2016, **358**, 30–33.

159 A. Foukis, O. A. Gkini, P. Y. Stergiou, V. A. Sakkas, A. Dima, K. Boura, A. Koutinas and E. M. Papamichael, *Bioresour. Technol.*, 2017, **238**, 122–128.

160 N. S. Rios, M. P. Pinheiro, J. C. S. dos Santos, T. de S. Fonseca, L. D. Lima, M. C. de Mattos, D. M. G. Freire, I. J. da Silva, E. Rodríguez-Aguado and L. R. B. Gonçalves, *J. Mol. Catal. B: Enzym.*, 2016, **133**, 246–258.

161 J. W. Shen, J. M. Qi, X. J. Zhang, Z. Q. Liu and Y. G. Zheng, *Org. Process Res. Dev.*, 2019, **23**, 1017–1025.

162 C. G. Spelmezan, L. C. Bencze, G. Katona, F. D. Irimie, C. Paizs and M. I. Tos, *Molecules*, 2020, **25**, 350–365.

163 C. Luna, V. Gascón-Pérez, F. J. López-Tenllado, F. M. Bautista, C. Verdugo-Escamilla, L. Aguado-Deblas, J. Calero, A. A. Romero, D. Luna and R. Estévez, *Catalysts*, 2021, **11**, 1350–1362.

164 J. M. Griffin, J. H. Atherton, M. I. Page and N. T. Powles, *J. Phys. Org. Chem.*, 2016, **29**, 768–772.

165 H. Tirunagari, L. Kuna, B. Shalini and K. Thenkrishnan, *Process Biochem.*, 2018, **65**, 109–114.

166 C. Wang, N. Wang, X. Liu, P. Wan, X. He and Y. Shang, *Fibers Polym.*, 2018, **19**, 1611–1617.

167 M. G. Yadav, M. R. Kavadia, R. N. Vadgama, A. A. Odaneth and A. M. Lali, *Prep. Biochem. Biotechnol.*, 2017, **47**, 1050–1058.

168 M. S. S. Googheri, M. R. Housaindokht and H. Sabzyan, *J. Mol. Graphics Modell.*, 2015, **57**, 9–19.

169 J. Błaszczyk and P. Kiełbasiński, *Crystals (Basel)*, 2020, **10**, 404–413.

170 V. Skouridou, H. Stamatis and F. N. Kolisis, *J. Mol. Catal. B: Enzym.*, 2003, **21**, 67–69.

171 C. Orellana-Coca, J. M. Billakanti, B. Mattiasson and R. Hatti-Kaul, *J. Mol. Catal. B: Enzym.*, 2007, **44**, 133–137.

172 U. Törnvall, C. Orellana-Coca, R. Hatti-Kaul and D. Adlercreutz, *Enzyme Microb. Technol.*, 2007, **40**, 447–451.

173 A. A. Tzialla, E. Kalogeris, A. Enotiadis, A. A. Taha, D. Gournis and H. Stamatis, *J. Mater. Sci. Eng. B*, 2009, **165**, 173–177.

174 M. Steinhagen, A. Gräbner, J. Meyer, A. E. W. Horst, A. Drews, D. Holtmann and M. B. Ansorge-Schumacher, *J. Mol. Catal. B: Enzym.*, 2016, **133**, S179–S187.

175 E. G. Ankudey, H. F. Olivo and T. L. Peeples, *Green Chem.*, 2006, **8**, 923–926.

176 M. Yolanda Ríos, E. Salazar and H. F. Olivo, *Green Chem.*, 2007, **9**, 459–462.

177 M. Markiton, S. Boncel, D. Janas and A. Chrobok, *ACS Sustainable Chem. Eng.*, 2016, **5**, 1685–1691.

178 D. González-Martínez, M. Rodríguez-Mata, D. Méndez-Sánchez, V. Gotor and V. Gotor-Fernández, *J. Mol. Catal. B: Enzym.*, 2015, **114**, 31–36.

179 A. Drozdz and A. Chrobok, *Chem. Commun.*, 2016, **52**, 1230–1233.

180 D. Méndez-Sánchez, I. Lavandera, V. Gotor and V. Gotor-Fernández, *Org. Biomol. Chem.*, 2017, **15**, 3196.

181 M. S. Melchiors, T. Y. Vieira, P. S. Pereira, B. A. M. Carciofi, P. H. H. De, A. Araújo, D. Débora De Oliveira and C. Sayer, *Ind. Eng. Chem. Res.*, 2019, **58**, 13918–13925.

182 A. F. Zanette, I. Zampakidi, G. T. Sotiroudis, M. Zoumpanioti, I. C. R. Leal, R. O. M. A. de Souza, L. Cardozo-Filho and A. Xenakis, *J. Mol. Catal. B: Enzym.*, 2014, **107**, 89–94.

183 G. Chávez, R. Hatti-Kaul, R. A. Sheldon and G. Mamo, *J. Mol. Catal. B: Enzym.*, 2013, **89**, 67–72.

184 P. G. Jessop, *Green Chem.*, 2011, **13**, 1391–1398.

185 F. P. Byrne, S. Jin, G. Paggiola, T. H. M. Petchey, J. H. Clark, T. J. Farmer, A. J. Hunt, C. R. Mcelroy and J. Sherwood, *Sustain. Chem. Processes*, 2016, **4**, 1–24.

186 C. J. Clarke, W. C. Tu, O. Levers, A. Bröhl and J. P. Hallett, *Chem. Rev.*, 2018, **118**, 747–800.

187 R. Matyáš, J. Selesovsky, V. Pelikán, M. Szala, S. Cudziło, W. A. Trzciński and M. Gozin, *Propellants, Explos., Pyrotech.*, 2017, **42**, 198–203.

188 S. Ranganathan, T. Gärtner, L. O. Wiemann and V. Sieber, *J. Mol. Catal. B: Enzym.*, 2015, **114**, 72–76.

189 S. Ranganathan and V. Sieber, *React. Chem. Eng.*, 2017, **2**, 885–895.

190 J. Clayden, N. Greeves, S. Warren and P. Wothers, *Organic Chemistry*, Oxford University Press, Oxford, First Edition., 2006.

191 P. Lindberg, A. Brndstrm, B. Wallmark, H. Mattsson, L. Rikner and K. J. Hoffmann, *Med. Res. Rev.*, 1990, **10**, 1–54.

192 S. Caron, R. W. Dugger, S. G. Ruggeri, J. A. Ragan and D. H. Brown Ripin, *Chem. Rev.*, 2006, **106**, 2943–2989.

193 D. S. Bhalerao, G. China Mala Kondaiah, N. Dwivedi, R. Kumar Mylavarappu, L. Amarnath Reddy, A. Roy, G. Nagaraju, P. Pratap Reddy, A. Bhattacharya, R. Bandichhor and S. Bhalerao, *Synth. Commun.*, 2010, **40**, 2983–2987.

194 H. Hou, X. Zeng and X. Zhang, *Angew. Chem., Int. Ed.*, 2020, **59**, 17356–17376.

195 M. Teranishi, S.-I. Naya and H. Tada, *J. Am. Chem. Soc.*, 2010, **132**, 7850–7851.

196 Y. Jiang, P. Ni, C. Chen, Y. Lu, P. Yang, B. Kong, A. Fisher and X. Wang, *Adv. Energy Mater.*, 2018, **8**, 1801909.

197 Y. Pang, H. Xie, Y. Sun, M. M. Titirici and G. L. Chai, *J. Mater. Chem. A.*, 2020, **8**, 24996–25016.

198 Y. Sun, L. Han and P. Strasser, *Chem. Soc. Rev.*, 2020, **49**, 6605–6631.

199 K. Dong, Y. Lei, H. Zhao, J. Liang, P. Ding, Q. Liu, Z. Xu, S. Lu, Q. Li and X. Sun, *J. Mater. Chem. A.*, 2020, **8**, 23123–23141.

200 X. Shi, S. Back, T. M. Gill, S. Siahrostami and X. Zheng, *Chem*, 2021, **7**, 38–63.

201 J. An, Y. Feng, Q. Zhao, X. Wang, J. Liu and N. Li, *Environ. Sci. Ecotechnology*, 2022, **11**, 100170.

202 Y. Wen, T. Zhang, J. Wang, Z. Pan, T. Wang, H. Yamashita, X. Qian and Y. Zhao, *Angew. Chem., Int. Ed.*, 2022, **61**, e202205972.

203 D. Hâncu, J. Green and E. J. Beckman, *Acc. Chem. Res.*, 2002, **35**, 757–764.

204 H. Li, B. Zheng, Z. Pan, B. Zong and M. Qiao, *Chem. Sci. Eng.*, 2018, **12**, 124–131.

205 G. Gao, Y. Tian, X. Gong, Z. Pan, K. Yang and B. Zong, *Chi. J. Catal.*, 2020, **41**, 1039–1047.

206 G. Xu, Y. Liang and F. Chen, *J. Mol. Catal. A: Chem.*, 2016, **420**, 66–72.

207 A. Torres-Pinto, M. J. Sampaio, C. G. Silva, J. L. Faria and A. M. T. Silva, *Catalysts*, 2019, **9**, 990.

208 Z. Haider, H. in Cho, G. hee Moon and H. il Kim, *Catal. Today*, 2019, **335**, 55–64.

209 L. Pi, J. Cai, L. Xiong, J. Cui, H. Hua, D. Tang and X. Mao, *Chem. Eng. J.*, 2020, **389**, 123420.

210 X. Zeng, Y. Liu, X. Hu and X. Zhang, *Green Chem.*, 2021, **23**, 1466–1494.

211 L. Wang, J. Zhang, Y. Zhang, H. Yu, Y. Qu and J. Yu, *Small*, 2022, **18**, 2104561–2104582.

212 Z. Chen, D. Yao, C. Chu and S. Mao, *Chem. Eng. J.*, 2022, **451**, 138489.

213 X. Yang and D. Wang, *ACS Appl. Energy Mater.*, 2018, **1**, 6657–6693.

214 A. Fujishima, T. N. Rao and D. A. Tryk, *J. Photochem. Photobiol., C*, 2000, **1**, 1–21.

215 M. Pelaez, N. T. Nolan, S. C. Pillai, M. K. Seery, P. Falaras, A. G. Kontos, P. S. M. Dunlop, J. W. J. Hamilton, J. A. Byrne, K. O'Shea, M. H. Entezari and D. D. Dionysiou, *Appl. Catal., B*, 2012, **125**, 331–349.

216 V. Maurino, C. Minero, G. Mariella and E. Pelizzetti, *Chem. Commun.*, 2005, **1**, 2627–2629.

217 V. Maurino, C. Minero, E. Pelizzetti, G. Mariella, A. Arbezzano and F. Rubertelli, *Res. Chem. Intermed.*, 2007, **33**, 319–332.

218 N. Kaynan, B. A. Berke, O. Hazut and R. Yerushalmi, *J. Mater. Chem. A*, 2014, **2**, 13822–13826.

219 M. Teranishi, S. I. Naya and H. Tada, *J. Phys. Chem. C*, 2016, **120**, 1083–1088.

220 X. Xiong, X. Zhang, S. Liu, J. Zhao and Y. Xu, *Photochem. Photobiol. Sci*, 2018, **17**, 1018–1022.

221 L. Zheng, H. Su, J. Zhang, L. S. Walekar, H. Vafaei Molamahmood, B. Zhou, M. Long and Y. H. Hu, *Appl. Catal., B*, 2018, **239**, 475–484.

222 R. Ma, L. Wang, H. Wang, Z. Liu, M. Xing, L. Zhu, X. Meng and F. S. Xiao, *Appl. Catal., B*, 2019, **244**, 594–603.

223 G. H. Moon, W. Kim, A. D. Bokare, N. E. Sung and W. Choi, *Energy Environ. Sci.*, 2014, **7**, 4023–4028.

224 X. Zeng, Z. Wang, G. Wang, T. R. Gengenbach, D. T. McCarthy, A. Deletic, J. Yu and X. Zhang, *Appl. Catal., B.*, 2017, **218**, 163–173.

225 X. Zeng, Z. Wang, N. Meng, D. T. McCarthy, A. Deletic, J. hong Pan and X. Zhang, *Appl. Catal., B.*, 2017, **202**, 33–41.

226 W. J. Ong, L. L. Tan, Y. H. Ng, S. T. Yong and S. P. Chai, *Chem. Rev.*, 2016, **116**, 7159–7329.

227 B. Zhu, L. Zhang, B. Cheng and J. Yu, *Appl. Catal., B*, 2018, **224**, 983–999.

228 S. Cao, J. Low, J. Yu and M. Jaroniec, *Adv. Mater.*, 2015, **27**, 2150–2176.

229 J. Fu, J. Yu, C. Jiang and B. Cheng, *Adv. Energy Mater.*, 2018, **8**, 1701503.

230 J. Lim, H. Kim, J. Park, G. H. Moon, J. J. M. Vequizo, A. Yamakata, J. Lee and W. Choi, *Environ. Sci. Technol.*, 2020, **54**, 497–506.

231 A. Guerrero-Corella, A. María Martinez-Gualda, F. Ahmadi, E. Ming, A. Fraile and J. Alemán, *Chem. Commun.*, 2017, **53**, 10463–10466.

232 M. Singh, A. K. Yadav, L. D. S. Yadav and R. K. P. Singh, *Tetrahedron Lett.*, 2018, **59**, 450–453.

233 H. Hao, Z. Wang, J. L. Shi, X. Li and X. Lang, *ChemCatChem*, 2018, **10**, 4545–4554.

234 C. Capello, U. Fischer and K. Hungerbühler, *Green Chem.*, 2007, **9**, 927–934.

235 S. Bormann, A. Gomez Baraibar, Y. Ni, D. Holtmann and F. Hollmann, *Catal. Sci. Technol.*, 2014, **5**, 2038–2052.

236 I. Bassanini, E. E. Ferrandi, M. Vanoni, G. Ottolina, S. Riva, M. Crotti, E. Brenna and D. Monti, *Eur. J. Org. Chem.*, 2017, **2017**, 7186–7189.

237 X. Wei, C. Zhang, X. Gao, Y. Gao, Y. Yang, K. Guo, X. Du, L. Pu and Q. Wang, *ChemistryOpen*, 2019, **8**, 1076–1083.

238 Y. Li, Y. Ma, P. Li, X. Zhang, D. Ribitsch, M. Alcalde, F. Hollmann and Y. Wang, *Chempluschem*, 2020, **85**, 254–257.

239 M. Hobisch, D. Holtmann, P. Gomez de Santos, M. Alcalde, F. Hollmann and S. Kara, *Biotechnol. Adv.*, 2021, **51**, 107615.

240 G. Carrea, B. Redigolo, S. Riva, S. Colonna, N. Gaggero, E. Battistel and D. Bianchi, *Tetrahedron Asymmetry*, 1992, **3**, 1063–1068.

241 F. Secundo, G. Carrea, S. Dallavalle and G. Franzosi, *Tetrahedron Asymmetry*, 1993, **4**, 1981–1982.

242 F. Zambianchi, P. Pasta, G. Carrea, S. Colonna, N. Gaggero and J. M. Woodley, *Biotechnol. Bioeng.*, 2002, **78**, 489–496.

243 S. Wei, G. Xu, L. Zhang, J. Zhou and Y. Ni, *Chem. Commun.*, 2022, **58**, 13246–13249.

244 K. Okrasa, E. Guibé-Jampel and M. Therisod, *Tetrahedron Asymmetry*, 2003, **14**, 2487–2490.

245 M. J. L. J. Fürst, A. Gran-Scheuch, F. S. Aalbers and M. W. Fraaije, *ACS Catal.*, 2019, **9**, 11207–11241.

246 N. M. Kamerbeek, D. B. Janssen, W. J. H. van Berkel and M. W. Fraaije, *Adv. Synth. Catal.*, 2003, **345**, 667–678.

247 C. E. Paul, D. Eggerichs, A. H. Westphal, D. Tischler and W. J. H. van Berkel, *Biotechnol. Adv.*, 2021, **51**, 107712.

248 C. E. Paul, D. Eggerichs, A. H. Westphal, D. Tischler and W. J. H. van Berkel, *Arch. Biochem. Biophys.*, 2014, **544**, 2–17.

249 G. E. Turfitt, *Biochem. J.*, 1948, **42**, 376–383.

250 D. B. Norris and P. W. Trudgill, *Biochem. J.*, 1971, **121**, 363–370.

251 N. A. Donoghue, D. B. Norris and P. W. Trudgill, *Eur. J. Biochem.*, 1976, **63**, 175–192.

252 S. Thodberg and E. H. J. Neilson, *Catalysts* , 2020, **10**, 329–349.

253 D. M. Ziegler and C. H. Mitchell, *Arch. Biochem. Biophys.*, 1972, **150**, 116–125.

254 R. D. Ceccoli, D. A. Bianchi, M. A. Carabajal and D. v. Rial, *Mol. Catal.*, 2020, **486**, 110875.

255 E. Malito, A. Alfieri, M. W. Fraaije and A. Mattevi, *Proc. Natl. Acad. Sci. USA*, 2004, **101**, 13157–13162.

256 S. Eswaramoorthy, J. B. Bonanno, S. K. Burley and S. Swaminathan, *Proc Natl Acad Sci U S A*, 2006, **103**, 9832–9837.

257 A. Alfieri, E. Malito, R. Orru, M. W. Fraaije and A. Mattevi, *Proc. Natl. Acad. Sci. USA*, 2008, **105**, 6572–6577.

258 E. Romero, J. R. Gómez Castellanos, G. Gadda, M. W. Fraaije and A. Mattevi, *Chem. Rev.*, 2018, **118**, 1742–1769.

259 M. Toplak, A. Matthews and R. Teufel, *Arch. Biochem. Biophys.*, 2021, **698**, 108732.

260 V. Piano, B. A. Palfey and A. Mattevi, *Trends Biochem. Sci.*, 2017, **42**, 457–469.

261 M. J. Fürst, F. Fiorentini and M. W. Fraaije, *Curr. Opin. Struct. Biol.*, 2019, **59**, 29–37.

262 L. A. Harwood, L. L. Wong and J. Robertson, *Angew. Chem., Int. Ed.*, 2021, **60**, 4434–4447.

263 I. Polyak, M. T. Reetz and W. Thiel, *J. Am. Chem. Soc.*, 2012, **134**, 2732–2741.

264 D. Sheng, D. P. Ballou and V. Massey, *Biochemistry*, 2001, **40**, 11156–11167.

265 R. M. Phelan, M. J. Abrahamson, J. T. C. Brown, R. K. Zhang and C. R. Zwick, *Org. Process Res. Dev.*, 2022, **26**, 1944–1959.

266 G. de Gonzalo and A. R. Alcántara, *Catalysts*, 2021, **11**, 605–629.

267 F. S. Aalbers and M. W. Fraaije, *ChemBioChem*, 2019, **20**, 20–28.

268 M. Bučko, P. Gemeiner, A. Schenkmayerová, T. Krajčovič, F. Rudroff and M. D. Mihovilovič, *Appl. Microbiol. Biotechnol.*, 2016, **100**, 6585–6599.

269 D. E. Torres Pazmiño, H. M. Dudek and M. W. Fraaije, *Curr. Opin. Chem. Biol.*, 2010, **14**, 138–144.

270 G. de Gonzalo, M. J. L. J. Fürst and M. W. Fraaije, *Catalysts*, 2017, **7**, 288–297.

271 J. Löwe, O. Blifernez-Klassen, T. Baier, L. Wobbe, O. Kruse and H. Gröger, *J. Biotechnol.*, 2019, **294**, 81–87.

272 J. Engel, K. S. Mthethwa, D. J. Opperman and S. Kara, *Mol. Catal.*, 2019, **468**, 44–51.

273 E. J. Seo, C. W. Kang, J. M. Woo, S. Jang, Y. J. Yeon, G. Y. Jung and J. B. Park, *Metab. Eng.*, 2019, **54**, 137–144.

274 H. R. Mansouri, M. D. Mihovilovic and F. Rudroff, *ChemBioChem*, 2020, **21**, 971–977.

275 G. X. Zhang, Z. N. You, J. M. Yu, Y. Y. Liu, J. Pan, J. H. Xu and C. X. Li, *ChemBioChem*, 2021, **22**, 1190–1195.

276 M. A. Graham, H. Askey, A. D. Campbell, L. Chan, K. G. Cooper, Z. Cui, A. Dalgleish, D. Dave, G. Ensor, M. Rita, G. Espinosa, P. Hamilton, C. Heffernan, L. v Jackson, D. Jing, M. F. Jones, P. Liu, K. R. Mulholland, M. Pervez, M. Popadynec, E. Randles, S. Tomasi and S. Wang, *Org. Process Res. Dev.*, 2021, **25**, 43–56.

277 R. Röllig, C. E. Paul, M. Claeys-Bruno, K. Duquesne, S. Kara and V. Alphand, *Org. Biomol. Chem.*, 2021, **19**, 3441–3450.

278 E. Erdem, L. Malihan-Yap, L. Assil-Companioni, H. Grimm, G. D. Barone, C. Serveau-Avesque, A. Amouric, K. Duquesne, V. de Berardinis, Y. Allahverdiyeva, V. Alphand and R. Kourist, *ACS Catal.*, 2022, **12**, 66–72.

279 J. Solé, J. Brummund, G. Caminal, G. Álvaro, M. Schürmann and M. Guillén, *Org. Process Res. Dev.*, 2019, **23**, 2336–2344.

280 P. B. Brondani, G. de Gonzalo, M. W. Fraaije and L. H. Andrade, *Adv. Synth. Catal.*, 2011, **353**, 2169–2173.

281 P. B. Brondani, H. Dudek, J. S. Reis, M. W. Fraaije and L. H. Andrade, *Tetrahedron Asymmetry*, 2012, **23**, 703–708.

282 S. Bordewick, A. Beier, K. Balke and U. T. Bornscheuer, *Enzyme Microb. Technol.*, 2018, **109**, 31–42.

283 B. P. Branchaud and C. T. Walsh, *J. Am. Chem. Soc.*, 1985, **107**, 2153–2161.

284 C. T. Walsh and Y. C. J. Chen, *Angew. Chem., Int. Ed.*, 1988, **27**, 333–343.

285 B. J. Ring, S. A. Wrighton, S. L. K. Aldridge, K. Hansen, B. Haehner and L. A. Shipley, *Drug Metab. Dispos.*, 1999, **27**, 1099–1103.

286 T. Taniguchi-Takizawa, M. Shimizu, T. Kume and H. Yamazaki, *Drug Metab. Pharmacokinet.*, 2015, **30**, 64–69.

287 N. Lončar, F. Fiorentini, G. Bailleul, S. Savino, E. Romero, A. Mattevi and M. W. Fraaije, *Appl. Microbiol. Biotechnol.*, 2019, **103**, 1755–1764.

288 S. P. Hanlon, A. Camattari, S. Abad, A. Glieder, M. Kittelmann, S. Lütz and M. Winkler, *Chem. Comm.*, 2012, **48**, 6001–6003.

289 Y. C. Chen, E. C. Holmes, J. Rajniak, J. G. Kim, S. Tang, C. R. Fischer, M. B. Mudgett and E. S. Sattely, *Proc. Natl. Acad. Sci. U. S. A.*, 2018, **115**, E4920–E4929.

290 G. Ottolina, S. Bianchi, B. Belloni, G. Carrea and B. Danieli, *Tetrahedron Lett.*, 1999, **40**, 8483–8486.

291 S. Colonna, V. Pironti, P. Pasta and F. Zambianchi, *Tetrahedron Lett.*, 2003, **44**, 869–871.

292 G. Catucci, I. Zgrablic, F. Lanciani, F. Valetti, D. Minerdi, D. P. Ballou, G. Gilardi and S. J. Sadeghi, *Biochim. Biophys. Acta, Proteins Proteomics*, 2016, **1864**, 1177–1187.

293 D. E. Torres Pazmiño, R. Snajdrova, D. v. Rial, M. D. Mihovilovic and M. W. Fraaije, *Adv. Synth. Catal.*, 2007, **349**, 1361–1368.

294 H. S. Choi, J. K. Kim, E. H. Cho, Y. C. Kim, J. il Kim and S. W. Kim, *Biochem. Biophys. Res. Commun.*, 2003, **306**, 930–936.

295 S. M. Ren, F. Liu, Y. Q. Wu, Q. Chen, Z. jun Zhang, H. L. Yu and J. H. Xu, *Biotechnol. Bioeng.*, 2021, **118**, 737–744.

296 C. Tolmie, R. do Aido-Machado, F. M. Ferroni, M. S. Smit and D. J. Opperman, *Catalysts*, 2020, **10**, 339–351.

297 Y. J. Li, Y. C. Zheng, Q. Geng, F. Liu, Z. J. Zhang, J. H. Xu and H. L. Yu, *Bioresour. Bioprocess.*, 2021, **8**, 1–10.

298 X. Xu, Y. Zhang, S. Wang, L. Xu, B. Su, L. Wang and J. Lin, *Bioorg. Chem.*, 2022, **125**, 105867.

299 W. R. F. Goundry, B. Adams, H. Benson, J. Demeritt, S. McKown, K. Mulholland, A. Robertson, P. Siedlecki, P. Tomlin and K. Vare, *Org. Process Res. Dev.*, 2017, **21**, 107–113.

300 N. Xu, J. Zhu, Y. Q. Wu, Y. Zhang, J. Y. Xia, Q. Zhao, G. Q. Lin, H. L. Yu and J. H. Xu, *Org Process Res Dev*, 2020, **24**, 1124–1130.

301 G. de Gonzalo, N. Loncar and M. Fraaije, *Biocatal. Biotransform.*, 2022, 1–7.

302 A. Riebel, G. de Gonzalo and M. W. Fraaije, *J. Mol. Catal. B: Enzym.*, 2013, **88**, 20–25.

303 F. Liu, C. Shou, Q. Geng, C. Zhao, J. Xu and H. Yu, *Appl. Microbiol. Biotechnol.*, 2021, **105**, 3169–3180.

304 Y. Zhang, Y. Q. Wu, N. Xu, Q. Zhao, H. L. Yu and J. H. Xu, *ACS Sustain Chem Eng*, 2019, **7**, 7218–7226.

305 G. de Gonzalo and A. Franconetti, *Enzyme Microb. Technol.*, 2018, **113**, 24–28.

306 T. Gul, M. Krzek, H. P. Permentier, M. W. Fraaije and R. Bischoff, *Drug Metab. Dispos.*, 2016, **44**, 1270–1276.

307 A. Rioz-Martínez, G. de Gonzalo, D. E. T. Pazmiño, M. W. Fraaije and V. Gotor, *Eur. J. Org. Chem.*, 2010, 6409–6416.

308 T. Heine, A. Scholtissek, S. Hofmann, R. Koch and D. Tischler, *ChemCatChem*, 2020, **12**, 199–209.

309 C. Holec, K. Neufeld and J. Pietruszka, *Adv. Synth. Catal.*, 2016, **358**, 1810–1819.

310 S. G. Allenmark and A. C. Andersson, *Tetrahedron Asymmetry*, 1993, **4**, 2371–2376.

311 A. N. Serreqi and R. J. Kazlauskas, *Can. J. Chem.*, 1995, **73**, 1357–1367.

312 P. Kiełbasiński, B. Zwanenburg, T. J. G. Damen, M. Wieczorek, W. R. Majzner and G. D. Bujacz, *Eur. J. Org. Chem.*, 1999, **10**, 2573–2578.

313 P. Kiełbasiński, M. Mikołajczyk, B. Zwanenburg and R. C. de Laet, *Phosphorus Sulfur Silicon Relat Elem*, 2009, **95**, 495–496.

314 M. Kwiatkowska, I. Janicki and P. Kiełbasiński, *J. Mol. Catal. B: Enzym.*, 2015, **118**, 23–28.

315 V. Guerrero De La Rosa, M. Ordóñez and J. M. Llera, *Tetrahedron Asymmetry*, 2000, **11**, 2991–3001.

316 Q. Chen, K. Wang and C. Yuan, *New J. Chem.*, 2008, **33**, 972–975.

317 J. H. Weiner, R. A. Rothery, D. Sambasivarao and C. A. Trieber, *Bioenergetics*, 1992, **1102**, 1–18.

318 M. Abo, M. Tachibana, A. Okubo and S. Yamazaki, *Bioorg. Med. Chem.*, 1995, **3**, 109–112.

319 M. Abo, M. Dejima, F. Asano, A. Okubo and S. Yamazaki, *Tetrahedron Asymmetry*, 2000, **11**, 823–828.

320 S. P. Hanlon, D. L. Graham, P. J. Hogan, R. A. Holt, C. D. Reeve, A. L. Shaw and A. G. McEwan, *Microbiology (N Y)*, 1998, **144**, 2247–2253.

321 M. Abo, M. Tachibana, A. Okubo and S. Yamazaki, *Biosci. Biotechnol. Biochem.*, 1994, **58**, 596–597.

322 H. R. Luckarift, H. Dalton, N. D. Sharma, D. R. Boyd and R. A. Holt, *Appl. Microbiol. Biotechnol.*, 2004, **65**, 678–685.

323 S. Boschi-Muller, A. Olry, M. Antoine and G. Branlant, *Biochim. Biophys. Acta, Proteins Proteomics*, 2005, **1703**, 231–238.

324 B. Jiang and J. Moskovitz, *Antioxidants* , 2018, **7**, 122–130.

325 S. L. dos Santos, I. Petropoulos and B. Friguet, *Antioxidants*, 2018, **7**, 191–212.

326 D. B. Oien and J. Moskovitz, *Biochim. Biophys. Acta, Mol. Basis Dis.*, 2019, **1865**, 1756–1762.

327 J. Moskovitz and A. Smith, *Amino Acids*, 2021, **53**, 1011–1020.

328 H. Y. Kim and V. N. Gladyshev, *Biochem. Biophys. Res. Commun.*, 2004, **320**, 1277–1283.

329 M. Reiterer, R. Schmidt-Kastner and S. L. Milton, *Free Radical Res.*, 2019, **53**, 1144–1154.

330 C. Achilli, A. Ciana and G. Minetti, *BioFactors*, 2015, **41**, 135–152.

331 L. Tarrago, A. Kaya, E. Weerapana, S. M. Marino and V. N. Gladyshev, *J. Biol. Chem.*, 2012, **287**, 24448–24459.

332 D. T. Le, B. C. Lee, S. M. Marino, Y. Zhang, D. E. Fomenko, A. Kaya, E. Hacioglu, G. H. Kwak, A. Koc, H. Y. Kim and V. N. Gladyshev, *J. Biol. Chem.*, 2009, **284**, 4354–4364.

333 F. M. Ranaivoson, M. Antoine, B. Kauffmann, S. Boschi-Muller, A. Aubry, G. Branlant and F. Favier, *J. Mol. Biol.*, 2008, **377**, 268–280.

334 N. Coudevylle, M. Antoine, S. Bouguet-Bonnet, P. Mutzenhardt, S. Boschi-Muller, G. Branlant and M. T. Cung, *J. Mol. Biol.*, 2007, **366**, 193–206.

335 X. X. Ma, P. C. Guo, W. W. Shi, M. Luo, X. F. Tan, Y. Chen and C. Z. Zhou, *J. Biol. Chem.*, 2011, **286**, 13430–13437.

336 A. Kriznik, S. Boschi-Muller and G. Branlant, *Arch. Biochem. Biophys.*, 2014, **548**, 54–59.

337 J. C. Lim, Z. You, G. Kim and R. L. Levine, *Proc. Natl. Acad. Sci. U. S. A.*, 2011, **108**, 10472–10477.

338 F. Misiti, M. E. Clementi and B. Giardina, *Neurochem. Int.*, 2010, **56**, 597–602.

339 J. Moskovitz, P. Maiti, D. H. J. Lopes, D. B. Oien, A. Attar, T. Liu, S. Mittal, J. Hayes and G. Bitan, *Biochemistry*, 2011, **50**, 10687–10697.

340 A. Kanayama, J. I. Inoue, Y. Sugita-Konishi, M. Shimizu and Y. Miyamoto, *J. Biol. Chem.*, 2002, **277**, 24049–24056.

341 J. A. Miernyk, M. L. Johnston, S. C. Huber, A. Tovar-Méndez, E. Hoyos and D. D. Randall, *Proteomics Insights*, 2009, **2**, 15–22.

342 D. B. Oien, G. A. Carrasco and J. Moskovitz, *J. Amino Acids*, 2011, **2011**, 1–6.

343 J. R. Erickson, M. ling A. Joiner, X. Guan, W. Kutschke, J. Yang, C. v. Oddis, R. K. Bartlett, J. S. Lowe, S. E. O'Donnell, N. Aykin-Burns, M. C. Zimmerman, K. Zimmerman, A. J. L. Ham, R. M. Weiss, D. R. Spitz, M. A. Shea, R. J. Colbran, P. J. Mohler and M. E. Anderson, *Cell*, 2008, **133**, 462–474.

344 D. B. Oien and J. Moskovitz, *Curr. Top. Dev. Biol.*, 2007, **80**, 93–133.

345 M. A. Bennett, *Sulfur Metabolism*, 1939, **3**, 1794–1797.

346 M. A. Rahman, H. Nelson, H. Weissbach and N. Brot, *J. Biol. Chem.*, 1992, **267**, 15549–15551.

347 J. Moskovitz, H. Weissbach and N. Brot, *Proc. Natl. Acad. Sci. U. S. A.*, 1996, **93**, 2095–2099.

348 Y. Chen, J. Zhuo, D. Zheng, S. Tian and Z. Li, *J. Mol. Catal. B: Enzym.*, 2014, **106**, 100–104.

349 J. Yang, Z. Yuan, Y. Zhou, J. Zhao, M. Yang, X. Cheng, G. Ou and Y. Chen, *J. Mol. Catal. B: Enzym.*, 2017, **133**, S588–S592.

350 C. Achilli, A. Ciana and G. Minetti, *Tetrahedron Lett.*, 2017, **58**, 4781–4782.

351 L. Peng, Y. Wen, Y. Chen, Z. Yuan, Y. Zhou, X. Cheng, Y. Chen and J. Yang, *ChemCatChem*, 2018, **10**, 3284–3290.

352 J. Yang, Y. Wen, L. Peng, Y. Chan, X. Cheng and Y. Chen, *Org Biomol Chem*, 2019, **17**, 3381–3388.

353 L. Tarrago and V. N. Gladyshev, *Biochemistry (Moscow)*, 2012.

354 Y. Wen, L. Peng, Y. Zhou, T. Peng, Y. Chen, X. Cheng, Y. Chen and J. Yang, *Catal. Commun.*, 2020, **136**, 105908.

355 V. Nosek and J. Míšek, *Angew. Chem.*, 2018, **130**, 9849–9852.

356 S. Bierbaumer, L. Schmermund, A. List, C. K. Winkler, S. M. Glueck and W. Kroutil, *Angew. Chem., Int. Ed.*, 2022, **61**, e2021171.

357 T. Peng, J. Tian, Y. Zhao, X. Jiang, X. Cheng, G. Deng, Q. Zhang, Z. Wang, J. Yang and Y. Chen, *Angew. Chem., Int. Ed.*, 2022, **61**, e202209272.

358 S. Boschi-Muller, S. Azza and G. Branlant, *Protein Sci.*, 2001, **10**, 2272–2279.

359 A. B. Taylor, D. M. Benglis, S. Dhandayuthapani and P. J. Hart, *J. Bacteriol.*, 2003, **185**, 4119–4126.

360 M. Antoine, S. Boschi-Muller and G. Branlant, *J. Biol. Chem.*, 2003, **278**, 45352–45357.

361 M. Quinternet, P. Tsan, F. Neiers, C. Beaufils, S. Boschi-Muller, M. C. Averlant-Petit, G. Branlant and M. T. Cung, *Biochemistry*, 2008, **47**, 8577–8589.

362 A. Gand, M. Antoine, S. Boschi-Muller and G. Branlant, *J. Biol. Chem.*, 2007, **282**, 20484–20491.

363 H. Weissbach, F. Etienne, T. Hoshi, S. H. Heinemann, W. T. Lowther, B. Matthews, G. st. John, C. Nathan and N. Brot, *Arch. Biochem. Biophys.*, 2002, **397**, 172–178.

364 S. Boschi-Muller, A. Gand and G. Branlant, *Arch Biochem Biophys*, 2008, **474**, 266–273.

365 S. Boschi-Muller and G. Branlant, *Bioorg. Chem.*, 2014, **57**, 222–230.

366 X. Robert and P. Gouet, *Nucleic Acids Res.*, 2014, **42**, W320–W324.

367 B. Ohtani, Y. Ogawa and S. Nishimoto, *J. Phys. Chem.*, 1997, **101**, 3746–3752.

368 H. Gnaser, M. R. Savina, W. F. Calaway, C. E. Tripa, I. v. Veryovkin and M. J. Pellin, *Int. J. Mass Spectrom.*, 2005, **245**, 61–67.

369 H. Wang, J. Niu, X. Long and Y. He, *Ultrason. Sonochem.*, 2008, **15**, 386–392.

370 R. Rahal, T. Pigot, D. Foix and S. Lacombe, *Appl. Catal., B*, 2011, **104**, 361–372.

371 X. Lang, J. Zhao and X. Chen, *Angew. Chem., Int. Ed.*, 2016, **55**, 4697–4700.

372 H. Hao, J. L. Shi, H. Xu, X. Li and X. Lang, *Appl. Catal., B*, 2019, **246**, 149–155.

373 J. Zhu, W. C. Yang, X. D. Wang and L. Wu, *Adv. Synth. Catal.*, 2018, **360**, 386–400.

374 X. Gu, X. Li, Y. Chai, Q. Yang, P. Li and Y. Yao, *Green Chem.*, 2013, **15**, 357–361.

375 H. Cui, W. Wei, D. Yang, Y. Zhang, H. Zhao, L. Wang and H. Wang, *Green Chemistry*, 2017, **19**, 3520–3524.

376 S. Sharma and A. Sharma, *Org. Biomol. Chem.*, 2019, **17**, 4384–4405.

377 T. Keshari, V. K. Yadav, V. P. Srivastava and L. D. S. Yadav, *Green Chem.*, 2014, **16**, 3986–3992.

378 S. S. Zalesskiy, N. S. Shlapakov and V. P. Ananikov, *Chem. Sci.*, 2016, **7**, 6740–6745.

379 J. Dad'ová, E. Svobodová, M. Sikorski, B. König and R. Cibulka, *ChemCatChem*, 2012, **4**, 620–623.

380 T. Neveselý, E. Svobodová, J. Chudoba, M. Sikorski and R. Cibulka, *Adv. Synth. Catal.*, 2016, **358**, 1654–1663.

381 L. A. Averianova, L. A. Balabanova, O. M. Son, A. B. Podvolotskaya and L. A. Tekutyeva, *Front. Bioeng. Biotechnol.*, 2020, 8, 1–23.

382 M. A. Santos, J. J. Garcia-Ramirez and J. L. Revuelta, *J. Biol. Chem.*, 1995, **270**, 437–444.

383 B. Mühldorf and R. Wolf, *Chem. Commun.*, 2015, **51**, 8425–8428.

384 E. Skolia, P. L. Gkizis, N. F. Nikitas and C. G. Kokotos, *Green Chem.*, 2022, **24**, 4108–4118.

385 P. R. Blakemore and M. S. Burge, *J. Am. Chem. Soc.*, 2007, **129**, 3068–3069.

386 N. Sakai, H. Maeda and Y. Ogiwara, *Synthesis (Stuttg)*, 2019, **51**, 2323–2330.

387 R. Isshiki, M. B. Kurosawa, K. Muto and J. Yamaguchi, *J. Am. Chem. Soc.*, 2021, **143**, 10333–10340.

388 M. M. Coulter, K. G. M. Kou, B. Galligan and V. M. Dong, *J. Am. Chem. Soc.*, 2010, **132**, 16330–16333.

389 C. R. Emerson, L. N. Zakharov and P. R. Blakemore, *Chem. Eur. J.*, 2013, **19**, 16342–16356.

390 M. S. Holzwarth, W. Frey and B. Plietker, *Chem. Commun.*, 2011, **47**, 11113–11115.

391 K. Lauder, S. Anselmi, J. D. Finnigan, Y. Qi, S. J. Charnock and D. Castagnolo, *Chem. Eur. J.*, 2020, **26**, 10422–10426.

392 K. Lauder, A. Toscani, Y. Qi, J. Lim, S. J. Charnock, K. Korah and D. Castagnolo, *Angew. Chem., Int. Ed.*, 2018, **57**, 5803–5807.

393 J. D. White and S. Shaw, *Chem. Sci.*, 2014, **5**, 2200–2204.

394 M. G. Civit, X. Sanz, C. M. Vogels, J. D. Webb, S. J. Geier, A. Decken, C. Bo, S. A. Westcott and E. Fernández, *J. Org. Chem.*, 2015, **80**, 2148–2154.

395 F. Zhao, K. Lauder, S. Liu, J. D. Finnigan, S. B. R. Charnock, S. J. Charnock and D. Castagnolo, *Angew. Chem., Int. Ed.*, 2022, **61**, e202202363.

396 J. Niu, H. Zhou, Z. Li, J. Xu and S. Hu, *J. Org. Chem.*, 2008, **73**, 7814–7817.

397 K. Trân, R. van den Hauwe, X. Sainsily, P. Couvineau, J. Côté, L. Simard, M. Echevarria, A. Murza, A. Serre, L. Théroux, S. Saibi, L. Haroune, J. M. Longpré, O. Lesur, M. Auger-Messier, C. Spino, M. Bouvier, P. Sarret, S. Ballet and É. Marsault, *J. Med. Chem.*, 2021, **64**, 5345–5364.

398 B. Hasdemir, H. Yaşa, T. Yıldız, H. B. Küçük and H. Ç. Onar, *ChemistrySelect*, 2020, **5**, 6035–6039.

399 N. Amri and T. Wirth, *J. Org. Chem.*, 2021, **86**, 15961–15972.

400 J. Yang, Y. Wen, L. Peng, Y. Chan, X. Cheng and Y. Chen, *Org. Biomol. Chem.*, 2019, **17**, 3381–3388.

401 S. Gan, J. Yin, Y. Yao, Y. Liu, D. Chang, D. Zhu and L. Shi, *Org. Biomol. Chem.*, 2017, **15**, 2647.

402 J. L. García Ruano, C. Alemparte, M. Teresa Aranda and M. M. Zarzuelo, *J. Chem. Soc., Perkin Trans. 1*, 1996, **3**, 173.

403 P. R. Blakemore, M. S. Burge and M. A. Sephton, *Tetrahedron Lett.*, 2007, **48**, 3999–4002.

404 M. Yadav, A. Bhunia, S. K. Jana and P. W. Roesky, *Inorg. Chem.*, 2016, **55**, 28.

405 R. C. Gadwood, I. M. Mallick and A. J. DeWinter, *J. Chem. Soc., Chem. Commun*, 1987, **52**, 4937.

406 S. Ruppenthal and R. Brückner, *J. Org. Chem.*, 2015, **80**, 897–910.

407 K. Motoshima, A. Sato, H. Yorimitsu and K. Oshima, *Bull. Chem. Soc. Jpn.*, 2007, **80**, 2229–2231.

408 S. Anselmi, S. Liu, S.-H. Kim, S. M. Barry, T. S. Moody and D. Castagnolo, *Org. Biomol. Chem.*, 2021, **19**, 156–161.

409 S. C. Davidson, G. dos P. Gomes, L. R. Kuhn, I. v. Alabugin, A. R. Kennedy and N. C. O. Tomkinson, *Tetrahedron*, 2021, **78**, 1–10.

410 A. M. Kulkarni, U. v. Desai, K. S. Pandit, M. A. Kulkarni and P. P. Wadgaonkar, *RSC Adv.*, 2014, **4**, 36702–36707.

411 S. Liu, B. Chen, Y. Yang, Y. Yang, Q. Chen, X. Zeng and B. Xu, *Electrochem. Commun.*, 2019, **109**, 106583.

412 T. Satoh, T. Fujii and K. Yamakawa, *Chem. Soc. Jpn.*, 1990, **63**, 1266–1268.

413 D. Plaza-Lozano, A. Conde-Gallardo and J. Olguín, *Eur. J. Inorg. Chem.*, 2021, **2021**, 2846–2856.

414 S. Kotha, N. K. Gupta and S. Ansari, *RSC Adv.*, 2022, **12**, 25154–25162.

415 S. S. Kim, K. Nehru, S. S. Kim, D. W. Kim and H. C. Jung, *Synthesis (Stuttg)*, 2002, 2484–2486.

416 J. K. Park and S. Lee, *J. Org. Chem.*, 2021, **86**, 13790–13799.

417 S. Gahlot, A. Gradone, M. Roy, M. Giorgi, S. Conti, P. Ceroni, M. Villa and M. Gingras, *Chem. Eur. J.*, 2022, **28**, e202200797.

418 T. Nakajima, K. Takano, H. Maeda, Y. Ogiwara and N. Sakai, *Chem. Asian J.*, 2021, **16**, 4103–4107.

419 E. Cruickshank, G. J. Strachan, J. M. Storey and C. T. Imrie, *J. Mol. Liq.*, 2022, **346**, 117094.

420 T. Sato, K. Nogi and H. Yorimitsu, *ChemCatChem*, 2020, **12**, 3467–3471.

421 M. Petsi and A. L. Zografos, *ACS Catal.*, 2020, **10**, 7093–7099.

422 Q. Liu, L. Wang, H. Yue, J. S. Li, Z. Luo and W. Wei, *Green Chem.*, 2019, **21**, 1609–1613.

423 Y. J. Ma, A. Doni, M. O. Skjoedt, C. Honoré, M. Arendrup, A. Mantovani and P. Garred, *J. Biol. Chem.*, 2011, **286**, 3405–3417.

424 R. Y. R. Wang, Y. Song, B. A. Barad, Y. Cheng, J. S. Fraser and F. DiMaio, *Elife*, 2016, **5**, 1–22.

425 M. J. Abraham, T. Murtola, R. Schulz, S. Páll, J. C. Smith, B. Hess and E. Lindah, *SoftwareX*, 2015, **1–2**, 19–25.

426 C. S. Ashvar, F. J. Devlin, K. L. Bak, P. R. Taylor and P. J. Stephens, *J. Phys. Chem.*, 1996, **100**, 9262–9270.

427 J. Tomasi, B. Mennucci and R. Cammi, *Chem. Rev.*, 2005, **105**, 2999–3093.

428 G. M. Morris, D. S. Goodsell, R. S. Halliday, R. Huey, W. E. Hart, R. K. Belew and A. J. Olson, *J. Comput. Chem.*, 1998, **19**, 1639–1662.

429 V. Hornak, R. Abel, A. Okur, B. Strockbine, A. Roitberg and C. Simmerling, *Proteins: Struct., Funct., Bioinf.*, 2006, **65**, 712–725.

430 B. Hess, H. Bekker, H. J. C. Berendsen and J. G. E. M. Fraaije, *J. Comput. Chem.*, 1997, **18**, 14631472.

431 T. Darden, D. York and L. Pedersen, *J. Chem. Phys.*, 1998, **98**, 10089.

432 F. Delaglio, S. Grzesiek, G. W. Vuister, G. Zhu, J. Pfeifer and A. Bax, *J. Biomol. NMR*, 1995, **6**, 293.

433 B. A. Johnson, in *Protein NMR Techniques*, ed. K. A. Downing, Humana Press, Second edition., 2004, vol. 278, pp. 313–352.

434 P. Gogoi, T. Kotipalli, K. Indukuri, S. Bondalapati, P. Saha and A. K. Saikia, *Tetrahedron Lett.*, 2012, **53**, 2726–2729.

435 A. Jalba, N. Régnier and T. Ollevier, *Eur. J. Org. Chem.*, 2017, **2017**, 1628–1637.

436 J. Tang, F. Huang, Y. Wei, H. Bian, W. Zhang and H. Liang, *Dalton Trans.*, 2016, **45**, 8061–8072.

437 A. Rioz-Martínez, M. Kopacz, G. de Gonzalo, D. E. Torres Pazmiño, V. Gotor and M. W. Fraaije, *Org. Biomol. Chem.*, 2011, **9**, 1337–1341.

438 F. Gelat, J. Jayashankaran, J. F. Lohier, A. C. Gaumont and S. Perrio, *Org. Lett.*, 2011, **13**, 3170–3173.

439 H. Sakuraba and H. Maekawa, *J. Inclusion Phenom. Macrocyclic Chem.*, 2006, **54**, 41–45.

440 F. Gelat, A. C. Gaumont and S. Perrio, *J. Sulfur Chem.*, 2013, **34**, 596–605.

# Appendices

## Appendix I. Copies of NMR spectra

### Sulfides NMR spectra

*Ethyl(phenyl)sulfane* ***27c***

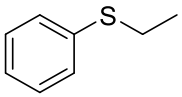


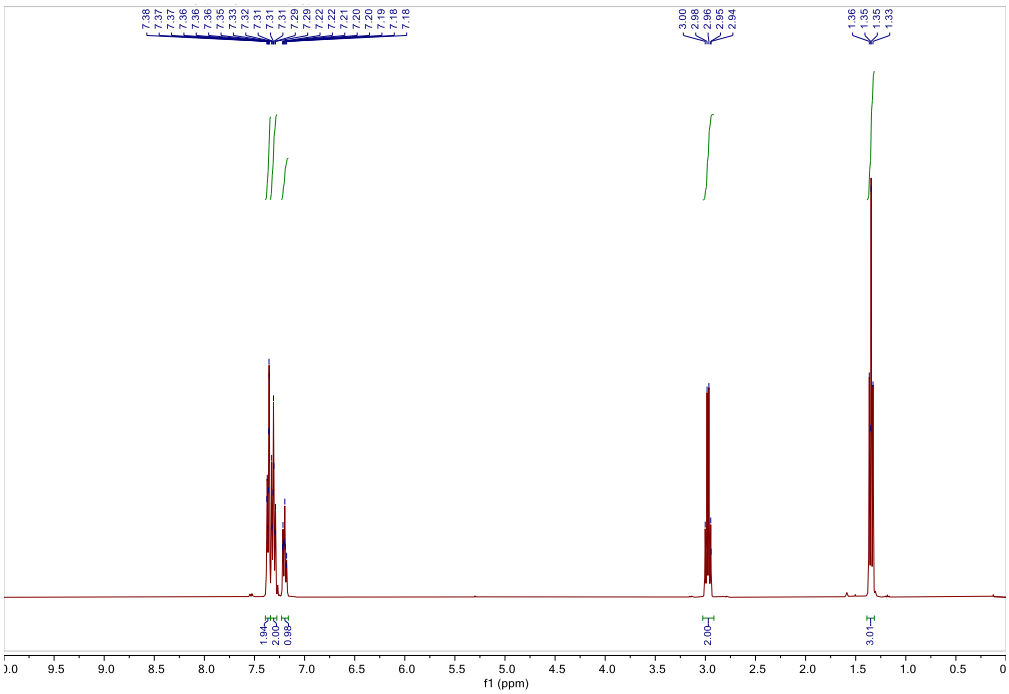


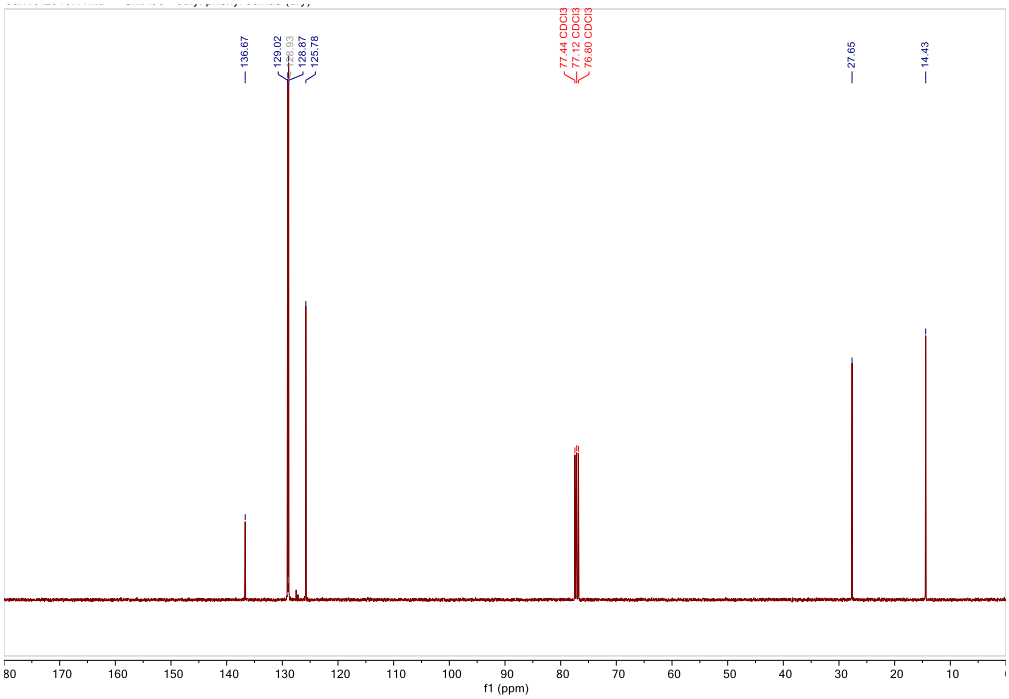

*Ethyl(p-tolyl)sulfane* ***27d***

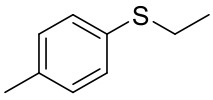


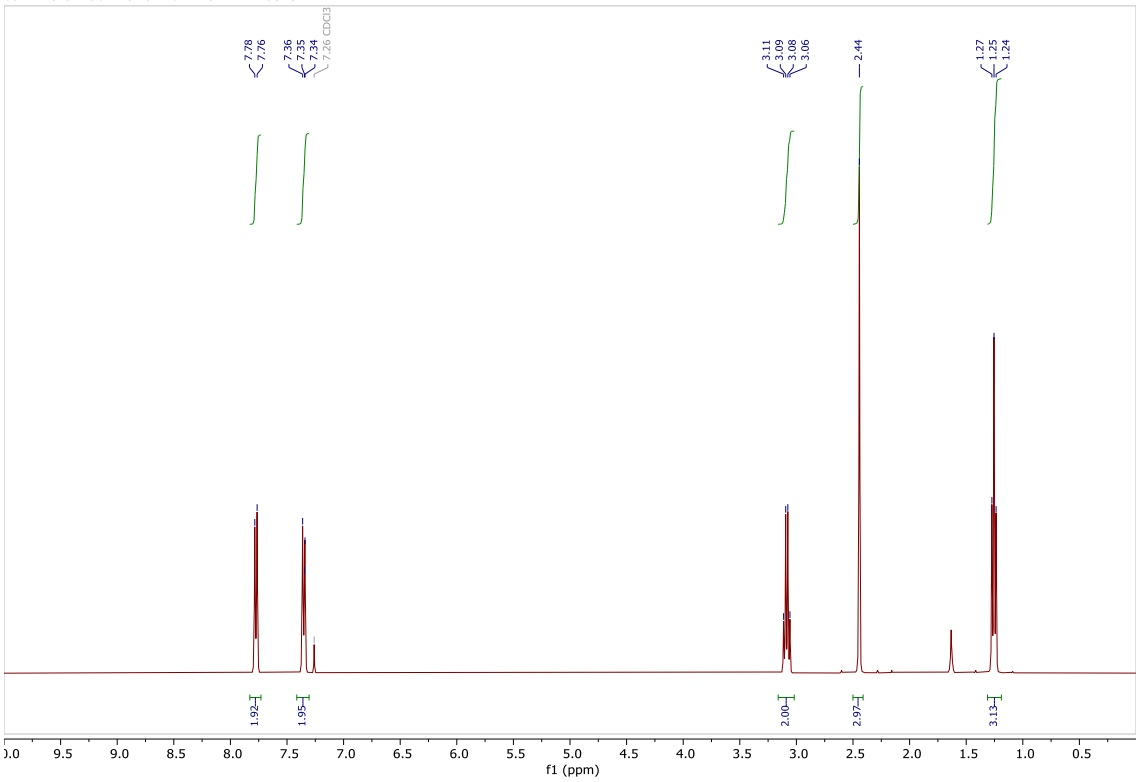


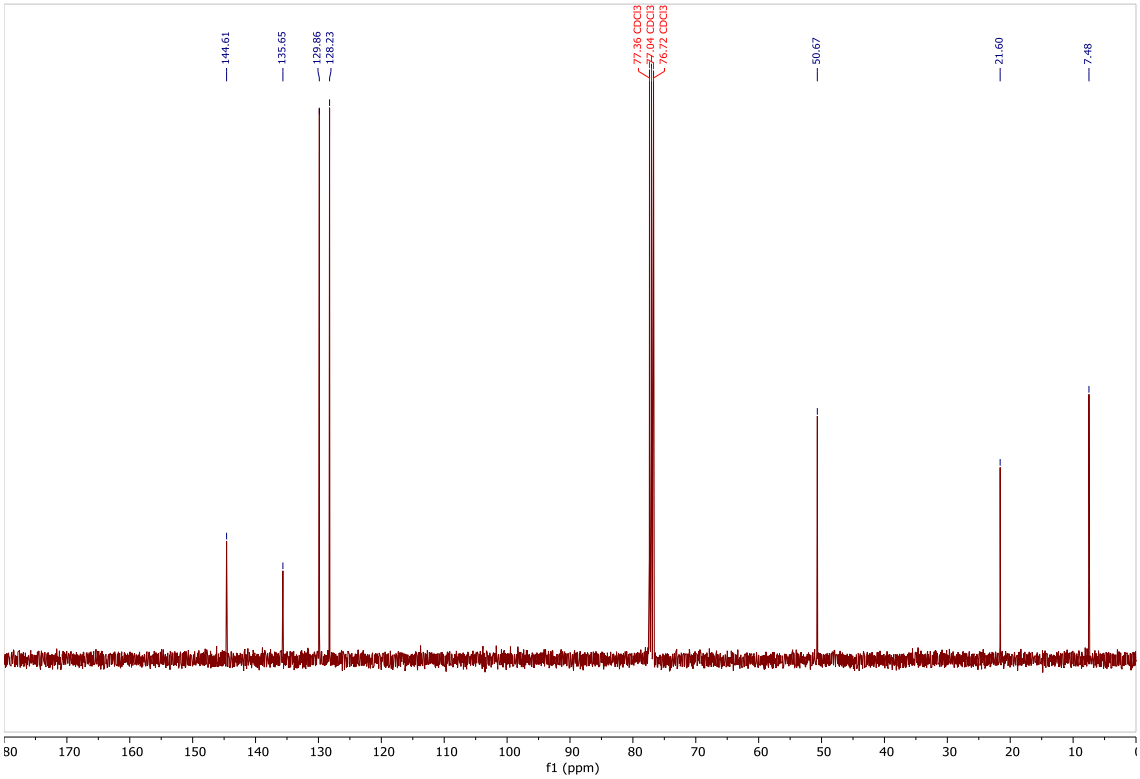

*Ethyl(4-methoxyphenyl)sulfane* ***27e***

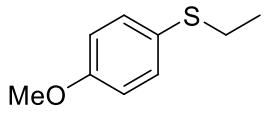


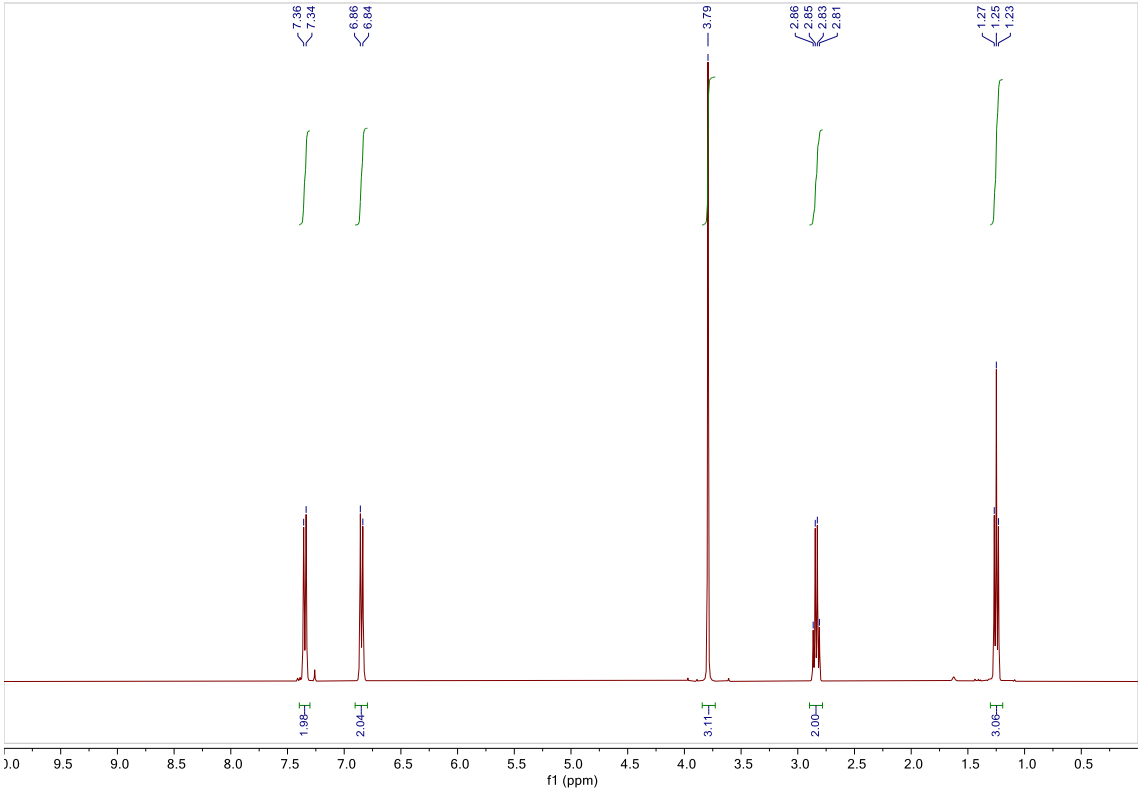


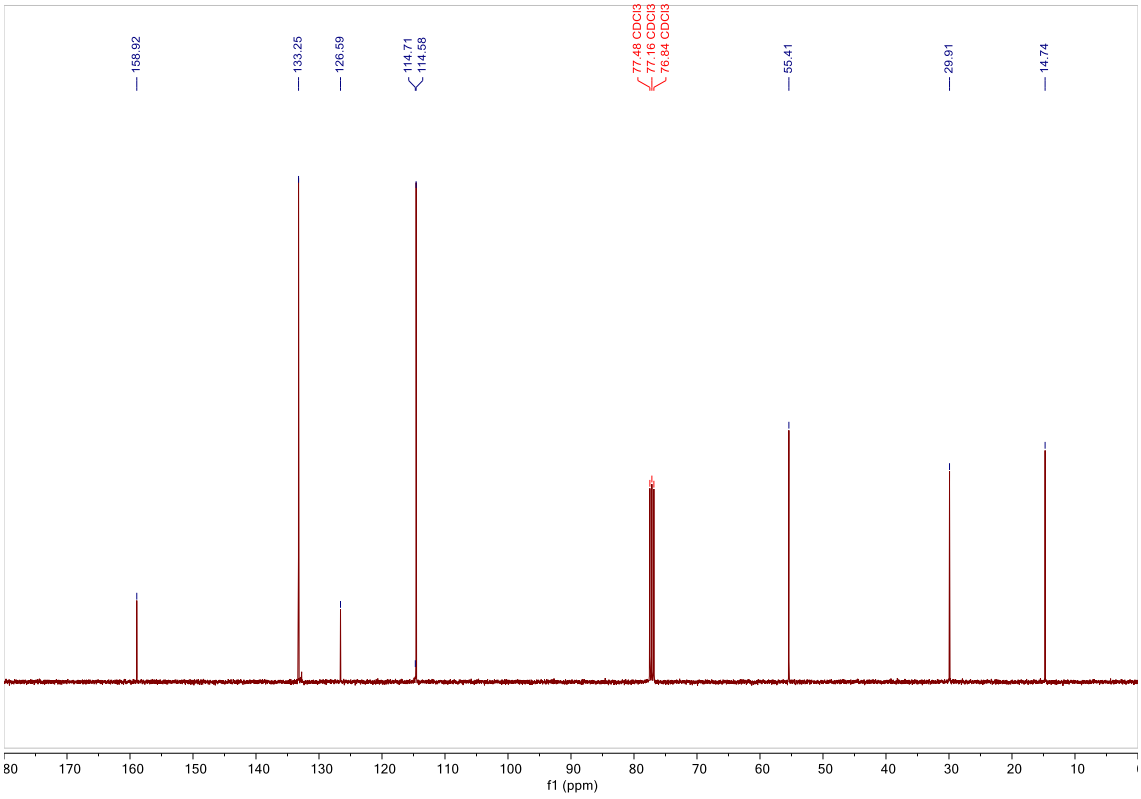

*(4-Chlorophenyl)(ethyl)sulfane* ***27f***

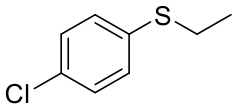


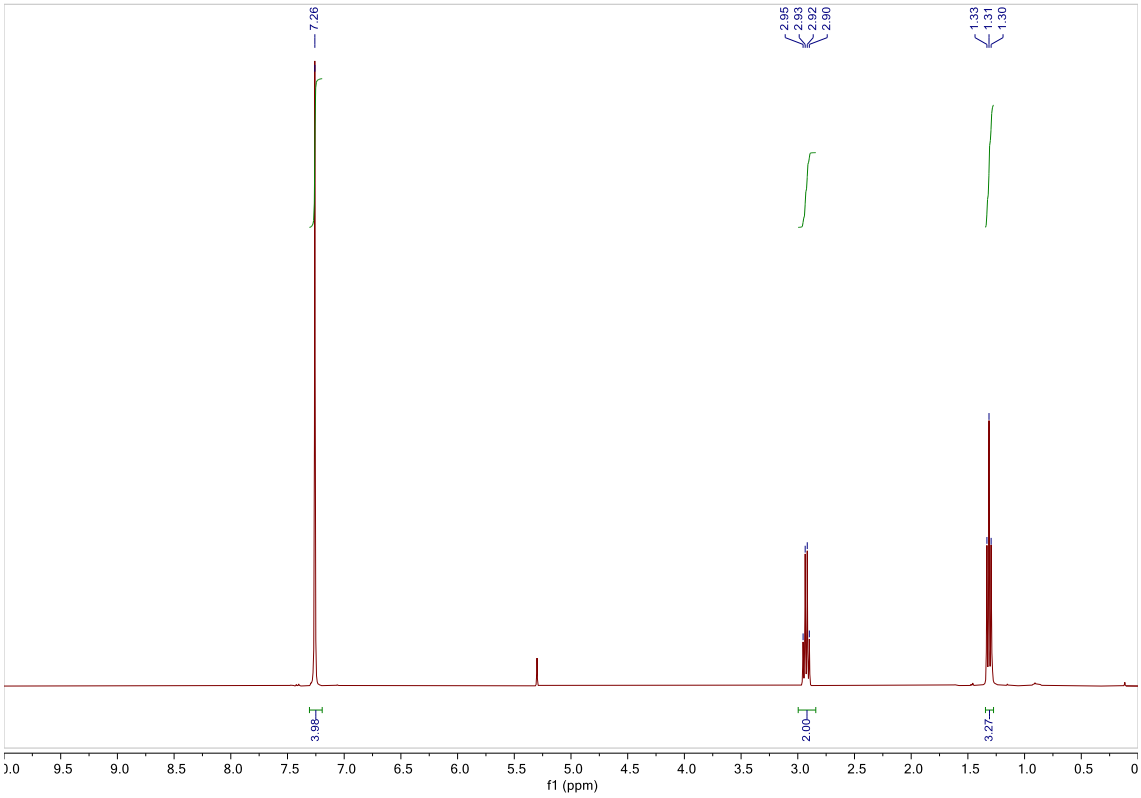


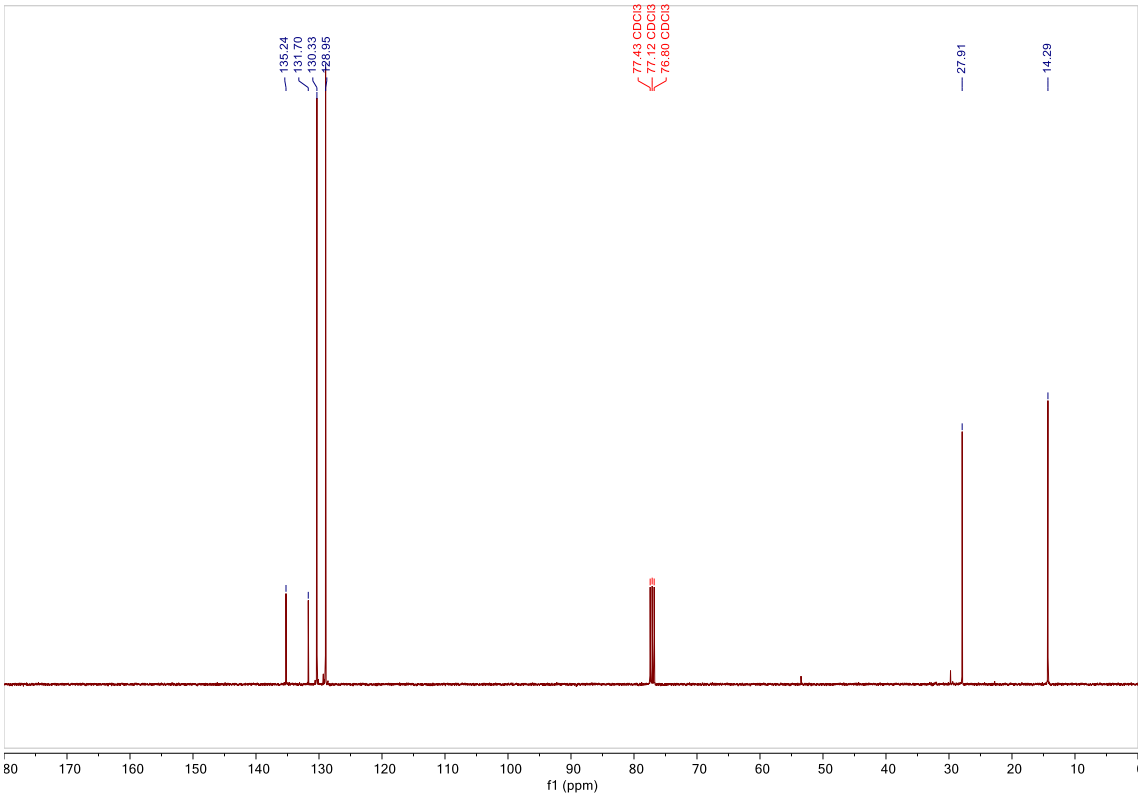

*(4-Bromophenyl)(ethyl)sulfane* ***27g***

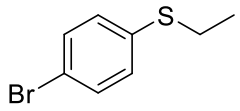


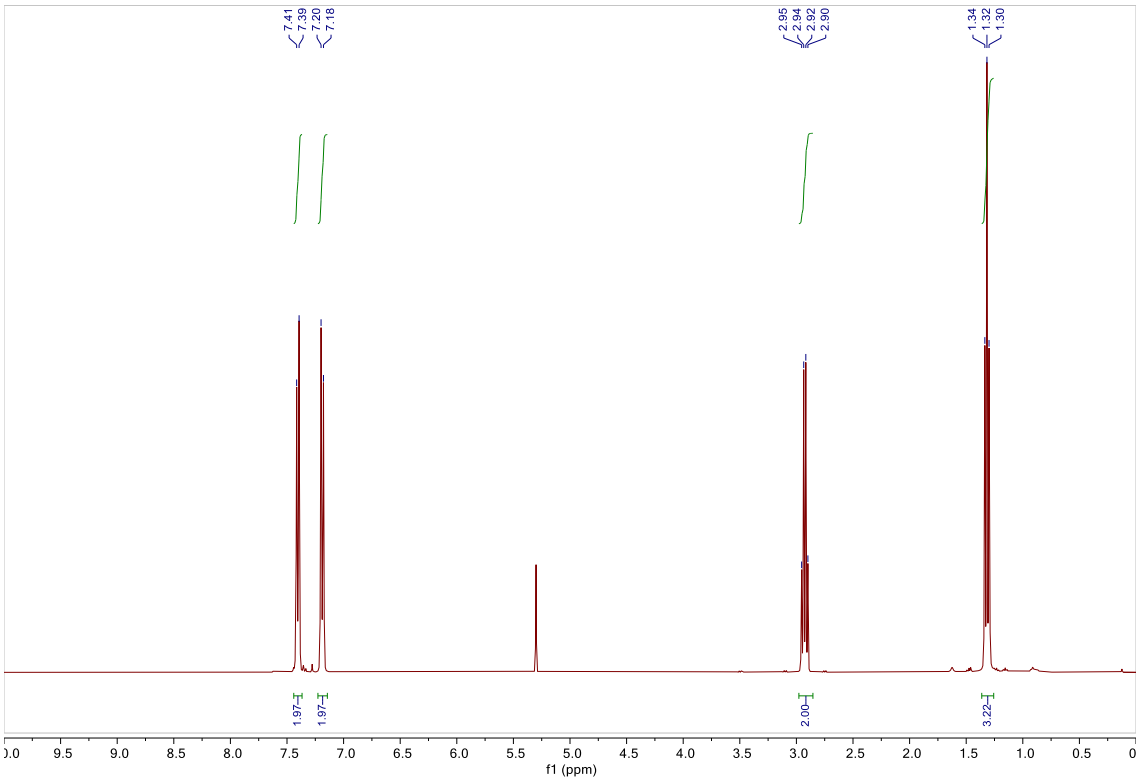


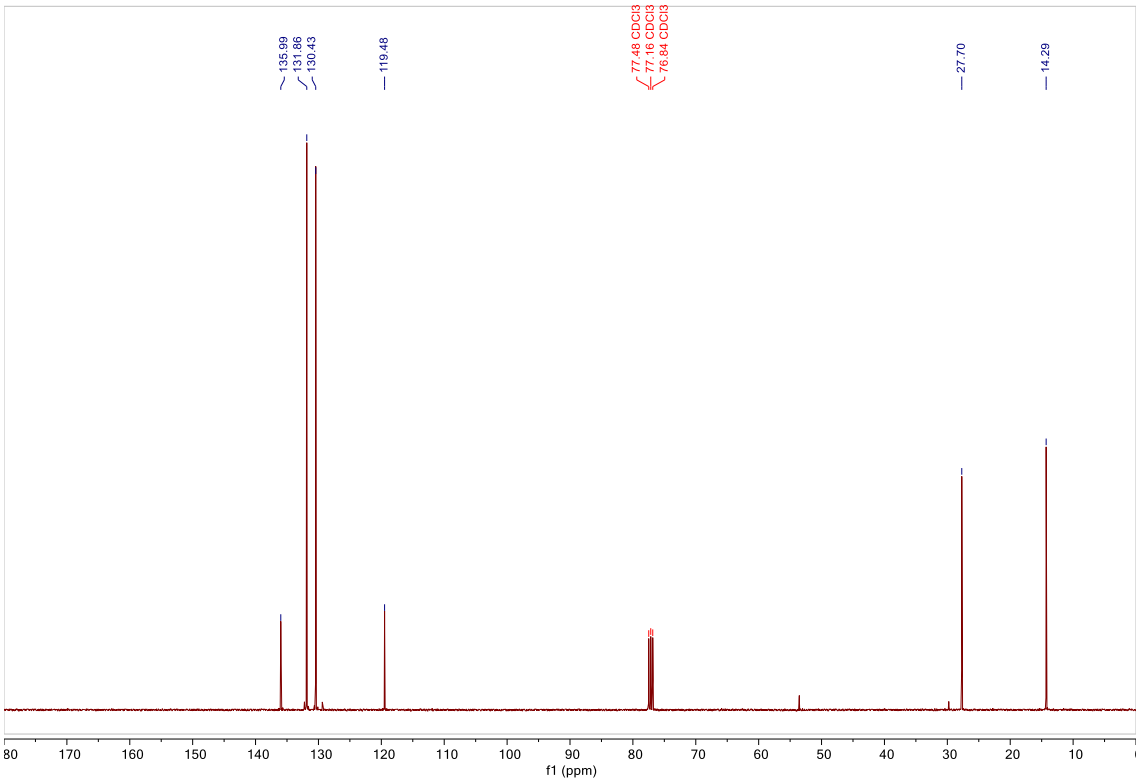

*(2-Chlorophenyl)(ethyl)sulfane* ***27h***

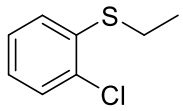


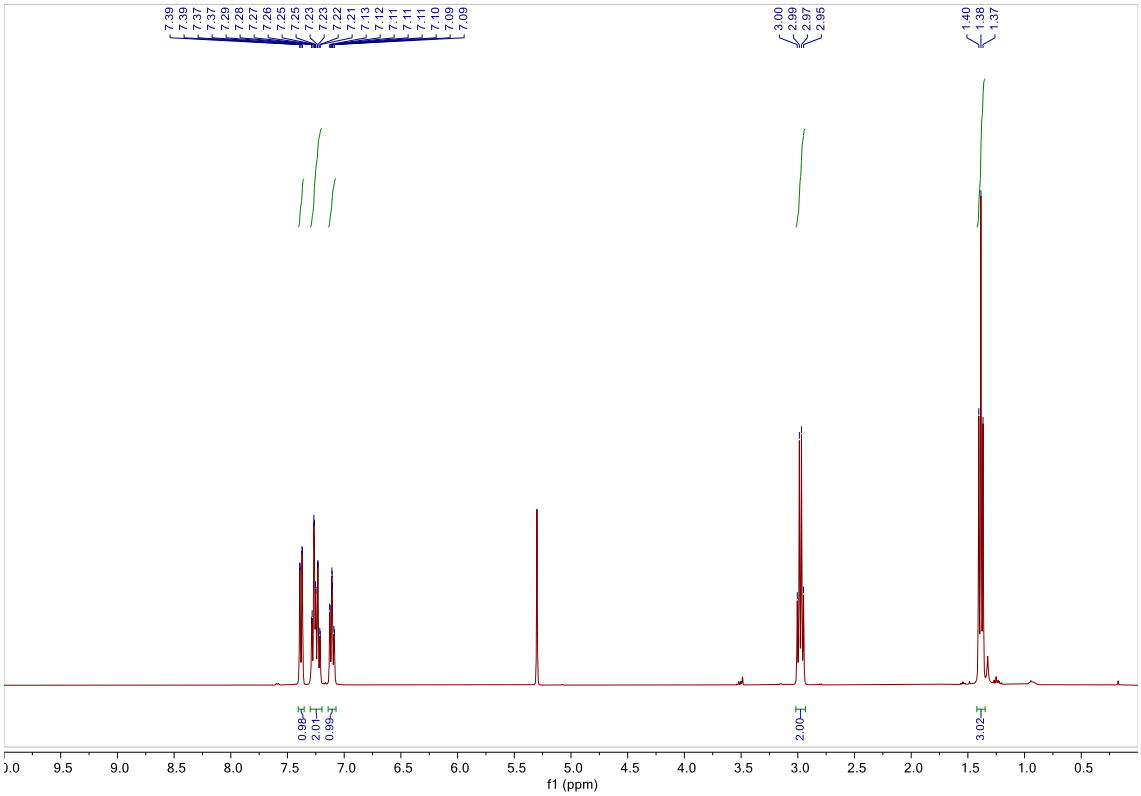


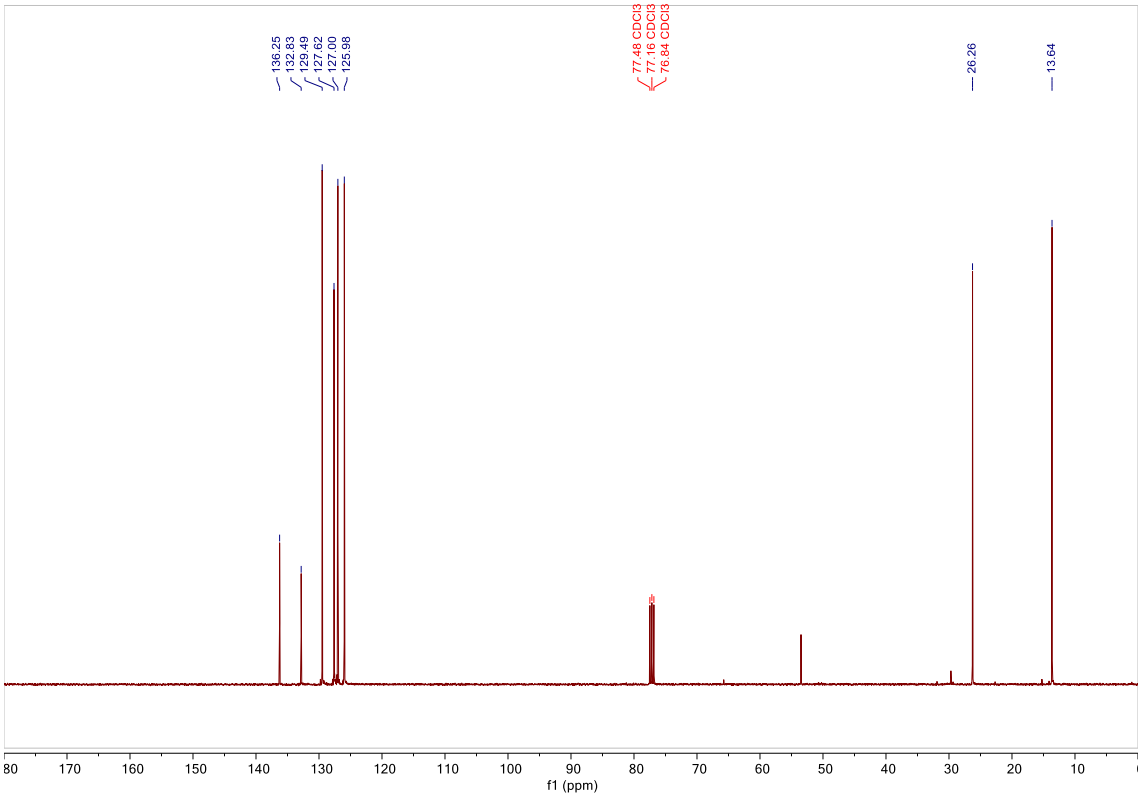

*(2-Bromophenyl)(ethyl)sulfane* ***27i***

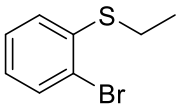


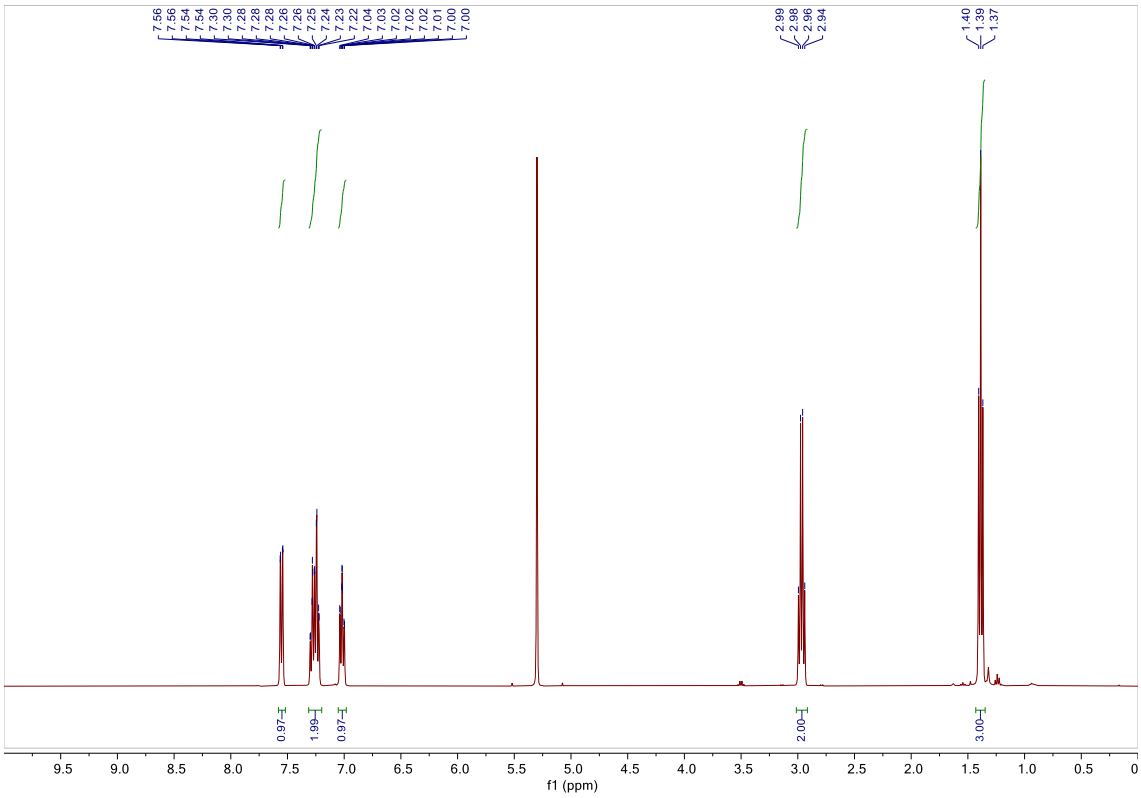


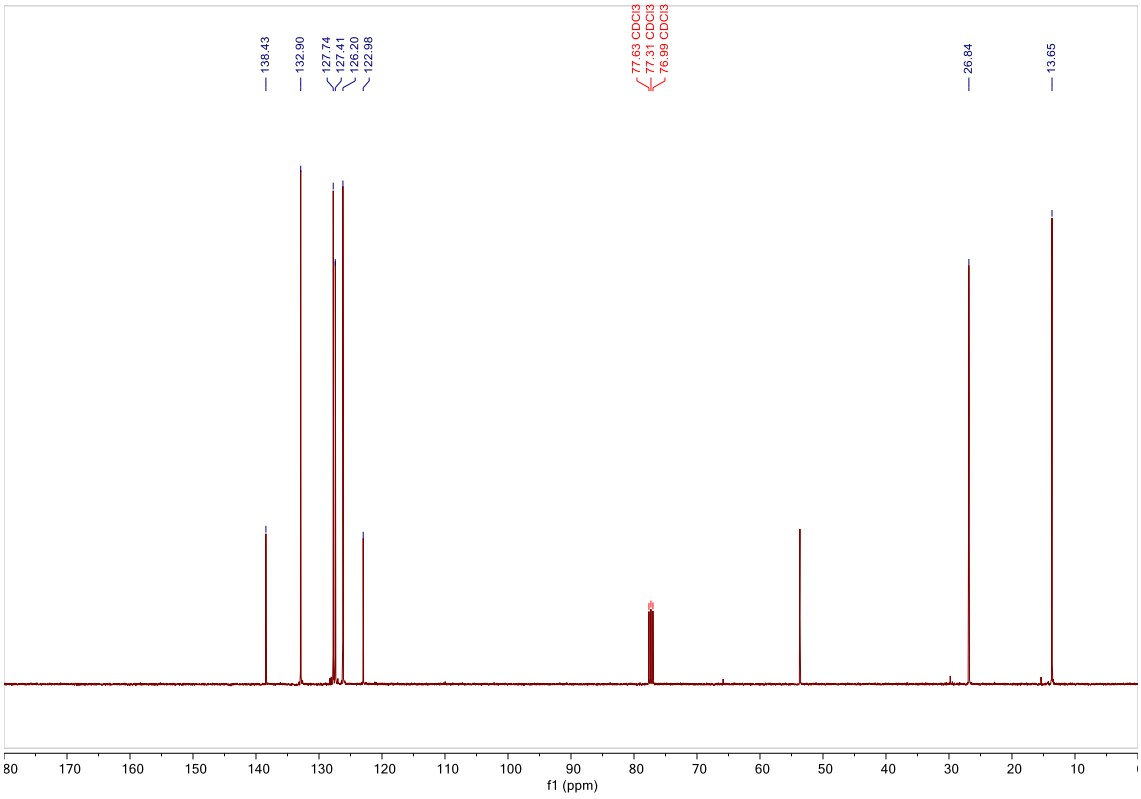

*(4-Methoxyphenyl)(propyl)sulfane* ***27j***

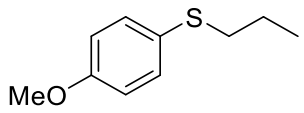


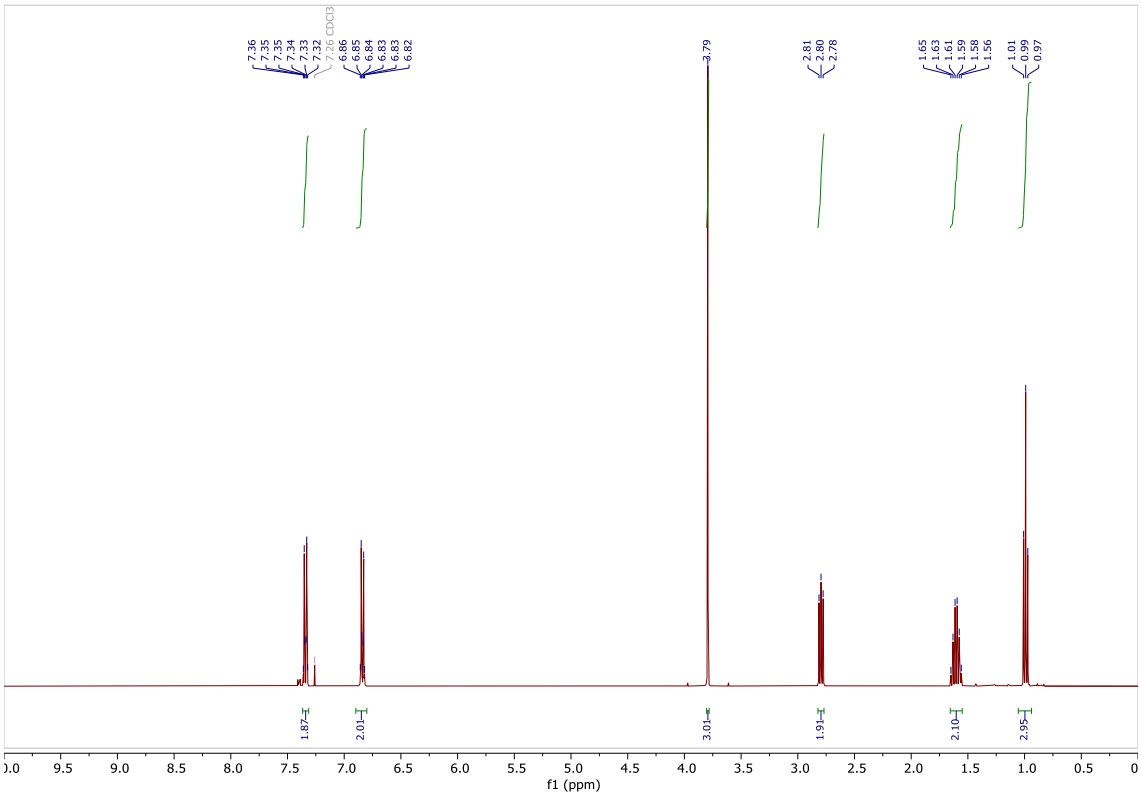


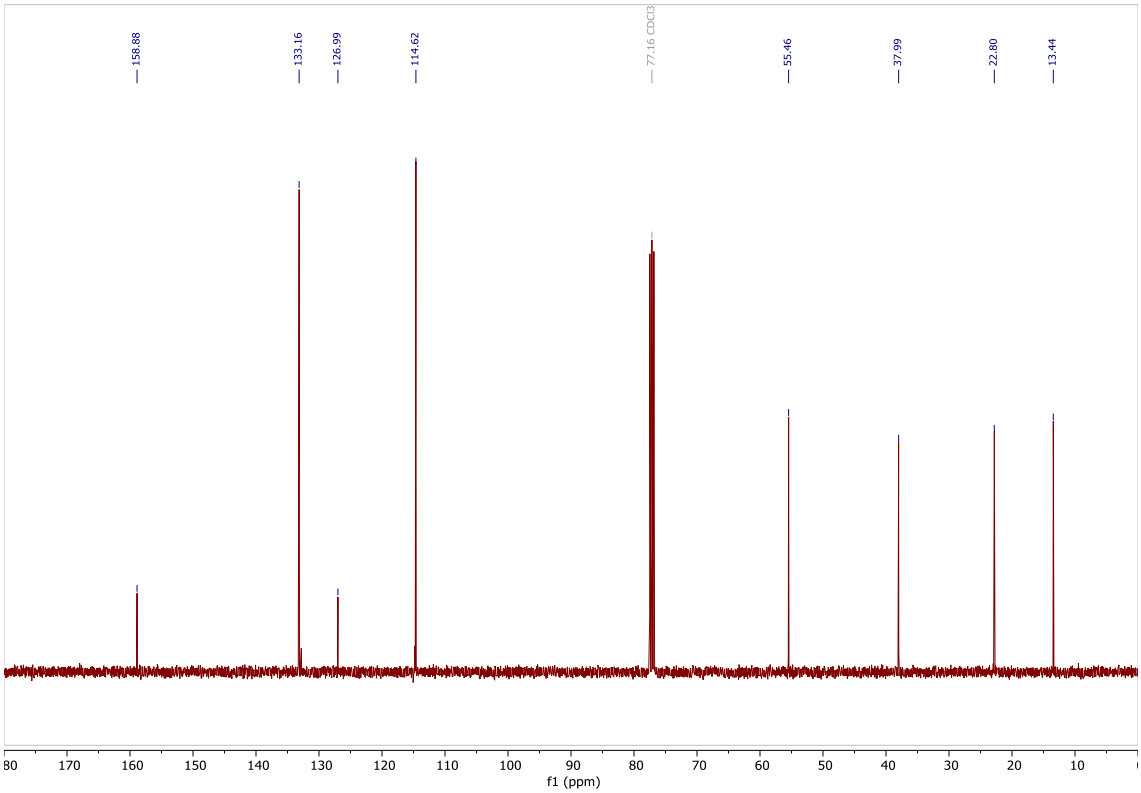

*Propyl(p-tolyl)sulfane* ***27k***

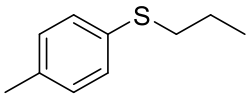


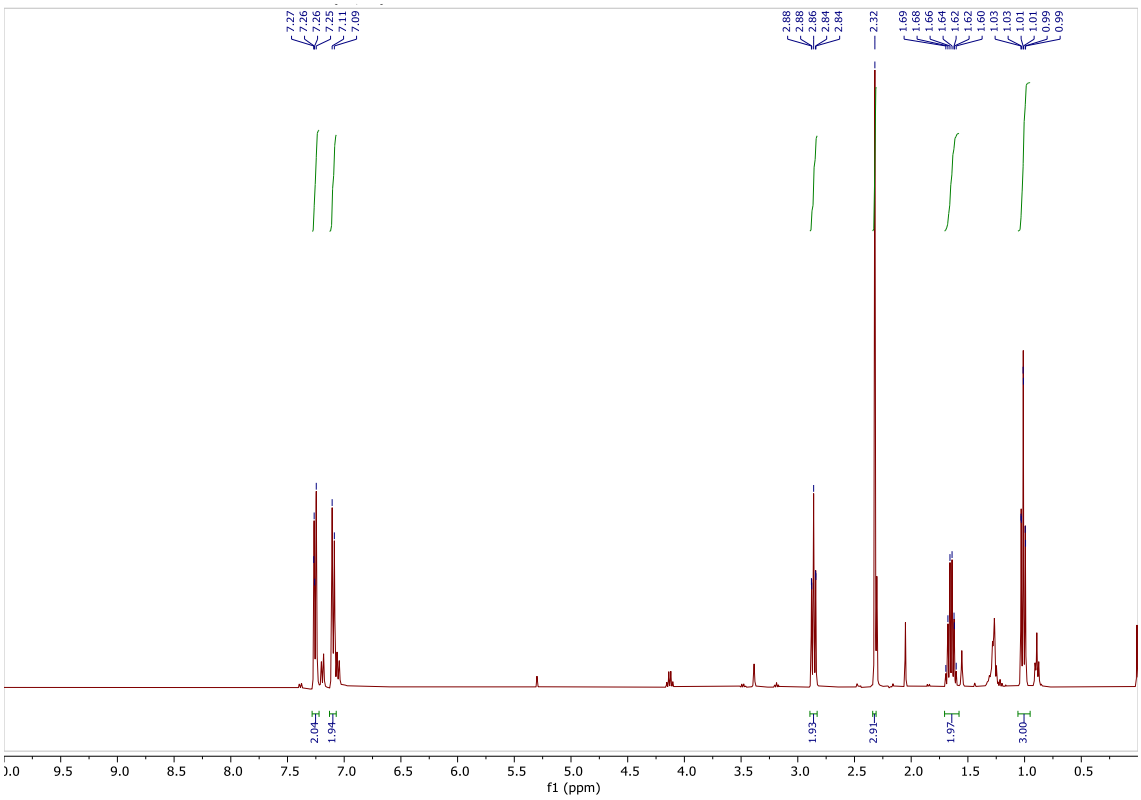


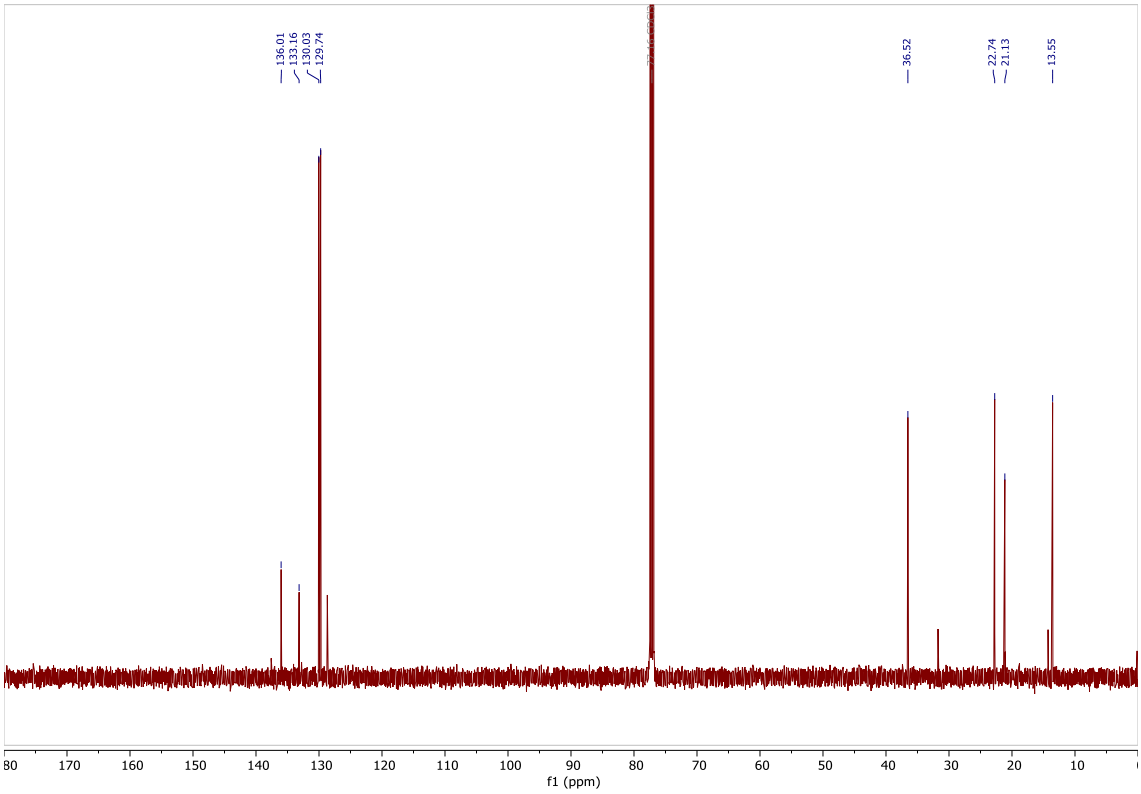

*Allyl(phenyl)sulfane* ***27l***

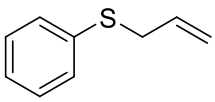


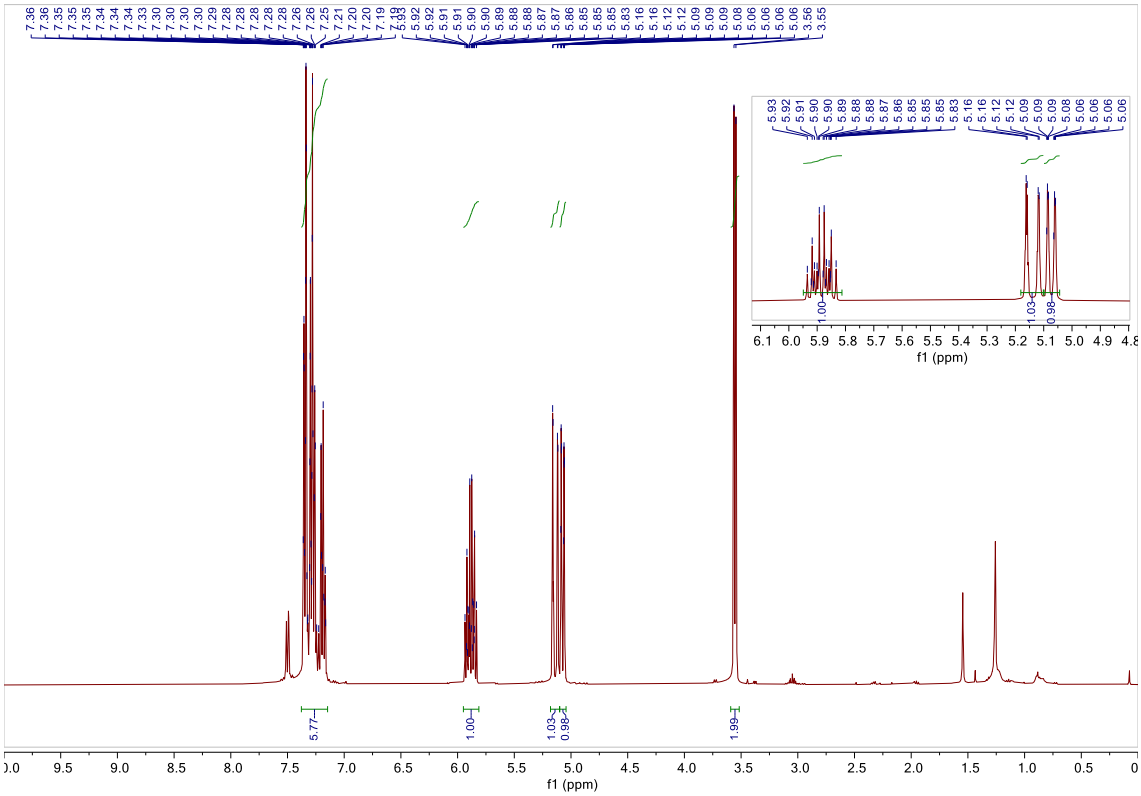


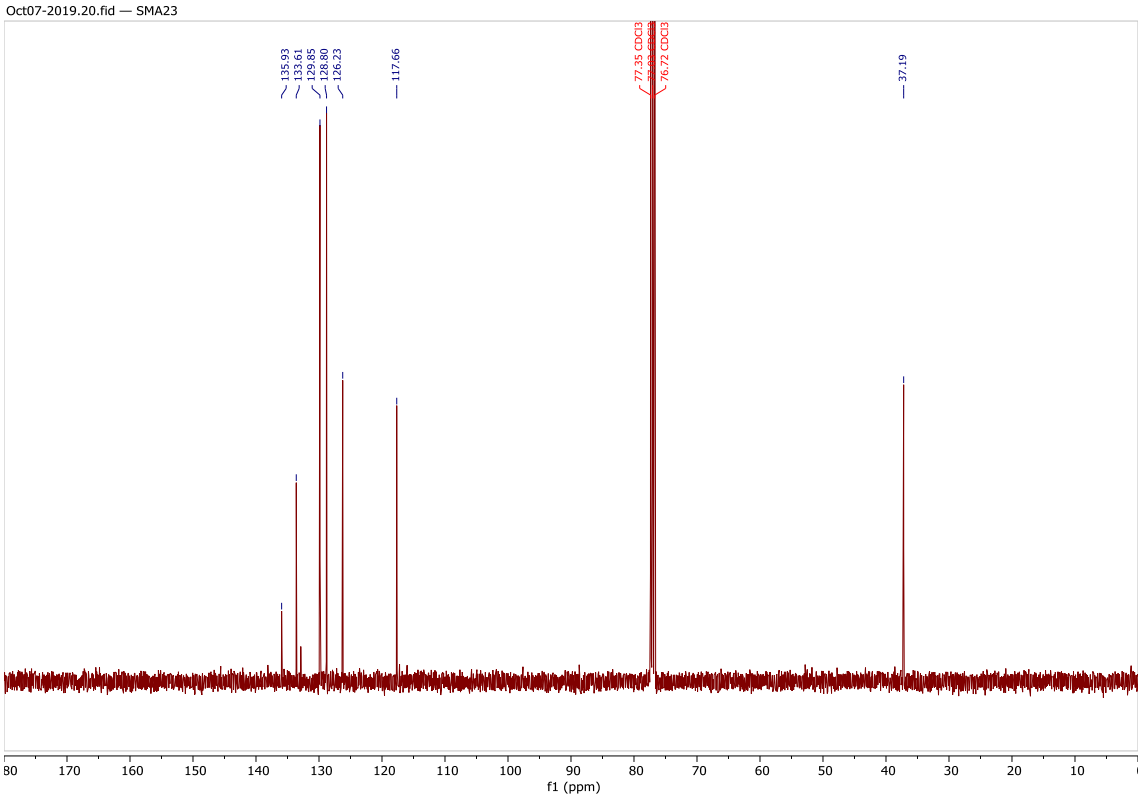

*But-3-en-1-yl(phenyl)sulfane* ***27m***

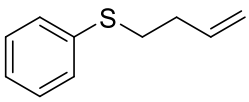


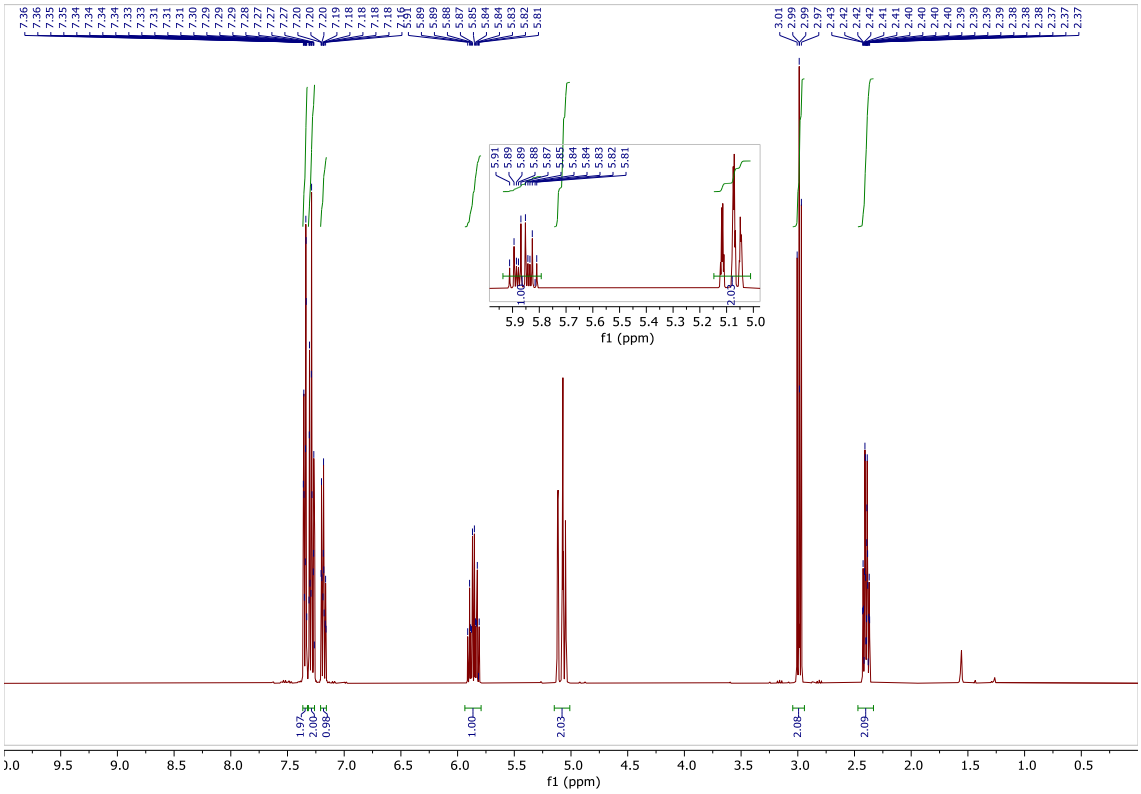


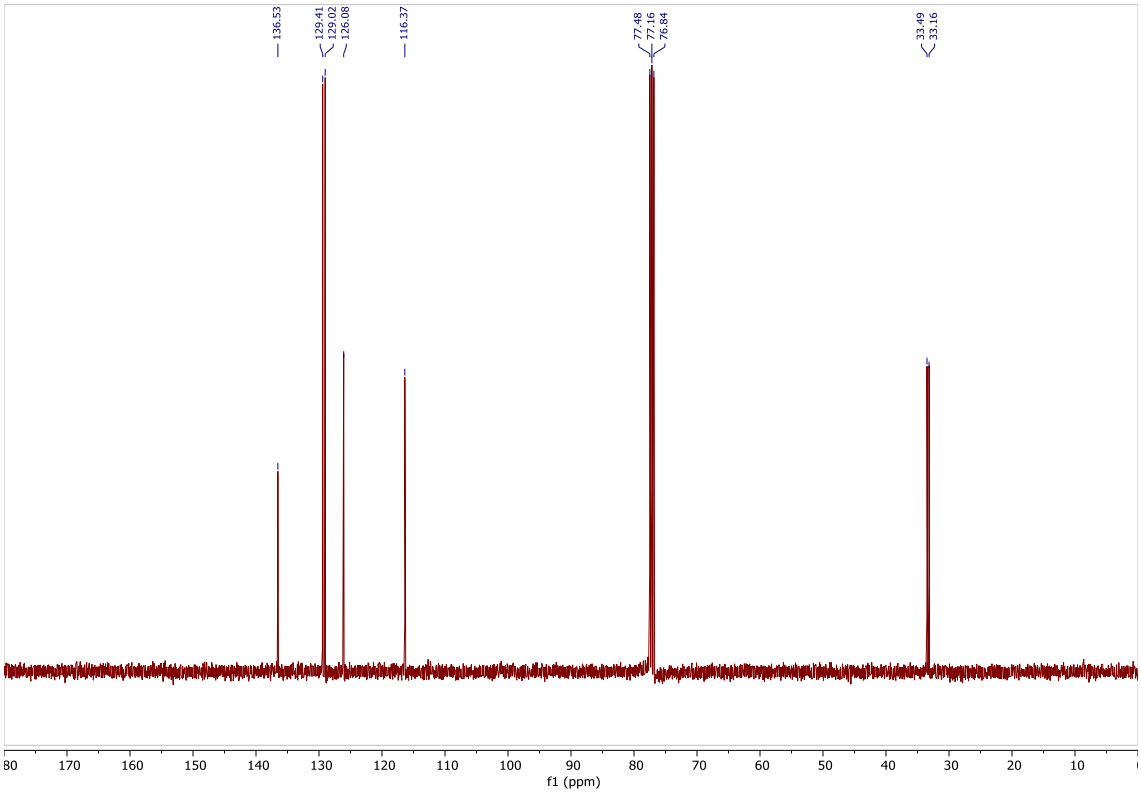

*But-3-en-1-yl(p-tolyl)sulfane* ***27n***

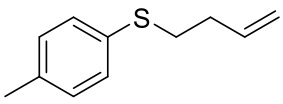


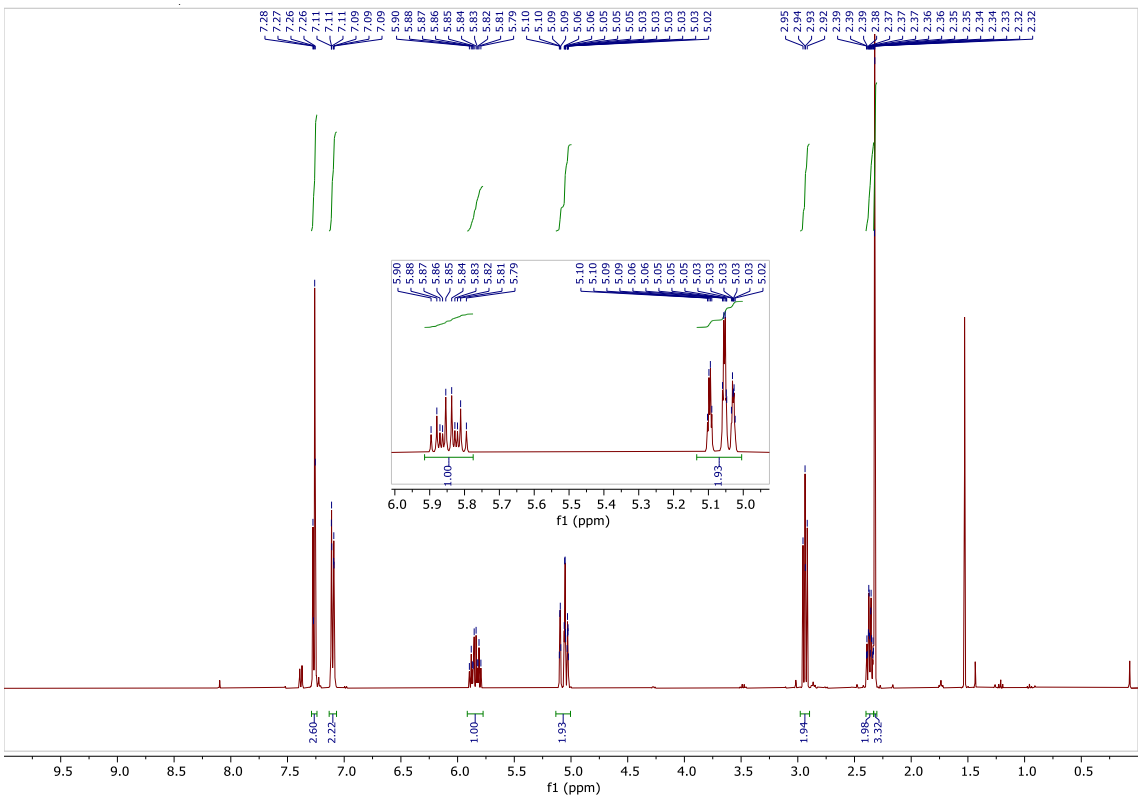


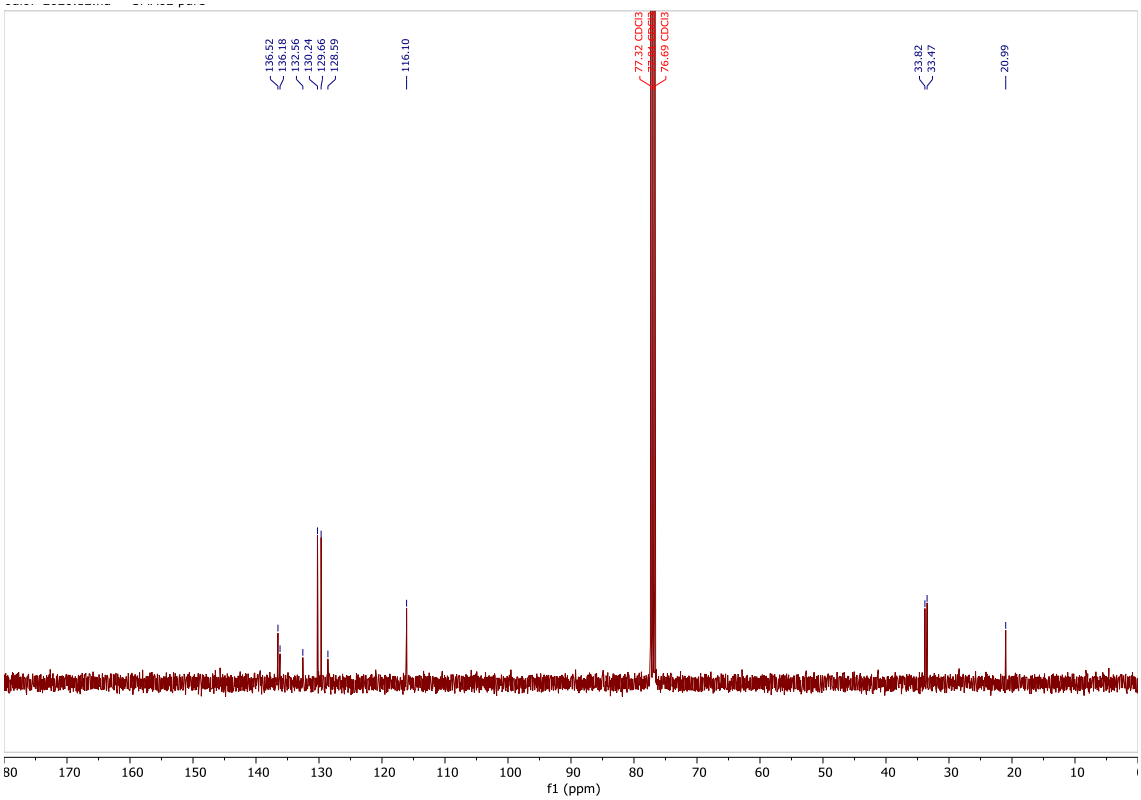

*Allyl(benzyl)sulfane* ***27p***

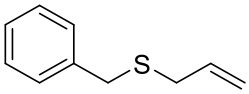


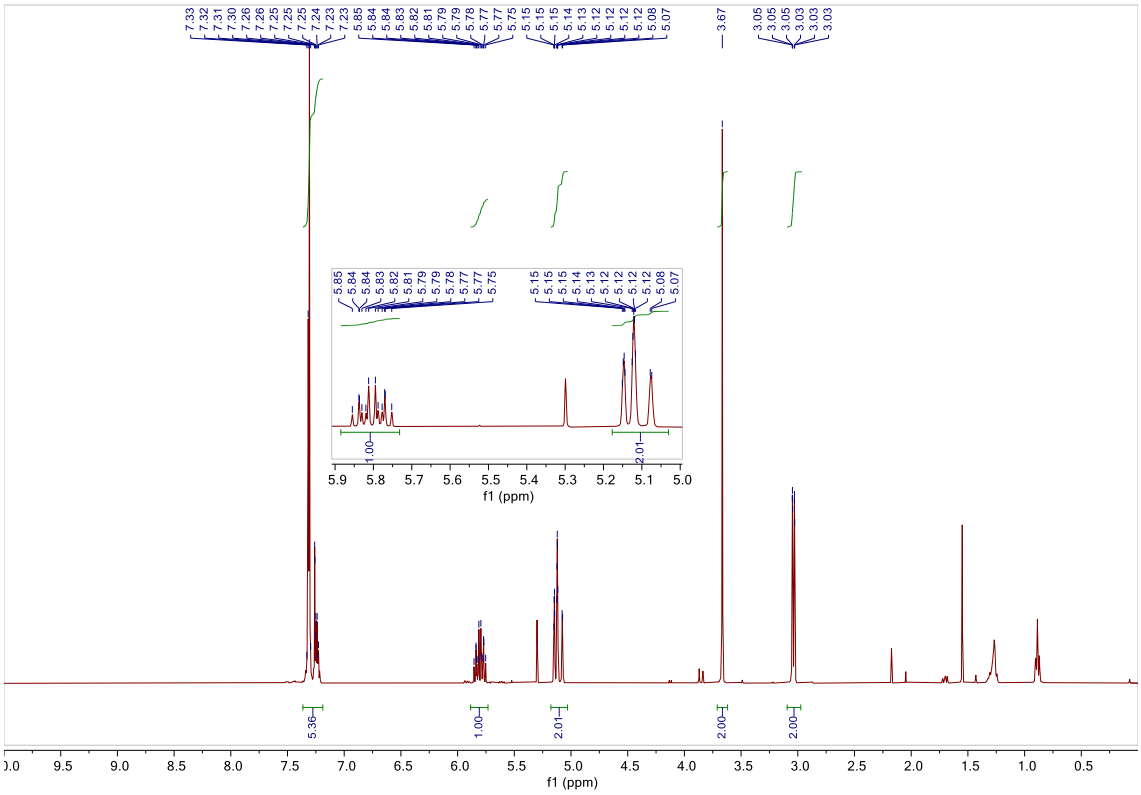


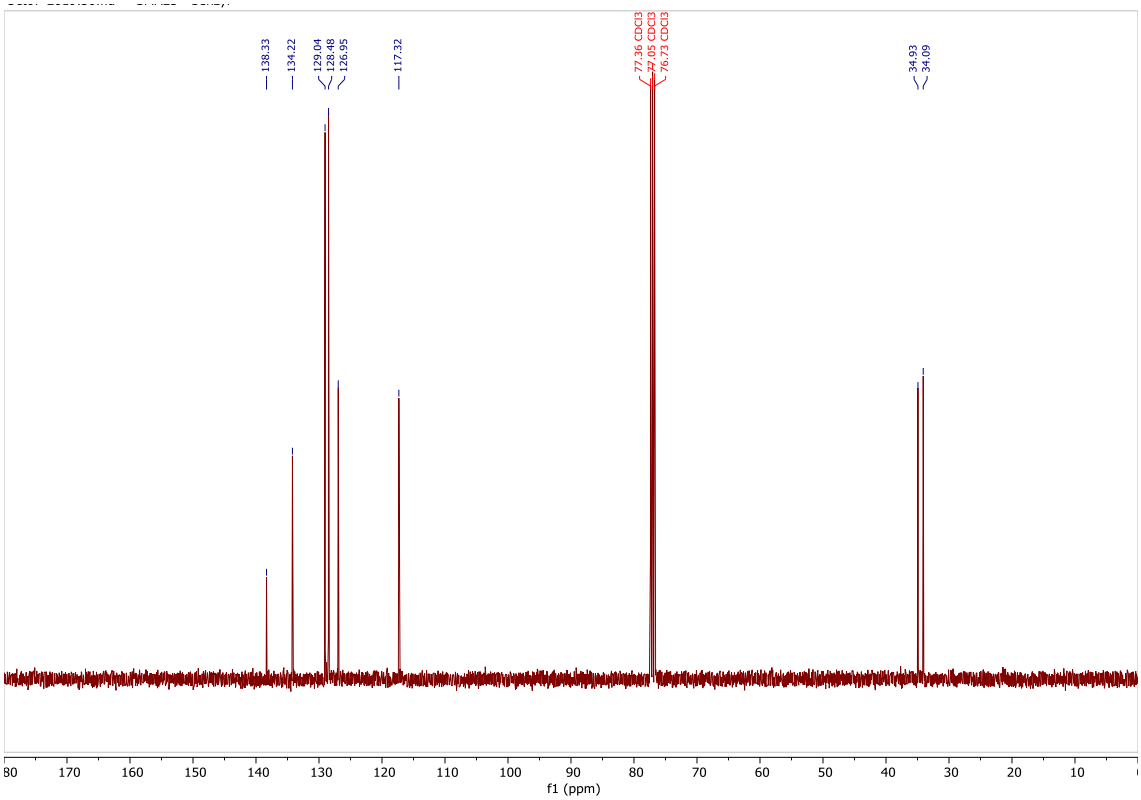

*2-(Phenylthio)propanenitrile* ***27q***

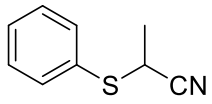


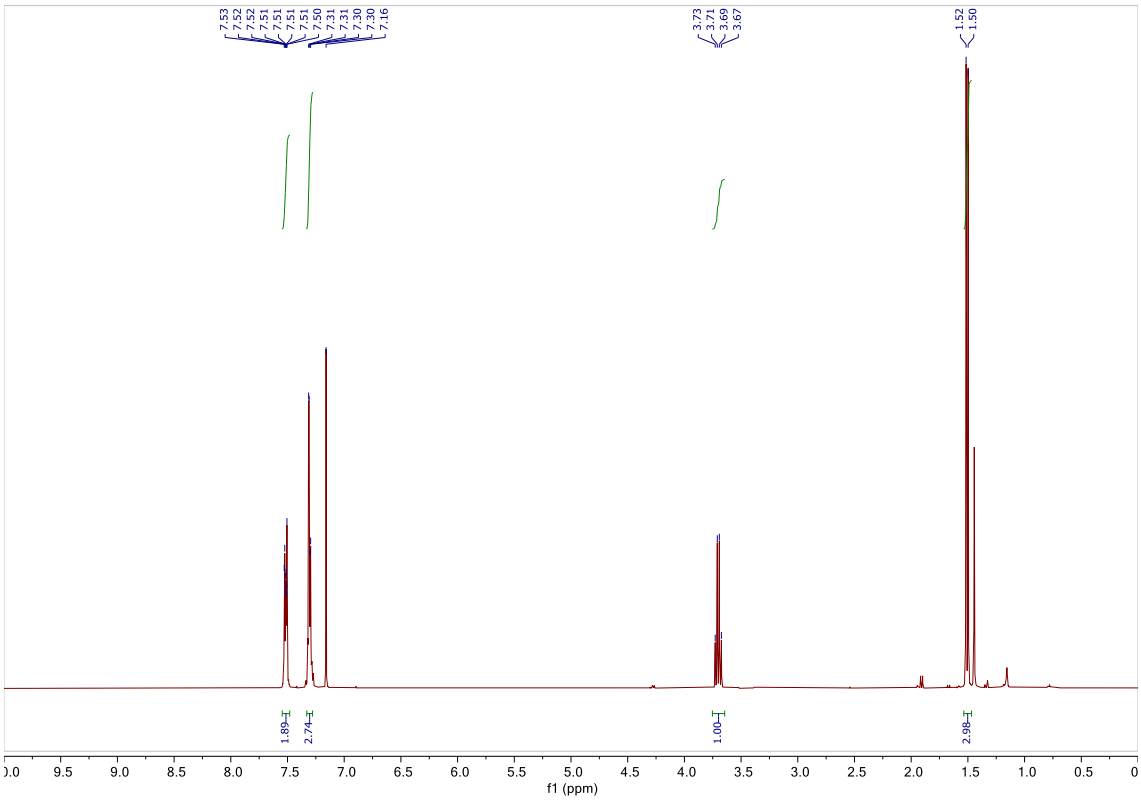


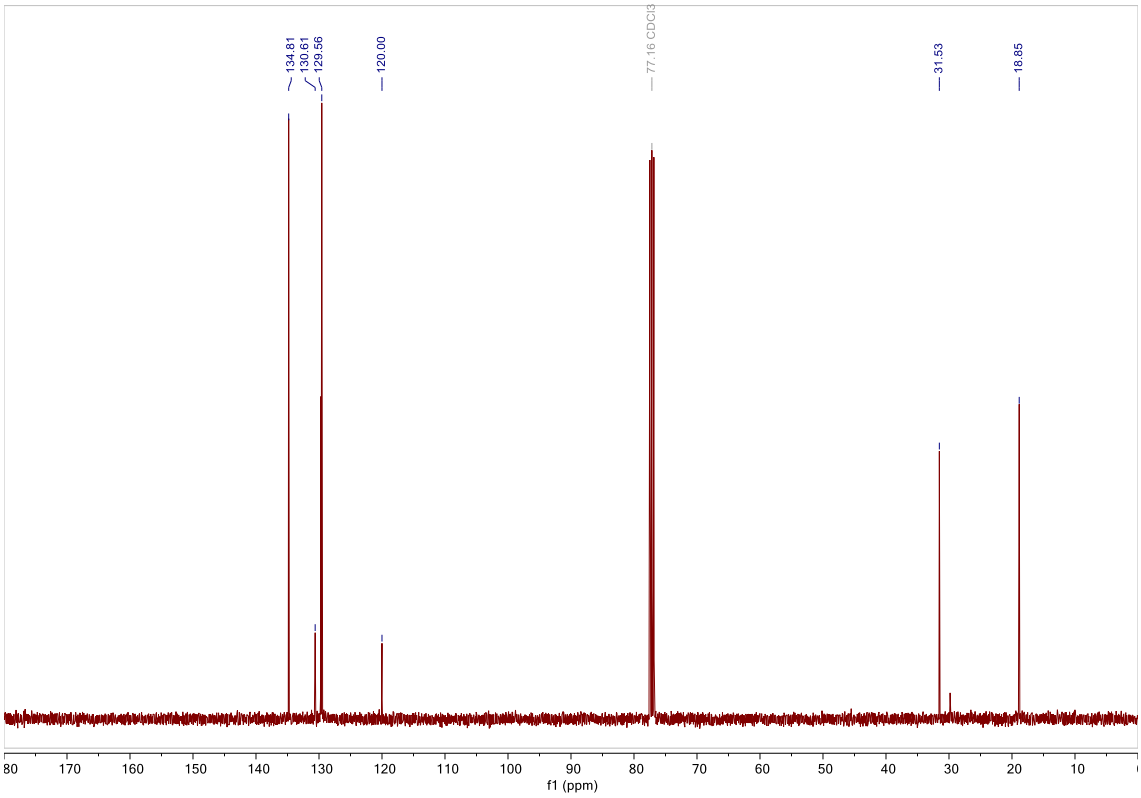

*2-((Propylthio)methyl)pyridine* ***27s***

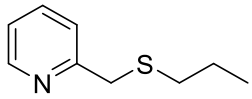


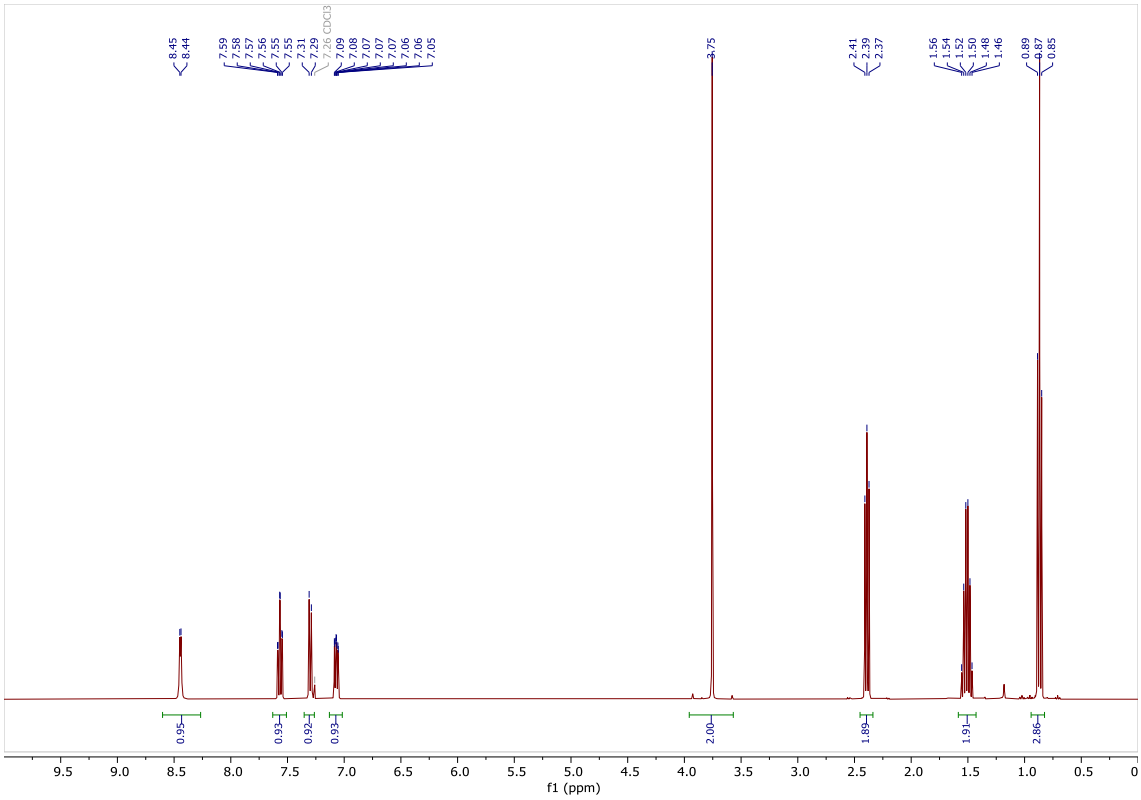


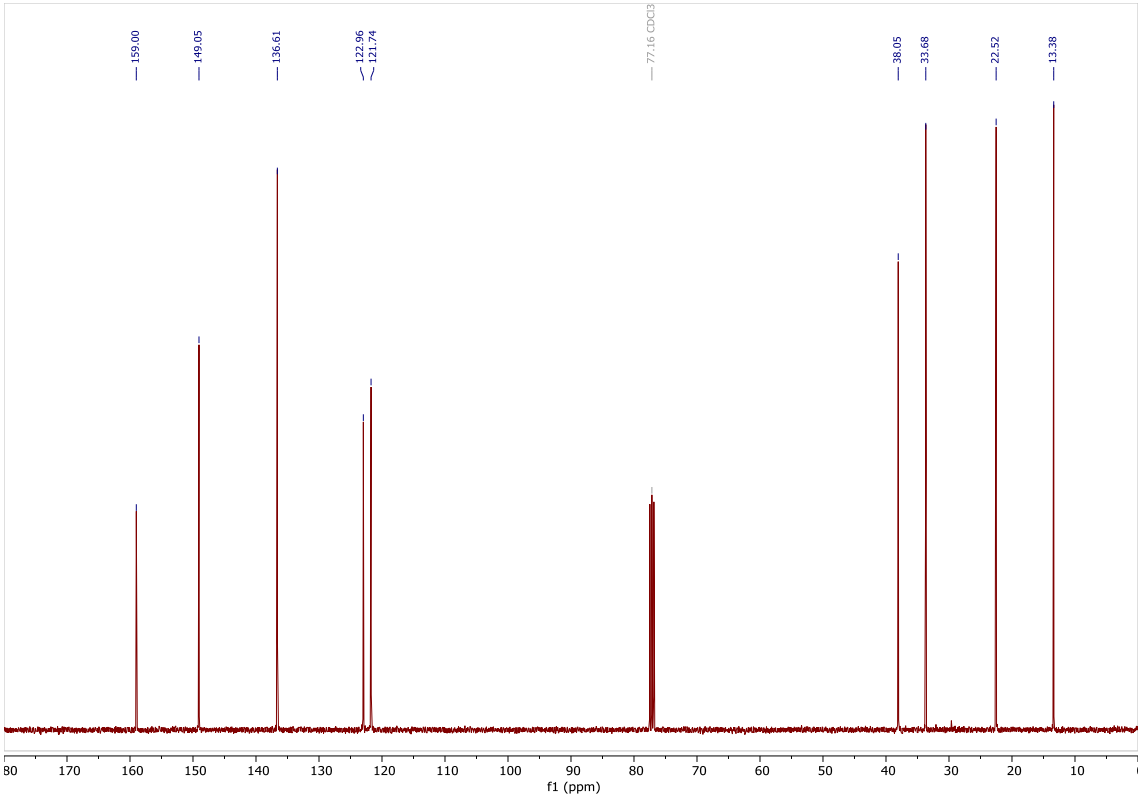

*2-((Ethylthio)methyl)pyridine* ***27t***

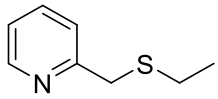


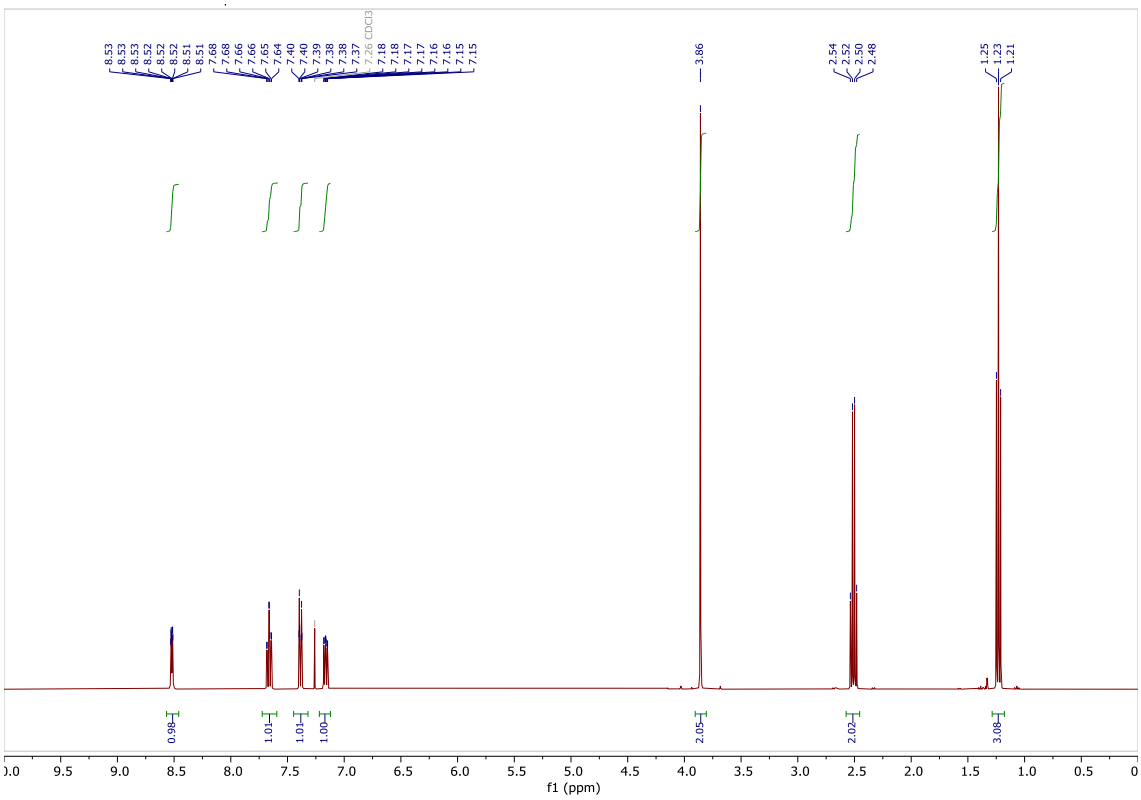


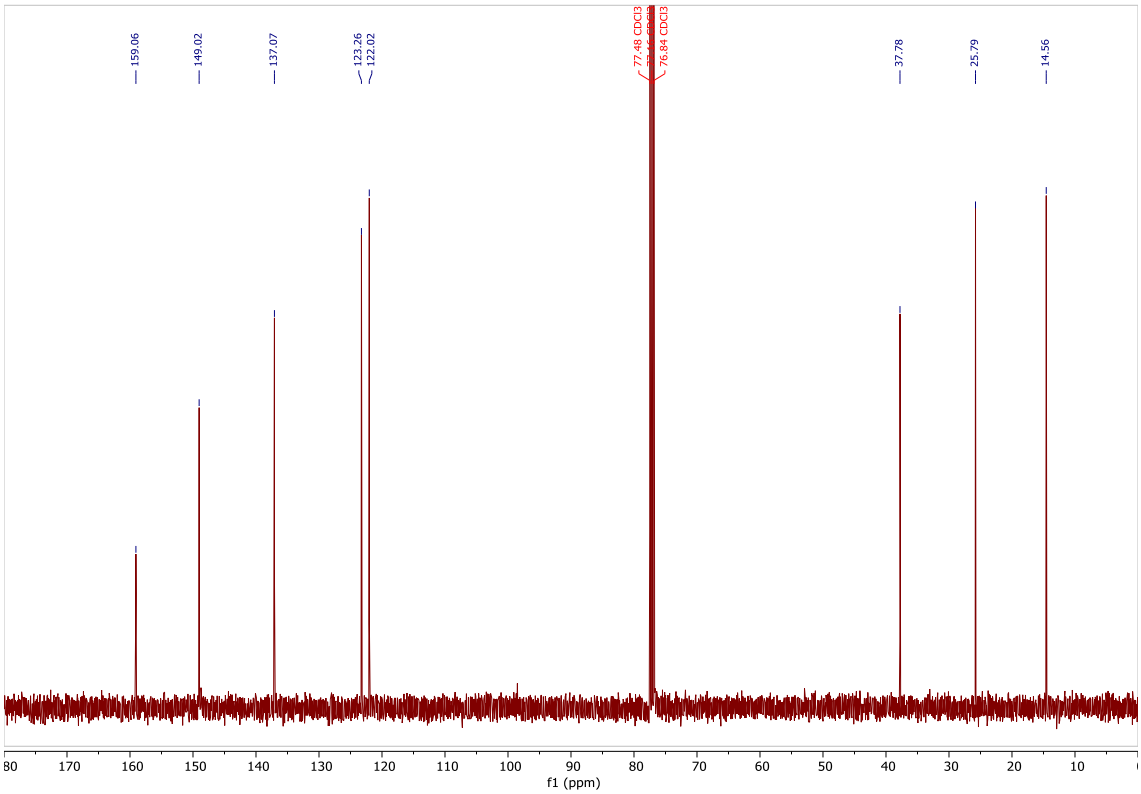

*2-((Benzylthio)methyl)pyridine* ***27u***

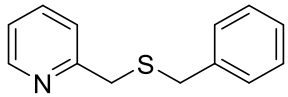


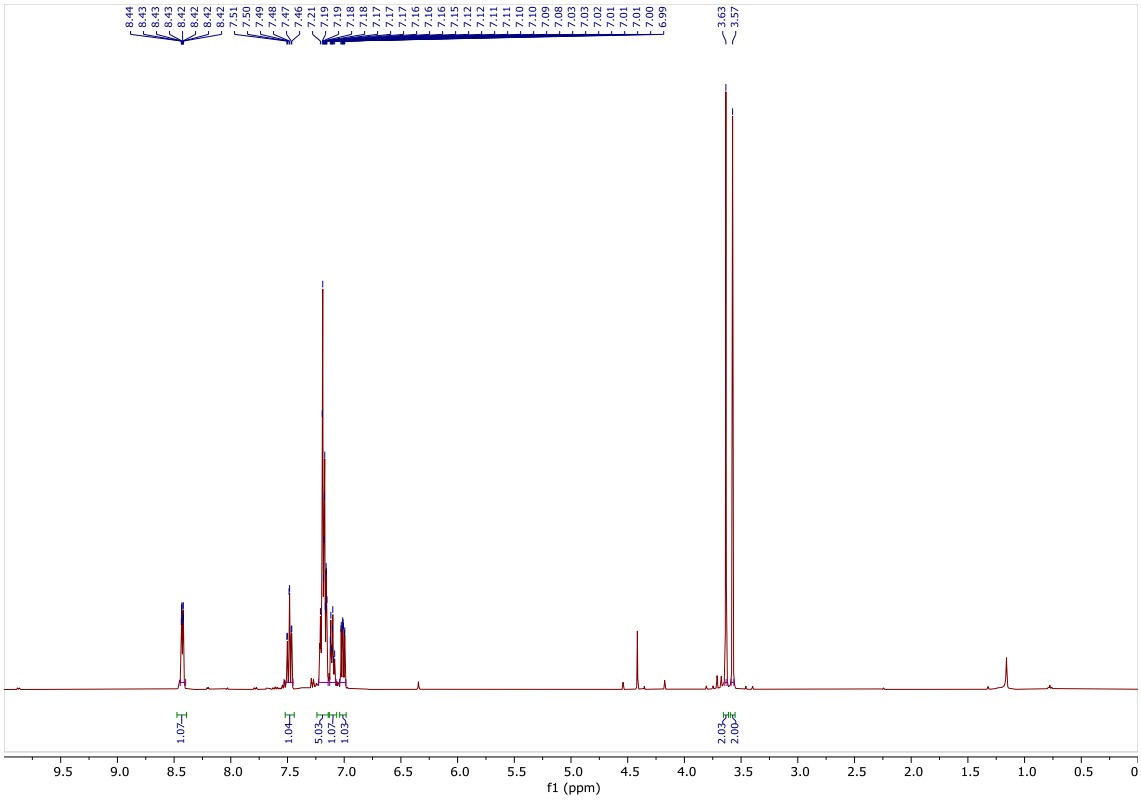


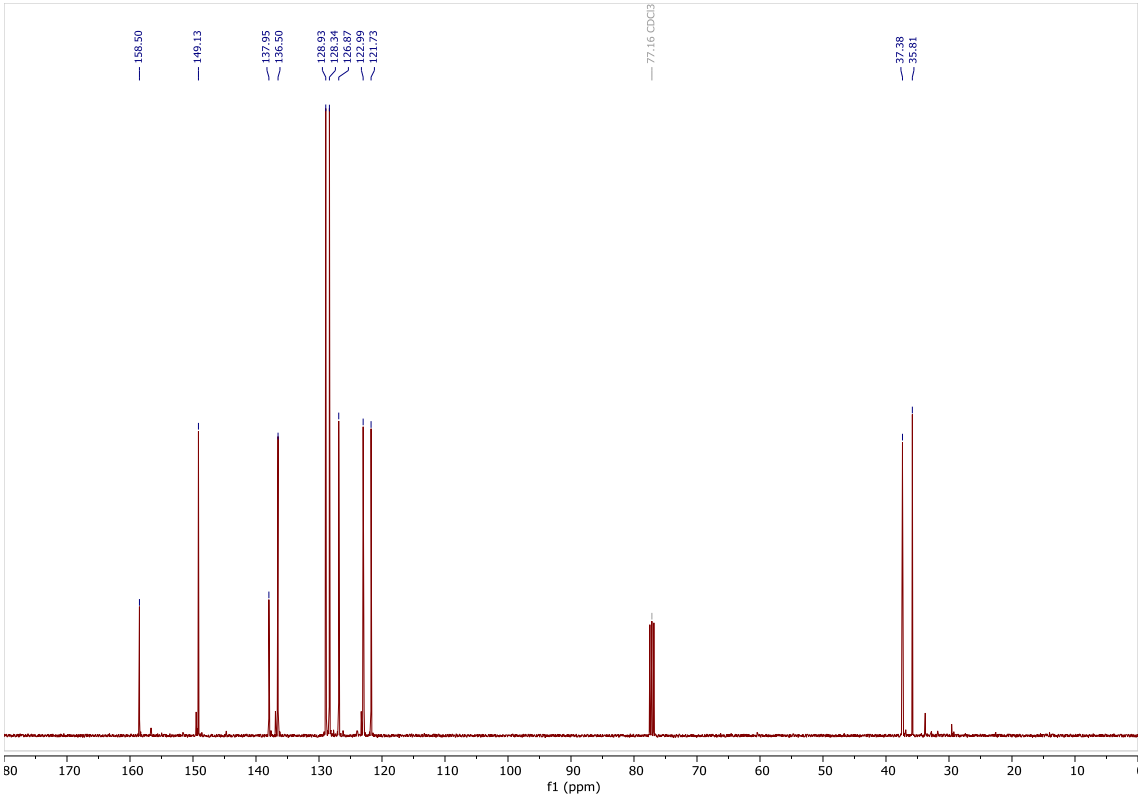

*Benzyl(ethyl)sulfane* ***27v***

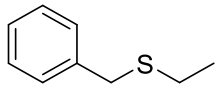

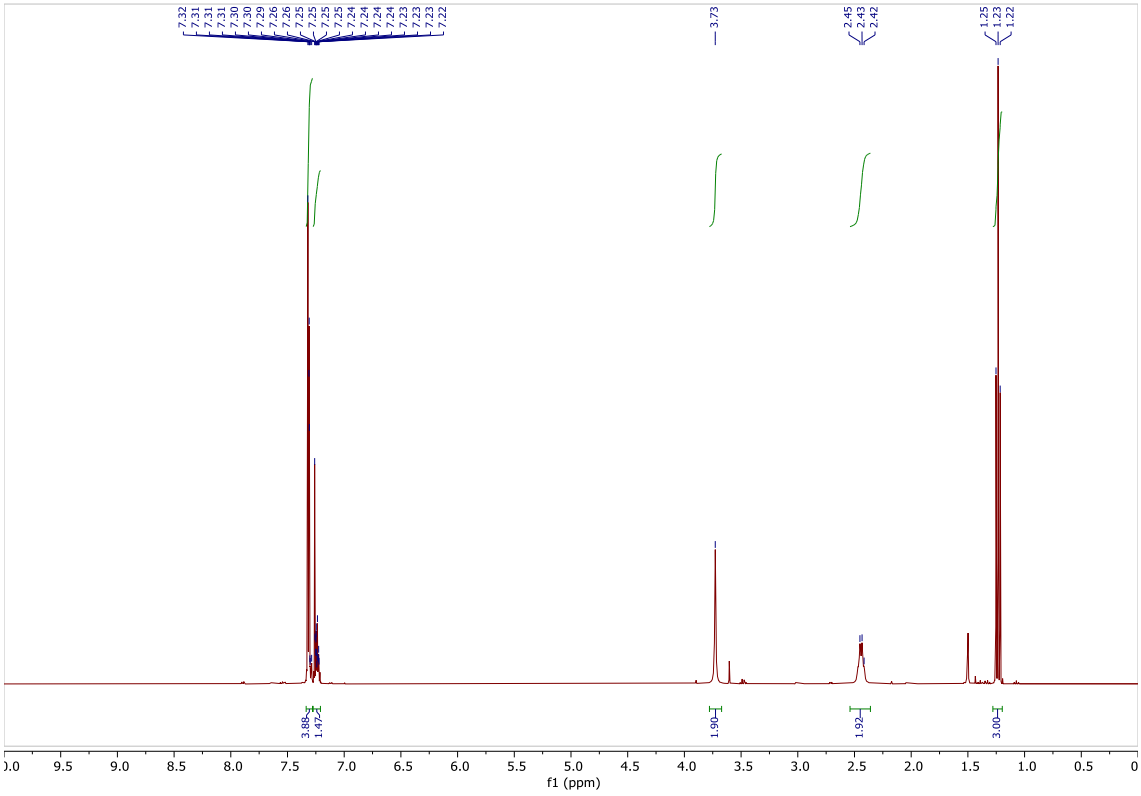


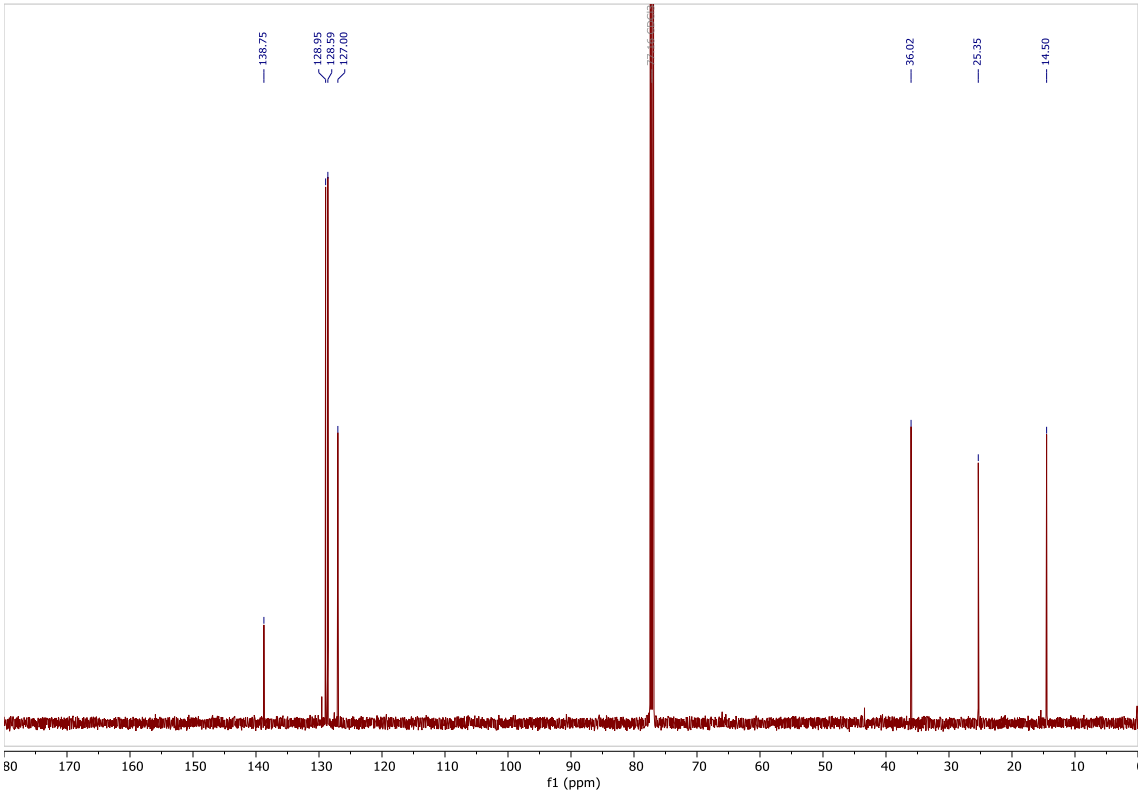

*Ethyl(phenethyl)sulfane* ***27w***

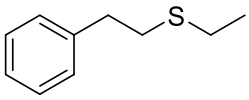


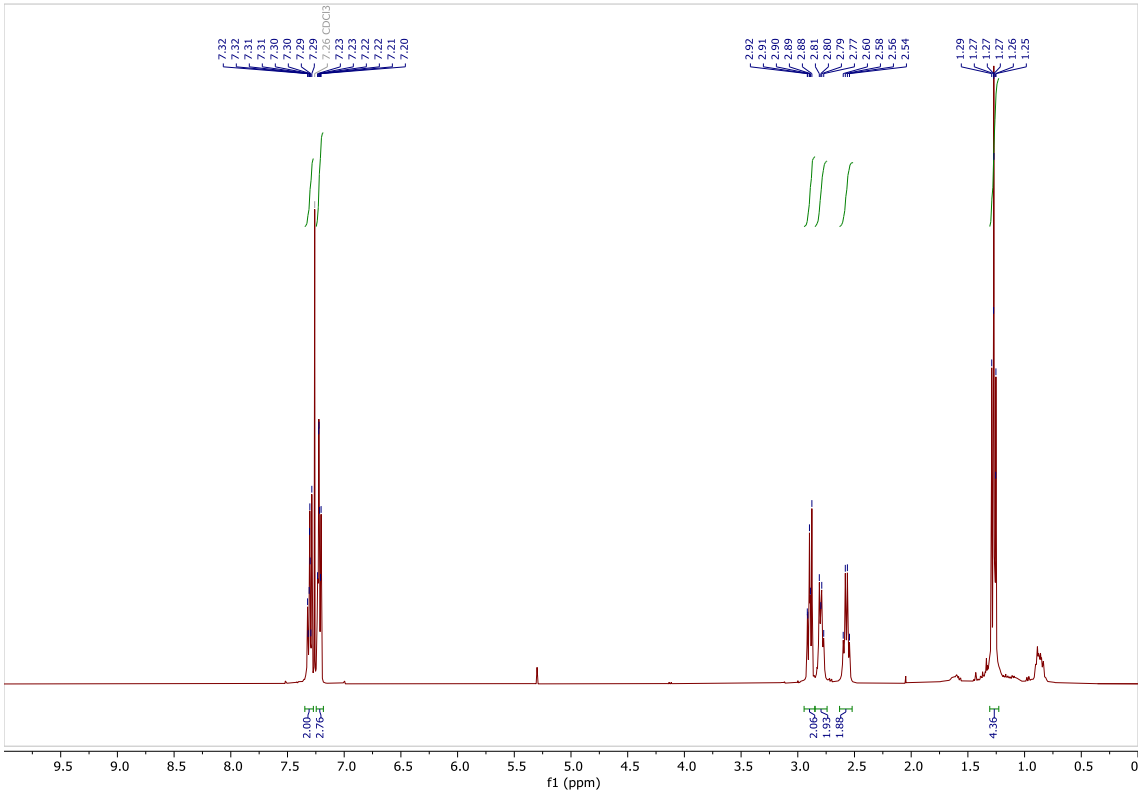


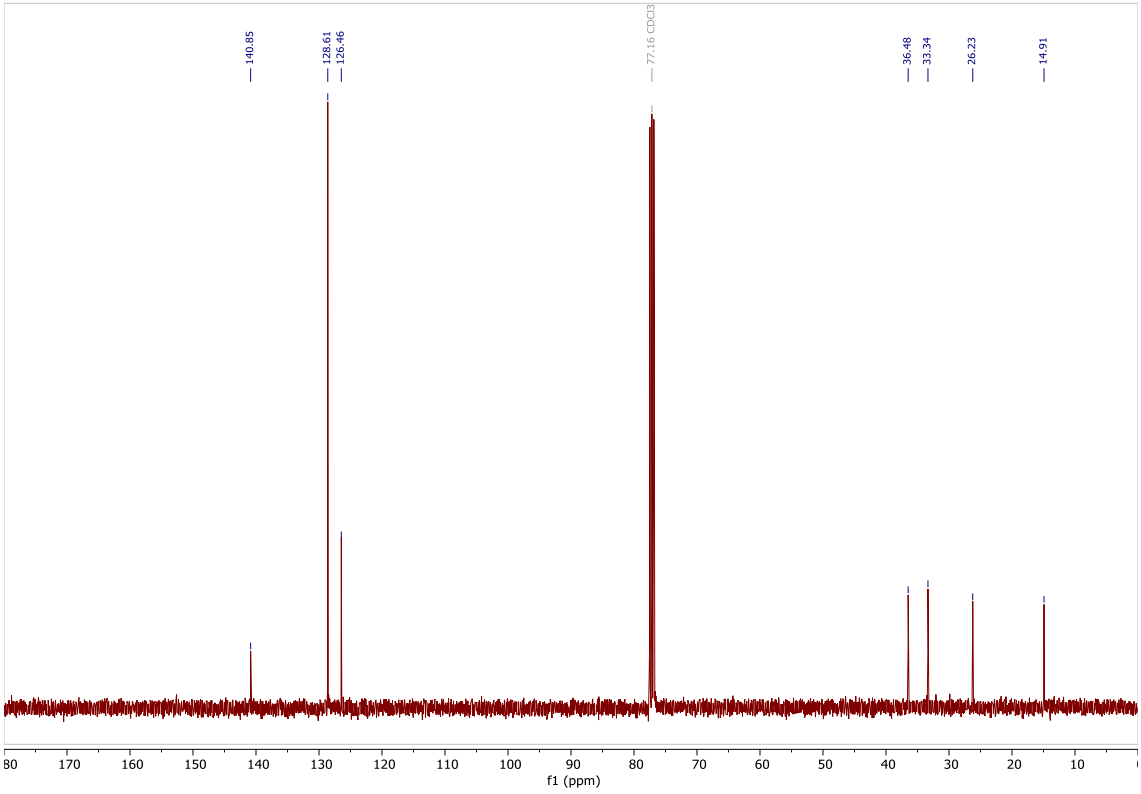

*Methyl(naphthalen-2-yl)sulfane* ***27ai***

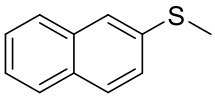


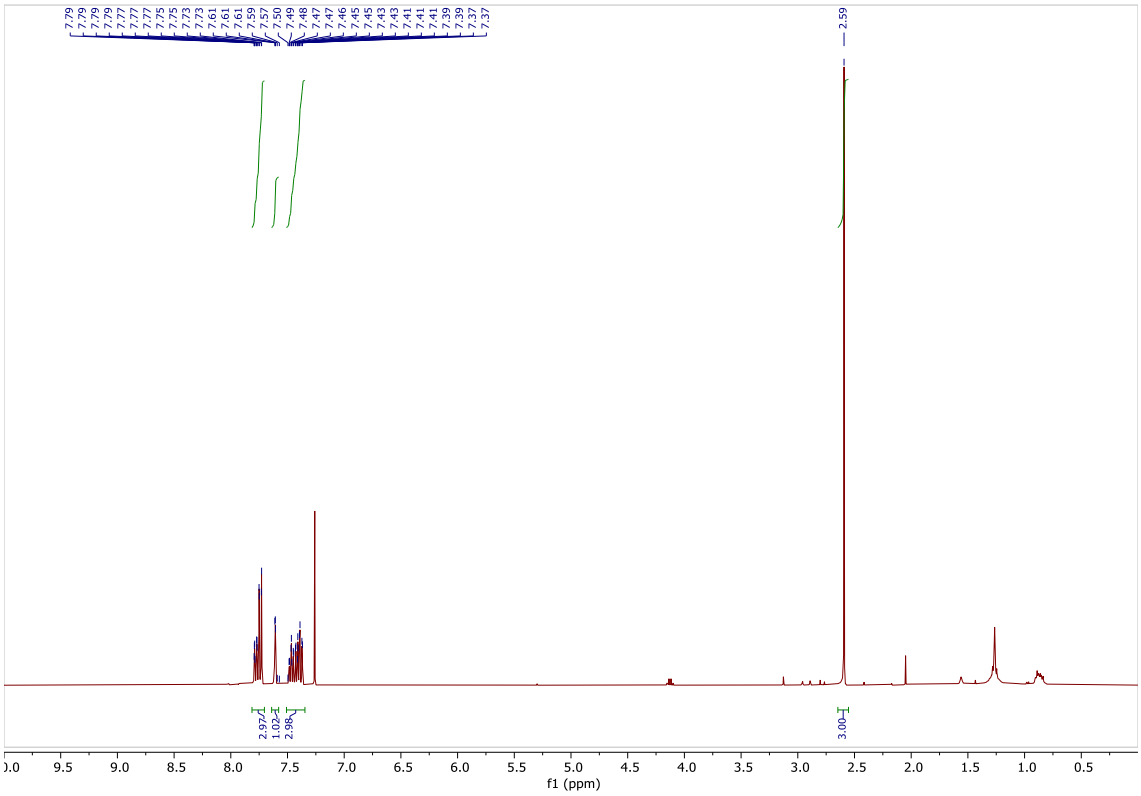


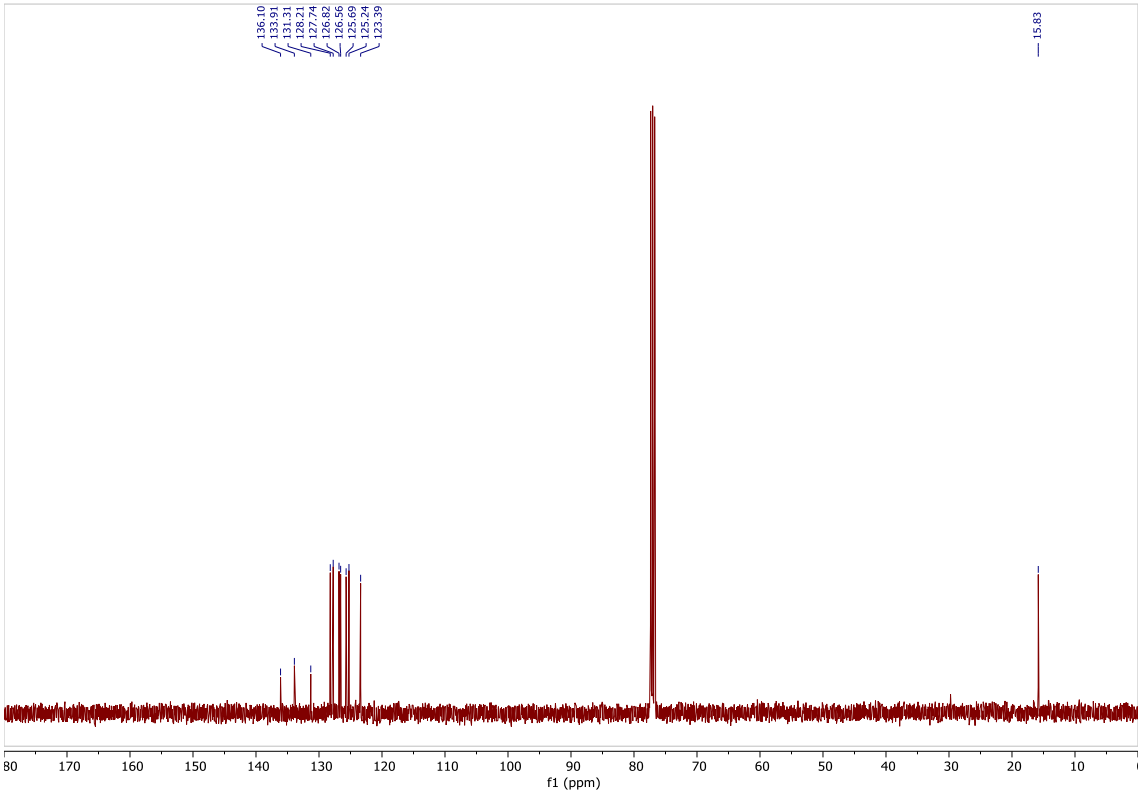

*Methyl(naphthalen-1-yl)sulfane* ***27aj***

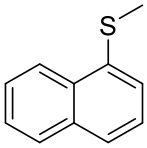


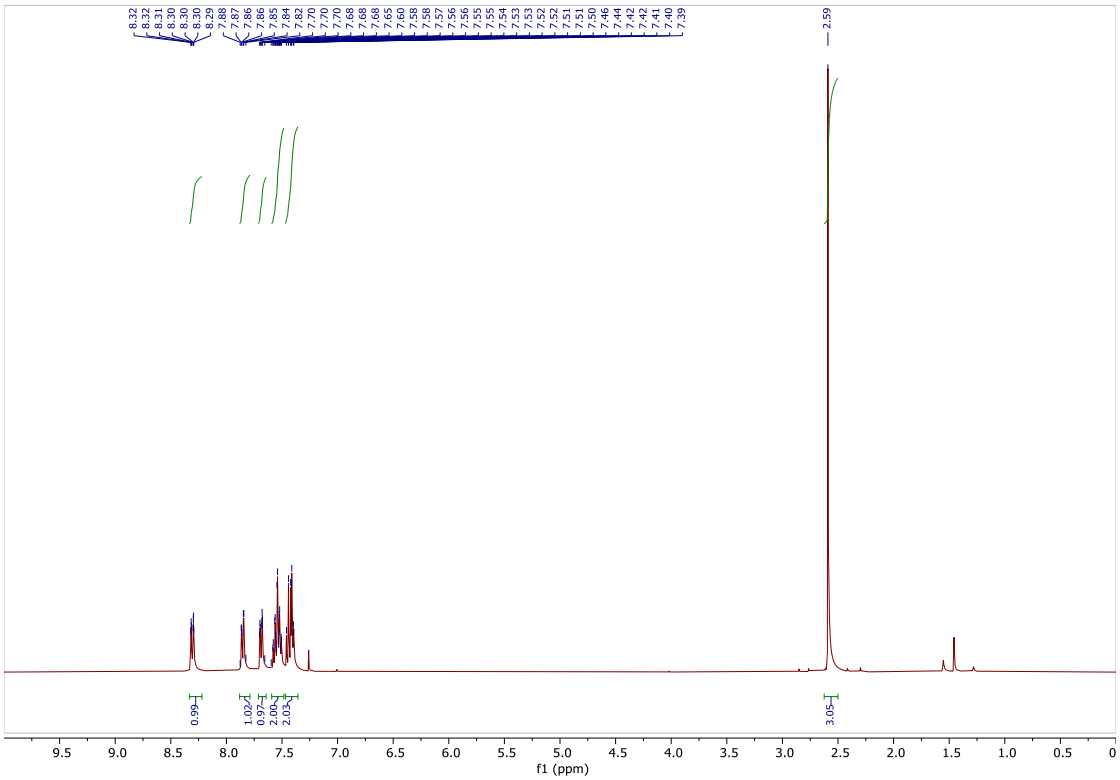


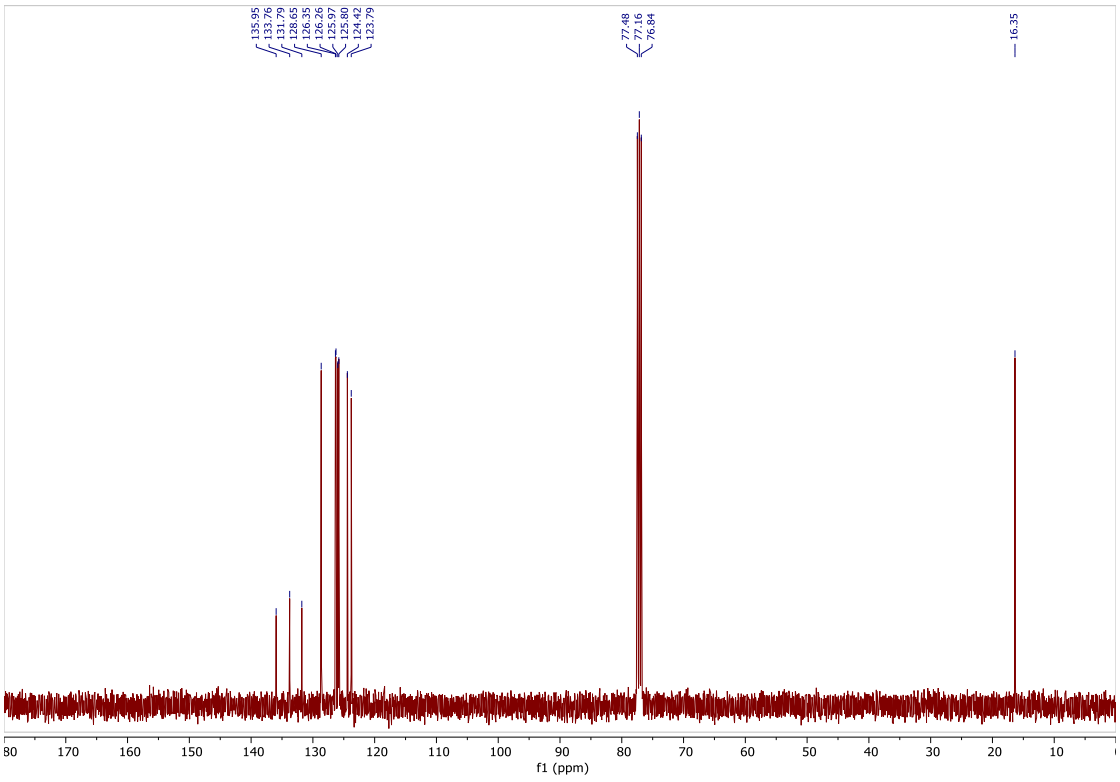

*Methyl(2-(phenylthio)ethyl)sulfane* ***27am***

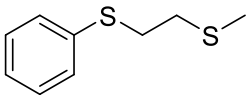


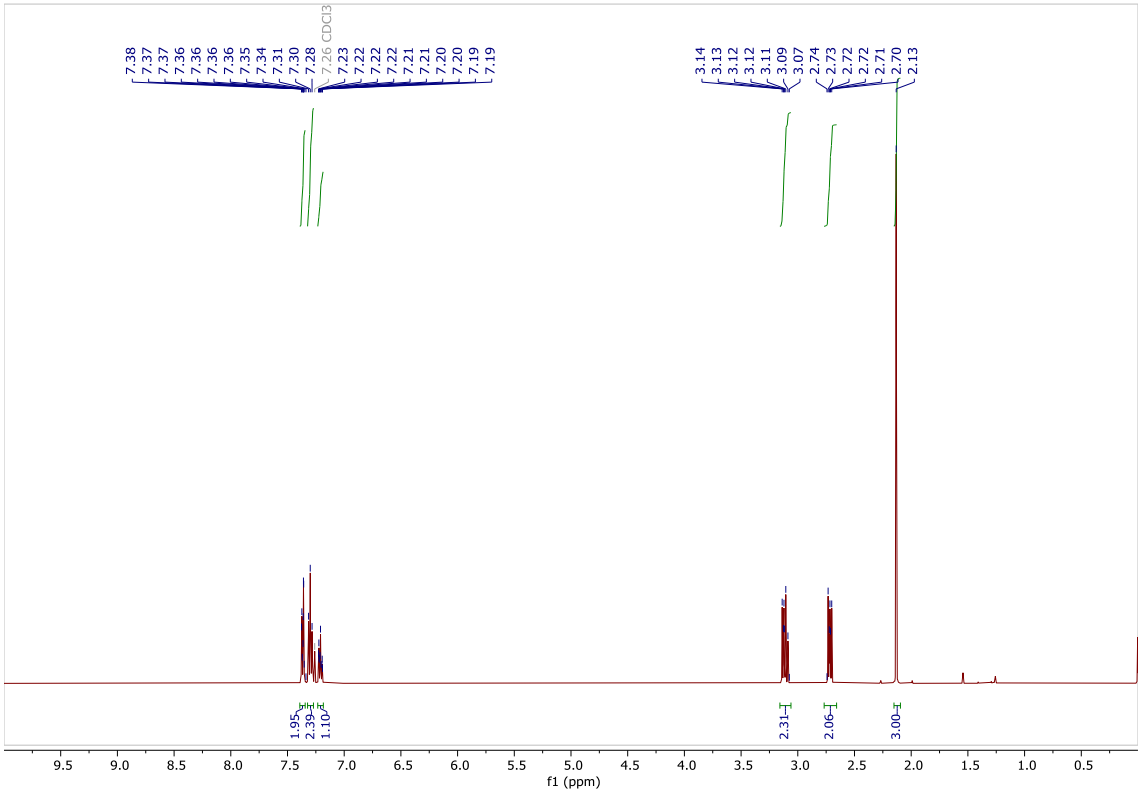


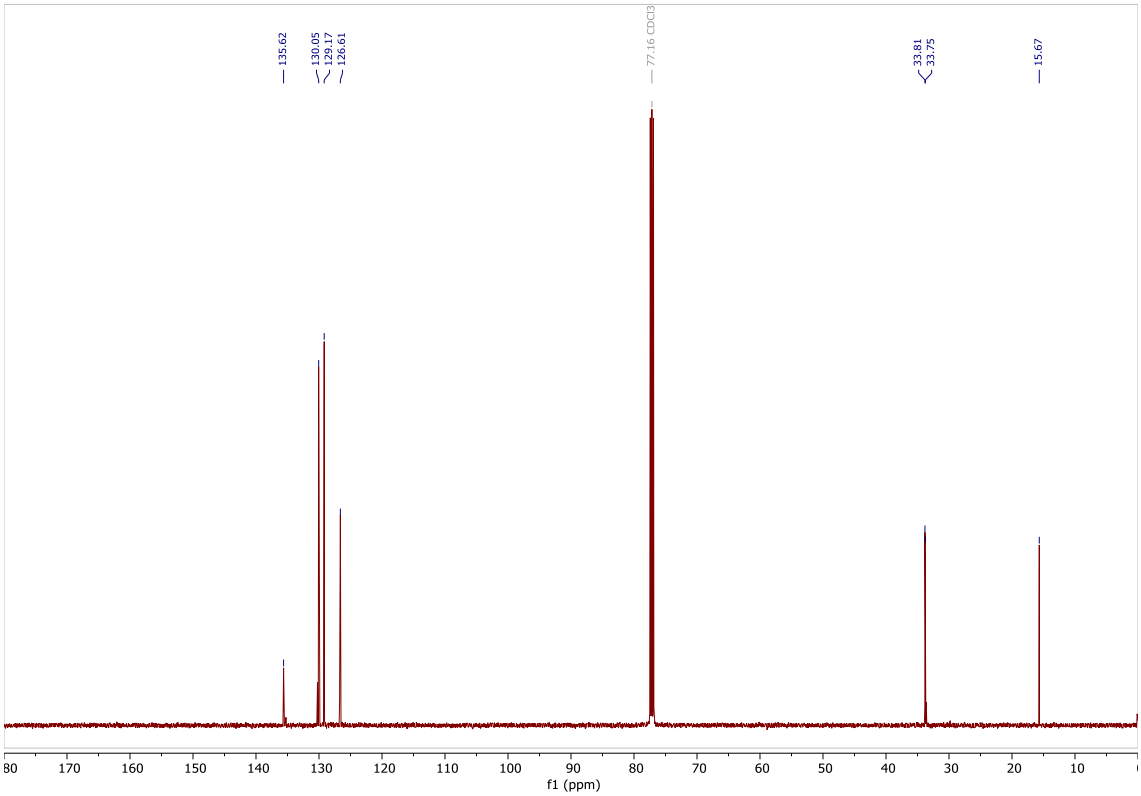

*Phenyl(propyl)sulfane* ***27an***

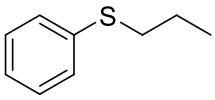


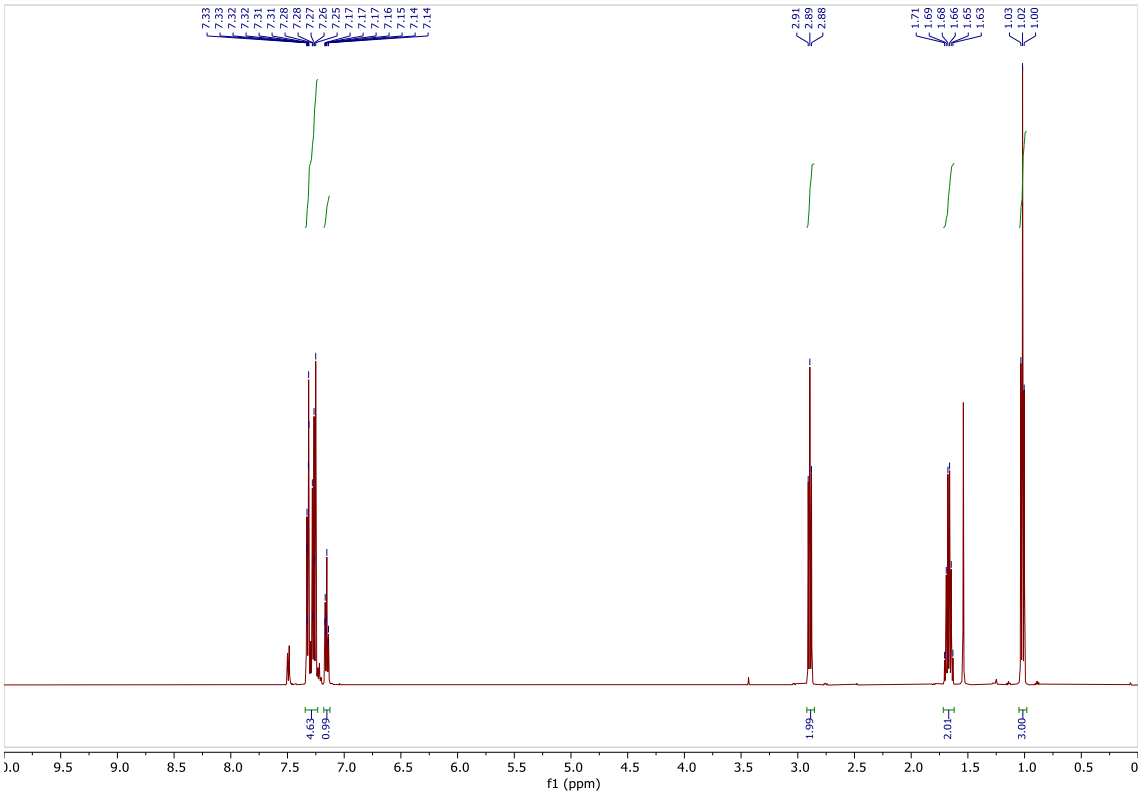

*(4-Chlorophenyl)(propyl)sulfane* ***27ao***

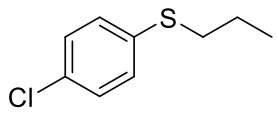


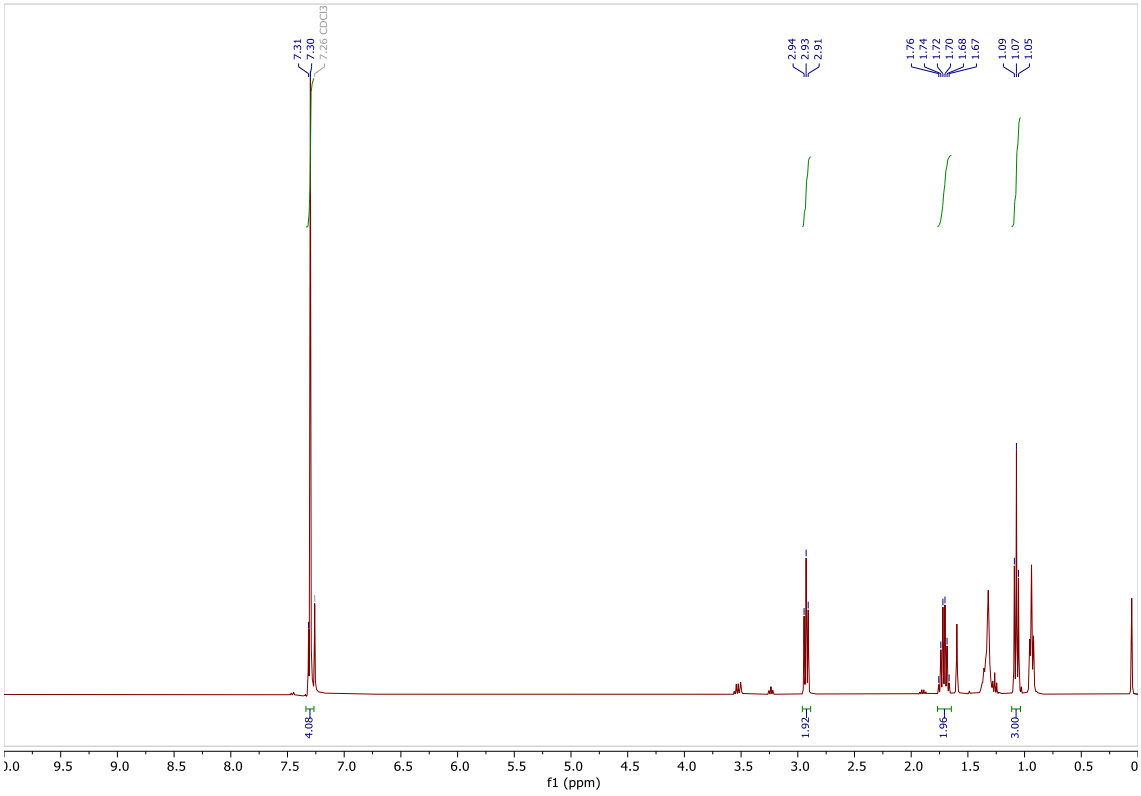


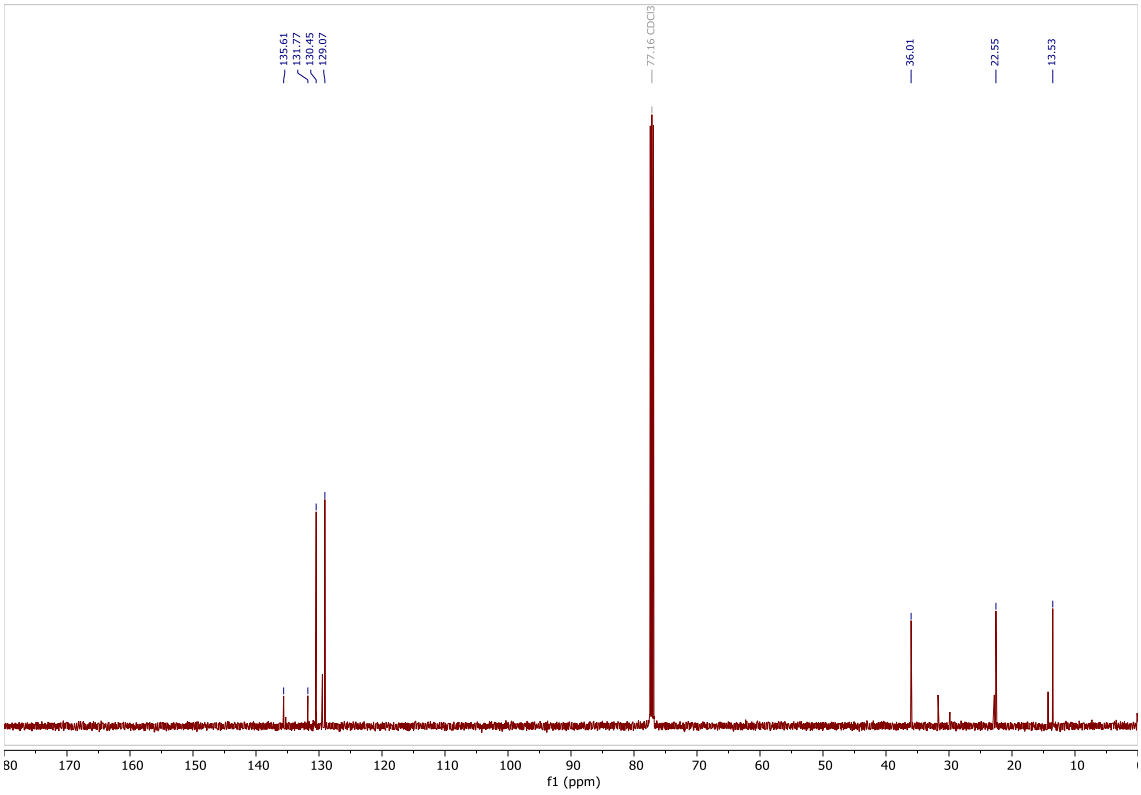

*(4-Bromophenyl)(propyl)sulfane* ***27ap***

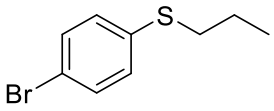


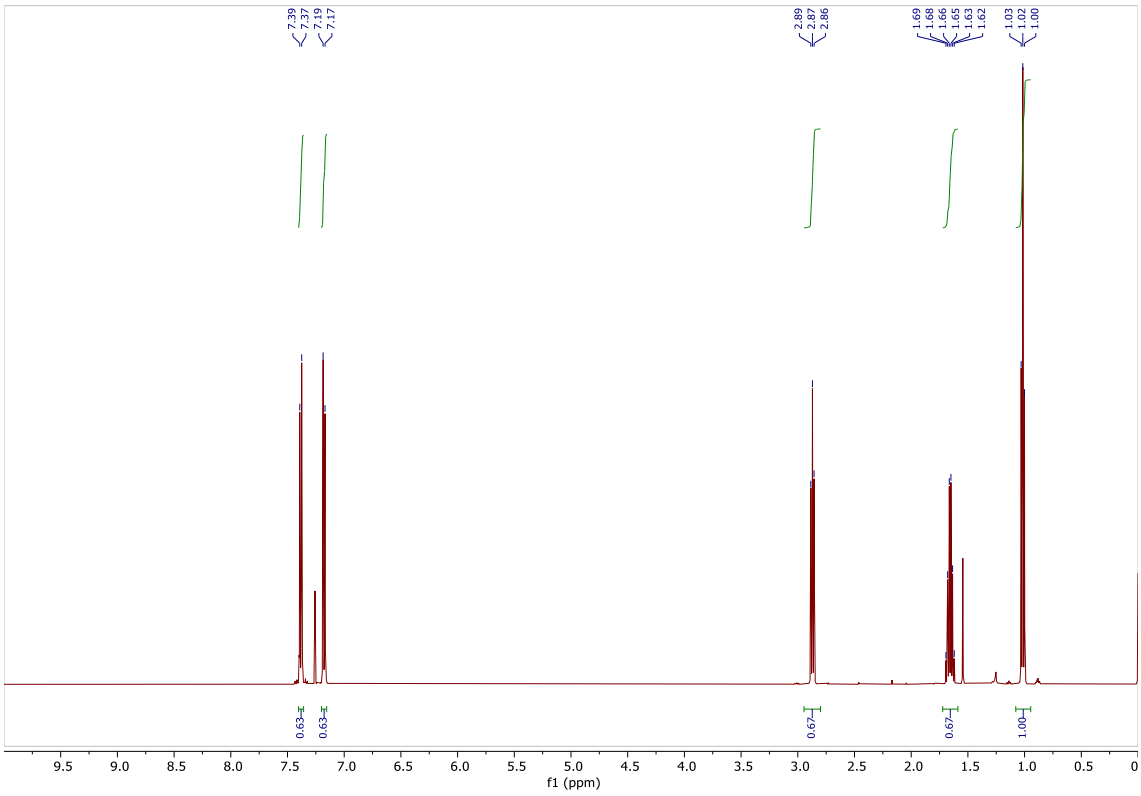


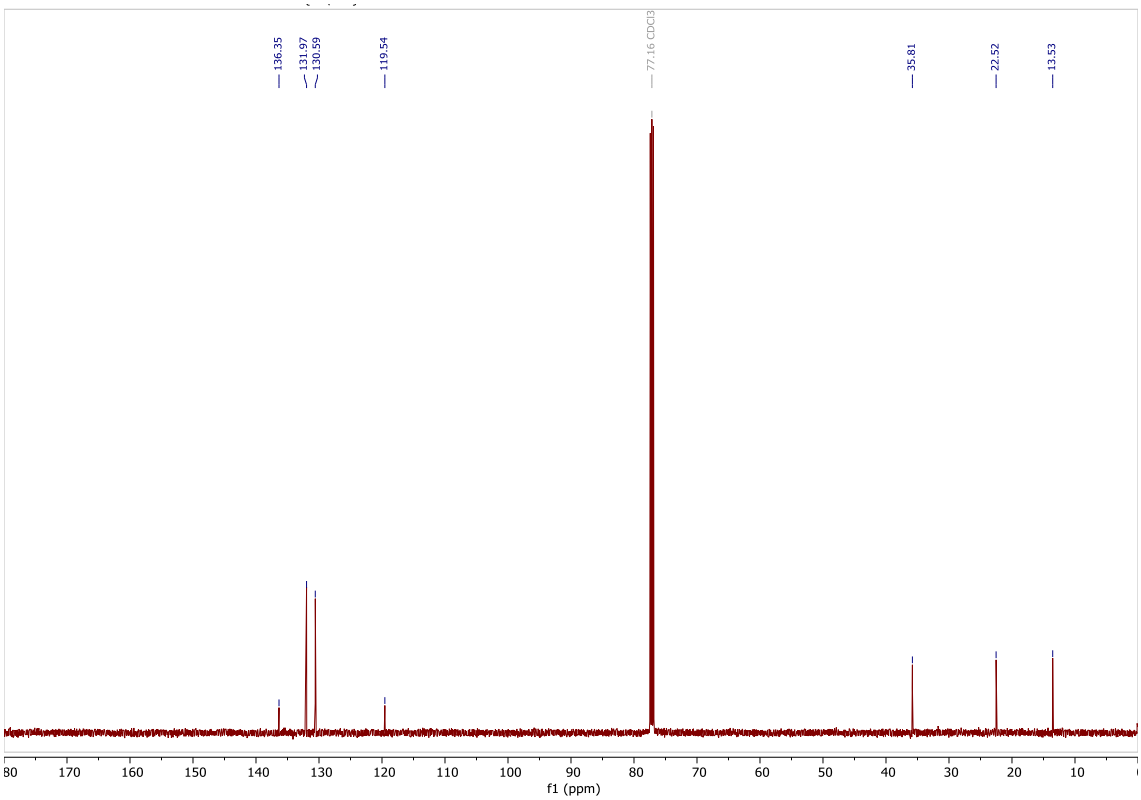

*(3-Methoxyphenyl)(propyl)sulfane* ***27aq***

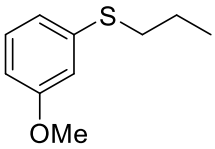


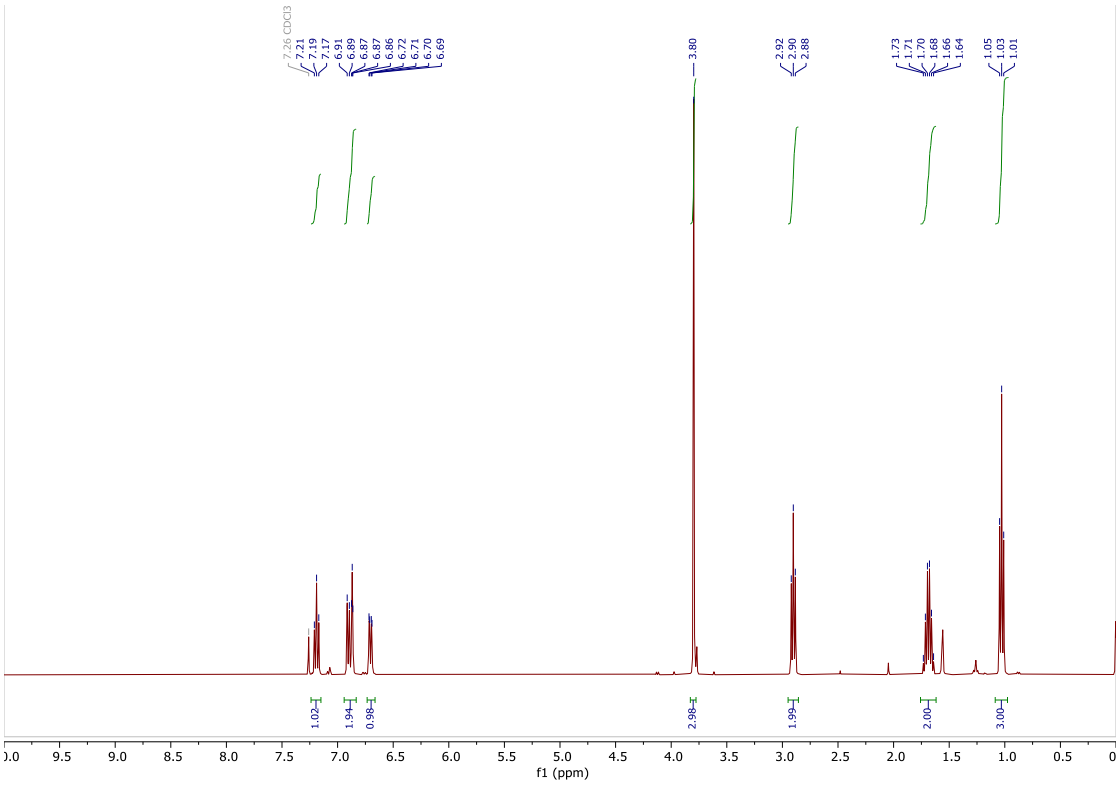


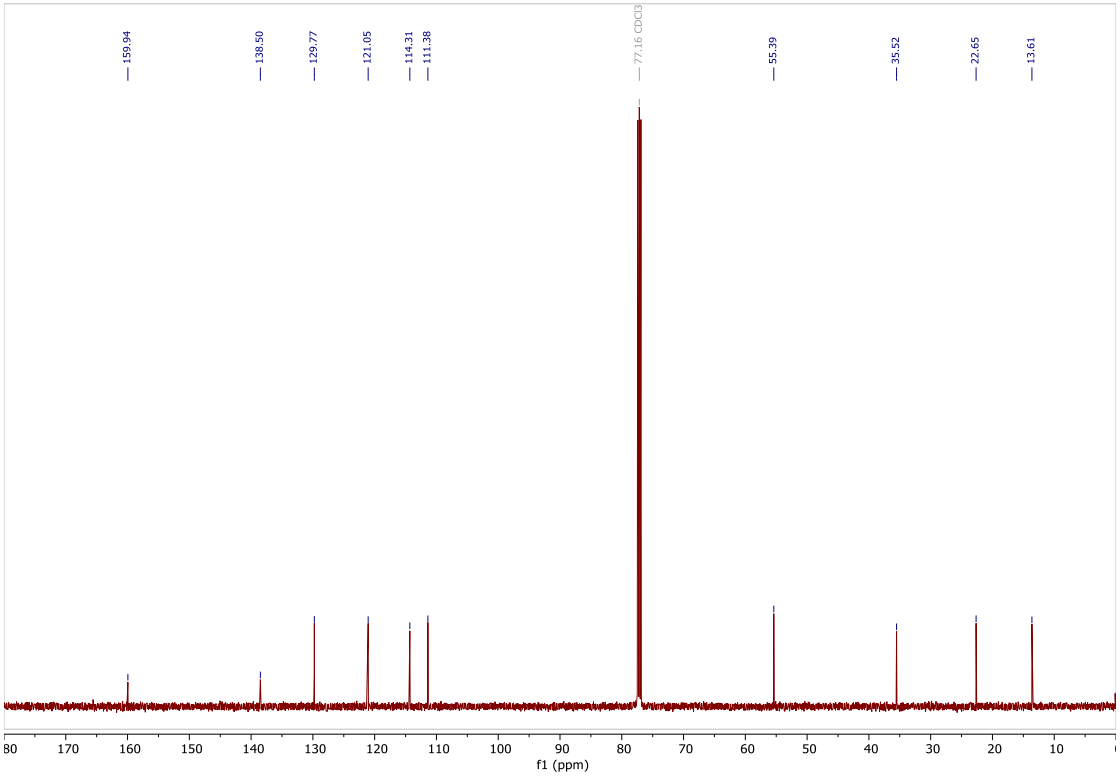

*Butyl(4-methoxyphenyl)sulfane* ***27ar***

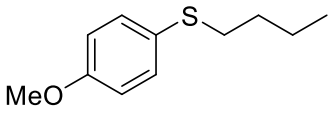


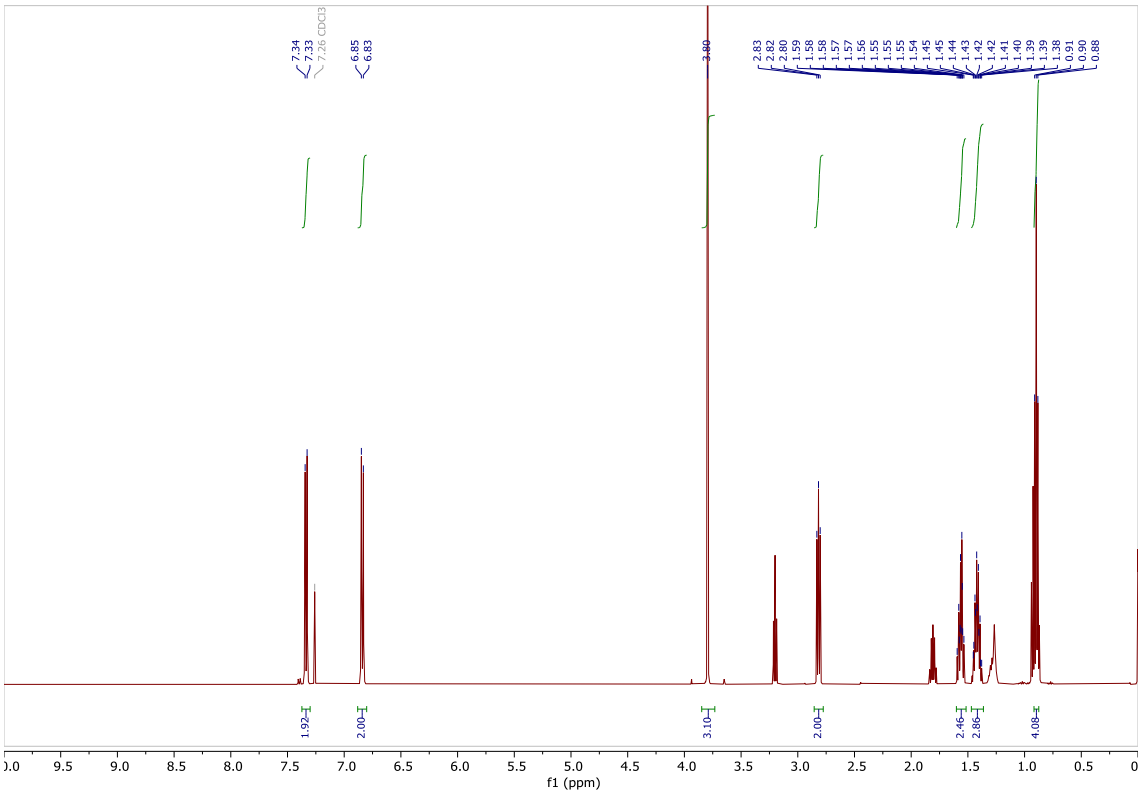


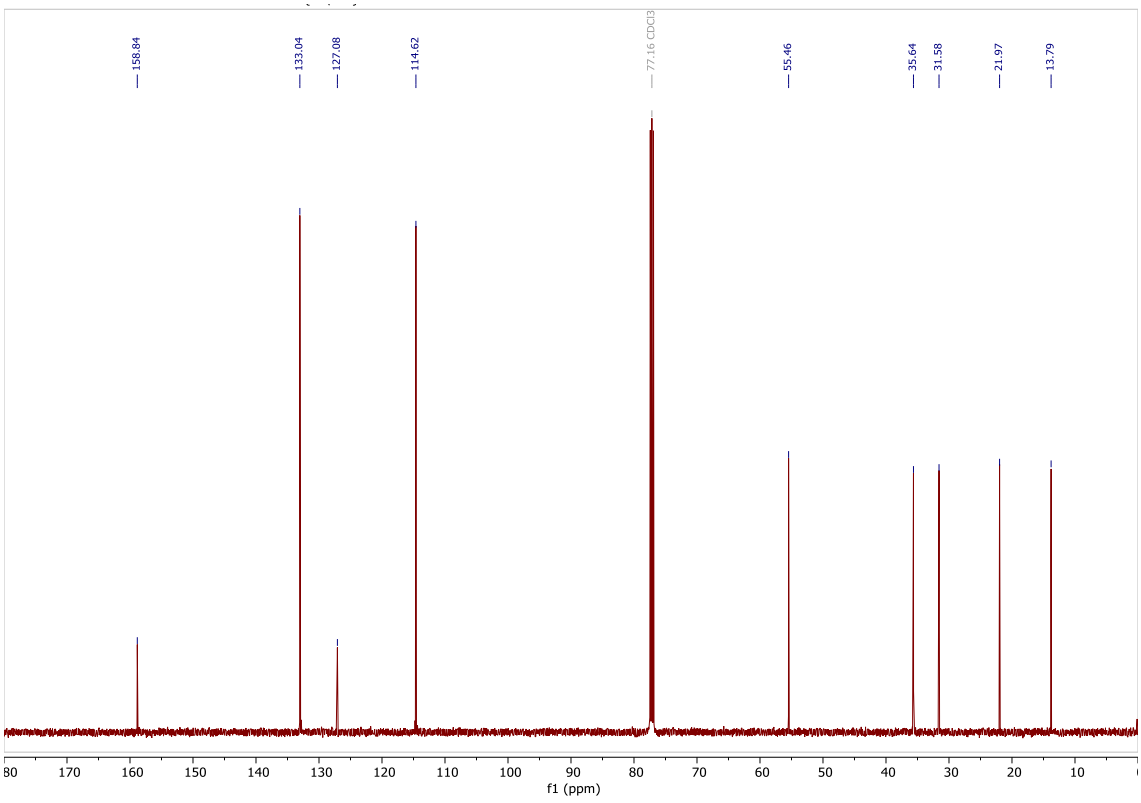

*1-(Phenylthio)propan-2-one* ***38d***

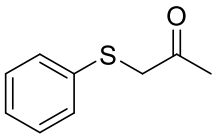


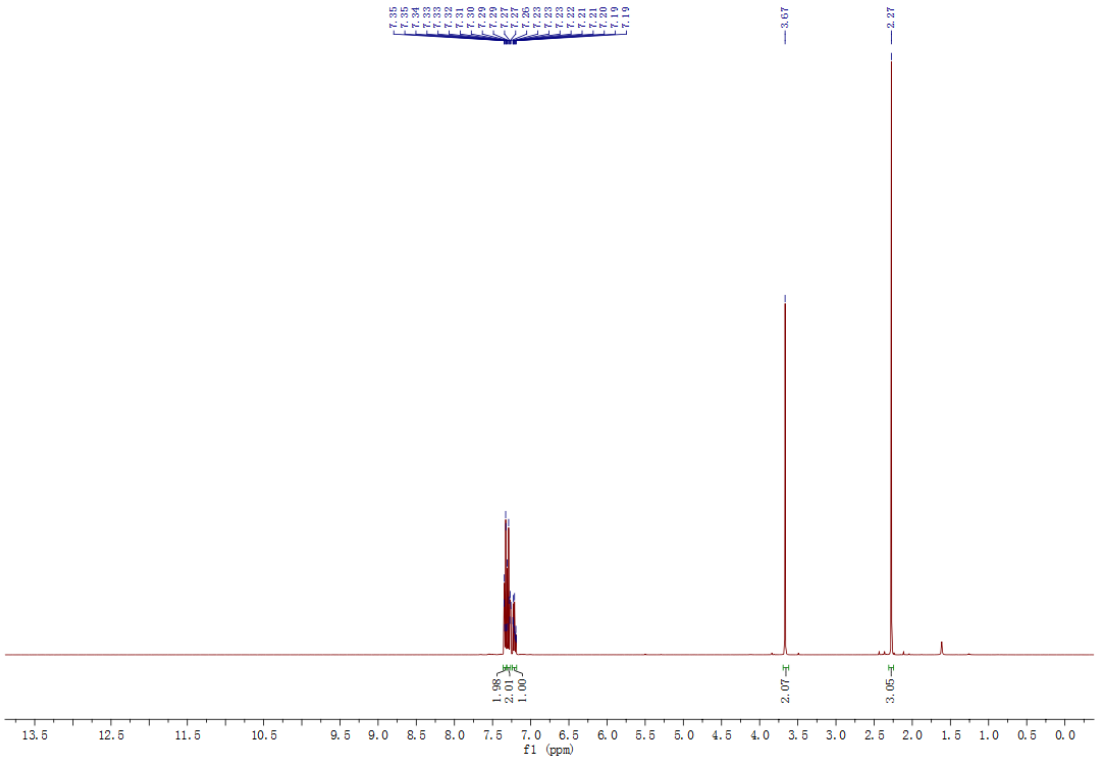


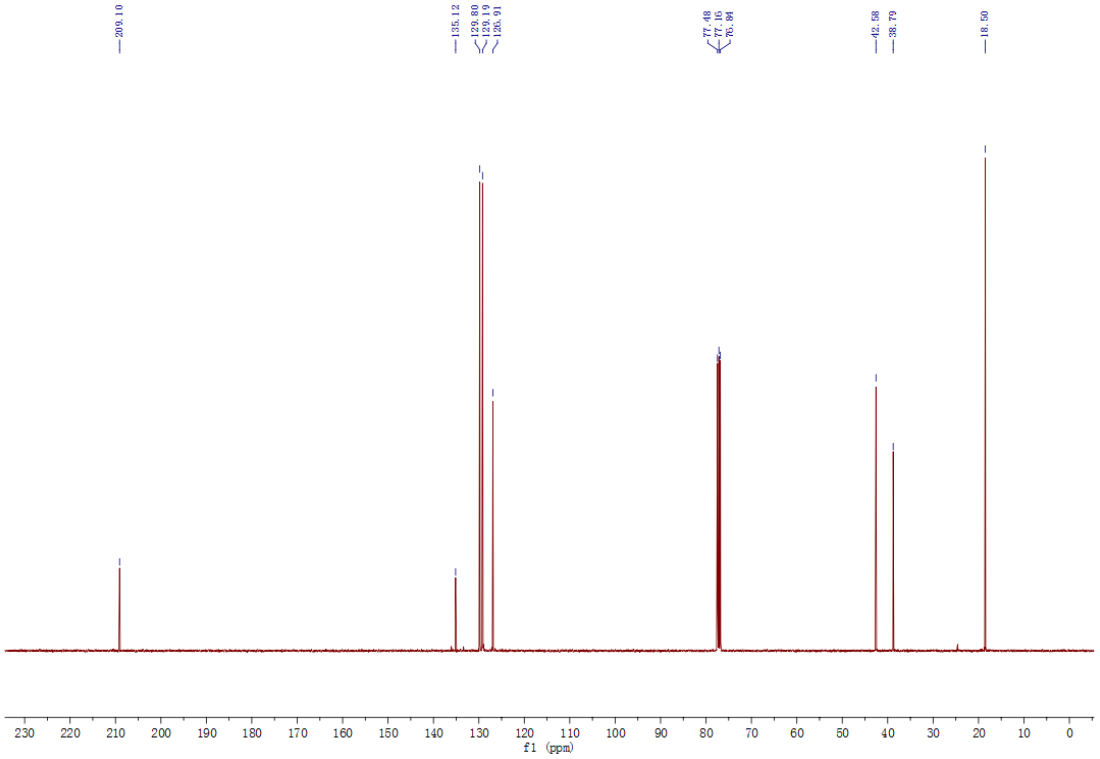

*1-(phenylthio)butan-2-one* ***38e***

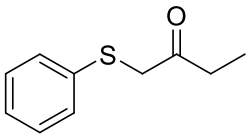


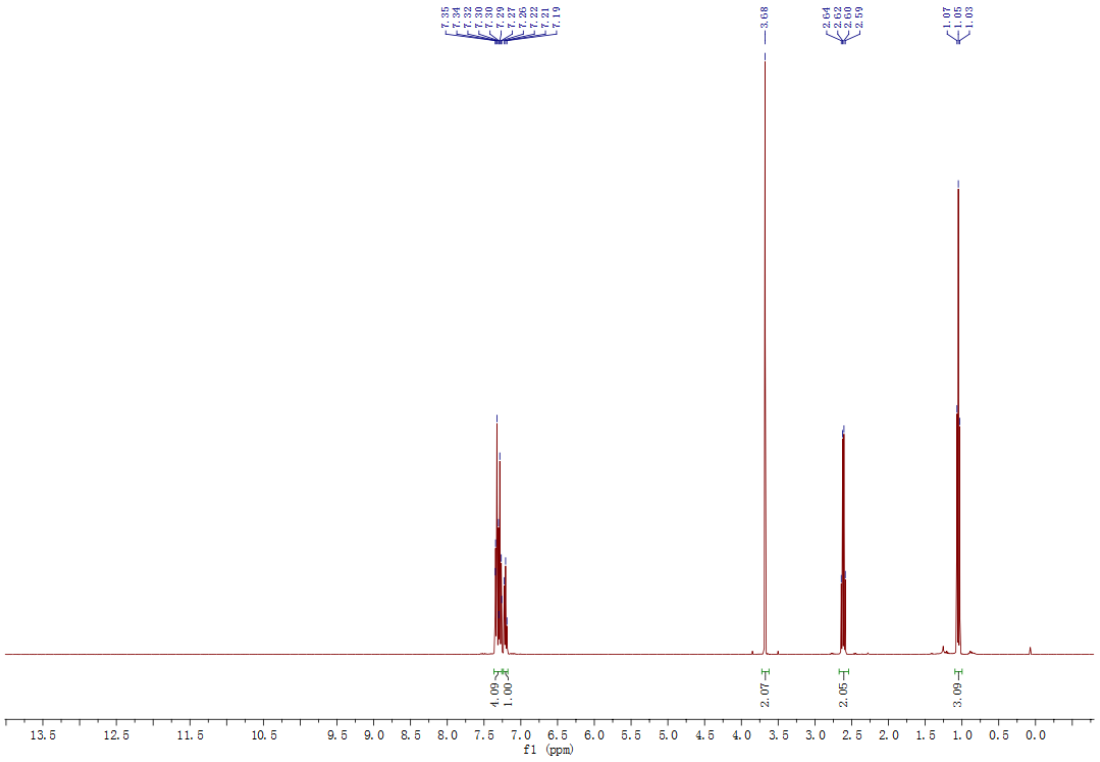


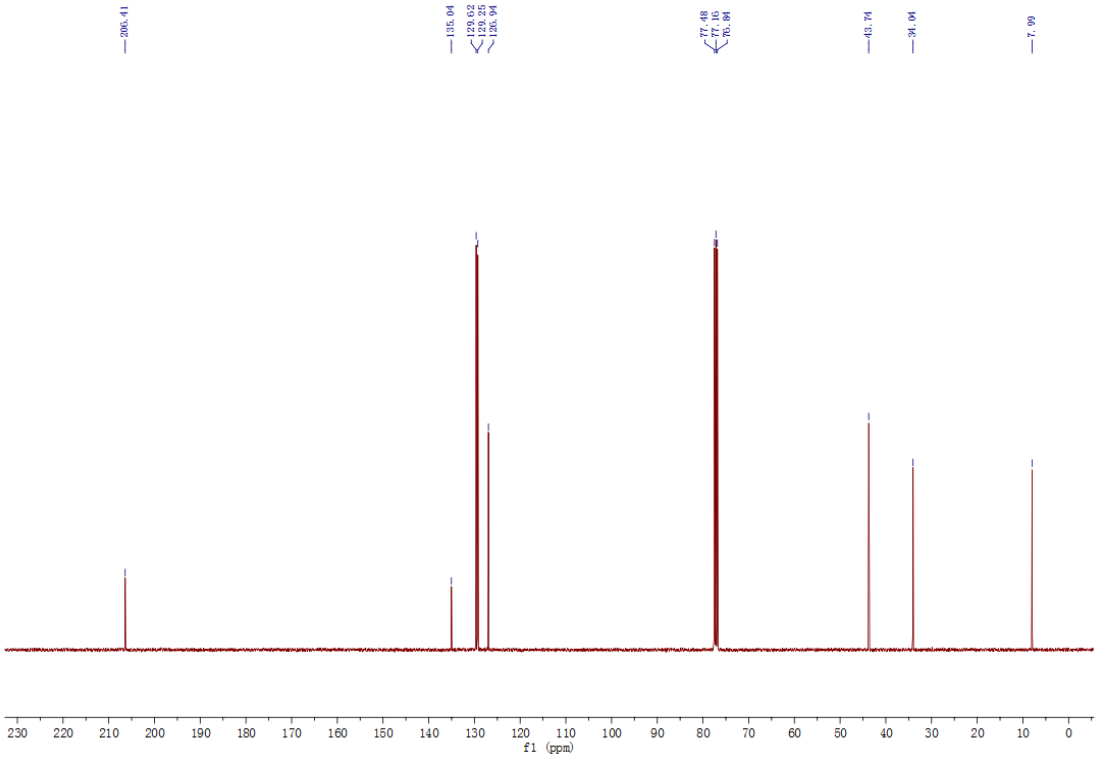

*3-Methyl-1-(phenylthio)butan-2-one* ***38f***

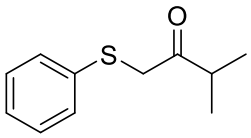


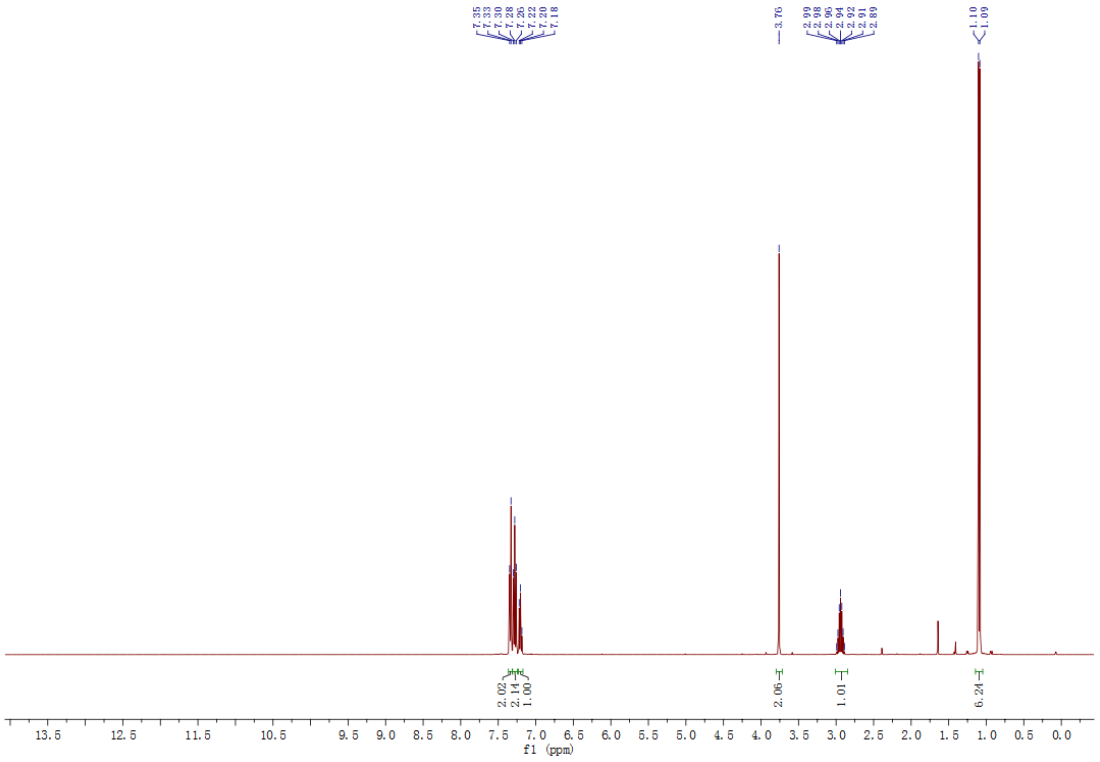


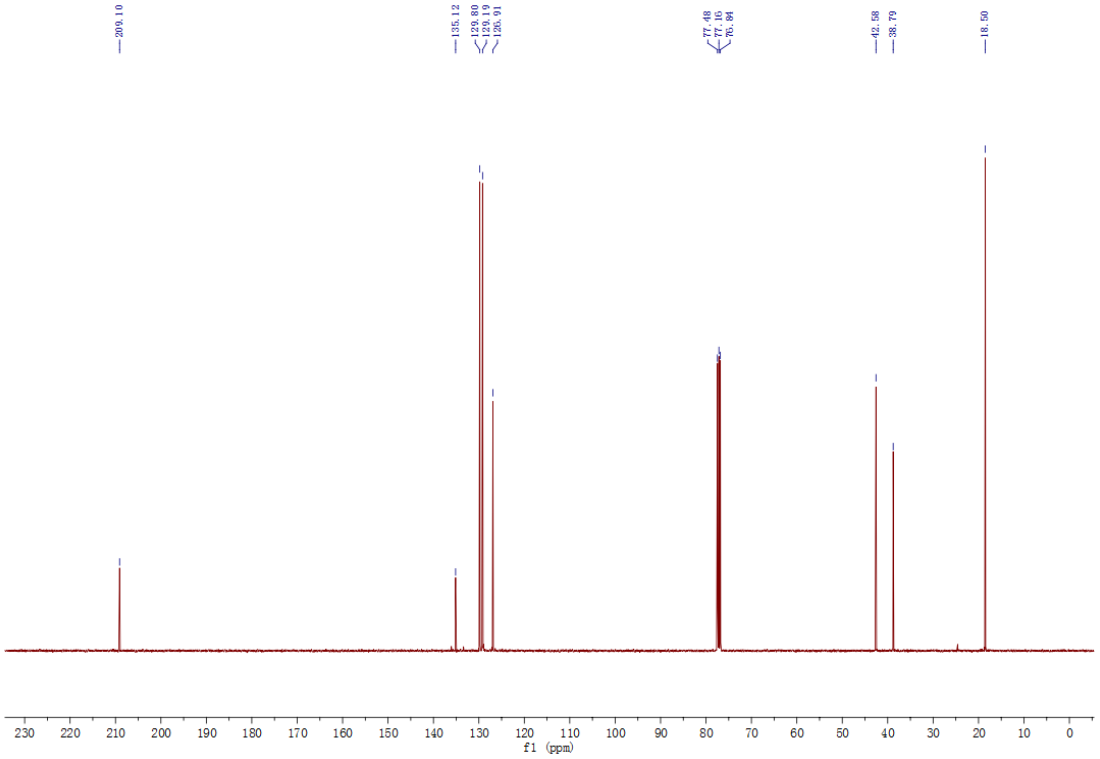

## Sulfoxides NMR spectra

*Methyl phenyl sulfoxide* ***28a***

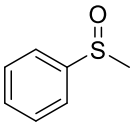


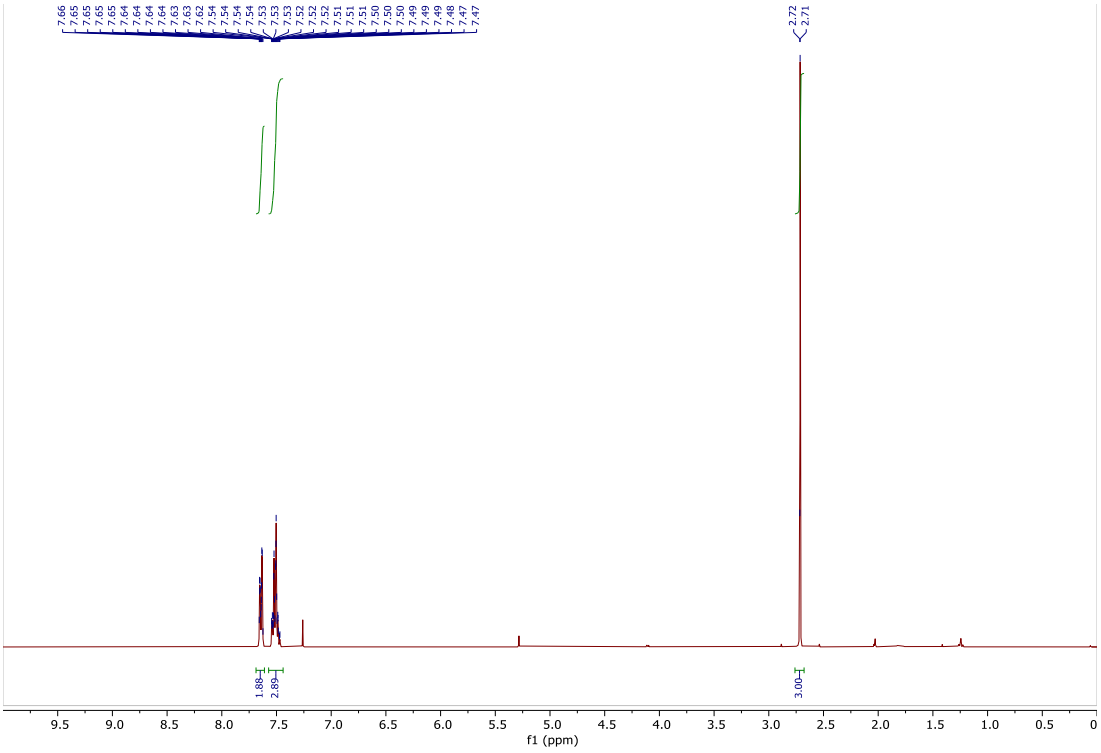


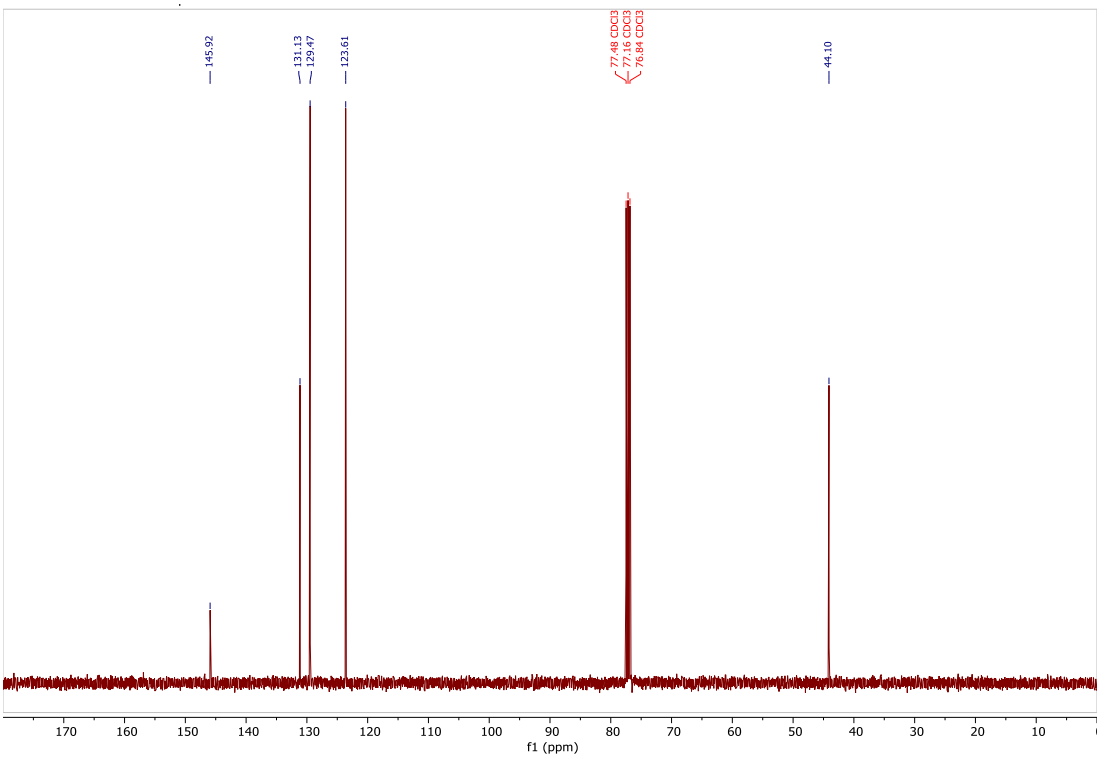

*1-Fluoro-4-(methylsulfinyl)benzene* ***28b***

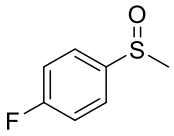


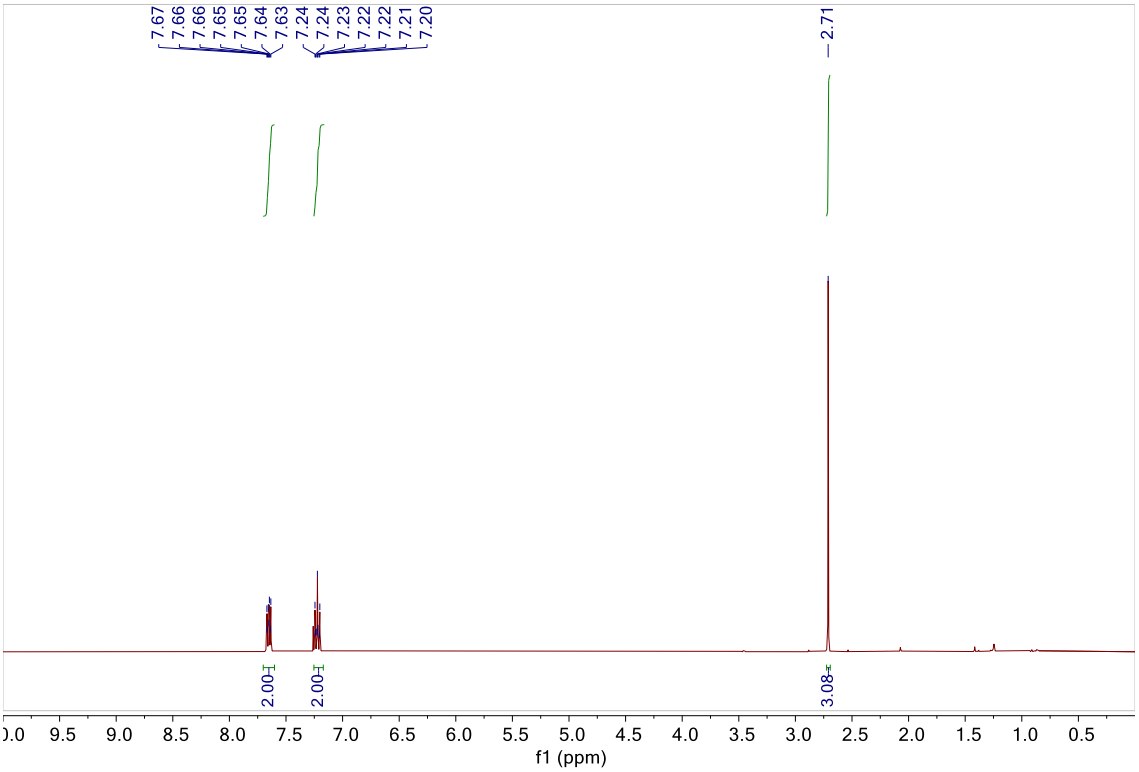


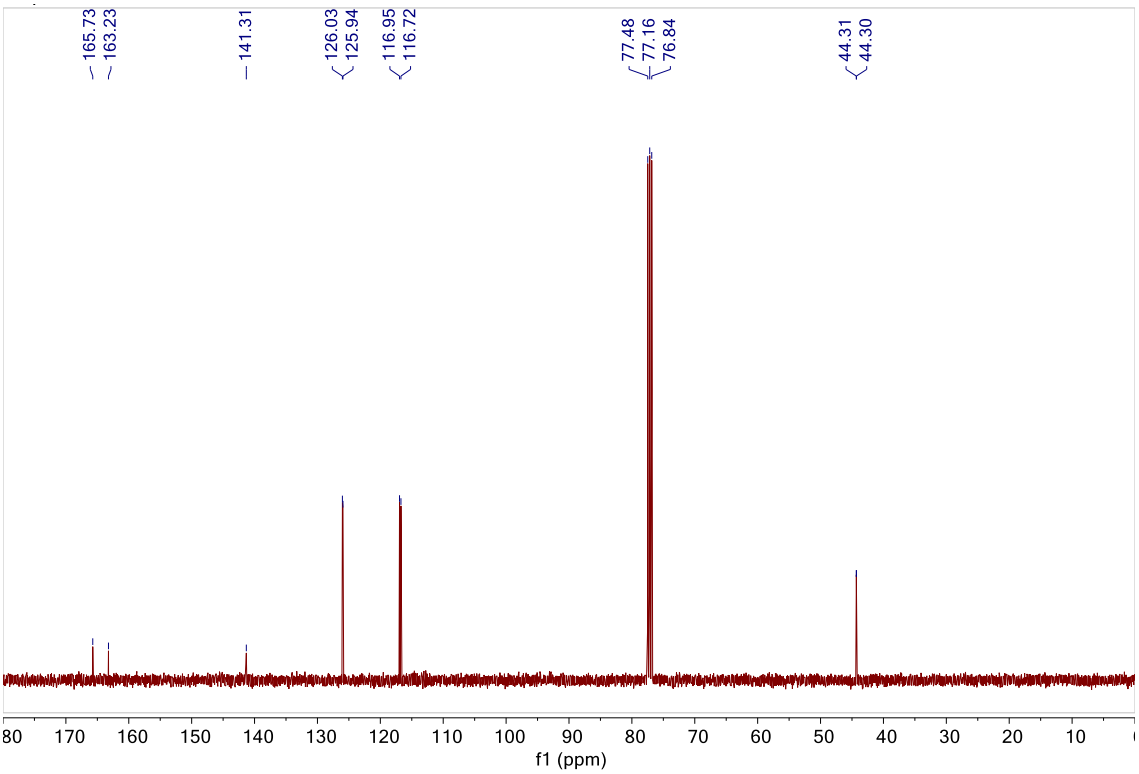

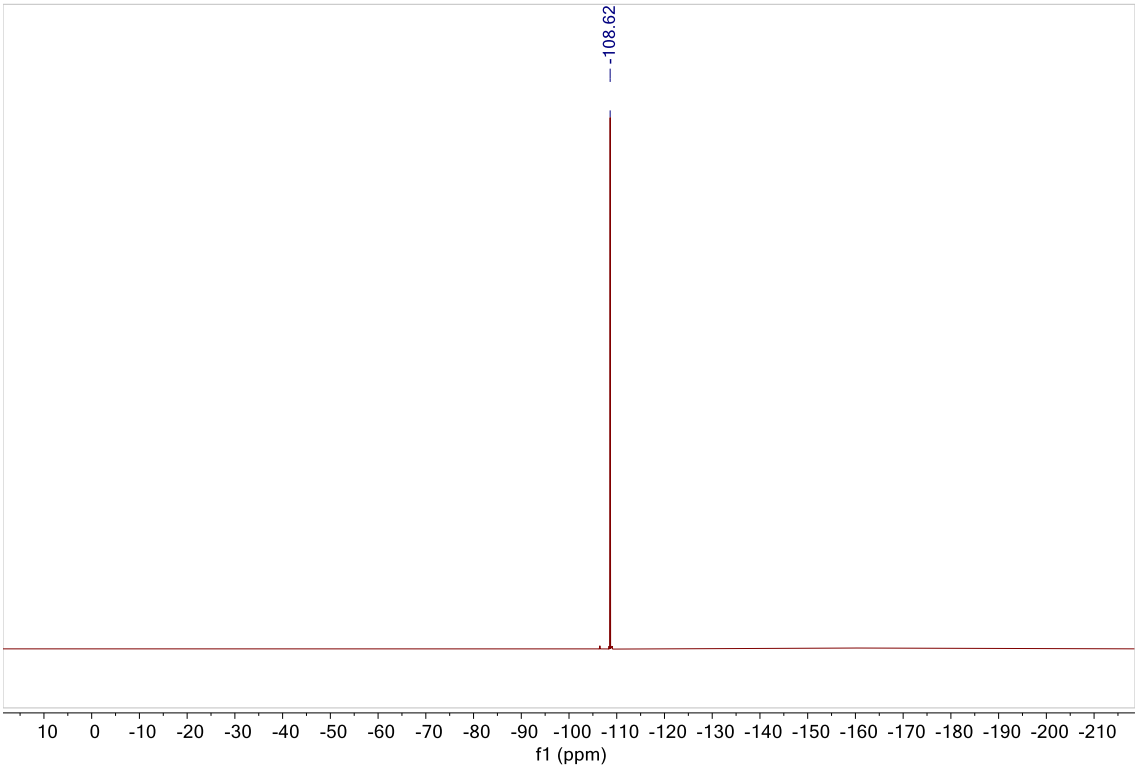
-108.62
10 0 -10 -20 -30 -40 -50 -60 -70 -80 -90 -100 -110 -120 -130 -140 -150 -160 -170 -180 -190 -200 -210
f1 (ppm)

*(Ethylsulfinyl)benzene* ***28c***

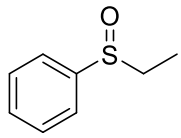

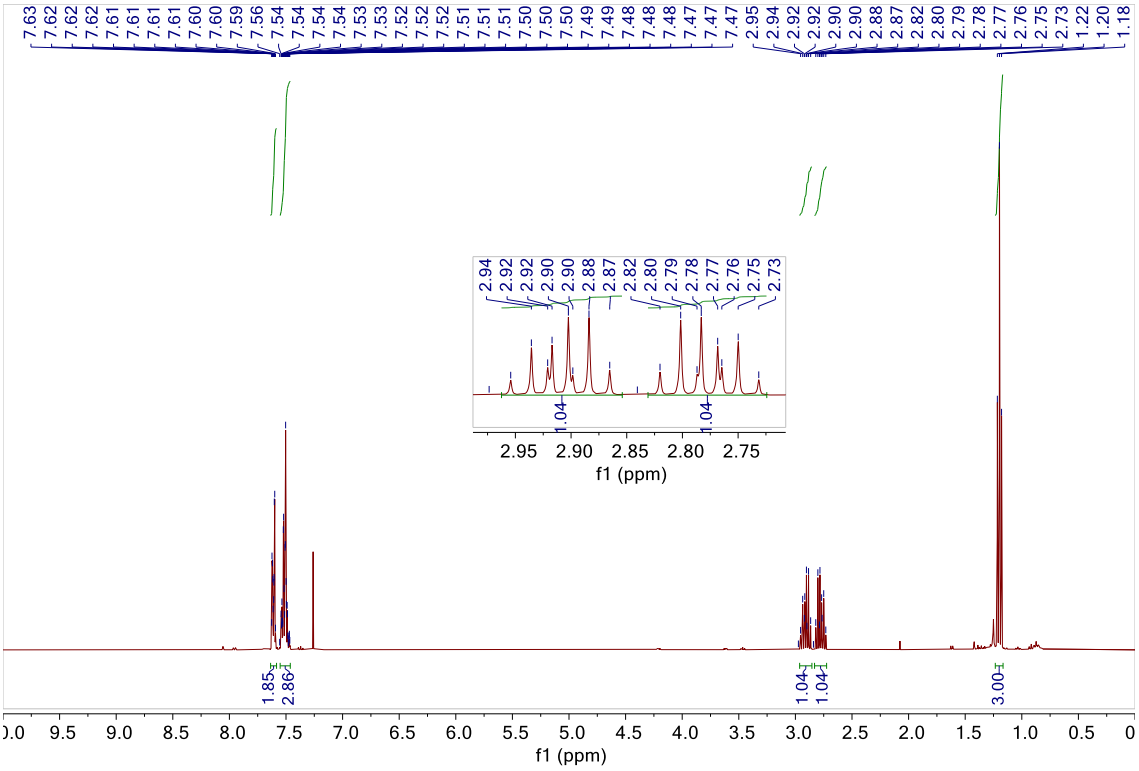


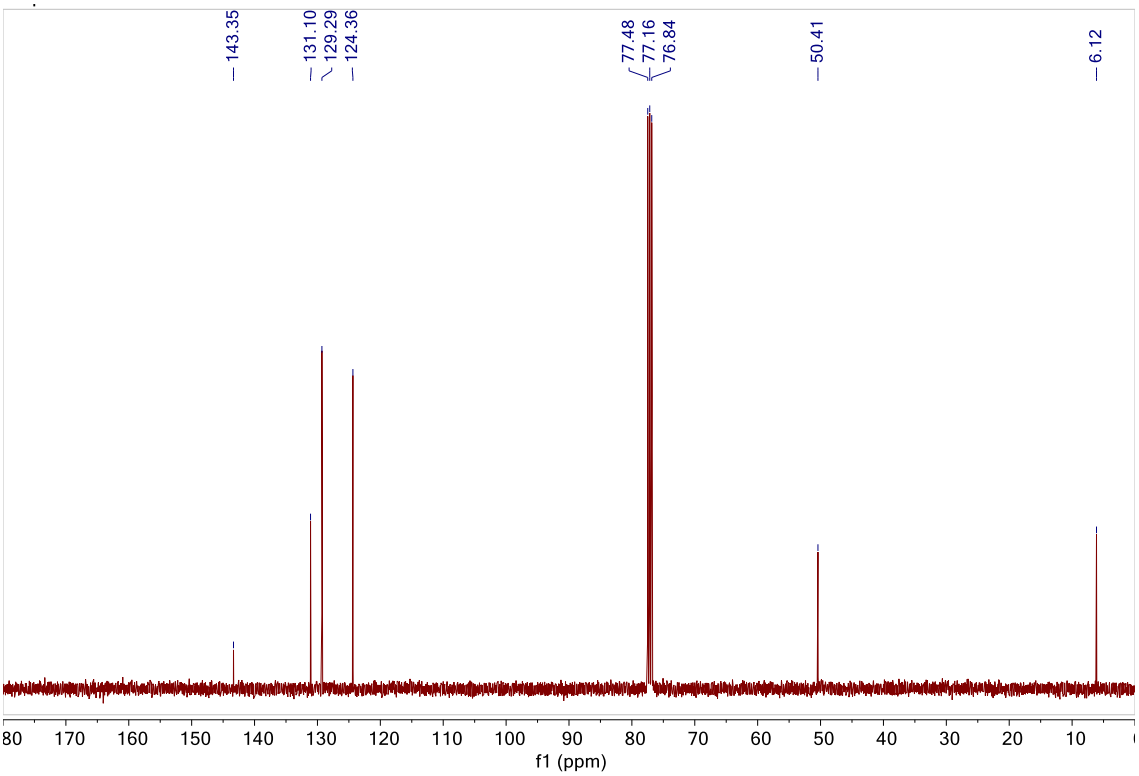

*1-(Ethylsulfinyl)-4-methylbenzene* ***28d***

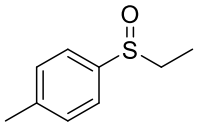

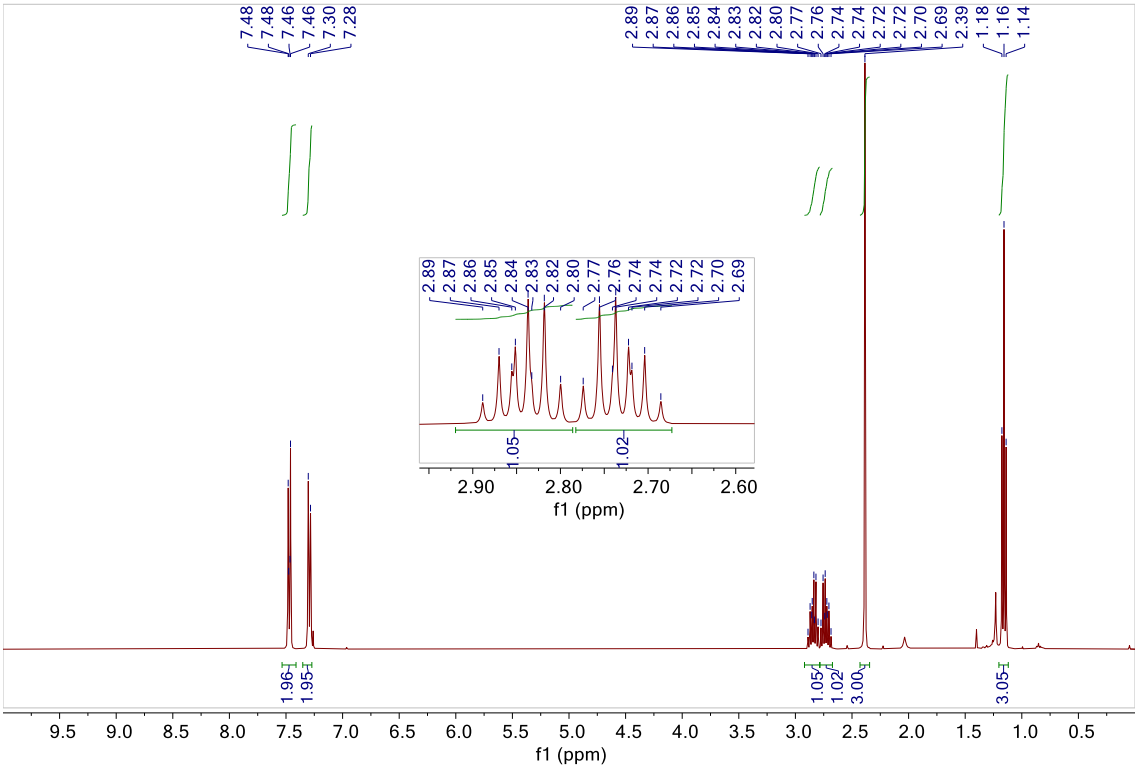


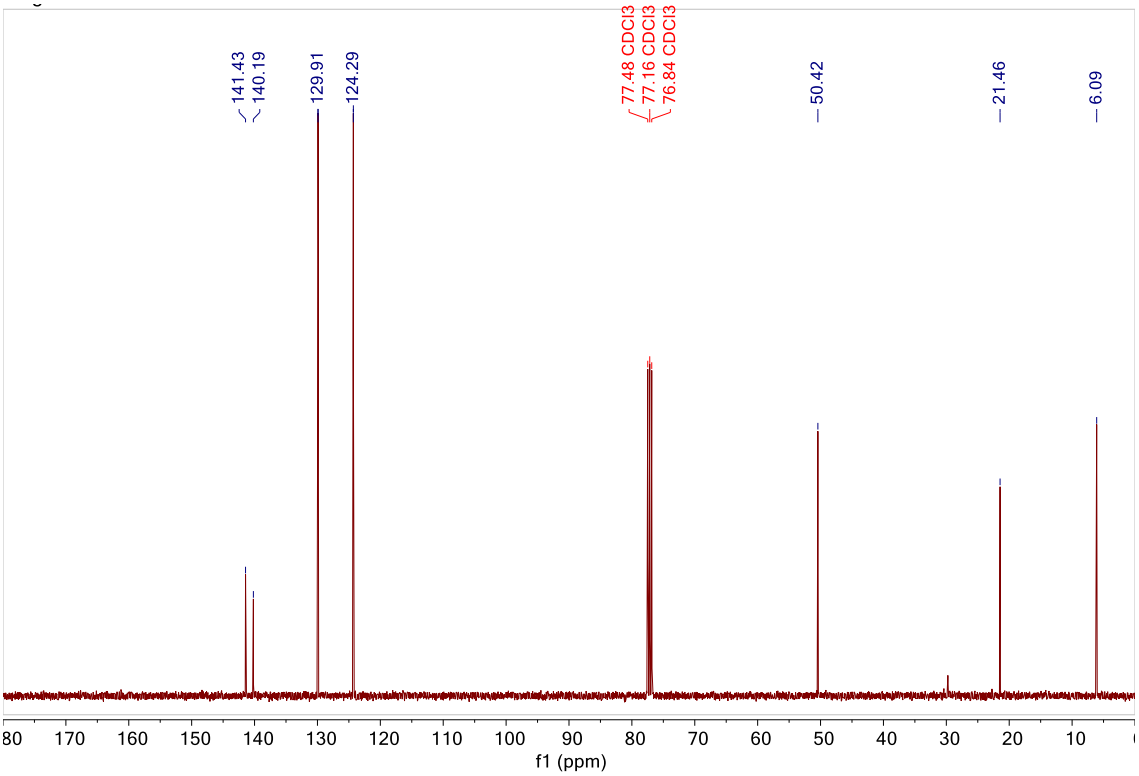

*1-(Ethylsulfinyl)-4-methoxybenzene* ***28e***

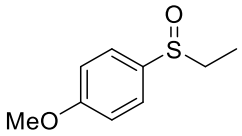


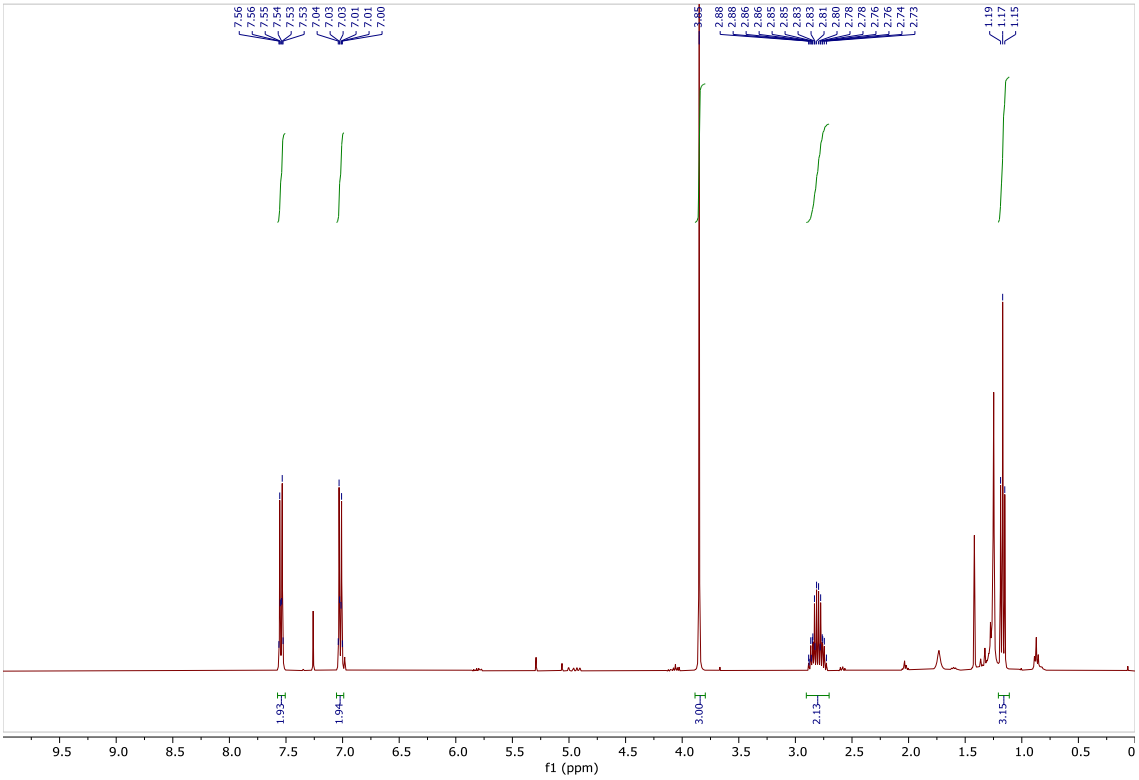


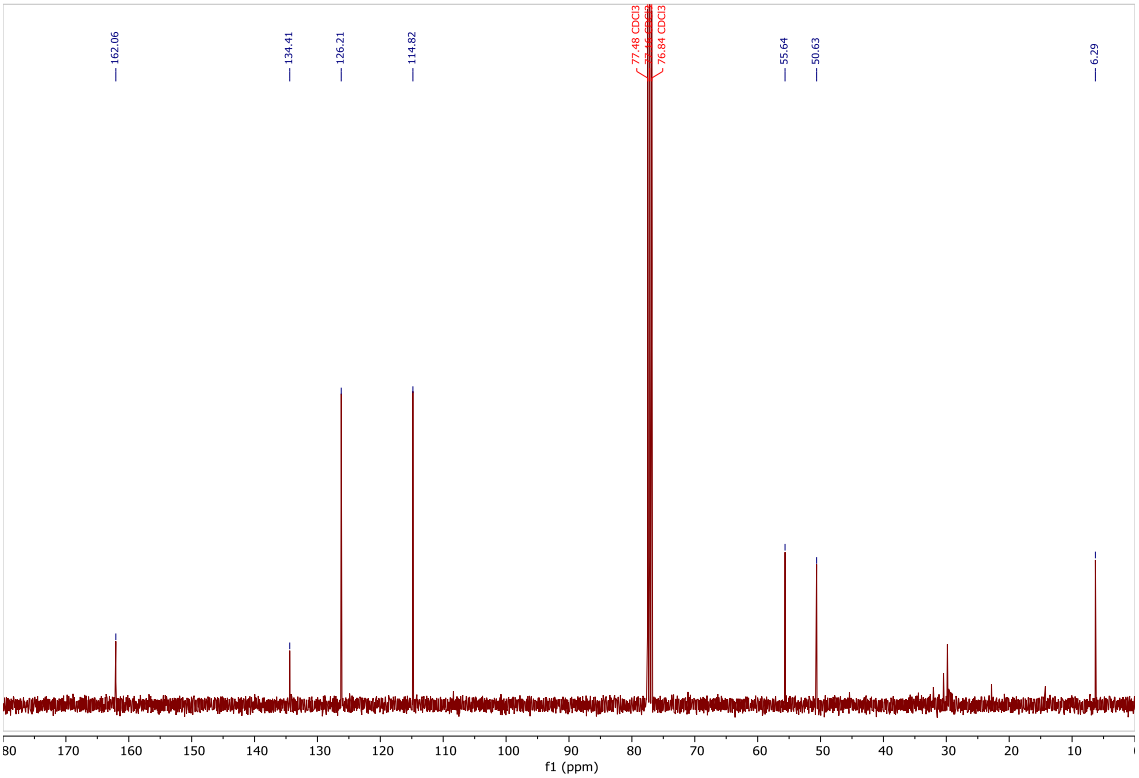

*1-Chloro-4-(ethylsulfinyl)benzene* ***28f***

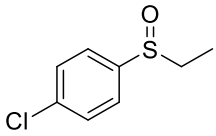


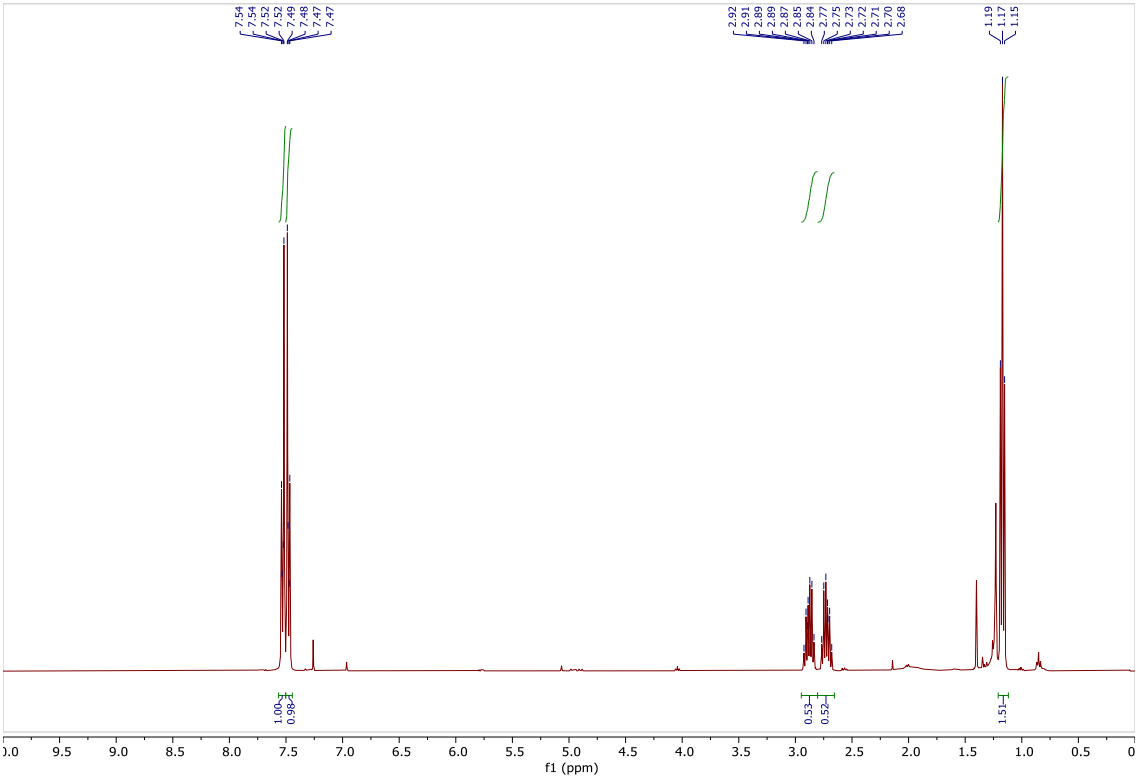


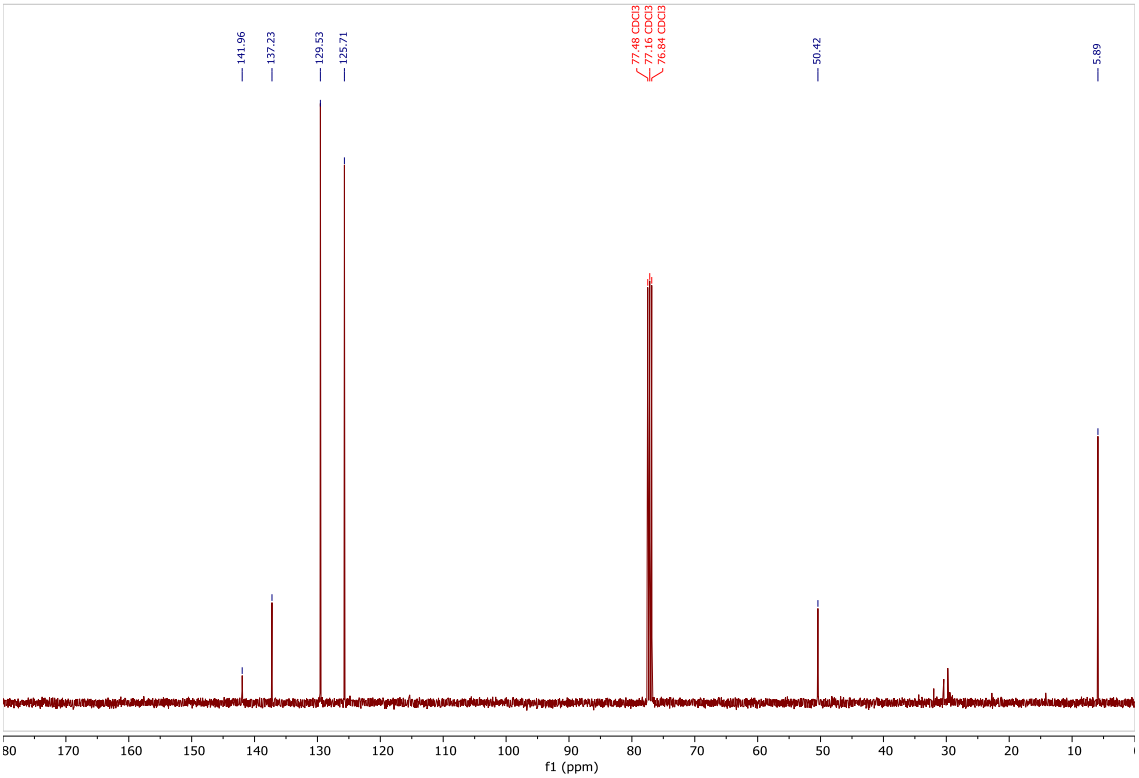

*1-Bromo-4-(ethylsulfinyl)benzene* ***28g***

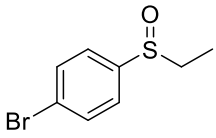


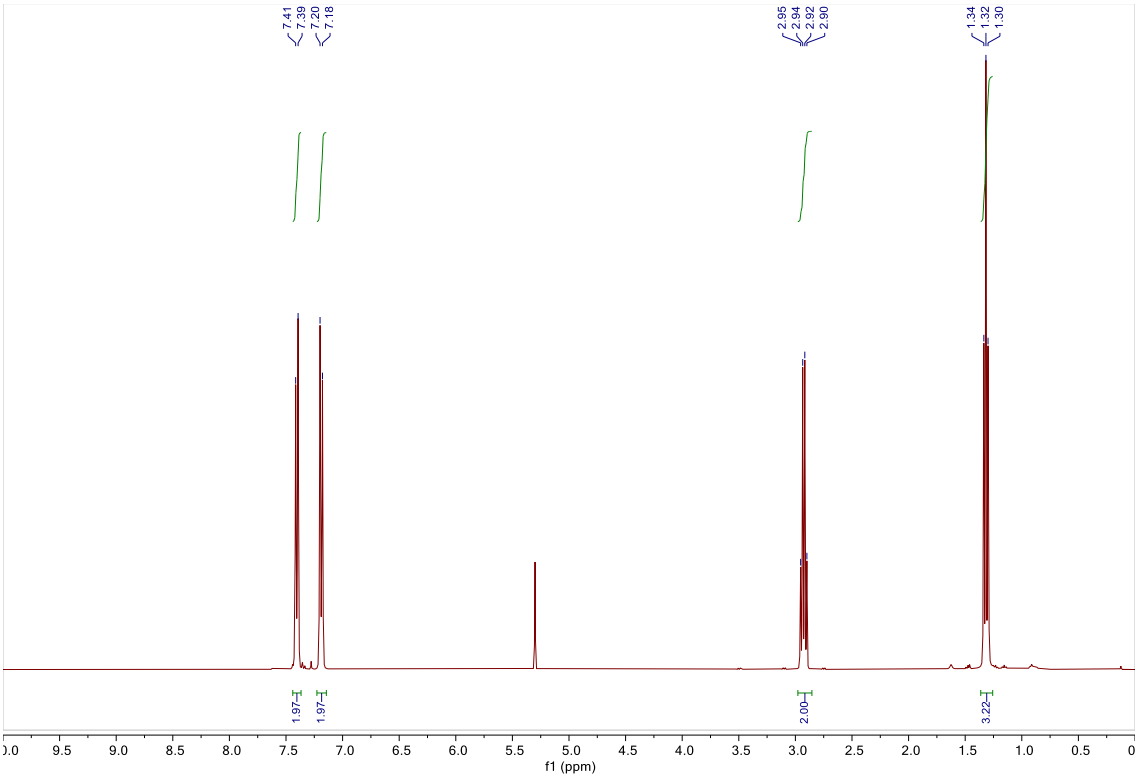


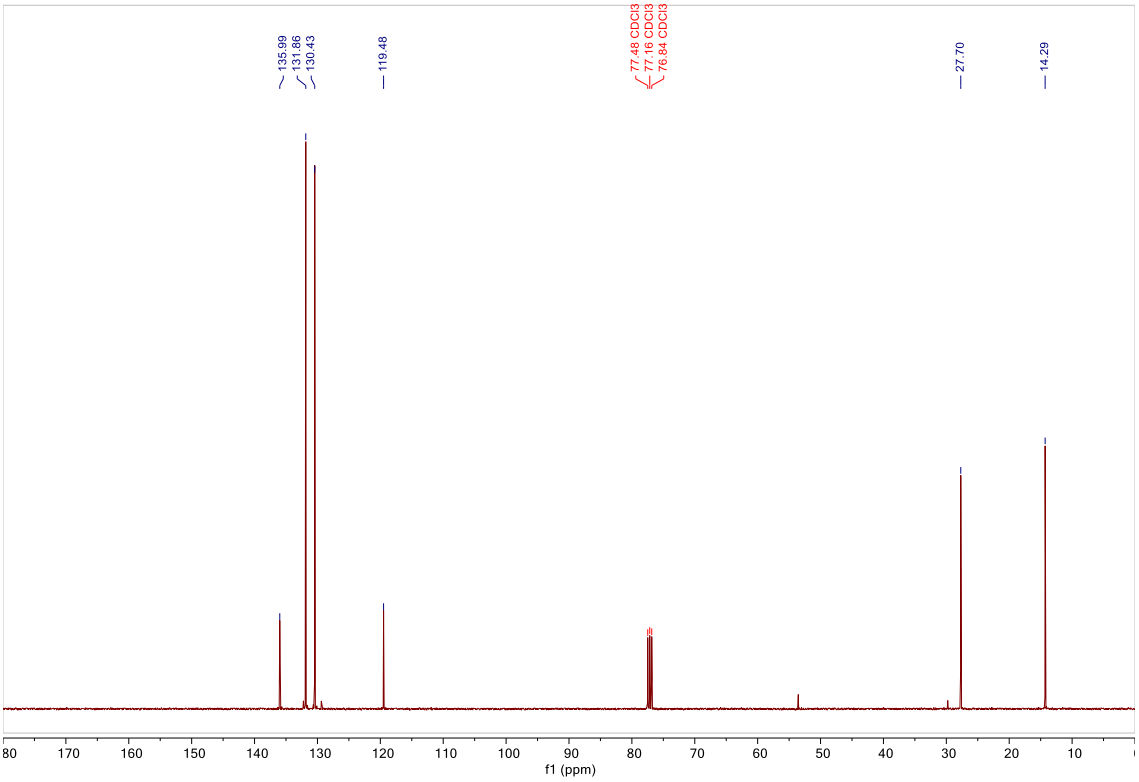

*1-Chloro-2-(ethylsulfinyl)benzene* ***28h***

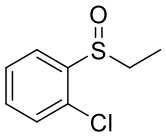


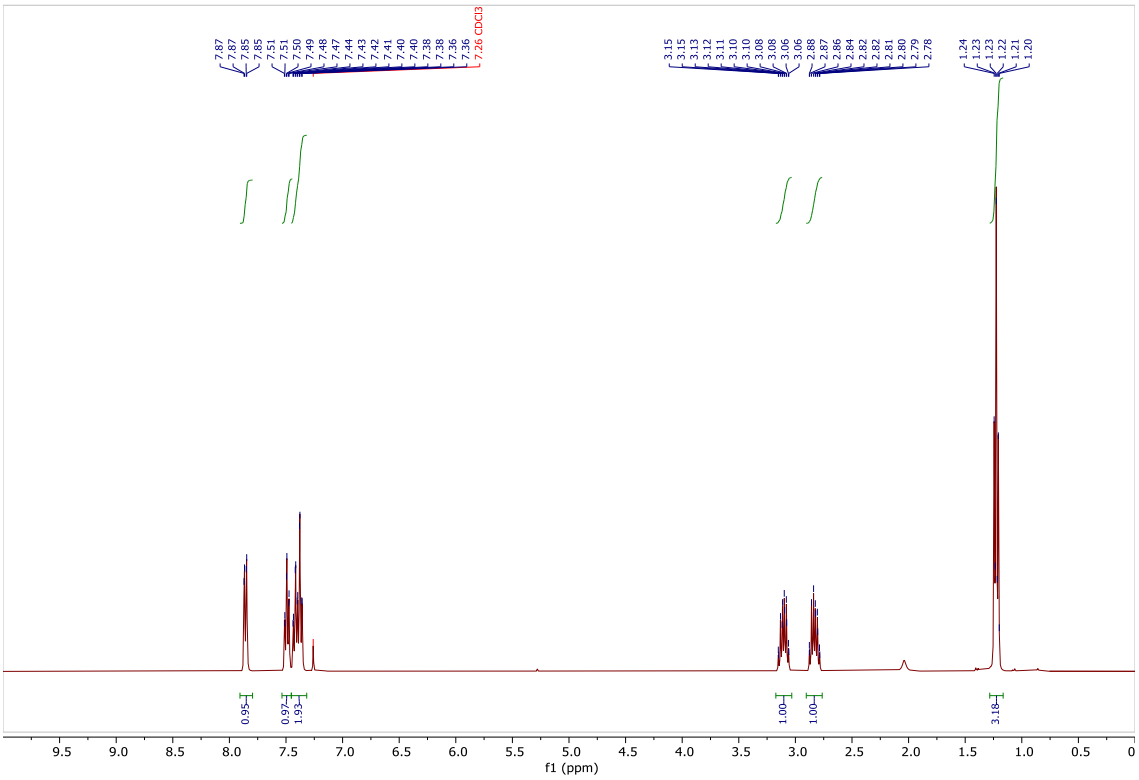


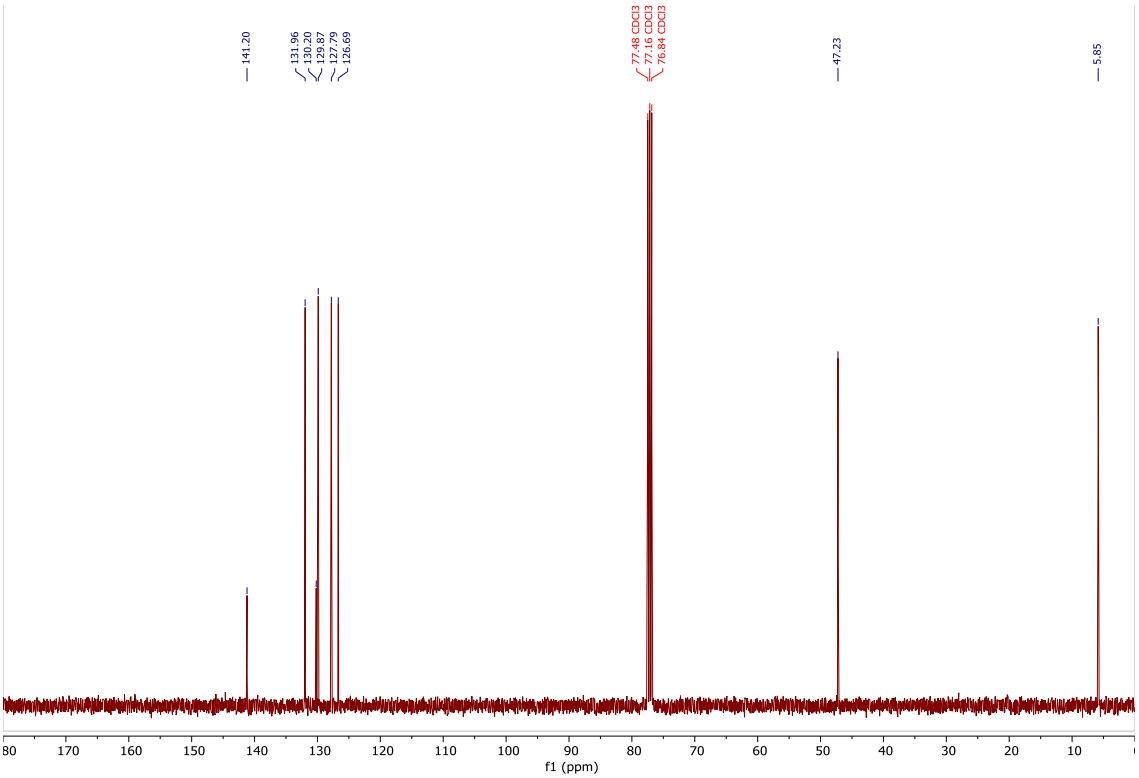

*1-Bromo-2-(ethylsulfinyl)benzene* ***28i***

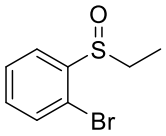


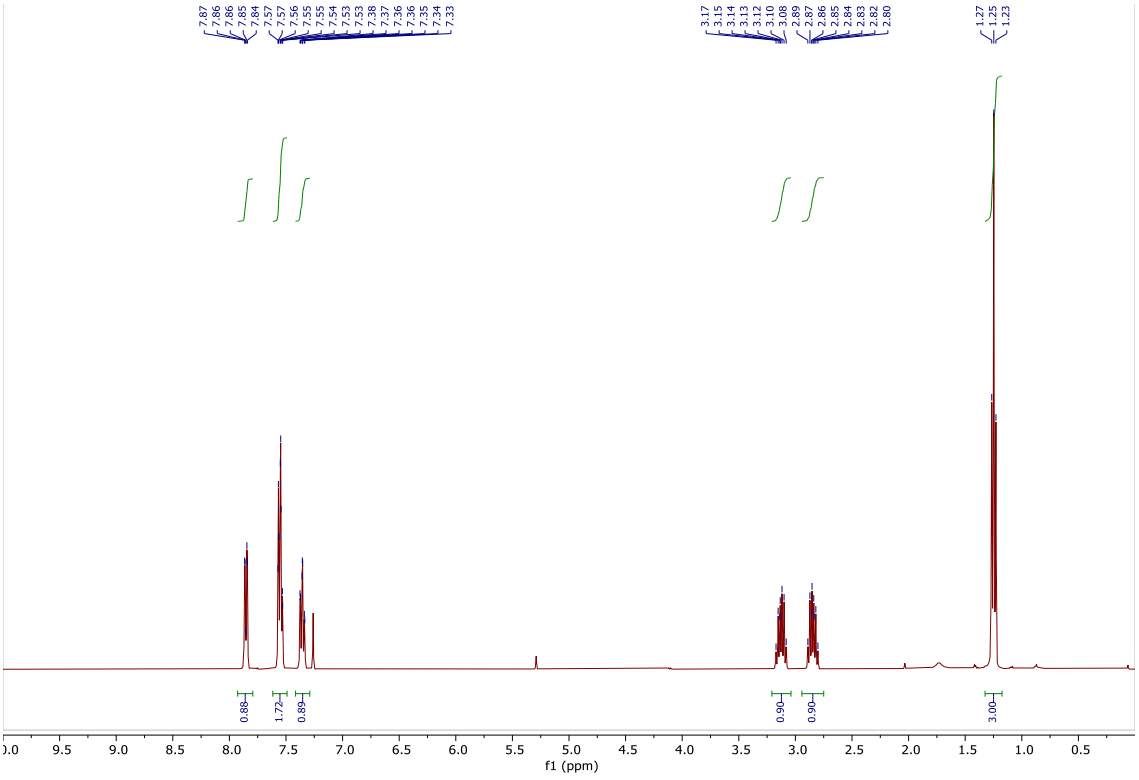


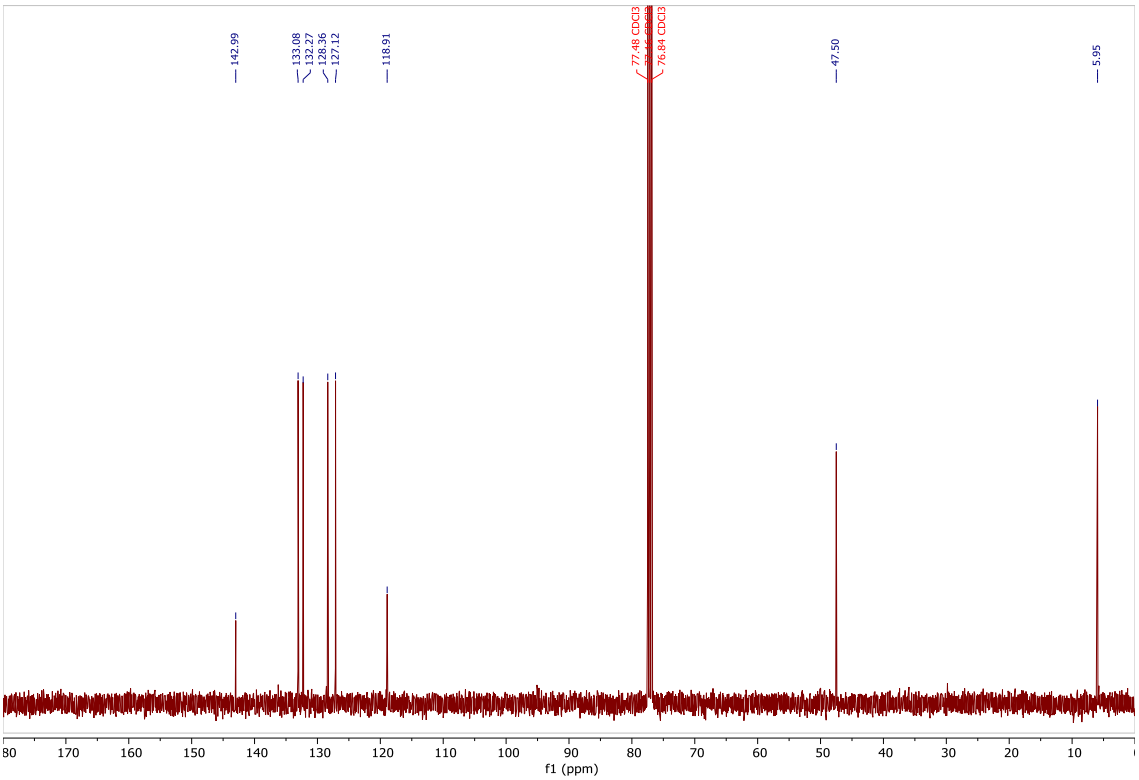

*1-Methoxy-4-(propylsulfinyl)benzene* ***28j***

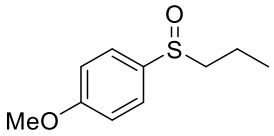


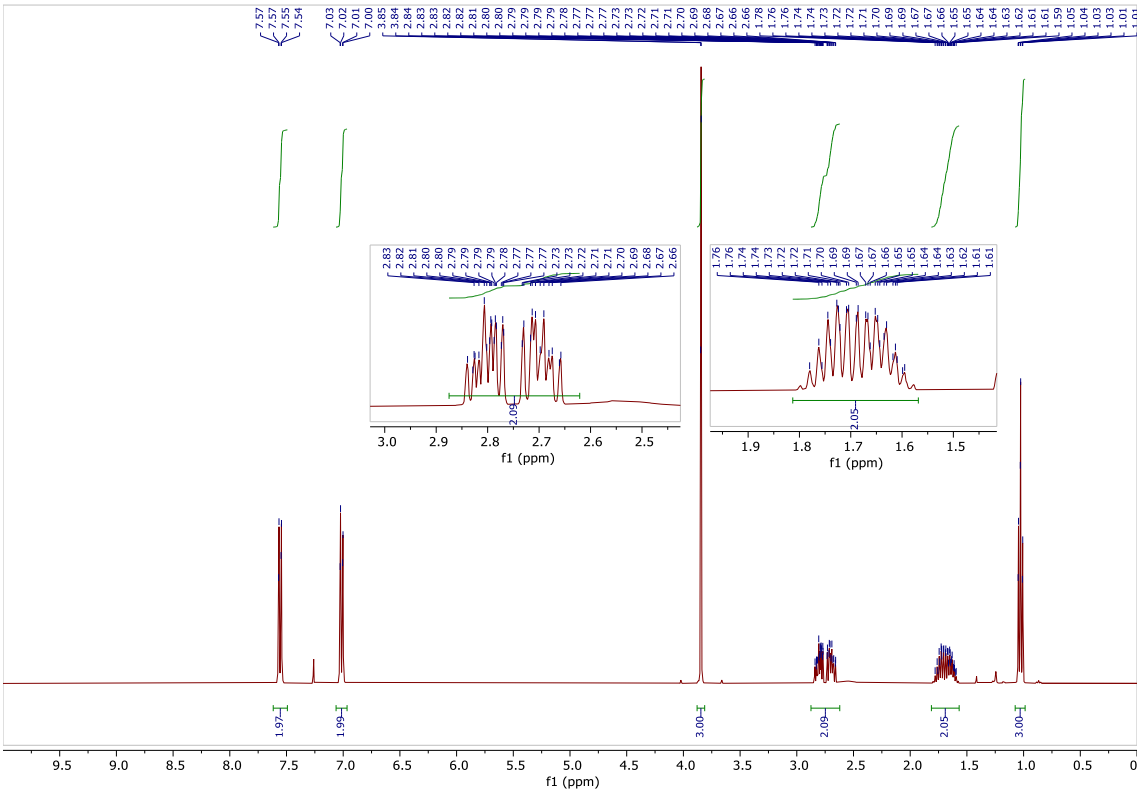


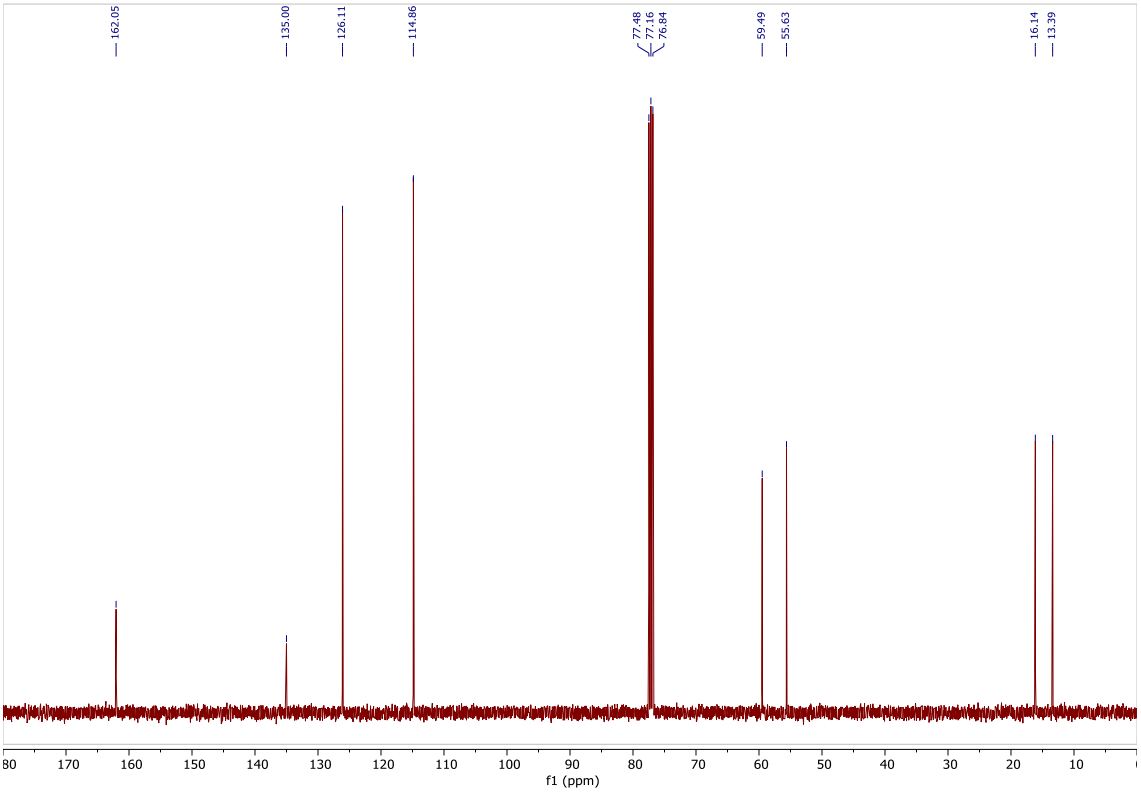

*1-Methyl-4-(propylsulfinyl)benzene* ***28k***

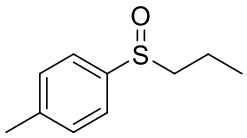

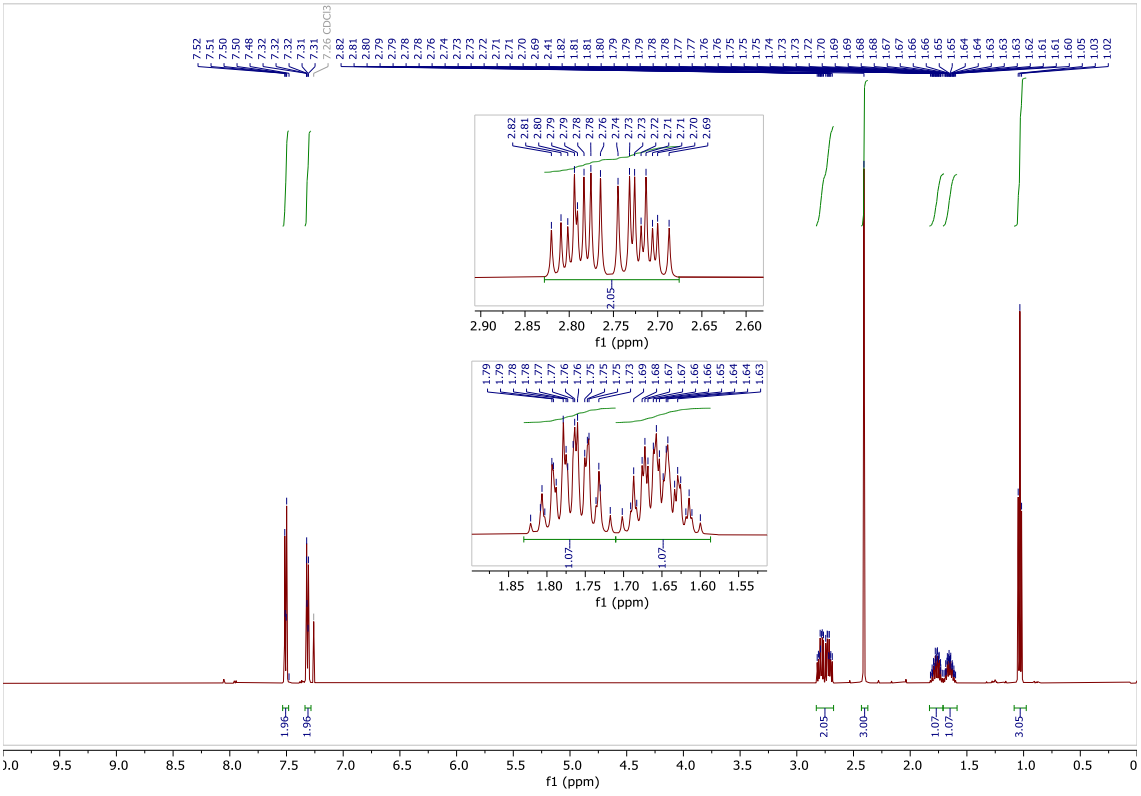


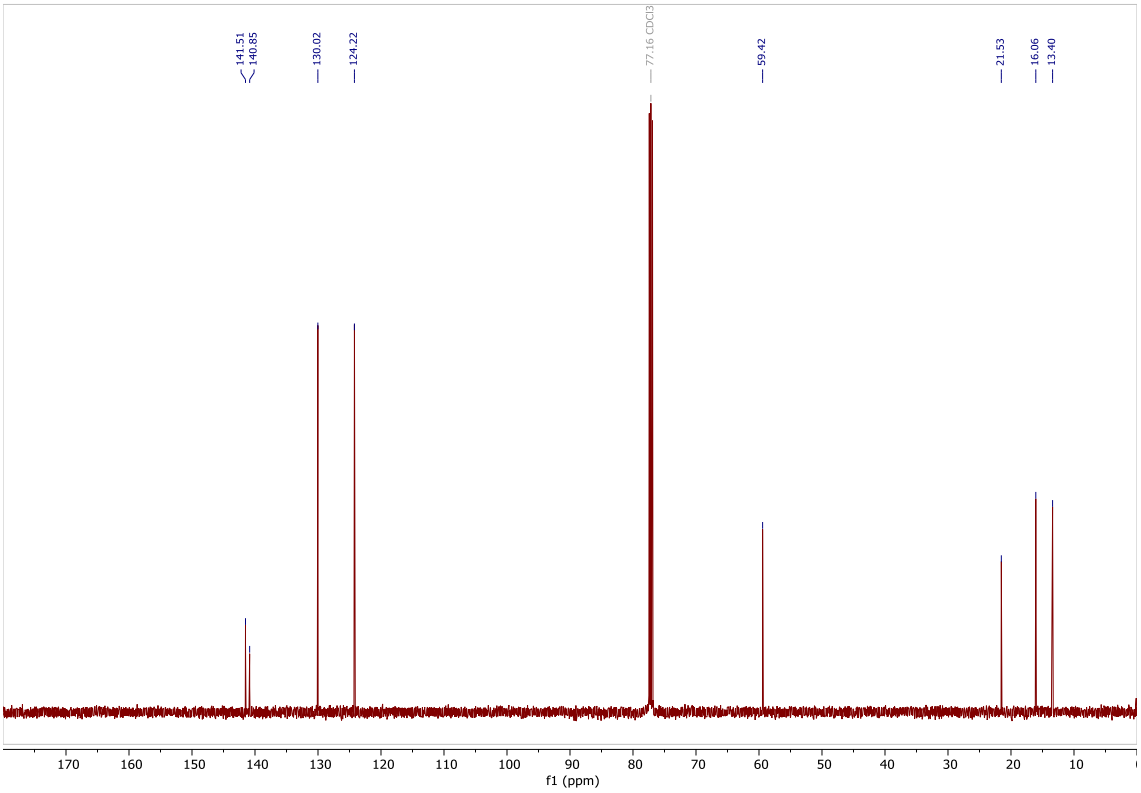

*Allyl phenyl sulfoxide* ***28l***

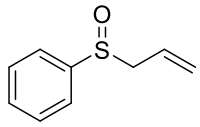

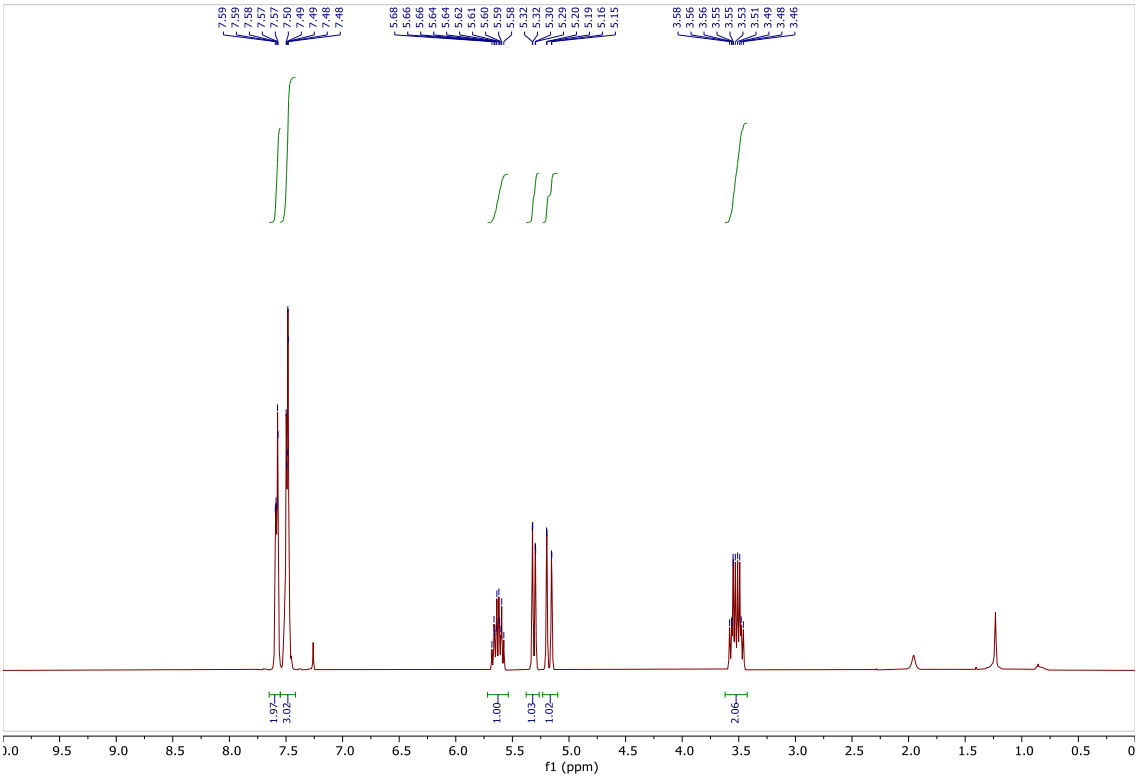


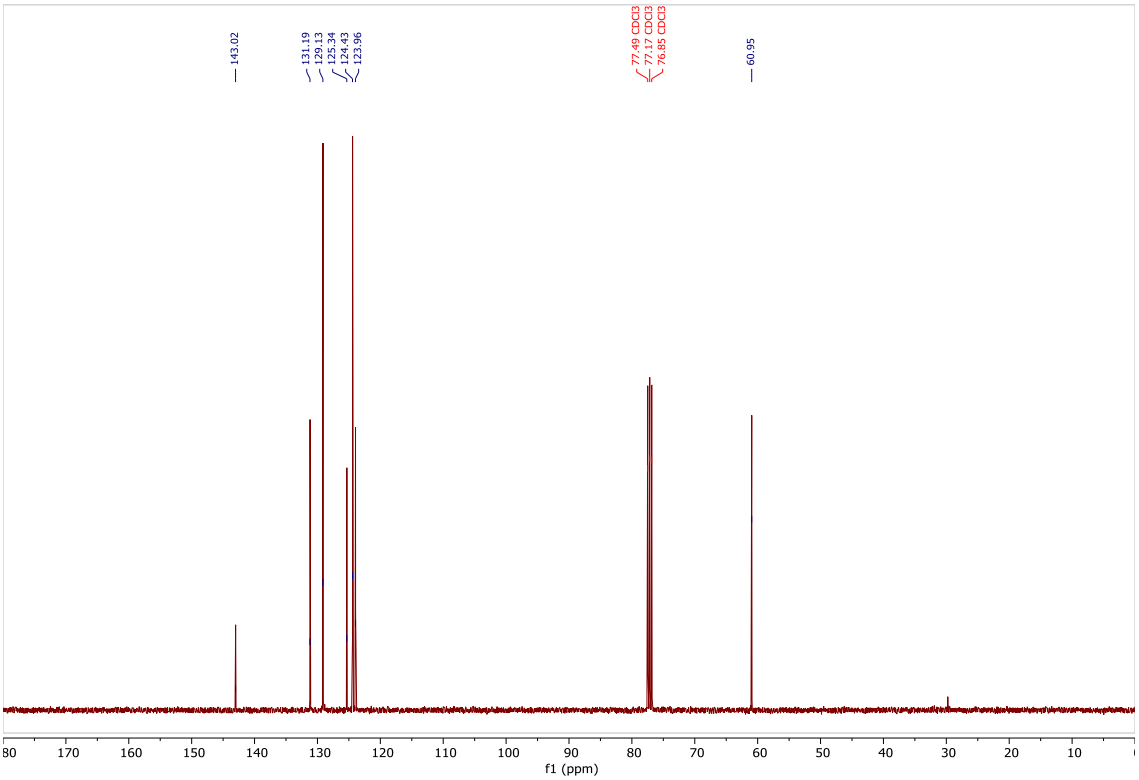

*(But-3-en-1-ylsulfinyl)benzene* ***28m***

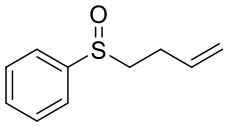

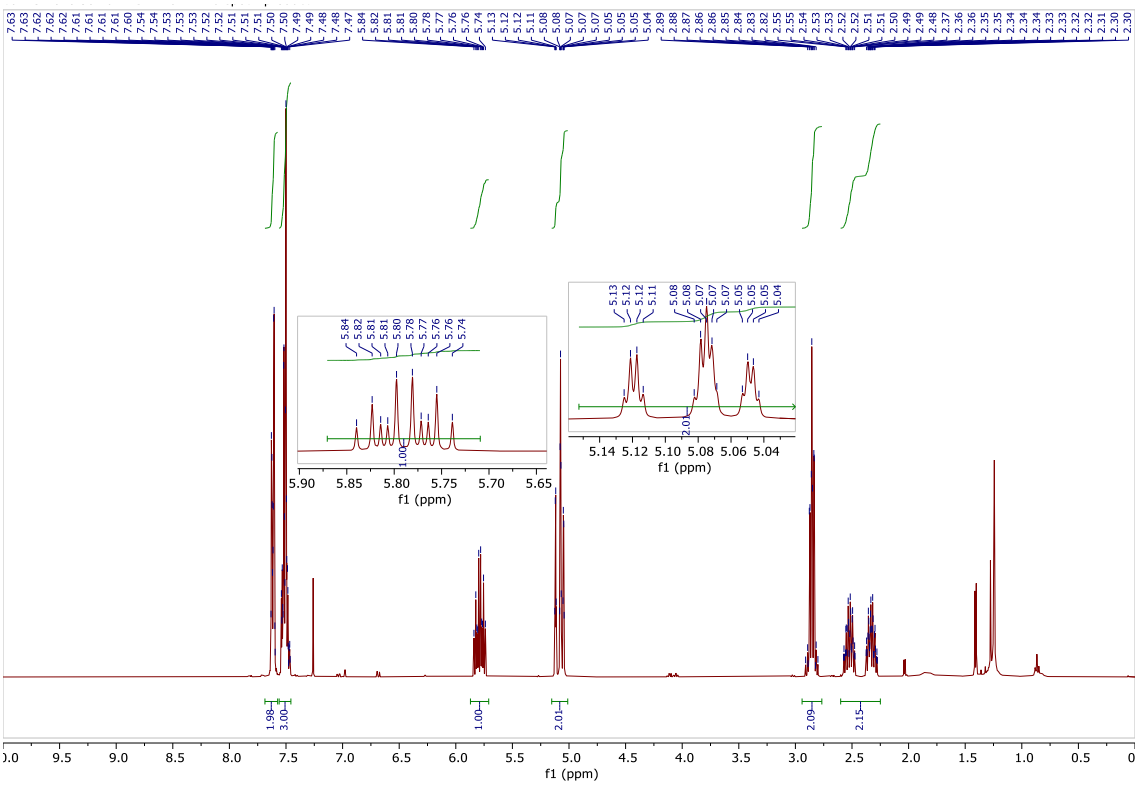

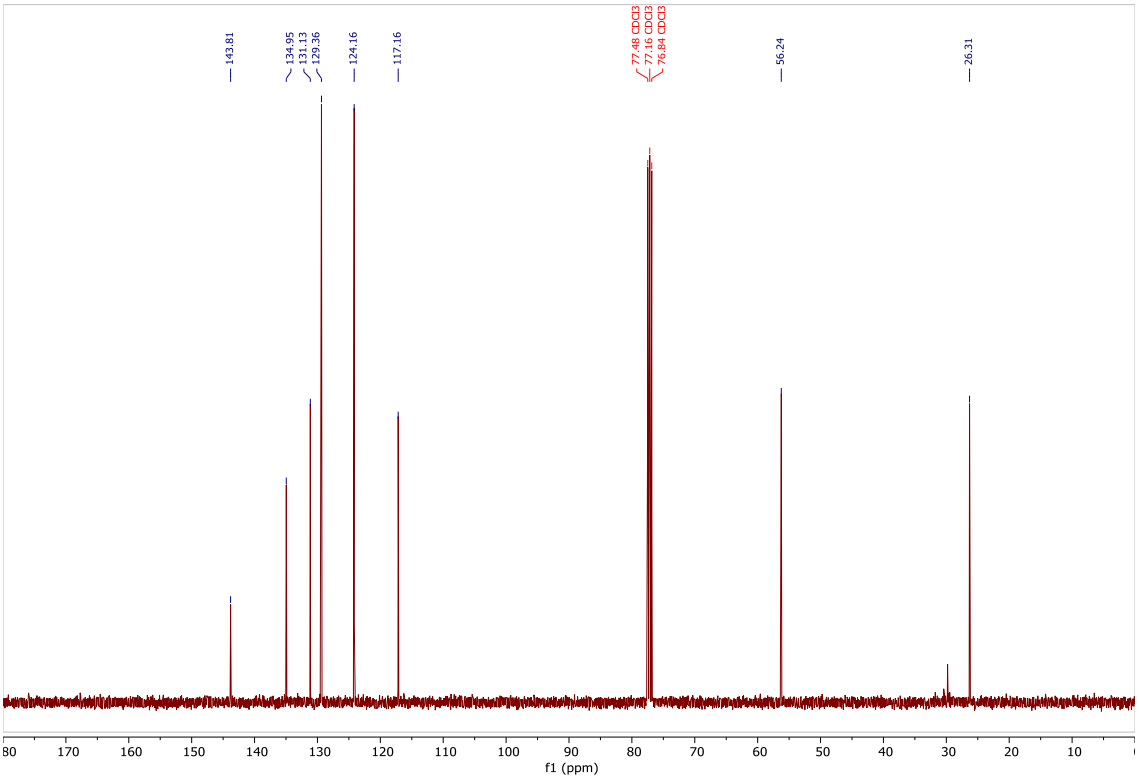

*1-(But-3-en-1-ylsulfinyl)-4-methylbenzene* ***28n***

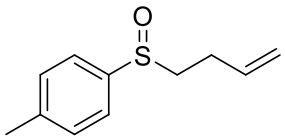

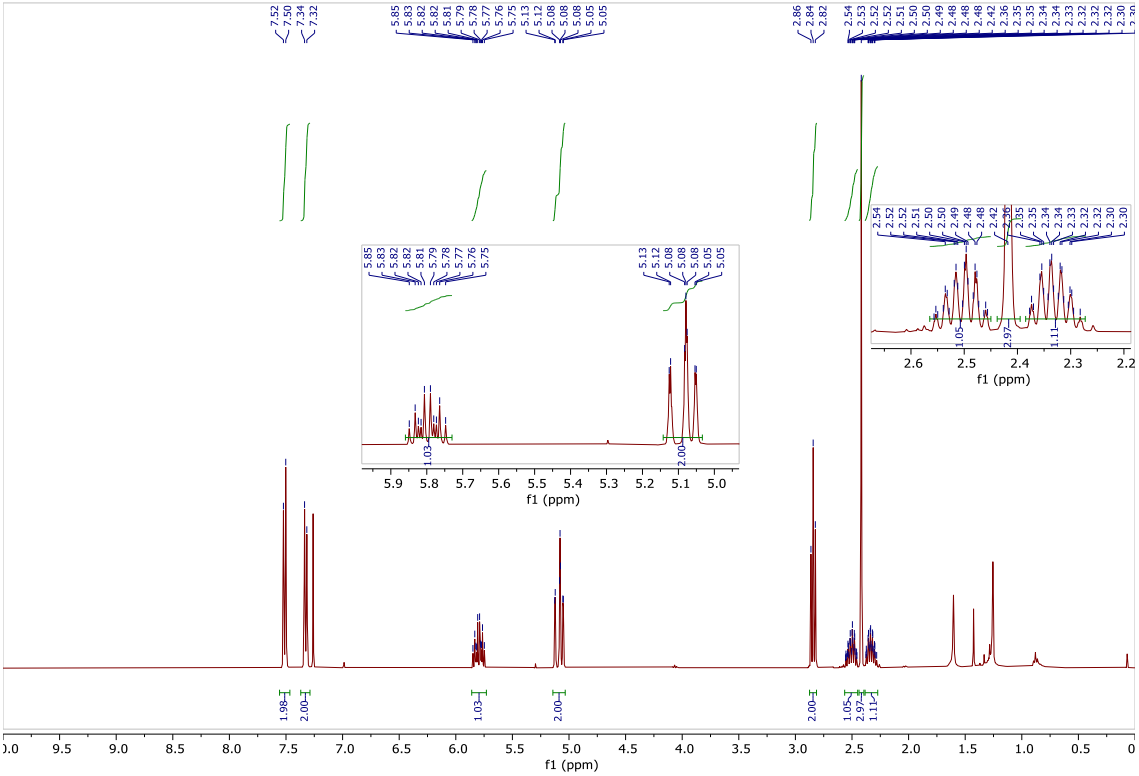

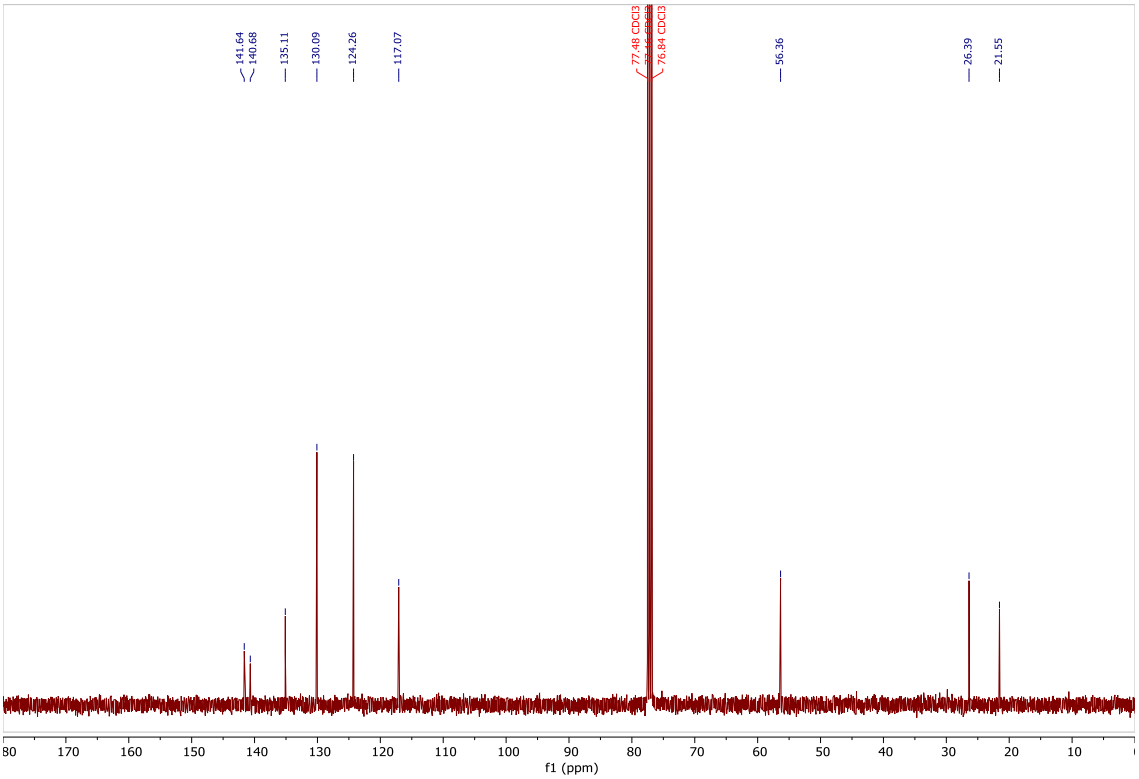

*Benzyl methyl sulfoxide* ***28o***

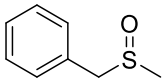

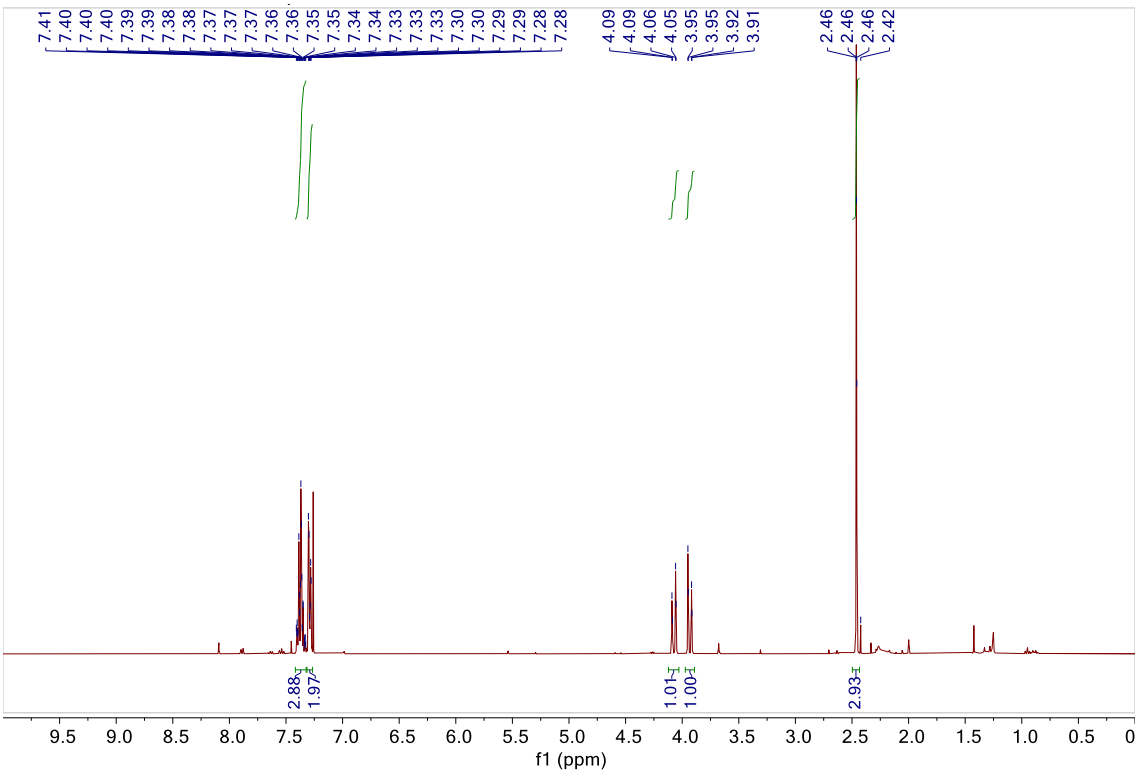


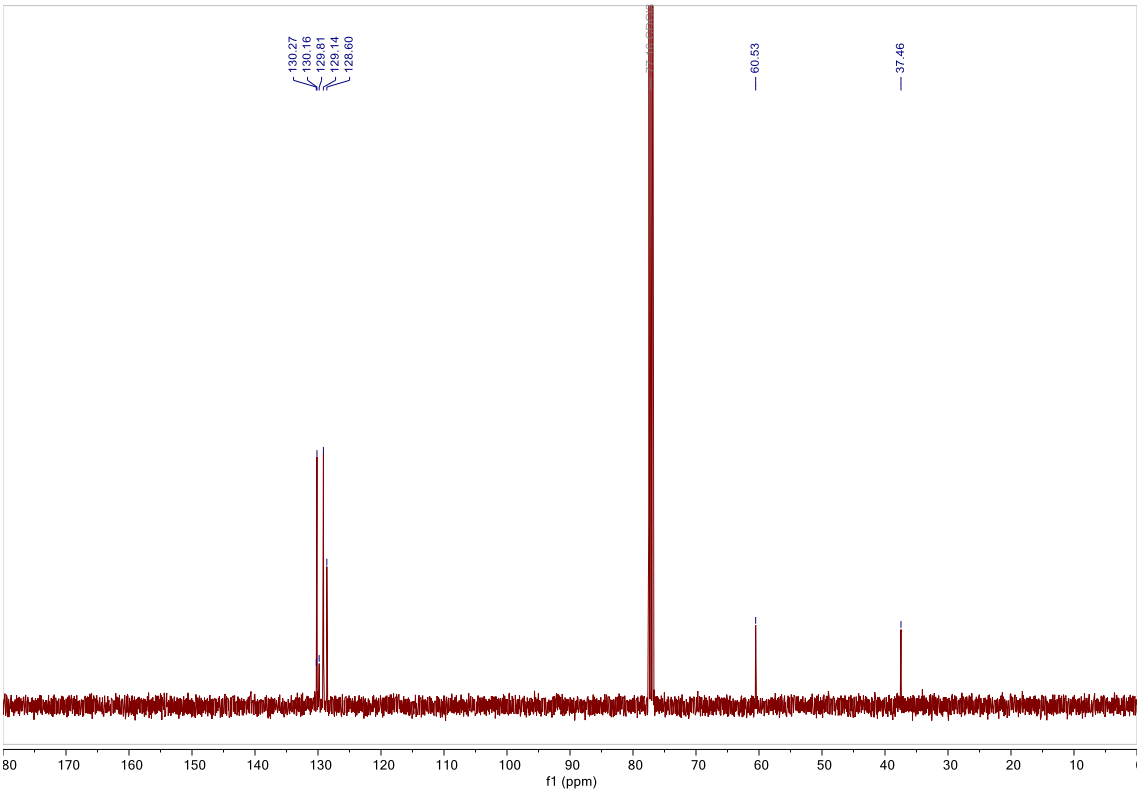

*Allyl benzyl sulfoxide* ***28p***

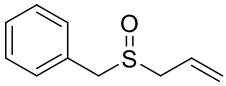

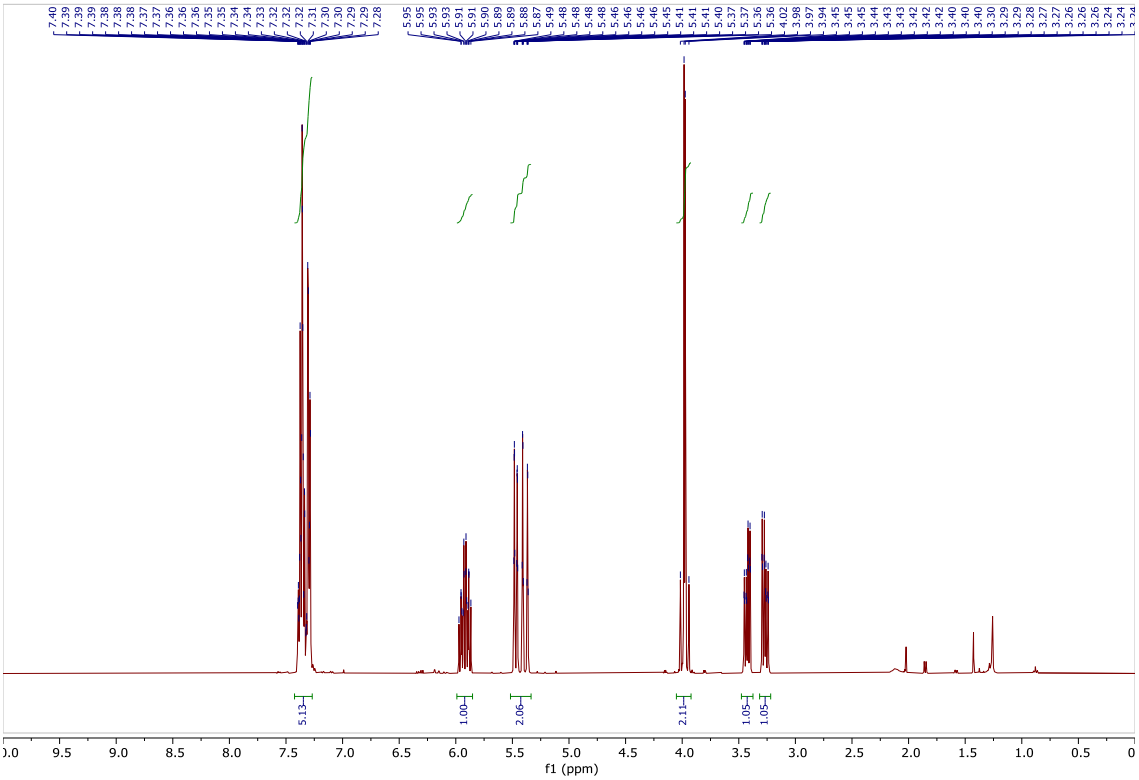


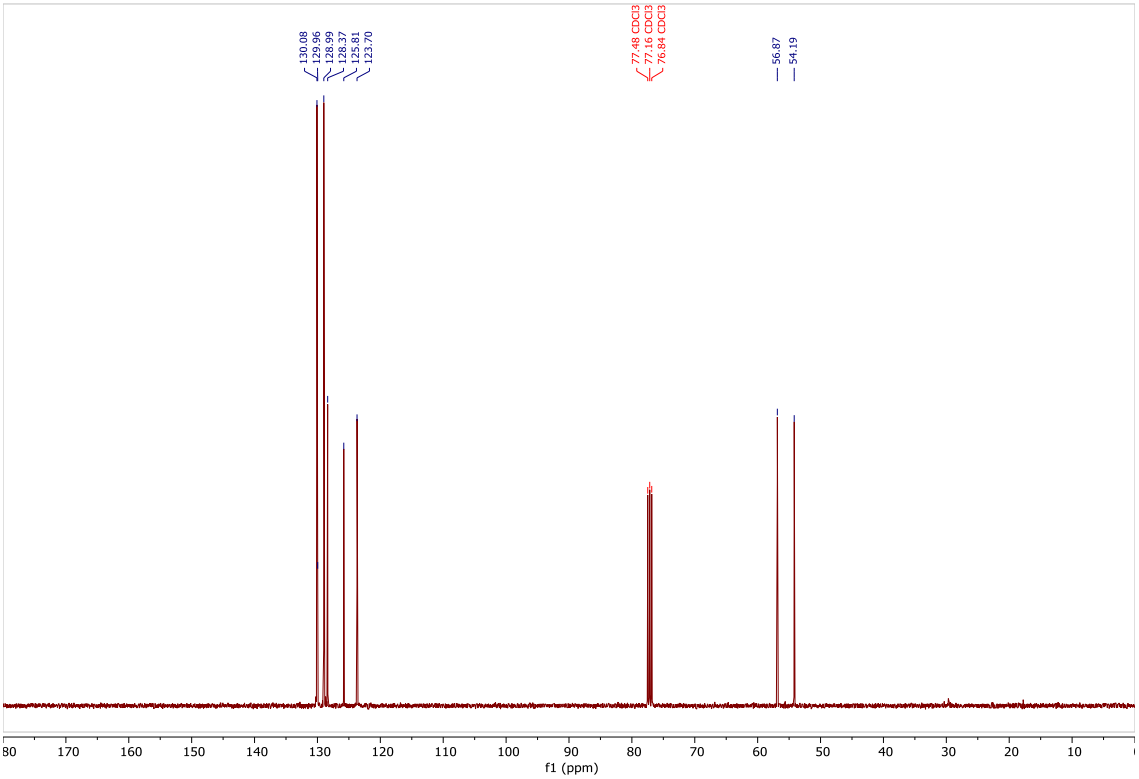

*2-(Phenylsulfinyl)propanenitrile* ***28q***

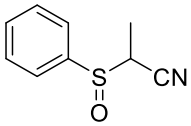


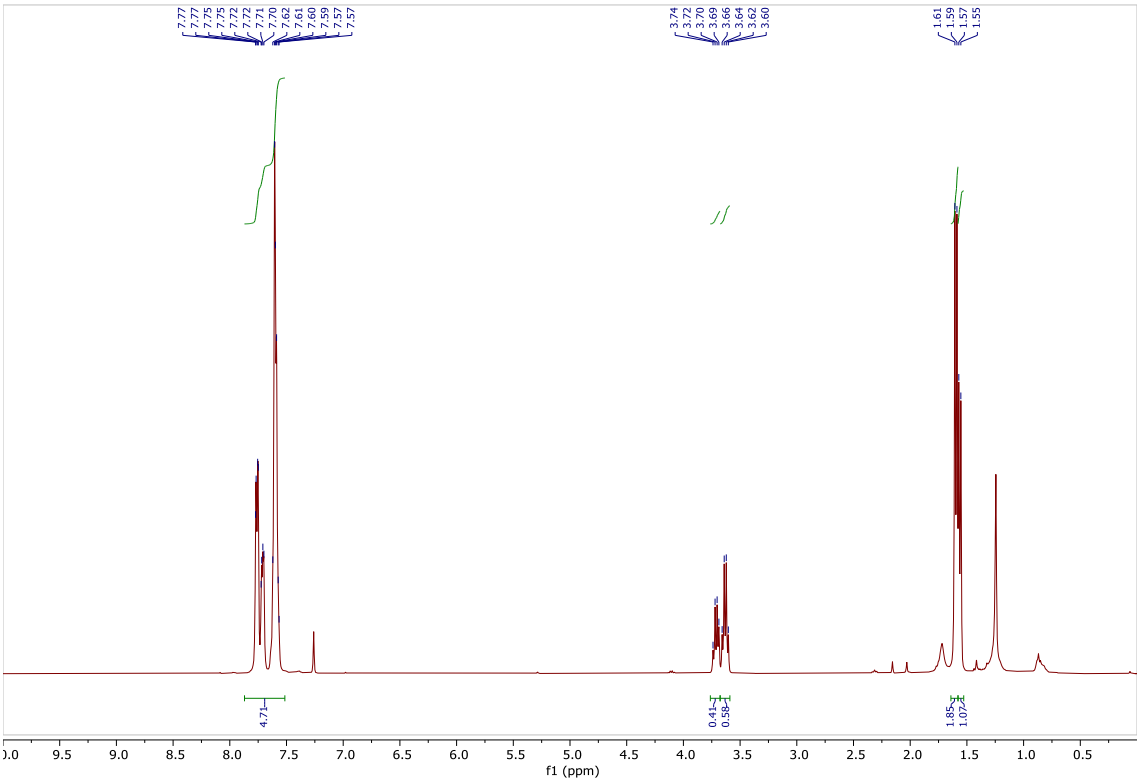


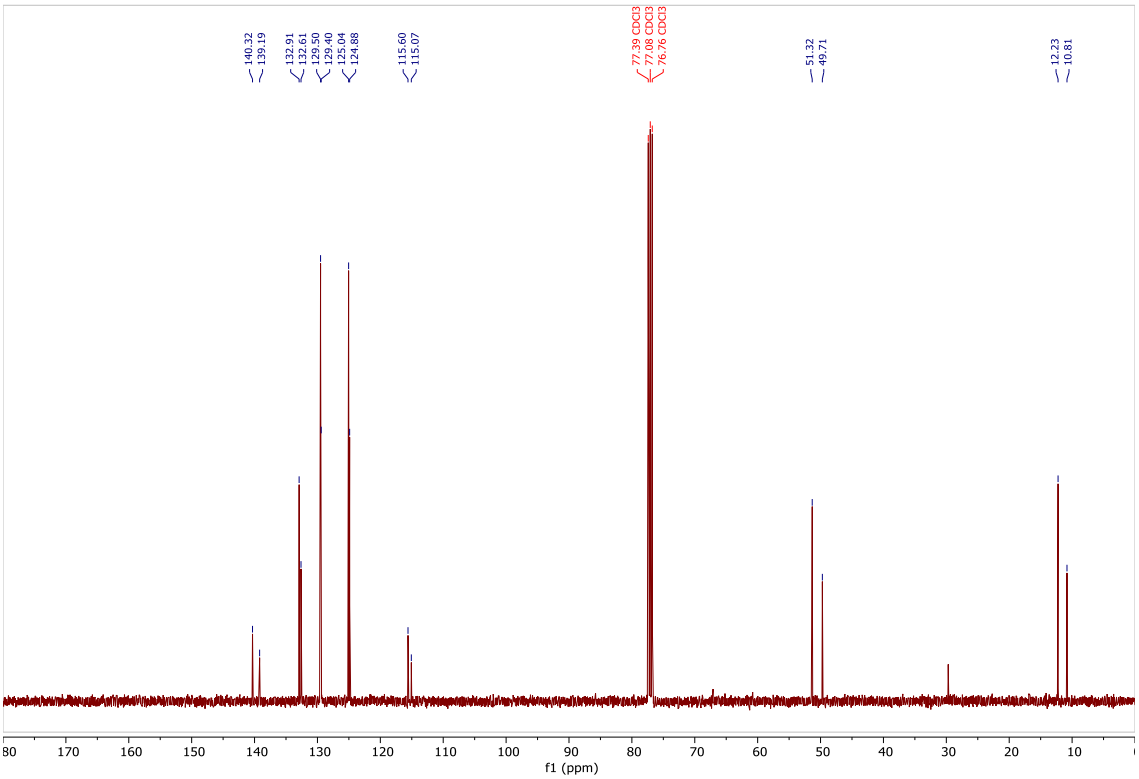

*1-(Butylsulfinyl)butane* ***28r***

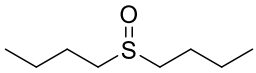

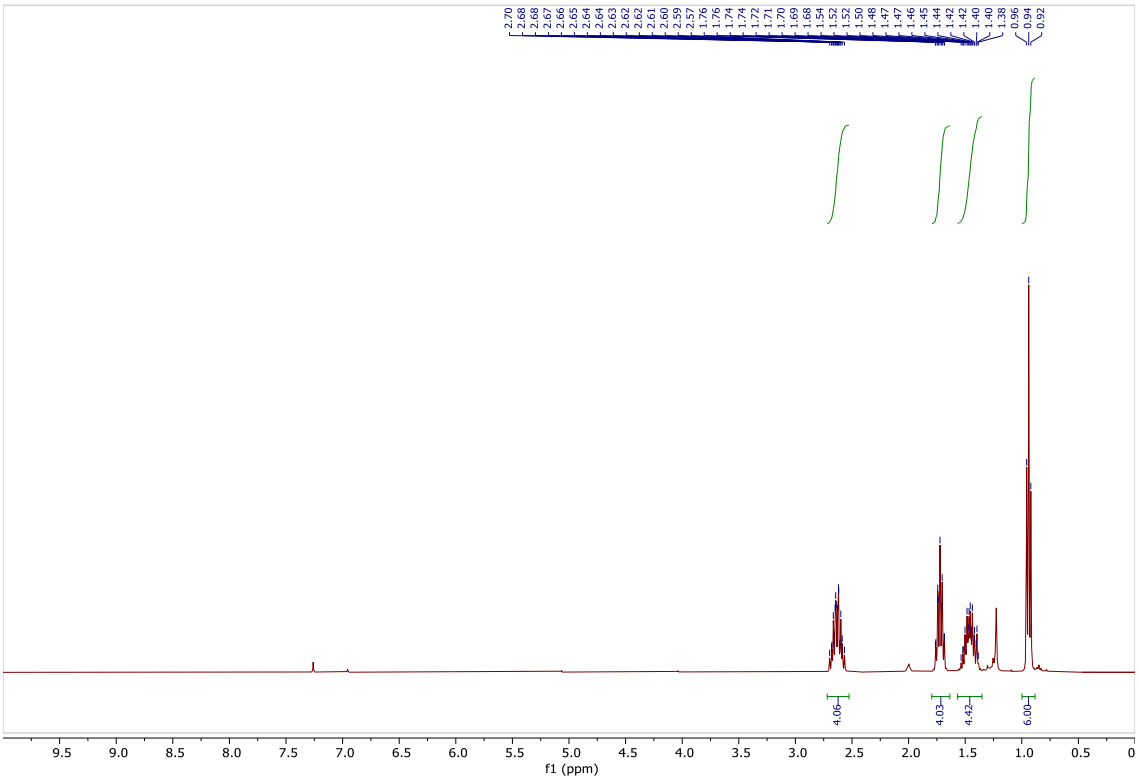


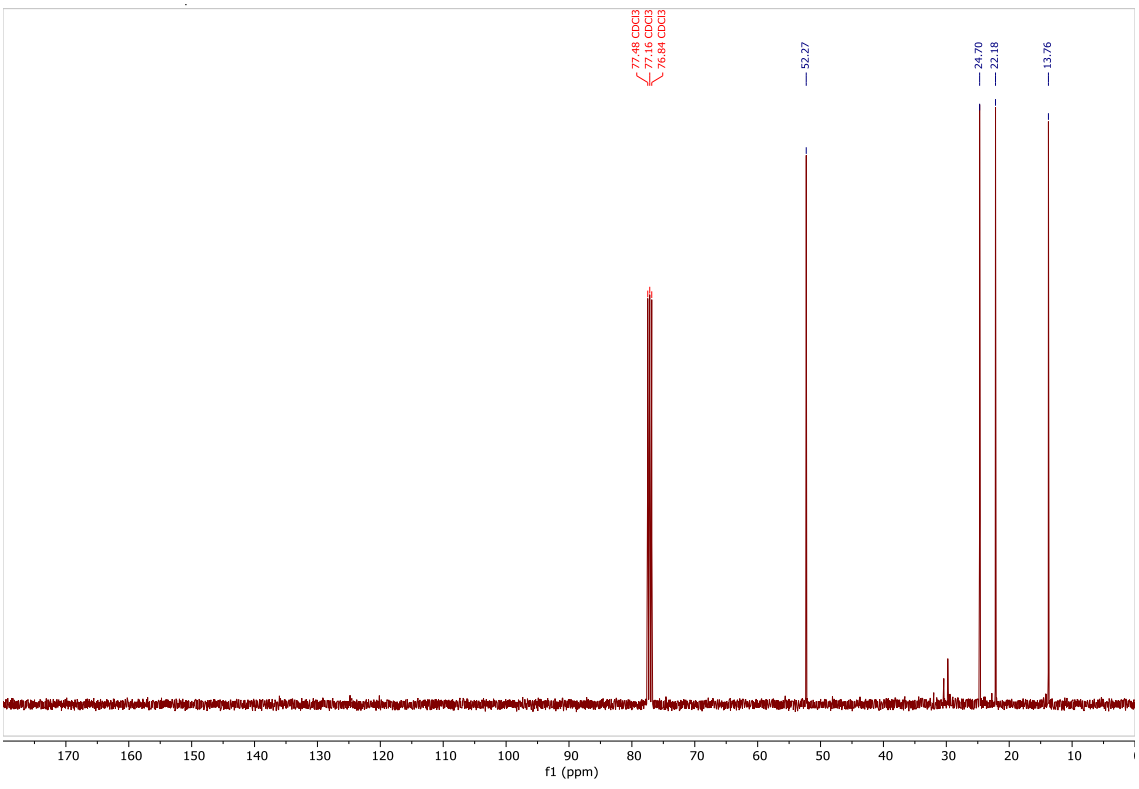

*2-((Propylsulfinyl)methyl)pyridine* ***28s***

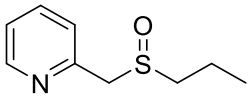


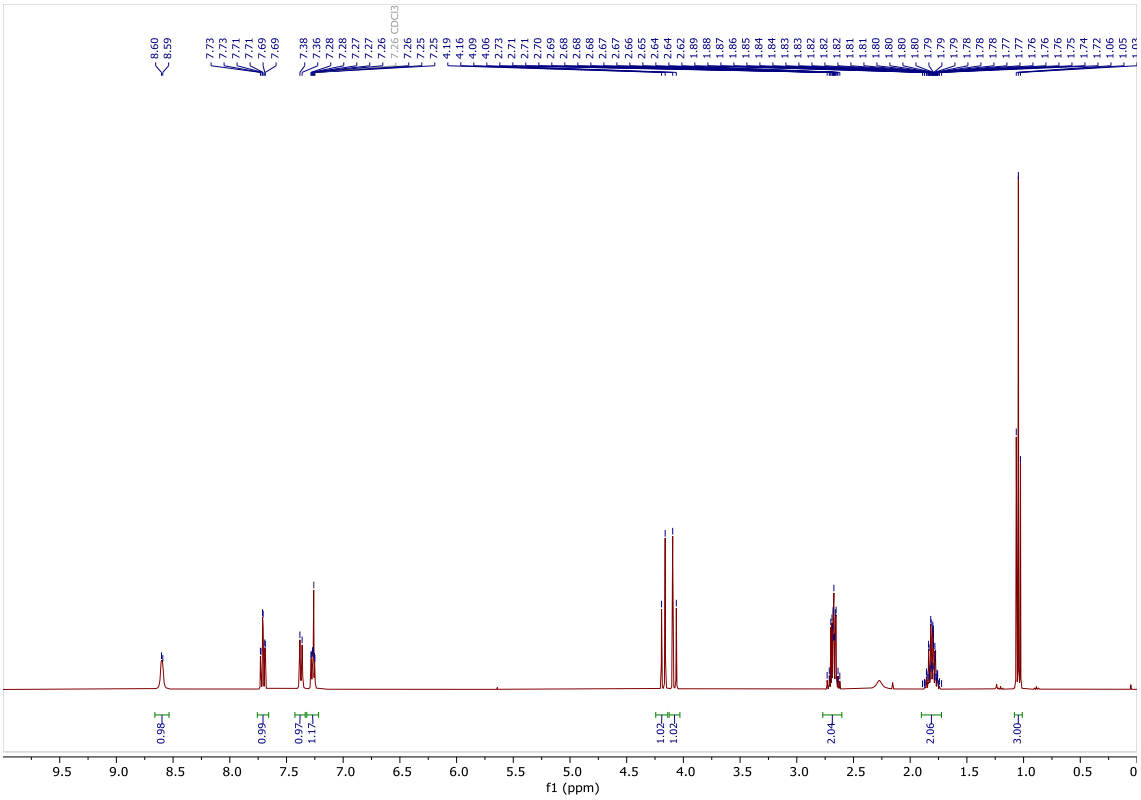


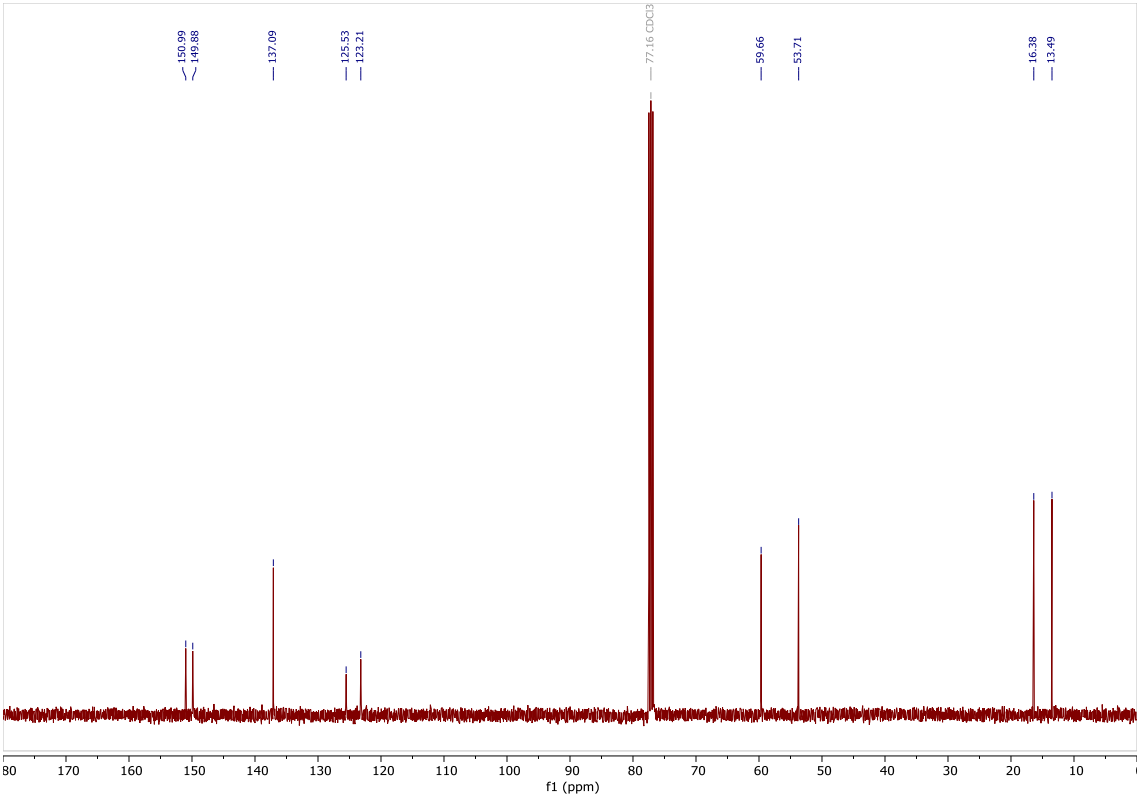

*2-((Ethylsulfinyl)methyl)pyridine* ***28t***

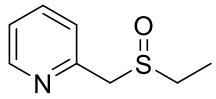


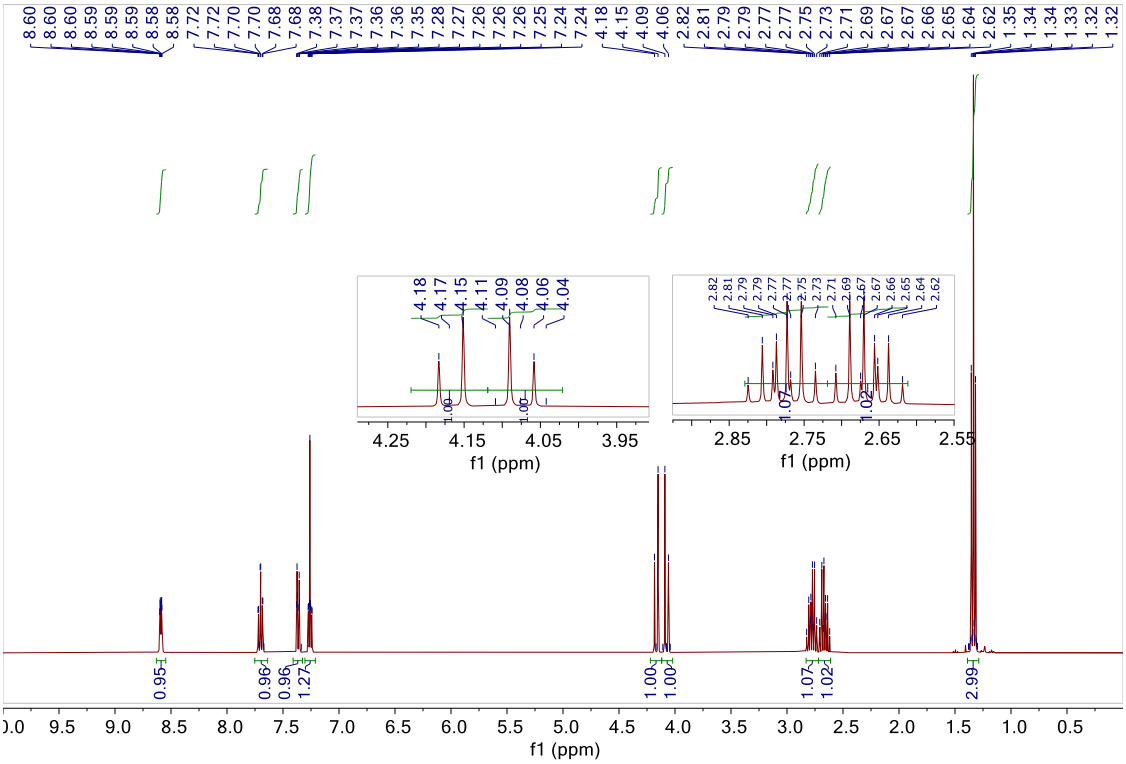


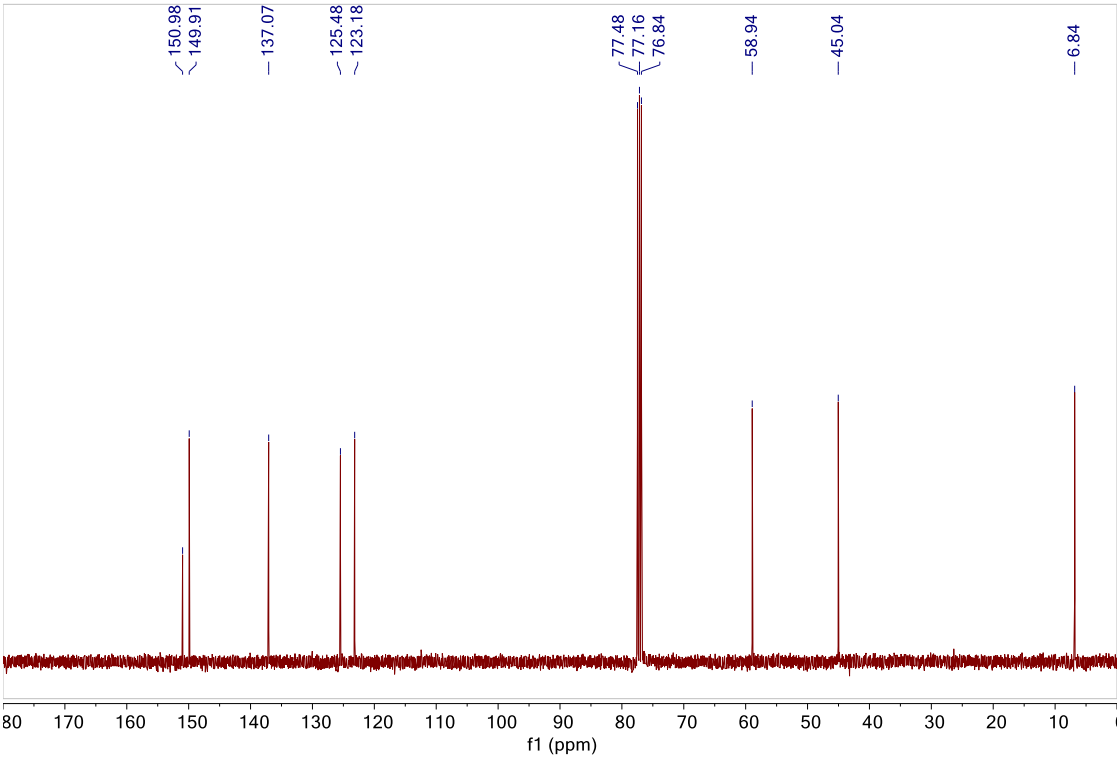

*2-((Benzylsulfinyl)methyl)pyridine* ***28u***

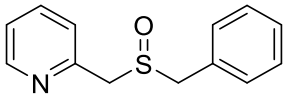


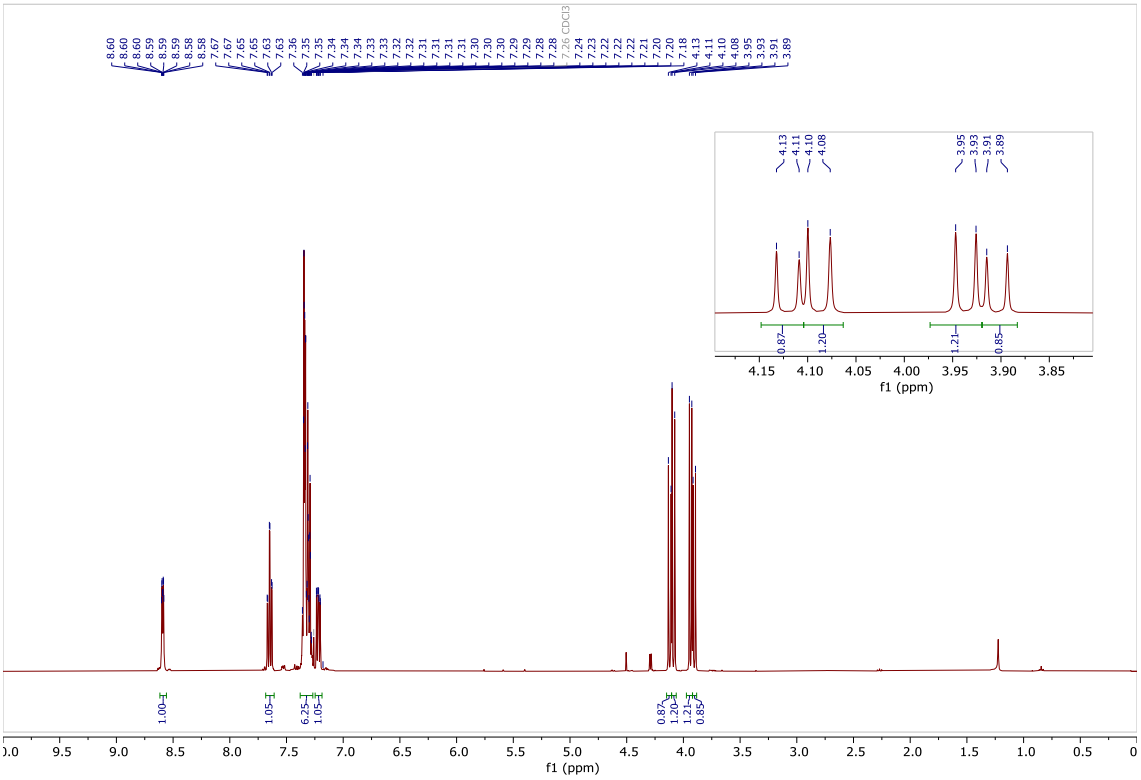


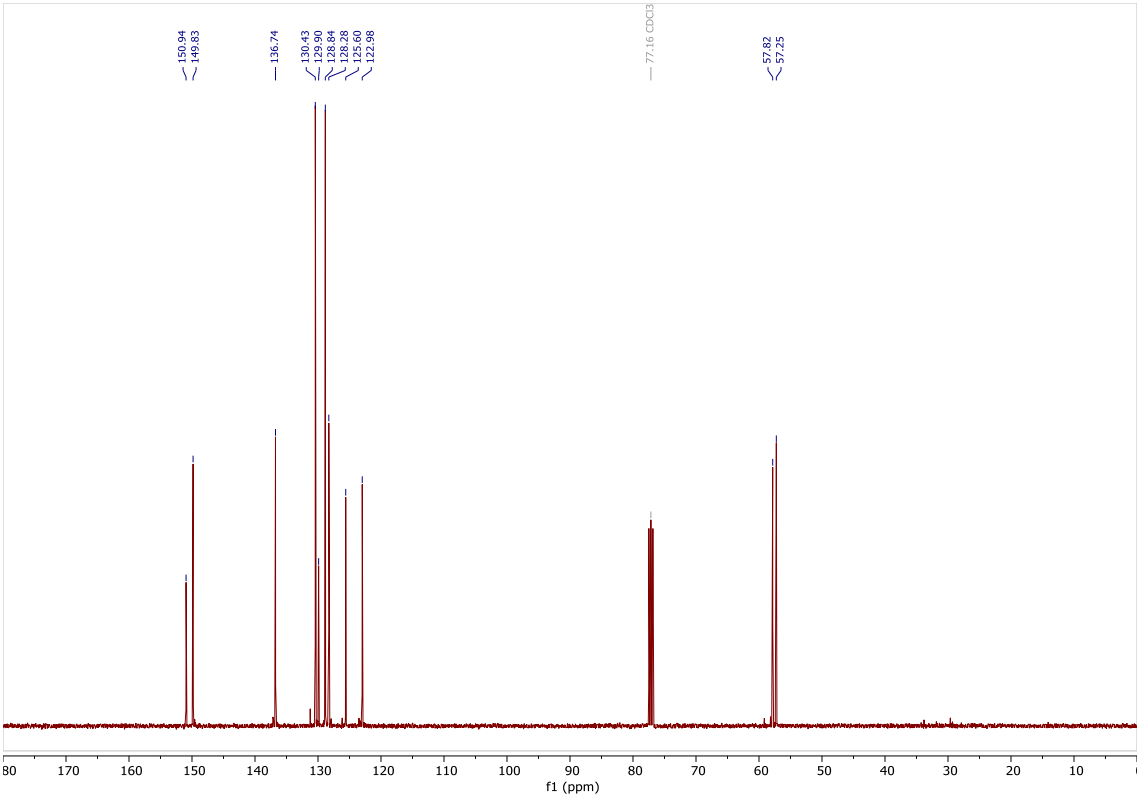

*((Ethylsulfinyl)methyl)benzene* ***28v***

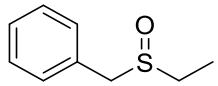

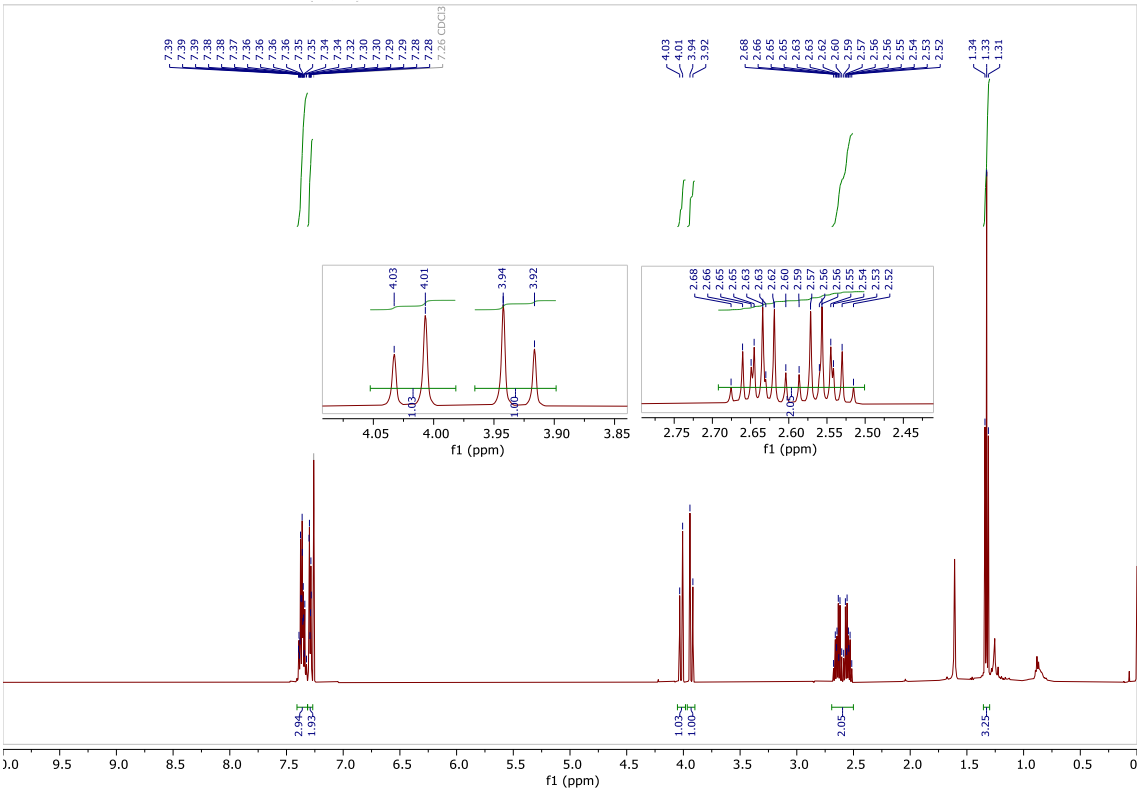

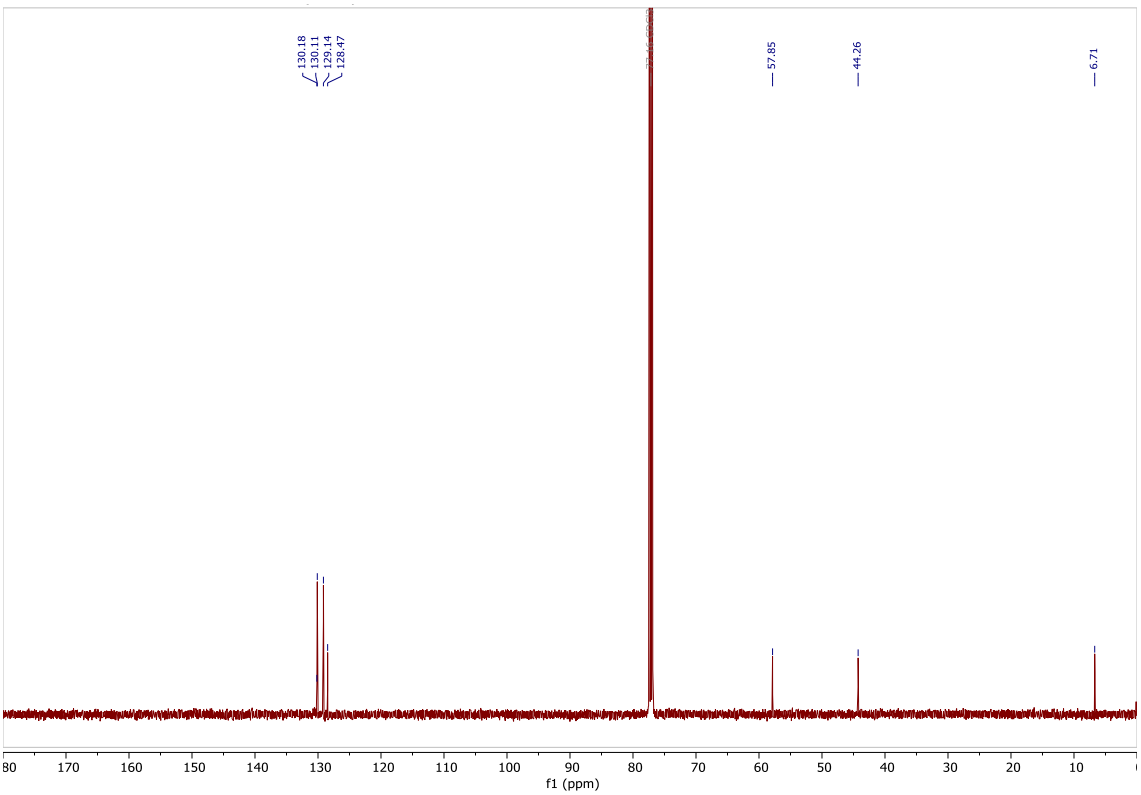

*(2-(Ethylsulfinyl)ethyl)benzene* ***28w***

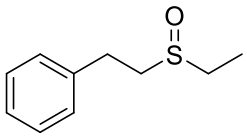

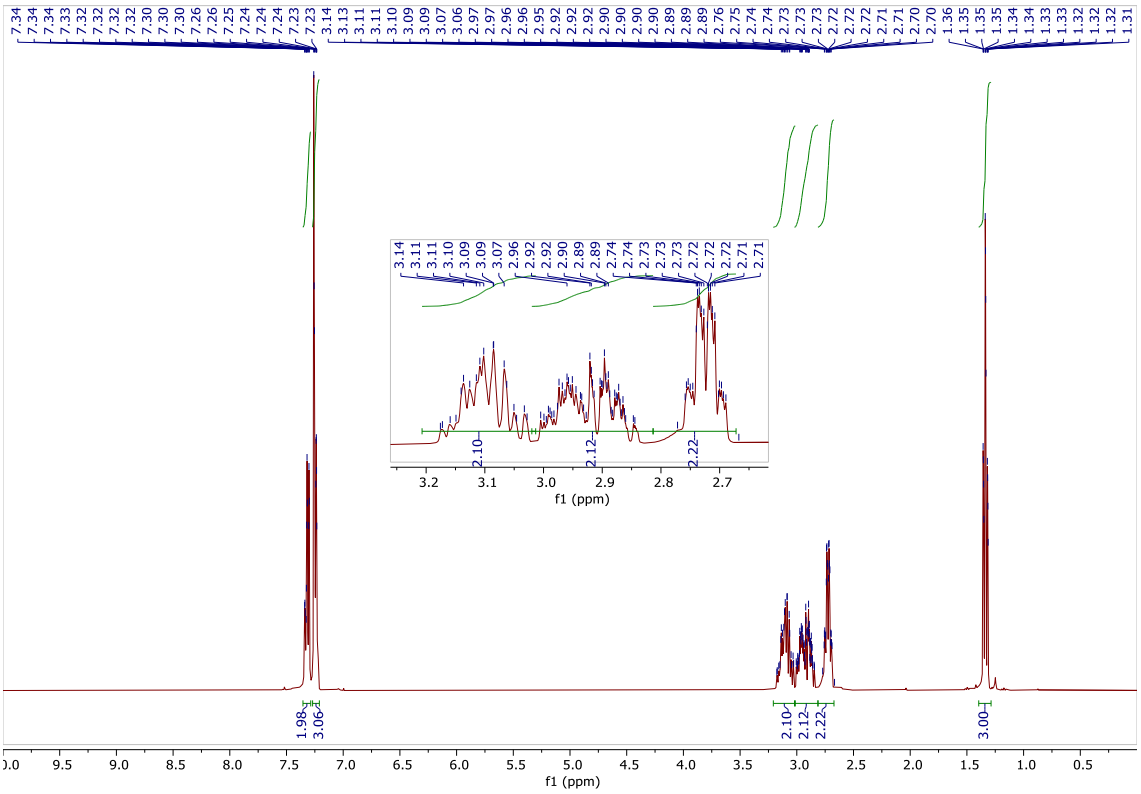

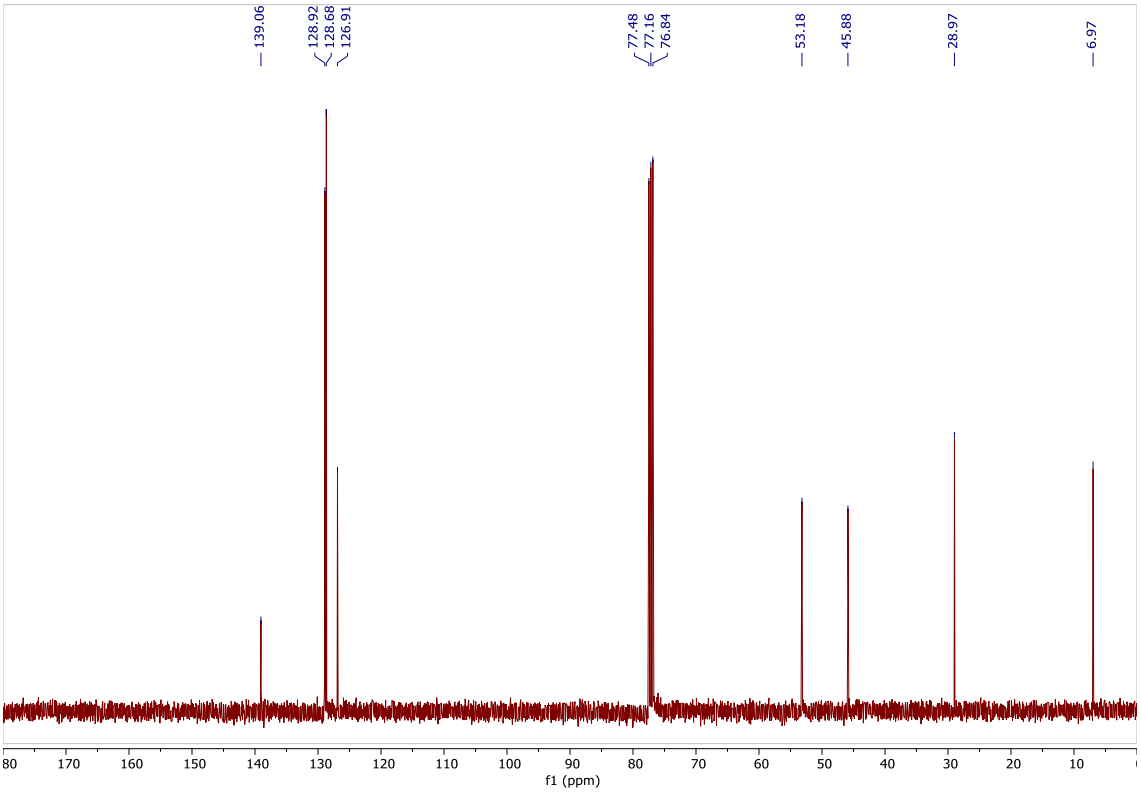

*1-Bromo-4-(methylsulfinyl)benzene* ***28x***

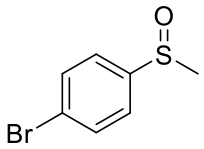


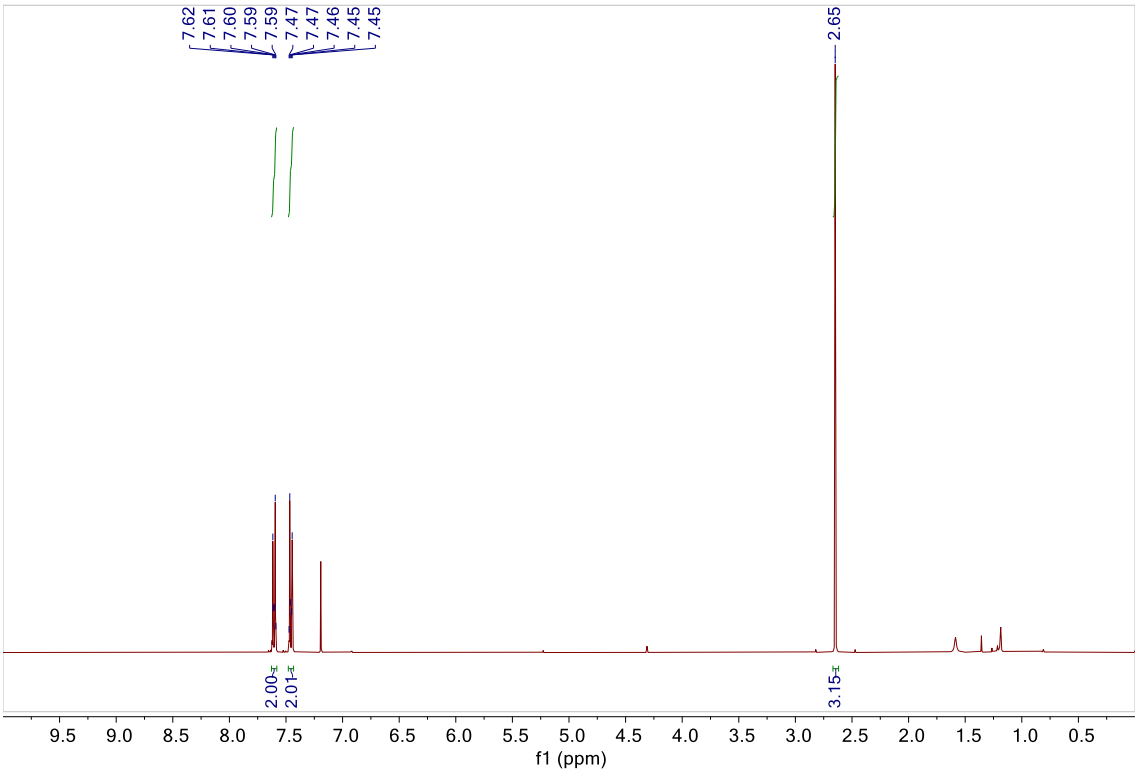


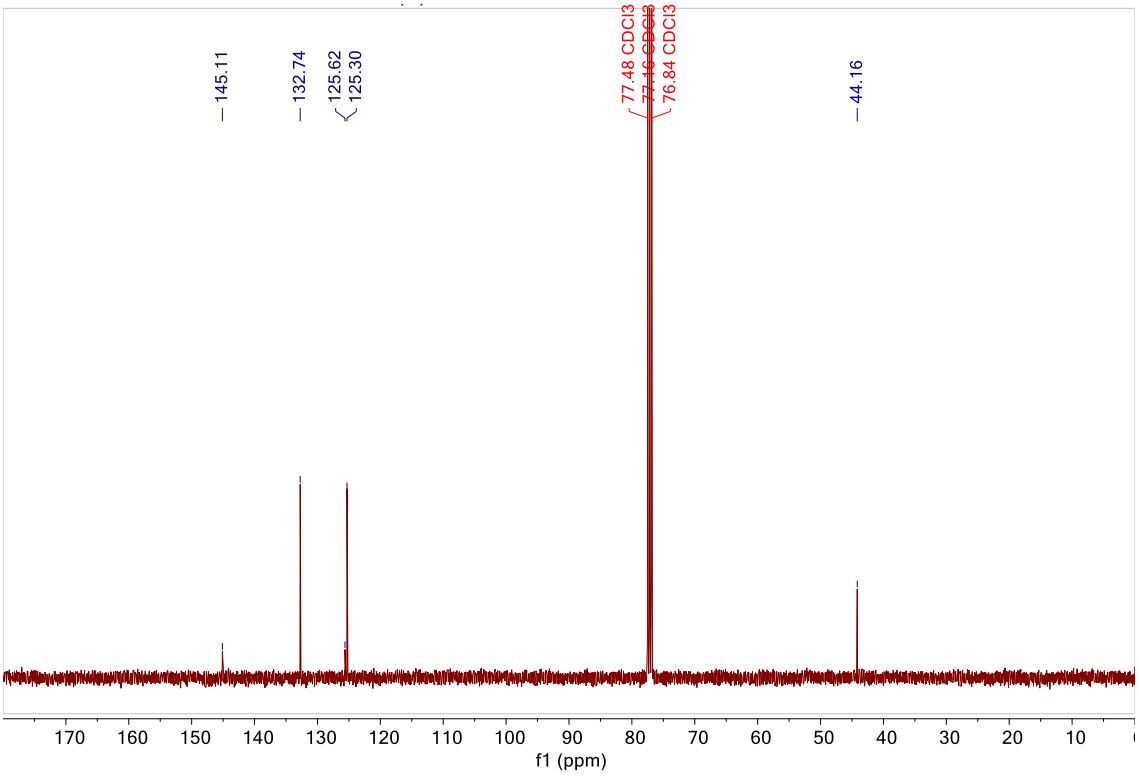

*1-Chloro-4-(methylsulfinyl)benzene* ***28y***

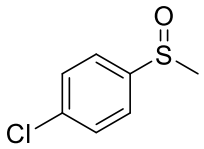


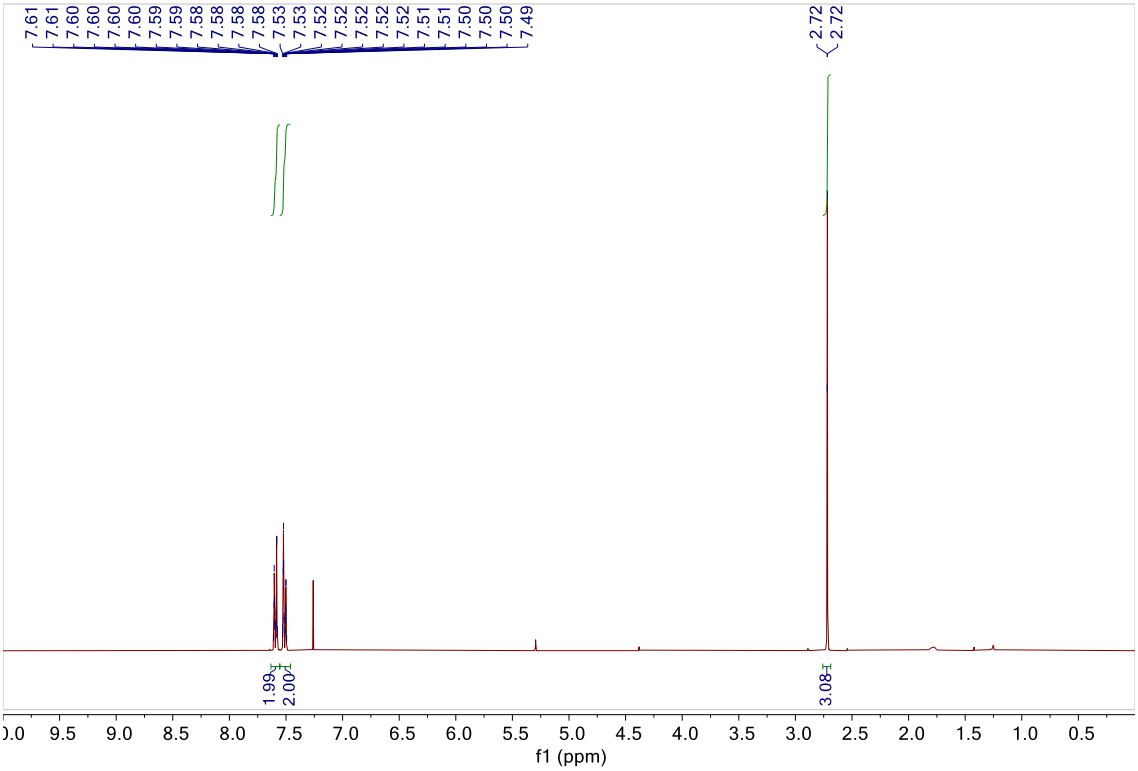


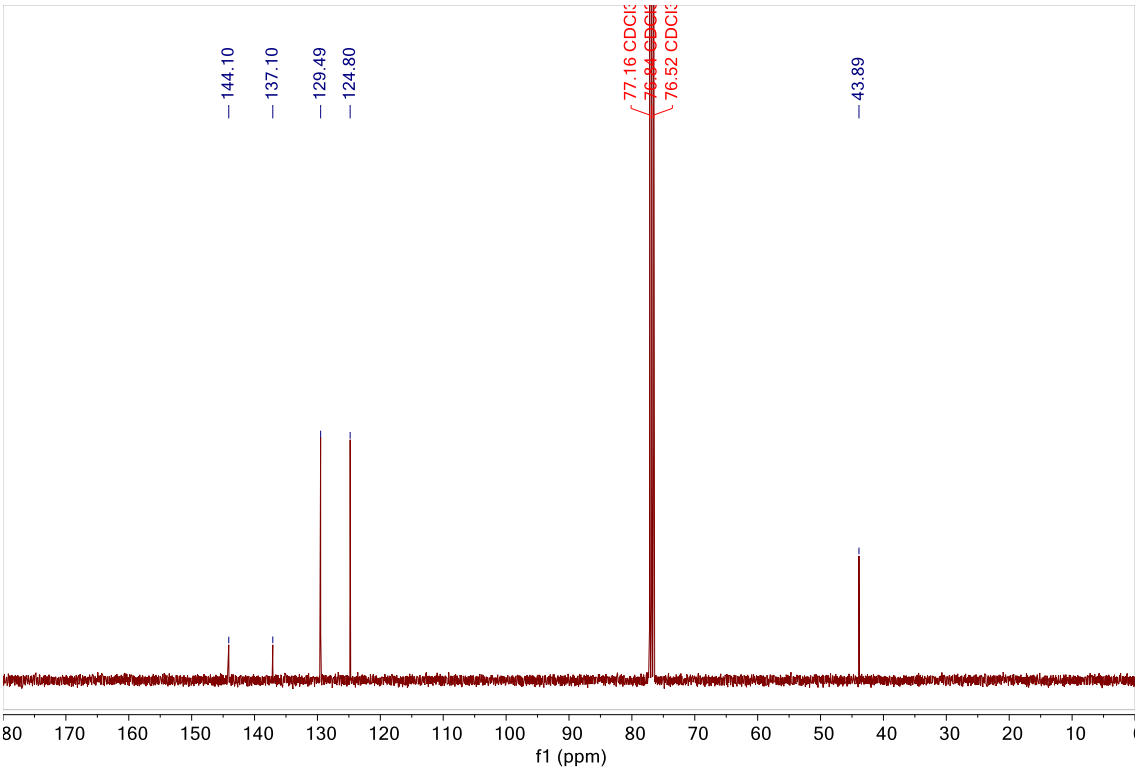

*1-Chloro-3-(methylsulfinyl)benzene* ***28z***

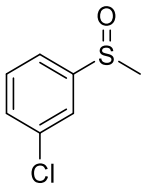


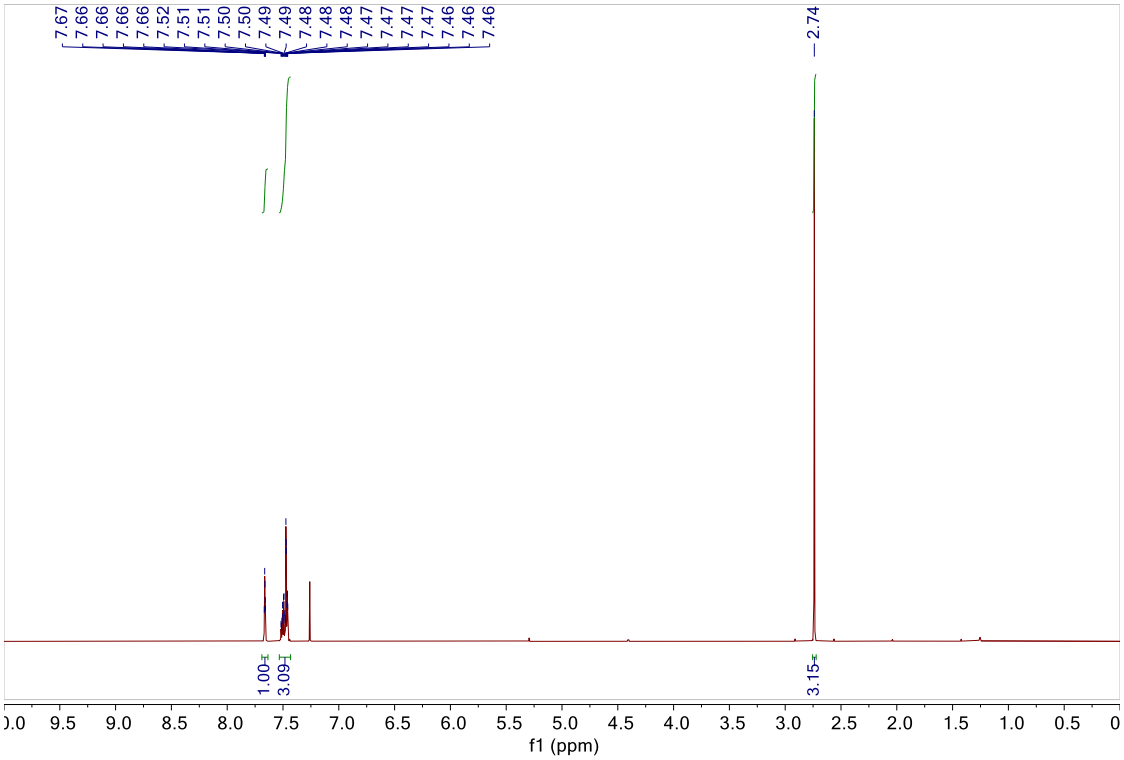


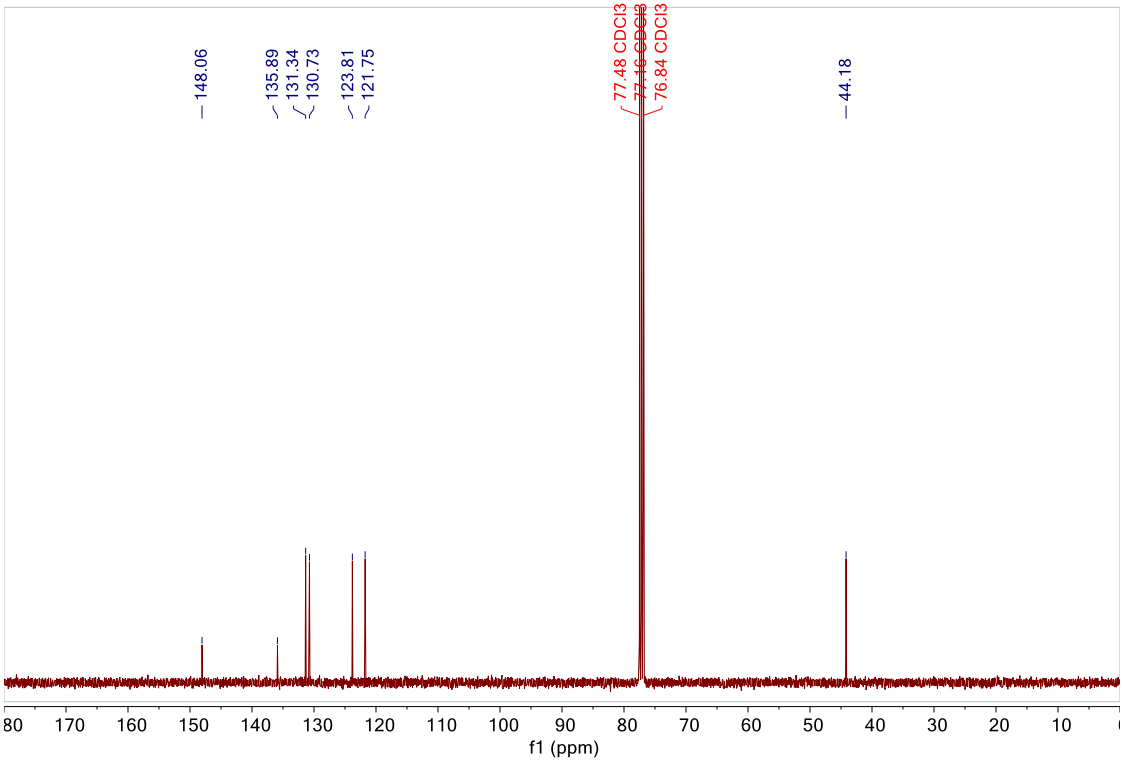

*1-Chloro-2-(methylsulfinyl)benzene* ***28aa***

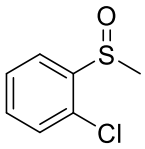


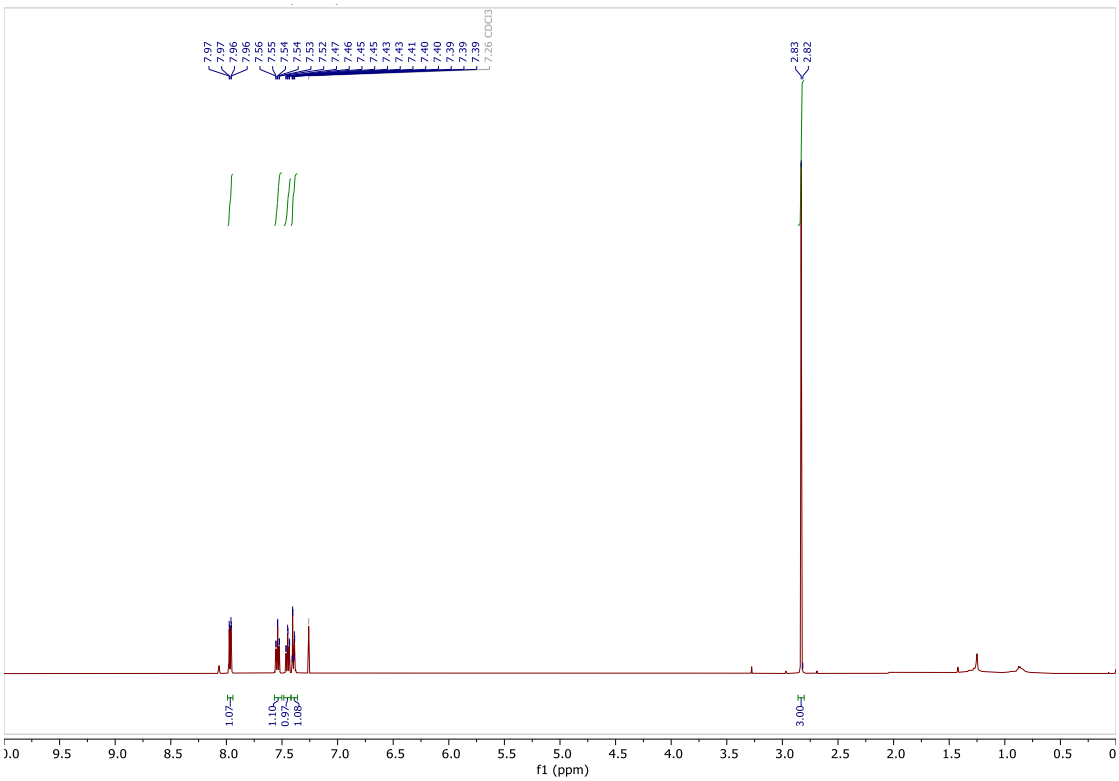


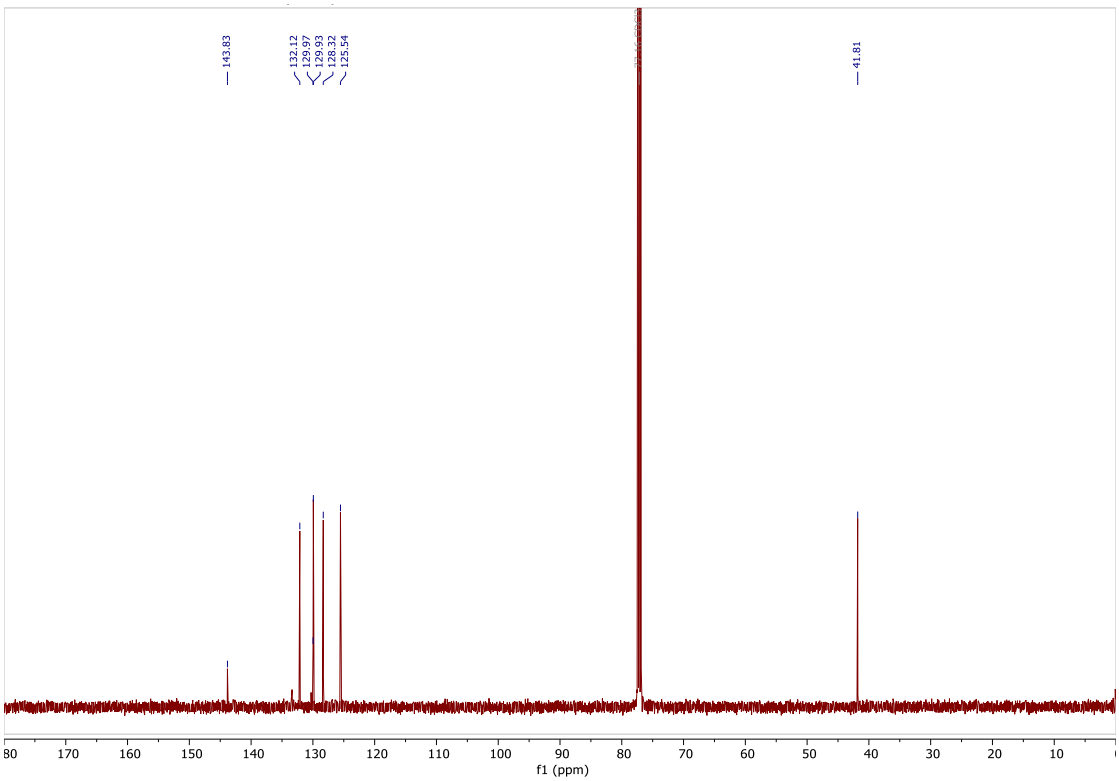

*1-(4-(Methylsulfinyl)phenyl)ethan-1-one* ***28ab***

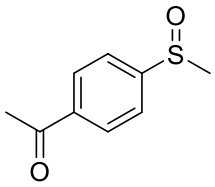

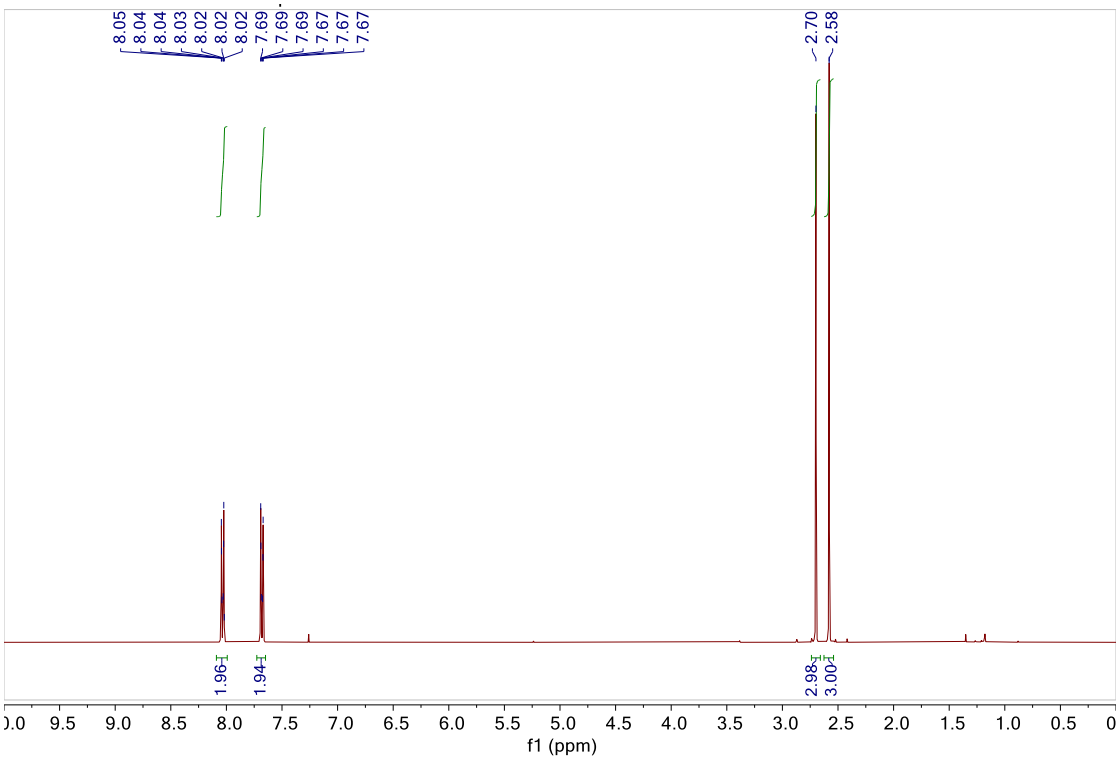


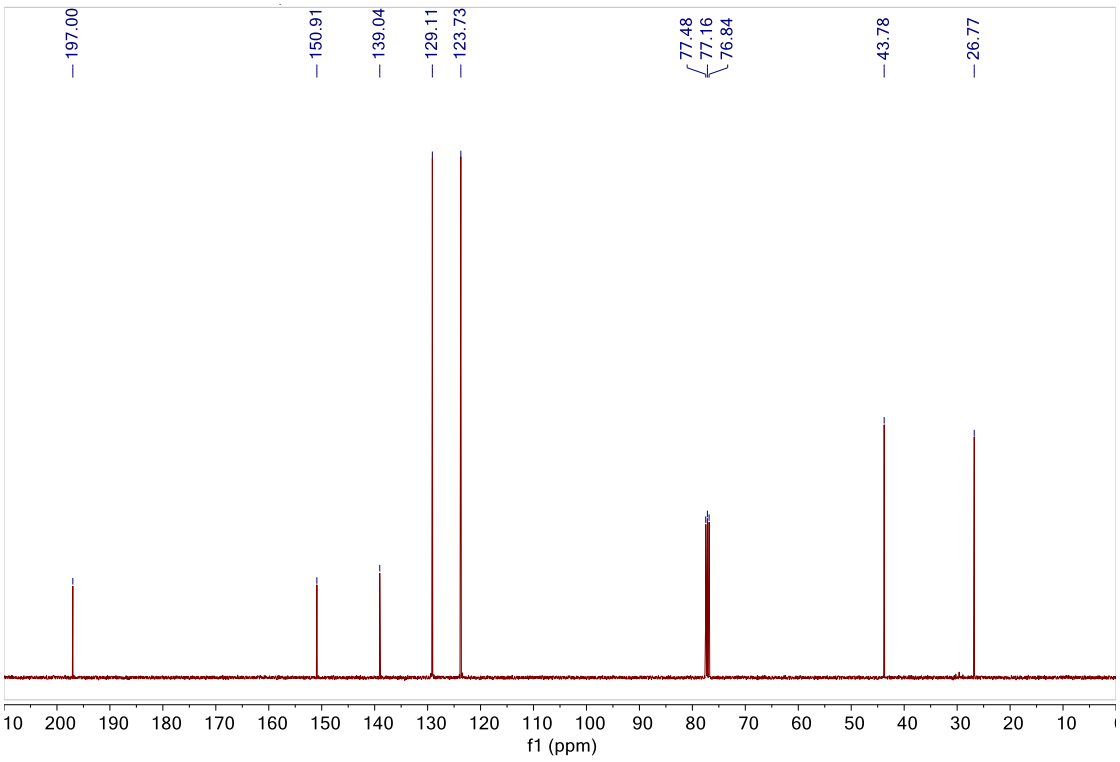

*1-Methyl-3-(methylsulfinyl)benzene* ***28ac***

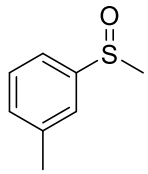


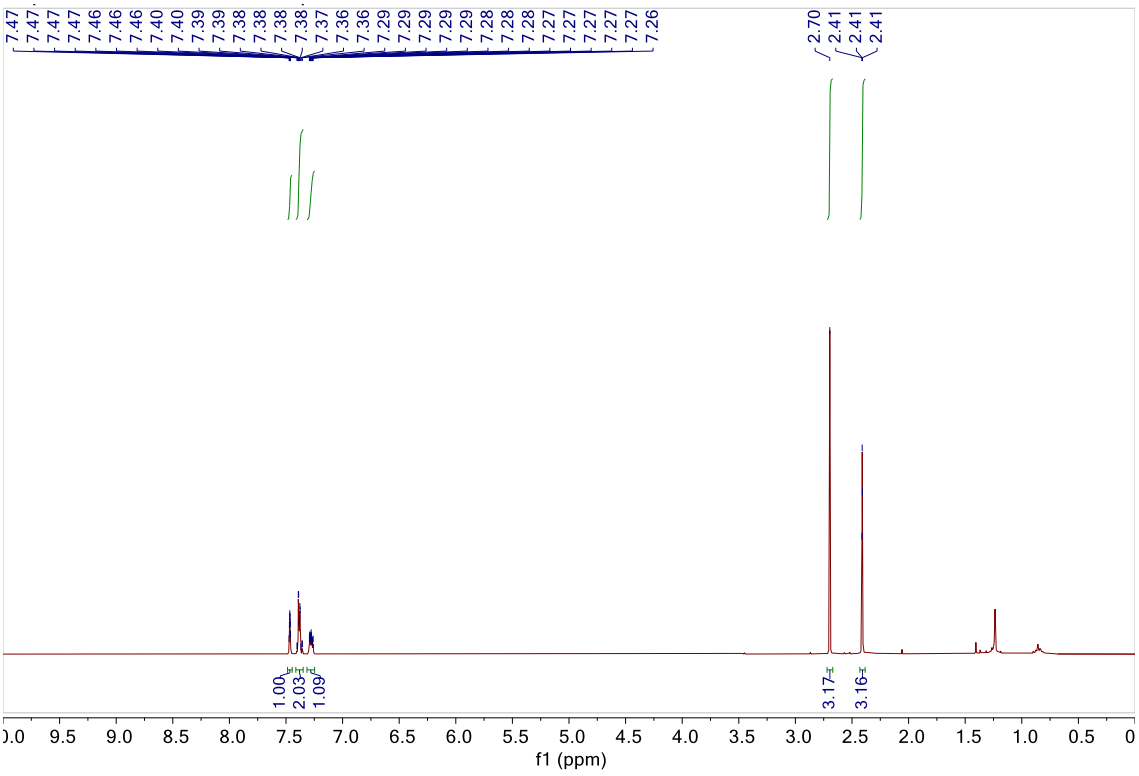


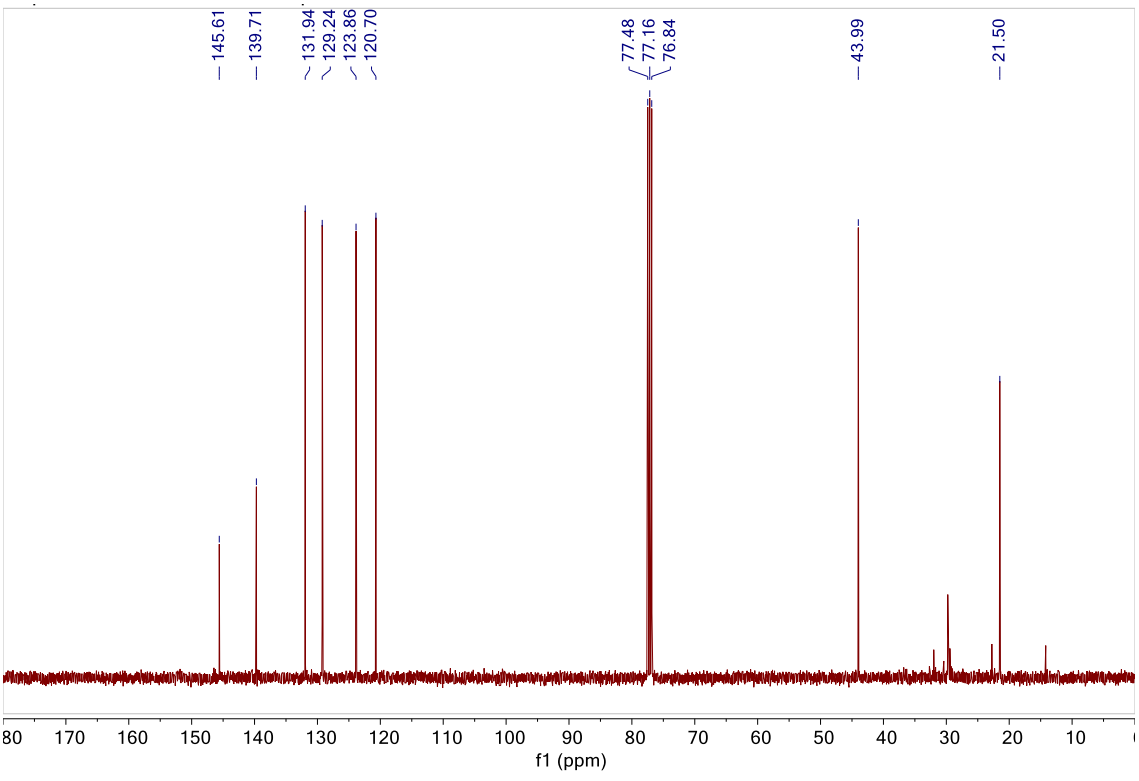

*2,4-Dimethyl-1-(methylsulfinyl)benzene* ***28ad***

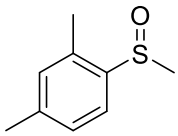


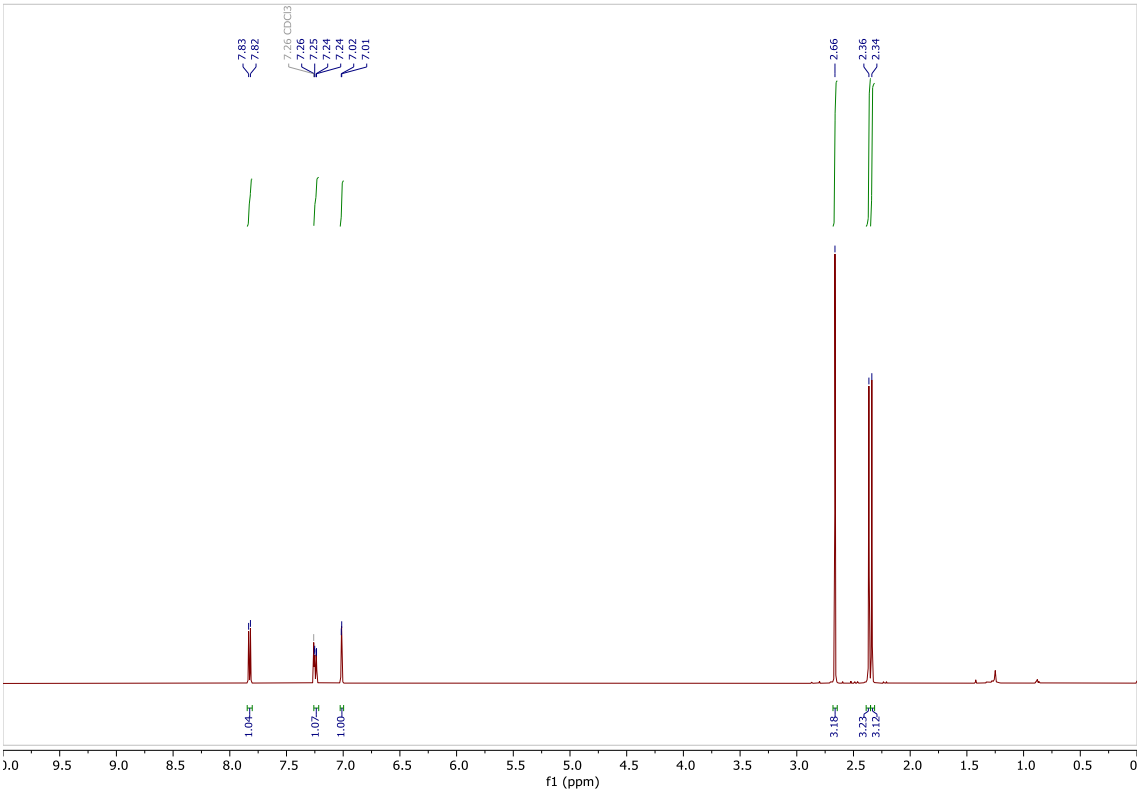


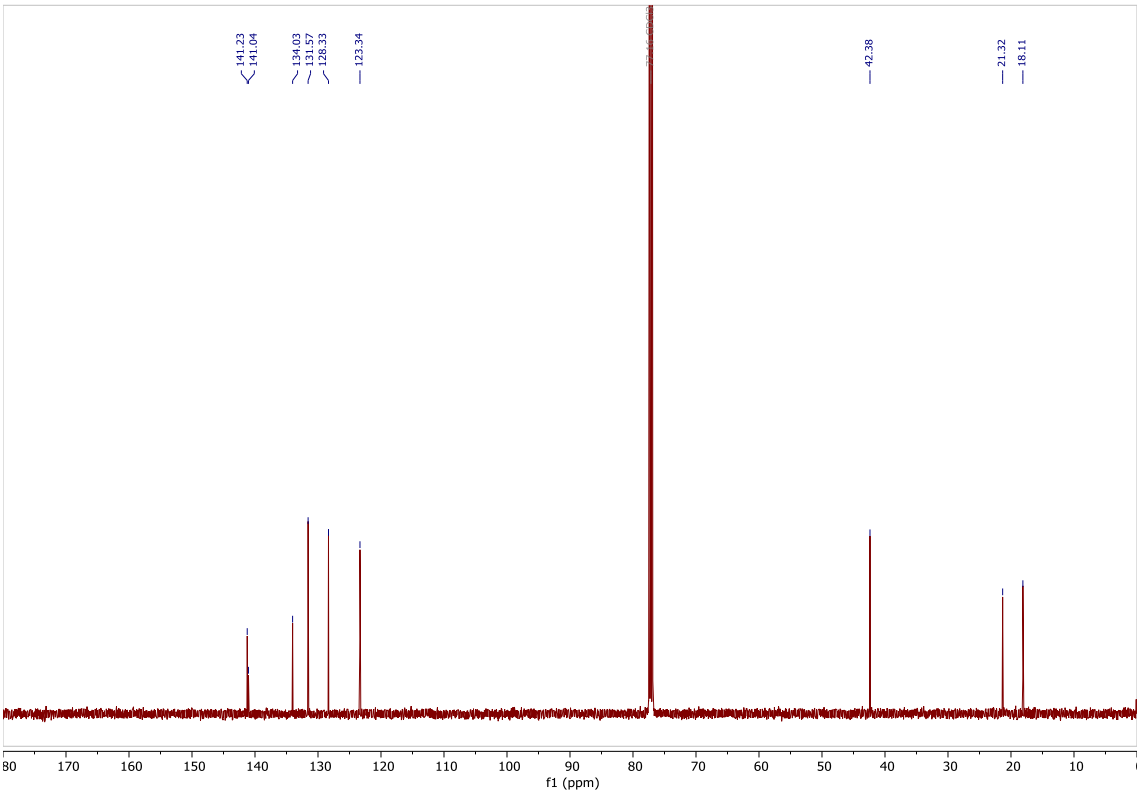

*1-Methoxy-4-(methylsulfinyl)benzene* ***21ag***

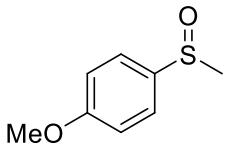


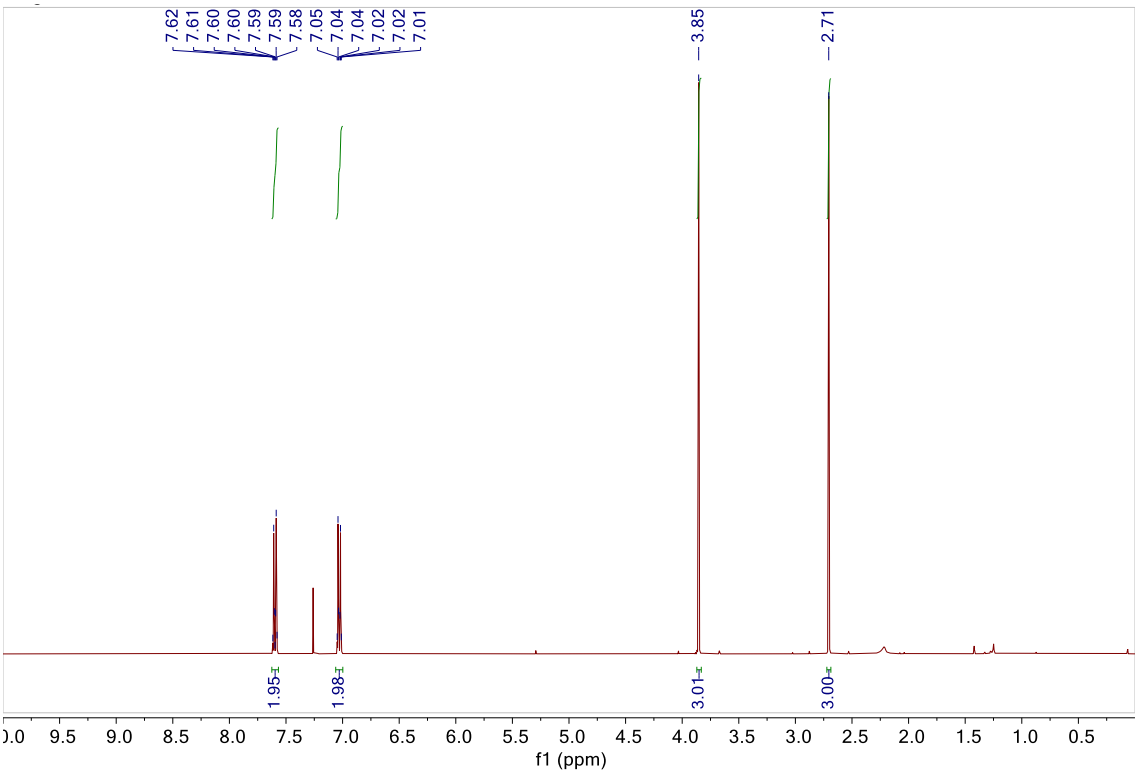


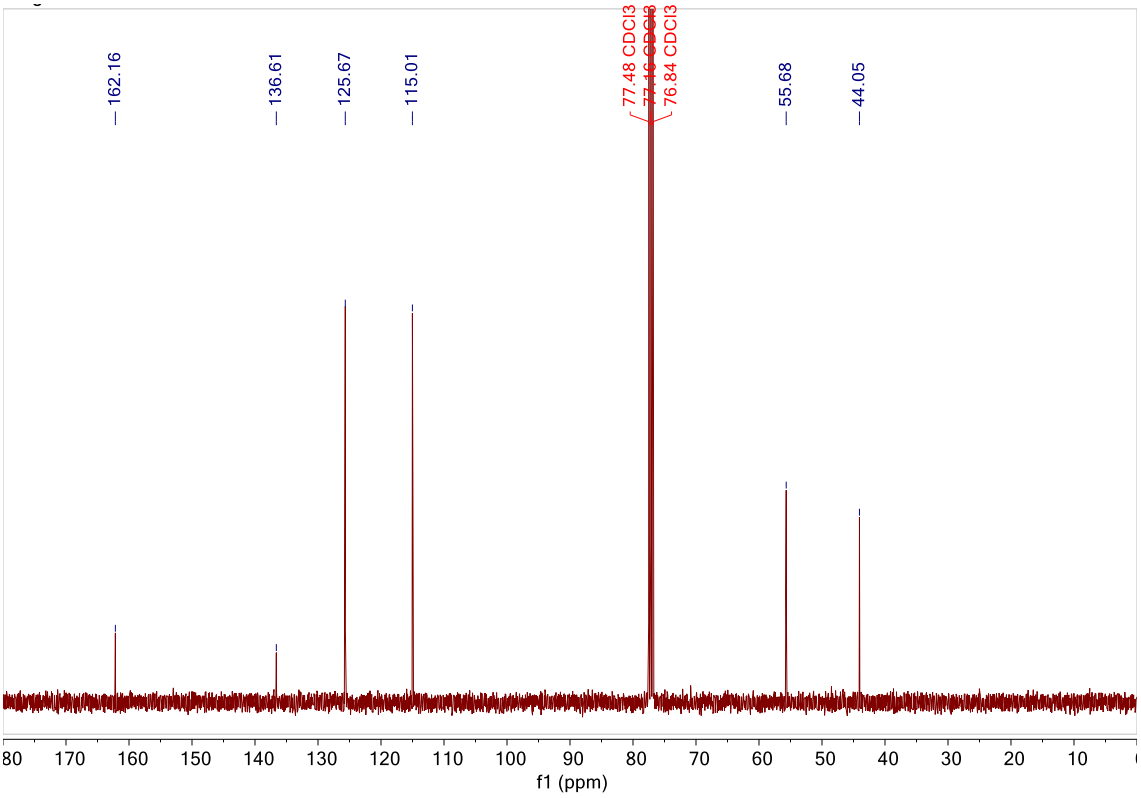

*1-Methoxy-3-(methylsulfinyl)benzene* ***21ah***

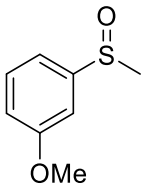


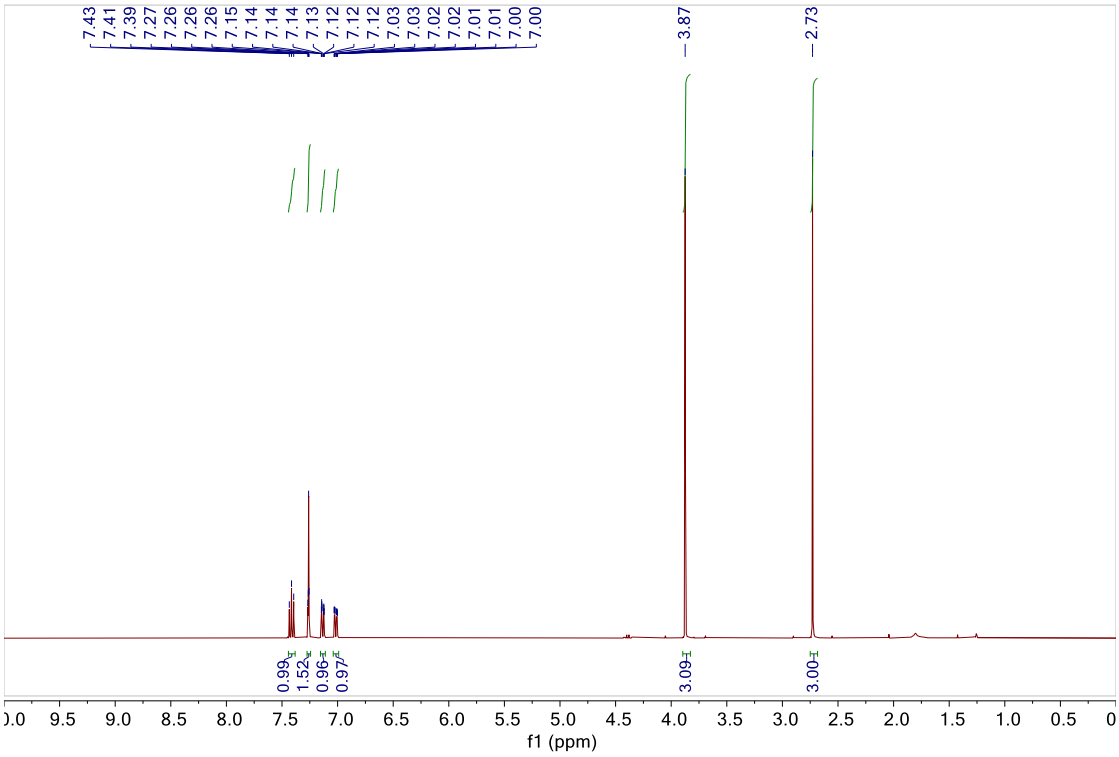


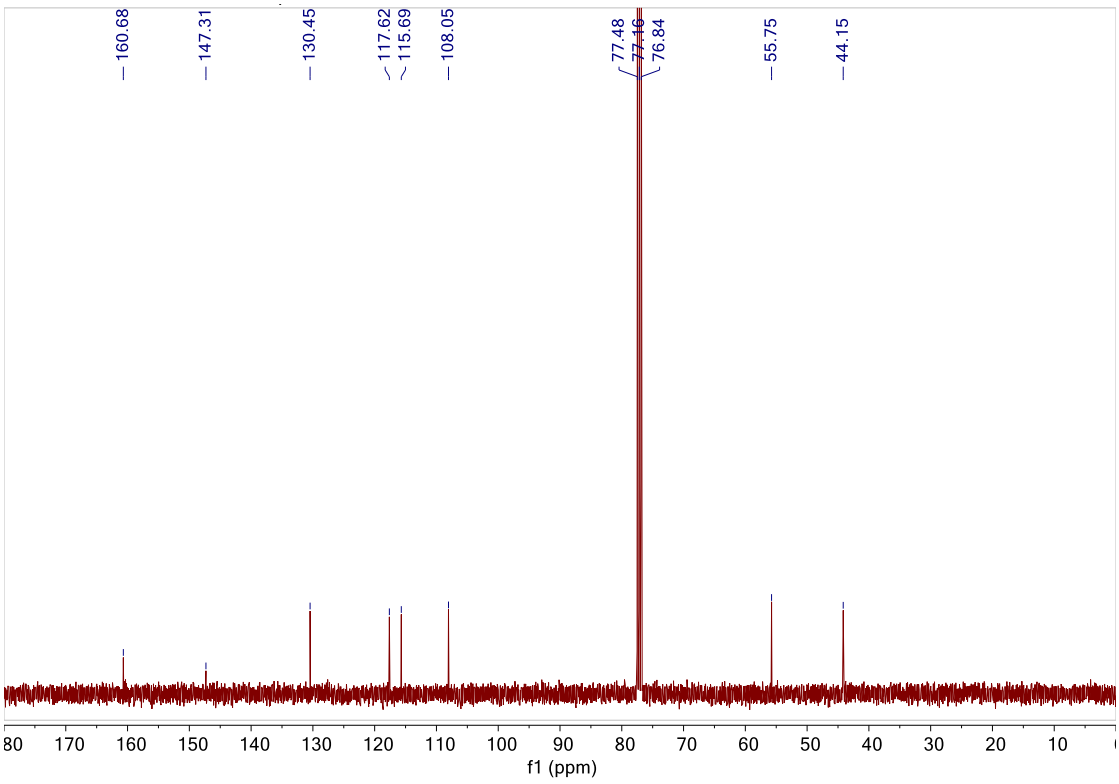

*2-(Methylsulfinyl)naphthalene* ***28ai***

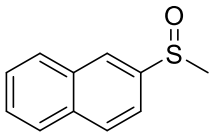

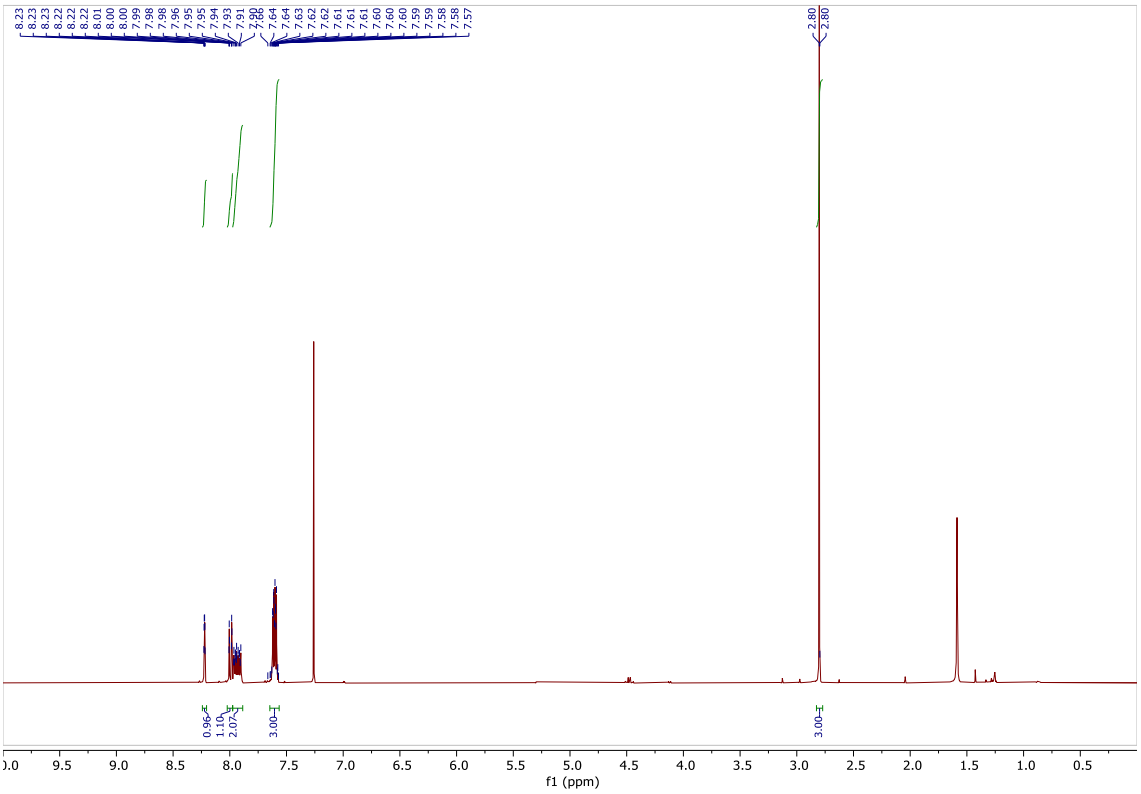


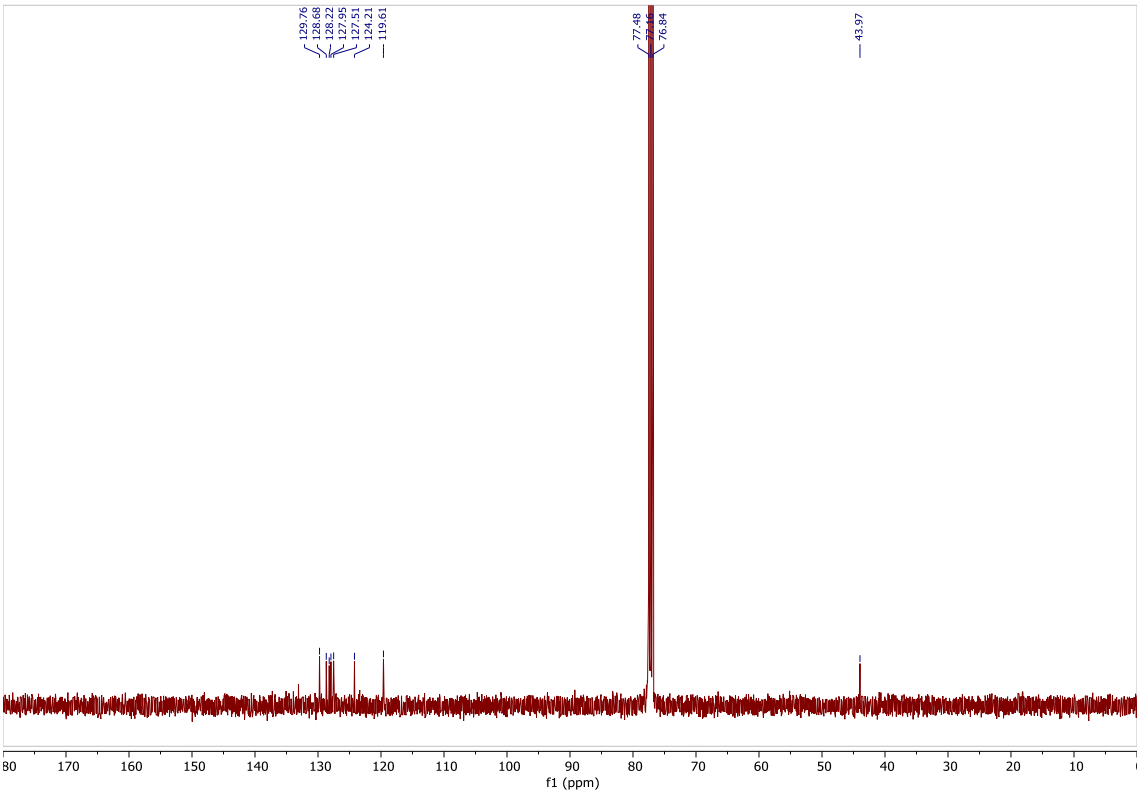

*1-(Methylsulfinyl)naphthalene* ***28aj***

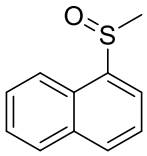


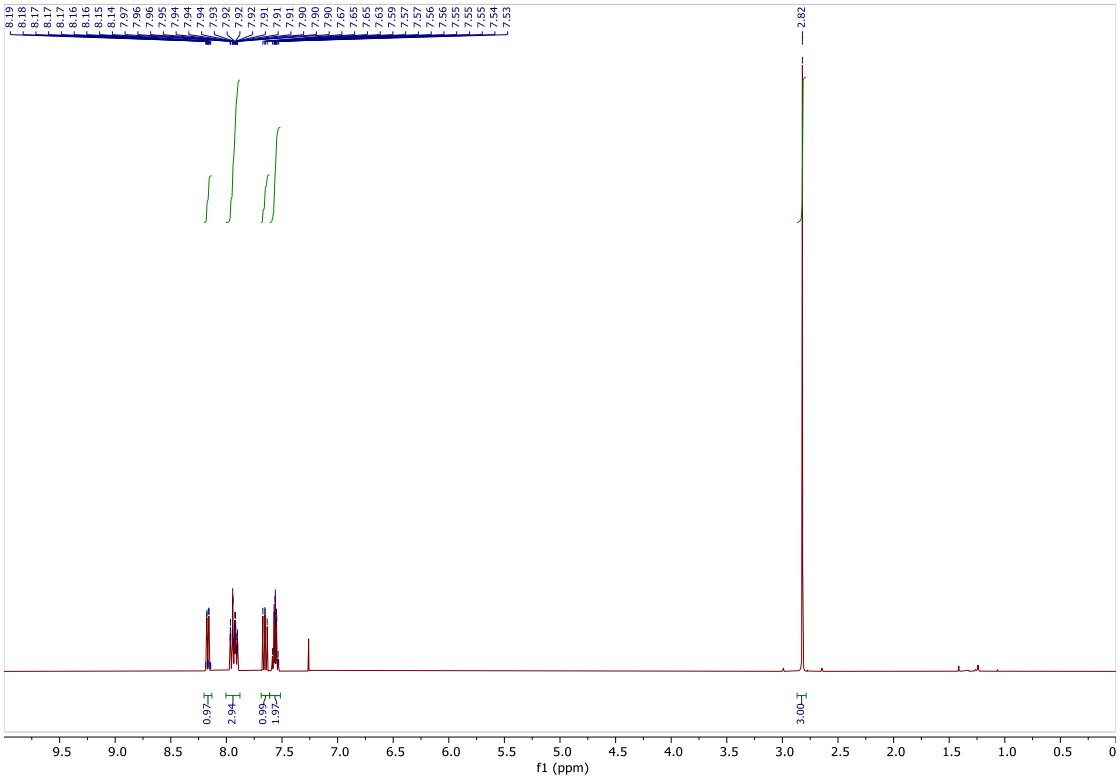


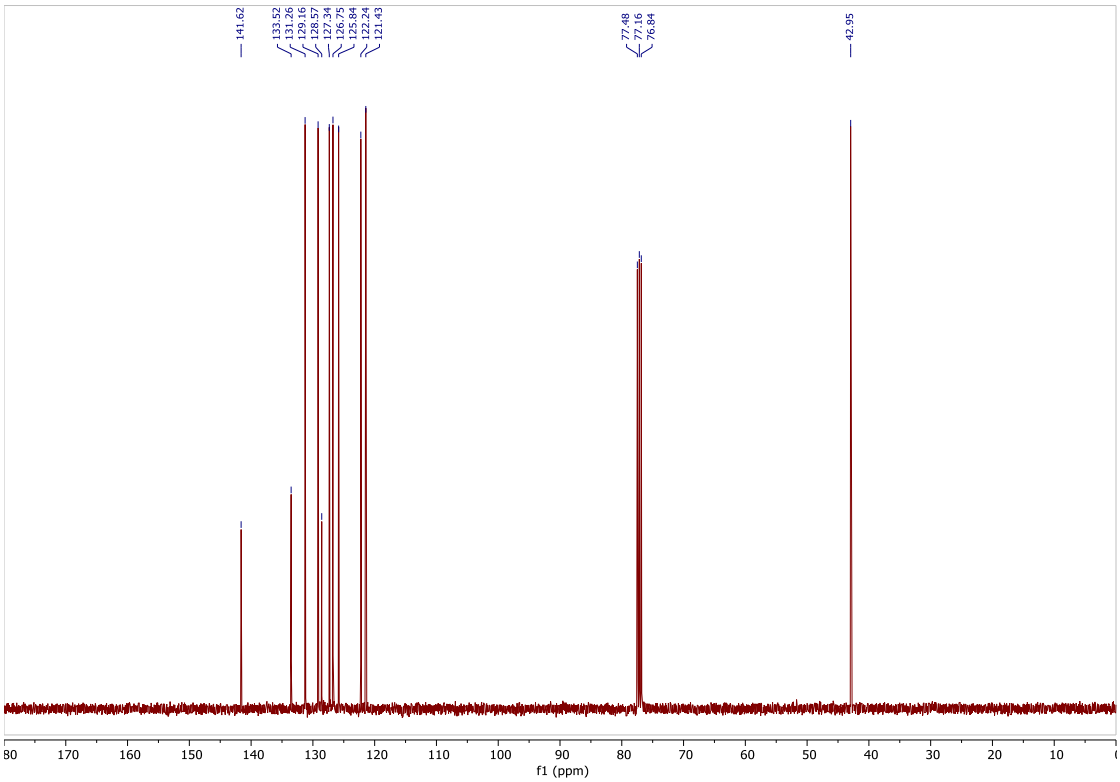

*4-(Methylsulfinyl)butan-2-one* ***28al***

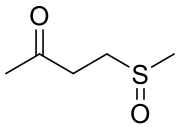

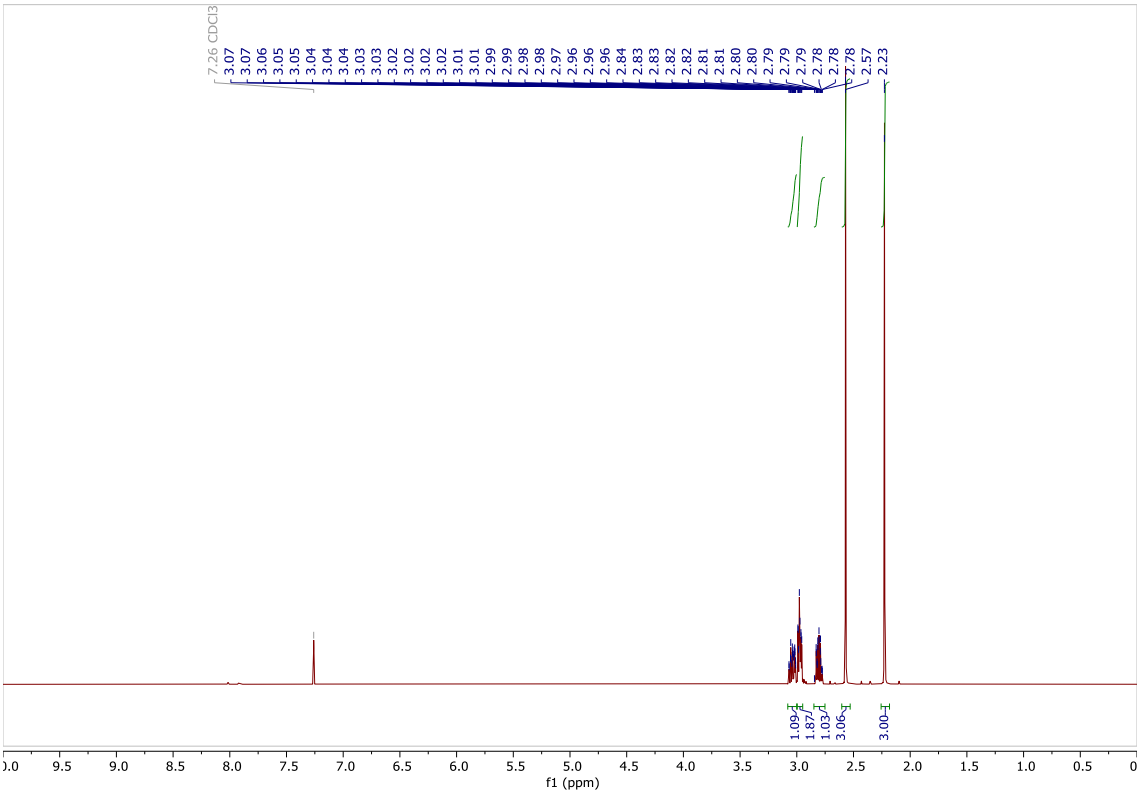


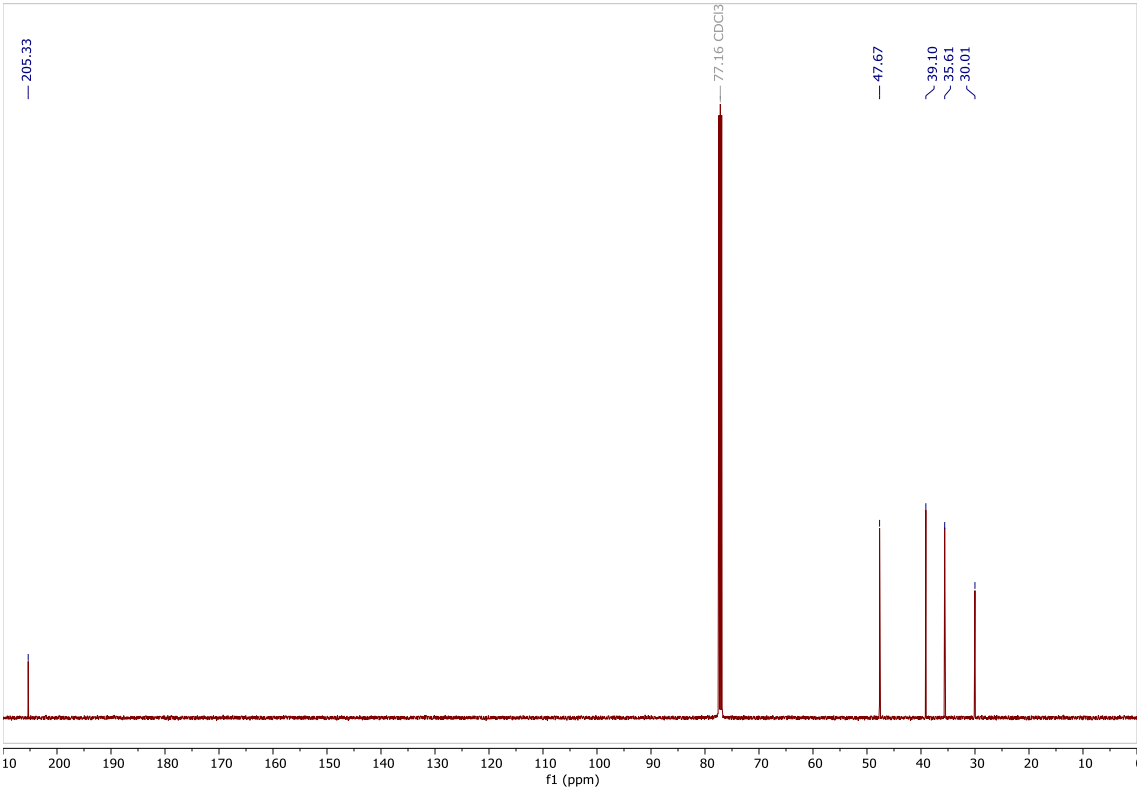

*((2-(Methylsulfinyl)ethyl)sulfinyl)benzene* ***28am***

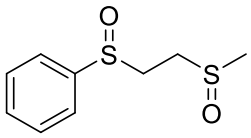

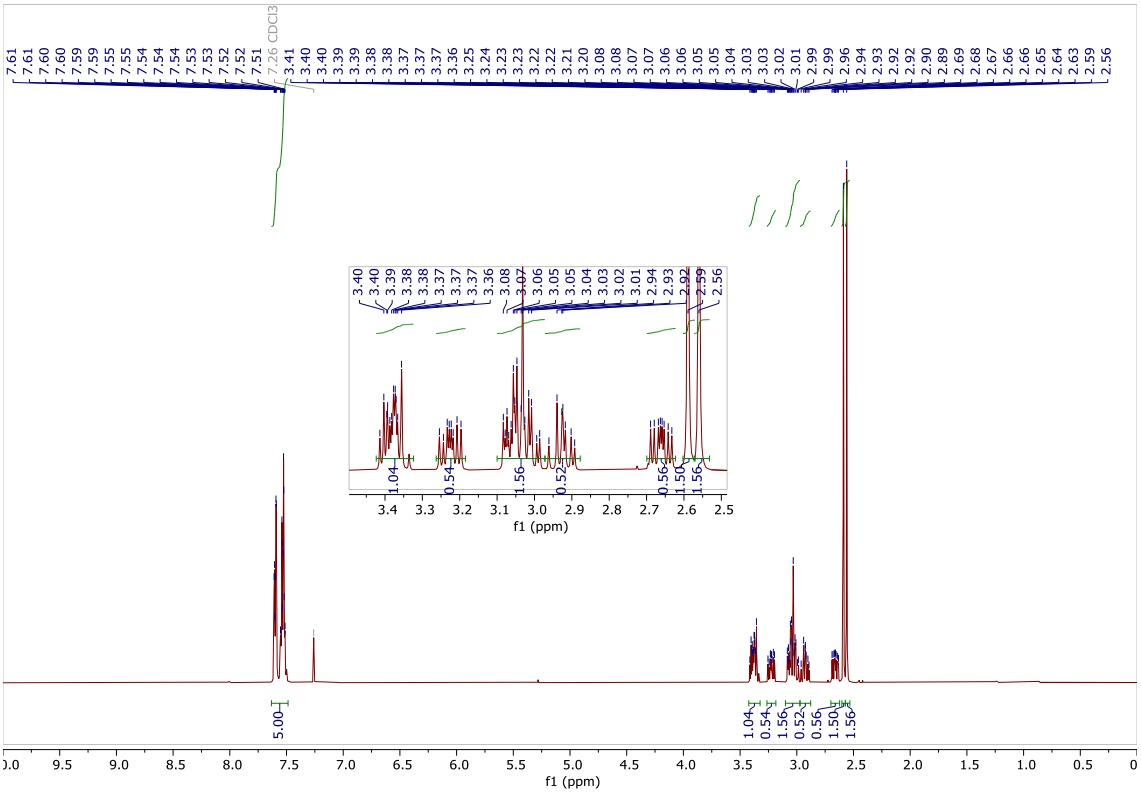


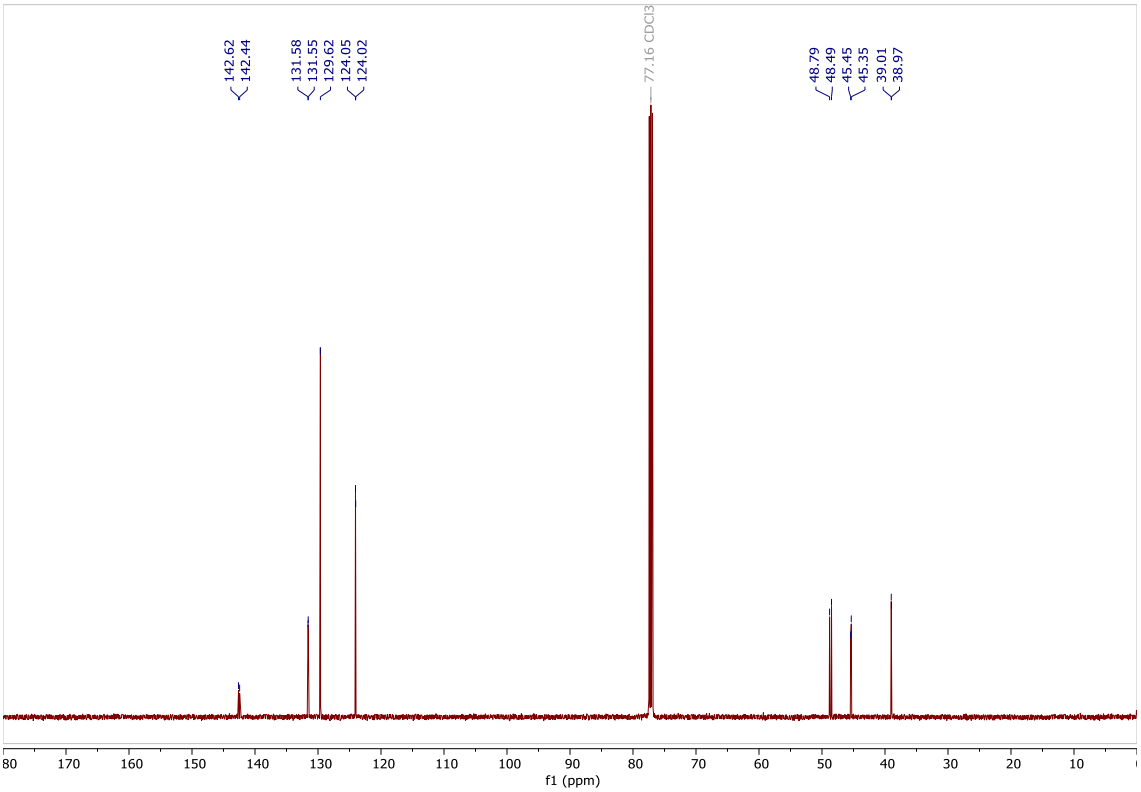

*(Propylsulfinyl)benzene* ***28an***

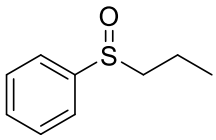

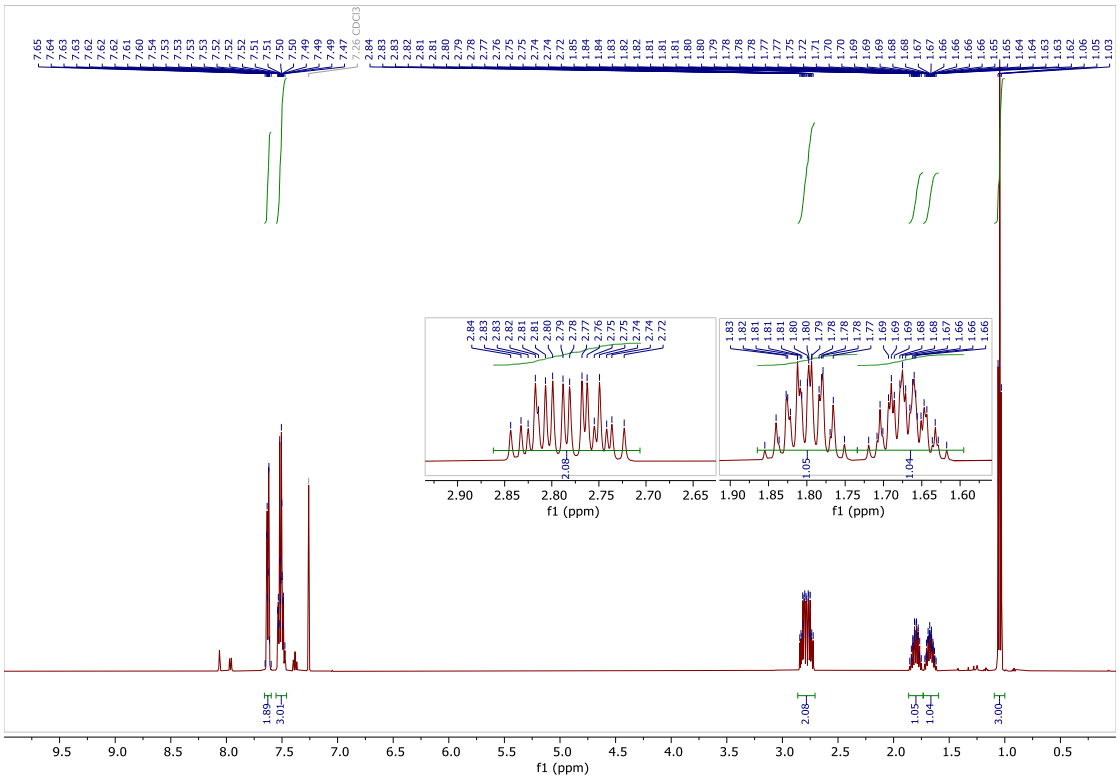


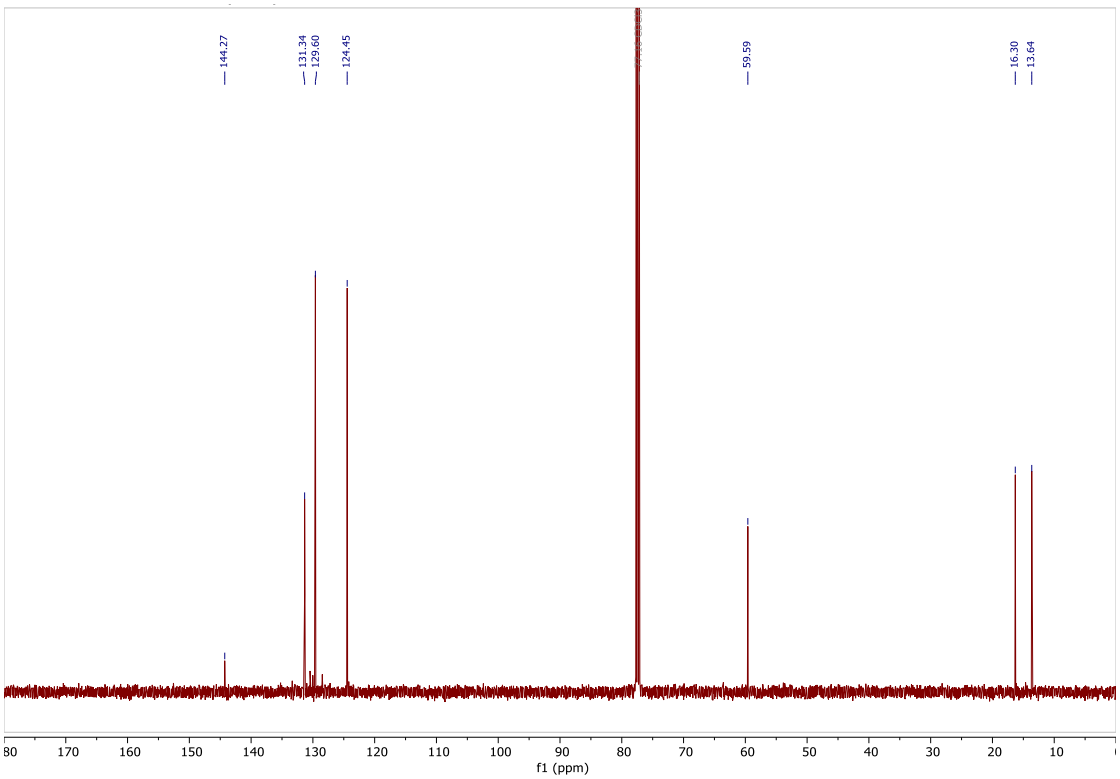

*1-Chloro-4-(propylsulfinyl)benzene* ***28ao***

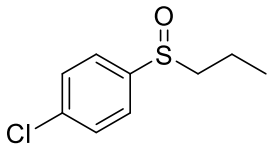


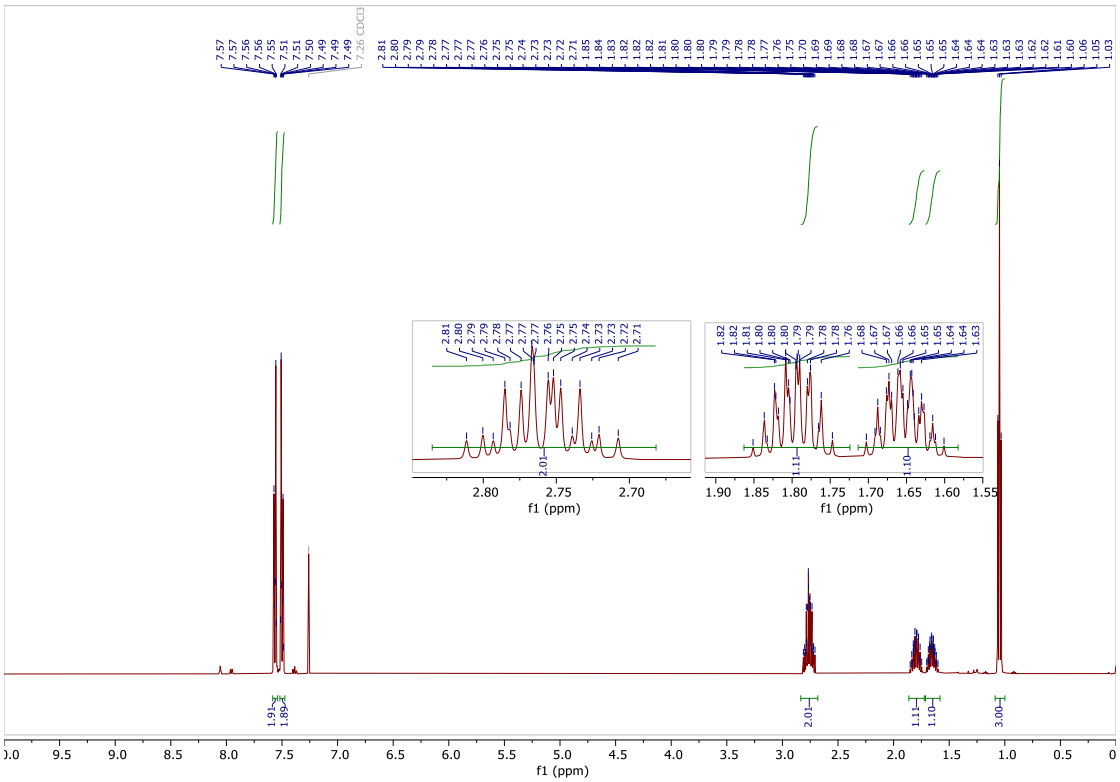


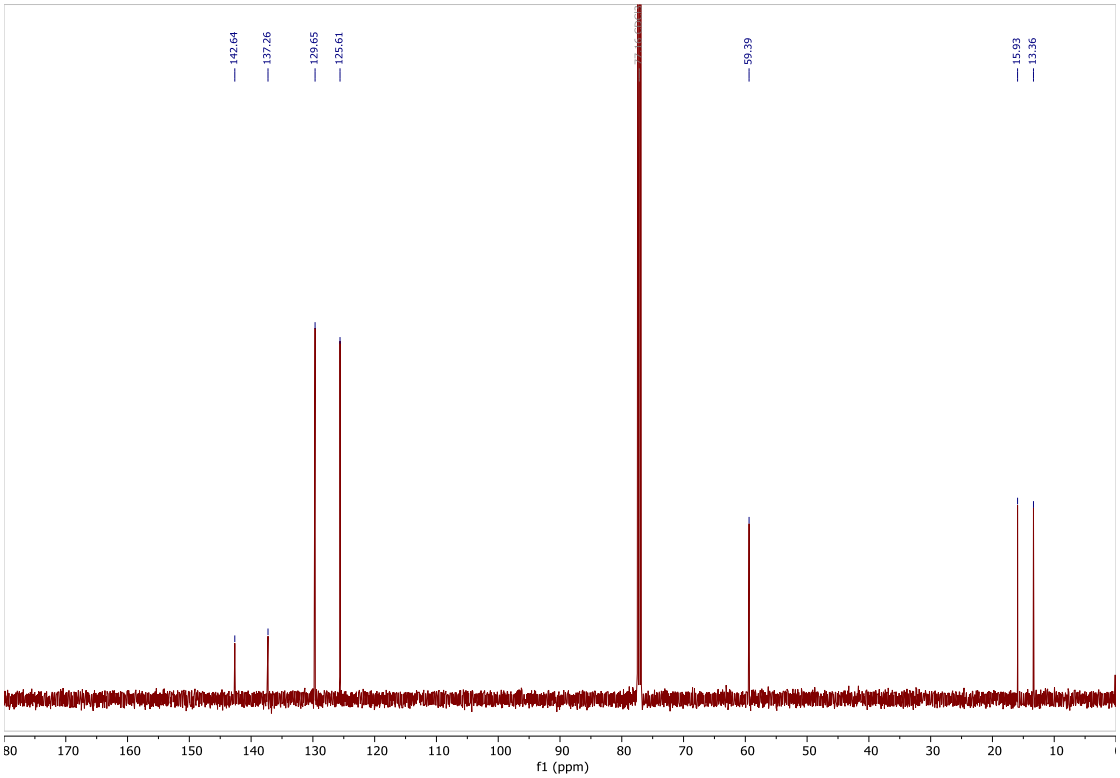

*1-Bromo-4-(propylsulfinyl)benzene* ***28ap***

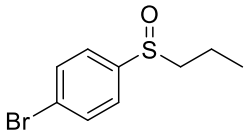


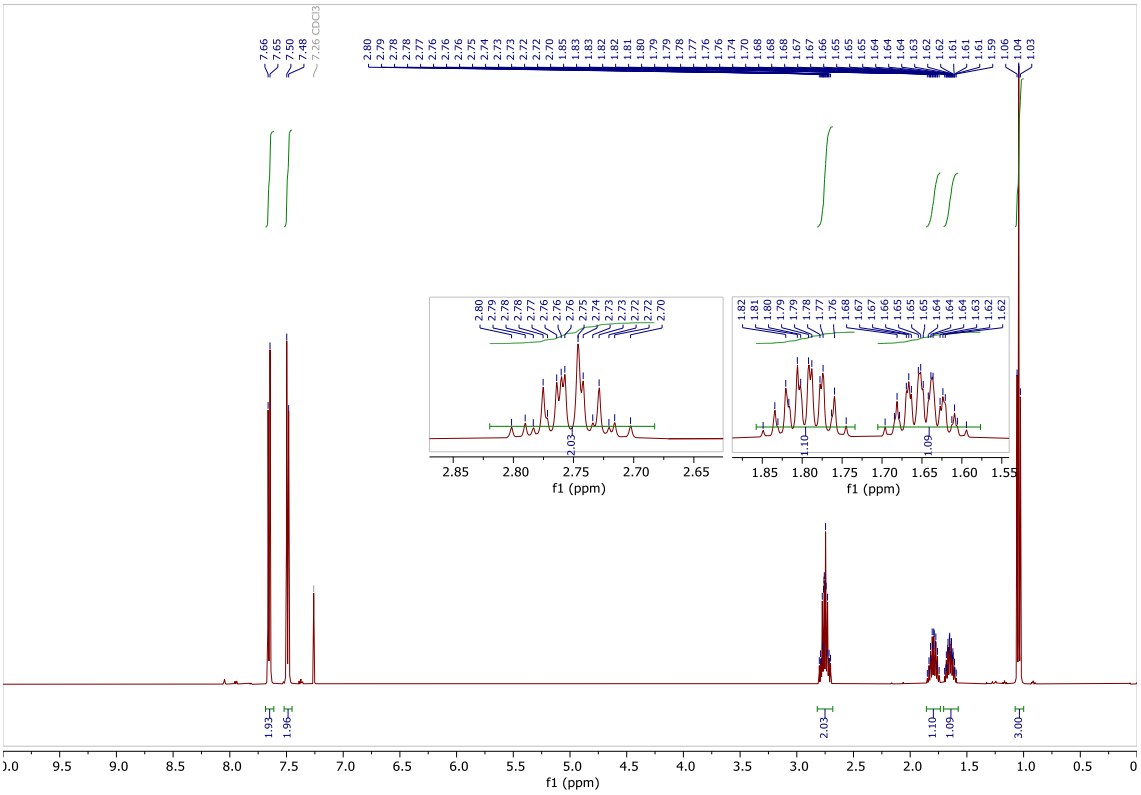


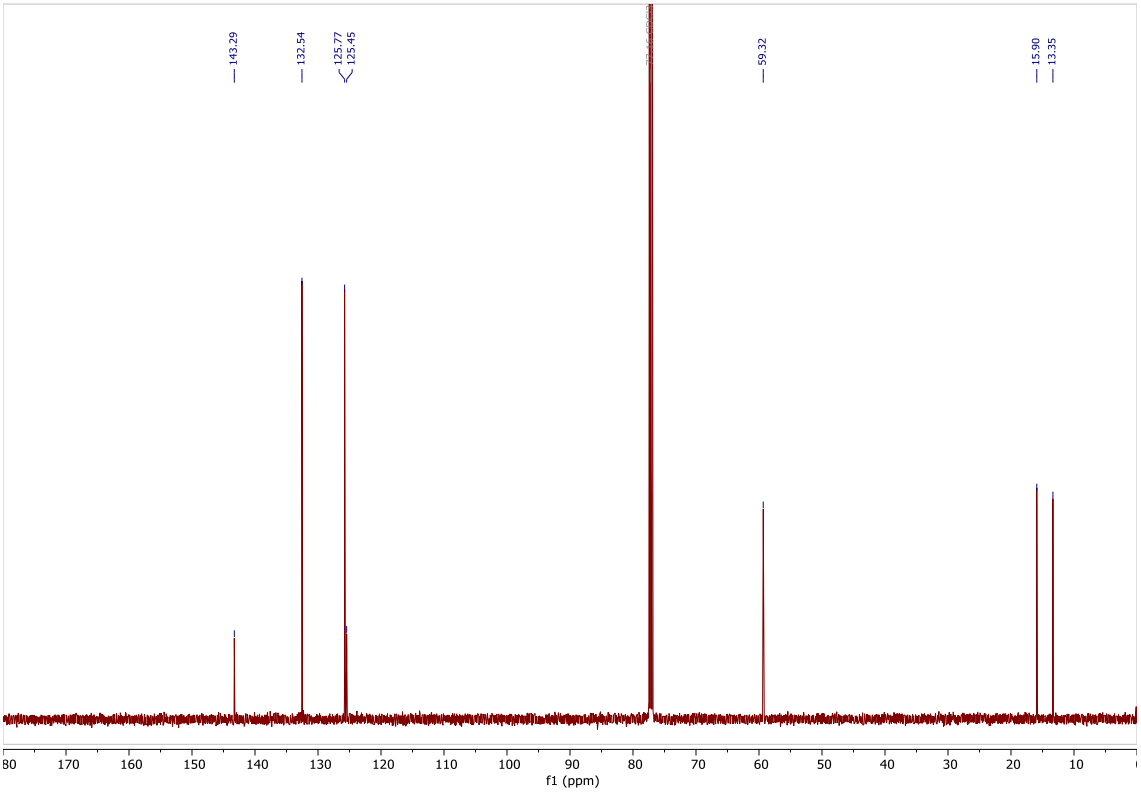

*1-Methoxy-3-(propylsulfinyl)benzene* ***28aq***

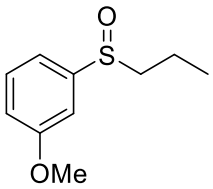


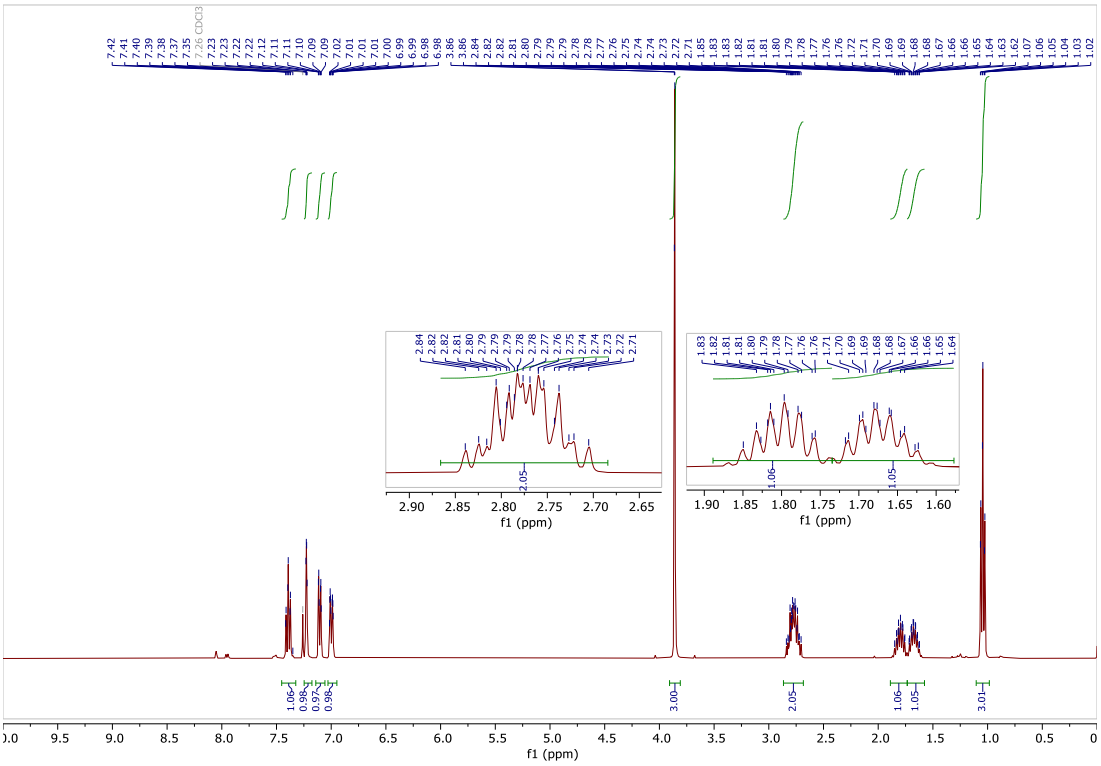


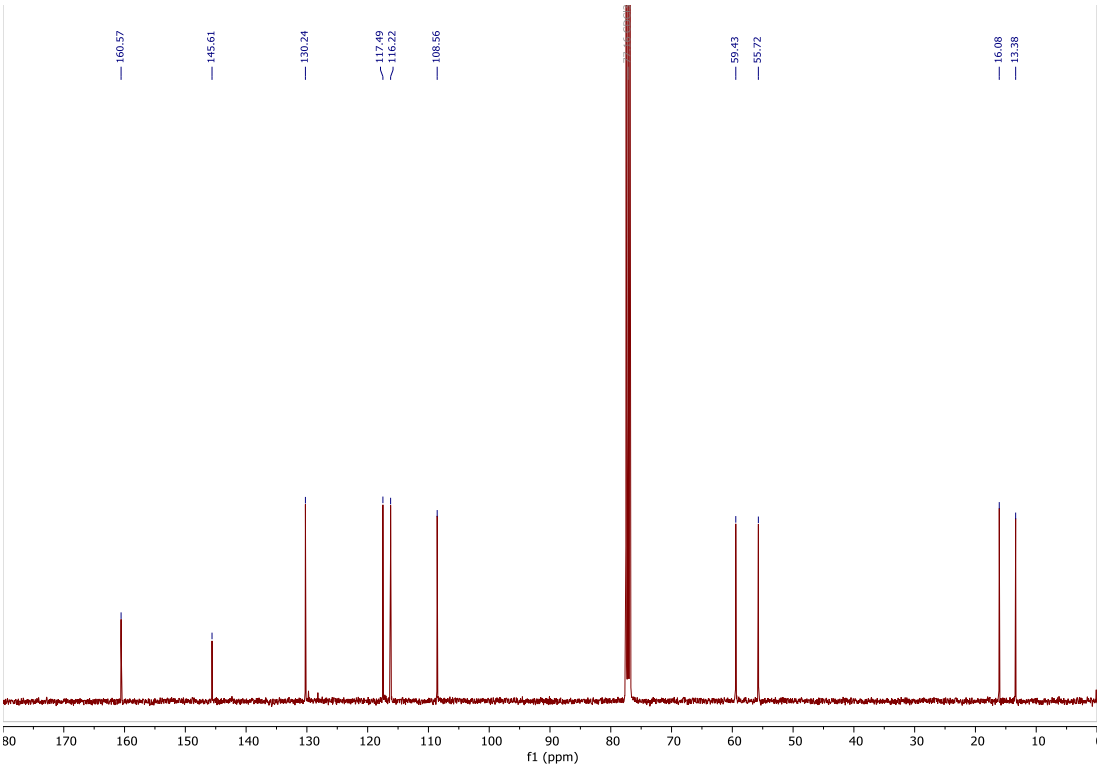

*1-Methoxy-4-(butylsulfinyl)benzene* ***28ar***

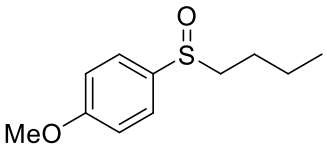


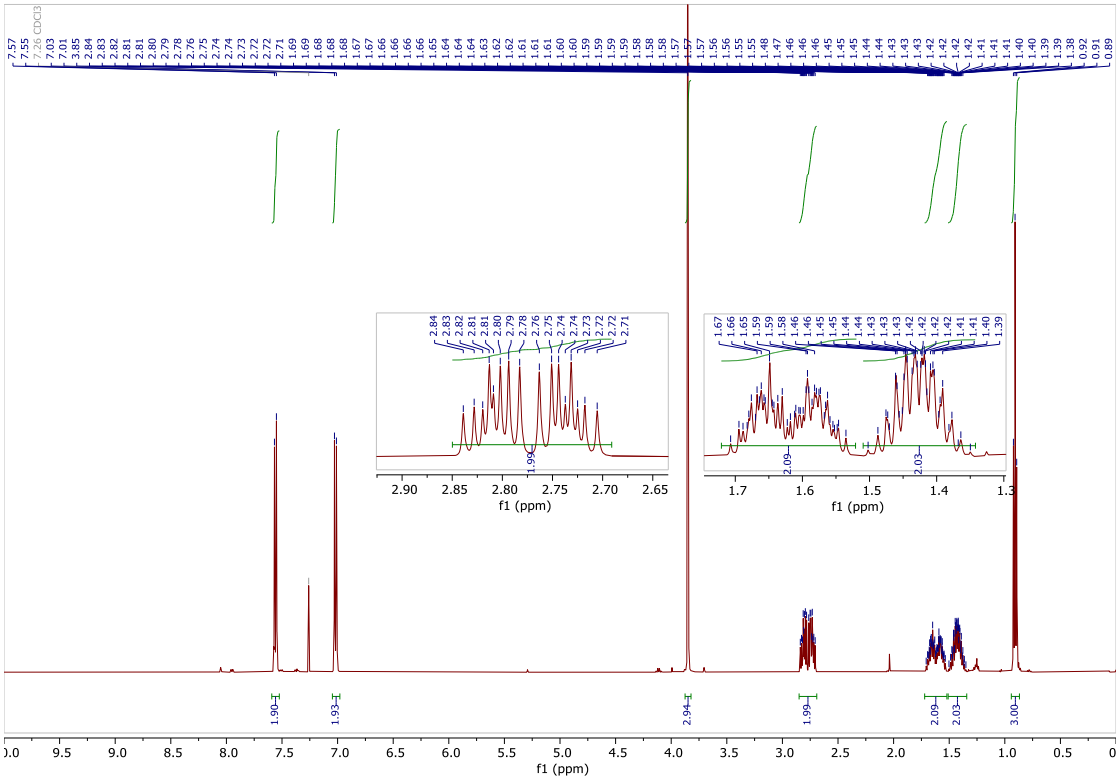


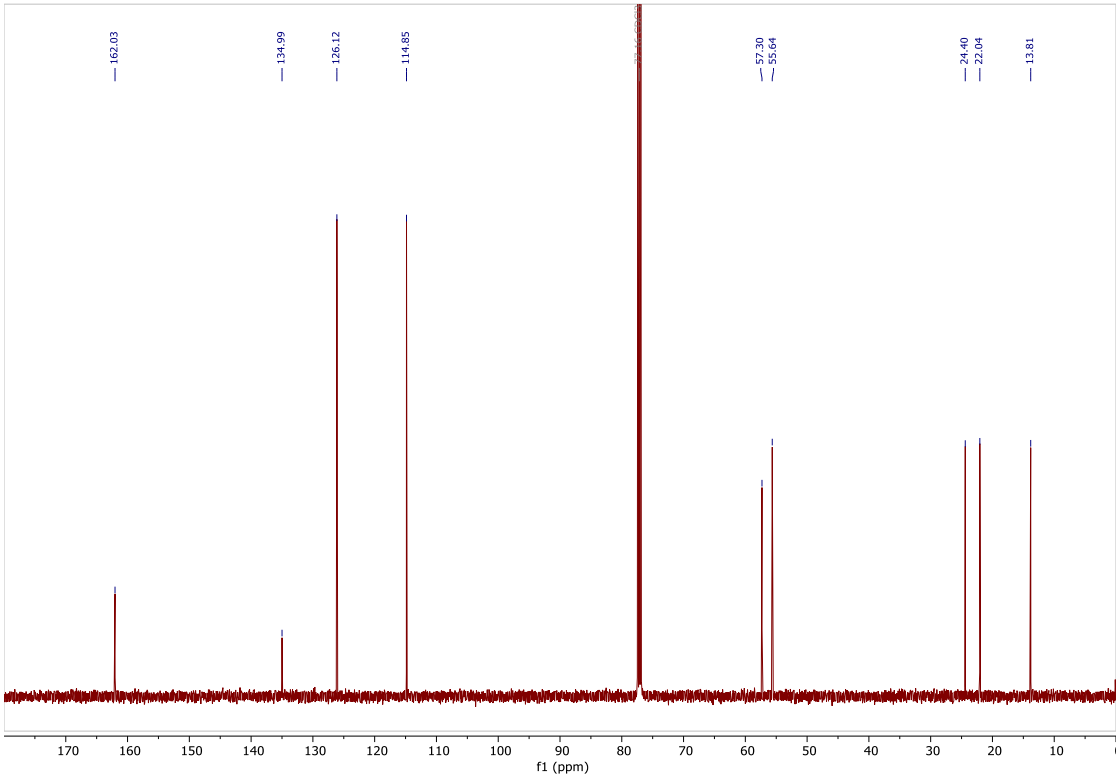

*4-(Phenylsulfinyl)butan-2-one* ***39a***

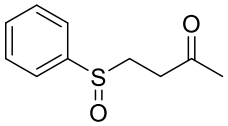


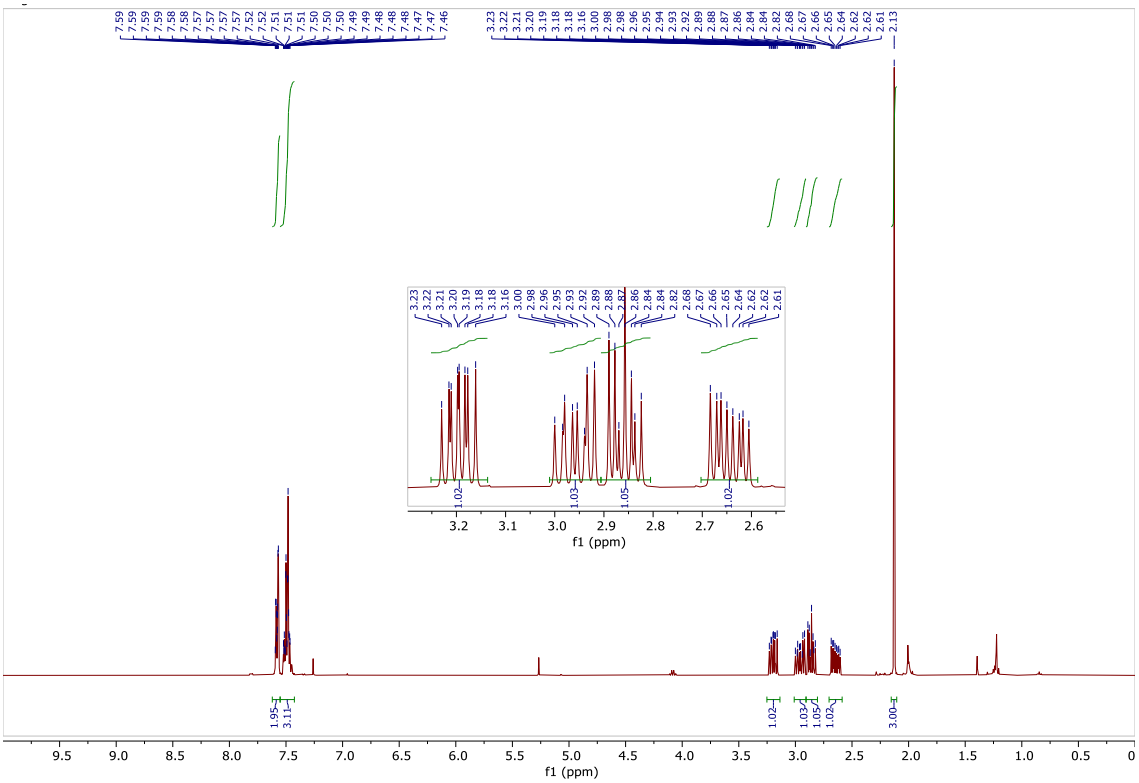


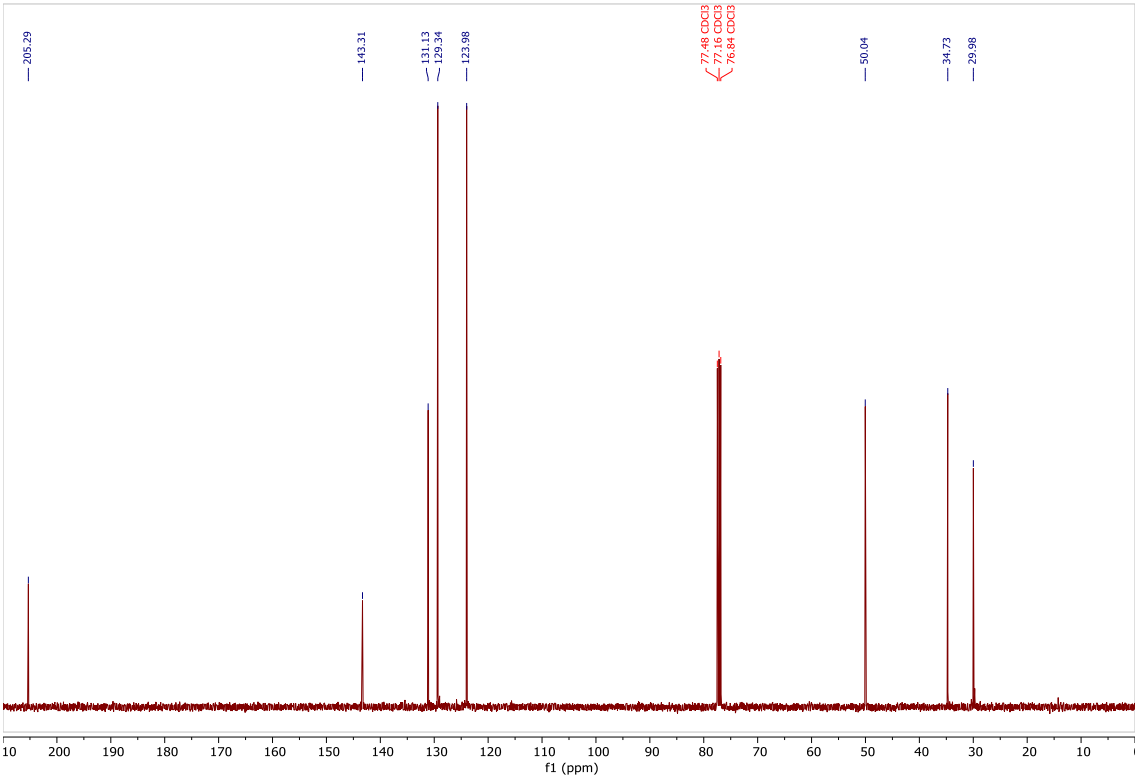

*4-(Phenylsulfinyl)pentan-2-one* ***39b***

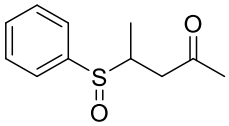

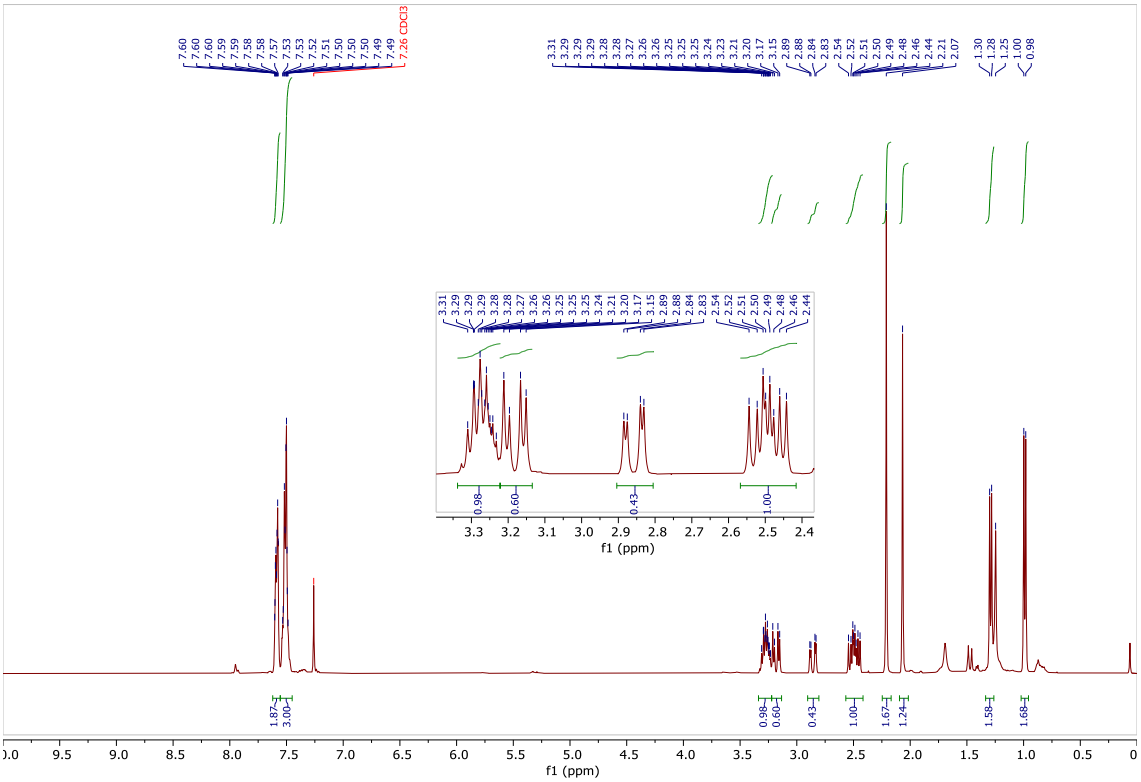


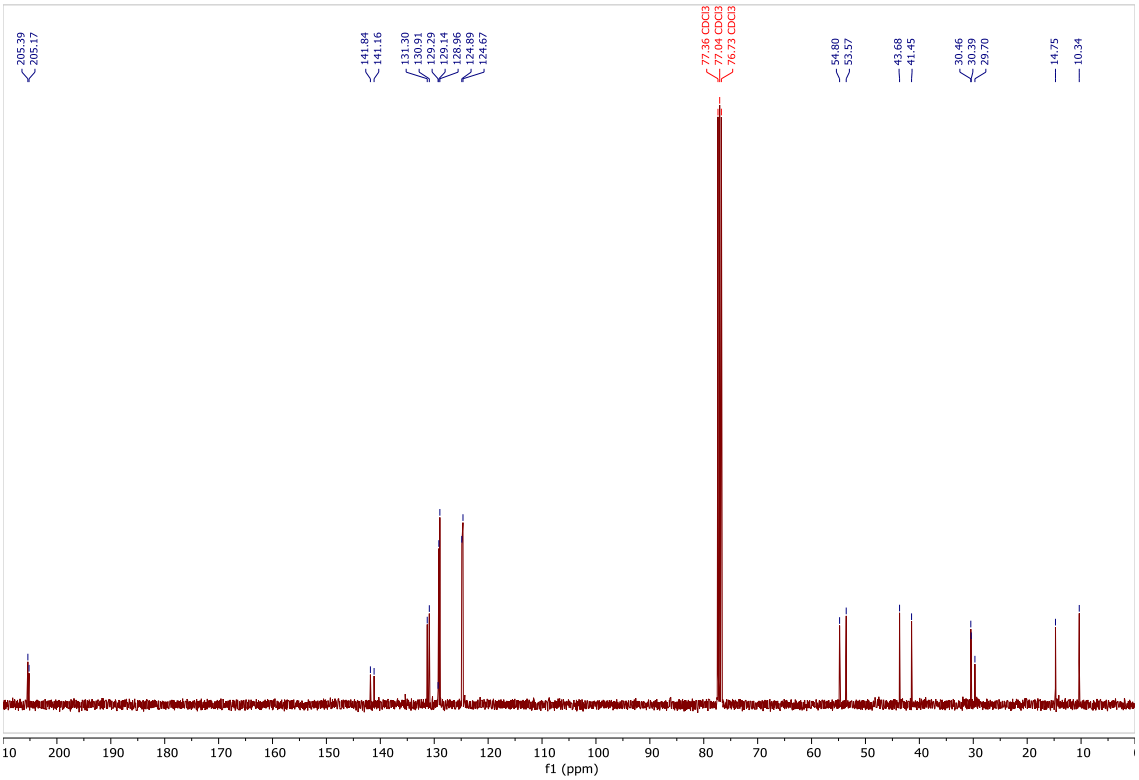

*1-(Phenylsulfinyl)propan-2-one* ***39d***

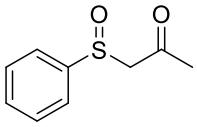

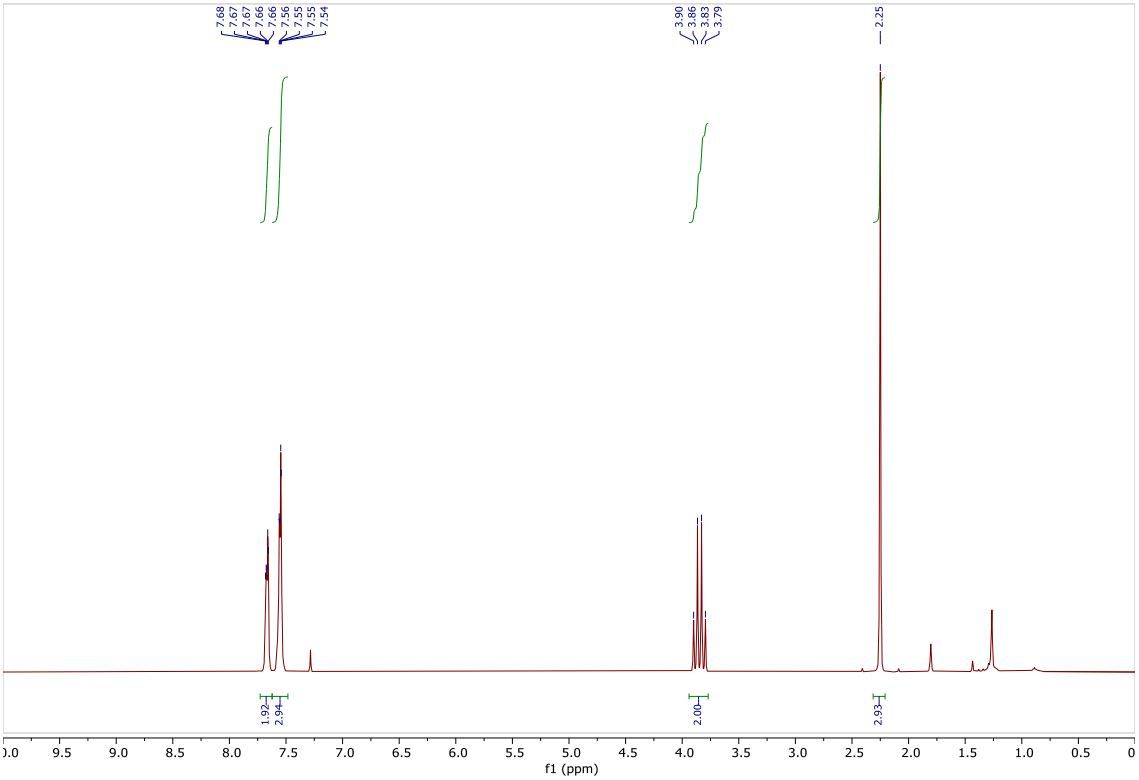


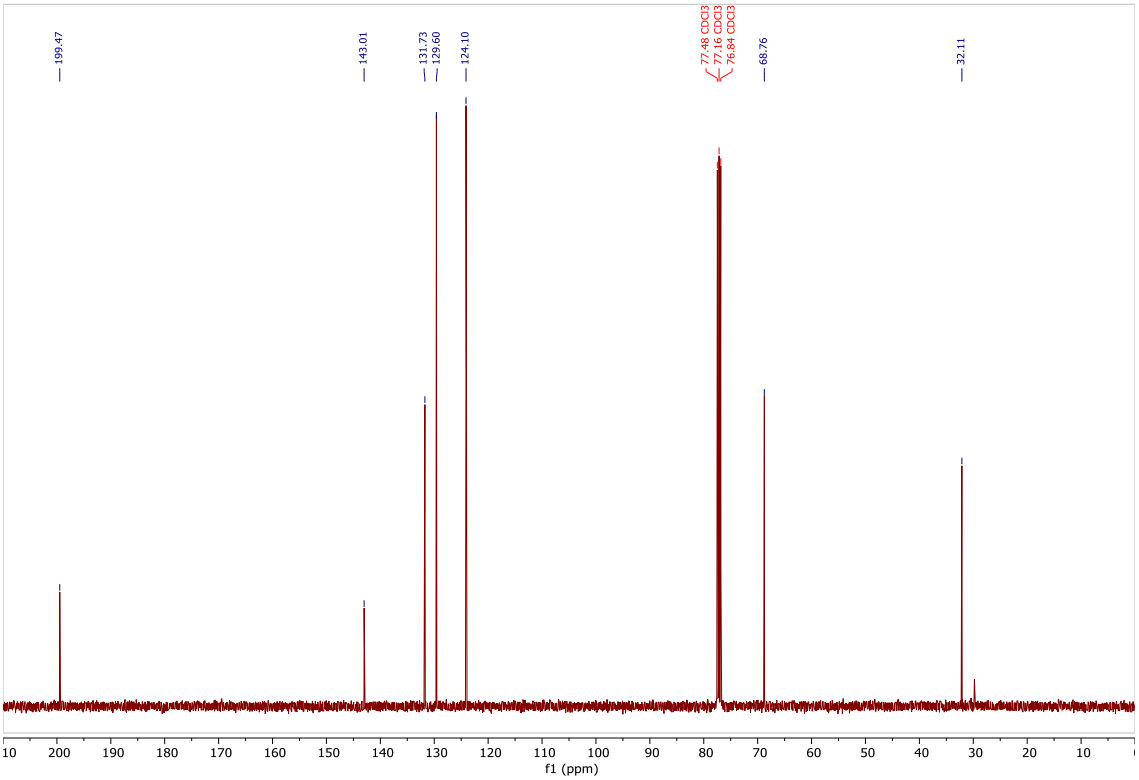

*1-(phenylsulfinyl)butan-2-one* ***39e***

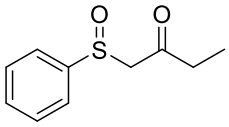

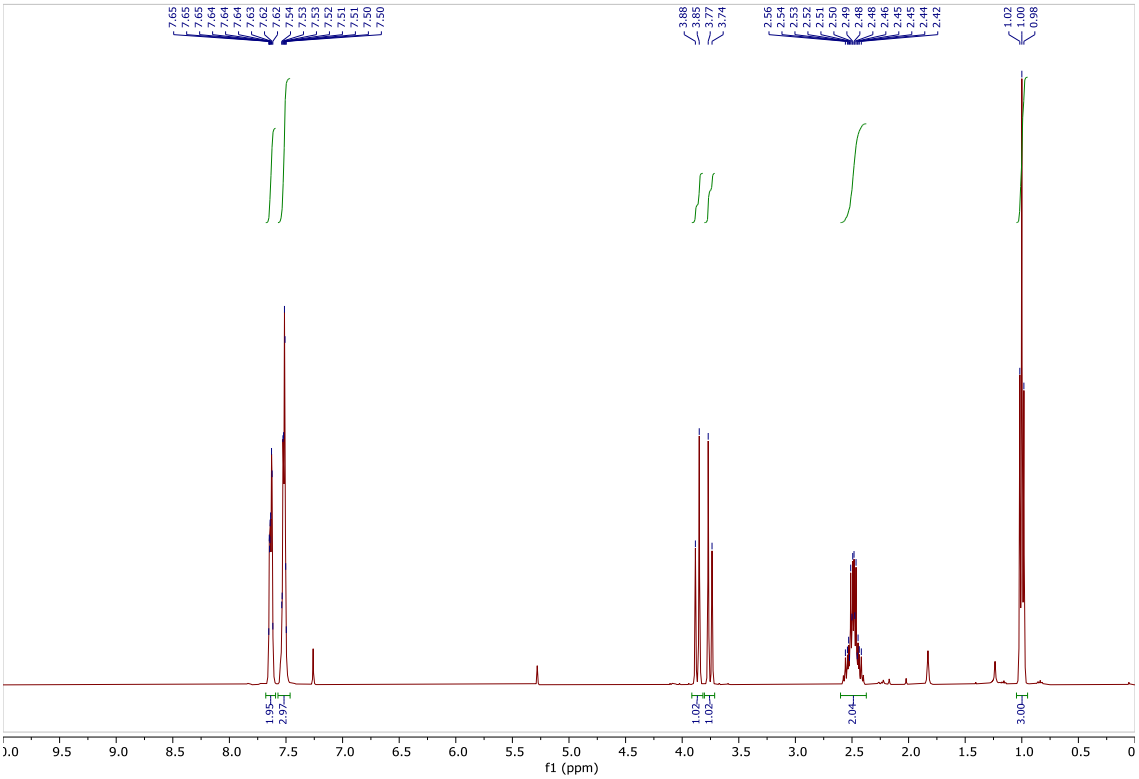


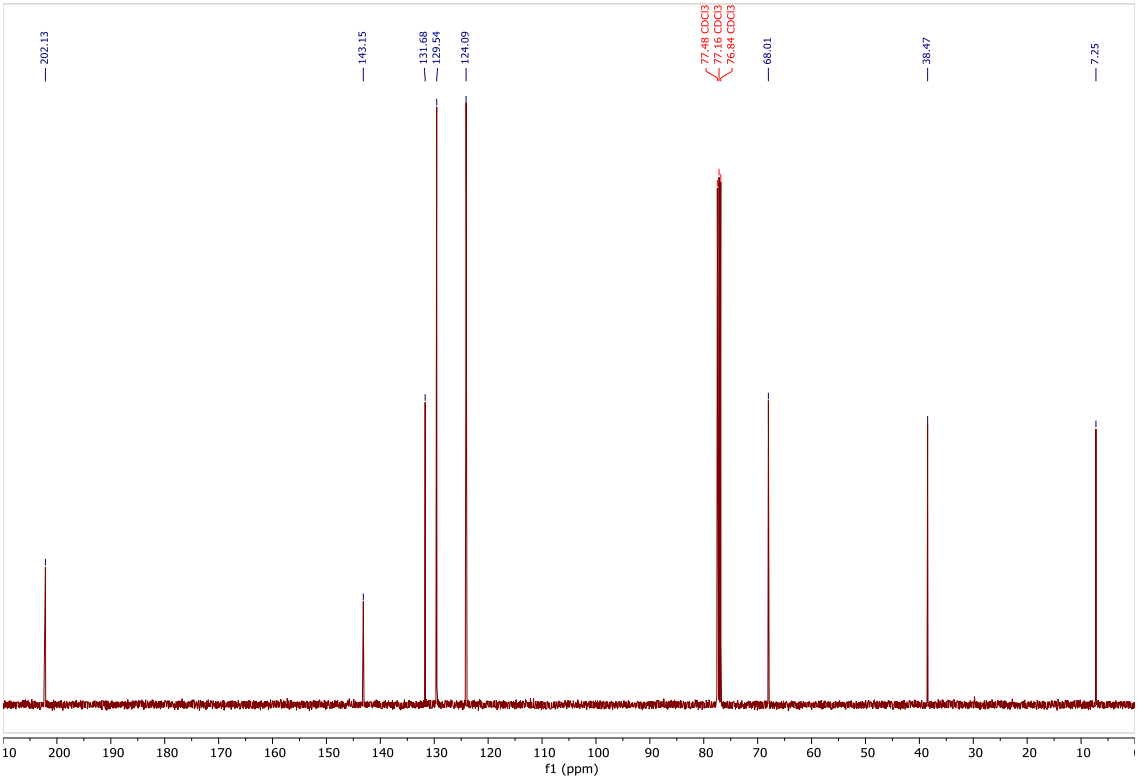

*3-Methyl-1-(phenylsulfinyl)butan-2-one* ***39f***

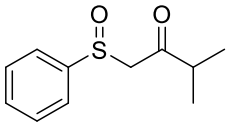

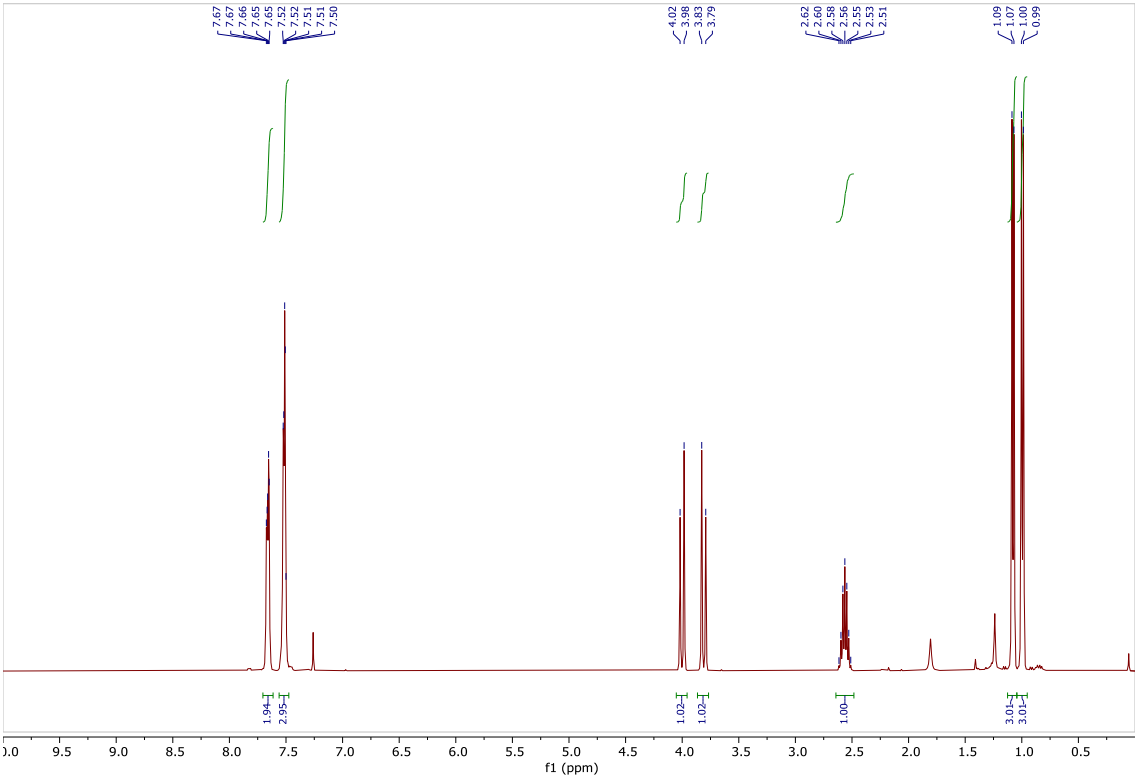


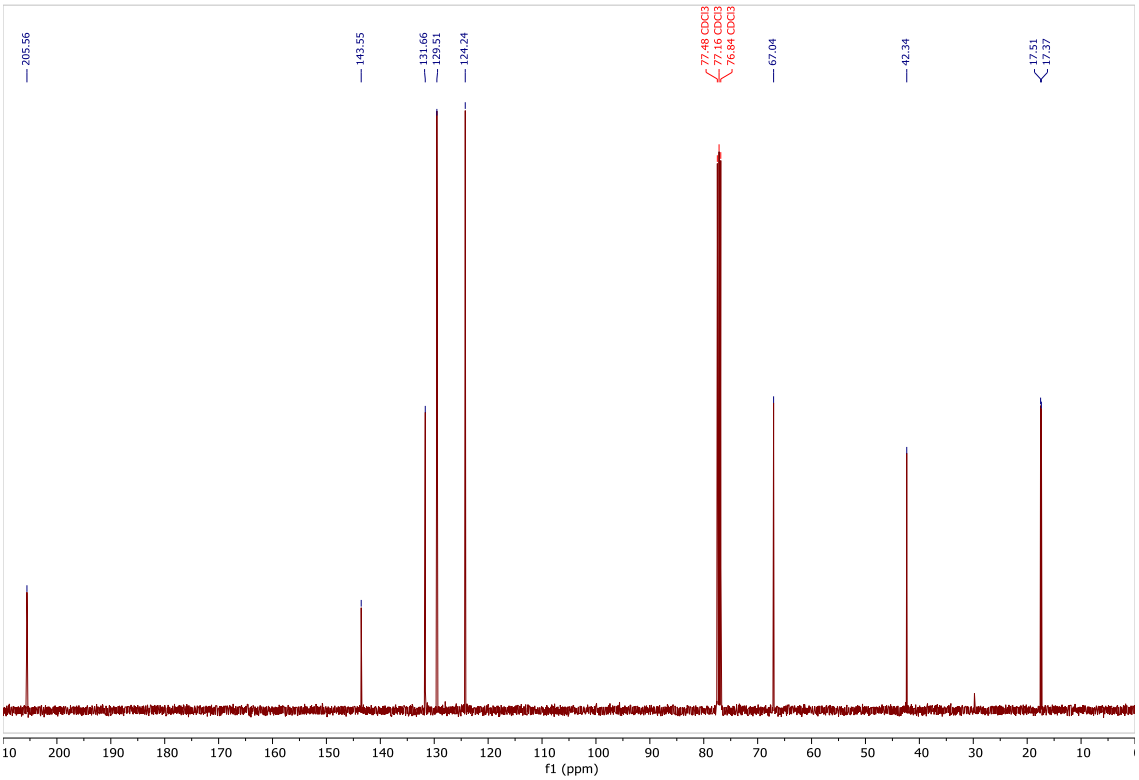

*4-(Phenylsulfinyl)butan-2-ol* ***41a***

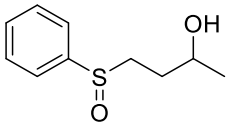


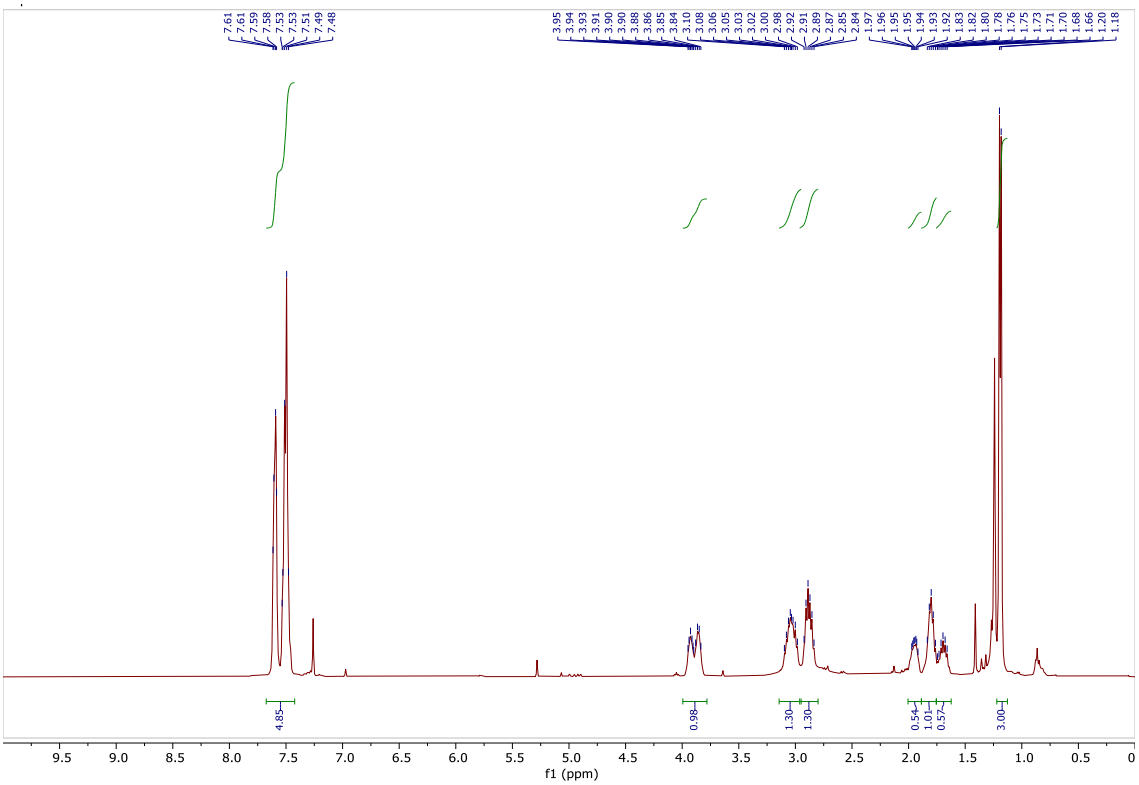


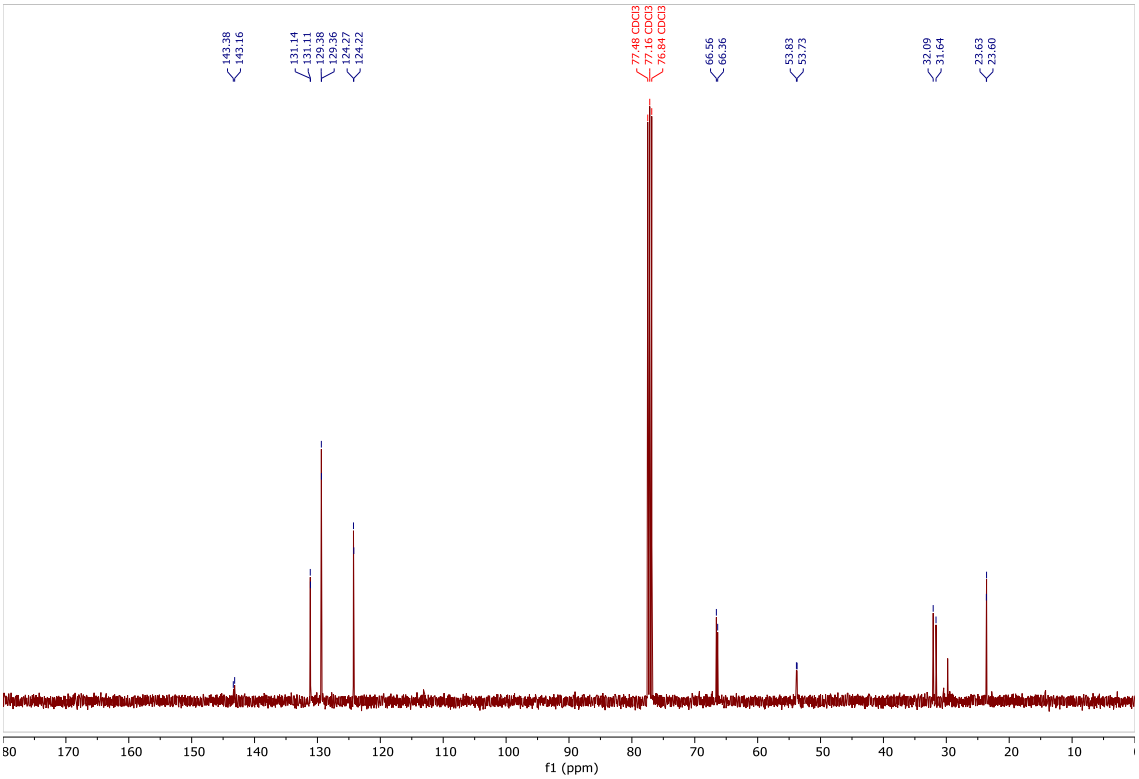

*3-(Phenylsulfinyl)butyl acetate* ***41b***

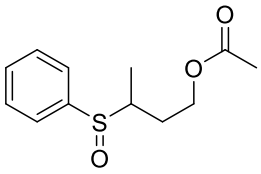

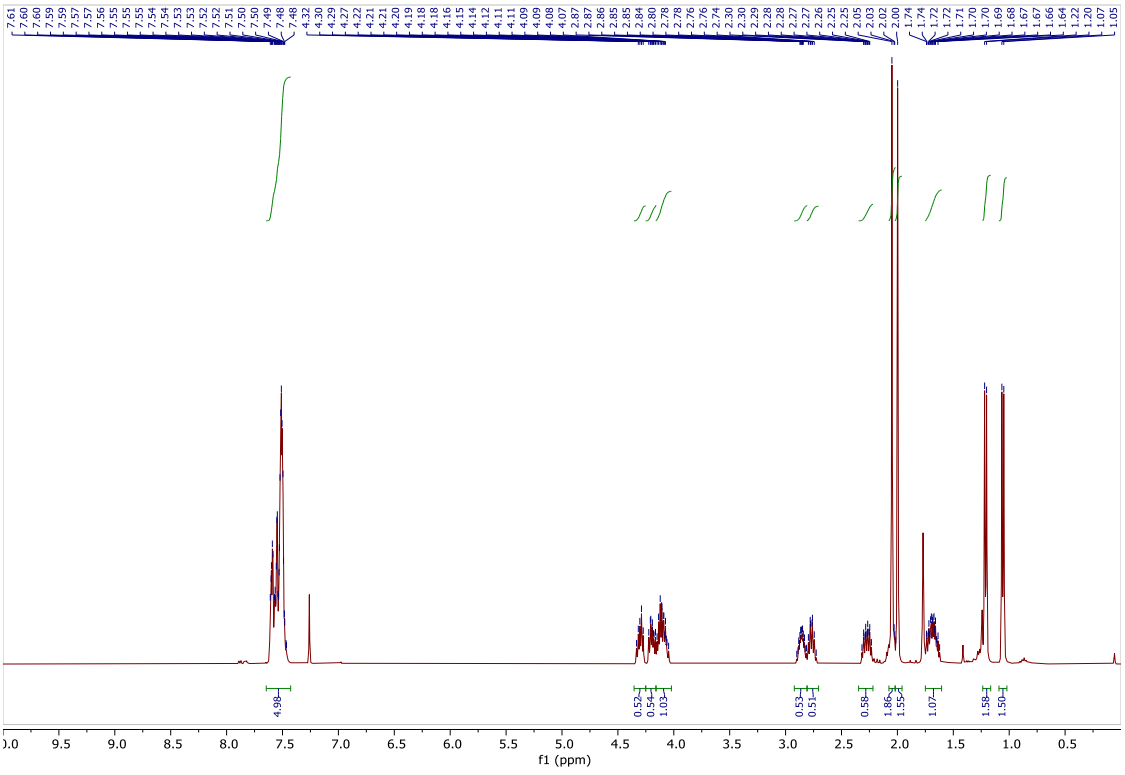


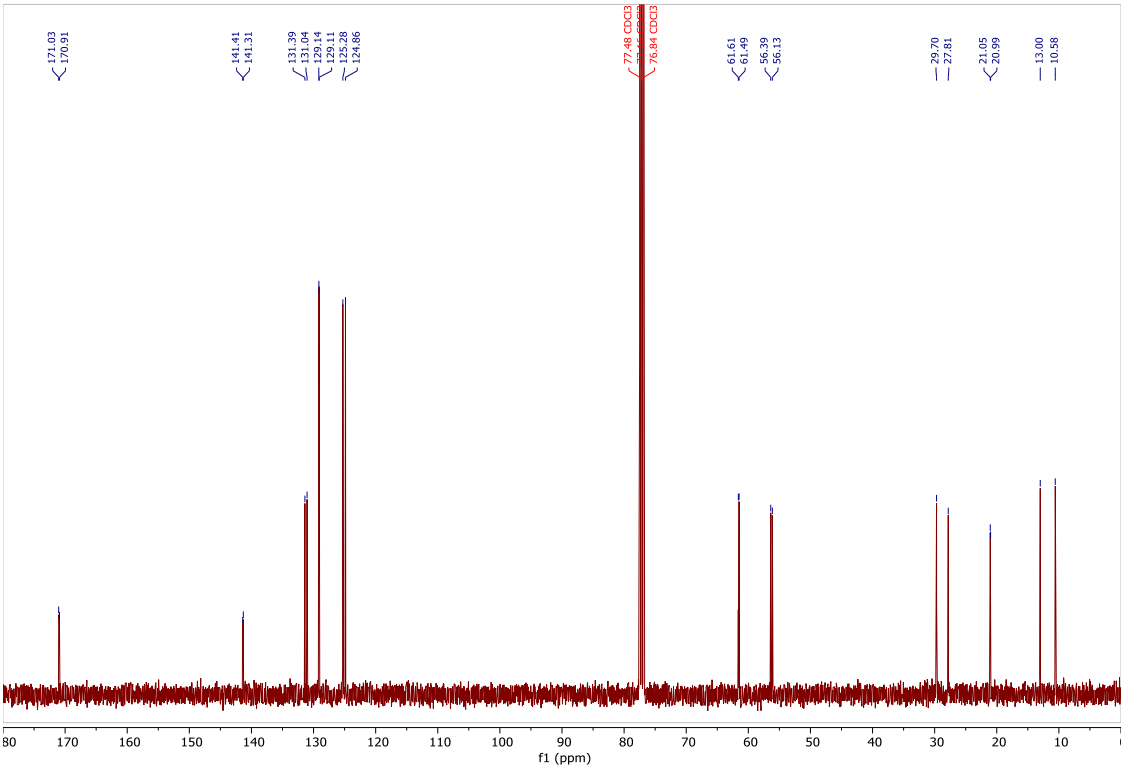

*Omeprazole* ***43***

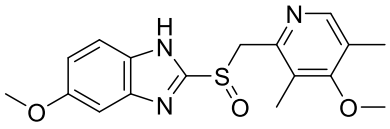

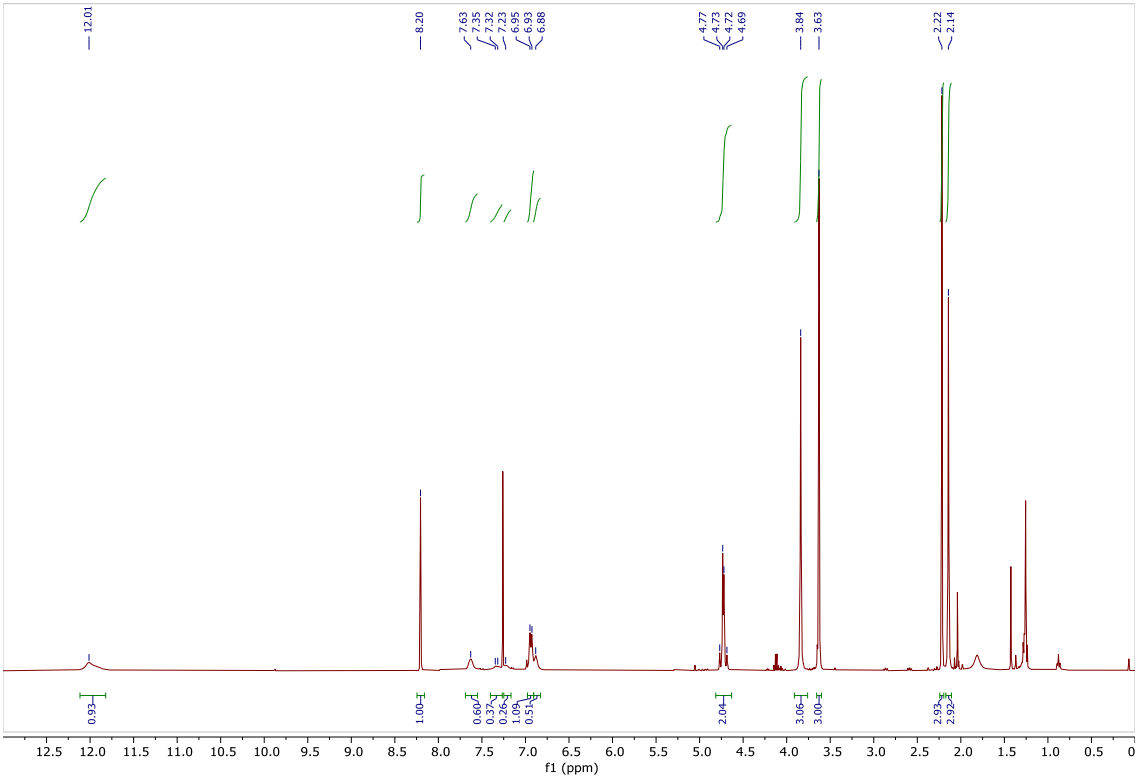


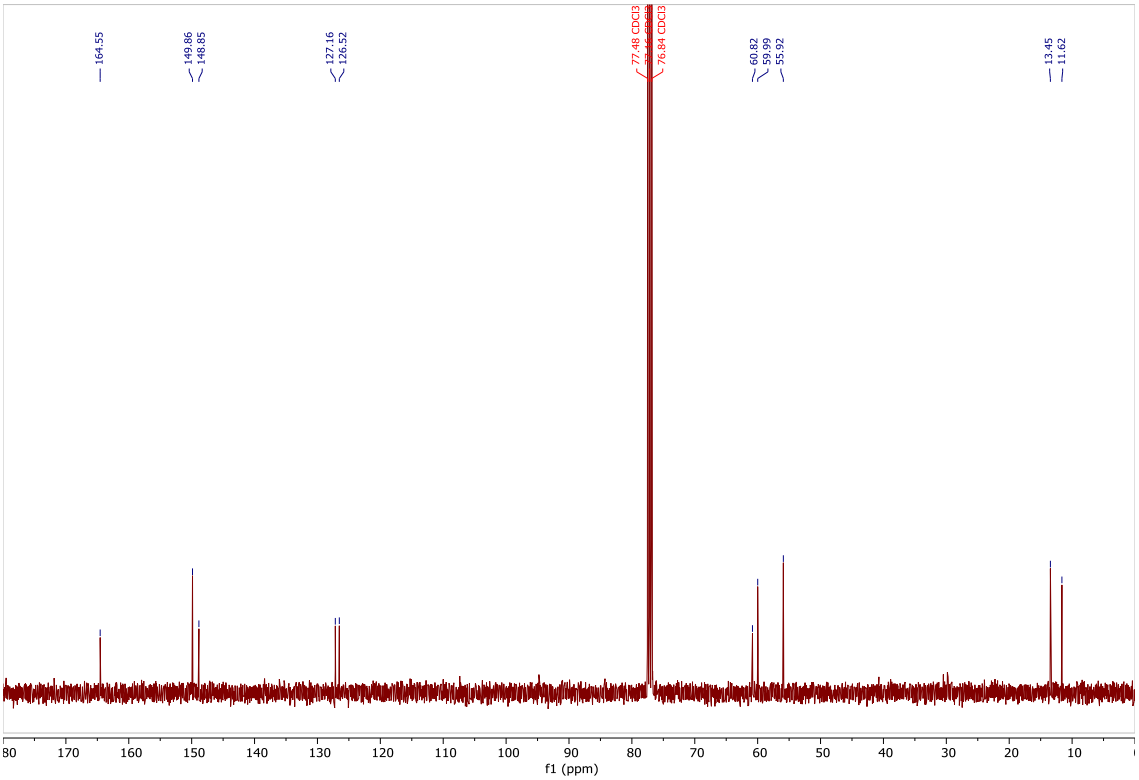

## Other compounds spectra

*(But-3-en-1-yloxy)benzene* ***33***

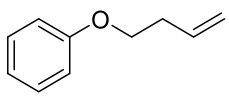

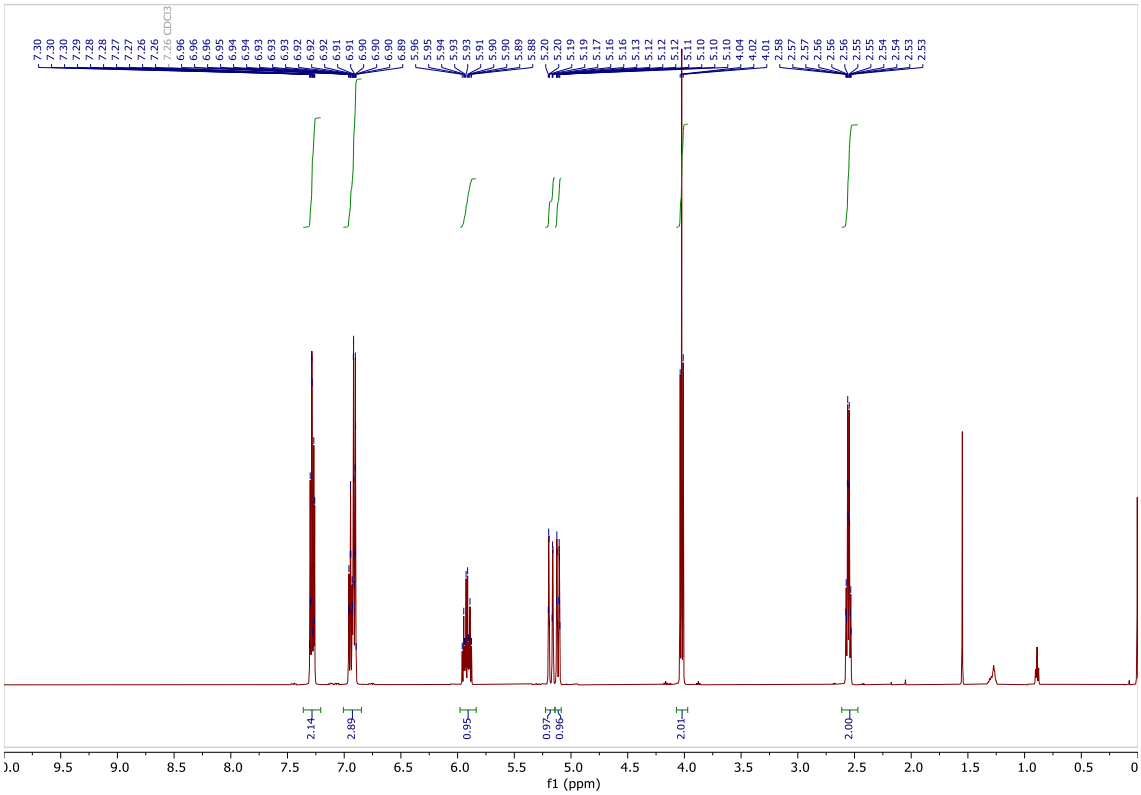

*Pivaloyl-L-proline* ***45***

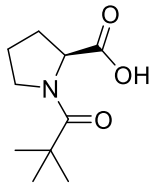


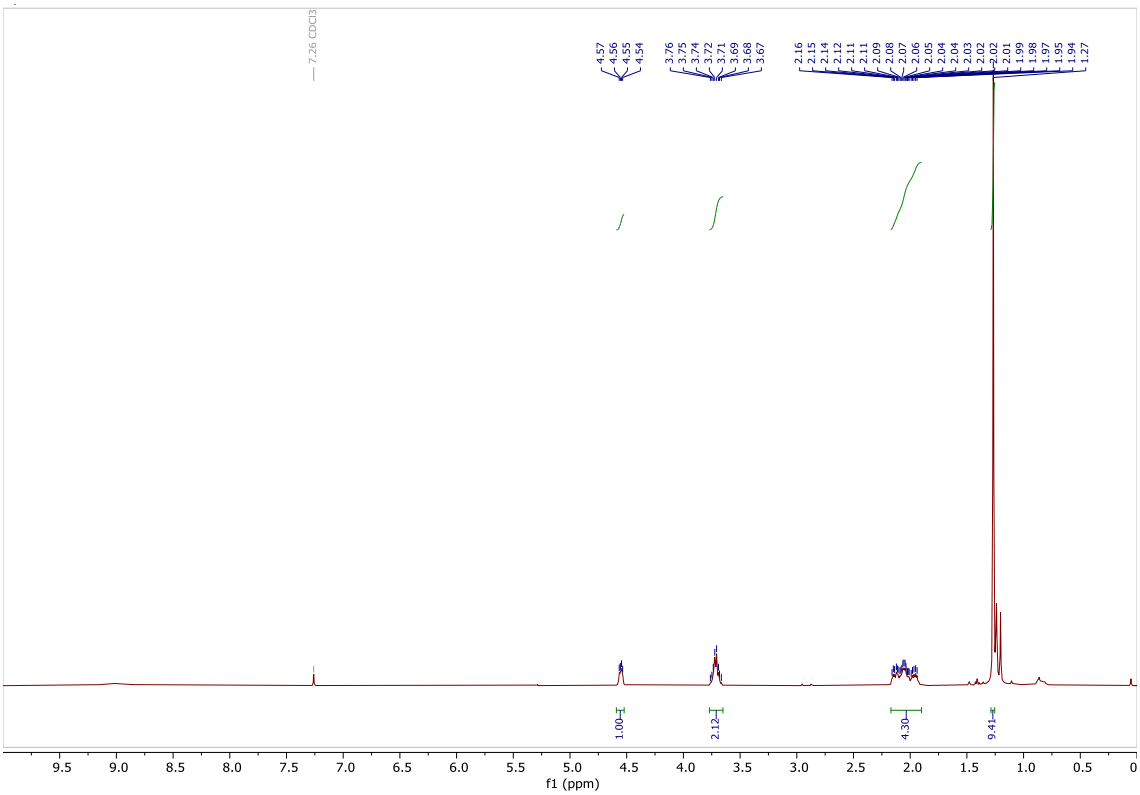

*Pivaloyl-L-phenylglycine* ***52***

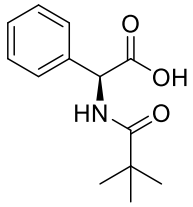


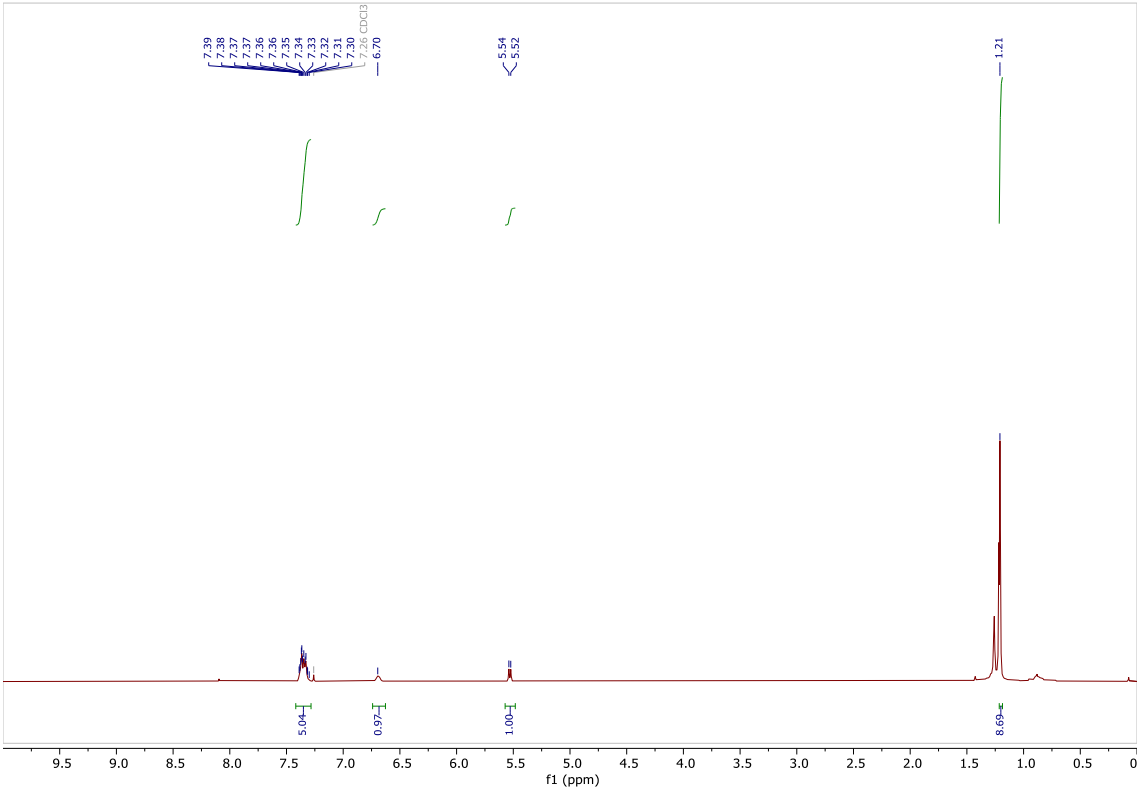

*Methyl(2-(phenylsulfinyl)ethyl)sulfane* ***27am-2***

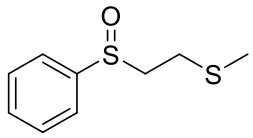

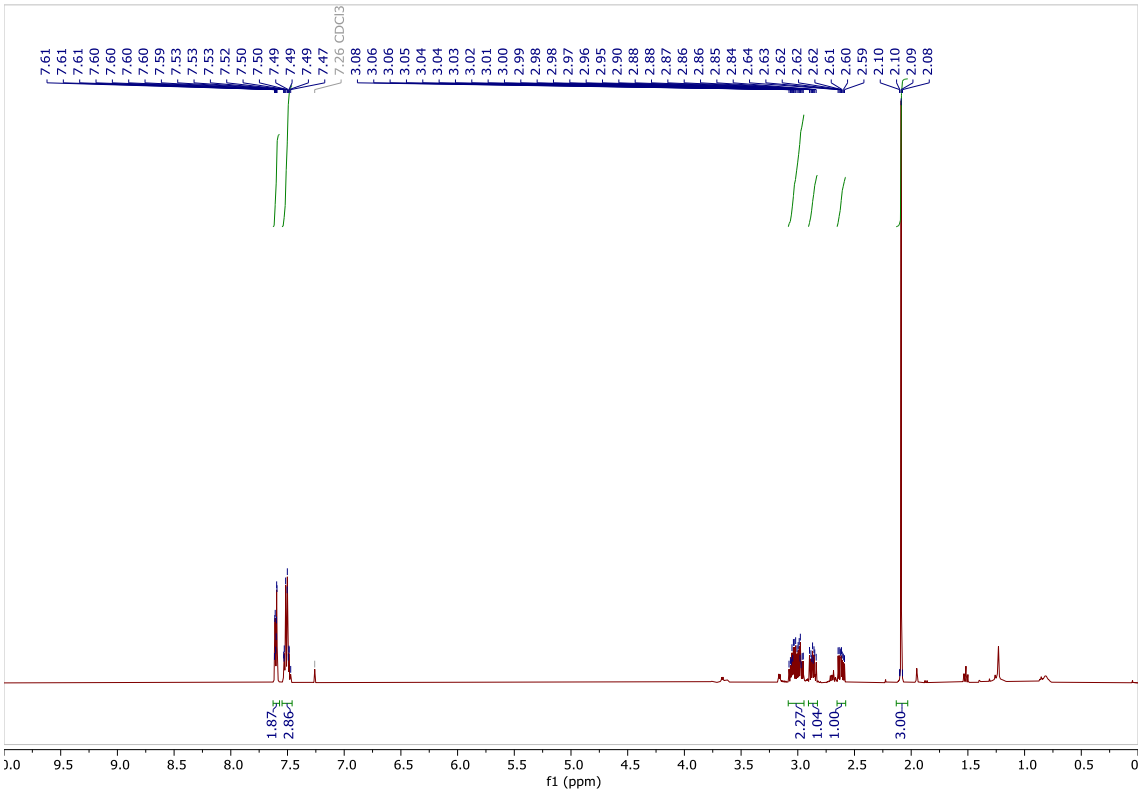


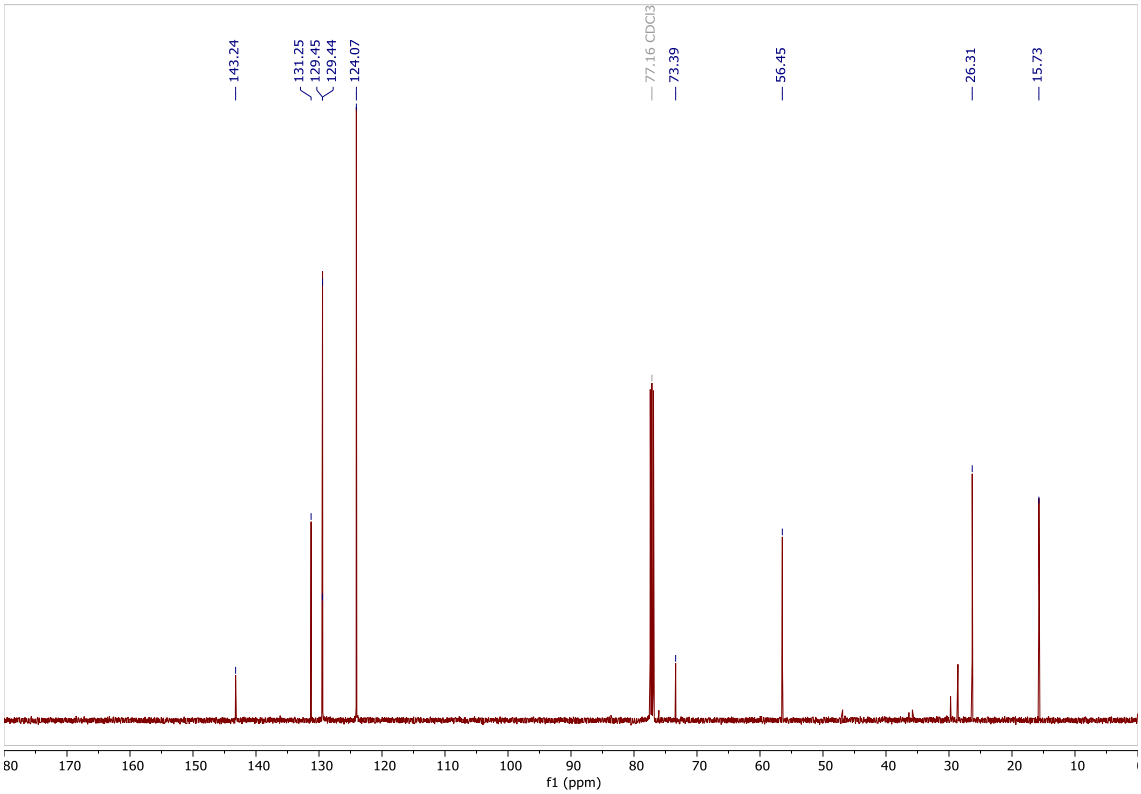

*Riboflavin tetraacetate (**RFTA**)*

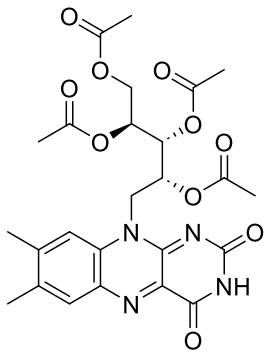

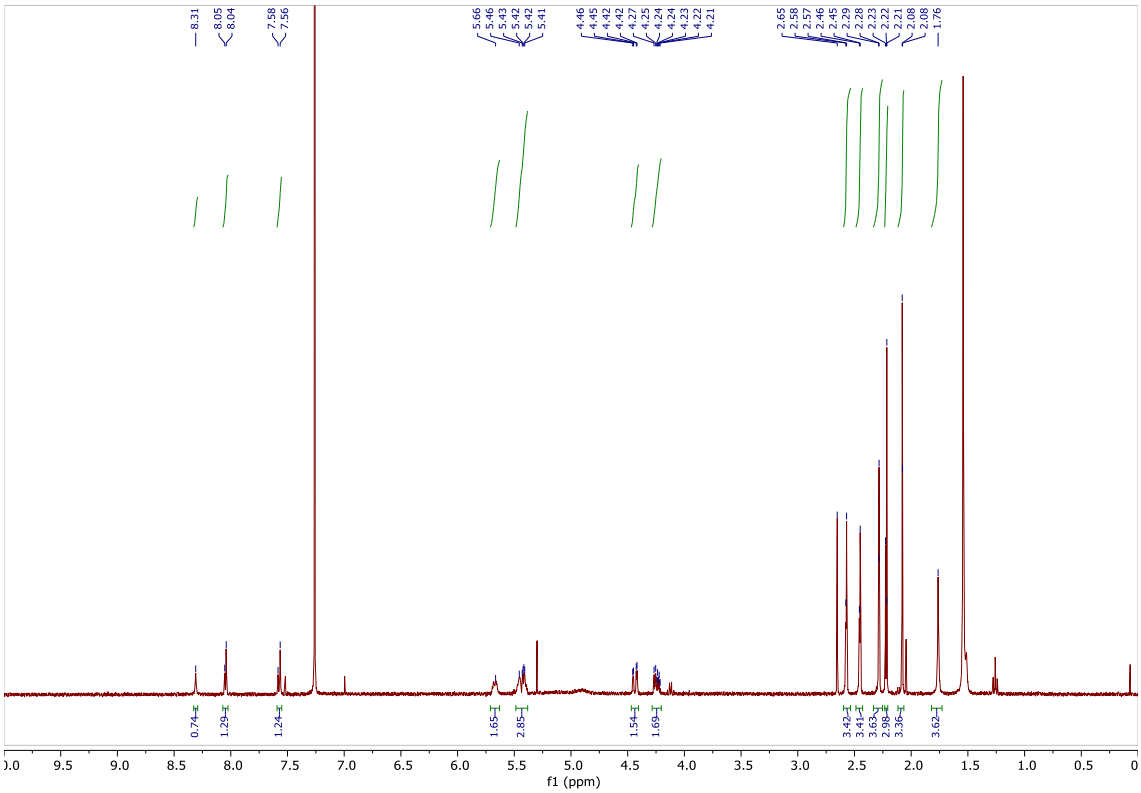

## Appendix II. Isolated yields and optical rotation data of (*R*)-sulfoxides 28 (Chapter 4)

| Compound | Mass / mg | Yield % | Optical rotation / $[\alpha]_D^{27}$ |
|---|---|---|---|
| **(*R*)-28af** | 11.6 | 48 | +169.8 (c 1.0, in $CHCl_3$)[355] |
| **(*R*)-28a** | 18 | 35 | +80.4 (c 1.0, in $CHCl_3$)[434] |
| **(*R*)-28b** | 18 | 26 | +46.8 (c 1.0, in $CHCl_3$)[400] |
| **(*R*)-28x** | 28 | 41 | +160.2 (c 1.0, in $CHCl_3$)[355] |
| **(*R*)-28y** | 17 | 38 | +82.8 (c 1.0, in $CHCl_3$)[435] |
| **(*R*)-28z** | 20 | 40 | +65.0 (c 1.0, in $CHCl_3$)[436] |
| **(*R*)-28aa** | 9 | 30 | +125.2 (c 1.0, in $CHCl_3$)[436] |
| **(*R*)-28ab** | 35 | 50 | +155.4 (c 1.0, in $CHCl_3$)[437] |
| **(*R*)-28ag** | 30 | 43 | +144.2 (c 1.0, in $CHCl_3$)[355] |
| **(*R*)-28ah** | 24 | 35 | +94.0 (c 1.0, in $CHCl_3$)[438] |
| **(*R*)-28ac** | 32 | 46 | +88.6 (c 1.0, in $CHCl_3$)[355] |
| **(*R*)-28ad** | 29 | 41 | +104.4 (c 1.0, in $CHCl_3$) |
| **(*R*)-28ai** | 40 | 55 | +88.6 (c 1.0, in $CHCl_3$)[400] |
| **(*R*)-28aj** | 61 | 87 | +58.4 (c 3.0, in $CHCl_3$)[439] |
| **(*R*)-28o** | 20 | 29 | +64.6 (c 1.0, in $CHCl_3$)[355] |
| **(*R*)-28ak** | 32 | 46 | -51.6 (c 1.0, in $CHCl_3$)[440] |
| **(*R*)-28am** | 34 | 49 | -96.0 (c 1.0, in $CHCl_3$) |
| **(*R*)-28c** | 33 | 47 | +137.6 (c 1.0, in $CHCl_3$)[434] |
| **(*R*)-28d** | 11 | 37 | +123.3 (c 1.0, in $CHCl_3$)[355] |
| **(*R*)-28g** | 18 | 55 | +94.6 (c 1.0, in $CHCl_3$)[434] |
| **(*R*)-28v** | 25 | 36 | +76.0 (c 1.0, in $CHCl_3$)[355] |
| **(*R*)-28w** | 28 | 40 | -44.8 (c 1.0, in $CHCl_3$) |

## Appendix III. Table of retention times and chiral column specification for compounds 28 (Chapter 3)

In order to determine the enantiomeric excess of the sulfoxides, Daicel Chiralpak chiral columns IC (0.46 cm x 25 cm) and IG (0.46 cm x 25 cm) were used in normal phase. All the methods described ran at 1.0 $mLmin^{-1}$, 25 $^{o}C$ with an isocratic eluent. Detection wavelengths were set at 254 and 240 nm for all compounds.

| Compound | Column | Eluent system | Retention time |
|---|---|---|---|
| **28s** | IC | *n*-hexane:IPA 7:3 | 29.3 (R), 33.9 (S) |
| **28t** | IC | *n*-hexane:IPA 6:4 | 14.8 (R), 16.4 (S) |
| **28v** | IC | *n*-hexane:IPA 8:2 | 20.8 (S), 23.0 (R) |
| **28a** | IC | *n*-hexane:IPA 8:2 | 19.8 (R), 22.0 (S) |
| **28b** | IC | *n*-hexane:IPA 8:2 | 16.2 (R), 17.4 (S) |
| **28z** | IG | *n*-hexane:IPA 8:2 | 10.1 (R), 12.6 (S) |
| **28ab** | IG | *n*-hexane:IPA 8:2 | 12.2 (S), 13.2 (R) |
| **28g** | IC | *n*-hexane:IPA 8:2 | 14.8 (R), 15.6 (S) |

## Appendix IV. Table of retention times and chiral column specification for compounds 28 (Chapter 4)

In order to determine the enantiomeric excess of the sulfoxides, Daicel Chiralpak chiral columns IC (0.46 cm x 25 cm), IG (0.46 cm x 25 cm), ID (0.46 cm x 25 cm) and Daicel Chiracel OD-H (0.46 cm x 25 cm) were used in normal phase. All the methods described ran at 1.0 $mLmin^{-1}$, 25 $^{o}C$ with an isocratic eluent. Detection wavelengths were set at 254 and 240 nm for all compounds and 210 nm for compounds **28ak** and **28al**.

| Compound | Column | Eluent system | Retention time |
|---|---|---|---|
| **28af** | IG | *n*-hexane:IPA 8:2 | 14.2 (R), 15.2 (S) |
| **28a** | IC | *n*-hexane:IPA 8:2 | 20.2 (R), 22.8 (S) |
| **28b** | IC | *n*-hexane:IPA 8:2 | 16.5 (R), 17.5 (S) |
| **28x** | IC | *n*-hexane:IPA 8:2 | 16.8 (R), 17.9 (S) |
| **28y** | IC | *n*-hexane:IPA 8:2 | 16.1 (R), 17.3 (S) |
| **28z** | IG | *n*-hexane:IPA 8:2 | 11.5 (R), 13.3 (S) |
| **28aa** | IG | *n*-hexane:IPA 8:2 | 11.5 (S), 13.5 (R) |
| **28ab** | IC | *n*-hexane:IPA 6:4 | 25.4 (S), 27.3 (R) |
| **28ag** | IG | *n*-hexane:IPA 8:2 | 25.4 (R), 27.0 (S) |
| **28ah** | IG | *n*-hexane:IPA 8:2 | 16.9 (R), 19.3 (S) |
| **28ac** | IG | *n*-hexane:IPA 8:2 | 11.7 (S), 12.3 (R) |
| **28ad** | IG | *n*-hexane:IPA 8:2 | 14.8 (R), 16.8 (S) |
| **28ai** | IG | *n*-hexane:IPA 8:2 | 19.1 (R), 21.0 (S) |
| **28aj** | IC | *n*-hexane:EtOH 8:2 | 13.6 (R), 15.7 (S) |
| **28o** | IC | *n*-hexane:IPA 7:3 | 16.7 (S), 17.5 (R) |
| **28ak** | IC | *n*-hexane:IPA 9:1 | 30.5 (R), 32.3 (S) |
| **28al** | IG | *n*-hexane:IPA 6:4 | 8.4 (S), 9.0 (R) |
| **28am** | IC | *n*-hexane:EtOH 1:1 | 12.9, 14.0, 16.8, 20.5 |
| **28c** | IC | *n*-hexane:IPA 8:2 | 17.2 (R), 20.0 (S) |
| **28d** | IG | *n*-hexane:IPA 8:2 | 14.4 (R), 15.7 (S) |
| **28g** | IC | *n*-hexane:IPA 8:2 | 14.6 (R), 15.5 (S) |
| **28v** | IC | *n*-hexane:IPA 8:2 | 21.3 (S), 23.5 (R) |
| **28w** | IG | *n*-hexane:IPA 8:2 | 13.2 (R), 17.3 (S) |
| **28t** | IC | *n*-hexane:IPA 6:4 | 15.8 (R), 17.5 (S) |
| **28an** | OD-H | *n*-hexane:EtOH 9:1 | 6.6 (R), 7.5 (S) |
| **28j** | IC | *n*-hexane:IPA 8:2 | 29.3 (S), 31.2 (R) |
| **28l** | IC | *n*-hexane:IPA 8:2 | 15.8 (R), 17.0 (S) |
| **28k** | IC | *n*-hexane:IPA 8:2 | 19.4 (S), 21.9 (R) |
| **28ao** | IG | *n*-hexane:EtOH 9:1 | 17.2 (S), 18.0 (R) |
| **28ap** | IG | *n*-hexane:IPA 8:2 | 11.4 (R), 12.0 (R) |
| **28aq** | ID | *n*-hexane:IPA 9:1 | 14.7 (R), 15.9 (S) |
| **28ar** | IC | *n*-hexane:IPA 8:2 | 28.3 (S), 30.8 (R) |

## Appendix V. HPLC traces

### Chapter 3

*2-((Propylsulfinyl)methyl)pyridine (**28s**)*

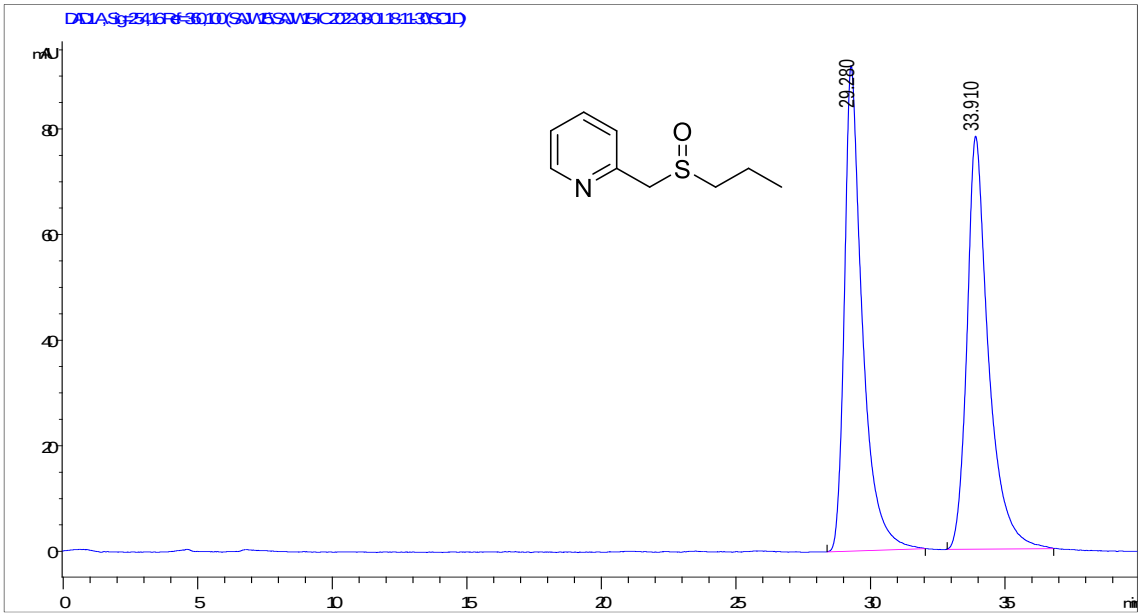


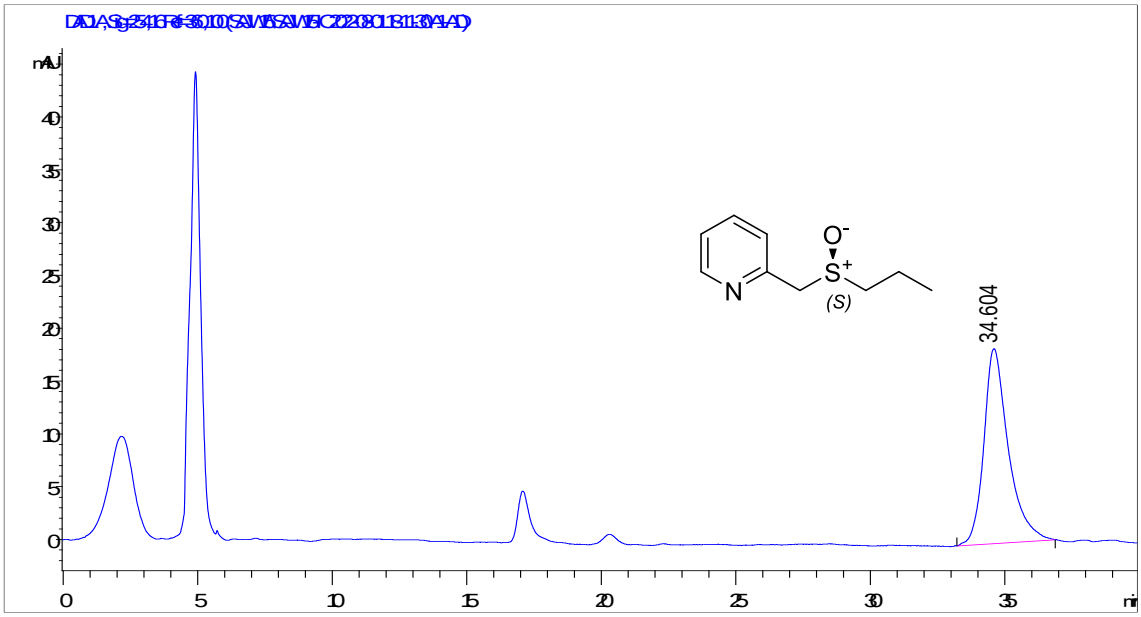

*2-((Ethylsulfinyl)methyl)pyridine (**28t**)*

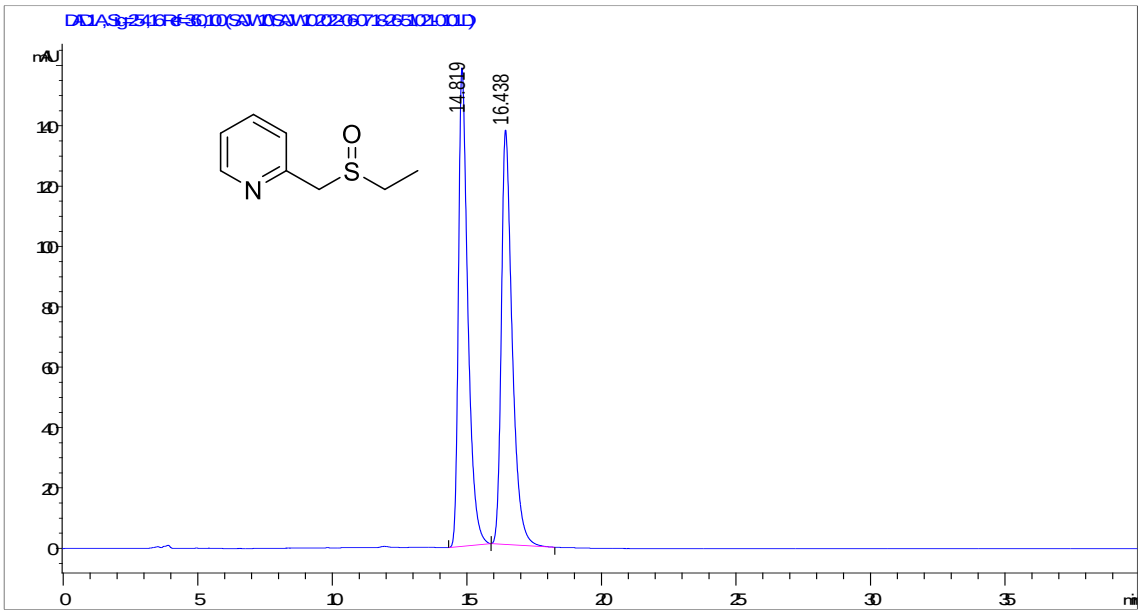


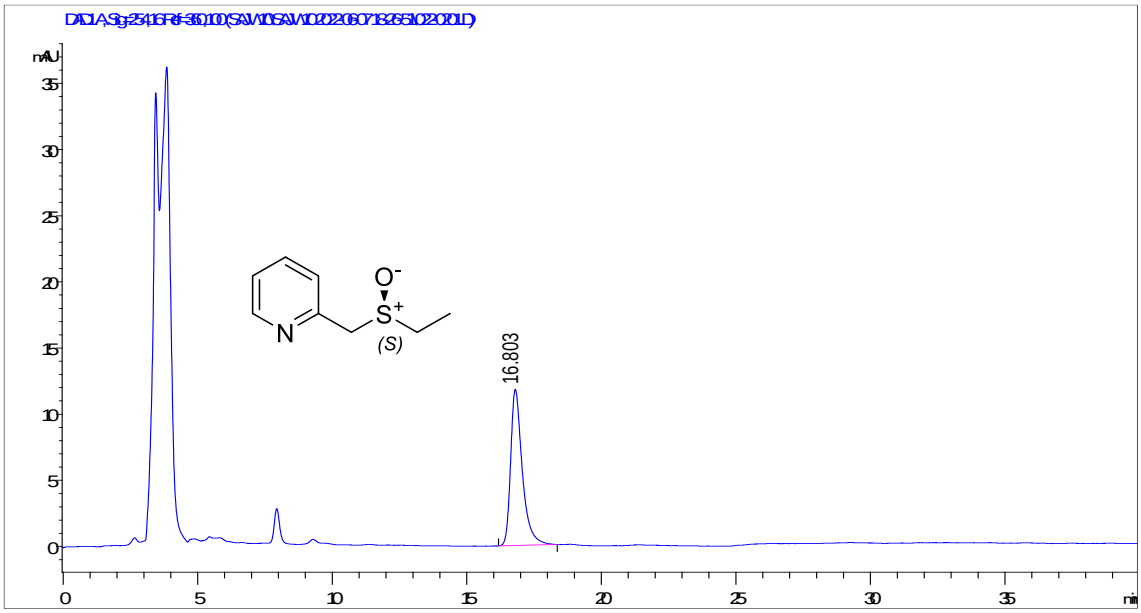

*((Ethylsulfinyl)methyl)benzene (**28v**)*

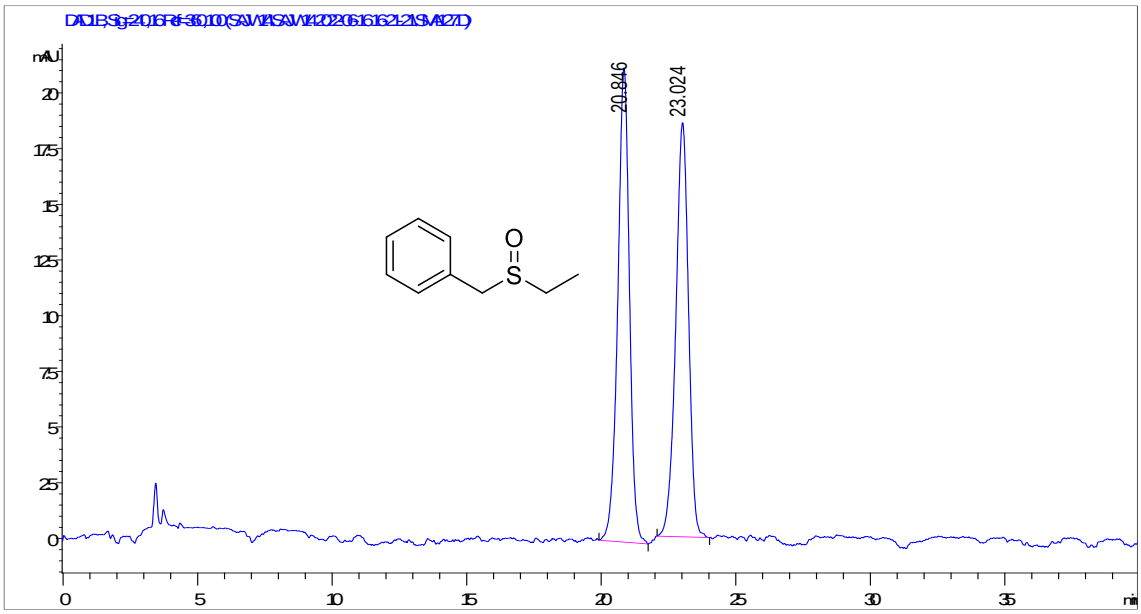


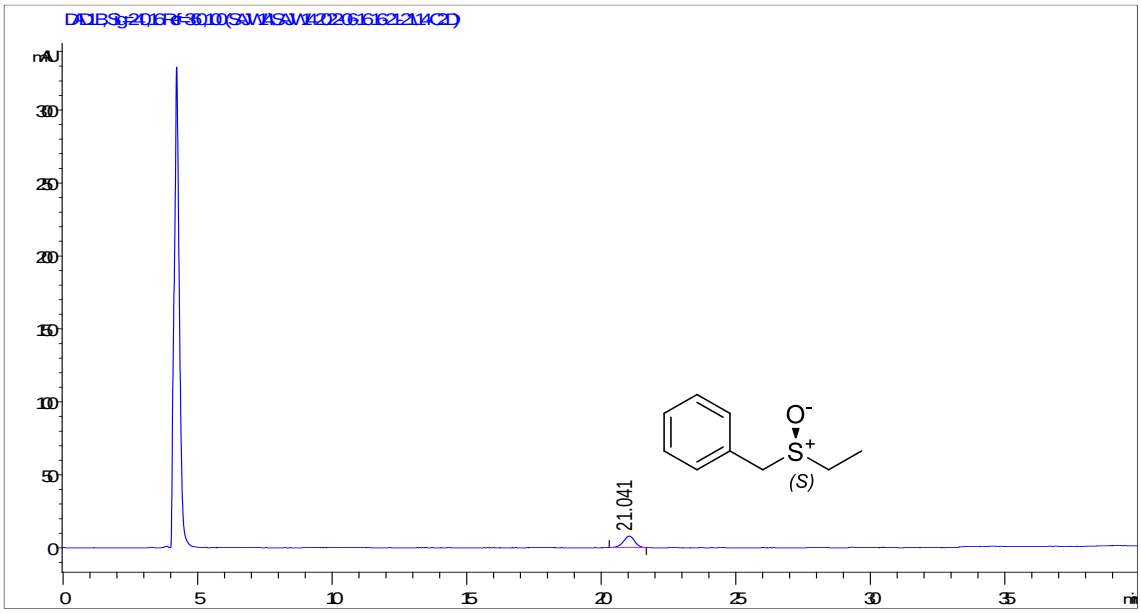

*(Methylsulfinyl)benzene (**28a**)*

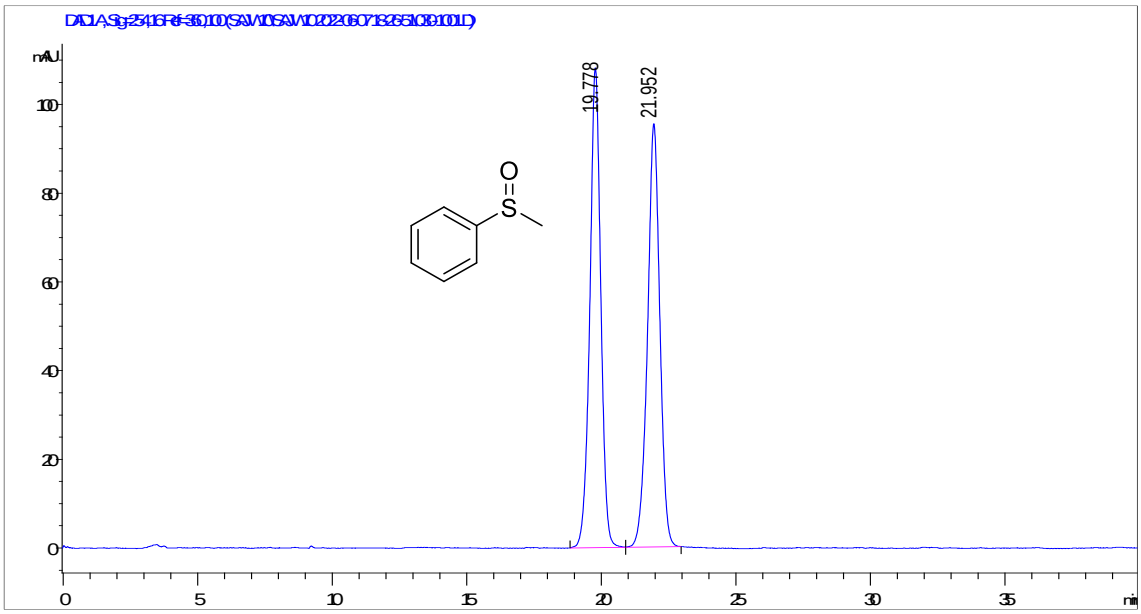


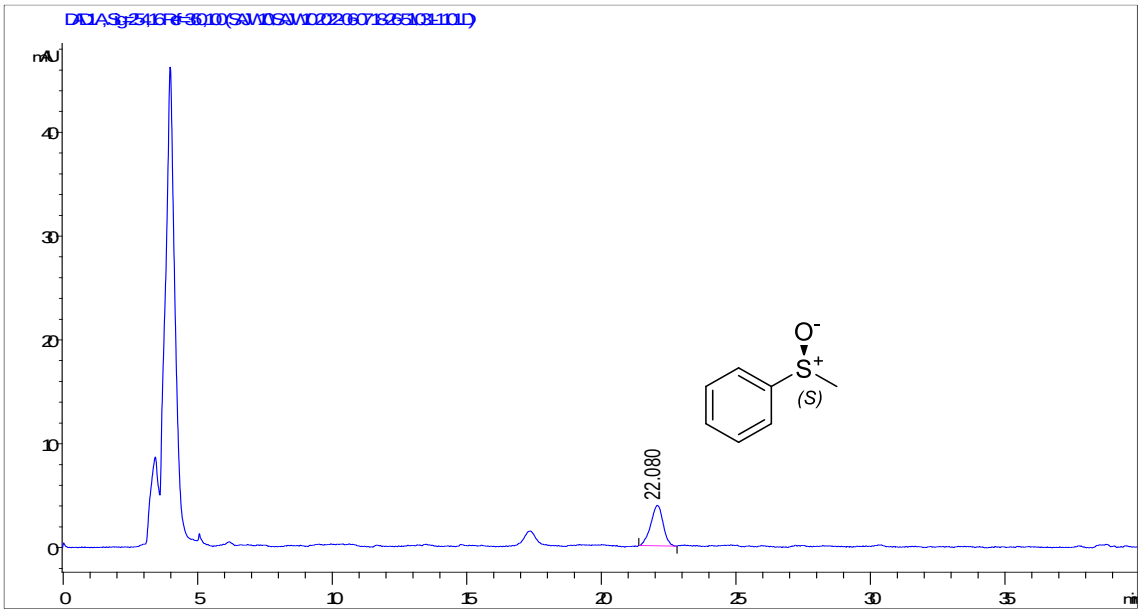

*1-Fluoro-4-(methylsulfinyl)benzene (**28b**)*

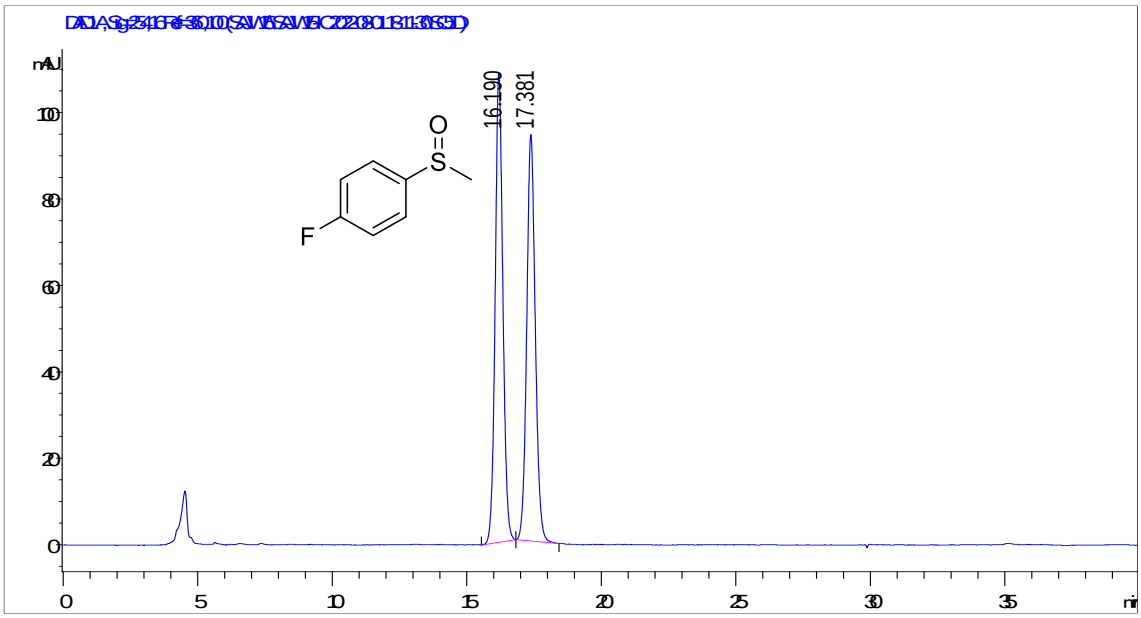


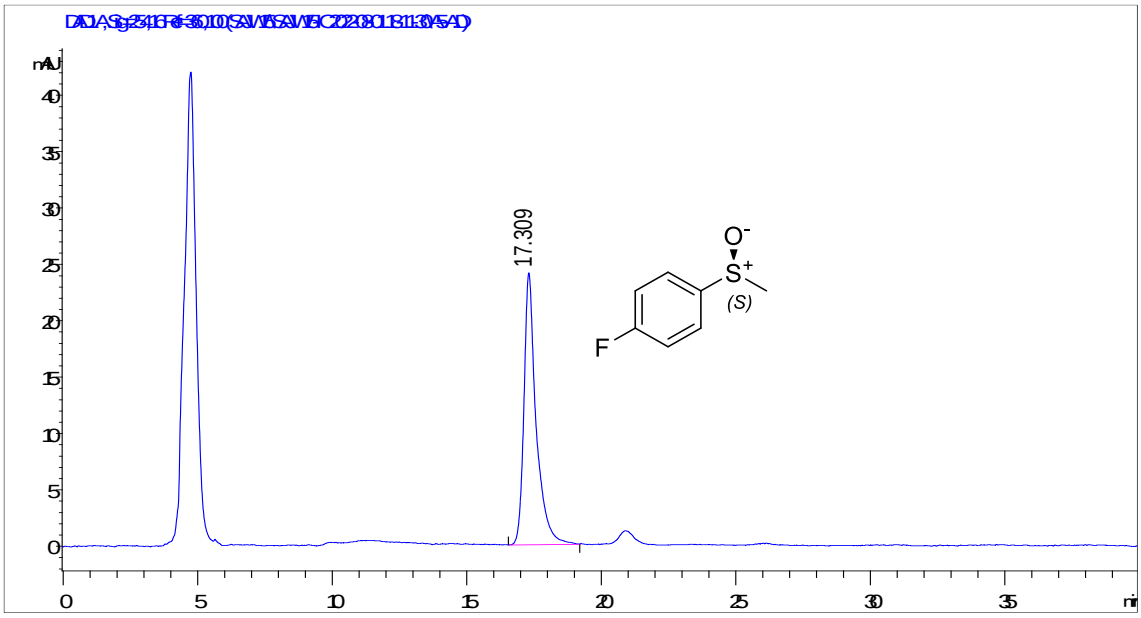

*1-Chloro-3-(methylsulfinyl)benzene (**28z**)*

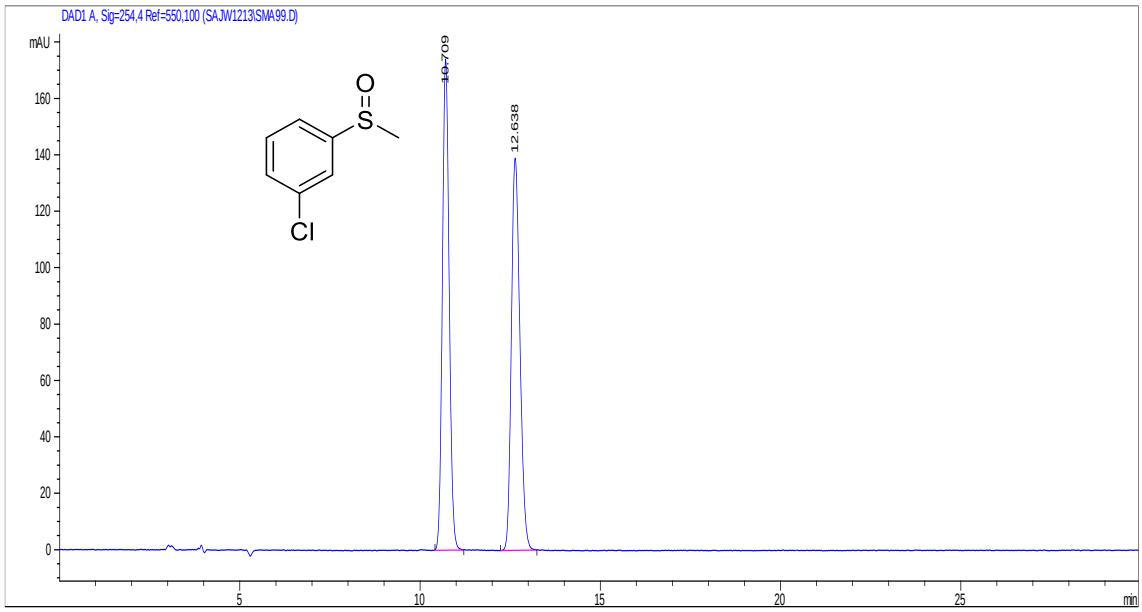


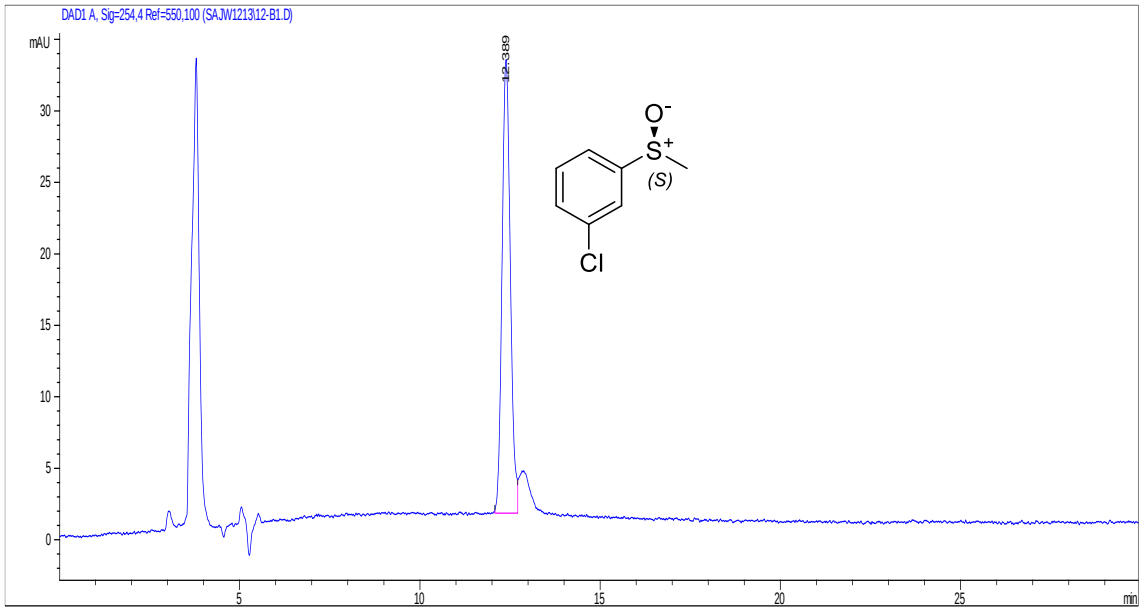

*1-Methyl-3-(methylsulfinyl)benzene (**28ac**)*

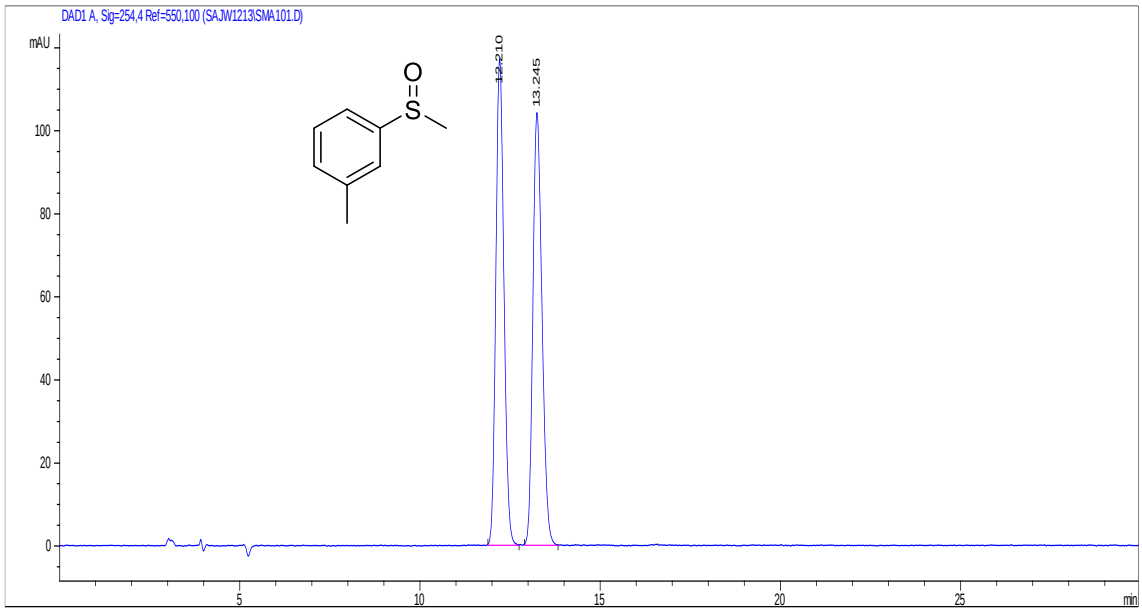


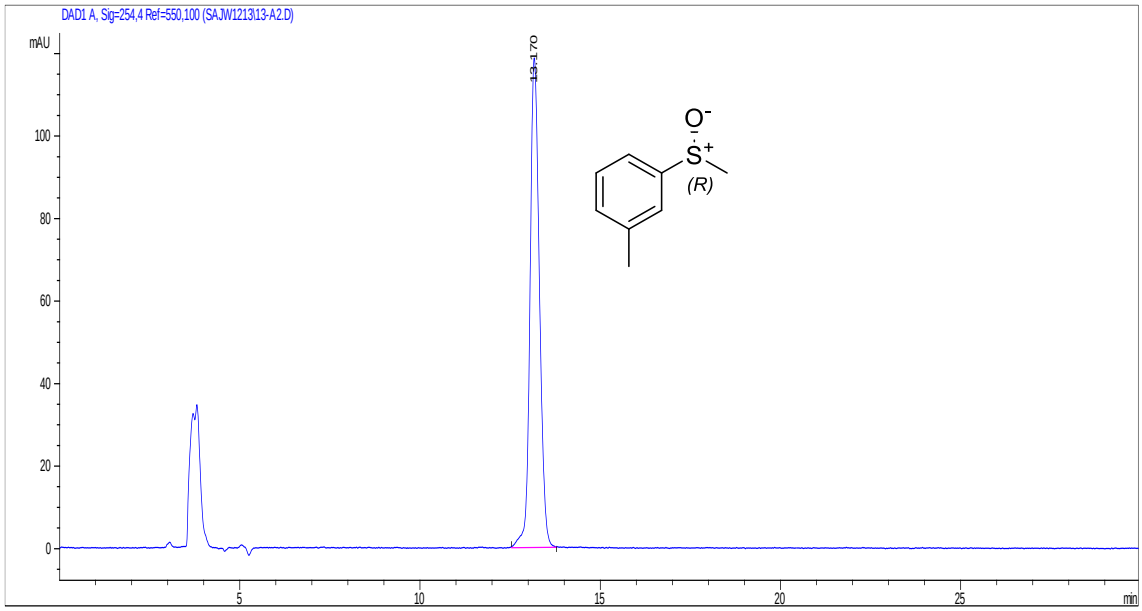

*1-Bromo-4-(ethylsulfinyl)benzene (**28g**)*

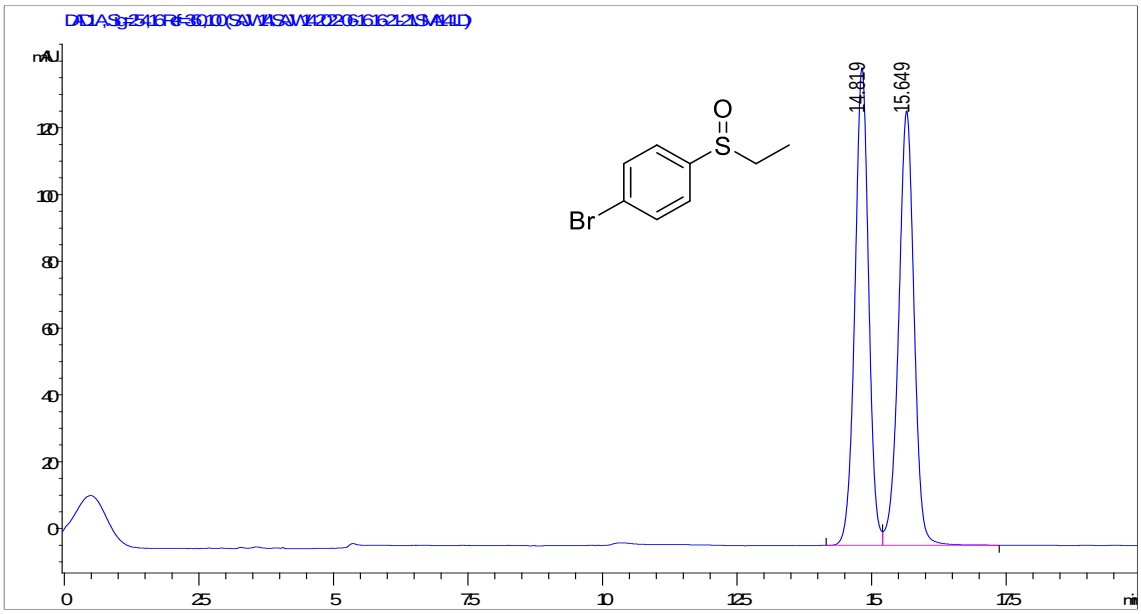


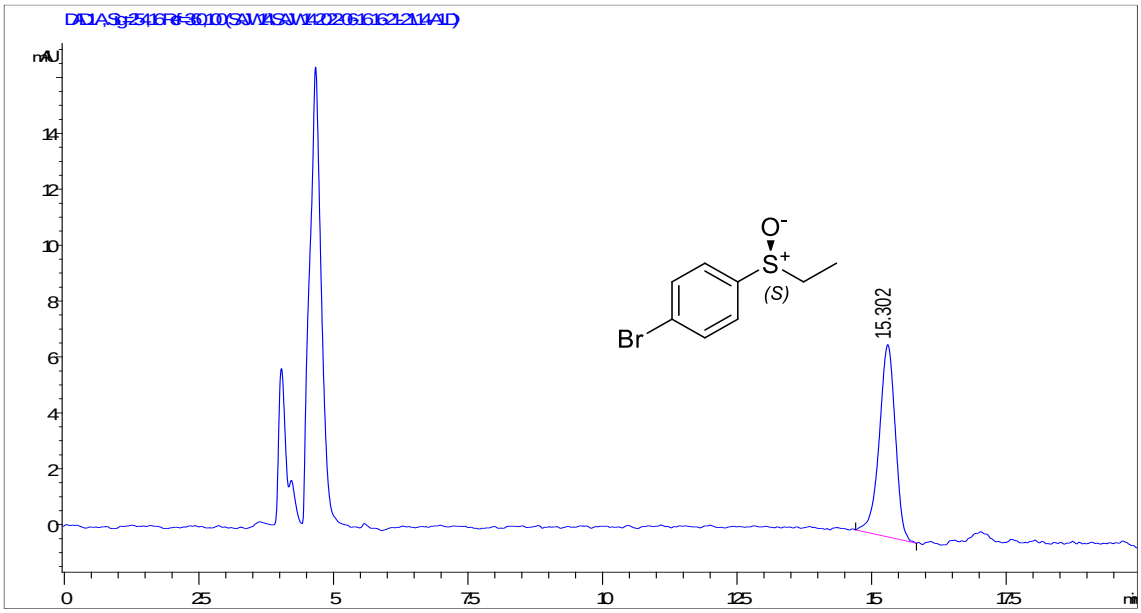

*1-Methyl-4-(methylsulfinyl)benzene (**28af**)*

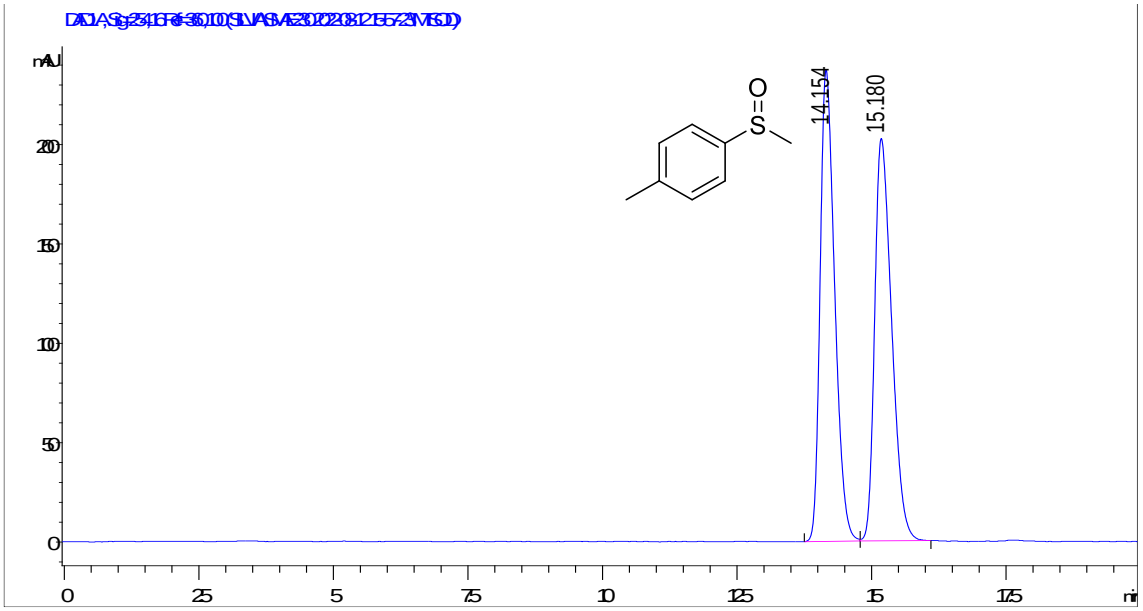


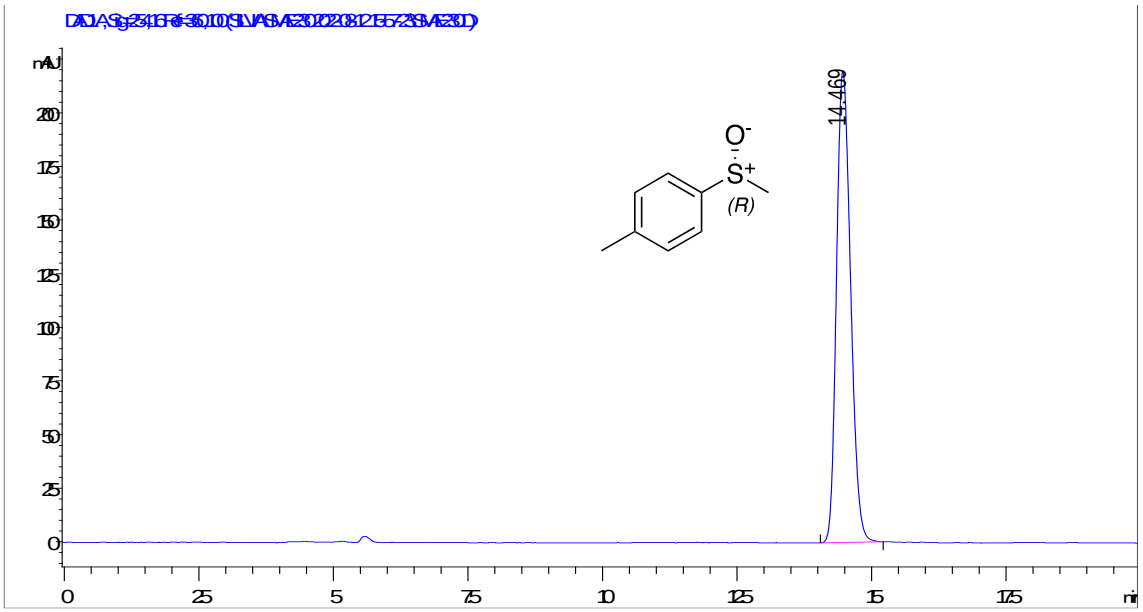

*(Methylsulfinyl)benzene (**28a**)*

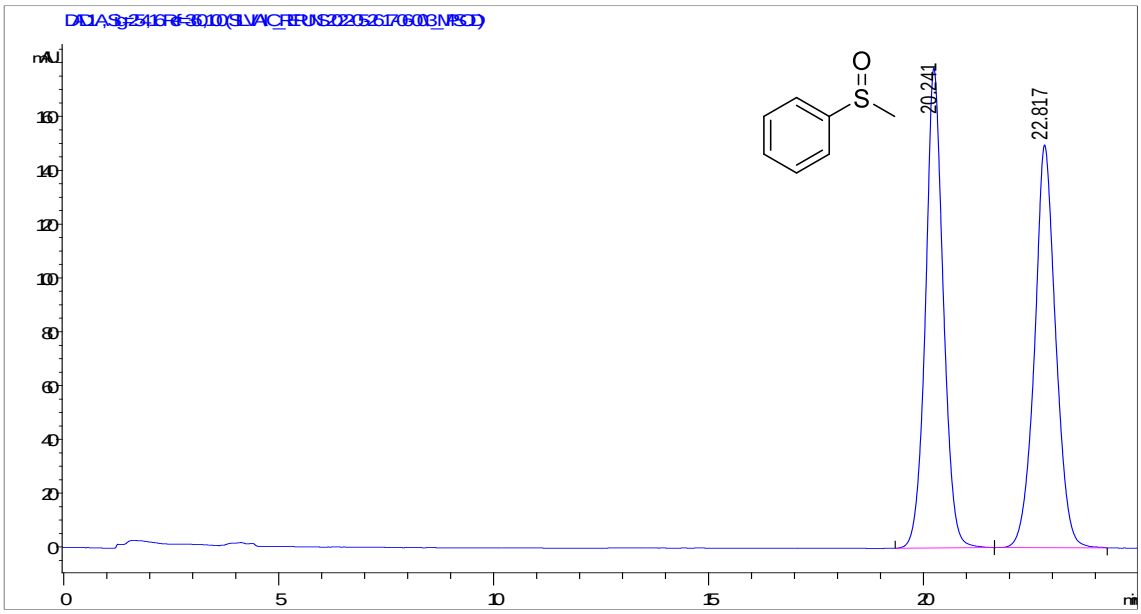


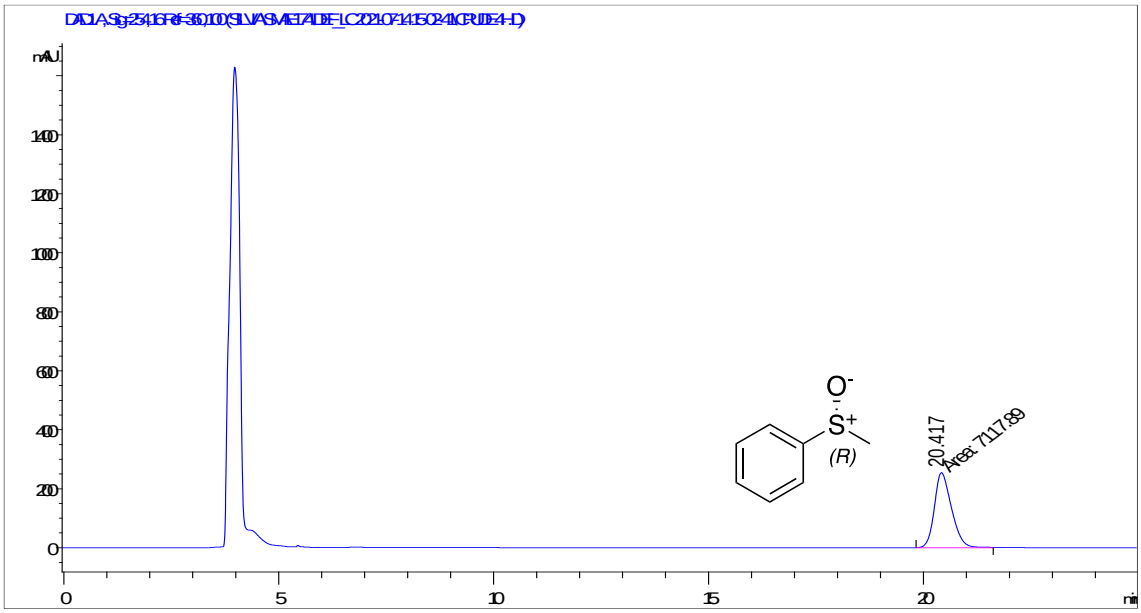

*1-Fluoro-4-(methylsulfinyl)benzene (**28b**)*

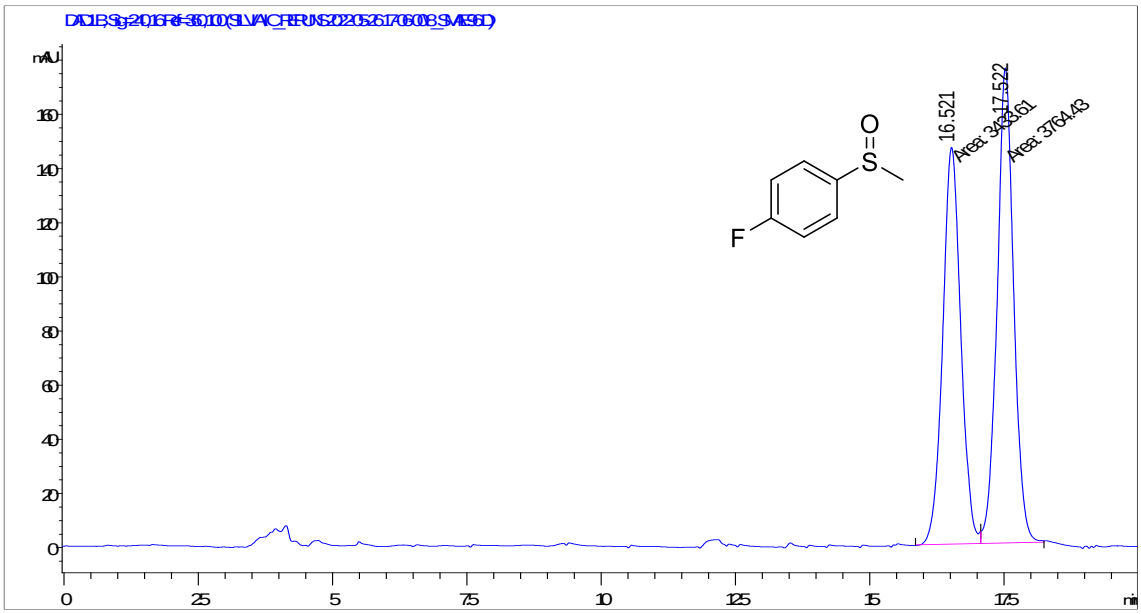


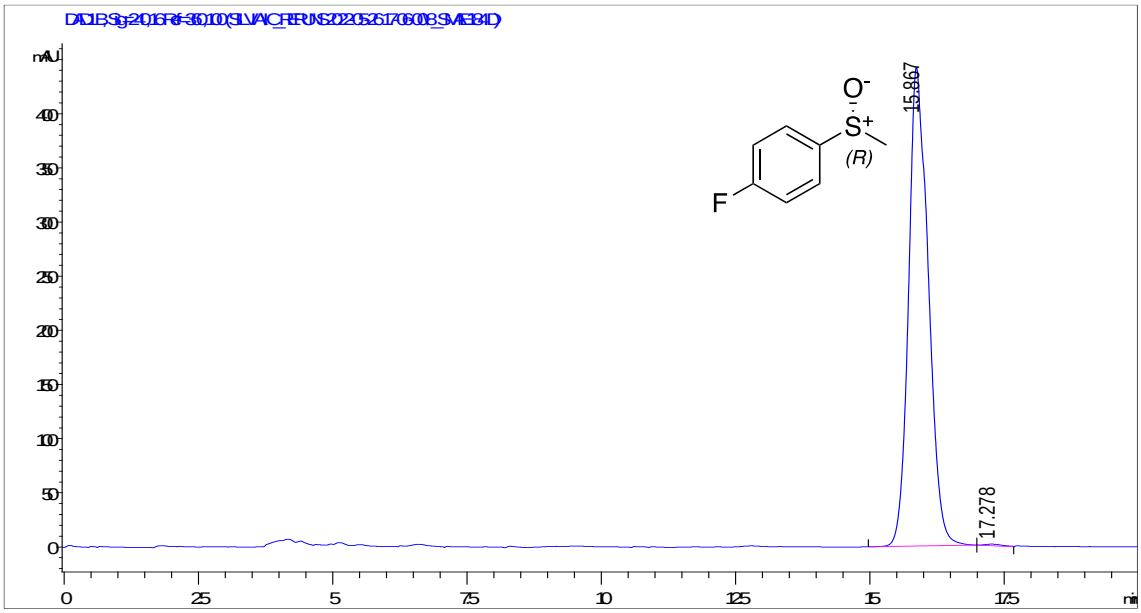

*1-Bromo-4-(methylsulfinyl)benzene (**28x**)*

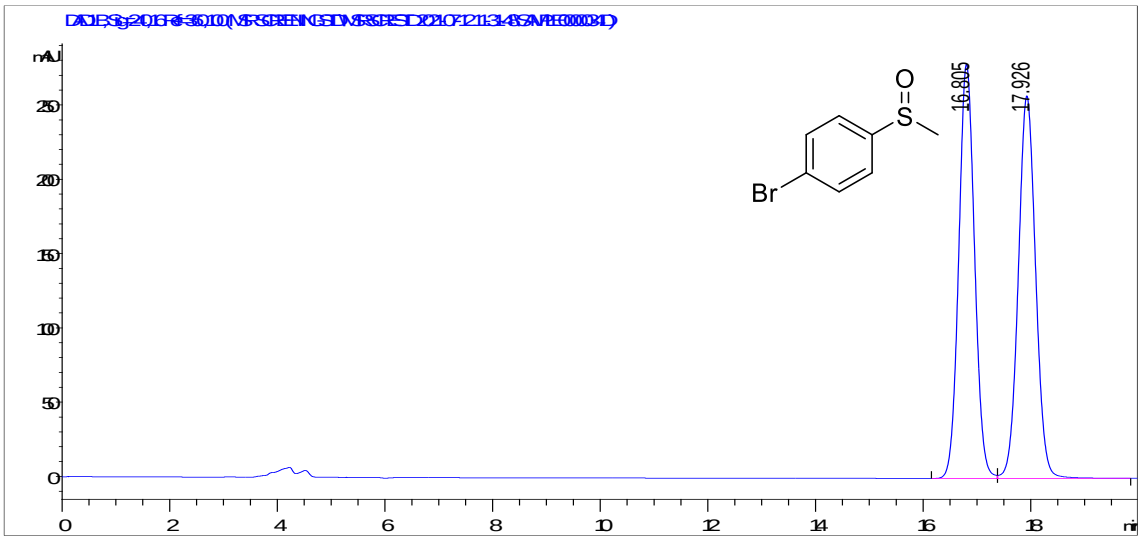


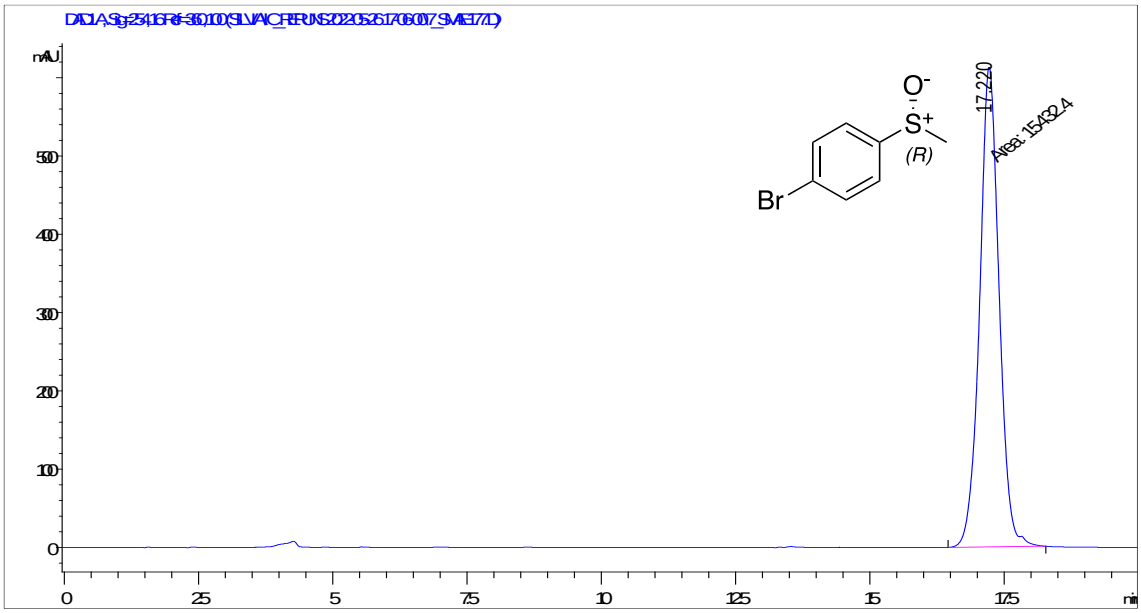

*1-Chloro-4-(methylsulfinyl)benzene (**28y**)*

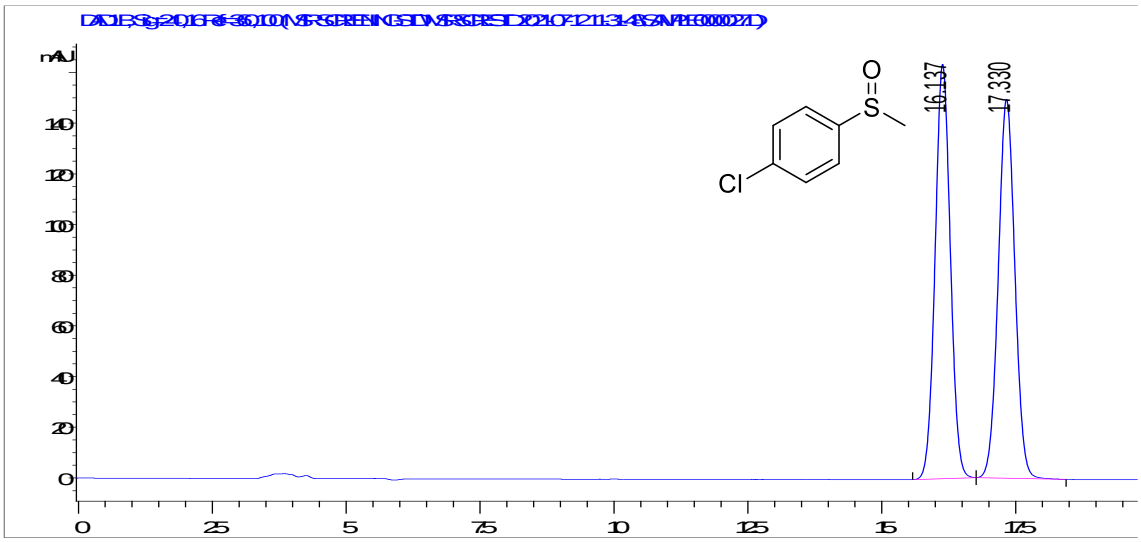


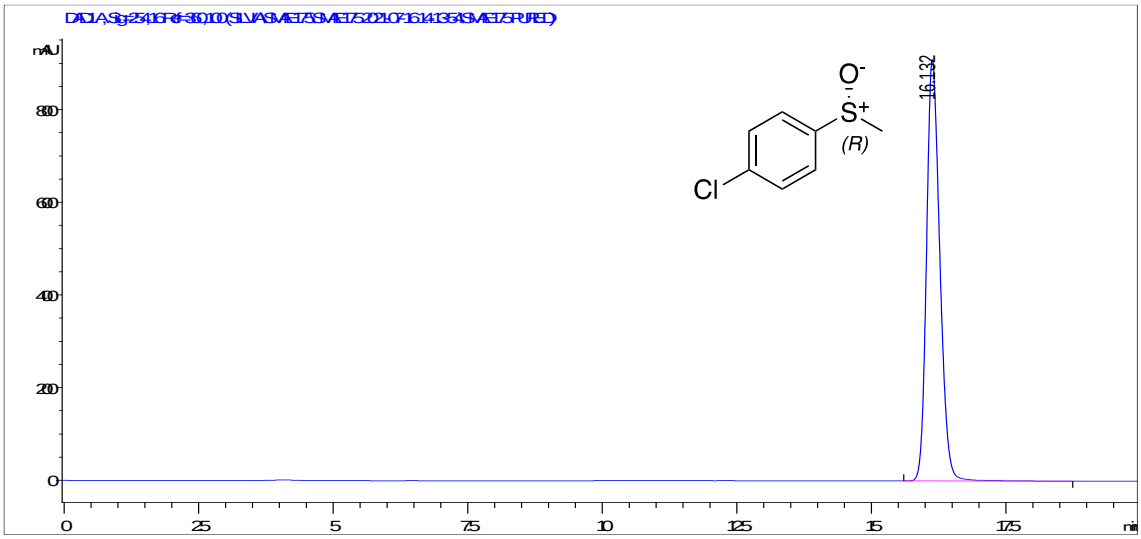

*1-Chloro-3-(methylsulfinyl)benzene (**28z**)*

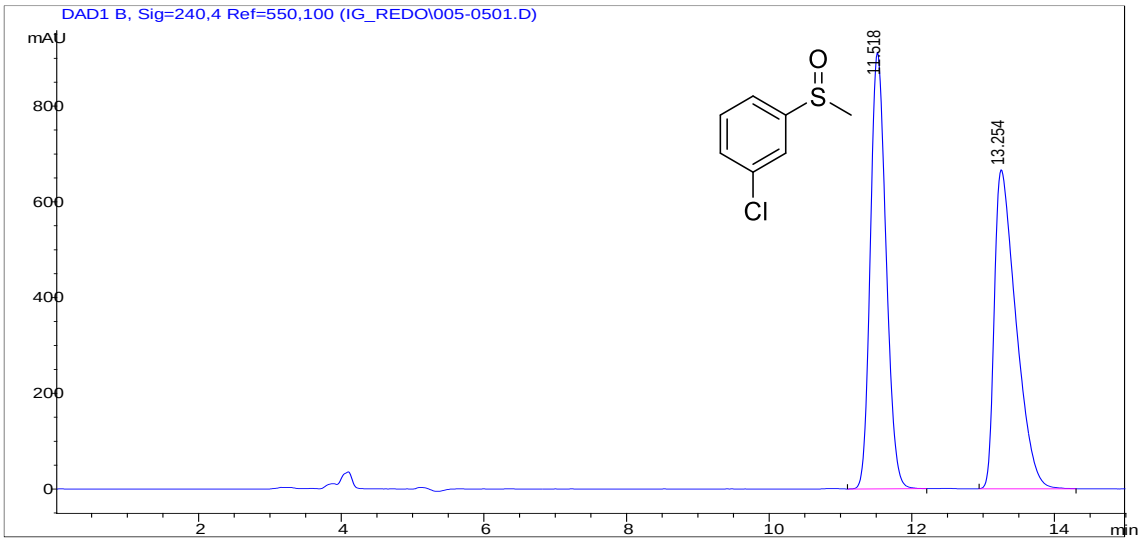


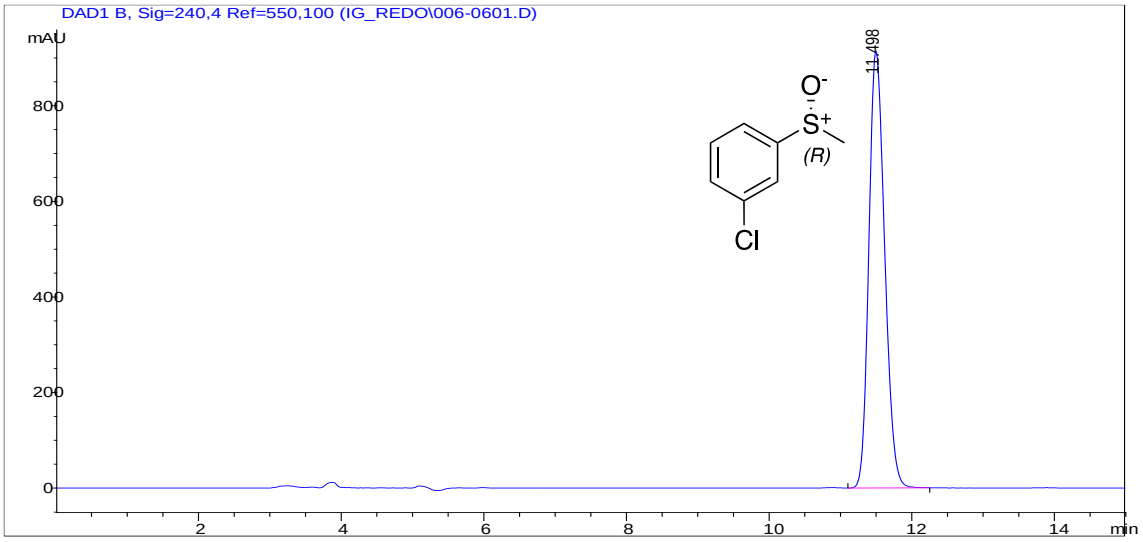

*1-chloro-2-(methylsulfinyl)benzene (**28aa**)*

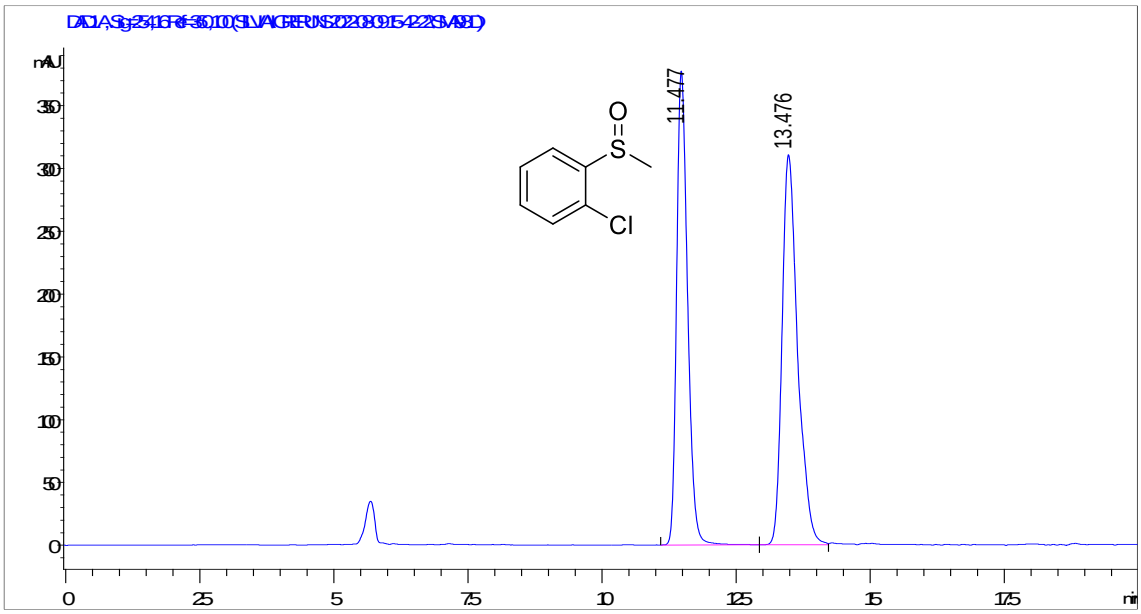


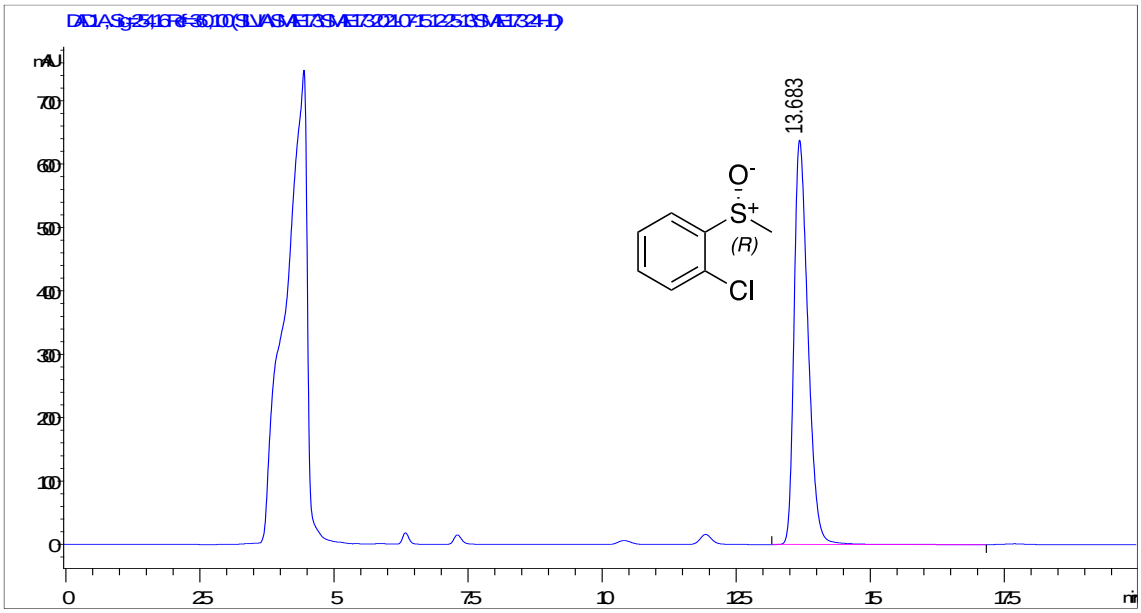

*1-(4-(Methylsulfinyl)phenyl)ethan-1-one (**28ab**)*

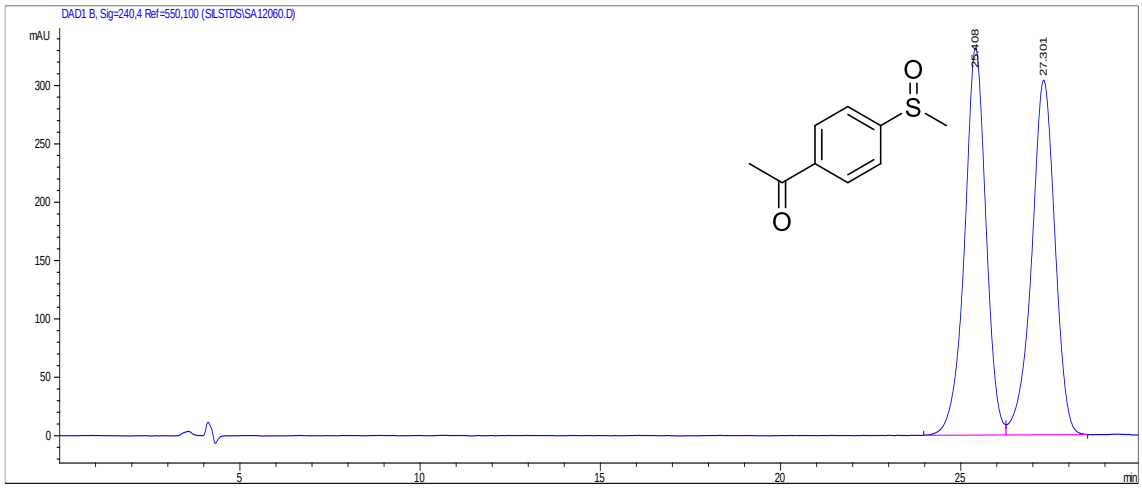


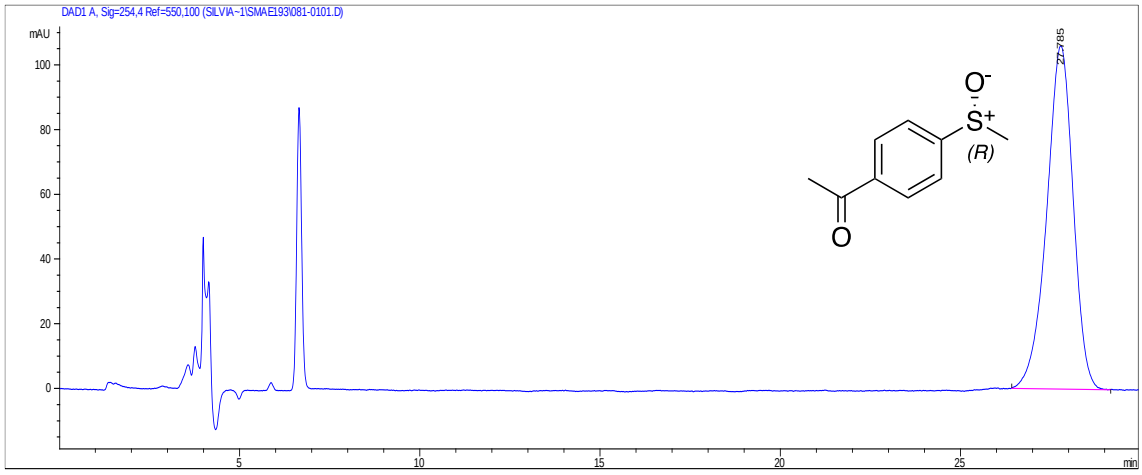

*1-Methoxy-4-(methylsulfinyl)benzene (**28ag**)*

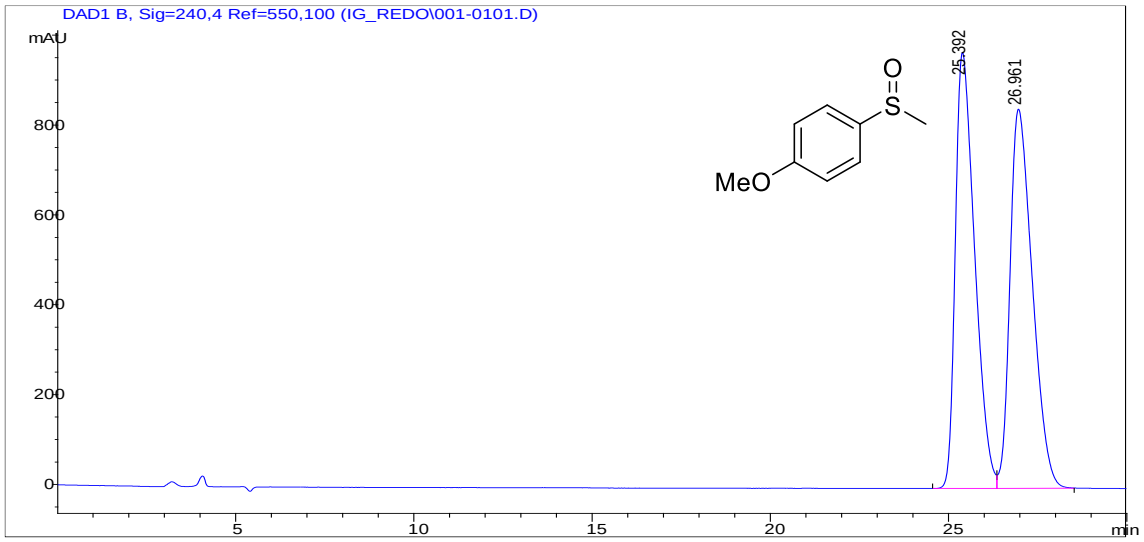


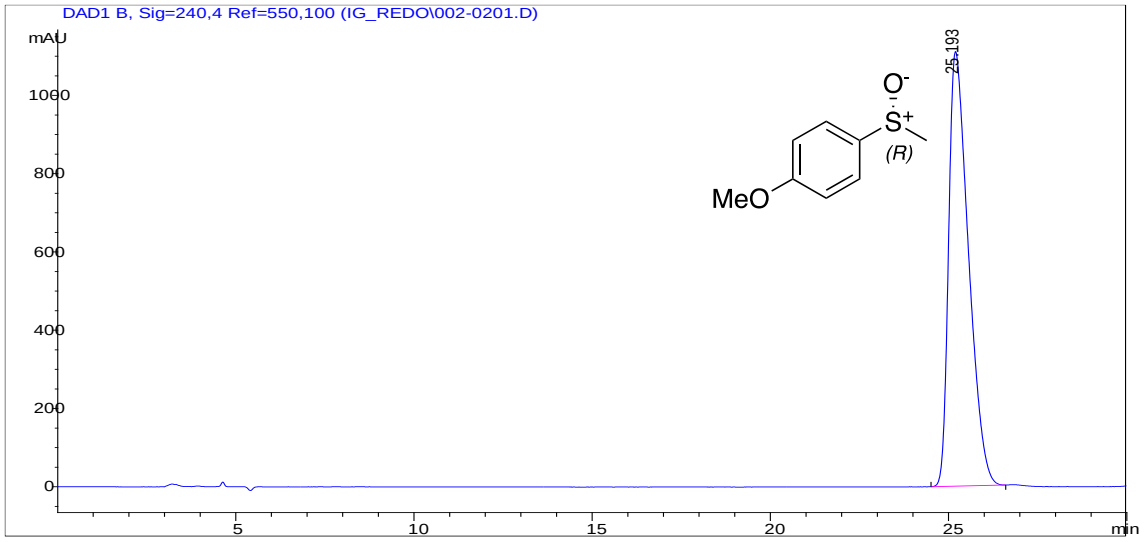

*1-Methoxy-3-(methylsulfinyl)benzene (**28ah**)*

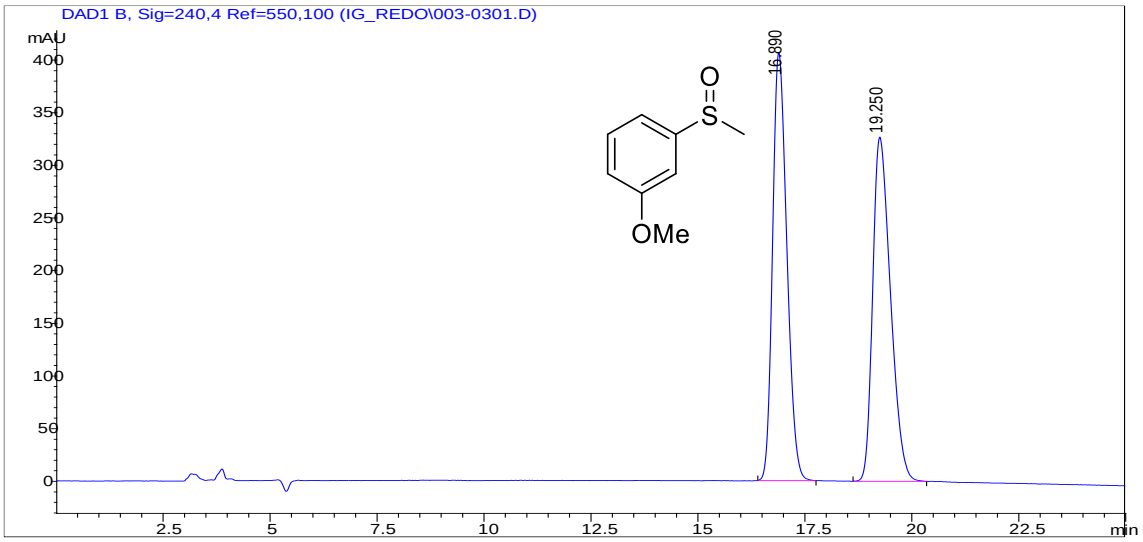


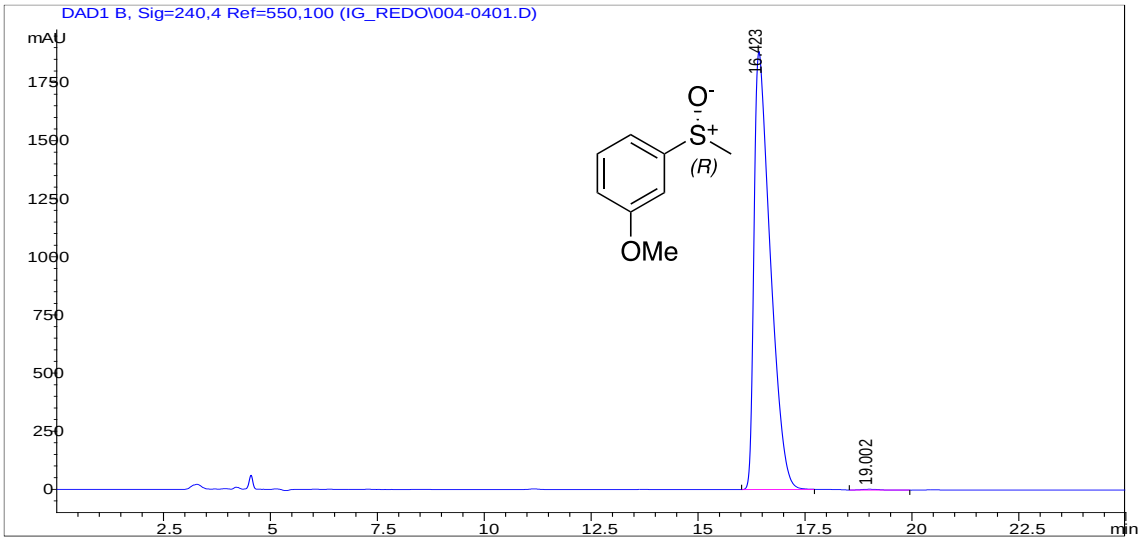

*1-Methyl-3-(methylsulfinyl)benzene (**28ac**)*

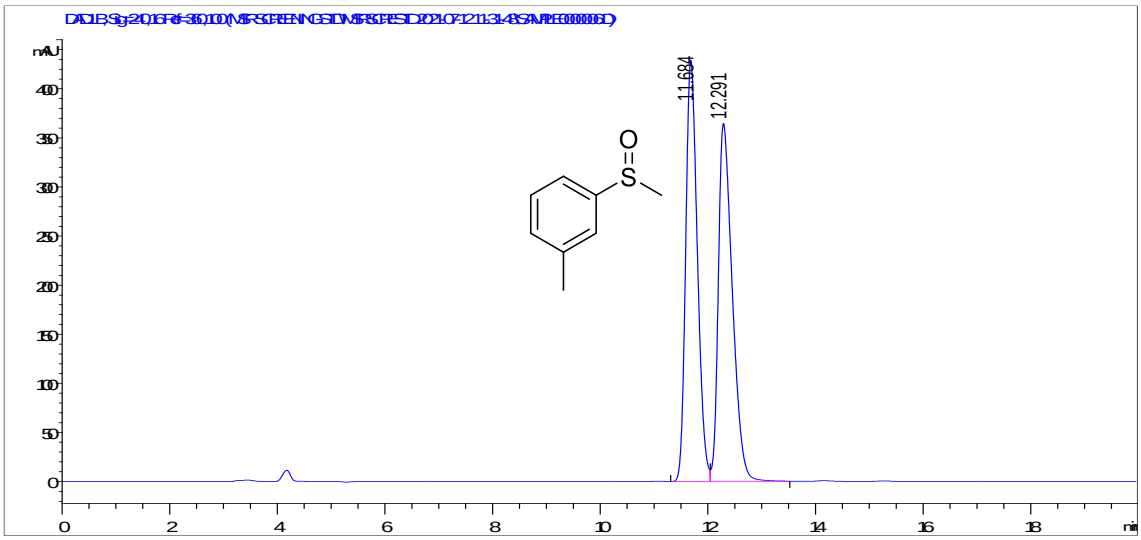


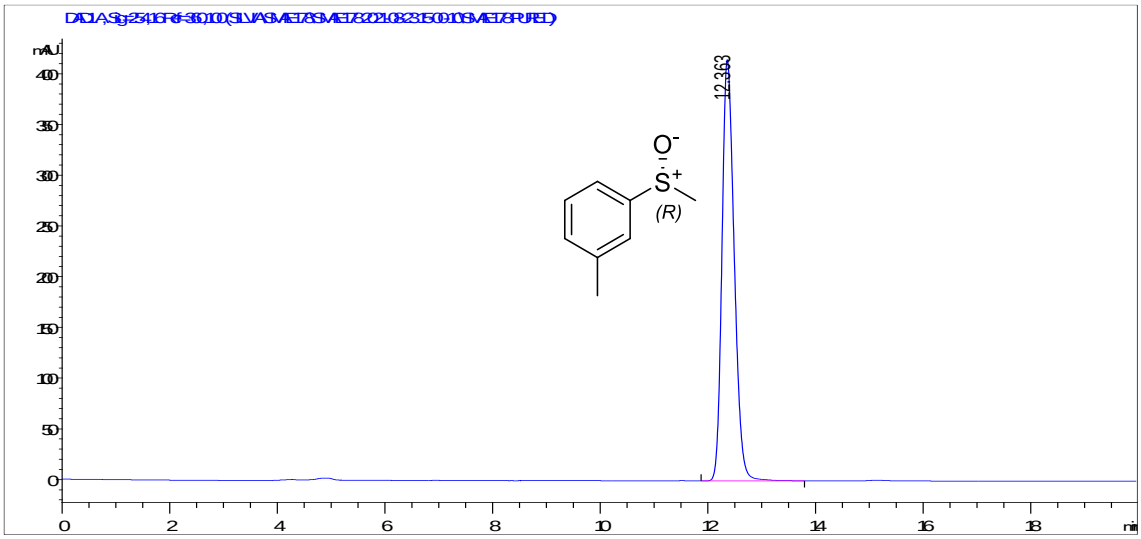

*2,4-Dimethyl-1-(methylsulfinyl)benzene (**28ad**)*

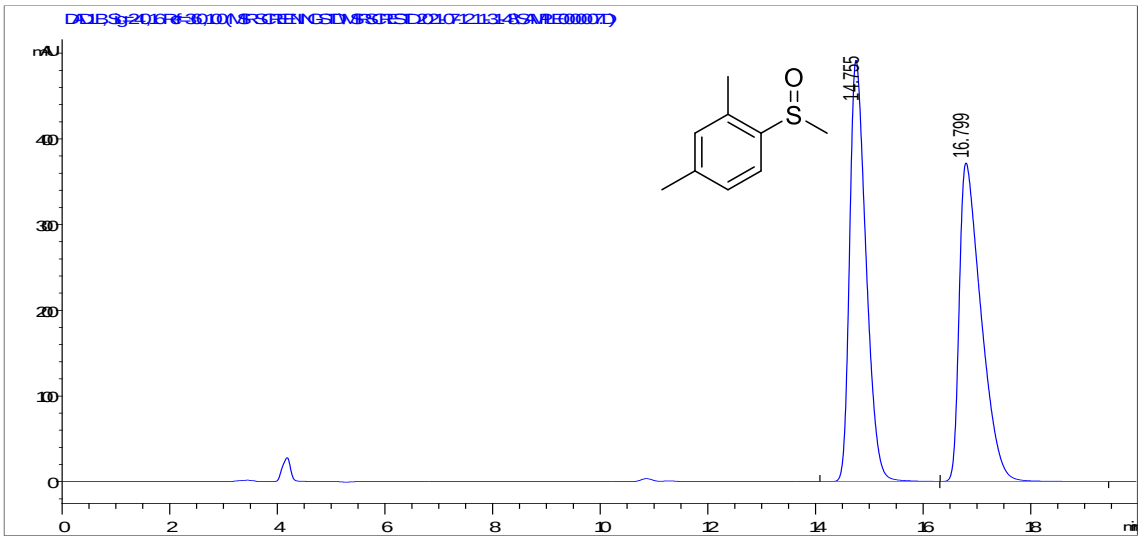


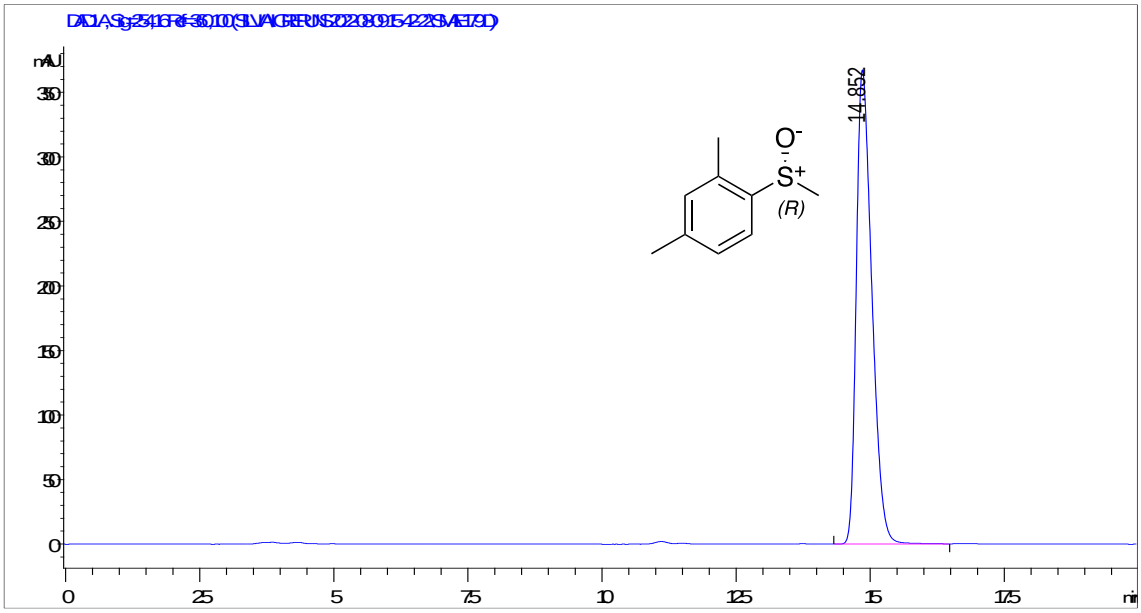

*2-(Methylsulfinyl)naphthalene (**28ai**)*

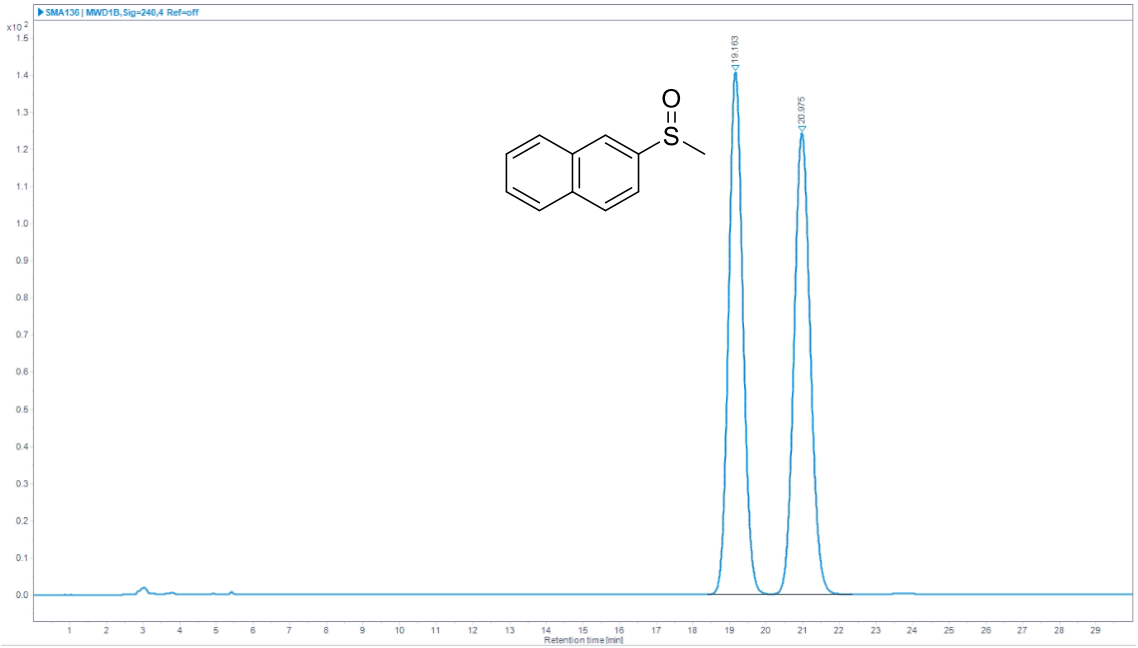


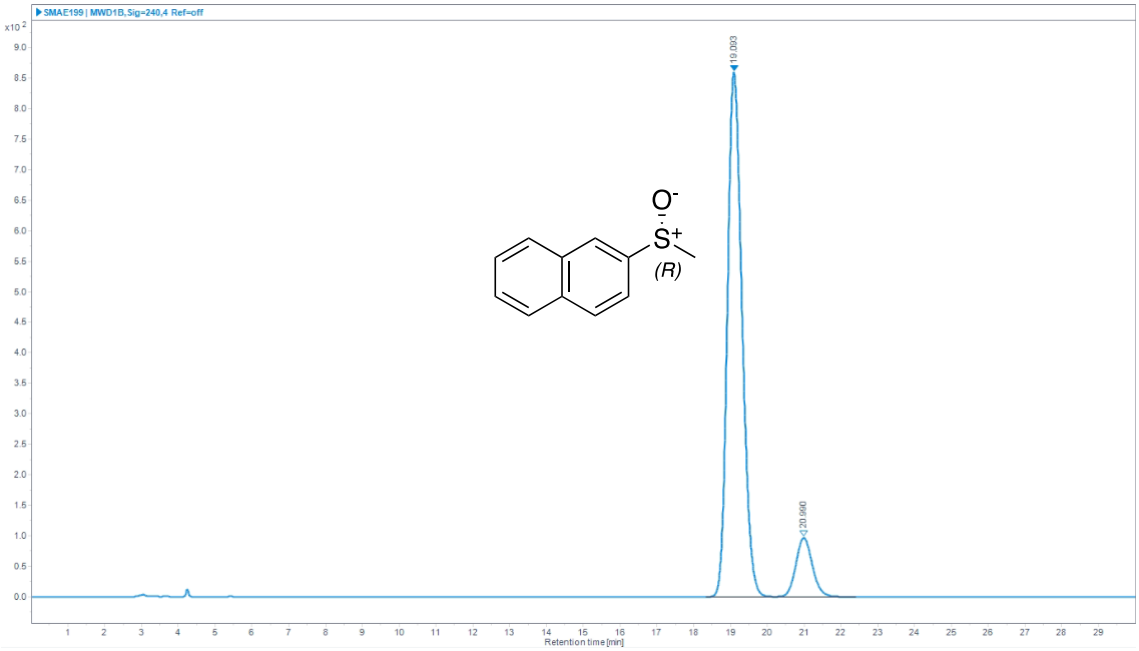

*1-(Methylsulfinyl)naphthalene (**28aj**)*

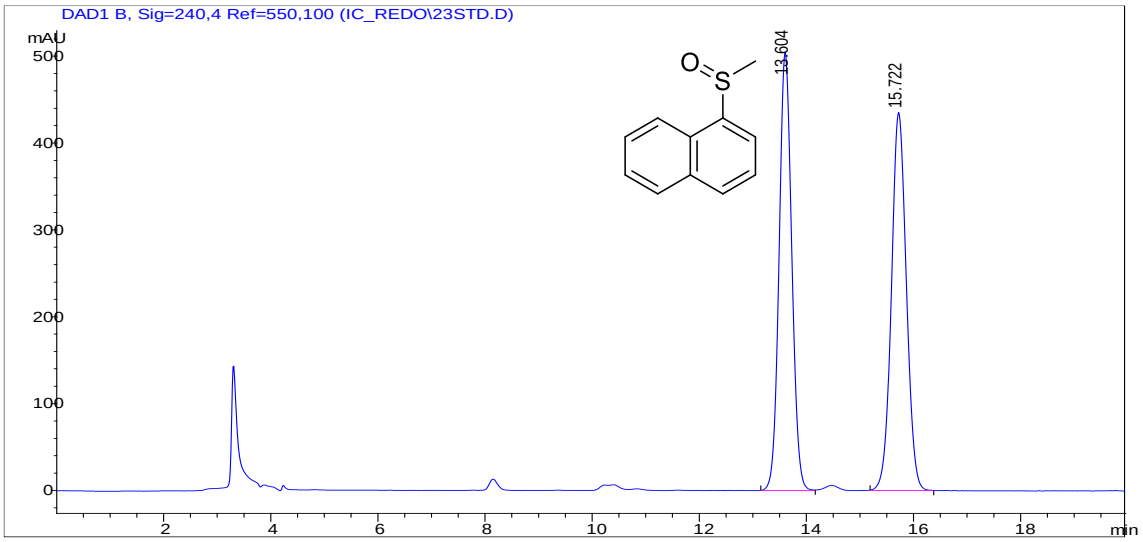


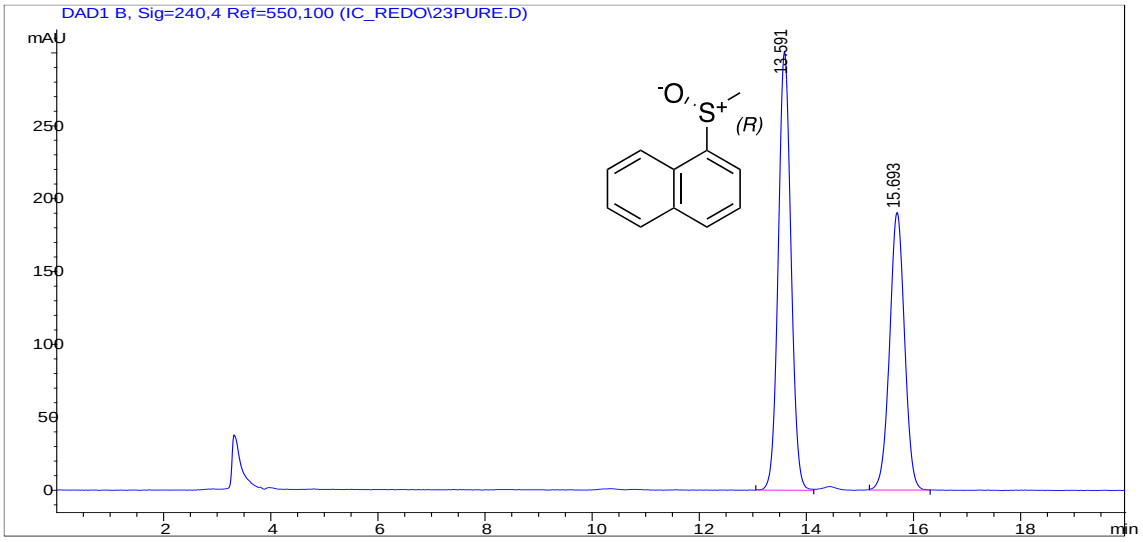

*((Methylsulfinyl)methyl)benzene (**28o**)*

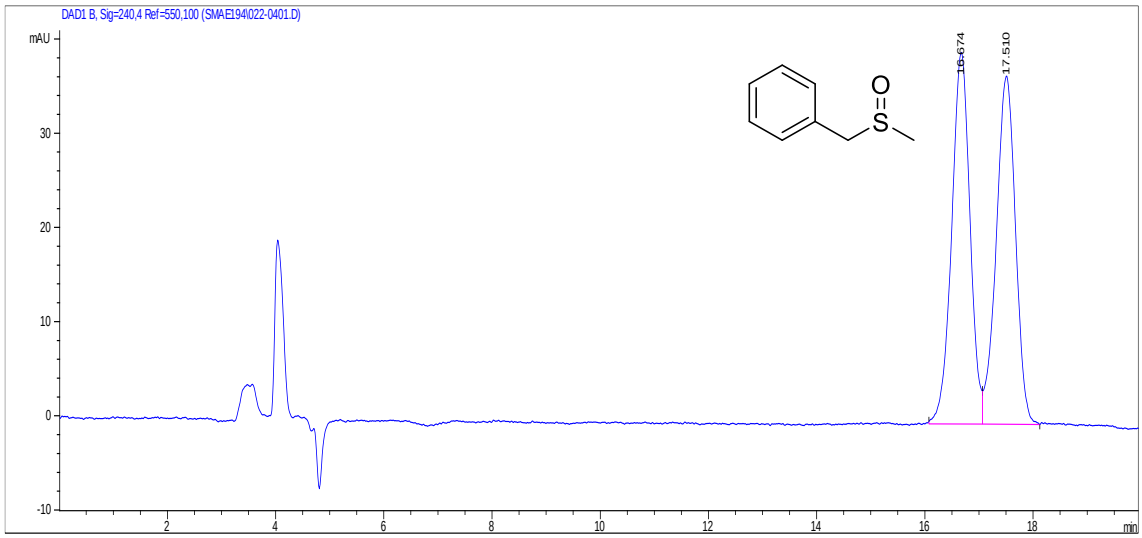


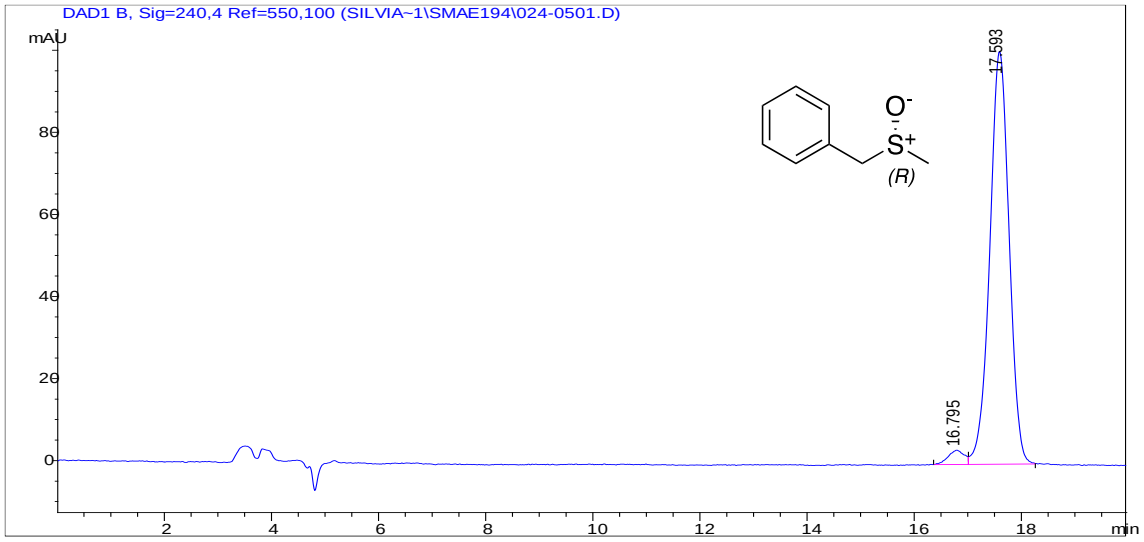

*1-(Methylsulfinyl)dodecane (**28ak**)*

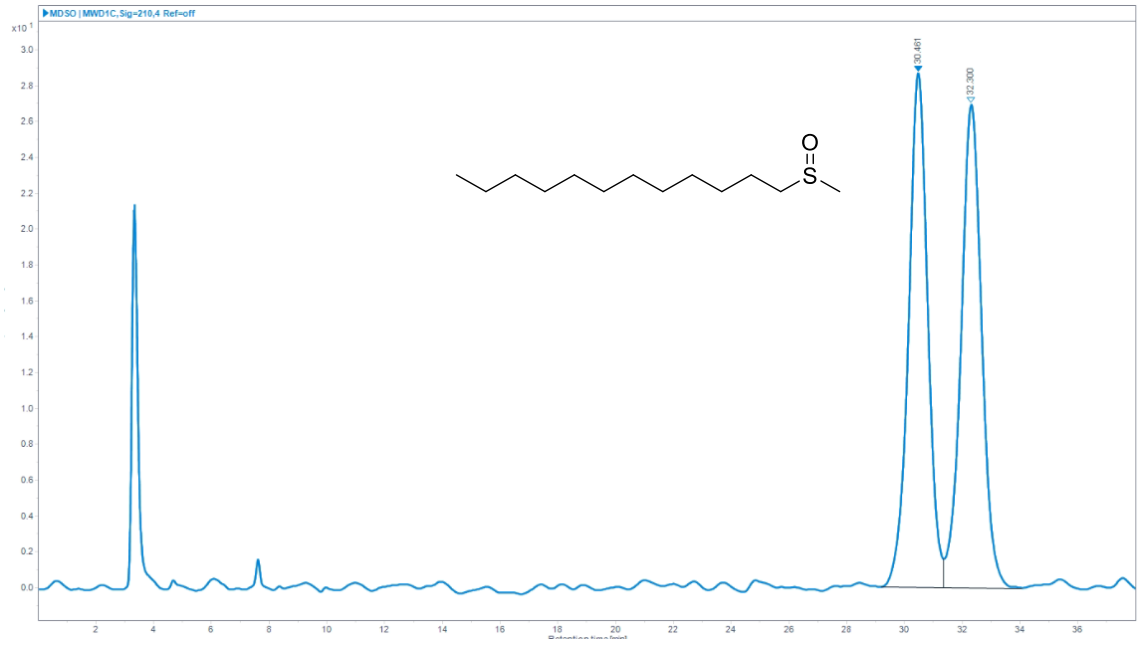


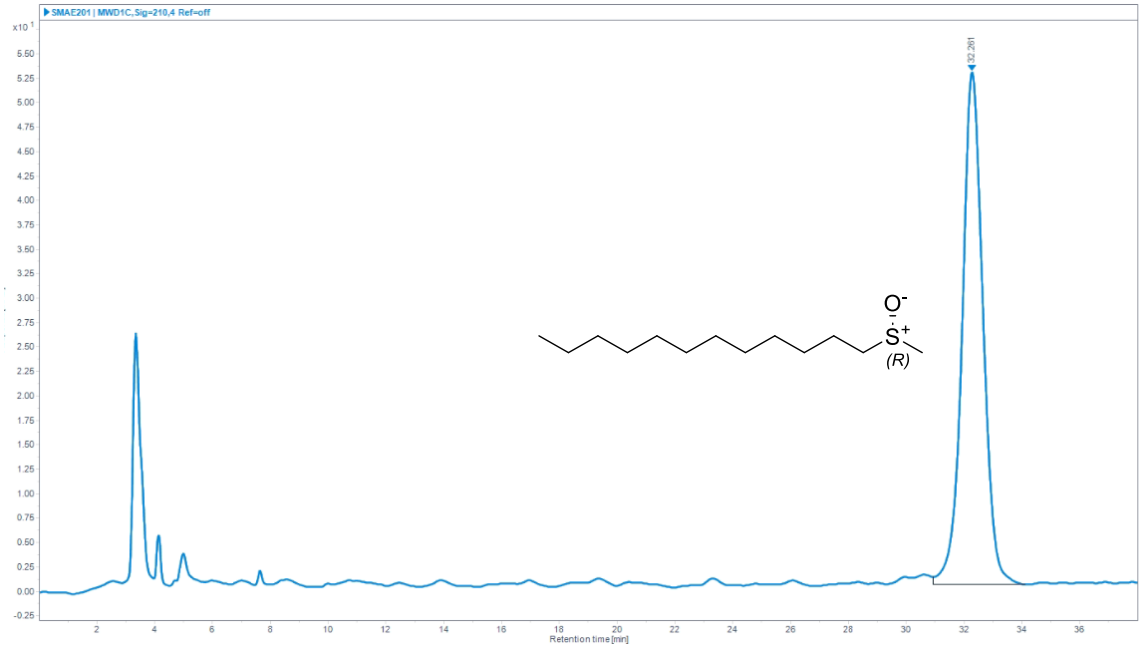

*4-(Methylsulfinyl)butan-2-one (**28al**)*

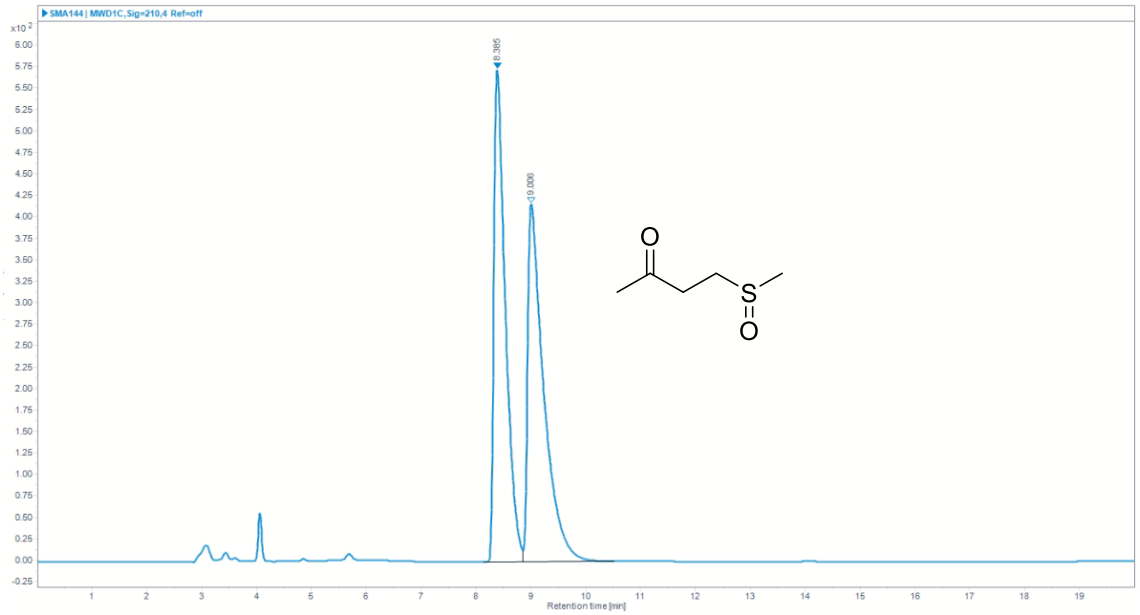


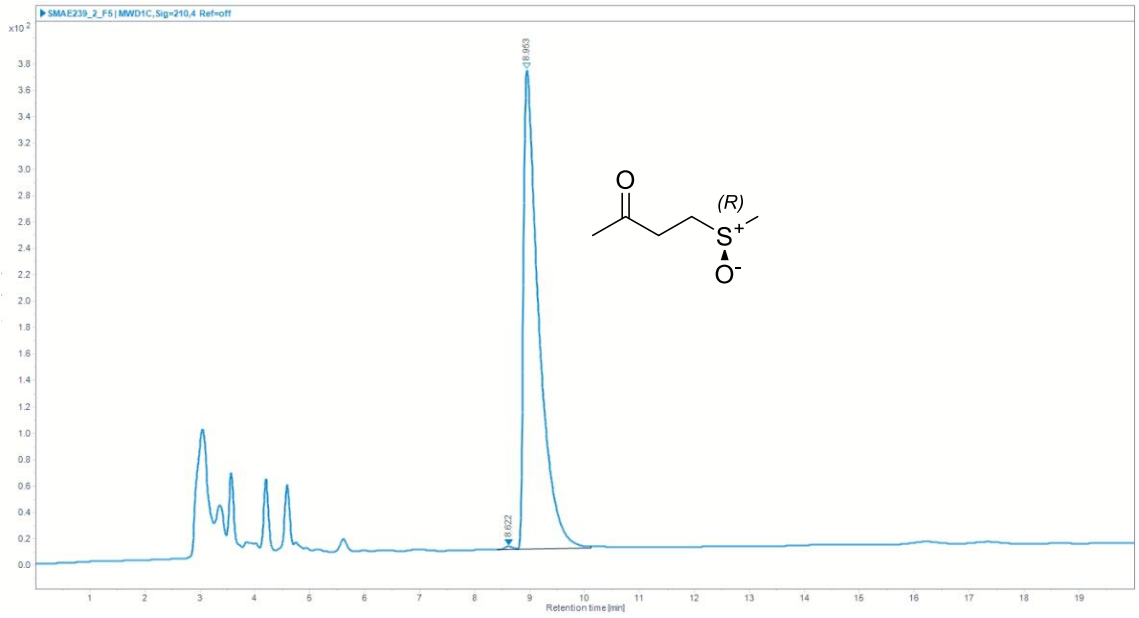

*((2-(Methylsulfinyl)ethyl)sulfinyl)benzene (**28am**)*

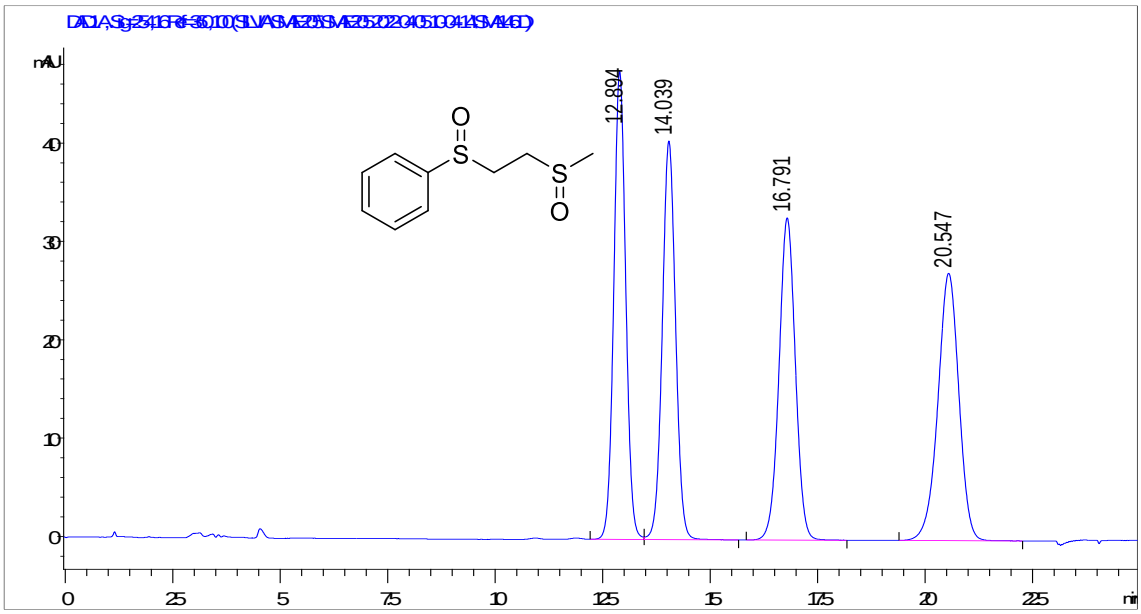


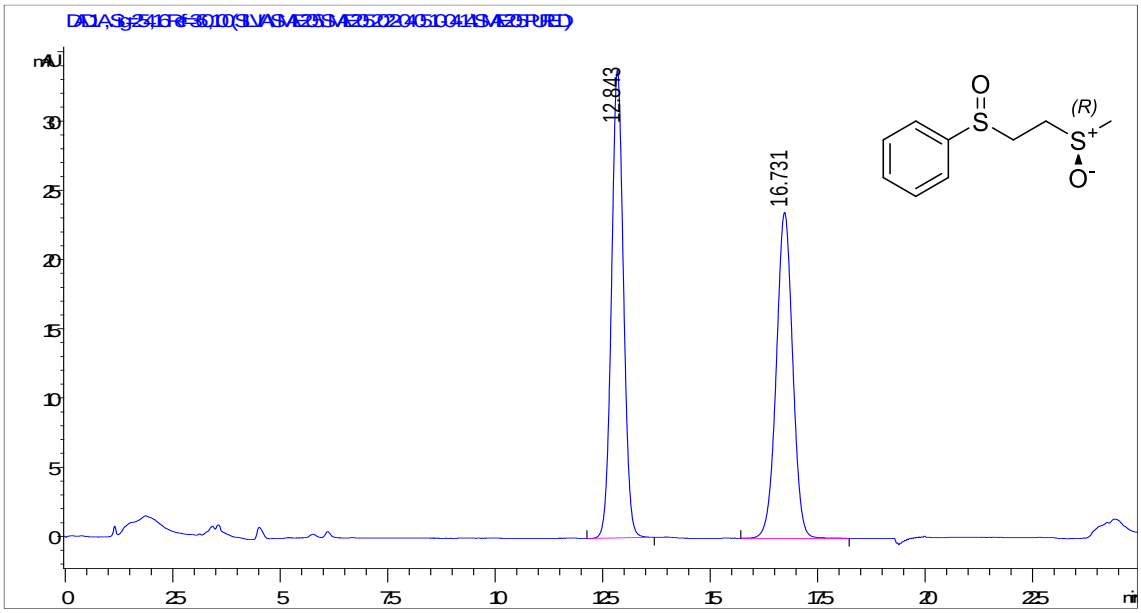

*(Ethylsulfinyl)benzene (**28c**)*

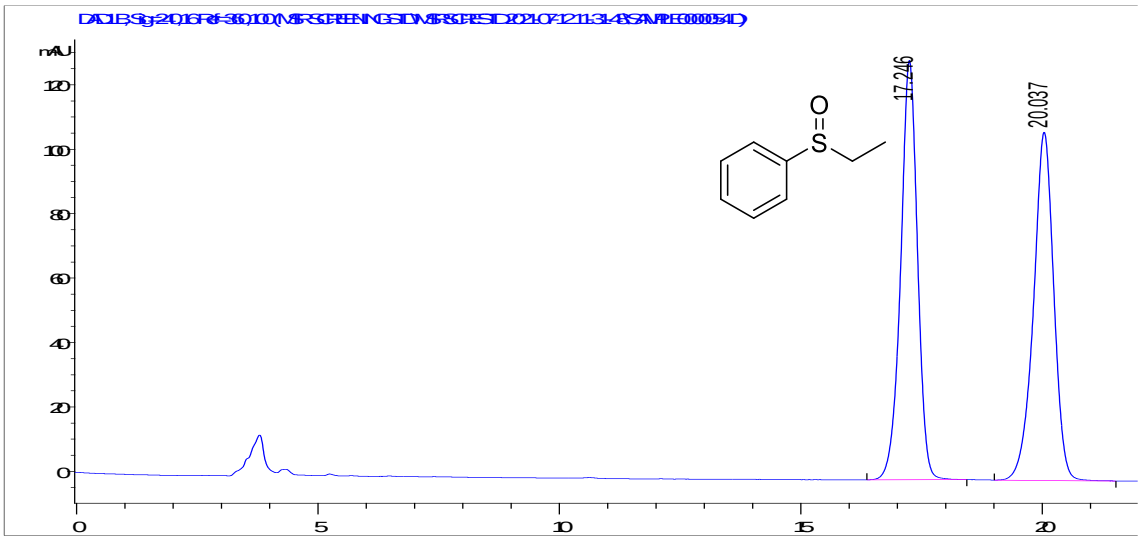


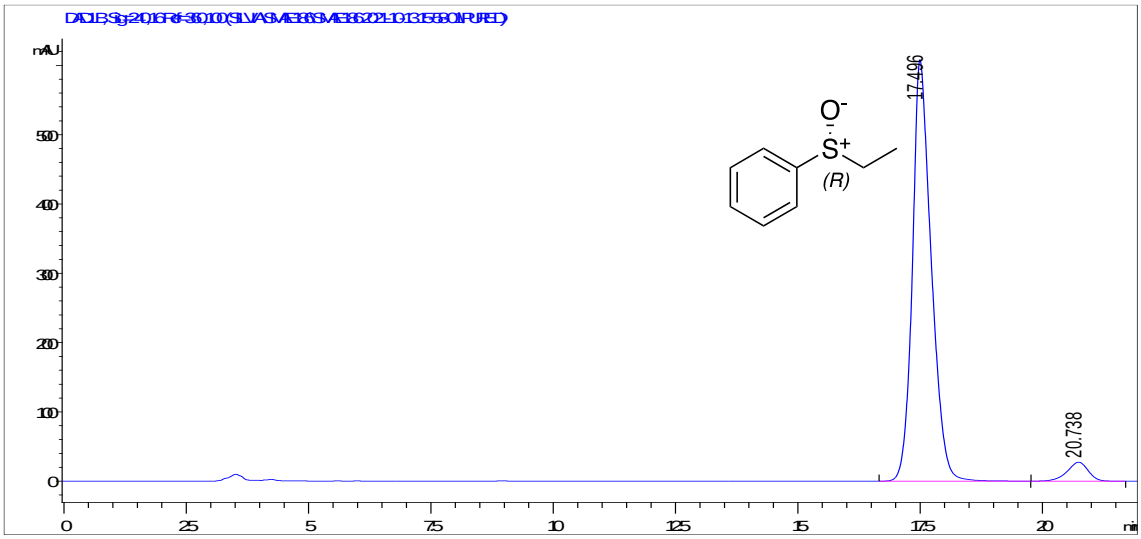

*1-Methyl-4-(ethylsulfinyl)benzene (**28d**)*

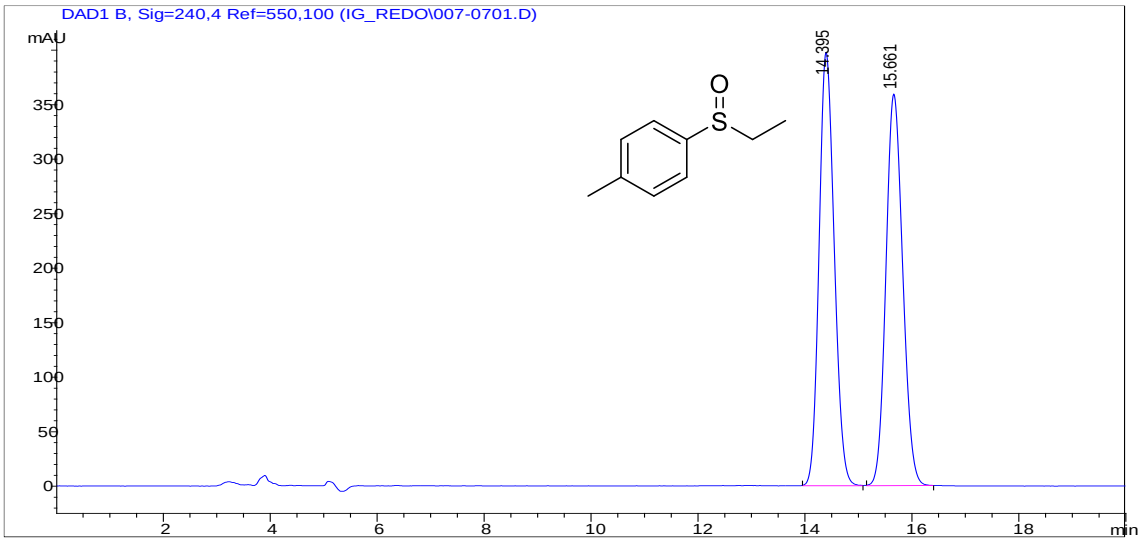


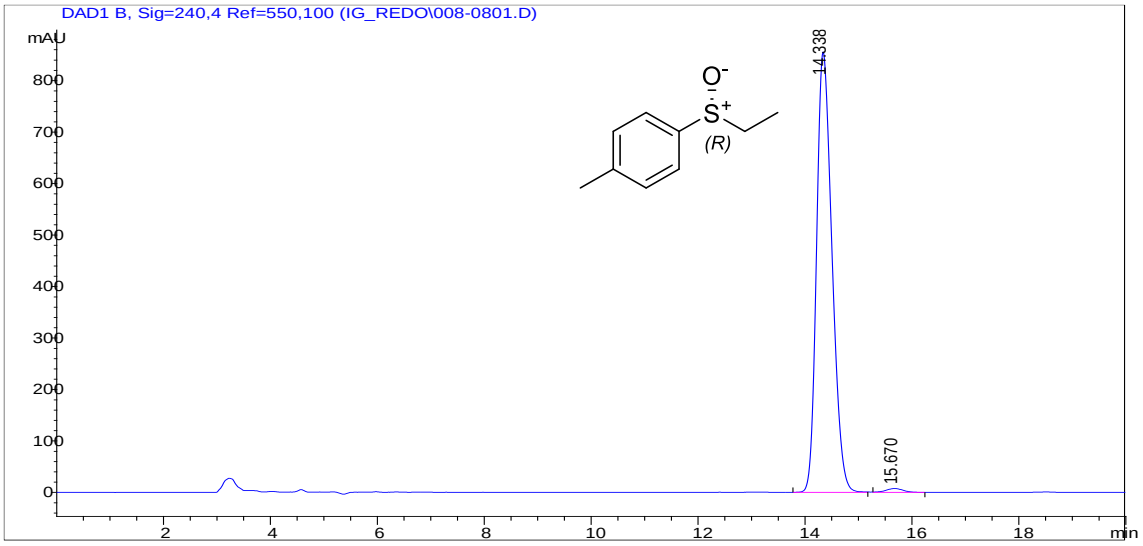

*1-Bromo-4-(ethylsulfinyl)benzene (**28g**)*

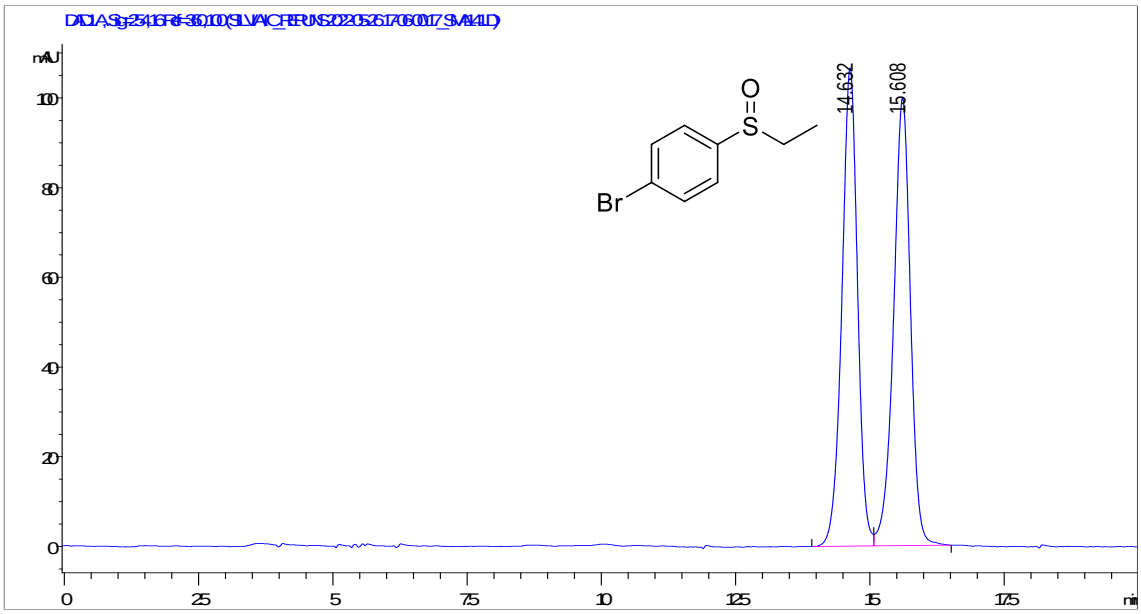


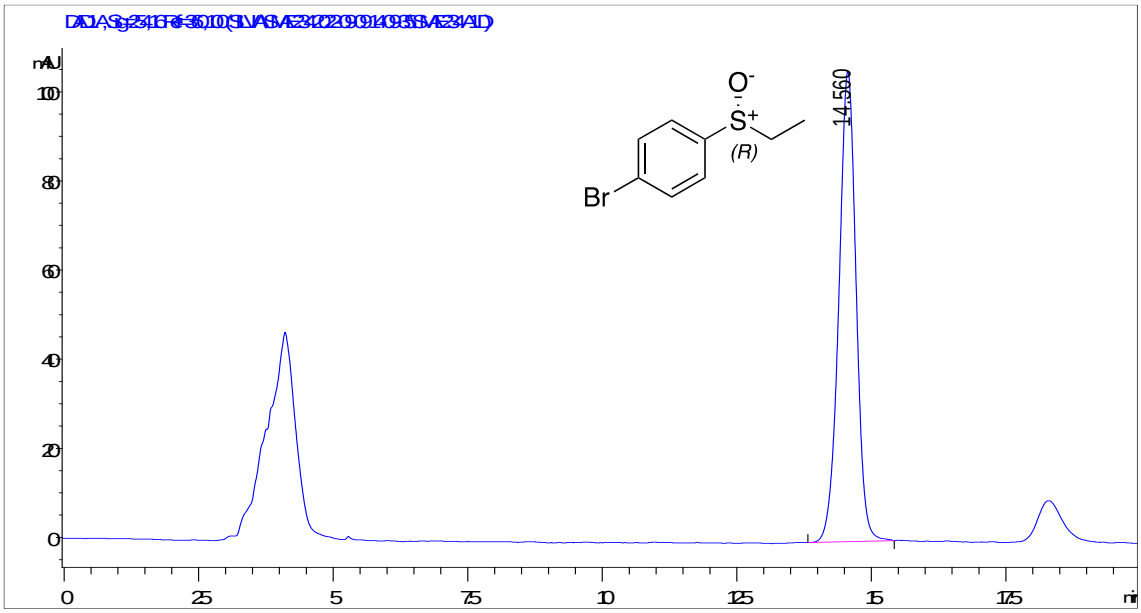

*((Ethylsulfinyl)methyl)benzene (**28v**)*

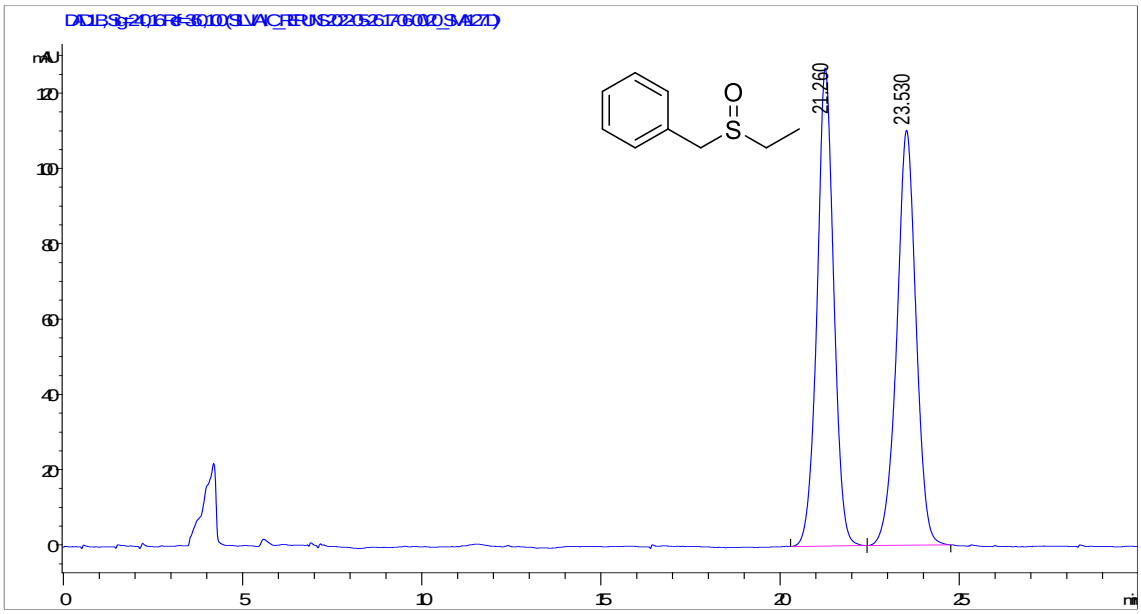


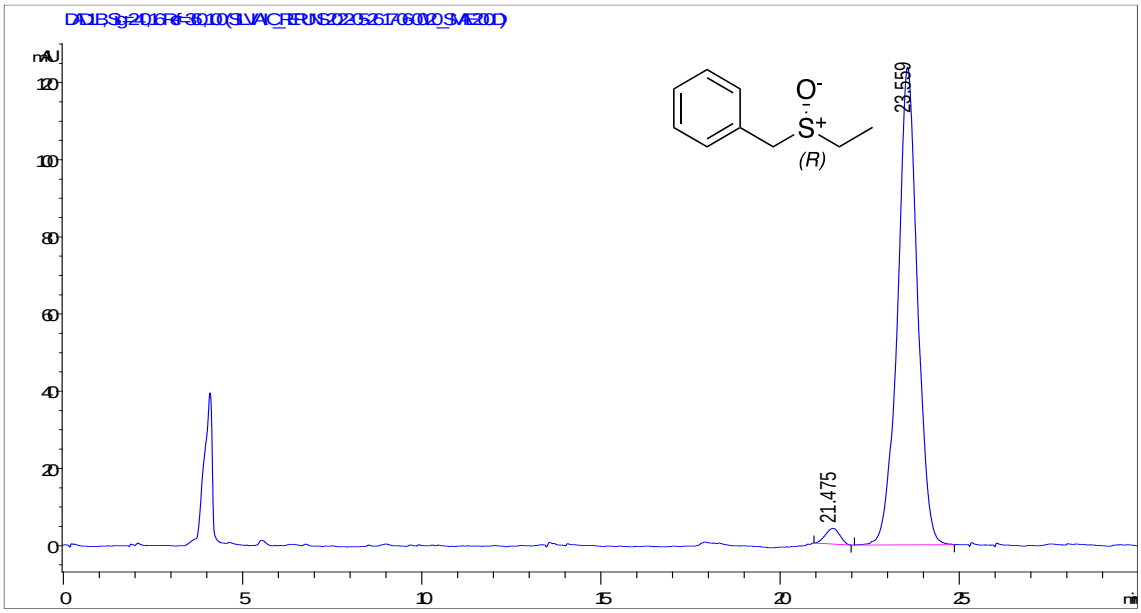

*(2-(ethylsulfinyl)ethyl)benzene (**28w**)*

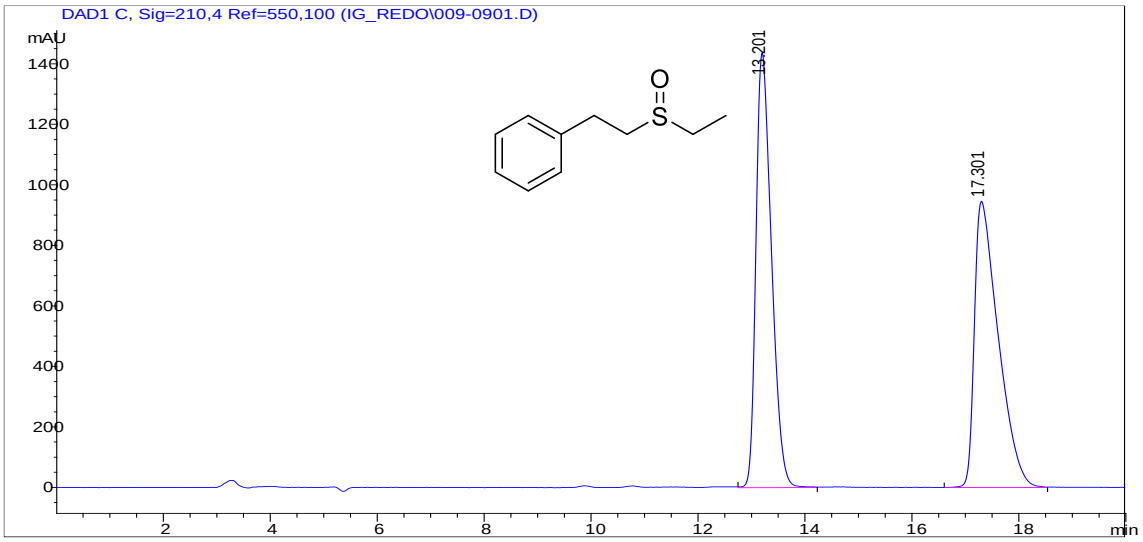


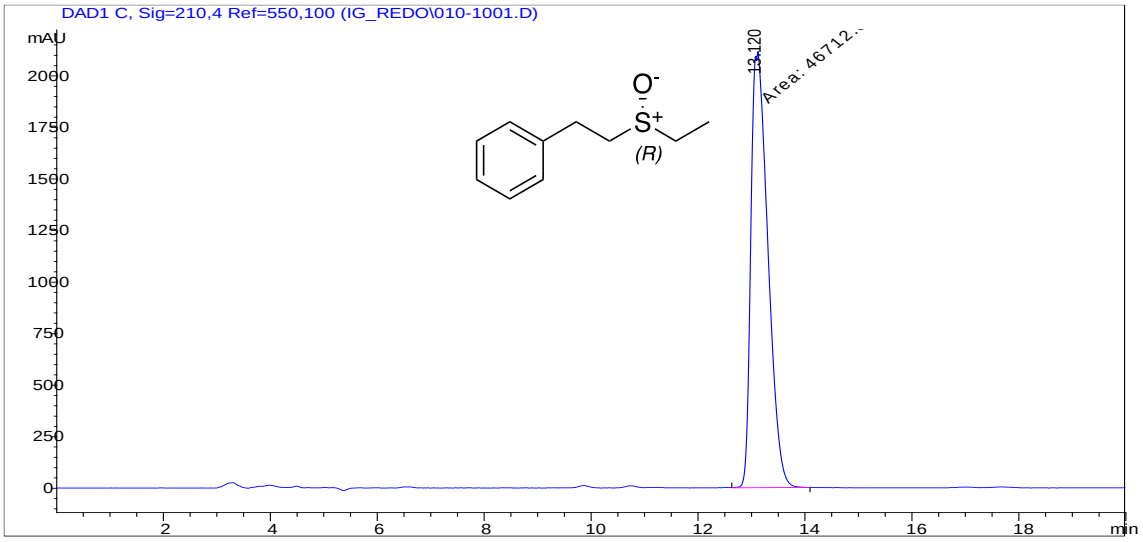

*2-((Ethylsulfinyl)methyl)pyridine (**28t**)*

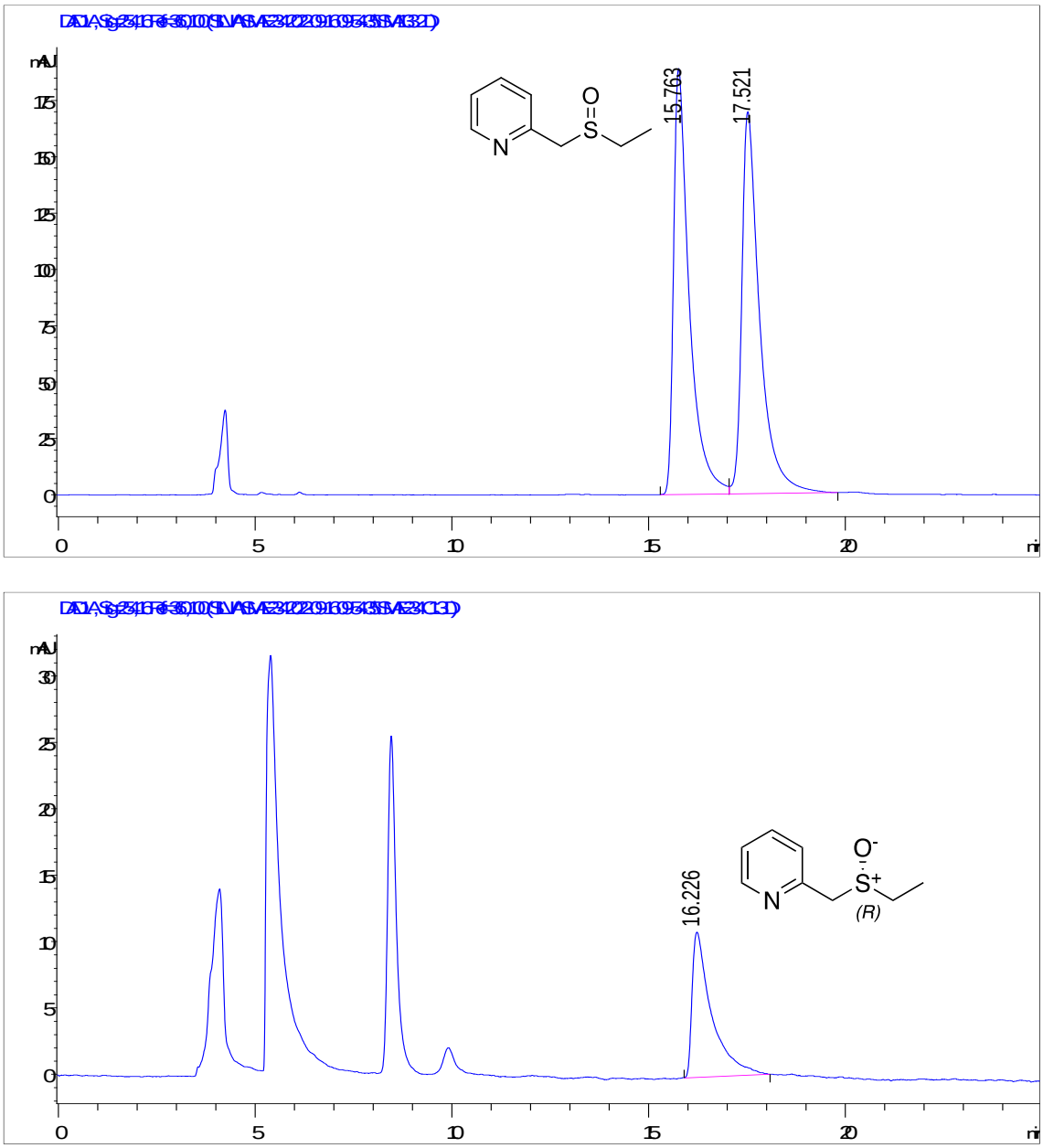


HPLC trace obtained from crude extract of the enzymatic reaction.

*(Propylsulfinyl)benzene (**28an**)*

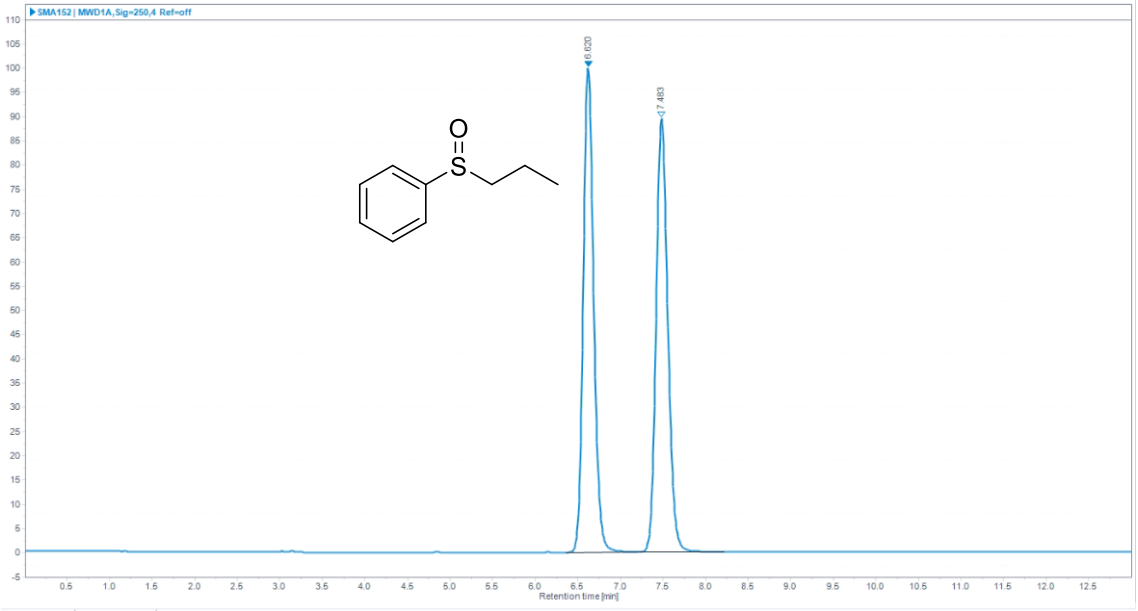


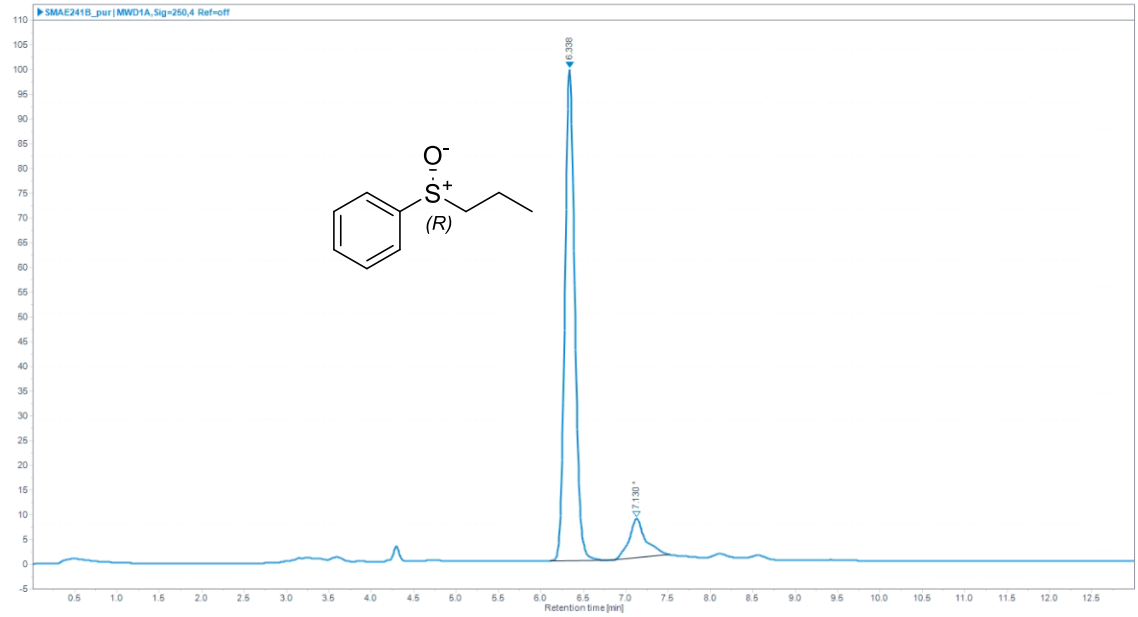

*1-Methoxy-4-(propylsulfinyl)benzene (**28j**)*

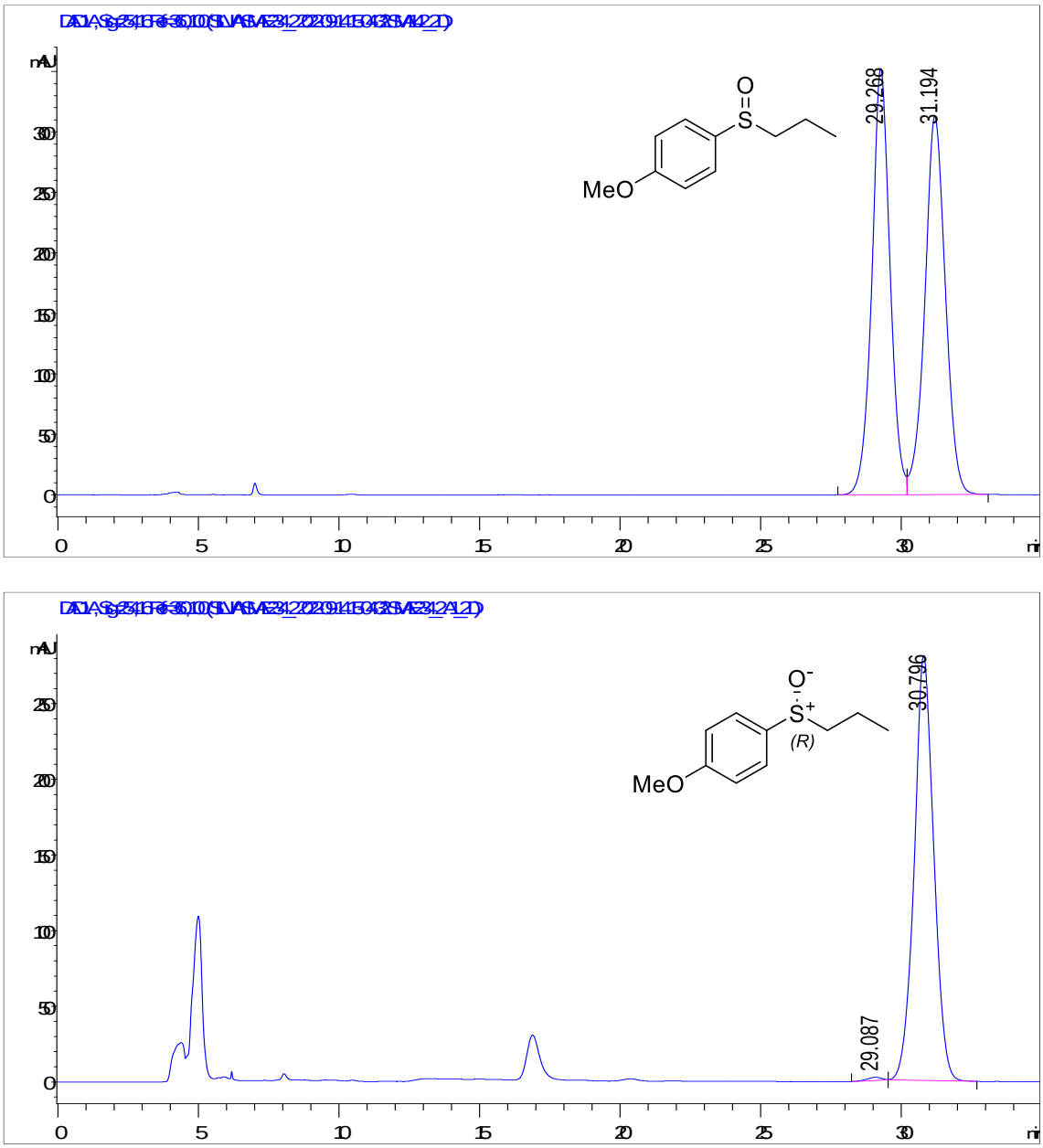


HPLC trace obtained from crude extract of the enzymatic reaction.

*(Allylsulfinyl)benzene (**28l**)*

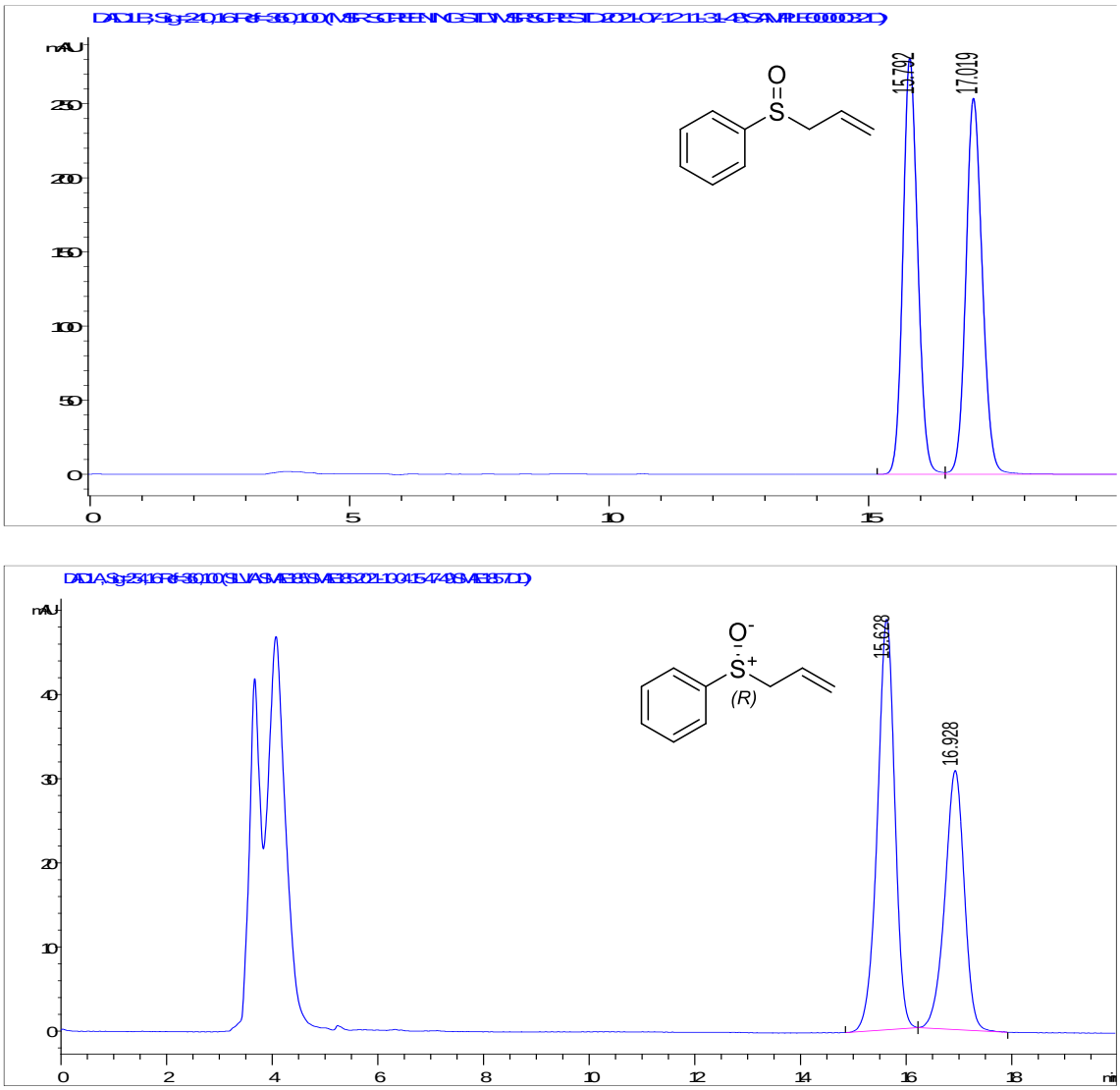


HPLC trace obtained from crude extract of the enzymatic reaction.

*1-Methyl-4-(propylsulfinyl)benzene (**28k**)*

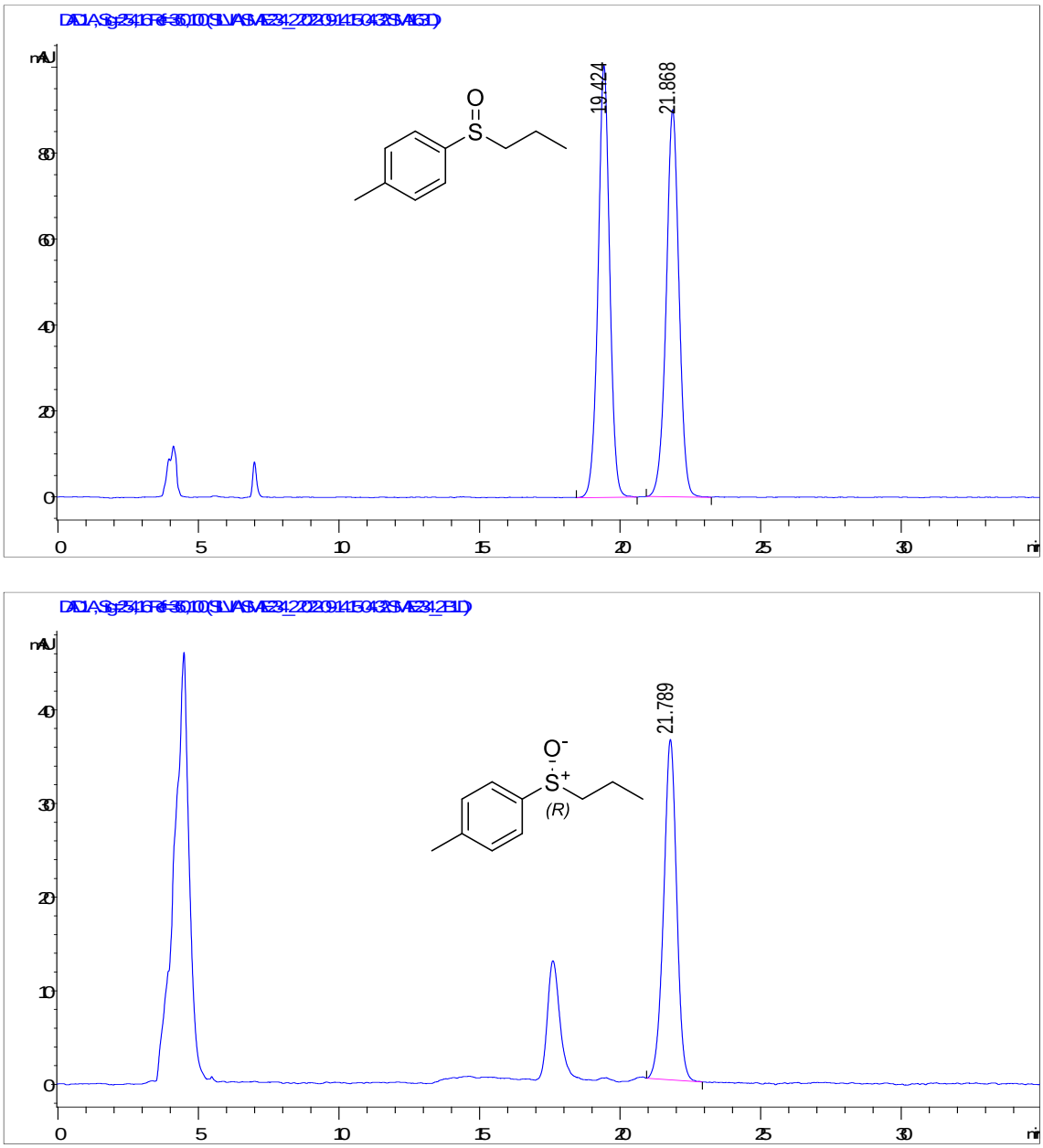


HPLC trace obtained from crude extract of the enzymatic reaction.

*1-Chloro-4-(propylsulfinyl)benzene (**28ao**)*

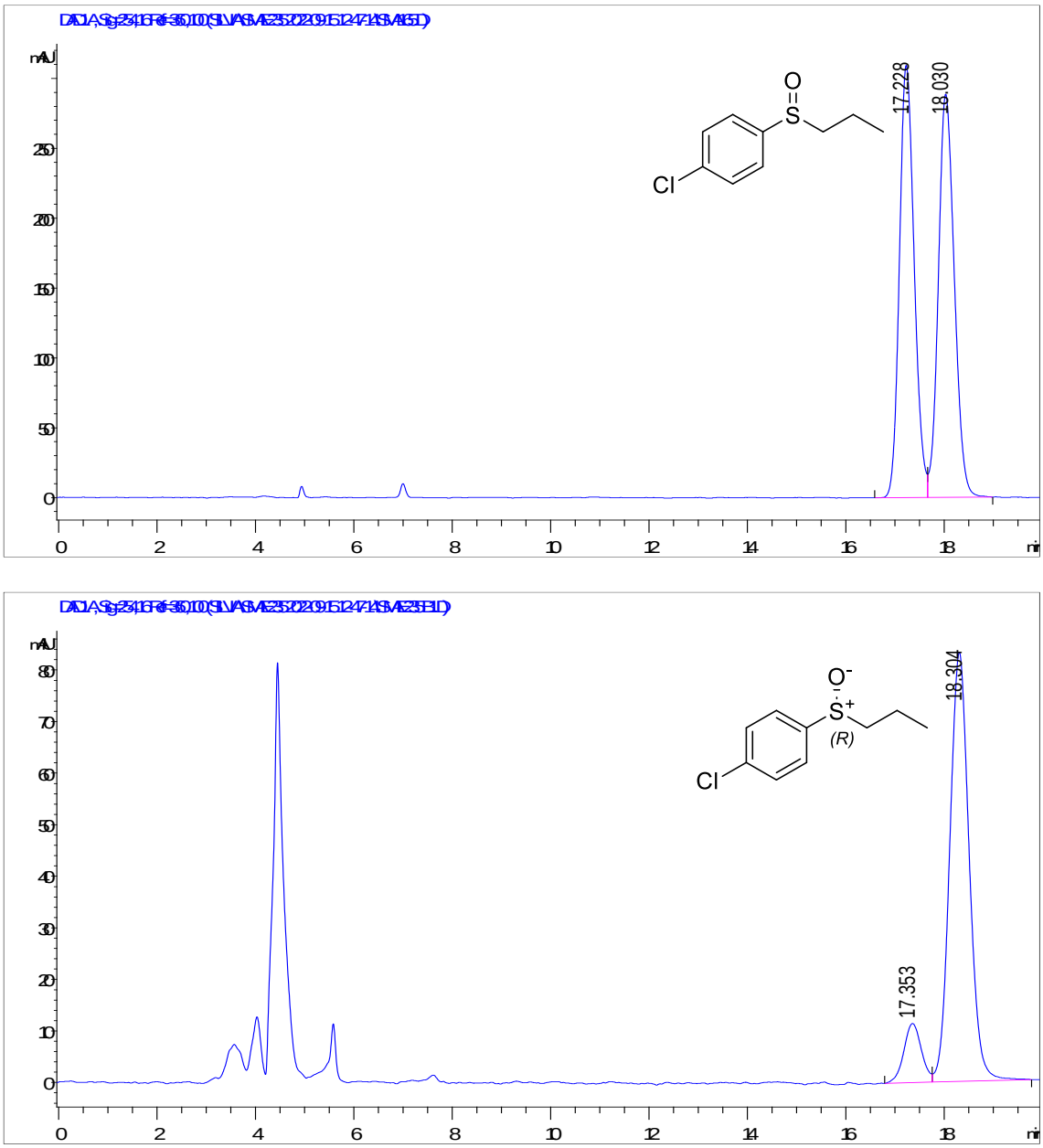


HPLC trace obtained from crude extract of the enzymatic reaction.

*1-Bromo-4-(propylsulfinyl)benzene (**28ap**)*

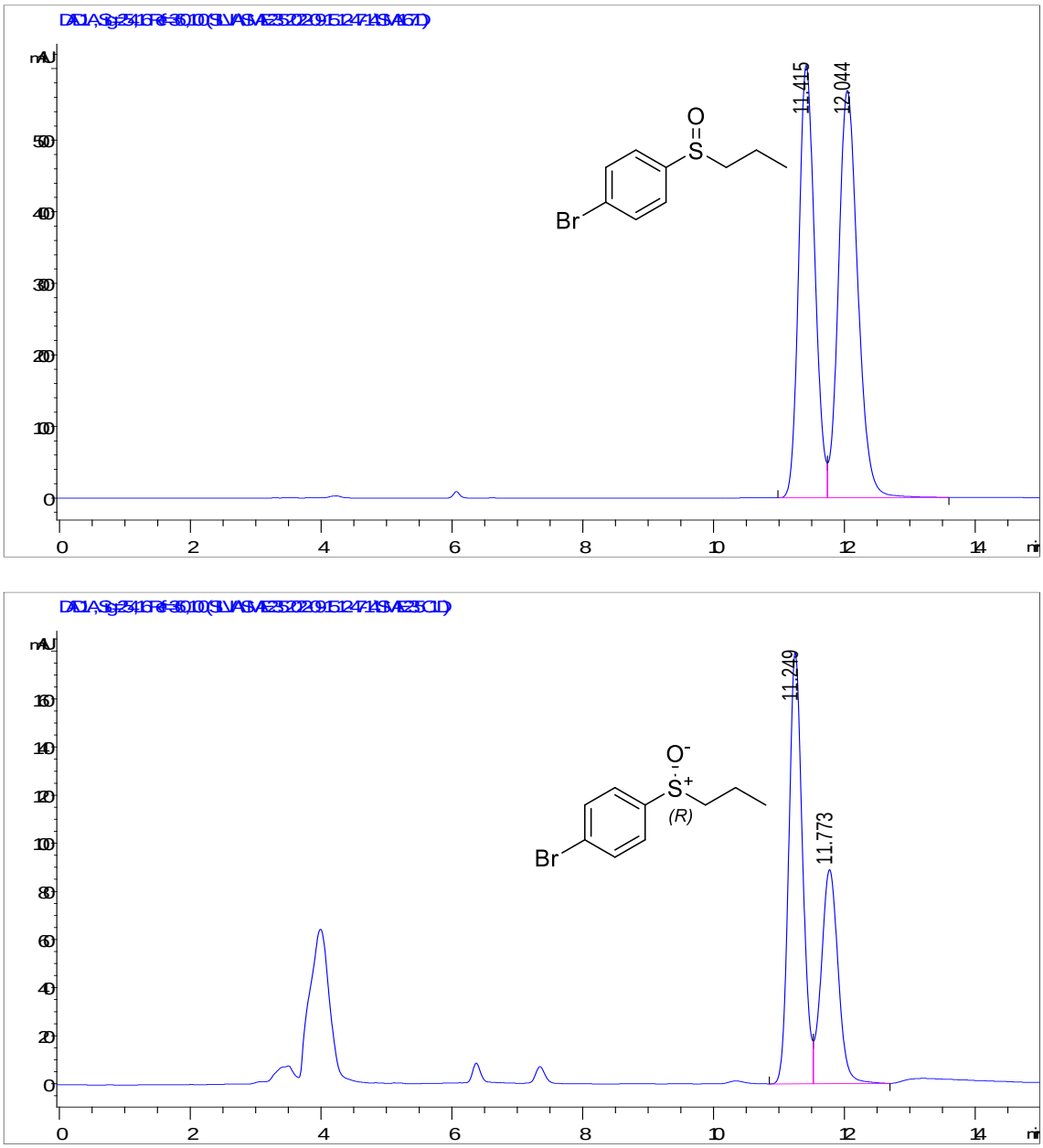


HPLC trace obtained from crude extract of the enzymatic reaction.

*1-Methoxy-3-(propylsulfinyl)benzene (**28aq**)*

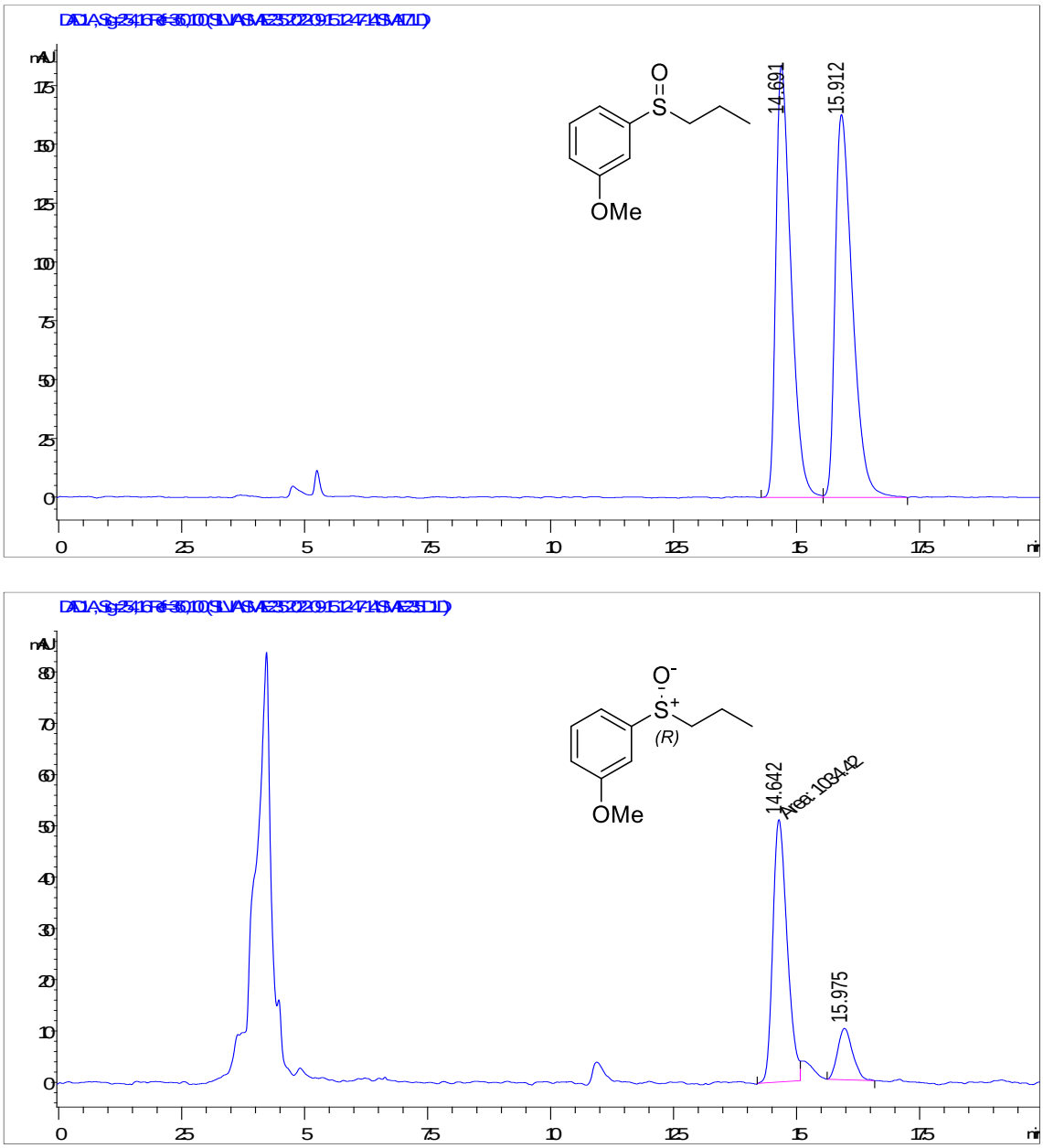


HPLC trace obtained from crude extract of the enzymatic reaction.

*1-(Butylsulfinyl)-4-methoxybenzene (**28ar**)*

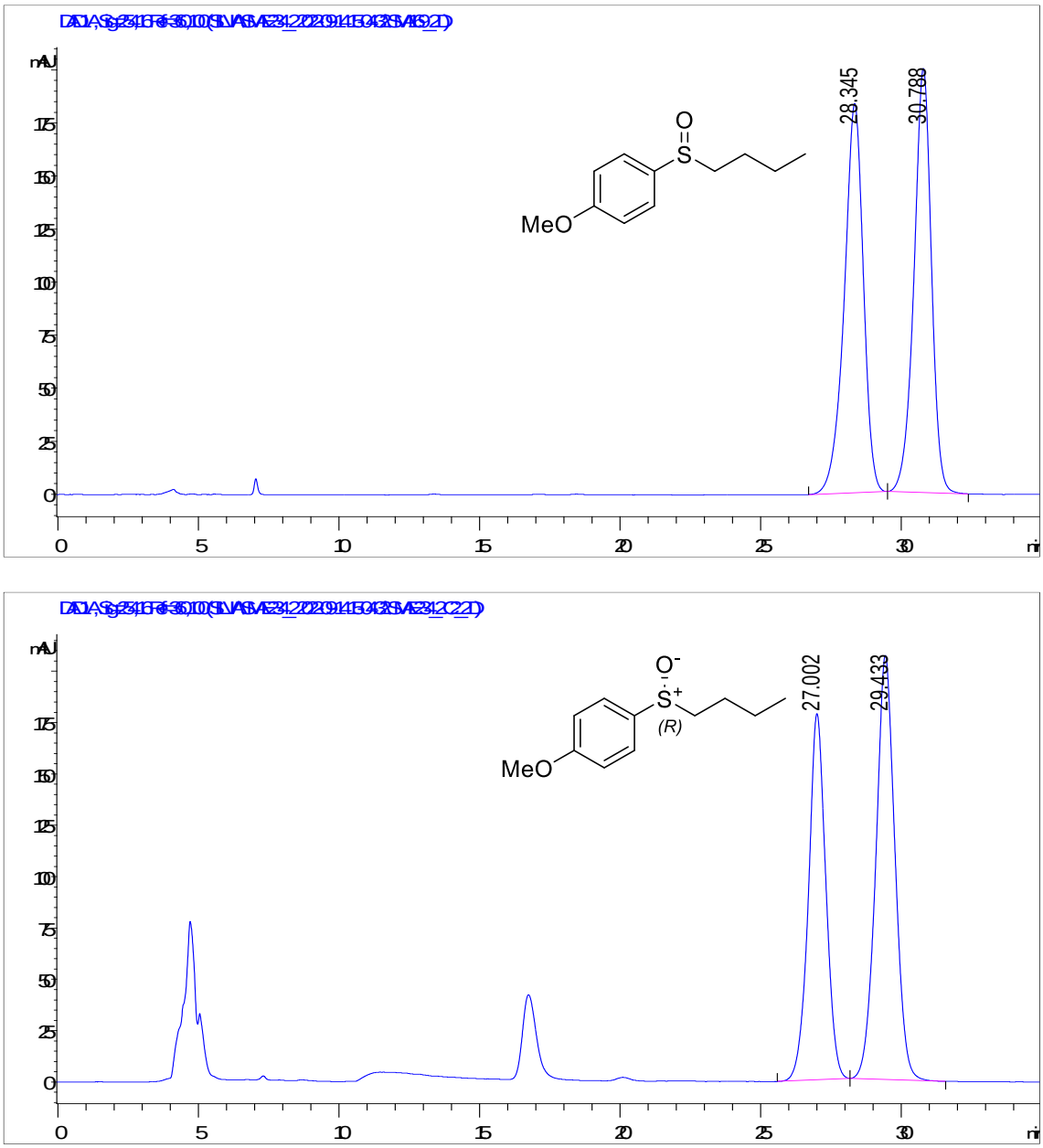


HPLC trace obtained from crude extract of the enzymatic reaction.

## Appendix VI. Calibration curves for HPLC conversions

A series of five solutions, where the concentration of the internal standard, methyl phenyl sulfoxide (MPSO) or methyl *p*-tolyl sulfoxide (MTSO), was kept at 8 mM and the concentration of the substrate sulfoxide varied between 12, 8, 4, 2 and 1 mM, was injected into an Agilent Eclipse Plus C18 (2.7 µm, 3.0x50 mm) reversed phase column in duplicate. The resulting ratios of the areas under the curve (auc) were averaged and used to calculate the calibration curve for each sulfoxide. Upon completion of the biocatalysed reaction, a 10 µL aliquot was reserved for calculating the ee of the sulfoxide, and 500-700 µL of $CH_3CN$ was added to the mixture to quench the reaction. Then, 1 eq. of internal standard was added, and the mixture was centrifuged at maximum speed to remove insoluble protein. The resulting clear solution was analysed by reversed phase HPLC to determine the ratio between the substrate sulfoxide and the internal standard and the HPLC yield was obtained using the calibration curves.

### Calibration curve for 28af

The retention time of **28af** was 5.73 min and the internal standard MPSO was 4.94 min. The detector was set at 240 nm.

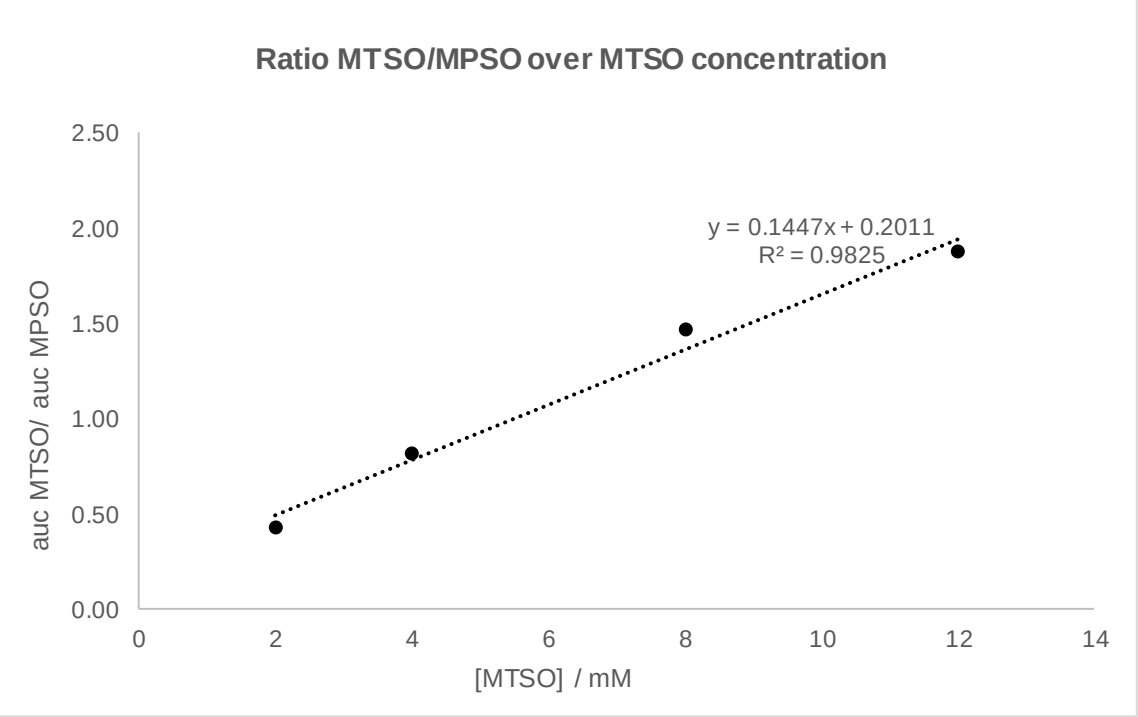

**Calibration curve for 28g**

The retention time of **28g** was 4.50 min and the internal standard MTSO was 4.45 min. The detector was set at 240 nm.

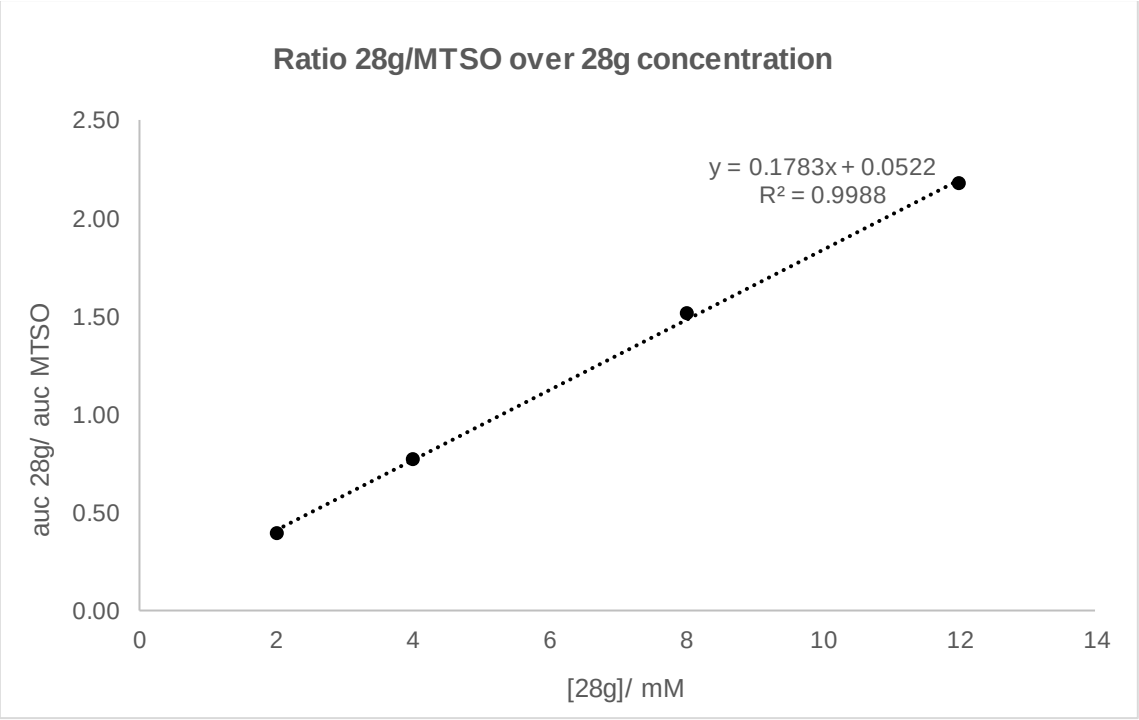


**Calibration curve for 28t**

The retention time of **28t** was 2.45 min and the internal standard MTSO was 4.45 min. The detector was set at 240 nm.

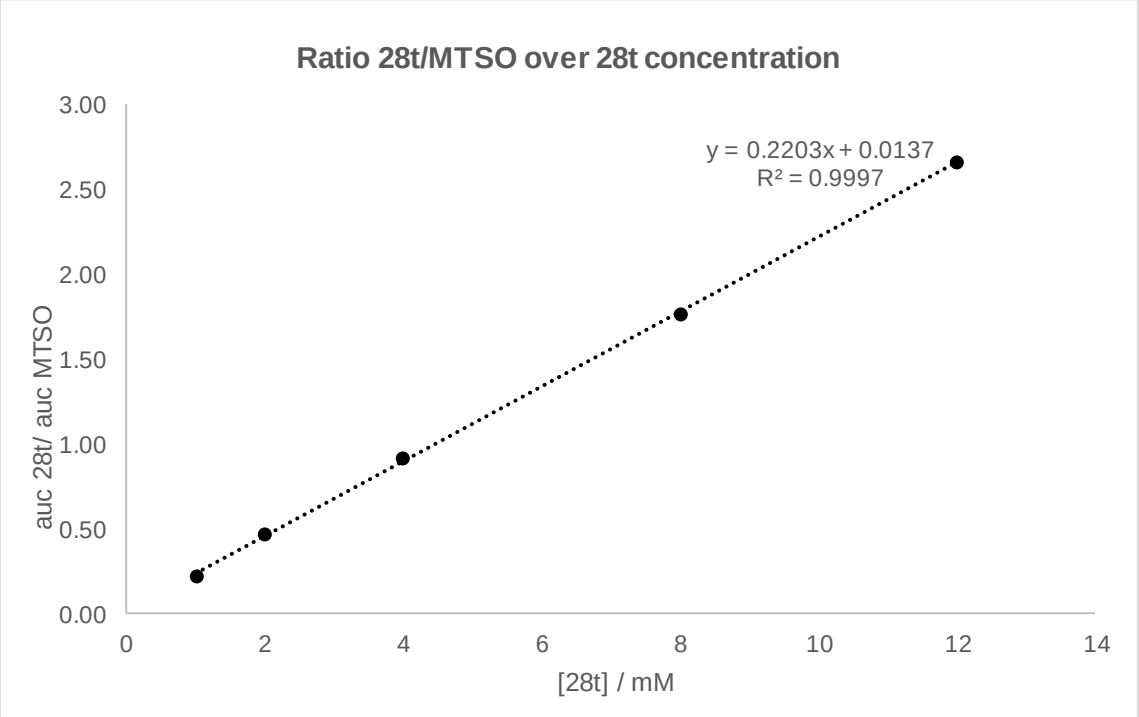

**Calibration** curve **for 28an**

The retention time of **28an** was 5.24 min and the internal standard MTSO was 4.45 min. The detector was set at 240 nm.

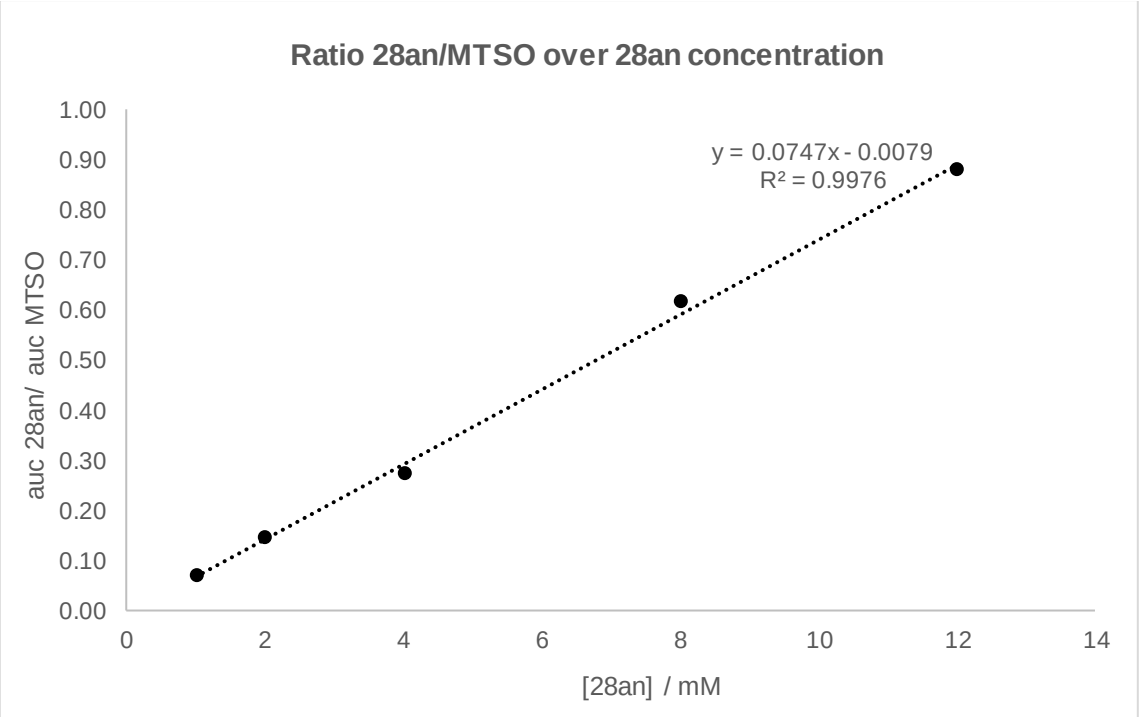


**Calibration curve for 28j**

The retention time of **28j** was 5.73 min and the internal standard MTSO was 4.45 min. The detector was set at 240 nm.

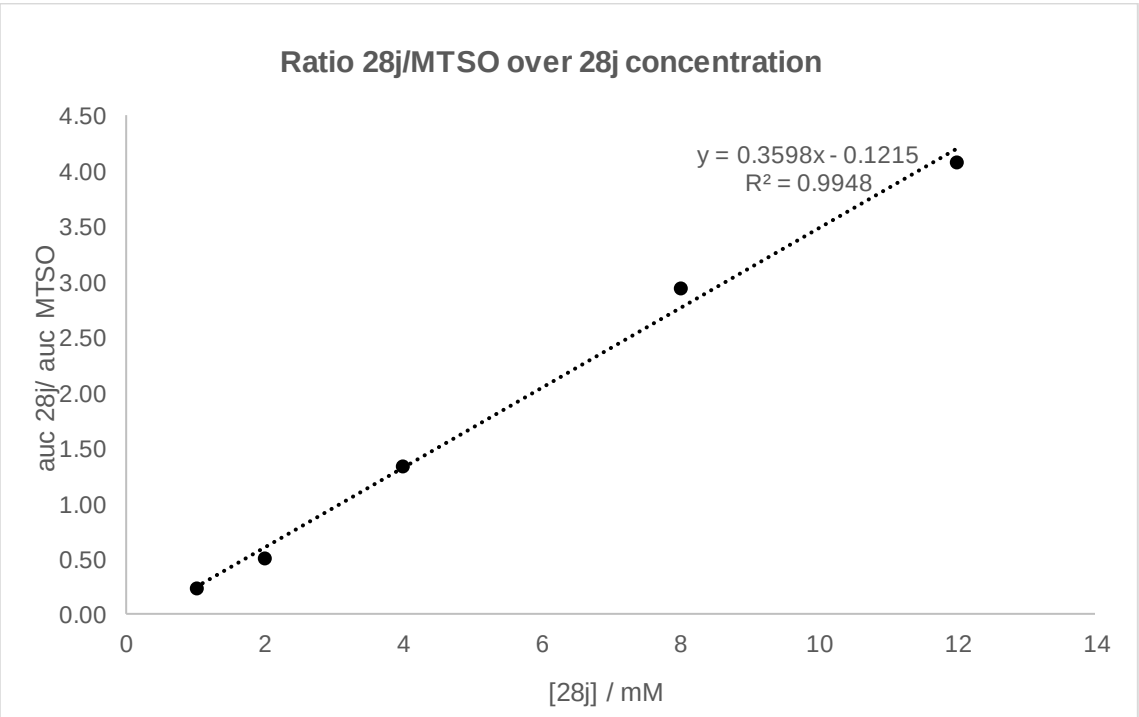

**Calibration curve for 28k**

The retention time of **28k** was 6.35 min and the internal standard MTSO was 4.45 min. The detector was set at 240 nm.

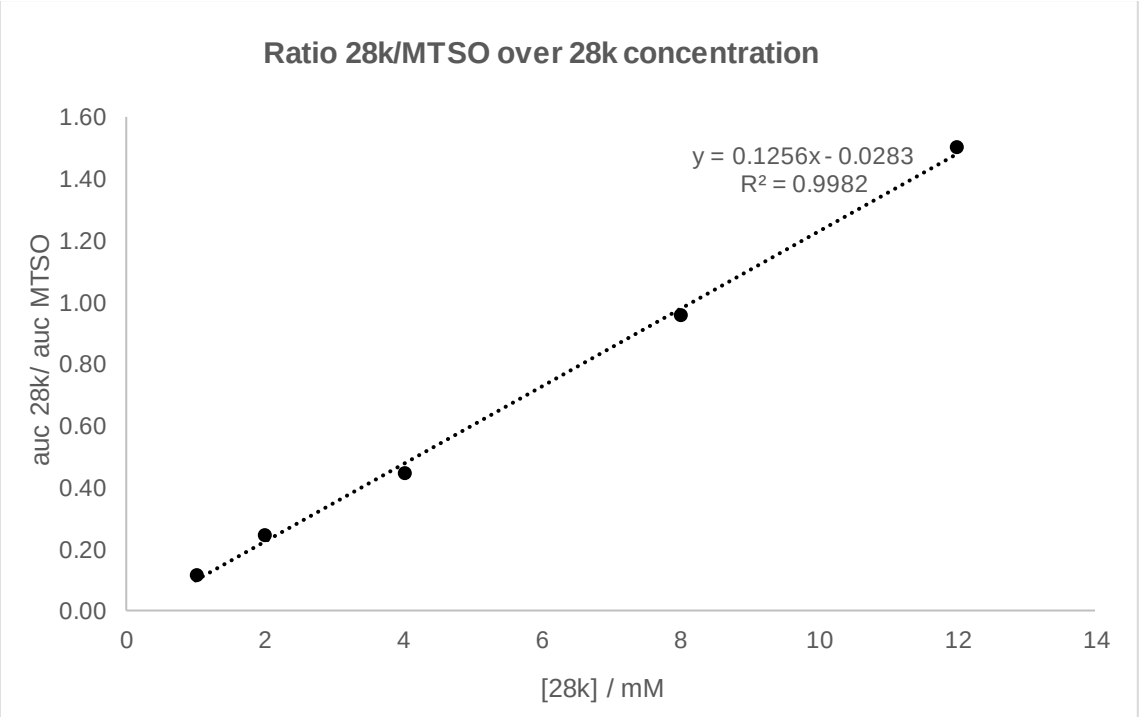


**Calibration curve for 28ao**

The retention time of **28ao** was 6.78 min and the internal standard MTSO was 4.45 min. The detector was set at 240 nm.

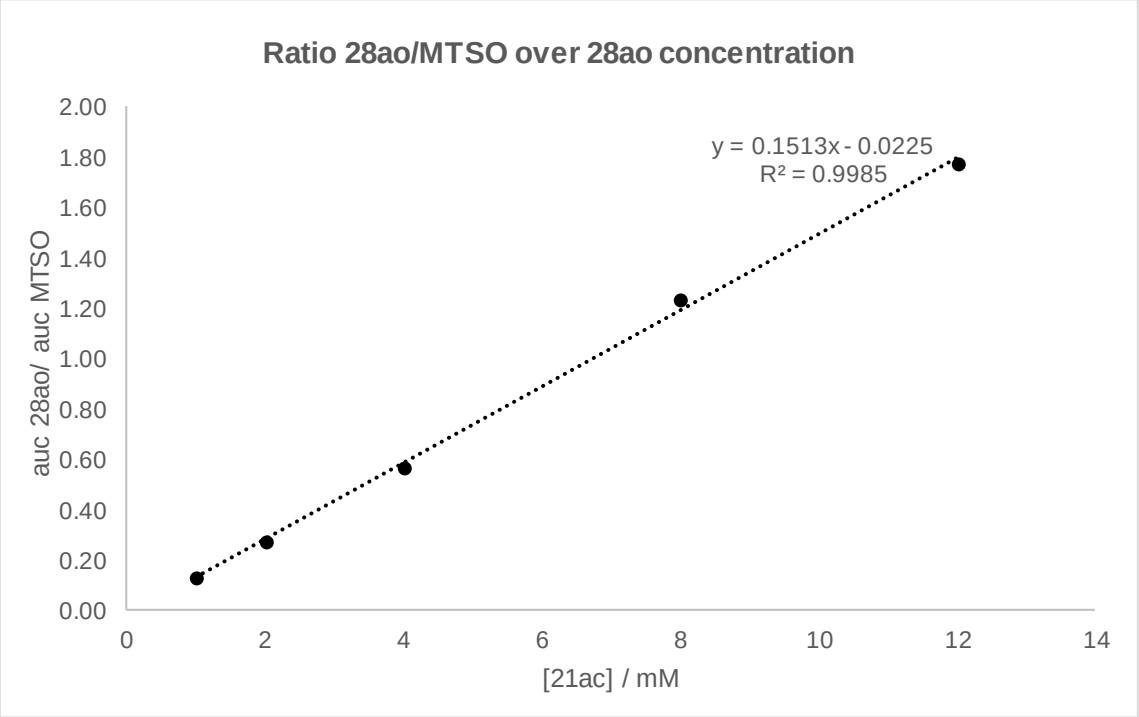

**Calibration curve for 28ap**

The retention time of **28ap** was 7.18 min and the internal standard MTSO was 4.45 min. The detector was set at 240 nm.

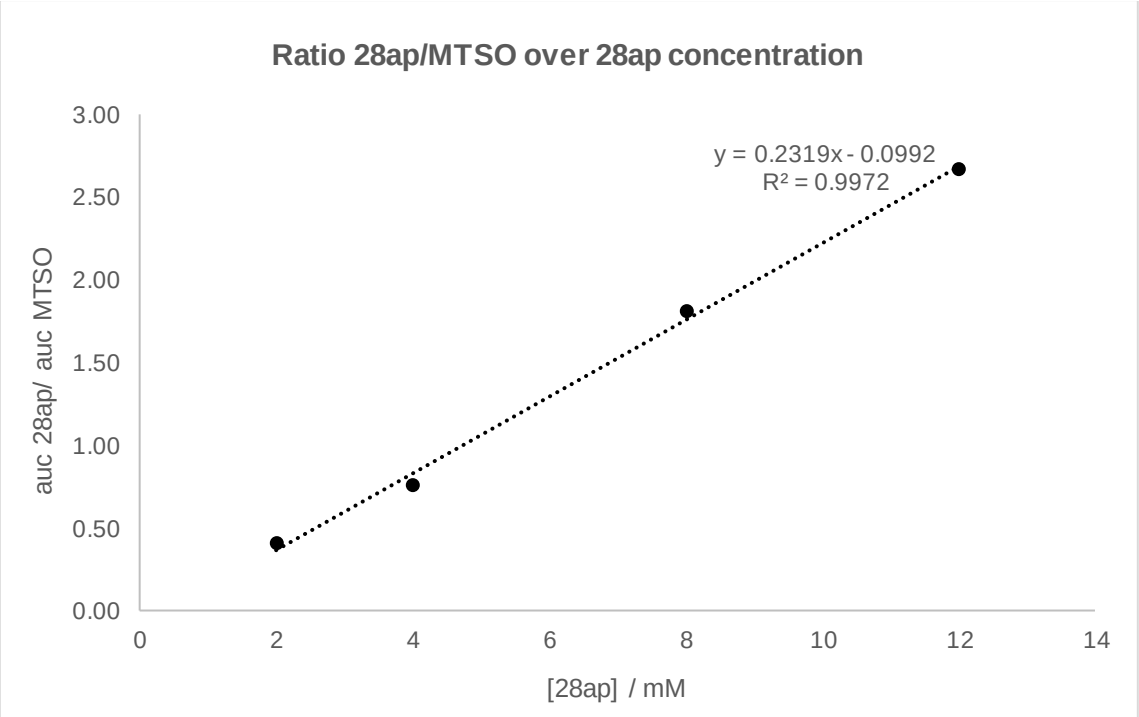


**Calibration curve for 28aq**

The retention time of **28aq** was 6.81 min and the internal standard MTSO was 4.45 min. The detector was set at 240 nm.

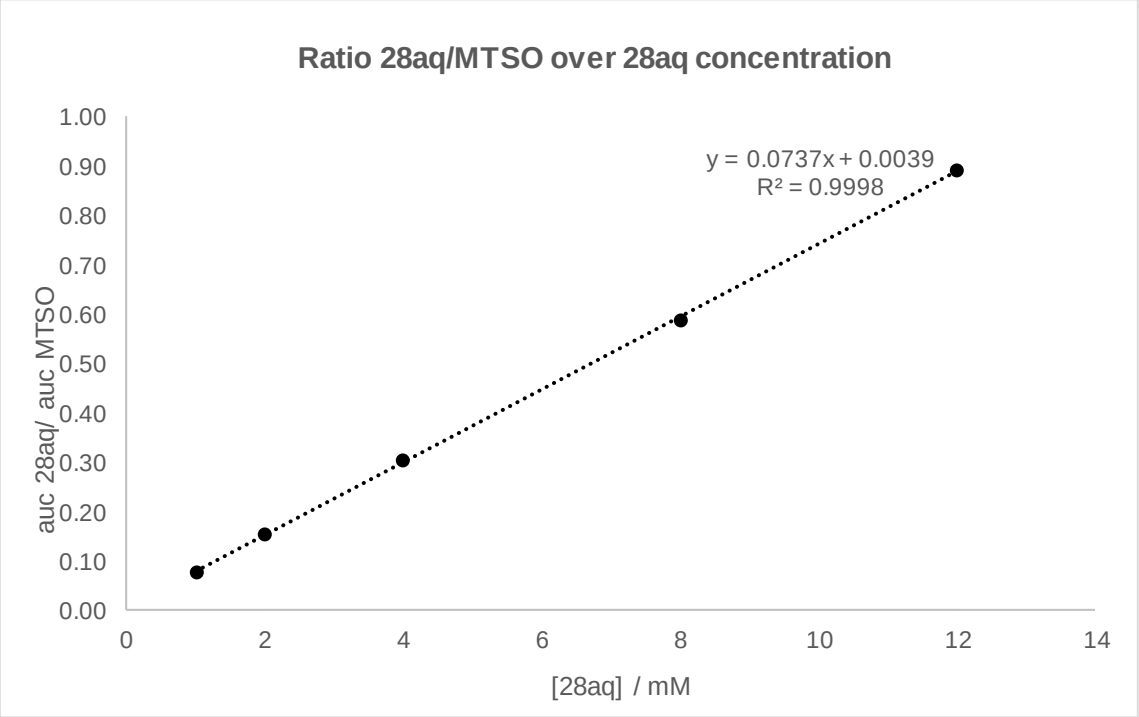

**Calibration curve for 28ar**

The retention time of **28ar** was 6.81 min and the internal standard MTSO was 4.45 min. The detector was set at 240 nm.

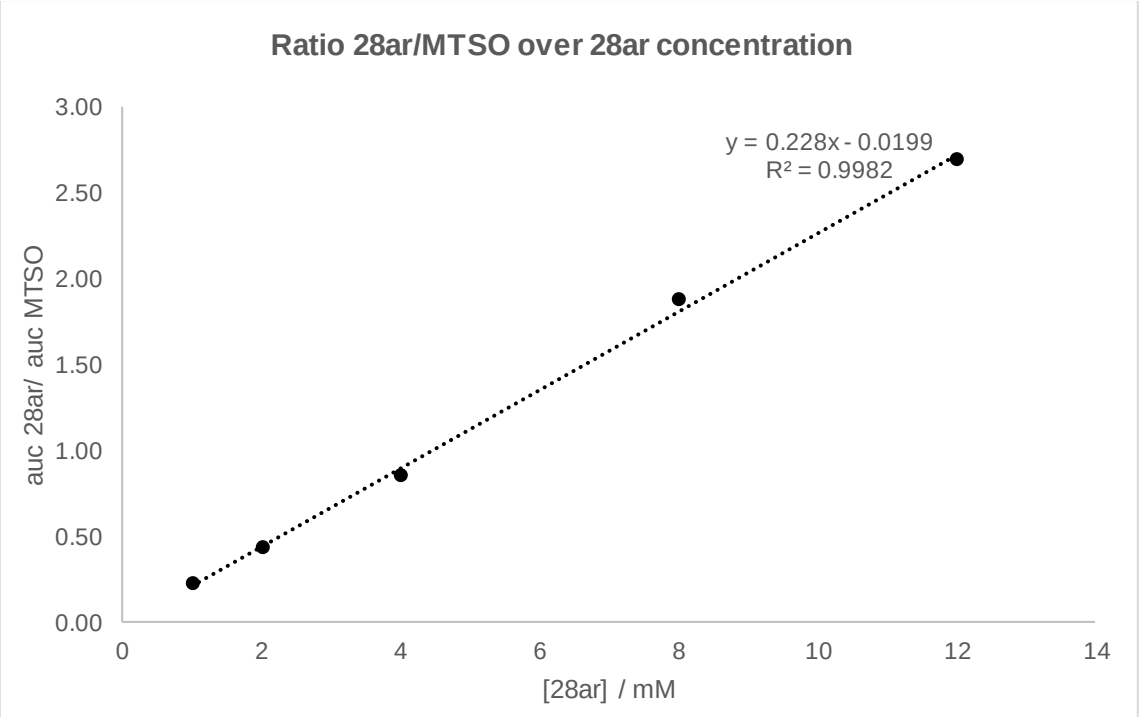

## Appendix VII. Bradford assay calibration curve
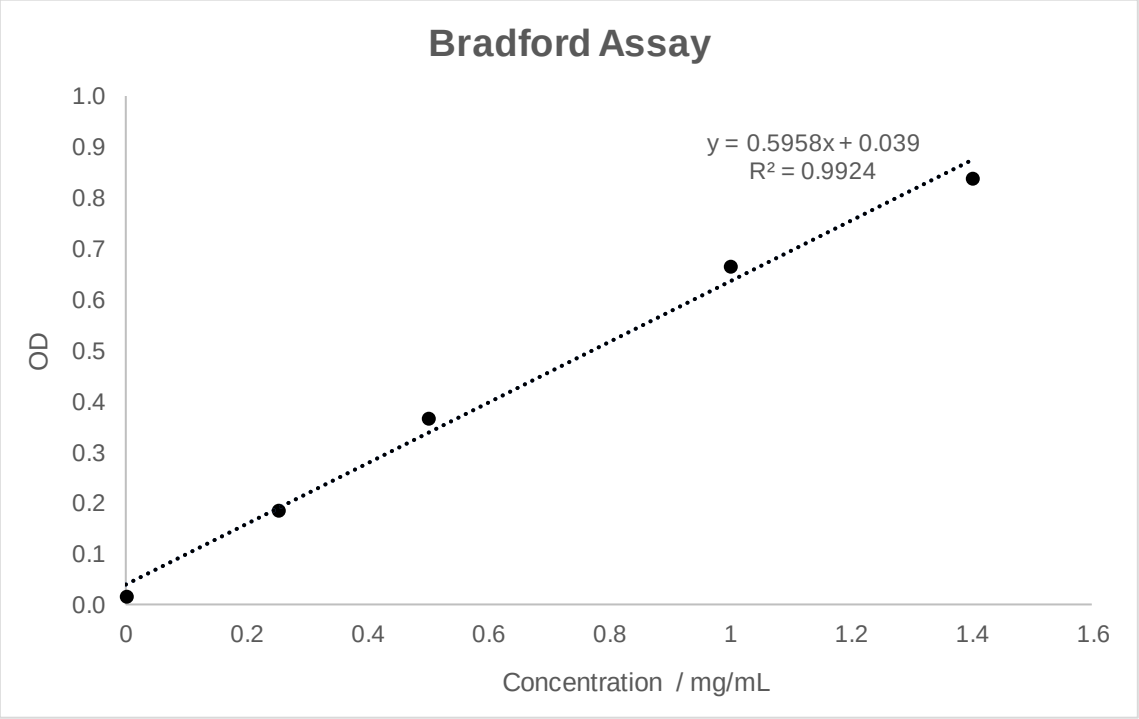
The Bradford method was used to calculate the concentration of MsrA02 protein in purified samples. The OD reading was taken at 595 nm.